RECONSTRUCTING POLLUTION HISTORY FROM INTERTIDAL REGIONS OF ESTUARIES ALONG MUMBAI COAST, INDIA

Ph.D THESIS

BY

LINA L. FERNANDES
M.Sc

JULY, 2012

RECONSTRUCTING POLLUTION HISTORY FROM INTERTIDAL REGIONS OF ESTUARIES ALONG MUMBAI COAST, INDIA

THESIS

SUBMITTED TO GOA UNIVERSITY FOR THE AWARD OF THE DEGREE OF

DOCTOR OF PHILOSOPHY

IN

MARINE SCIENCE

BY

LINA L. FERNANDES
M.Sc

RESEARCH GUIDE

PROF. G. N. NAYAK

Department of Marine Sciences,
Goa University,
Taleigao, Goa – 403206

JULY, 2012

STATEMENT

As required under the University ordinance OB.9.9 (iv), I state that the present thesis entitled "**RECONSTRUCTING POLLUTION HISTORY FROM INTERTIDAL REGIONS OF ESTUARIES ALONG MUMBAI COAST, INDIA**", is my original contribution and the same has not been submitted for any other degree, diploma, associateship, fellowship or similar titles in any universities or institutions on any previous occasion. To the best of my knowledge, the present study is the first comprehensive work of its kind from the area mentioned.

The literature related to the problem investigated has been cited. Due acknowledgements have been made wherever facilities and suggestions have been availed of.

Place: Goa University
Date:

Ms. Lina L. Fernandes

CERTIFICATE

This is to certify that the thesis entitled, "**RECONSTRUCTING POLLUTION HISTORY FROM INTERTIDAL REGIONS OF ESTUARIES ALONG MUMBAI COAST, INDIA**", submitted by Ms. Lina L. Fernandes for the award of the Degree of Doctor of Philosophy in Marine Science is based on her original studies carried out by her under my supervision. The thesis or any part thereof has not been previously submitted for any other degree, diploma, associateship, fellowship or similar titles in any universities or institutions. This thesis represents independent work carried out by the student.

Place: Goa University

Date:

Prof. G. N. Nayak
(Research Guide)
Dean, Faculty of Life science and Environment,
Head, Department of Marine Sciences,
Goa University, Goa

Acknowledgements

I have been extremely fortunate for having been surrounded by helpful, kind and knowledgeable people throughout this study. During my research many people have supported me and together we have made this thesis into what it is now. I am indebted to all of them but I want to thank a number of people in particular.

This thesis would not have been possible without the support and guidance from my research guide and advisor Dr. G. N. Nayak. Special thanks to him for suggesting this topic and granting me the opportunity to research on it. I thank him for his scientific advice and knowledge and many insightful discussions and suggestions. He patiently guided me through the process, never accepting less than my best efforts.

I would like to express my gratitude to the FRC committee, comprising of Dr. Borole, Dr. H. B. Menon and Dr. G. N. Nayak, for their suggestions and encouragements during the course of my degree.

This research was supported by grants funded by the Ministry of Earth Sciences, for the first two years, through funded research project entitled, “Reading Pollution History, Paleoclimate and Sea Level changes from the study of Mudflats, Central West Coast of India”. I am thankful to them. I also gratefully acknowledge the support of the Council of Scientific and Industrial Research (CSIR), New Delhi, through the award of Senior Research Fellowship.

My special thanks to Mr. D. Ilangovan, Scientist at National Institute of Oceanography, for his support in my field work, soil analysis, patience and unfailing willingness to assist and providing helpful inputs throughout the study.

I am grateful to Dr. S. R. Shetye, Director, National Institute of Oceanography (NIO), Goa, India, for allowing me to utilize the required facilities at the Institute. Special thanks to Dr. Borole, Retired Scientist from NIO, Goa, for Pb dating analysis. Other NIO scientists, Dr. Pratima Kessarkar, Dr. P. C. Rao and technical officer Mr. Prabhu, all from NIO, are thanked for their cooperation and technical support in analysis of clay mineral and Magnetic susceptibility analyses and the discussions of the results.

My profound gratitude to all my teachers of Department of Marine Sciences, Goa University, Dr. V. M. Matta, Dr. S. Upadhyay, Dr. H. B. Menon, Dr. Aftab Can and Dr. C. U. Rivonkar, for

their encouragements and support. I thank the Head of Department (HOD) of Marine Sciences for providing the required laboratory facilities for carrying out the research work.

Furthermore, I thank all my colleagues at the Marine Science Department of the University, who were not only directly or indirectly involved in the science of this thesis, but who made my stay at the department and the conferences visited into unforgettable events. I especially thank Ratnaprabha, Deepti, Cheryl, Maria, Shilpa, Bhavya, Tanu, Soniya, Samida, Anant, Maheshwar, Mahabaleshwar, Shrivardan, Dinesh, Rahul, Sweety, Ganesh, Renosh, Nutan, Santosh, Tomchou, Abhilash, Conchita, Vinay and Vidya. I wish you all the best and thank you for your support.

I am thankful to the non-teaching staff of the Department of Marine Science, Goa University, viz, Mr. Rosario, Mr. Yashwant, Mr. Ashok, Mr. Narayan, Mr. Shatrugan, Mr. Achut, Mr. Samrat, for their kind help, required during the course. Also my thanks go to Mr. Serrao, Mr. Martin and Mr. Ulhas for rendering the required help during the course.

Lastly and most importantly, I would like to say a big thank you to my family and friends for their endless support and encouragement over the past few years and for just being there. I feel a deep sense of gratitude for my parents who formed part of my vision, taught me the good things that really matter in life and made me what I am today.

Ms. Lina L. Fernandes

Table of Contents

List of Tables

List of Figures

Preface

One of the major global concerns in recent times has been the monitoring of environmental changes to understand the implications of various anthropogenic activities in the post-industrial era. The Estuarine environment and its associated sub-environments, such as mudflats and mangroves, play an important role in sediment deposition which acts as a sink for particle associated contaminants such as heavy metals. Heavy metals contamination in aquatic environment is of critical concern, due to their accumulation in aquatic habitats and toxicity of metals. Heavy metals in contrast to most pollutants are not biodegradable and enter ecological cycle. The concentration and the particular form of a heavy metal and its interaction with components of the sediment, determine its potential to cause toxic effects in biological systems. For the past few decades, it has been recognised that the environmental impact of these heavy elements is determined not by the total concentration but by their physical and chemical forms within an environmental system. For these reasons the speciation of a heavy metal is crucial to its behaviour in sediments and its toxicity.

Mumbai is a highly urbanised and industrialised region. Owing to the rapidly expanding industrial and urban areas, it is subjected to the effects and influences of these developments. Total metal concentrations of the sediments in the region have been reported earlier, which found increased level of contaminant. In recent years, many studies about the quality of creek sediments have been undertaken in this region and showed contamination problems concerning heavy metal pollution. However, all these studies were restricted to surface sediments of some selected stretches of the Mumbai coast. Systematic investigations of the subsurface sediments along the estuarine and creek systems were not conducted so far. Further, understanding the geochemical dynamics is an important factor for interpreting transport and ultimate fate of metals in the creek environment. Therefore, in the present study, an attempt has been made to understand the processes affecting the distribution and concentration of sediment components and metals by studying the spatial as well as temporal sediment analysis, which will help to reconstruct the pollution history of the region. However, determination of the total metal concentration in sediments is inadequate to fully understand bioavailability, mobility, and toxicity of metals, but is generally useful as an indicator of contamination in aquatic environments. Therefore, in the present study, speciation studies are also adopted. Although sediment geochemistry provides plenty of information of past conditions in the sites studied, the present study involving a multi-proxy approach, gives a more comprehensive picture of the ecosystem structure and functioning.
The thesis is divided into five chapters.

In the first chapter, the importance and the use of the different proxies employed to interpret the results of the study are presented. A general background on the literature survey carried out in the study area and also in the country and around the world, which is related to most of the work currently undertaken on pollution, is presented. The objectives of the work which comprises studying the spatial and temporal variations of the different sediment parameters along with the probable sources and factors accountable for the observations are

also presented. A description of the study area which includes the different sampling sites, geology and industrialised zones is also provided in this chapter.

The second chapter gives the methodology, covering in detail the sampling protocols and the various analytical techniques used in the investigation. The sampling locations with the latitudes and longitudes recorded, and the visual characteristic of the cores sampled are provided. The principle of the methods used, followed by the step by step process employed are also explained. Brief account of instruments used is also presented. Statistical approaches including pollution indices used are presented.

The third chapter is about the distribution of trace metals in different sub-environments of intertidal regions. This chapter describes the spatial and temporal variations in sediment characteristics and metal concentrations in sediments. C/N ratios calculated from the ratio of percentages of Total Organic Carbon (TOC) and Total Nitrogen (TN) provides insight into the relative contributions of algal vs. terrestrial organic matter to the sediment. Temporal analysis of heavy metals and stable Pb isotope variability highlights that most of the metals are being significantly enriched from anthropogenic sources especially in recent years, with high enrichment factors. The correlation and principal component analyses are attempted to get an understanding of the various geochemical factors and processes determining the fate of metals in sediments. Brief account of instruments used is also presented. Statistical approaches including pollution indices used are presented.

The fourth chapter summarises the results of the metal speciation studies in sediments. Seven metals namely Fe, Mn, Cu, Pb, Co, Zn and Cr are studied in vertical sections of selected cores in the estuarine and creek regions. The abundance and distribution of metals along with their bio-available fractions in sediments have been investigated and discussed.

The salient features of the present study are summarized in fifth Chapter with the main conclusions drawn and future research directions are listed. The references are given at the end of the thesis.

Chapter 1

INTRODUCTION

1.1. Introduction

Contamination of the environment and in particular the coastal marine environment by heavy metals has received considerable attention as evidenced by an increase of publications appearing in the literature (Chandra, 2002). The term "heavy metal" is used to describe metals having density greater than 5-6 g cm^{-3} (Sedgwick, 2005). Heavy metals are often referred to as trace metals, occurring naturally in low concentrations in water, soil and in organisms (Furness and Rainbow, 2000). Heavy metals can be divided into two groups namely; i) metals essential to some organisms (micronutrients) such as As, Cr, Cu, Ni, and Zn and ii) non-essential heavy metals with no known biological function which include Hg, Pb and Cd (Furness and Rainbow, 2000; Denton et al., 2001). Even though micronutrients are essential to some forms of life, they become toxic at high concentrations (Sedgwick, 2005). Heavy metals occur naturally as they are components of the lithosphere and are released into the environment through volcanism and weathering of rocks (Fergusson, 1990). However, large-scale release of heavy metals to the aquatic environment is often a result of human intervention (Mance, 1987; Denton et al., 1997). Almost all industrial processes that produce waste discharges are potential source of heavy metals to the aquatic environment (Denton et al., 2001) such as mining, smelting and refining. A proportion of the total anthropogenic metal input in sediments in nearshore waters, adjacent to urban and industrial growth centres, comes from the combustion of fossil fuels. Domestic wastewater, sewage sludge, urban runoff and leachate from solid waste disposal sites are also sources of heavy metals into rivers, estuaries and coastal waters (Mance, 1987). Other potential sources include ports, harbours, marinas and mooring sites, also recreational, commercial, and occasionally, military, boating, and shipping activities (Denton et al., 1997). Agricultural activities contribute to the overall heavy metal loadings to the environment through the spreading of fertilisers, pesticides, wood preservatives and sewage sludges (Alloway, 1995; Bradl, 2005).

In aquatic systems metals are partitioned amongst soluble phases, suspended and bottom sediments and biota (Gangaiya et al., 2001). The strong affinity of metals for particulates typically results in metals being retained for extended periods of time, before they are released back into the dissolved phase, and enter the water surrounding sediment particles (sediment porewater). The partitioning behaviour of heavy metals is such that they tend to accumulate in sediments to levels that are several orders of magnitude higher than the surrounding waters (Denton et al., 1997). Therefore, the analysis of heavy metals in the sediments permits detection of contaminants that may be either absent or present in low concentrations in the water column. It is said that sediments are a major carrier phase for pollutants and provide useful spatial and temporal information (Birch et al., 2000; Birch, 2003; Singh and Nayak, 2009; Fernandes and

Nayak, 2009). Sediment is a matrix of materials, made up of detritus, inorganic and organic particles and is relatively heterogeneous in terms of its physical, chemical and biological characteristics (Sarkar et al., 2004) and consists of wide range of particle sizes, including gravel, sand, silt and clay (Fergusson, 1990). Sediment grain size is an important factor in influencing the concentration of heavy metals, with metal concentrations significantly enriched in fine grained sediments, mainly clay and silt, which have high absorption capability due to their large specific surface area. Sediments are well known to act as a major sink for many of the more persistent organic and inorganic chemicals introduced into the aquatic environment by atmospheric deposition, erosion of the geological matrix or from anthropogenic sources such as industrial effluents, mining wastes, etc. (Pempkowiak et al., 1999; Sarkar et al., 2004; Calace et al., 2005). Being formed by the deposition of fine particles with their associated contaminants, each layer of buried sediment represents a record of the environmental conditions, reflecting the water quality and possible effects of anthropogenic contamination at a certain period (Von Gunten et al., 1997). Sediments can also act as potential sources of pollution for the surrounding water and benthic flora and fauna by releasing sorbed contaminants back to the overlying water column if remobilization occurs through any disturbance (Denton et al., 1997; Sarkar et al., 2004; Adamo et al., 2005). Human activities such as dredging and reclamation in coastal environments can remobilize heavy metals from sediments into the seawater column (Lee and Cundy, 2001). The resuspension of sediment might lead to the release of metals into the overlying water or due to the transport of porewater metals into this water or through metal desorption from sediment into this water (Calmano et al., 1994; Cantwell et al., 2002; Eggleton and Thomas, 2004; Zwolsman et al., 1997). Spatial and temporal fluctuations in metal concentrations may also be caused by changing environmental processes/parameters, such as water flow rate, pH, salinity, turbidity, temperature and organic matter (Baeyens et al., 2005; Byrne et al., 1988; Hatje et al., 2003, Teasdale et al., 2003).

The growing apprehension about the potential effects of sediment toxicity to marine fauna and flora and the risk posed to the environment by the contaminants accumulated in the sediments have aroused an increase in research interests in marine sediments (Vernet, 1991; Calace et al., 2005). In aquatic environments, since a large proportion of the metals are associated with suspended particulates and bottom sediments, high concentrations of heavy metals are often detected in sediments of many industrialized harbours and coastal regions around the world (Miller et al., 2000; Chen et al., 2001; Feng et al., 2004; Wang et al., 2007). The concentrations of metals in aquatic systems may vary greatly between locations depending on the proximity to natural and anthropogenic sources. A large and increasing proportion of the world's population

are concentrated in coastal areas. Therefore, pollution levels are often elevated along the coast because of nearby land based pollution sources (Fergusson, 1990; Angelidis, 1995) and decrease rapidly with distance from a source, due to dilution and dispersion (Aguilera and Amils, 2005; Baeyens et al., 2005; Teasdale et al., 2003). Therefore, the chemical analysis of sediments is very important from the environmental pollution point of view. Further, sediment concentrates metals from aquatic systems, and represents an appropriate medium for monitoring of environmental pollution (Denton et al., 1997; Sarkar et al., 2004).

Trace metal cycling and its fate in coastal wetland, a typical dynamic ecosystem, have fascinated many researchers, because they not only reveal the evolution processes of natural environment (Wang and Liu, 2003), but also indicate the intensity of human activities (Rabouille et al., 2007). The process of sediment deposition is common in intertidal flats of estuaries. Intertidal areas comprising of mud/sand flats and mangroves are highly dynamic systems which are constantly influenced by local energy levels and, especially in the case of high energy sand flat areas, exhibit a micro-structure which is governed by repeated erosion and deposition during the reworking of the sediment (Swart, 1983). Mudflats and sheltered intertidal sand flats reflect low energy conditions which are characterised by: particles of a small medium diameter, shallow slope, high water content, high sorting coefficient, low permeability and generally low porosity, high organic content and therefore high reducing conditions, high carbon to nitrogen ratio, high microbial population and high sediment stability. Sub-tidal mobile sandbanks and exposed intertidal sands are found in high energy areas which are characterised by: particles of a high median diameter, low sorting coefficient, high permeability, generally high porosity (depending on compaction), low organic content, high oxygen content and therefore low reducing conditions, low carbon to nitrogen ratio, small microbial population and low sediment stability. Intertidal mudflats develop in low energy areas, while sub-tidal mobile sandbanks develop especially as the result of the physiography and large-scale current patterns producing gyres. The above hydrographic and sedimentary processes on intertidal mud/sand flats control the mixing and dispersal of sediment bound contaminants (Dolphin et al., 1995). Mangroves are one among the world's most productive ecosystem and form an important part of the coastal and estuarine environment. Living at the interface between the land and the sea, the mangrove plants have morphological and physiological adaptations to survive in harsh saline environment. Mangroves produce organic carbon well in excess of the ecosystem requirement and contribute significantly to global carbon cycle. They have enormous ecological value. They protect and stabilize coast lines, enrich coastal waters, yield commercial products and support coastal fisheries.

The Estuarine environment and its associated mudflats and mangroves play an important role in sediment deposition which acts as a sink for particle associated contaminants such as heavy metals. Although natural and anthropogenic activities introduce trace metals to aquatic regions, the anthropogenic effects may seriously degrade the environment at local to regional scale (Siegel, 2002). Estuarine systems often have higher concentrations of naturally occurring metals than adjacent open water, as they receive riverine inputs (Apte and Day, 1998; Munksgaard and Parry, 2001). Marine organisms that inhibit estuaries can often tolerate higher metal concentrations than those living in the open ocean. This is because there are greater concentrations of inorganic and organic metal complexing ligands e.g. Fe and Mn hydroxides, humic and fulvic acids or because historical exposure has lead to the evolution of tolerance mechanisms (Apte et al., 2000; Nies, 1999; Rijstenbil and Gerringa, 2002). Estuaries which are more open and have larger tidal ranges usually have greater rates of flushing, decreasing the likelihood of metal enrichment (Deeley and Paling, 1999). Human activities on land and immediately adjacent to coast, pose a significant threat to the health, productivity and biodiversity of the marine environment (Chandra, 2002).

1.2. Speciation

Environmental pollution with toxic metals is becoming a global phenomenon. Metal contaminants are distinctive as they are persistent in the environment and are not removed by degradation. Instead they undergo conversions between different chemical forms (Hirose, 2006; Smith et al., 2002). These conversions may be mediated by both biotic (micro and macro-organisms) and abiotic (environmental) mechanisms (Hirose, 2006; Van Cappellen and Wang, 1996; Santschi et al., 1990). Though the total metal concentration in sediment is a valuable index of pollution, it does not give an indication of the available metal concentrations. The distribution of metals among the different forms or species is referred to as metal speciation (Apte et al., 2005; Batley et al., 2004; Byrne, 1988). Chemical species may vary due to differences in isotopic composition, electronic or oxidation state and/or molecular structure (Smith et al., 2002; Templeton et al., 2000). The elements ability to be mobilised and transported between the environmental compartments and become potentially available is directly related to its speciation. The species that are available for uptake in organisms are considered to be the bio-available fractions. The term bioavailability reflects the rate and the amount of toxic substances that may be taken up in an organism. The chemical partitioning of heavy metals among different sedimentary forms is very important in determining their bio-availability (Luoma, 1983). Since total concentration does not yield information on mobility, origin or bioavailability of elements, study of metals in sediments have to be associated with the different fractions present. There is a

need to understand the chemical forms of heavy metals as well as their complexes so as to better evaluate the environmental impact of contaminated sediments. Speciation is therefore very useful for determining the degree of association of the metals in the sediments and to what extent they may be remobilized into the environment.

Factors affecting metal speciation

Metal speciation is influenced by many factors in aquatic systems, including the chemical/physical form of the metal released into the waters from natural/anthropogenic sources, physico-chemical properties of the water, the concentration and type of metal complexing ligands and environmental processes, all of which may vary between locations and over time (Heugens et al., 2003; Vasconcelos et al., 2002). For metals, as water pH decreases, the partitioning between dissolved and particulate forms favours the dissolved phase (Calmano et al., 1994; Hatje et al., 2003; Riba et al., 2004). This is due to hydrogen (H^+) ions competing with metals for binding sites on particulate matter. Changes in H^+ concentrations may cause changes in metal speciation by altering the structure of environmental ligands and metals bound to them. Although increased H^+ concentration generally causes an increase in dissolved metals, increasing in organism toxicity do not necessarily occur, as there is also increased competition between H^+ and dissolved metals for uptake sites on the organism (De Schamphelaere and Janssen, 2004; Wilde et al., 2006).

Water salinity has a large effect on the speciation of metals such as Cd, Ni, Hg, due to complexation with chloride and/or competition with major salinity ions (Cl^-, Na^+, K^+) for the binding sites for biological ligands and particulates (Hatje et al., 2003; Riba et al., 2004). Changes in metal speciation often occur when the salinity is in the range of 0-15 PSU (Hatje et al., 2003; Zwolsman et al., 1997; Baeyens et al., 2005). In estuaries, increase in salinity often cause the removal of significant amounts of Dissolved organic carbon into the particulate phase, through flocculation induced by changes in ionic strength and pH that accompany the mixing of riverine and saline waters (Fox and Wofsy, 1983; Morris and Bale, 1981; Sholkovitz, 1976). This flocculation may lead to the transfer of a significant amount of the metal from the dissolved to the particulate form (Sholkovitz, 1978; Teasdale et al., 2003; Stordal et al., 1996). Increase in salinity often decreases the toxic effects of metal exposure to organisms due to the competitive and complexing effects of major ions with trace metals (De Schamphelaere et al., 2004; Erickson et al., 1996; Riba et al., 2004).

Oxygen and oxidised compounds generally become depleted with sediment depth due to low oxygen penetration into the sediments, as well as oxygen and oxygen-rich compounds (NO_3, FeOOH, MnO_2) being utilized as electron acceptors by bacteria for coupling with organic matter oxidation. This causes the redox potential of the sediment to decrease as the speciation of compounds (both metals and non-metals) favours reduced forms, particularly as the depth of sediment increases and results in vertical stratification of metal speciation (Clark et al., 1998; Kristensen, 2000; Wang and Van Cappellen, 1996). In the surficial layer of sediments, a large proportion of metals are bound by oxidised species such as Fe and Mn (hydr)oxides, as well as organic carbon (Clark et al., 1998; Simpson and Batley, 2003). As the sediment depth increases, organic matter and oxidised compounds become depleted and metals increasingly exist in reduced forms. Sulphide is the dominant metal binding phase at depth, due to the reduction of sulphate, which is usually freely available to bacteria (Santschi et al., 1990).

Sequential extraction (Tessier et al., 1979) techniques can provide information about the identification of the main binding sites, the strength of metal binding to the particulates and the phase associations of trace elements in sediment. This helps in providing information on evaluation of metal bio-availability and identification of binding sites of metals for assessing metal accumulation, pollution and transport mechanisms thereby understanding the geochemical processes governing the heavy metal mobilization and the potential risks induced. Single and sequential extraction schemes have been designed for the determination of binding forms of trace metals in sediments (Sahuquillo et al., 1999). Different sequential extraction schemes have been proposed and most of these include a number of steps between 3 and 8. One of the first and most applied sequential extraction procedure proposed is a five-step procedure published by Tessier et al. (1979). Several other procedures followed the Tessier procedure, and now there are a wide variety of sequential extraction procedures available based on different sequence of extractants and different operational conditions. The principle of these procedures is based on the selective extraction of heavy metals in different physico-chemical fractions of a material using specific solvents (Bruder-Hubscher et al., 2002).

1.3. Magnetic parameters

Magnetic minerals present in soils or sediments may be either inherited from parent materials, or be produced by pedogenic processes via fluvial and eolian transportation, or stem from anthropogenic activities (Boyko et al., 2004). Magnetic susceptibility is a potentially useful proxy measure of heavy metal contamination in soils and sediments. This is on the basis of the fact that many anthropogenic impacts on the environment are accompanied by significant

emission of strong magnetic particles, which causes an increase in magnetic susceptibility. Since industrialization, however, magnetic spherules originating from anthropogenic fly-ashes from factories and vehicles may also significantly contribute to the magnetic properties of marine sediments. This is especially common in coastal settings and marginal seas adjacent to heavily populated and industrialized areas (Horng et al., 2009). The magnetic enrichment in marine sediment was found to be caused by fine-grained iron oxides derived from industrial and urban sources (Versteeg et al., 1995; Chan et al., 1998, 2001; Petrovsky and Elwood, 1999; Hanesch and Scholger, 2002). In recent years, magnetic susceptibility has been successfully used to map the spatial distribution of pollutants, for example, toxic metals in soils from industrial activities and dust deposition around power plants (Kapicka et al., 1999) or along roads (Hoffmann et al., 1999; Goddu et al., 2004; Gautam et al., 2004), as well as to differentiate emission types and sources in atmospheric particulates and sediments (Hanesch and Scholger, 2002; Hanesch et al., 2003; Lecoanet et al., 2003; Moreno et al., 2003). Additionally, Strzyszcz and Magiera (1998) studied the magnetic susceptibility of soils in different regions of Poland and found that the regional magnetic susceptibility distribution pattern was closely correlated to the concentration of heavy metals. In another case, Lu (2003) presented a comprehensive overview of magnetic monitoring methods in pollution studies. Combined analysis of chemical and magnetic data has proved close relationship between magnetic susceptibility and heavy metal concentrations in marine and river sediments (Chan et al., 1998; Desenfant et al., 2004) and soils (Petrovsky et al., 2001). Magnetic measurements as a proxy for industrial contamination, petroleum hydrocarbons and polycyclic aromatic hydrocarbons in coastal environment have also been employed (Goddu et al., 2004; Dessai et al, 2009; Alagarsamy, 2009; Sangode et al., 2010; Venkatachalapathy et al., 2011b; Blaha et al., 2011). Magnetic mineral analyses have also been successfully used to investigate on depositional environment, sediment fluxes and sediment sources and on their paleo-climatic and paleo-environmental associations (Bloemendal et al., 1992; Stoner et al., 1995; Maher and Thompson, 1999).

1.4. Sediment chronology

Compared with most environmental archives, coastal sediments may provide more favourable conditions for the preservation of historical pollution records. This is because marine sedimentation is usually a reasonably continuous and steady process and sediment layers can be dated by fallout radionuclides such as ^{210}Pb and ^{137}Cs to establish a reliable sediment chronology. Methods using stable Pb isotope ratios are gaining importance because the variations of these ratios are not altered by chemical and physical processes and can thus be used to trace the sources of anthropogenic contaminants associated with Pb (Gallon et al., 2005, 2006;

Hou et al., 2006). The total ^{210}Pb activity in estuarine sediments has two components. Supported ^{210}Pb is that component of the activity, which derives from in-situ decay of the parent isotope ^{226}Ra within the individual soil or rock particles. It is transported into the water bodies in particulate form (along with the associated ^{226}Ra) as a part of erosive input from the catchment. The second component, called unsupported ^{210}Pb derives from a fraction of the ^{222}Rn atoms formed in the atmosphere due to interstitial diffusion through the soil into the atmosphere, where they decay through a sequence of short-lived isotopes to ^{210}Pb. This is removed from the atmosphere by precipitation or dry deposition falling on to land surface or into lakes or oceans. ^{210}Pb falling directly into estuaries is scavenged from the waters and is deposited on the bed of the estuary along with the sediments. In most situations, the supported ^{210}Pb can be assumed to be in radioactive equilibrium with the supported ^{226}Ra activity, and the unsupported activity at any level is obtained by subtracting ^{226}Ra activity from the total ^{210}Pb activity. The unsupported ^{210}Pb in each sediment layer declines with its age in accordance with the usual radioactive decay law and can be used to date the sediment. The determination of ^{210}Pb content can be effected either through a simple radiochemical separation scheme based on an anionic ion exchange followed with Pb-chromate precipitation and beta counting of ^{210}Bi or through ^{210}Pb leaching followed with alpha measurement of its grand- daughter ^{210}Po deposited on a Silver planchette (Godoy et al., 1998).

1.5. Literature review

Studies carried out using different sediment parameters in the recent past are given in Table 1.1 below,

Table 1.1. Literature survey of studies carried out in India and the world

Authors	Parameters analysed	Observations
Choi et al., 2012	Metal analysis	To investigate the status of metal contamination in the sediments of coastal marine areas of South Korea, Cr, Ni, Cu, Zn, As, Cd, Pb and Hg were determined in twelve study sites. According to the average Enrichment Factor values, the most contaminated metal was Hg. Overall, the metal contaminations of surface and bottom sediment in the South Korean harbours was regarded as medium-low to medium-high-priority sites.
Neser et al., 2012	Organic matter and Metal analysis	Concentrations of heavy metals and organic carbon in sediment of the Aliaga Bay were investigated. Comparison of metal concentrations with average shale values revealed that most of the samples from the Aliaga were polluted with Hg, Cd, Pb, Cr, Cu, Zn, Mn and Ni. According to the Metal Pollution Index (MPI), highest MPI values were observed for coastal stations. Based on the enrichment factors, the metal pair ratios clearly reflected maximum enrichment of Hg, Cd, Pb, Cu and Mn. The main metal source was atributed to

		shipping activity, ship-breaking industry, steel works (iron smelters and roller mills) and petrochemical complex.
Blaha et al., 2011	Magnetic parameters, Polycyclic Aromatic Hydrocarbon (PAH), Metal contents, ^{210}Pb dating technique, Scanning Electron Microscopy (SEM)	The onset and rise of urban and industrial pollution in Mumbai region was reconstructed from an anthropogenically contaminated mudflat sediment profile (1.8 m) from adjacent Thane creek. In this study, magnetic methods were used for delineation of both anthropogenic PAH as well as anthropogenic metal contamination. ^{210}Pb dating revealed that water and air polluting industrial activities significantly increased in the mid 1950s. SEM investigation of magnetic extracts from the contaminated sediments revealed the presence of fly ash particles probably originating from the local coal-fired power plant.
Davutluoglu et al., 2011	Grain size, Total organic matter, Metals, Speciation analysis	Chemical fractionation of seven heavy metals (Cd, Cr, Cu, Mn, Ni, Pb and Zn) was studied using a modified three-step sequential procedure, to assess their impacts in the sediments of the Seyhan River, Turkey. Metal fractionation showed that, except for Mn and Pb, the majority of metals were found in the residual fraction regardless of sampling time, indicating that these metals were strongly bound to the sediments. Based on RAC classification, Cd and Cr posed no risk, Cu and Ni posed low risk, Pb and Zn were classified as medium risk metals, while the environmental risk from Mn was classified as high.
Ghrefat et al., 2011	Grain size, Metals, XRD analysis	Sediment pollution, in this study, was assessed using Enrichment Factor (EF) and Geo-accumulation index (Igeo). The results indicated that the Igeo calculations were more reliable than those of EF. The EF results demonstrated that metals in the study area were enriched. Based on Igeo values, the surface, cut-bank and dam bank sediments were uncontaminated with respect to Ni, Co, Cr, Cu and Mn; moderately to strongly contaminated with Pb and strongly to extremely contaminated with Cd and Zn. Mineralogical analysis showed the presence of clay minerals (illite, kaolinite), calcite, dolomite, quartz, orthoclase and microcline.
Suresh et al., 2011	Grain size analysis, Radioactivity (gamma-ray spectrometer), Mineralogical measurement, Heavy metals	The concentration and spatial distribution of heavy metals (Pb, Cr, Cu, Zn and Ni) were studied to understand the metal contamination and its level of toxicity. Studied metal concentrations, except Cr, Pb and Pollution Load Index (PLI) were increased towards the mouth of the river, which was due to the increasing content of clay and human activities. Statistical analyses showed that the clay mineral kaolinite was the major factor for absorbed dose rate and PLI.
Venkatachal apathy et al., 2011a	Magnetic parameters, Heavy metals	In this study, environmental magnetic, heavy metal and statistical analyses were conducted on 21 surface sediments collected from Chennai coast, India, to examine the feasibility of heavy metal pollution using magnetic susceptibility (χ). The Chennai coastal sediment samples were dominated by ferrimagnetic minerals corresponding to magnetite-like minerals. The percentage of frequency dependent magnetic susceptibility reflected the presence of super-paramagnetic/single domain magnetic minerals. Significant correlations between heavy metals and χ indicated the potential of magnetic screening/monitoring for simple and rapid proxy indicator of heavy metal pollution in marine sediments.

Venkatachal apathy et al., 2011b	Petroleum HydroCarbon (PHC), Metals	In this study, four sediment cores (C1, A1, T1 and K1) from the northeast coast of Tamil Nadu, India were statistically analysed to examine the feasibility of PHC using magnetic susceptibility. The C1 and A1 cores reveal a clear horizon of increase in PHC above 35 and 50 cm respectively, suggesting that excess anthropogenic loading occurred in the recent past. Magnetic properties which were enhanced in the upper parts of the sediment cores were the result of ferrimagnetic minerals from anthropogenic sources. Factor analysis confirmed that the input of magnetic minerals and PHC in Chennai coastal sediments was derived from the same sources.
Fang and Yang, 2010	Metals	Data on heavy metals (Cd, Cr, Cu, Ni, Pb and Zn) in river sediments in Taiwan, China, Japan, India and Vietnam during 1999 to 2009 was reviewed and discussed. The results showed that the sources of heavy metal pollution came mainly from a variety of anthropogenic activities which included domestic and industrial wastewater, as well as e-waste recycling, chemical, electric plating and refining industries.
Hani and Kariminejad, 2010	Heavy metals	A study was carried out to determine the spatial pattern of Cd, Cu, Pb, Mn, Zn and Ni in Kaveh industrial city using multivariate and geostatistical analysis, to attain the industrialization effect on heavy metal pollution in soils. A high significant correlation was observed between Zn and Cd, indicating that they were from same origin. The results of principal component analysis indicated that Cd, Zn and Pb were likely affected by pedogenic factors, while the concentration of Cu and Mn was related to pedogenic (e.g., background values) and anthropogenic factors (e.g., the discharge of industrial waste). Ni concentration was related to anthropogenic factors such as industrial effluents and wastes and had high risks for environmental pollution and human health.
Harikumar and Jisha, 2010	pH, Electrical conductivity, Organic carbon and Metals	Study was carried out to investigate the concentrations and spatial distribution of trace metals in the sediments of Kottuli wetland, the south west coast of India. Pollution load index value (PLI) of the studied area ranged from 0.10 to 58.78 which indicated that the wetland sediments were polluted. From the study, PLI of the downstream area of the wetland had the highest values of Cu, Mn, Cd, Zn and Cr.
Ho et al., 2010	Grain size, pH, Organic matter, Clay minerals, Total sulphur, Metals	The distribution, controlling geochemical factors and contamination status of heavy metals in estuarine sediments near Cua Ong Habour, Ha Long Bay (Vietnam) were investigated. The results illustrated that the distribution patterns of As, Cd, Cr, Cu, Ni, Pb and Zn were mainly controlled by organic matter and clay minerals and determined by the distribution of the fine-grained fraction (< 63 μm) in the sediments. In contrast, Fe and Mn compounds seemed to exert some control on the distribution of Co. Carbonates partly controlled the distribution of Mn, but were not important with respect to the other studied heavy metals. Among the studied heavy metals, only As was of concern.
Huan et al., 2010	^{7}Be and ^{210}Pb activities	Sediment cores (~40-100 cm) were collected at 12 locations in the western Bohai Bay, the Haihe River estuary, the Yongding River estuary and the Tianjin Harbour, China and analyzed for ^{7}Be and ^{210}Pb activities. From ^{7}Be and ^{210}Pb profiles, the temporal and spatial variations of these radionuclides

		supported a non-steady state depositional environment in the study area. ^{210}Pb inventories in the sediments implied that there was a net on-shore transport of sediments and the sediments were mass-balanced in the entire study area. Overall, the results suggested that the sediments were retained in the estuaries and the western Bohai Bay despite local variability in sediment dynamics and disturbance due to human activities.
Jain et al., 2010	pH, Organic matter, Metals, Chemical Speciation	Fractionation of metal ions was studied on the bed sediments of Hussainsagar Lake in order to determine the ecotoxic potential of metal ions. The quality of Hussainsagar Lake has degraded due to the municipal and industrial discharges from the lake catchment area. Although the total content of heavy metals in the sediments was much higher, the bio-available quantity of heavy metals was comparatively low. About 20-30% of majority of metals studied were associated with the residual fraction. The metals associated with this fraction cannot be remobilized under normal conditions encountered in nature.
Lepane et al., 2010	Metals, Organic matter, Chemical Speciation	A sequential extraction procedure was used to study the partitioning of metals (Ca, Mn, Fe, Cu, Zn and Cd) between operationally defined fractions in the interval covering the last 150 years of sediment record from Lake Peipsi, Estonia. The results indicated decreased total and bio-available Cu and Zn levels from the 1980s to the present and increased Cd levels. The variability in Mn and Fe concentrations was possibly induced by changes in redox conditions at the bottom of the lake. This study revealed increasing trends for general sediment characteristics (organic matter, dissolved organic carbon and absorbance ratio) since the 1960s, together with some molecular characteristics (peak areas of humic and high molecular weight fractions). Statistical cluster analysis revealed that metal concentration data in combination with some chromatographic and spectrometric parameters can be used to reveal periods with similar characteristics in Lake Peipsi sediments.
Praveena et al., 2010	Metals	This study was carried out to investigate the dynamics of heavy metals concentration. The results revealed relatively higher concentrations of heavy metals at high tide compared to low tide. This observation was complexed by other factors such as redox condition, presence of hydroxides and oxy-hydroxides. The major source of heavy metals in mangrove surface sediment was of anthropogenic origin such as from agricultural, aquaculture and industrial activities.
Ratheesh et al., 2010	Texture, pH, Total Carbon, Hydrogen, Nitrogen, Sulphur and Heavy metals	Heavy metals in the surface sediments of two coastal ecosystems of Cochin, southwest India were assessed. The analysis of enrichment factor indicated a minor enrichment for Pb and Zn in mangrove sediments, while extremely severe enrichment for Cd, moderate enrichment for Zn and minor enrichment of Pb were observed in estuarine system. The geo-accumulation index exhibited very low values for all metals except Zn, indicating the sediments of the mangrove ecosystem were unpolluted to moderately polluted by anthropogenic activities. The observations suggested that the mangrove ecosystems were relatively unpolluted but the estuarine stations were under the threat of severe

		accumulation of the toxic trace metals.
Singare et al., 2010	Bulk density, Moisture content, pH, Electrical conductivity, Alkalinity, Chlorinity, Heavy metals	In this investigation, heavy metal pollution in soil samples collected along Thane Creek were analysed for various parameters. The values recorded were observed to be high during dry seasons and low during rainy season. The soil samples were also analyzed for their heavy metal contents like Ni, Zn, Cd, Cu, Fe, As and Hg. It was observed that the concentration of these heavy metals increased gradually in dry seasons, followed by sharp decrease during the rainy season. The authors suggested need of regular monitoring of water resources and further improvement in the industrial waste water treatment methods.
Essien et al., 2009	Grain size analysis, Total organic carbon, Total organic nitrogen, Heavy metals	The concentration and distribution of selected heavy metals in epipelic and benthic sediments of Cross River Estuary mangrove swamp were studied to determine the extent of anthropogenic inputs from industrial activities and to estimate the effects of seasonal variations on geochemical processes in the estuarine ecosystem. Lowest metal concentrations were found during the dry season, compared to the wet season. Pollution load index and index of geo-accumulation revealed overall low values but the enrichment factors for Cr, Zn and V were high and this reflected the intensity of anthropogenic inputs related to industrial discharge into the estuary.
Garcia et al., 2009	Grain size, Total organic matter, Metals	The research work investigated the distribution, the factors controlling concentrations and toxicity risks of the metals (Co, Cr, Cu, Li, Mn, Ni, Pb, Zn, Al and Fe) in surface sediments of four rivers. Toxicity was evaluated using the consensus-based Sediment Quality Guidelines for freshwater ecosystems. Concentrations of metals in all samples were below the TEC (threshold effect concentration), indicating that for these trace metals adverse effects on aquatic biota should rarely occur. Metal enrichments due to anthropogenic influence were only observed at three sites. At other site, enrichment factors were indicative of a large predominance of naturally occurring metals in the sediments.
Madiseh et al., 2009	Grain size, Organic matter, Metals	The study was conducted to investigate the metal contents of sediments of several creeks in Persian Gulf that discharged into coastal waters using the Risk index. All of the studied creeks showed moderate to considerable contamination level for heavy metals in sediment.
Rathod and Patil, 2009	Water temperature, Suspended solids, pH, Dissolved oxygen, Salinity, Biochemical oxygen demand (BOD), Phosphate-phosphorus (PO_4-P), Nitrate-nitrogen (NO_3-N), Silicate-silicon	In this study, physical and chemical variables of water were monitored month-wise in the year 2004-2005 in Ulhas estuary, Mumbai. The entire stretch of estuary showed high values of BOD, PO_4-P, NO_3-N, Suspended solids and hypoxia suggesting deterioration of the estuary.
Zourarah et al., 2009	Dissolved and particulate heavy metal, Particulate organic carbon, Grain size, ^{137}Cs and ^{210}Pb activities, Metals in	A dated estuarine core from inter-tidal area of Oum Er Bia estuary was assessed using ^{210}Pb and ^{137}Cs data. The data indicated that the mean sedimentation rates were 0.38-68 cm/yr. The analytical and the radiodating results of sediment cores showed extremely high concentrations of Zn, Pb and Cu that were ascribed mostly to the discharge of the liquid

	sediment	effluent from the sewage since the late 1960s, decreasing towards the present day. The pollution intensity of the estuary determined by the enrichment factors showed that the estuary was in moderately polluted to unpolluted class.
Benson et al., 2008	Metals, Chemical speciation	An analysis of the distribution and chemical forms of selected metals Pb, Cd and Cu appeared to be the most abundant metal in the sediments of the systems and were predominantly associated with the residual, organic and oxidisable phases. Results indicated that there were also insignificant components that are bound to both the exchangeable and carbonate fractions. Speciation results indicate that metal contamination in the ecosystems investigated primarily comes from human-mediated sources.
Lu et al., 2008	pH, Heavy metals, Magnetic parameters, XRD analyses	The magnetic properties and magnetic mineralogy of a weathering sequence of soils developed on basalt parent material from eastern China were studied by rock magnetism, X-ray diffraction and soil chemical analyses, to establish the connection between mineral magnetic properties and pedogenic development in a subtropical region. Rock magnetism analysis showed that the major magnetic carriers in the weakly weathered soil profiles were magnetite and/or maghemite, and the highly developed soil profiles were generally enriched in magnetite/maghemite grains of pedogenic origin and the magnetically hard haematite, indicating that the magnetic component was transformed from a ferromagnetic phase (magnetite) to antiferromagnetic phase (hematite) during pedogenic development. Results indicated that some of the magnetic parameters of soils, (χ_{fd}), were useful for pedogenic comparisons and age correlations in the weathering sequence of soil. It was thus suggested that multiparameter rock magnetic investigations represented a more powerful approach for pedogenesis.
Palanques et al., 2008	Grain size, Dry bulk density, Heavy metals, Carbonate, ^{210}Pb and ^{137}Cs analyses	Anthropogenic trace-metal concentrations and inventories were studied on the Llobregat continental margin, from the Llobregat river mouth to the Foix submarine canyon. This study correlated shelf sediment contamination with the adjacent submarine canyon sediment contamination and demonstrated that physical processes can contribute to an efficient off-shelf particulate trace-metal transfer through submarine canyons that could become a sink for them. The study also showed that anthropogenic contamination in the Mediterranean was affecting not only the littoral and continental shelf sediments, but also deeper areas through submarine canyons.
Sheng-Gao et al., 2008	Metals, Magnetic susceptibility, SEM analysis	Concentrations of Cu, Zn and various magnetic parameters in contaminated urban roadside soils were investigated using chemical analysis and magnetic measurements. The results revealed highly elevated Cu and Zn concentrations as well as magnetic susceptibility (χ) in the roadside soils. Cu and Zn concentrations of the soils had highly significant linear correlations with χ.
Borkar et al., 2007	Methods used: Quadrant method and Visual estimation	The study on the distribution of mangroves and the associate plants along Ulhas river estuary and the Thane creek during the period September 2001 to August 2002, showed presence of 8 genera and 14 species of mangroves and 11 genera and 12 species of mangrove associates. The dominant mangrove type

		was *Avicennia marina* where as *Acanthus ilicifolius* was the major associate type. When compared with the earlier data, it was apparent that the mangrove cover was significantly reduced. The main threat to mangroves was due to anthropogenic activities, like cutting for fuel; reclamation for various purposes such as industry, agriculture, sand landing (Retibunder), solid waste dumping, aquaculture ponds, construction of housing colonies, roads and bridges violating the CRZ regulation.
Hu et al., 2007	pH, Magnetic parameters, Heavy metals	To study the feasibility of using magnetic techniques for monitoring soil pollution in Shanghai, magnetic properties and heavy metals in topsoils of an urban site (Songnan Town) and a less-urbanized agricultural site (Luojing Town) in Baoshan District, Shanghai, were studied. Compared with the background, magnetic signals of the urban topsoils were extremely enhanced with magnetic susceptibility (χ) while those of the agricultural topsoils were only slightly increased. It suggested that the urban topsoils received some coarse ferrimagnetic particles. Heavy metals were highly enriched in the magnetic fractions of the topsoils. Geochemical properties of the magnetic fraction of urban topsoils were significantly different from those of agricultural topsoils, indicating that the extra magnetic minerals accumulated in the urban topsoils were neither inherited from soil parent materials nor from pedogenic processes, but originated from anthropogenic activities. Significant correlations between heavy metals and magnetic parameters (χ_{lf}, χ_{arm}, SIRM, SOFT and HIRM) of the topsoils indicated that the magnetic techniques can be used for monitoring soil pollution.
Karbassi et al., 2006	Metals, Chemical Speciation	In this study, bulk and chemical partitioning of elements in the Shefa-Rud riverbed sediments were studied. Higher elemental concentrations were observed in estuarine zone when compared with the Riverine sediments (except for Al, Fe, Pb and Mn). Geochemical Index and Enrichment Factor values were indicative of a clean environment throughout the river course. These values were in well agreement with the results of chemical partitioning data.
Mendiguchía et al., 2006	Total organic matter and Metals	The study was carried out in the Bay of Cádiz (SW Spain) where several intensive marine aquaculture facilities are located. The data obtained was statistically treated to determine whether the spatial and temporal gradients in heavy metals and organic matter in sediments are related to aquaculture. The results suggested that trace metal enrichment in the sediments may be attributed to the fish farm effluents.

1.6. Objectives

To identify and quantify the metal forms, to gain a precise understanding of the potential and actual impacts of elevated metal levels in the sediment, the present study was carried out on sediment cores collected from intertidal regions along Mumbai estuary and creeks with the following objectives:

1. To study the spatial and temporal variations of sediment characteristics, trace metals in bulk sediment and metal species of sediments.

2. To understand the environmental forcing parameters that control the distribution pattern of trace metals and their species with space and time.
3. To assess the relative scale of recent and historical contaminant input to the estuaries thereby determining pollution history of the area.

1.7. Study area

Coastal regions are some of the most sensitive environments and yet they are subject to growing human pressures (David, 2003) because of increasing urbanization, industrial development and recreational activities. Maharashtra, one of the coastal states of India, located along the west coast of India, is endowed with a coastline of 720 km. Mumbai is the largest city and capital of the state, covering an area of about 438 km^2 with a population of 11.9 million as per 2001 census records (Vijay et al., 2010). It lies between $18^o55'$ to $19^o20'$ N latitudes and $72^o45'$ to $73^o00'$ E longitudes. Many parts of the city lie just above sea level, with elevations ranging from 10 to 15 m. The coastline in Mumbai is indented with numerous creeks and marshy areas. Mumbai lies at the mouth of the Ulhas River. The area has rich natural resources like lakes, coastal forests, wetlands and mangroves. Mumbai experiences tropical savanna climate with heavy south-west monsoon rainfall, measuring 2166 mm on an average every year. The place experiences the onset of the monsoon in the month of June and receives the monsoon till the end of September. The temperature ranges from 16.5^oC to 34.7^oC, with marginal changes between summer and winter months whereas relative humidity ranges from 54.5 % to 85.5 % (MPCB, 2005). Mumbai has at its northern end the Ulhas River; on the south-eastern end the Thane creek and on the west the Arabian Sea. Mumbai and adjacent marine environment, harbours >60 %, out of total mangrove cover along the Central West Coast of India (Jagtap et al., 1994).

Geologically, Mumbai-Thane region is part of the Deccan trap that was formed by volcanic effusions at the end of the cretaceous period (Blasco, 1975). Differential weathering of the inter-layered soft tuffs and resistant basaltic flows (Deccan Traps) by seawater has created several bays and creeks around Mumbai; the prominent among them being the Thane Creek- Mumbai Harbour, Mahim, Versova and Bassein Creeks. The northern shores of the region are predominantly rocky with mud-patches in-between, while the central and the southern zones are largely sandy with occasional rock outcrops.

Mumbai is the industrial hub varying from textiles to petrochemicals, with total 36,048 industrial units. About 11,494 industries are located within the city and remaining 24,554 industries are located in suburbs. Most of the industries in Mumbai region are clustered in three large industrial

areas namely Thane-Belapur belt, Kalyan-Ulhasnagar-Ambernath belt, Western shore of Thane creek and around Patalganga River. These industries manufacturing a wide range of products such as dyes, pharmaceuticals, fine chemicals, plastics, petro and agrochemical, fertilizers and refined petroleum products release their waste water to Thane creek, Ulhas and Patalganga rivers. A rough estimate of industrial wastewater generated by these industries is about 5 x 105 m^3/d. The domestic wastewater generated in Mumbai city which amounts to 2 x 10^6 m^3/d is released untreated or partially treated to the marine environment transporting 450 tons of BOD, 63 tons of nitrogen, 11 tons of phosphorus, 0.18 tons of Cu, 0.36 tons of Zn and 0.09 tons of Pb every day (Zingde, 1989). In addition, many industries located at other places of Mumbai release their waste waters to nearby rivers, estuaries and creeks which act as conduits to the coastal zone. It generates sewage of about 2,000 million litres per day (mld). Therefore, large amounts of these untreated/partially treated industrial and domestic effluents are released into the coastal and marine environment. As a result, voluminous amounts of industrial and domestic effluent are released to coastal water in and around Mumbai and are under the grip of pollution. According to Dhage et al. (2006), coastal region around Mumbai has deteriorated due to discharge of wastewater through creeks, rivers, nallahs/drains and various non-point sources.

The region has been subject to a number of studies aiming to quantify the concentrations of pollutants present within the creeks, bays, estuaries and its tributaries. As a result, the transport and distribution of trace metals as well as radionuclides in water, suspended particulate matter and sediment in inshore areas of Mumbai have been extensively studied (Patel et al., 1975, 1985; Zingde and Desai, 1981; Bhosale and Sahu, 1991; Sharma et al., 1994; Jha et al., 2003). Also, several studies have been undertaken in coastal sediments along the Mumbai coast, for the determination of magnetic parameters and petroleum hydrocarbons, as indicators of historical pollution level (Blaha et al., 2011; Chouksey et al., 2004). Although few studies on surface sediment contamination in some stretches of the Thane creek and Ulhas estuary have been performed (Bhosale and Sahu, 1991; Ram et al., 1998, 2003, 2009) in the past, systematic investigations of the subsurface sediments along the estuarine and creek systems of the region have not been conducted so far. The study of concentration and distribution of trace metals in sediments play a key role in detecting sources of pollution in aquatic systems and have a direct implication on the health of estuaries, affecting both the flora and fauna and also humans. Therefore, in the present study, an attempt has been made to understand the processes affecting the distribution and concentration of sediment components and metals, which will help to reconstruct the history of pollution of the region. Although trace element pollution is a key environmental problem in Mumbai, no study on the speciation of trace elements in the sediments

i.e. studies of metal distribution among various geochemical phases of sediment such as carbonates, oxides, organic matter and others, of this region has been previously undertaken. Therefore, in the present study, speciation studies are also adopted.

Ulhas Estuary

Ulhas River, about 135 km long, rises in the rainy ravines of the Bhor Ghat and after flowing through hilly tracks and mountainous terrain of the Western Ghat finally reaches the Arabian Sea at Vasai creek (Bhosale and Sahu, 1991). The river is shallow having sandy basin, since the land runoff carries huge amounts of sediments from its catchment area. An outlet of the river touches the head of the Thane creek, south of Mumbra. Dredging activities near Mumbra resuspend the finer sediments and disturb the normal distribution of particulate and dissolved materials along its course. The estuary is strongly influenced by tides, with spring tidal range varying from about 4.5 to 2.8 m at the mouth and upstream end, respectively. Extensive mudflats are formed along both the banks, characterized by good growth of mangroves. During the dry season, barrages constructed upstream of the estuary and its associated tributaries allow only a limited river discharge to flow. The Ulhas River is mainly a monsoon fed river and the fresh water flow dwindles down during the non-monsoon seasons. The river is characteristic in its environmental conditions due to the shallow depth, tidal currents, mangrove vegetation, salinity gradient, diurnal temperature variation and large land runoff carrying huge quantity of sediments from its catchment area and human habitations. There are a number of industries situated along either banks of the river, adding their effluents at various localities namely Ambivli, Ulhas Nagar, Dombivli, Bhiwandi and Thane City and loading the water body heavily with pollutants. A considerable load of the sewage from Thane city is also added affecting aquatic organisms (Lala, 2004; Athalye et al., 2003; Mishra, 2002; Zingde, 2002; Mohapatra and Rehgarajan, 2000; Tandel, 1986; Patil, 1982; Metcalf and Eddy, 1979; Durve and Bal, 1961). Several industrial complex and estates located in Mumbra-Ambarnath segment in the upstream, release wastewater into the estuary either directly or indirectly. The fisheries of the estuary have been dwindling to threatening status (Rathod et al., 2002; Mutsaddi, 1964). The estuarine flushing time varies between 73 and 211 tidal cycles (NIO, 1994) during the dry season (October to May), which suggests that there might be a possibility of contaminant build-up inside the estuary. However, the estuary is well flushed during the monsoon season.

Thane creek

Spanning an area of about 147 km², the Thane city is located at an elevation of 7 m from sea level. Extending from Ulhas River to the head of Mumbai harbour bay is the Thane creek. It is a

triangular mass of brackish water which widens out and opens to the Arabian Sea in the South. The creek is narrow at the Northern end, where it is fed partially by the Ulhas River in the north, Panvel River in the middle and Patalganga River in the south. The creek could be considered as an estuary during southwest monsoon period when the land drainage and river run-offs are considerable. This area is also highly bio-productive and yields about 2,000 to 3,000 metric tonnes of fish annually. The creek is narrow and shallow at the riverine end and broader and deeper towards the sea. The creek is fringed with mangroves along both the banks coupled with heavy industrialization and urbanization. It receives about 294 mld and 145 to 260 mld of industrial and domestic wastes, respectively, within Thane city limits (TMC-ES, 2000). This area was developed by the state government essentially for the chemical industries towards the beginning of the sixties. At present about 25 large industries and about 300 medium and small scale units using hazardous chemicals are located, out of the total of 2,000 industrial units located in this zone. The diversified industries along the banks of the creek, which include chemical, textile, pharmaceutical, engineering and major fertilizer complexes, release through their effluents high levels of nitrates and phosphates into the creek (Quadros et al., 2009). The main water source for the industrial consumption is Maharashtra Industrial Development Corporation (MIDC). The industrial area utilizes about 45,000 m^3/day of fresh water. The effluent discharge, treated and untreated amounts to 28,750 m^3/day, i.e. 64 % of the total industrial effluents generated in the Thane creek area. Except for few major industries, the medium and the small scale industries discharge their treated or untreated effluents through the unlined surface drains into the Thane creek. In addition to this, domestic sewage discharge from suburbs of Mumbai City meets the Thane creek from the west side. Also, atmospheric fallout from the chimneys and stacks and vehicle exhausts estimated to be 22,000 tons/day over the city, reach the creek after washout. The problem is further aggregated by unrestricted dumping of solid waste, construction debris and other wastes. Because of all this, the soil as well as water of the Thane creek region has become severely polluted. This has created health hazards not only for local population but also resulted in disturbances of the mangrove ecosystem.

Mangrove species in Ulhas estuary consists of *Avicennia marina, Rhizophora mucronatta* while in the Thane creek species present are *Avicennia marina, Bruguiera cylindrica, Rhizophora mucronata, Sonneratia apetala* and the mangrove associates, *Sesuvium portulacastrum, Salvadora persica and Aeluropus lagopoides* (Borkar et al., 2007). In both the regions, *Avicennia marina* is found to be the dominant mangrove species.

Manori creek

Manori creek, which lies between 19°11' N; 72°47' E and 19°15' N; 72°50' E, is drained by the Dahisar River. The region receives an average rainfall of about 2470 mm, of which around 90 % falls during the monsoon (July and August) season. Semidiurnal tides with spring and neap of 3.5 m and 1.8 m in the mouth area, results in good tidal flushing of the lower reaches. The tidal column fluctuates in the range of 0.32-5.10 m (Anon, 2006). The minimum and maximum atmospheric temperatures in the area vary from 19^{o}C in January to 33^{o}C in May (IMD, 2007). The creek is characterised by abundant mudflats and exhibits good coverage of mangroves. However, in recent years, the mangrove areas are being intensively targeted for dumping garbage, disposal of sewage and also overexploited by salt industries, fishing, navigation and recreational activities. In the past, the only source of wastewater to the creek was from domestic discharge. But in recent years, development of nearby areas for residential purposes and industrial complexes has resulted in increasing level of pollution in the creek. Kulkarni et al (2010) studied biological and environmental characteristics of mangrove habitats around the creek and found *Avicennia marina* to be the dominant mangrove species. Because of poor abundance and diversity of mangroves, the area was considered as a highly stressed environment. The dominance of stress tolerant phytoplankton species such as *Skeletonema costatum* and benthic fauna such as *Polychaetas* further strengthened their observations. The dominance of *polychaeta* in the study area was attributed to increased salinity, temperature and heavy metal concentrations in the creek.

Versova and Nhava Sheva creeks

The Versova creek is a tidal creek of Mumbai with a depth of about 1 to 1.5 m and has a width ranging from 30 to 40 m. The dominant vegetation of the region is the mangrove species *Avicennia alba* which has a height of 1 m. During flood tide flow of sea water towards the upstream progressively inundates the creek and during extensive high tides, even the swamp vegetation is submerged.

Nhava Sheva region is the 6th largest port and the largest container port in India. The geographical position of Nhava is at 18°57′28.5″N and 72°59′11.45″E and Sheva is at 18°56′05.34″N and 72°57′39.98″E. Located in Maharashtra, the port on the Arabian Sea is accessed via the Thane Creek. Nhava- Sheva is located on the Konkan mainland across from the island city of Mumbai. Spread over 10 km^2, it was developed to relieve pressure on Mumbai Port and inaugurated on May 26, 1989.

Chapter 2

METHODOLOGY

2.1. Introduction

The primary objective of survey and sampling is to collect data that represents the site of study. The samples are collected by planning carefully, selecting the appropriate sampling locations, taking measures to avoid contamination, using proper devices and procedures and examining data to determine if they address the study objectives. The basic criteria for sample size, that is, the number of samples, should include consideration of the representativeness of the system as well as the amount required for measurement. An overview of the methods employed in the present study is illustrated in the form of a flow chart in Figure 2.1.

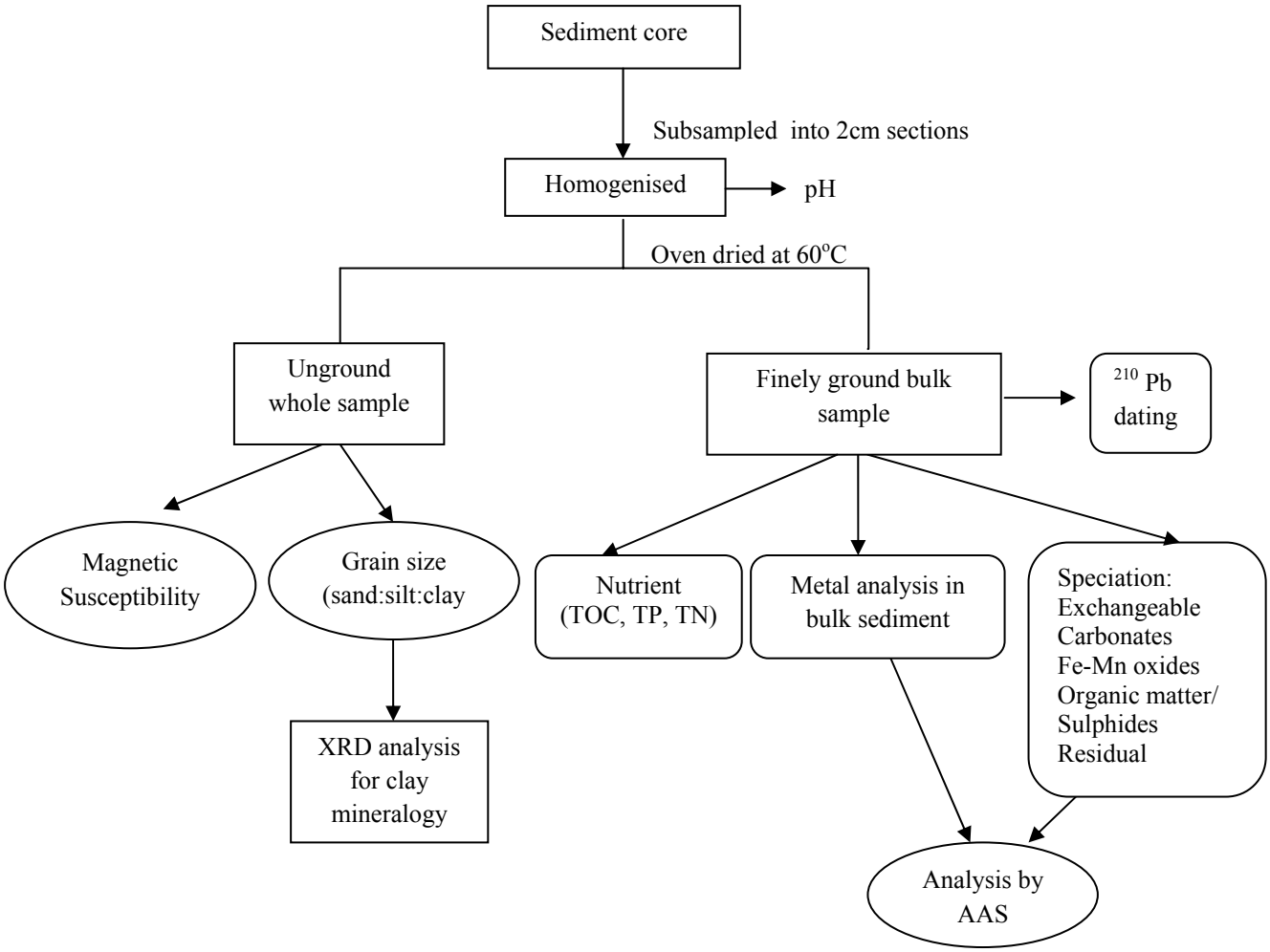

Fig. 2.1. Flowchart of sample preparation and analysis

After the collection of the samples at the field site, they must be transported to the laboratory under conditions that do not compromise the subsequent planned analysis. This may involve special steps to maintain cold temperature, to reduce potential contamination and to minimize mixing for biological, chemical, and physical analyses, respectively. Further, sample preparation for starting analysis generally involves the following steps: (1) drying or rewetting, (2)

homogenizing and sieving, (3) storage, and, occasionally, (4) grinding. The laboratory analysis characterizes the physical and chemical properties of the sample.

2.2. Field methods

2.2.1. Sediment sampling

To achieve the objectives defined, five semi-enclosed water bodies were chosen which ensure undisturbed sedimentation conditions. In September 2008, 22 sediment cores were collected from intertidal regions along southeast (Thane creek), west (Manori and Versova creeks) and northern (Ulhas estuary) parts of Mumbai (Fig. 2.2).

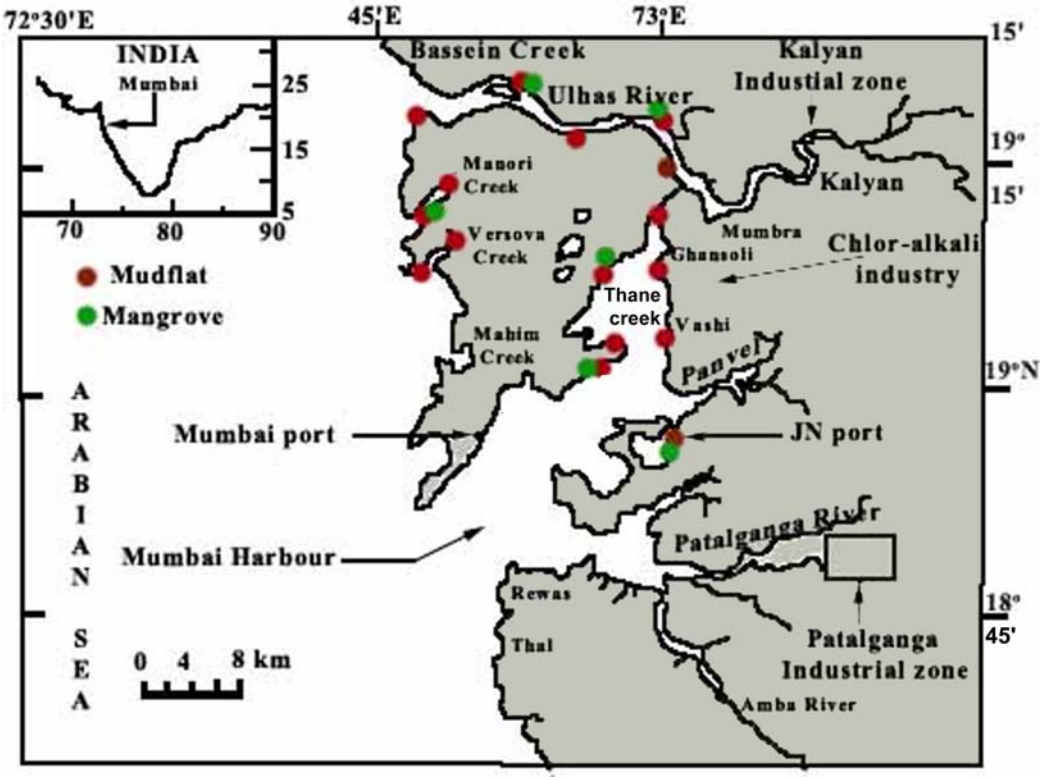

Fig. 2.2. Map showing the sampling locations

From the estuarine and creek environments, mudflat and mangrove cores were collected, maintaining a distance of about 50 m between the sub-environments. A global positioning system (GPS) was used for locating and recording positions of all the sampling sites. The sampling locations are shown in Figure 2.2. Core samples were collected at low tide, with the help of a PVC corer of 150 cm length and 5 cm diameter, which was gently pushed into the sediment and retrieved back. The cores were transported to the laboratory in a horizontal position. In the laboratory, core length was measured and a brief description of sedimentary characteristics of the cores was noted, with distinct changes in colour, the type of sediment (sandy or muddy) and shells present. Data, including the appropriate latitude and longitude, core

number, core length, sediment colour and other visual descriptions recorded are presented in Table 2.1.

Table 2.1. Details of the cores collected

Stations	Lat. and Long.	Core Length (cm)	Colour
THANE CREEK			
T I - Mudflat	19^{0}11′48″ N, 72°59′01″ E	46	0-46 – Black
T II - Mudflat	19°09′10.5″ N, 72°58′05″ E	28	0-18 – Black 18-22 – Mixed – brown + black 22-28 – Dark brown
T II - Mangrove		34	0- 34 – Mixed- brown + grey
T III - Mudflat	19°3′35.1″ N ,72°57′39.2″ E	60	0-20 – Brown 20-60 – Dark brown
T IV- Mudflat	19°01′41.8″ N, 72°57′10.6″ E	46	0-8 – Brown 8-46 – Mixed - brown + black
T IV- Mangrove		68	0-18 – Brown 18-46 – Mixed - brown + black 46-68 – Dark brown
TV- Mudflat	19°03′50″ N, 72°58′44″ E	62	0- 62 – Brown
TVI - Mudflat	19°09′17.28″ N, 72°59′14″ E	80	0-80 – Black
ULHAS RIVER			
U I - Mudflat	19°18′31.56″ N, 72°47′38″ E	26	0-22 – Brown 22-26 – Mixed – brown + black
U II - Mudflat	19°17′18.4″ N, 72°53′52.2″ E	60	0-30 – Brown 30-60 – Mixed – brown + black
U III - Mudflat	19°14′35.4″ N, 72°59′54″ E	70	0-14 – Brown 14-70 – Grey
U IV - Mudflat	19°17′29.8″ N, 73°00′10.1″ E	60	0-16– Brown 16-26 – Brown (Sandy) 26-60 – Dark brown
U IV - Mangrove		40	0-2 – Brown 2-28 – Grey 28-34 – Brown (Sandy) 34-40 – Grey
UV - Mudflat	19°19′43.4″ N,72°52′43.3″ E	28	0-10 – Brown 12-28 – Mixed - brown + grey
UV - Mangrove		58	0-44 – Brown 44-58 – Dark brown
MANORI CREEK			
Man I- Mudflat	19°14′ N, 72°49′25″ E	50	0-14 – Brown 14-50- Mixed - brown + grey
Man II- Mudflat	19°11′42.2″ N, 72°48′05.4″ E	42	0-18 – Brown 18-42 – Grey
Man II- Mangrove		38	0-8 – Brown 8-38 - Mixed – brown +black
VERSOVA CREEK			
VI - Mudflat	19°08′14.6″ N, 72°47′44.1″ E	86	0-58 – Grey 58-86 – Dark grey
VII - Mudflat	19°10′14.7″ N, 72°49′46.6″ E	40	0-32 – Black 32-40 – Mixed – brown + black
NHEVA SHEVA			
NS-Mudflat	18°56.09′22″ N,72°57′55.4″ E	24	0-10 – Brown 10-16 – Grey/Black

			16-24 – Grey
NS-Mangrove		34	0-28 – Brown 28-34 – Dark brown

2.2.2. Sub-sampling

The cores were sub-sampled at 2 cm intervals and stored in the refrigerator at 4°C till further analysis. A part of each homogenized sub-sample was used to determine the sediment components i.e. sand: silt: clay ratio, clay mineralogy and magnetic susceptibility. Another part of the sample was finely ground with an agate mortar and pestle, and homogenized for the determination of total organic carbon, total nitrogen, total phosphorus, total metal analysis, metal speciation and ^{210} Pb dating

2.3. Laboratory Methods

The laboratory methods employed throughout the course of this study are detailed below. Before performing the experiments, all the glassware's were soaked in chromic acid, prepared by adding potassium dichromate to concentrated H_2SO_4, followed by rinsing with copious amounts of de-ionised water and then oven dried. All the chemicals used were of analytical reagent grade. Milli-Q water was used for all dilutions throughout the study. All plastic containers were cleaned by soaking in 10 % (v/v) nitric acid for 24 hrs and then rinsing with distilled water prior to use.

#

2.3.1. pH

pH of each sub-sample was measured by using a pH meter (Thermo Orion 420 A^+ model). The pH electrode was calibrated with standard buffers of pH 4.0, pH 7.0 and pH 9.2.

2.3.2. Porosity and Bulk density

The dry bulk density (ρ_d) and porosity (n) of sediments were calculated from natural moisture content (m) and grain specific gravity (G_s) values using equations of soil mechanics (Budhu, 1999). Grain density or specific gravity of sediment was determined using a displacement method where an aliquot of dry sediment (~10 g) was added to a 25 ml specific gravity bottle with a known volume of deionized water. Natural moisture content of subsamples was determined in the laboratory using standard oven drying method. The procedure and equations involved in determining porosity and dry bulk density are as follows:

a) Natural moisture content(m) = Mass of water in the sediment/Mass of dry sediment
   It is expressed in percentage by multiplying by 100.

b) Void ratio (e), ratio of volume of voids to volume of solids:

$$e = (\text{natural moisture content}) \times (\text{specific gravity}) = m * G_s$$

c) Porosity (n) = e/(1+e)

It is expressed in percentage by multiplying by 100.

d) Dry bulk density(ρ_d) = (G_s * ρ_w)/(1+e)

where, ρ_w is density of water. The value of seawater density (ρ_w) is taken as 1.03g/cm^3.

2.3.3. Sediment grain size analysis (Sand: Silt: Clay)

Variation of the grain size can be an important indicator of changes occurring in erosion of the hinterland and river discharge which influence the amount and sedimentary composition of the detrital sediment. Grain size analysis to determine the sand (>63μm): silt (2-63 μm): clay (<2 μm) ratio was carried out by pipette method adopted from Folk (1974) which is based on Stoke's settling velocity principle.

15 g of oven dried (60^0 C) bulk sediment sample was weighed and transferred to 1000 ml beaker. Distilled water was added to this beaker and stirred. Sediment was then allowed to settle. The next day, water from the beaker was decanted by using a decanting pipe. This step was repeated at least 4 to 5 times to remove the salinity. After decanting, 10 ml Sodium Hexameta-phosphate (NaP_2O_5) was added which acts as a dispersing agent and the samples were gently agitated for 1 minute before being left to stand for 24 hrs. On the next day, 5 ml of 30 % of hydrogen peroxide (H_2O_2) was added to oxidize organic matter and left to stand overnight. Contents of the beaker were then poured over 63-micron (230 mesh) sieve and the filtrate was collected in 1000 ml cylinder. The contents from the beaker were washed till the solution became clear and then the cylinder volume was made up to 1000 ml with distilled water. The solution from the cylinder was used for pipette analysis. Before withdrawal, the contents were homogenized by stirring for about 2 minutes using a stirrer. This was then allowed to settle for certain time according to the room temperature. Stirring time was noted down and pipetting time was accordingly calculated by referring Table 2.2.

25 ml of the solution was pipetted out at 8 ϕ by inserting pipette up to 10 cm depth into the cylinder. Pipetted solution was then transferred into preweighed 100 ml beaker and dried at 60^{0}C overnight. After drying, the beaker containing clay was weighed. The sand, which remained on the sieve, was transferred to a preweighed beaker. This was then dried and kept in desiccator to remove any moisture and then weighed.

Table 2.2. Time schedule to be used for pipette analysis

Size Ø	Depth to which pipette is to inserted (cm)	Time after which water is to be pipetted out Hours: Minutes: Seconds				
		28^0C	29^0C	30^0C	31^0C	32^0C
4	20	0:00:48	0:00:46	0:00:46	0:00:44	0:00:44
5	10	0:01:36	0:01:34	0:01:32	0:01:29	0:01:28
6	10	0:06:25	0:06:15	0:06:06	0:06:57	0:05:52
7	10	0:25:40	0:25:02	0:24:25	0:24:49	0:23:27
8	10	1:42:45	1:40:13	1:37:42	1:37:15	1:33:51
9	10	6:30:00	6:40:40	6:32:50	6:32:10	6:11:30
10	10	27:06:00	26:30:00	-	-	-

Percentage of sand, silt and clay were calculated as follows

% Sand = (Wt. of sand / Total Wt) * 100

% Clay = {[(Wt. of clay / Total Wt)*(1000/25)]-1} * 100

% Silt = 100 - (% of sand + % of clay)

2.3.4. Clay Mineral Analysis

During pipette analysis, the sediment sample from the cylinder was pipetted out at 9 ϕ by inserting pipette till 10 cm depth and transferring the pipette solution into 500 ml beaker. To this beaker, 5 ml of acetic acid and 10 ml of 30 % hydrogen peroxide was added, to confirm the removal of carbonates and oxidise organic matter, and then stirred well. The contents from the beaker were then kept overnight for settling. The next day, the top clear liquid was decanted and distilled water was added. This step was repeated several times to free clay from the excess reagents. Slide preparation for clay mineral analysis was carried out by pipetting 1 ml of the clay solution and spreading uniformly over a pre-numbered slide. The slides were then air dried. For XRD analysis, the dried slides were exposed to ethylene glycol vapours at 100^0 C for 1 hr. The slides were then scanned from 3^0 to 15^0 2θ at 1.2^0 2θ/min on X-ray diffractometer using nickel-filtered CuKα radiation. Also, samples were scanned again in the range of 24^0 to 26^0 2θ at 0.5^0 2θ/minute to distinguish kaolinite and illite peaks. The percentage of different clay minerals were computed by measuring the integrated peak areas of basal reflections in the glycolated X-ray diffractograms by semi-quantitative method given by Biscaye (1965).

2.3.5. Total Organic Carbon (TOC) in sediment

Total organic carbon was determined for all the sediment samples by using the Walkley-Black method (1934), adopted and modified by Jackson (1958). It was mainly determined to assess the role played by the organic component of the sediment in the transport, deposition and retention

of trace metals. The Walkley-Black method utilizes exothermic heating and oxidation with potassium dichromate and sulphuric acid (H_2SO_4), which involves the following steps.

An aliquot of the sample (0.5 g) was treated with a known excess of the standard dichromate solution (10 ml) and 20 ml of concentrated H_2SO_4 with silver sulphate (Ag_2SO_4) in a conical flask. This was then mixed by gently rotating the flask for about 1 minute. The mixture was then allowed to stand for 30 minutes. After 30 minutes, the same solution was treated with 200 ml milli-Q water, 10 ml of 85 % phosphoric acid (H_3PO_4) and 0.2 g of sodium fluoride (NaF). This solution was then back titrated with standard ferrous ammonium sulphate solution using diphenylamine as an indicator to a one-drop end point (brilliant green). Silver sulfate was used to prevent the oxidation of chloride ions. A Standardization blank without sample was run following the same above procedure. Dextrose was taken as a reference standard for the determination of organic carbon.

Percentage of total organic carbon was calculated as follows

Total organic carbon (%) = 10 (1-T/S) * F

Where, S = Standardization blank titration, ml of ferrous solution

T = Sample titration, ml of ferrous solution

F = Factor which is derived as follows:

F = (1.0 N) * 12/4000 * 100/Sample weight

= 0.6, when sample weight is exactly 0.5 g

Where, 12/4000 = m. eq. wt. carbon

2.3.6. Total Nitrogen (TN) in sediment

Sediment digestion: 1g of the dried and finely ground sediment sample was autoclaved in an oxidation flask with a mixture of potassium persulfate and boric acid in sodium hydroxide solution for 30 minutes. The solution of the flask was then cooled.

1 ml of this solution was made to 50 ml with milli-Q water and then passed through a cadmium reductor column and analyzed for nitrogen as azo dye, measured at 543 nm (Grasshoff**,** 1999). The concentration of nitrogen was computed from the calibration curve constructed with standard potassium nitrate, and sulphaninyl amide and alpha napthyl amine hydrochloride as reagents.

2.3.7. Total Phosphorous (TP) in sediment

The procedure used to determine phosphorous in sediments is given by Murphy and Riley **(**1962**)**. It is based on the reaction of orthophosphate ions with an acidified molybdate reagent to form a phospho-molybdenum complex, which is then reduced with ascorbic acid to form molybdenum-blue, in the presence of potassium antimony tartarate. The brief procedure is given below,

5 ml of digested sediment sample (procedure for sediment digestion is same as that given for TN), was taken and made up to 50 ml with milli-Q water. To this, 1 ml of mixed reagent (ammonium molybdate solution + H_2SO_4 + potassium antimony tartarate) and 1 ml of ascorbic acid was added. The solution was thoroughly mixed after each addition of the reagent. The intensity of the colour was measured at 880 nm against a reagent blank after 30 minutes. The concentration of phosphorous was computed from the calibration curve constructed with standard potassium dihydrogen orthophosphate. A Shimadzu UV-VIS spectrophotometer was used to determine TN and TP concentrations.

Equipment: Ultraviolet-visible (UV-vis) spectroscopy is used to obtain the absorbance spectra of a compound in solution or as a solid. The basic parts of a spectrophotometer are a light source, a holder for the sample, a diffraction grating in a monochromator or a prism to separate the different wavelengths of light and a detector. Hydrogen or deuterium lamps provide the source of light for ultraviolet measurements. Tungsten lamps provide the light for visible measurements. These light sources generate light at specific wavelengths. Deuterium lamps generate light in the UV range (190 to 380 nm). Tungsten-halogen lamps generate light in the visible spectrum (380 to about 800 nm). Xenon lamps which can produce light in the UV and visible portions of the spectrum are used to measure both UV and visible spectra. In UV spectroscopy, a beam of light is split into a sample and reference beams. As its name implies, the sample beam is allowed to pass through the target sample. Alternately, the reference beam passes through the control solvent or a portion of the solvent that does not contain the actual target. Once the light passes through the target sample of interest it is measured by a special meter termed a spectrometer designed to compare the difference in the transmissions of the sample and reference beams.
The Beer-Lambert Law, equation given below, is the principle behind absorbance spectroscopy.

$$A = \varepsilon bc$$

For a single wavelength, A is absorbance (unitless, usually seen as arb. units or arbitrary units), ε is the molar absorptivity of the compound or molecule in solution ($M^{-1}cm^{-1}$), b is the path length of the cuvette or sample holder (usually 1 cm) and c is the concentration of the solution (M).

2.3.8. Magnetic Susceptibility Measurements

Sample preparation: A known weight of sediment sample was packed in a 10 cc plastic sample container, which was wrapped with 'cling' film to reduce the possibility of cross contamination and to keep the sediment fixed thereby reducing all movements within the sample container to a minimum while handling the sample. The containers containing the packing material were pre-measured for mass and susceptibility and the values were corrected.

Equipment: A Bartington MS2 system was used for magnetic susceptibility (χ) measurements. Both the high (4.7 kHz) and low (0.47 kHz) frequency measurements were performed using a dual frequency Bartington MS2 susceptibility meter. Magnetic susceptibility was measured 3 times on each sample on 0.1 range and the average of 3 measurements are presented as mass specific values. Frequency dependent susceptibility ($\chi_{fd\ \%}$) was calculated using the formula (χ_{lf}-χ_{hf}) / χ_{hf} * 100, where χ_{lf} is magnetic susceptibility at low frequency and χ_{hf} is susceptibility at high frequency. Anhysteretic remanent magnetization (ARM) was imparted to the samples by superposing a DC biasing field of 0.05 mT on a smoothly decreasing alternating field with a peak of 100 mT using a Molspin A.F. demagnetizer. ARM created within the sample was then measured using Molspin spinner magnetometer. Isothermal remnant magnetization (IRM) was acquired by first exposing the samples to series of successively larger fields along one direction and then in the opposite direction (backfields, -20mT, -30mT, -40mT, -50mT, -100mT, -200mT, -300mT, -500mT, -800mT and -1000mT) using a Pulse magnetizer (Magnetic measurements Ltd.). After each forward and reverse field (DC demagnetization), samples were measured using the Molspin spinner magnetometer. The IRM achieved at 1T is referred as the saturation isothermal remnant magnetization (SIRM).

Using the above magnetic parameters various other parameters were evaluated in terms of magnetic concentration, mineralogy and grain size as summarized by Thomson and Oldfield (1986) and Oldfield (1999). The descriptions of different magnetic parameters are presented in Table 2.3.

Table 2.3. The different magnetic parameters, definitions and their applications

Magnetic parameters	Definitions / formulae	Significance
1.Magnetic Susceptibility, χ (10^{-8} m^3/kg)	It is a measure of the ease with which a material is magnetized. $\chi = M/H$. Where, M is the volume magnetization induced in a material of susceptibility and H is the applied field.	Gives the concentration of magnetic minerals.
2. Frequency dependent susceptibility, χ_{fd} (%)	Variation in χ between low (0.47 kHz) and high frequency (4.7 kHz).	It is representative of magnetic grain size. Higher the value finer is the grain size. χ_{fd} % of ~10 % or 5-10 % indicates a large fine viscous (magnetite) component of super paramagnetic range.
3. Anhysteretic remnant magnetization, **ARM** (10^{-5} Am^2/kg^{-1})	It is achieved by subjecting a sample to a strong alternating field which is decreased to zero in the presence of small steady field.	ARM gives an estimation of the concentration of fine grain minerals.
4. Susceptibility of ARM, χ_{ARM} (10^{-8} m^3/kg^{-1})	It is a form of normalized ARM for the strength of a steady field.	It reflects concentration and grain size.
5. Saturation isothermal remnant magnetization, **SIRM** (10^{-5} Am^2/kg^{-1})	It is measured as the highest volume of magnetic remnence that can be produced in a sample by applying a very high field.	It is a characteristic of mineral type and concentration.
6. **S-ratio** (%)	It is defined as $IRM_{(-0.3T)}$/SIRM	S-ratio provides a measure of the relative proportions of higher coercive magnetic minerals (haematite) to lower coercive minerals (magnetite).
7. Hard IRM, **HIRM** (10^{-5} Am^2/kg^{-1})	Difference between SIRM and IRM_S in a reverse field of 300 mT, HIRM = SIRM-IRM_{-300mT}	It is a measure of high coercivity minerals.
8. **ARM/χ** (10^2Am^{-1})	It is the ratio of Anhysteretic remnant magnetization to magnetic susceptibility.	High values indicate significant stable single domain (magnetite) grains.

2.3.9. Sediment digestion for Total metal analysis

Sediment digestion was achieved by placing 0.2 g finely ground dried sediment sample into Teflon beakers. The samples were treated with 10 ml of 7:3:1 of HF, HNO_3 and $HClO_4$ mixture and heated at 150^oC till completely dried (Jarvis and Jarvis, 1985). After the samples were cooled at room temperature, 5 ml of the same acid mixture was added. Samples were again heated for 1 hour, cooled at room temperature and then 2 ml of concentrated HCL was added and dried completely. This was followed by addition of 10 ml of 50 % HNO_3 and the samples were warmed for an additional 10 minutes. Finally the samples were made upto 50 ml volume with milli-Q water. Metals were analyzed using Atomic Absorption Spectrophotometer (AAS). The instrument used in the present study had the facility to directly display the concentration of the

metal in the sample under analysis. From the knowledge of the sediment content taken for digestion and dilution of the digest, the concentration of the metal in sediment was calculated and expressed on dry weight basis. The digested samples were aspirated for Al, Ca, V, Fe, Mn, Cu, Pb, Co, Ni, Zn and Cr while the extracts from the different sediment fractions were analysed for Fe, Mn, Cu, Pb, Co, Zn and Cr with the help of Varian AA 240 FS flame Atomic Absorption Spectrometry (AAS) with an air/acetylene flame for all of the above elements except for Al, Ca and V for which nitrous oxide/acetylene flame was employed at specific wavelengths. The instrument was calibrated by running blank and standard solutions prior to each element analysis. Standard working solutions of the element analysed were prepared from the corresponding 1000 mg/l Merck stock solutions. Recalibration check was performed at regular intervals. All chemicals used in the study were of analytical grade as mentioned earlier. Together with the samples, certified reference standard from the Canadian National Bureau of Standards (BCSS-1) was digested and run, to test the analytical and instrument accuracy of the method. The recoveries were between 86-91 % for Fe, Cu, Ni and Al; 87-92 % for Mn and Co; 80-85 % for Pb and Zn; 90-95 % for Cr; 82-90 % for V and Ca, with a precision of +6%.

Equipment: Atomic Absorption Spectrophotometry (AAS) is an important technique for analyzing metals in water and sediments. The general method involves atomization of samples by thermal sources and the absorption of a specific wavelength by the atomic source as it is excited. The radiation used is a hollow cathode lamp containing, as its cathode, the same element under analysis. The quantity of the same element absorbed by the atomic vapour is proportional to the concentration of the atoms in the ground state. Atomic absorption is the determination of the presence and concentrations of metals in liquid samples. Typical concentrations range in the low mg/l (ppm) range. In AAS, light of a specific wavelength is passed through the atomic vapour of an element of interest, and measurement is made of the attenuation of the intensity of the light as a result of absorption. Quantitative analysis by Atomic Absorption depends on:
(1) Accurate measurement of the intensity of the light
(2) The assumption that the radiation absorbed is proportional to atomic concentration.

Metals will absorb ultraviolet light in their elemental form when they are excited by heat, either by flame or graphite furnace. Each metal has a characteristic wavelength that will be absorbed. The AAS instrument looks for a particular metal by focusing a beam of UV light at a specific wavelength through a flame and into a detector. The sample of interest is aspirated into the flame. If that metal is present in the sample, it will absorb some of the light, thus reducing its

intensity. The instrument measures the change in intensity. A computer data system converts the change in intensity into an absorbance.

The following components make up the Atomic Absorption Spectrometer:

i) *Hollow cathode lamp*: Source of the analytical light line for the element of interest. It gives a constant and intense beam of that analytical line.

ii) *Nebulizer*: Sucks up liquid sample at a controlled rate and creates a fine aerosol spray for introduction into the flame. It also mixes the aerosol, fuel and oxidant thoroughly for introduction into the flame.

iii) *Flame*: Destroys any analyte ions and breakdown complexes. Create atoms of the element of interest.

iv) *Monochromator*: Isolates the analytical line photons passing through the flame. Removes scattered light of other wavelengths from the flame. By doing this, only a narrow spectral line impinges on the PMT.

v) *Photomultiplier tube (PMT)*: This is the detector. The PMT determines the intensity of photons of the analytical line exiting the monochromator. The PMT is the most commonly used detector for AAS. High tech electronics amplify, filter and process the electrical signal, using a series of chips and microprocessors, transmitting the result to an internal or external computer which deals with all data-handling and display.

2.3.10. Metal Speciation

The chemical speciation of heavy metals in sediments was determined using the sequential extraction after Tessier et al. (1979). A schematic presentation of the sequential extraction procedure is given in Figure 2.3. The procedure involves following five steps, which are referred here as fractions. The details of the procedure are as follows:

- **Fraction 1** is a soluble, exchangeable fraction in which the metals are weakly adsorbed to the clays and organics in the sediment via electrostatic attraction. From a biological availability standpoint, metals in this fraction are readily available (Tessier et al., 1979; Patrick et al., 1977).

Step 1, Exchangeable fraction: 1 g of oven-dried sediment sample was placed in 50 ml polypropylene centrifuge tube to which 8 ml of Magnesium chloride, adjusted to pH 7, was added. The tube was then shaken continuously for 1 hour at room temperature of 22 ± 5^0C. The extract from the tube was separated from the solid phase by centrifugation at 6,000 rpm for 10 minutes. The supernatant liquid was transferred into a 50 ml plastic bottle and stored in a

refrigerator at 4^0C prior to analysis. The residue was then washed with 10 ml of de-ionized water and shaken for 10 minutes at 6,000 rpm.

- **Fraction 2** metals are bound to carbonates. These particular metals are very susceptible to changes in the temperature and pH of the solution and are therefore the next most readily available (Tessier et al., 1979).

Step 2, Acid-soluble fraction - bound to carbonates: To the residue from step 1, 8 ml of 1M Sodium acetate, adjusted to pH 5 with acetic acid, was added and then shaken continuously for 5 hours at room temperature of 22 ± 5^0C. The extract was separated from the solid phase by centrifugation at 6,000 rpm for 10 minutes. The supernatant liquid was transferred into a 50 ml plastic bottle and stored in a refrigerator at 4^0C prior to analysis. The residue was washed with 10 ml of de-ionized water and shaken for 10 minutes at 6,000 rpm.

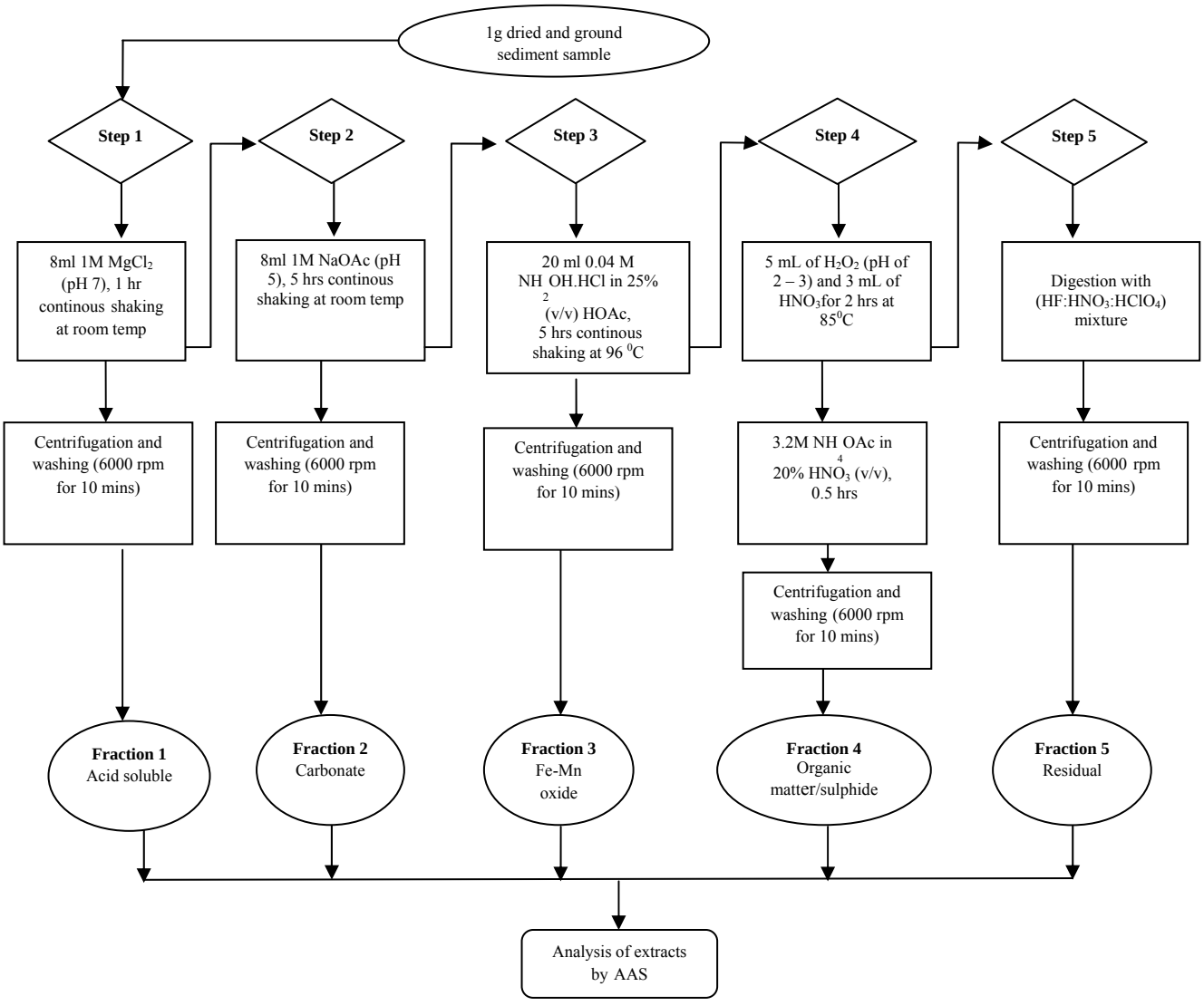

Fig. 2.3. Schematic representation of sequential extraction procedure

- **Fraction 3** metals are bound to Fe and Mn hydroxides. They exist in sediment as cement, nodules and concretions and tend to be thermodynamically unstable in anoxic conditions. They are most susceptible to changes in redox conditions i.e. Eh (increased availability at low Eh). These metals are most biologically available under reducing conditions (Tessier et al., 1979; Patrick et al., 1977).

Step 3, Reducible fraction - bound to Fe and Mn oxides: To the residue from step 2, 20 ml of 0.04 M Hydroxylamine hydrochloride ($NH_2OH.HCl$) in 25 % (v / v) acetic acid was added and then shaken continuously for 5 hours at 96 ± 3^0C. The extract was separated from the solid phase by centrifugation at 6,000 rpm for 10 minutes. The supernatant liquid was transferred into a 50 ml plastic bottle and stored in a refrigerator at 4^oC prior to analysis. The residue was washed with 10 ml of de-ionized water and shaken for 10 minutes at 6,000 rpm.

- **Fraction 4** metals are bound to various forms of organic matter and these bonds are strong. These metals are released when the oxidizing environment changes, degrading the organic matter. Metals in the organic matter fraction are the least biologically available (Tessier et al., 1979).

Step 4, Oxidizable fraction - bound to organic matter and sulphides: To the residue from step 3, 5 ml of hydrogen peroxide (pH of 2-3) and 3 ml of 0.02 M Nitric acid (HNO_3) was added carefully. The lid were unscrewed and the tube placed in 85 ± 3 °C hot water bath for 2 hours. During this time the tubes were agitated slightly by hand every 15 minutes. After the 2 hours, an additional 3 ml of hydrogen peroxide was added to the tube. The tube was left in the water bath and agitated by hand for 3 more hours at 85 ± 3 °C. The tubes were removed from the bath, cooled and 5 ml of 3.2M Ammonium acetate solution, prepared in 20 % (v/v) HNO_3, was added to the tube and the lids replaced. The tube was then shaken continuously for 30 minutes on orbital shaker. The extract was separated from the solid phase by centrifugation at 6,000 rpm for 10 minutes. The supernatant liquid was transferred into a 50 ml plastic bottle and stored in a refrigerator at 4^0C prior to analysis. The residue was washed with 10 ml of de-ionized water and shaken for 10 minutes at 6,000 rpm.

- **Fraction 5** is the residual fraction and includes metals incorporated into the crystal structure of the primary and secondary minerals. These metals are not biologically available and can only be released with the use of a very strong acid such as HF (Tessier et al., 1979; Patrick et al., 1977).

Step 5, Residual: The residue from fraction 4 was washed with deionised water and was transferred into acid washed teflon beaker and then digested completely following the same procedure used for the total digestion of sediment.

Equipment: The centrifuging machine used for the sequential extraction procedure was Remi Cooling Compufuge (model CPR 24). The Orbital shaker used for agitation of samples was Orbital shaking incubator (model RC2100).

Determinations of the various form of heavy metals was conducted using fast sequential Atomic Absorption Spectrometer. The recovery of each metal species from sequential extraction procedure was calculated using the following formula.

$$\text{Recovery (\%)} = \frac{\text{Fraction 1+ Fraction 2+ Fraction 3 + Fraction 4+ Fraction 5}}{\text{Total metal concentration obtained after total acid digestion}} \times 100$$

The recovery rates of the metals were found to range between 85 and 110%.

2.3.11. ^{210}Pb dating

Dry ground sediment samples of selected cores were stored for more than a year to allow secular equilibrium between ^{210}Pb and its grand-daughter ^{210}Po. The ^{210}Pb activity was measured following the standard radiochemical procedure given by Flynn (1968). For analysis by alpha spectroscopy, ^{210}Po must be separated from other alpha emitting isotopes. In this method, ^{208}Po (half life = 2.9 yr) has been used as a yield tracer which serves as an excellent internal standard to monitor the quality of the analysis. The procedure used for separation is described below.

1 g of dried finely ground sediment sample was transferred into a Teflon vessel and 15 ml of water and 1 ml of ^{208}Po tracer was added. Then 6 ml of HF was added and kept on hot plate until it dried and this step was repeated three times. Later, 5 ml of Conc. $HClO_4$, 1 ml of Conc. HNO_3, 1 ml of Conc. HCl and 10 ml of water was added and kept for drying. After drying, 5 ml of Conc. HNO_3 and 3 ml of Conc. HCl was added and kept on hot plate. This was followed by addition of 5 ml of 6 N HCl and kept on hot plate till it dried completely. Care was taken not to bake the residue. To the dried sample, 8 ml of 6 N HCl and 72 ml of distilled water was added. Also ~50 mg of Ascorbic acid was added to mask the Fe^{3+} ions in solution. The Po isotopes (^{210}Po and ^{208}Po) were then auto-plated onto a 1.5 cm diameter silver disc. The plating was carried out for 3 hours during which the temperature of the solution was maintained at 65^0C. After plating, the silver disc was rinsed with distilled water, dried and alpha activities of the Po isotopes (^{210}Po and ^{208}Po) were assayed using a silicon surface barrier detector of 450 mm^2 connected to an EG & G ORTEC 1024 multi-channel analyzer.

^{210}Po was measured by isotope dilution alpha spectrometry. Each radioactive decay of ^{210}Po emits an alpha particle that has energy of 5.3 MeV. The energy of the ^{208}Po alpha particle is about 5.1 MeV. Particles emitted at these two energies can be identified using an alpha spectrometry. The samples were counted for periods of 0.25 to 2 days depending upon the activity of ^{210}Po in the samples. The activity of ^{210}Po in the sample is determined from the ratio of the total counts of ^{208}Po to^{210}Po and from the quantities of sediment and ^{208}Po added to the sample. Blanks and standards were measured to verify the performance of all aspects of the procedures and the instrumentation. Unsupported ^{210}Pb activity was determined by subtracting the background ^{210}Pb activity obtained for the lower zones of the core, with the assumption of constant supported ^{210}Pb activity along the sediment column. ^{210}Pb age can be calculated for any specified depth in the sediment profile using the following formula,

$$A_d = A_o e^{-\alpha t}$$

Where A_d = activity of ^{210}Pb at depth d

A_o = activity of ^{210}Pb at a higher reference point

α = decay constant of ^{210}Pb (0.03114 y^{-1})

t = age of sediment sample,

$$t = (1/\alpha)\,[\ln(A_o/A_d)]$$

2.4. Data processing

Data was plotted with Excel 2007 (Microsoft Office) and Grapher 6.0 software. All mathematical and statistical computations were done using Excel 2007 and Statistica software. The data was standardised to give a normal distribution with a mean of 0 and a variance of 1. Sample means were standardised by subtracting the mean of their distribution and dividing by standard error (SE) or square root of the variance. Correlation coefficients analysis was applied in order to determine the strength of the association between the parameters analysed in the samples. Relations among variables were also assessed using principal component analysis (PCA) with varimax rotation. Principal components analysis describes the variation of a set of multivariate data as a reduced set of uncorrelated variables, each of which is a particular linear combination of the original variables.

The pollution status of the region was assessed by computing pollution indices such as Enrichment factor (Feng et al., 2004) and Geoaccumulation Index (I_{geo}) by (Muller, 1979). In addition, Ecotoxicological effects of heavy metal contaminations in sediments on biota was determined using sediment quality guidelines (SQGs) defined by MacDonald et al. (2000). SQG

values referred to as the threshold effect level (TEL) and the probable effect level (PEL) provide a reliable basis for assessing sediment quality conditions in aquatic ecosystems. TEL defines values below which harmful effects are unlikely to be observed, while PEL defines values above which harmful effects are likely to be observed. The potential ecological risk to the aquatic system by heavy metals in sediments was also assessed. In relation to this, the Effects Range Low (ERL) and Effects Range Median (ERM) concentrations were considered. The ERL represents chemical concentrations below which adverse biological effects are rarely observed, while the ERM represents concentrations above which effects are more frequently observed (Long et al., 1995; 1998). Further, based on metal speciation results, Risk Assessment Code (RAC) has been used to assess environmental risks and estimate possible damage to benthic organisms caused by contaminated sediments. The RAC considers the percentage fraction of metals that are exchangeable and associated with carbonates. The RAC classification defines risk levels as zero, low, medium, high and very high, depending on the percentage value obtained (Jain, 2004; Perin et al., 1985).

Chapter 3

RESULTS AND DISCUSSION

SECTION 1: THANE CREEK

Eight sediment cores, six from mudflats and two from mangrove areas, were collected from the intertidal regions covering the entire Thane creek from the head to the mouth, including western and eastern banks, during September 2008 (Fig. 3.1A.1). The creek head region is represented by core TI, upper middle creek region by cores TII (western bank) and TVI (eastern bank), lower middle creek region by cores TIII (western bank) and TV (eastern bank) while core TIV lies near the creek mouth. All these six cores were sampled from the mudflats of the main channel of the creek except for core TII, in the upper middle region, which was collected from a sub-channel of the main creek.

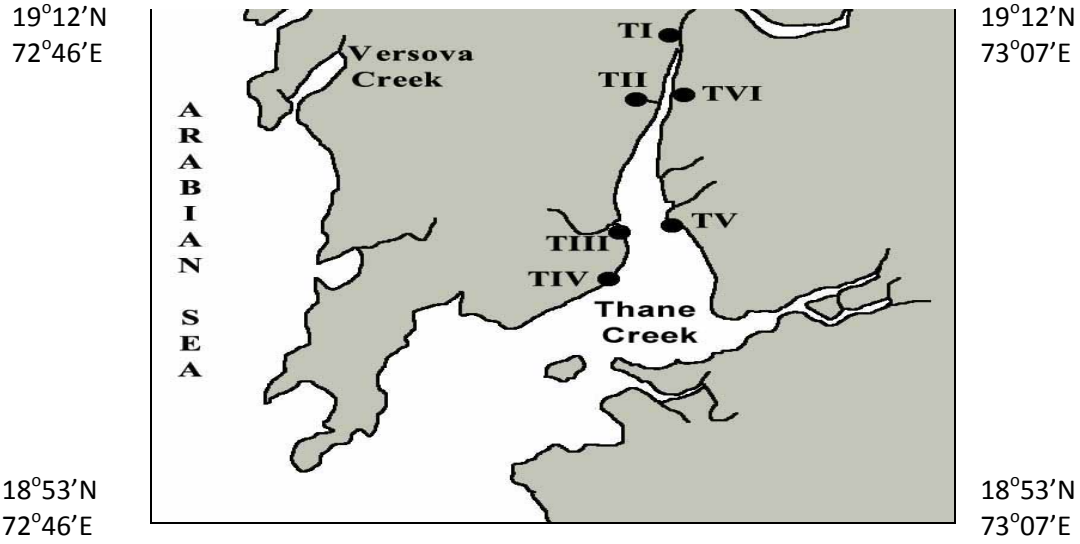

Fig. 3.1A.1. Map showing the sampling locations in Thane creek

3.1A. Mudflats

3.1A.1. Visual description

The sediments of core TI (46 cm long) collected from the head region and core TVI (80 cm long) from the upper middle creek region consists of uniform black colour. The other core (TII-28 cm long) from upper middle creek region shows dark brown colour from the bottom to 22 cm depth. Further above, from 22 to 18 cm, the sediments are a mix of brown and black colour. The remaining portion in core TII, i.e. 18 cm till the surface, is black in colour. Also, few shells appear in the top few centimeter of the core. Cores TIII (60 cm long) and TV (62 cm long) sampled from the lower middle creek region exhibit a variation in colour distribution. Core TIII shows dark brown colour from the bottom to 20 cm depth and further above a uniform brown colour is observed, while core TV exhibits brown colour throughout the length of the core. Core TIV (46 cm long) on the other hand, sampled from the creek mouth, displays a mixture of brown

and black colour from the bottom to 8 cm depth, while further above till the surface brown colour is seen.

3.1A.2. Sediment components (sand, silt, clay)

The grain size distributions of sediments show considerable spatial variability with respect to location within the estuary as well as temporal variability. In general, clay is found to be the dominant sediment component with average percentage > 60 % while sand is present in low percentage (< 2 %), except for core TIII, which shows higher sand percentage. In the entire creek, sand ranges from 0.05-23.54 %, while silt and clay vary from 5.97-44.82 % and 43.36-90.80 % with averages of 2.28 %, 30.21 % and 67.51 % respectively. The depth-wise distribution pattern of sediment components are shown in Fig. 3.1A.2- 3.1A.4.

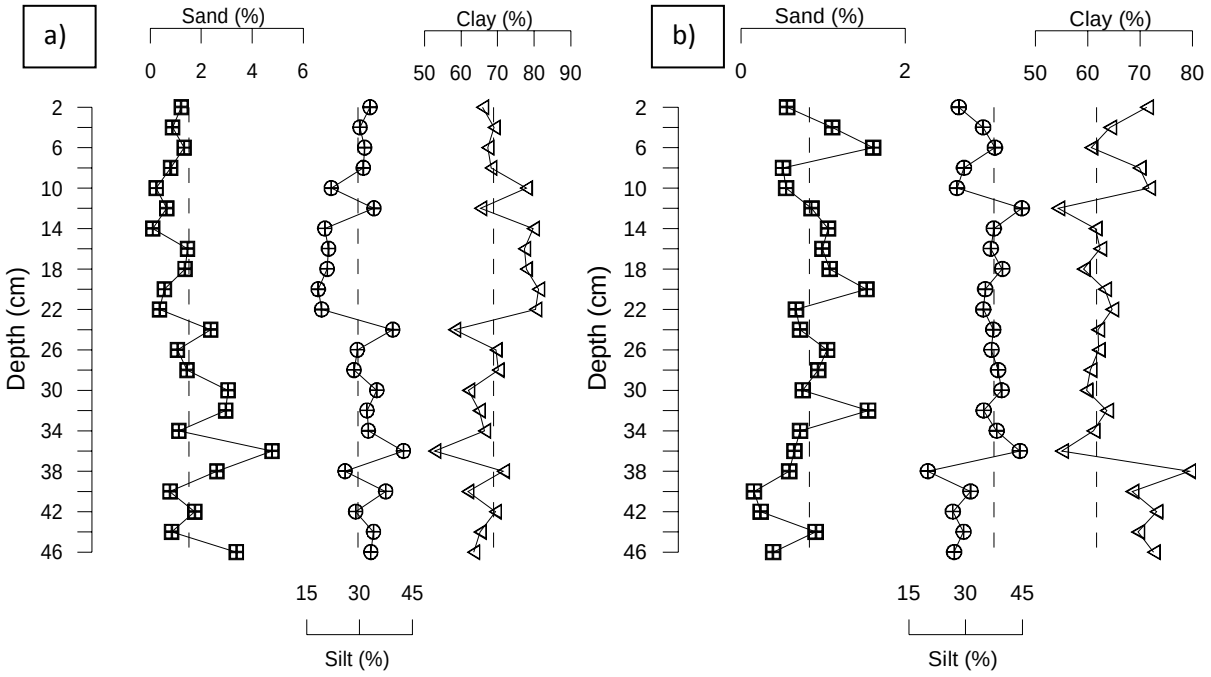

Fig. 3.1A.2. Vertical profiles of sediment components near the creek a) head (core TI) and b) mouth (core TIV)

In core TI sand, silt and clay range from 1.10-4.77 %, 18.24-42.42 % and 52.80-81.20 % with average values of 1.52 %, 29.54 % and 68.94 %, respectively. The vertical profiles of all the components exhibit irregular fluctuations. Sand and silt show a decrease from the bottom to mid-depth and then increase upto the surface. On the other hand, clay does not deviate much from its average value. Near the creek mouth (core TIV), sand, silt and clay range from 0.16-1.61 %, 20.01-44.82 % and 54.32-79.40 % with average values of 0.83 %, 34.34 % and 64.82 %, respectively. Sand shows a fluctuating trend with an overall increase towards the surface while clay initially decreases from the bottom to 36 cm, remains constant till 12 cm and then increases upto the surface. Silt increases from the bottom to 36 cm. Further above it remains constant till 12 cm depth and then fluctuates at the surface.

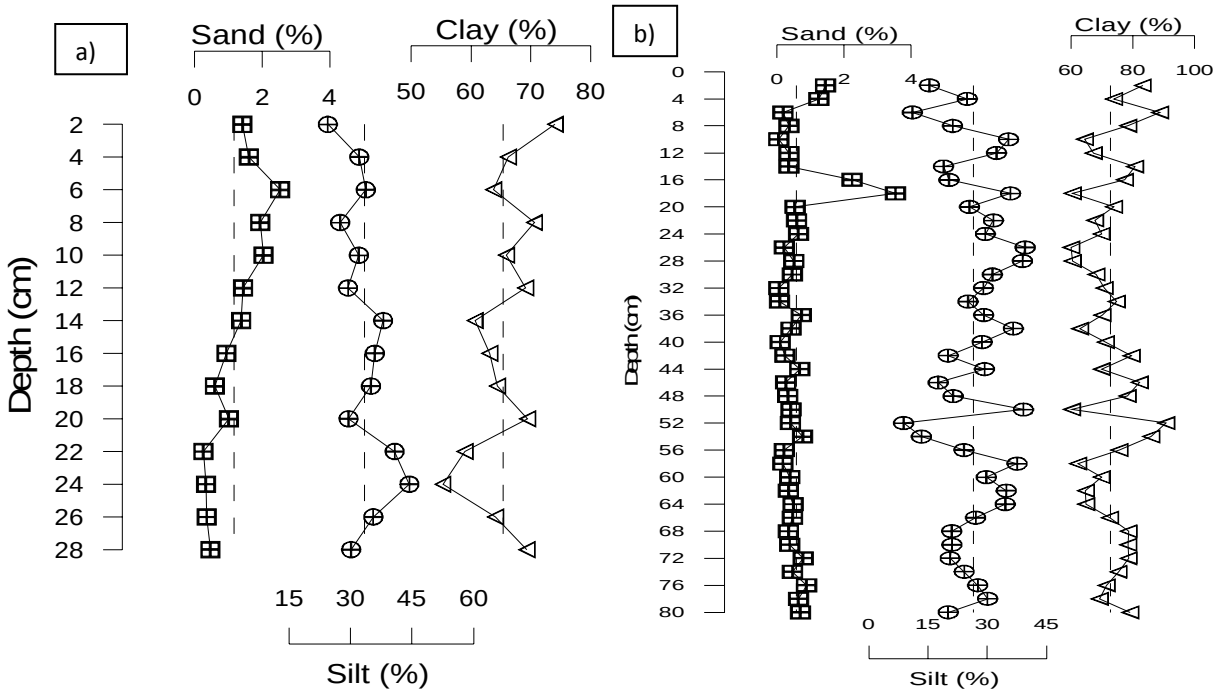

Fig. 3.1A.3. Vertical profiles of sediment components in upper middle creek region: a) core TII and b) core TVI

In the case of upper middle creek region, the ranges for cores TII and TVI are, 0.25-2.52 %; 0.05-3.53 % for sand, 24.51-44.39 %; 8.79-39.62 % for silt and 55.28-74.08 %; 60.16-90.80 % for clay with averages of 1.16 %; 0.59 % for sand, 33.48 %; 26.56 % for silt and 65.35 %; 72.85 % for clay, respectively. Sand in core TII shows an increasing trend from the bottom to the surface while in core TVI, sand distribution is found to be more or less constant except for a positive peak seen at 18 cm depth. Silt profile exhibits a decrease from the bottom to the surface in core TII whereas in core TVI, it shows an erratic distribution with a large range for the entire length, however with a general decreasing trend. Clay increases from the bottom towards the surface with some fluctuations in core TII, while in core TVI large fluctuations in the depth profile are observed, but with a general increasing trend.

In the lower middle creek region, sand, silt and clay vary from 0.20-23.54 %, 5.97- 42.93 % and 43.36-86.32 % for core TIII with average values of 9.04 %, 23.93 % and 67.03 %, respectively, while in core TV the range is 0.17-1.18 % for sand, 25.52-41.84 % for silt and 57.68-74.00 % for clay with average values of 0.53 %, 33.43 % and 66.04 %, for the corresponding components. Core TIII shows an increase in sand percentage from the bottom to 14 cm and then decrease at the surface, while core TV shows a uniform distribution from the bottom to 20 cm and above it the values fluctuate showing an increasing trend. The silt and clay profiles, in general, in both the cores show erratic distributions but largely compensate each other. The silt profiles in all the

cores studied, show large variations. Also, in all the cores, silt and clay are found to show a corresponding opposite trend to each other.

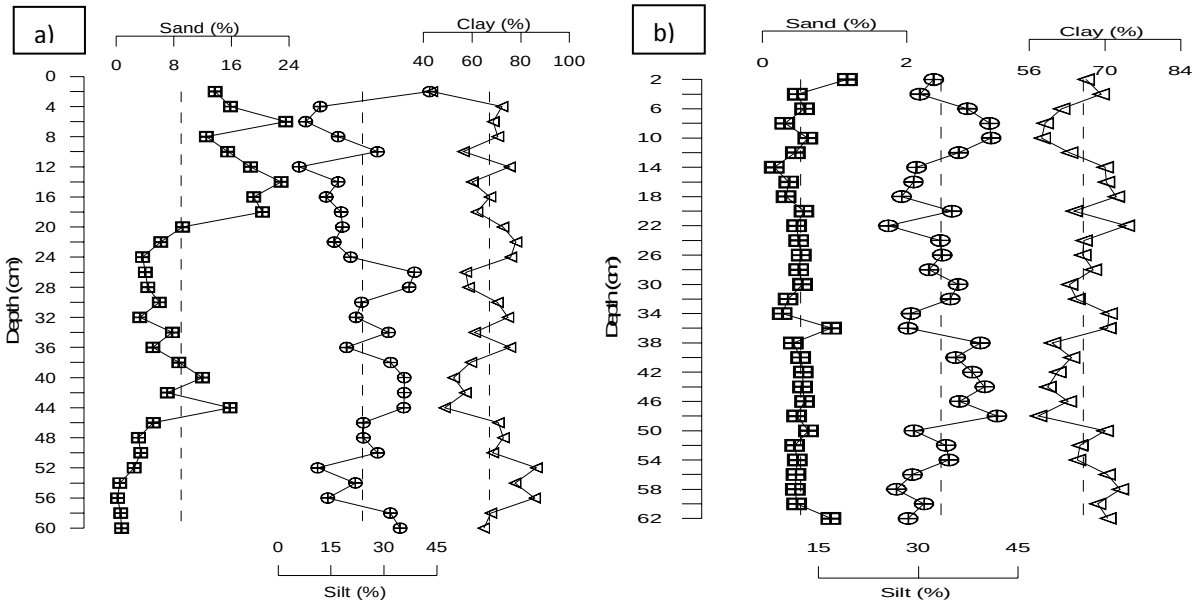

Fig. 3.1A.4. Vertical profiles of sediment components for lower middle creek region: a) core TIII and b) core TV

From the head to the mouth of the creek, a gradual decrease in sand and clay percentage and an increase in silt percentage are observed. However, core TIII, collected from the lower middle creek region shows higher amounts of average sand percentage (9.04) as compared to the other cores. Also, core TVI from the upper middle creek region, exhibits highest average clay percentage (72.85). The high accumulation of coarser sediments at core TIII may be due to the high energy available from the incoming tidal currents whereas the site for core TVI is located on the eastern side of the creek, sheltering the area and hence becoming a favourable area of deposition for finer sediments. In coastal environments with low hydrodynamic energy, fine particulates tend to be trapped, while in areas where hydrodynamic energy is high, fine particulates are flushed out (Williamson et al., 2003).

Further, in order to understand the hydrodynamic condition of the depositional environment of the study area, ternary diagram proposed by Pejrup (1988) has been used. The diagram (Fig. 3.1A.5) describes the hydrodynamic conditions by using clay percentage in the mud fraction represented by sections I to IV, which reflects increasing violent hydrodynamic conditions. Additionally, the sediments are also classified according to their sand percentage represented by four sections, viz, A to D. In the present study, it is seen that the sediment components from cores TI, TII, TV and TIV fall largely under group II of section D (Fig. 3.1A.5a, b, c and d), indicating that the sediment deposition took place under relatively less violent conditions. Subsamples from the upper middle creek region (core TVI) fall in group I and II of section D

(Fig. 3.1A.5b), reflecting that the sediment deposition occurred under less violent to calmer conditions. On the other hand, the subsamples from core TIII (Fig. 3.1A.5c), representing the lower middle creek region fall in group I and II of sections C and D. Such an observation depicts presence of coarser sediments, although the depositional environments range from less violent to calm conditions. These observations are in accordance with the sediment profile seen earlier.

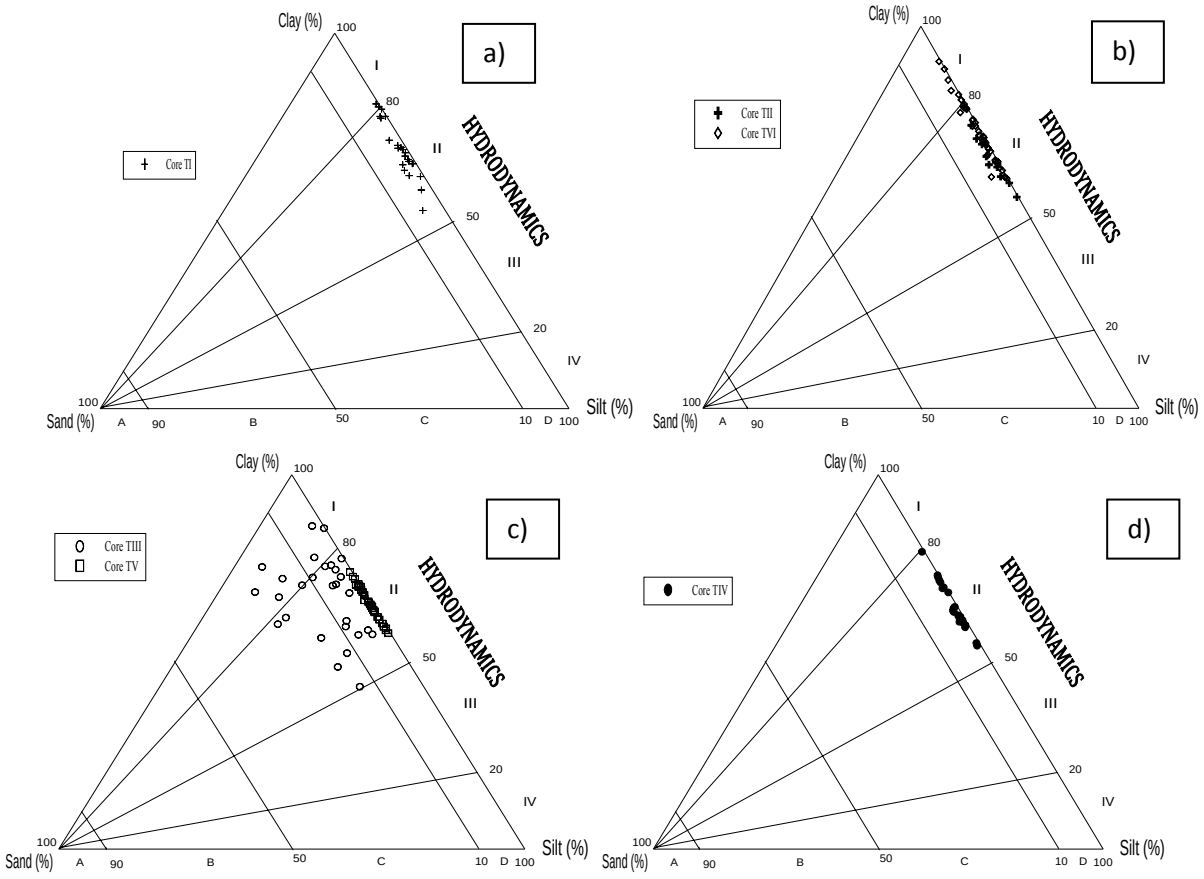

Fig. 3.1A.5. Ternary plots after Pejrup, (1988) for cores from the a) creek head (TI), b) upper middle (TII, TVI), c) lower middle (TIII, TV) and d) near the creek mouth (TIV).

Also textural class of sediment is understood in more detail by plotting the sediment component data on the ternary diagram proposed by Reineck and Siefert (1980). In this diagram, muddy intertidal sediments are commonly subdivided into Sand flats, Mixed flats, Mudflats and Mature Mudflats on the basis of sand or mud contents. When the data points are plotted (Fig. 3.1A.6a), it is observed that the sediments fall largely in the Mature Mudflat class. Another sediment classification using ternary diagram introduced by Flemming (2000) was also applied to the data set. This diagram is distinguished into six textural classes on the basis of simple sand/mud mixtures, Sand (<5 % mud content) and Mud (>95 % mud content) being the respective end-members. The plot (Fig. 3.1A.6b) shows that almost all the subsamples of the creek region fall in the Mud class, except for core TIII from the lower middle creek region, which falls between slightly Sandy Mud and Mud class. The higher amounts of sand content in core TIII as compared

to the other cores must have resulted in this observation. Therefore, it is observed that the three different ternary plots employed have helped in understanding the hydrodynamic conditions of sediment deposition as well as textural trends and classification of sediments within the creek.

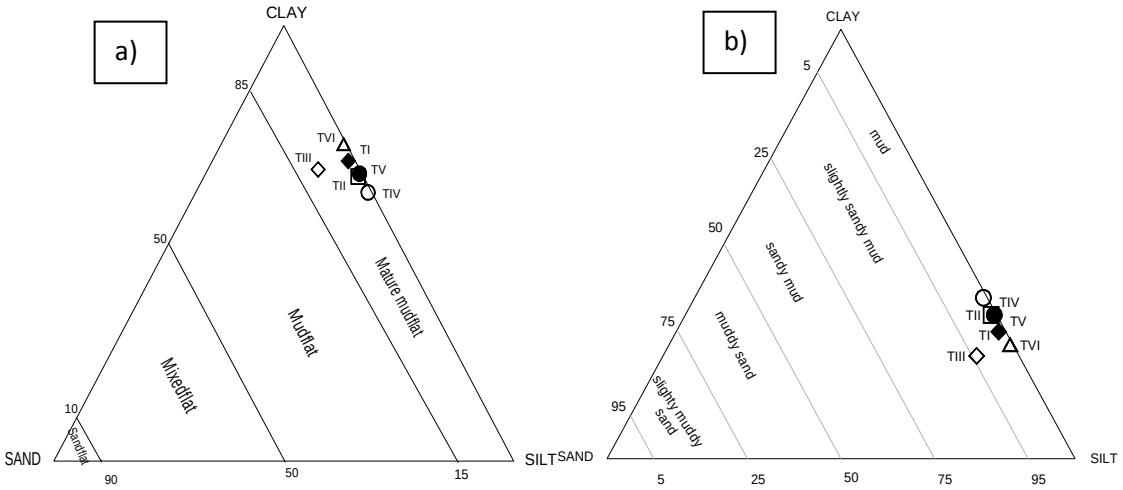

Fig. 3.1A.6. Ternary plots by a) Reineck and Siefert (1980) and b) Flemming (2000)

3.1A.3. Clay mineralogy

Clay mineral analysis using XRD was performed on subsamples of selected cores namely, from the head (core TI), the upper middle region (core TII) and the lower middle region (core TV) of the creek.

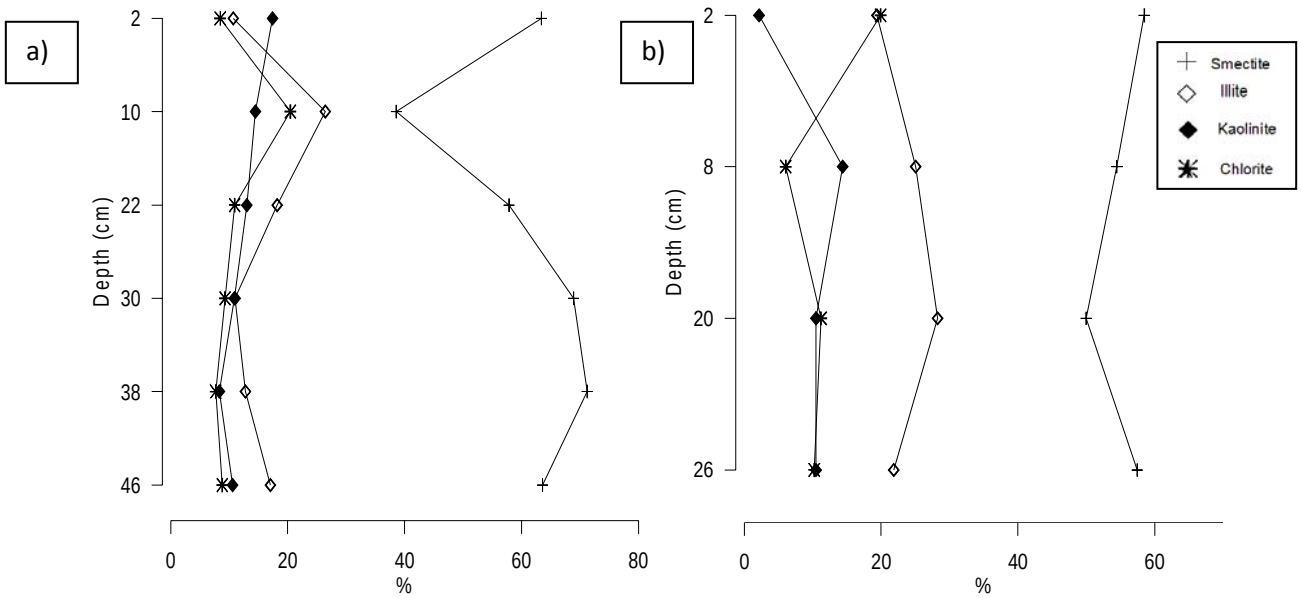

Fig. 3.1A.7. Depth-wise distribution of clay minerals in a) core TI and b) core TII

Sample composition is found to be consistent among selected cores, with smectite (avg. 62.85 %) as the major constituent clay mineral followed by illite (avg. 16.91 %), kaolinite (avg. 10.59 %) and chlorite (avg. 9.65 %). The results largely agree with the study of Bhosale and Sahu (1991), who carried out clay mineral analysis in the creek region and reported that the sediment mineralogy was dominated by montmorillonite, degraded chlorite, illite, and to some extent

silica. In the creek region, the percentage ranges are 38.59-79.73 % for smectite, 7.48-28.26 % for illite, 0.94-19.97 % for kaolinite and 4.77-20.48 % for chlorite. The vertical distribution profiles for the cores are shown in figures 3.1A.7 and 3.1A.8.

In core TI, near the creek head region, illite and chlorite range from 10.72-26.44 % and 7.69-20.48 % with averages of 16.03 % and 10.95 %, respectively. Both the minerals show a similar increasing trend from the bottom to the surface, with an increased peak at 10 cm depth. However, a decline is seen towards the surface. Kaolinite ranges from 8.31-17.42 % with an average of 12.44 % and exhibits a gradual increase from the bottom to the surface, while smectite varies from 38.59-71.20 % with an average of 60.58 %. It initially increases from the bottom to 38 cm, then decreases till 10 cm depth. Further above, an increase is observed. For the core collected from the upper middle region of the creek (TII), the clay mineral types are smectite (range- 50-59 %, avg. 55 %), illite (range- 19.41-28.26 %, avg. 23.64 %), kaolinite (range- 2.17-14.39 %, avg. 9.39 %) and chlorite (6.07-19.93 %, avg. 11.86 %). In general, kaolinite and illite initially increase at the bottom and then decrease towards the surface while smectite and chlorite after showing a decrease at the bottom, increase towards the surface.

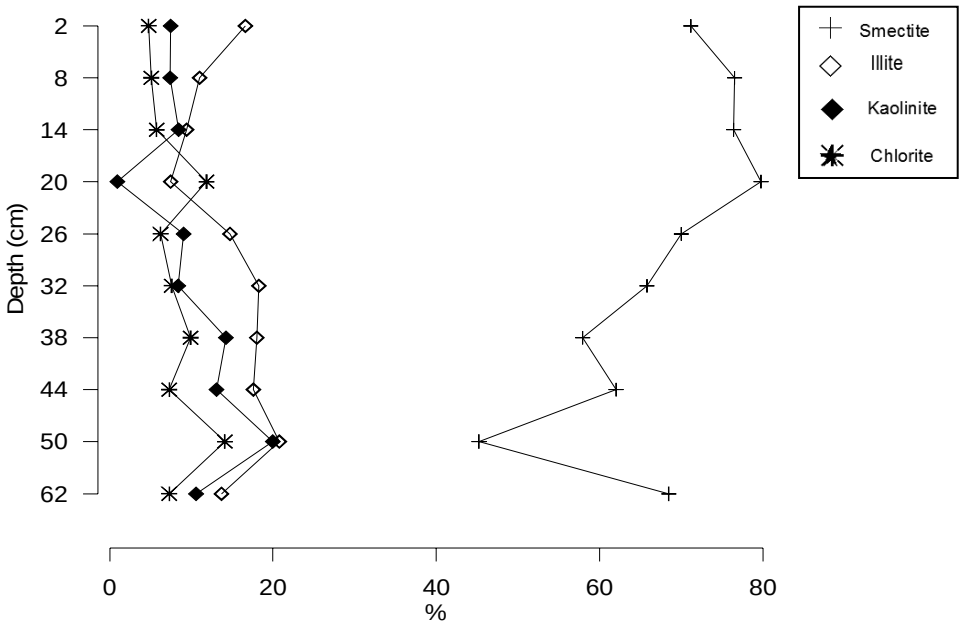

Fig. 3.1A.8. Depth-wise distribution of clay minerals in core TV

In the case of lower middle creek region represented by core TV, kaolinite (range- 0.94-19.97 %, avg. 9.96 %) and chlorite (range- 4.77-14.09 %, avg. 7.99 %) show similar increasing and decreasing trends from the bottom to 26 cm. Above this depth, chlorite shows an increased peak while kaolinite displays a decreased peak. Above 14 cm, both the clay minerals project a stable trend upto the surface. On the other hand, smectite (range- 45-80 %, avg. 67 %) and illite (range- 7.48-20.75 %, avg. 14.75 %) show corresponding opposite trends to each other. Smectite, after

fluctuating from the bottom to 38 cm, follows a gradual increasing trend till 20 cm depth. Further above, it decreases till the surface. Illite on the other hand, increases from the bottom to 50 cm and then decreases till 20 cm. Above this depth, an increase is observed till the surface.

Clay minerals in the marine environment are found to be largely detrital and widely dispersed (Biscaye, 1965). However, in the present case, the bulk clay mineralogical analyses, in general, show a remarkable consistency in the sediment mineralogy among the sites. Factors such as source and transport of clay materials to the creek seem to be responsible for the distribution with time. The observations also suggest that there is not much change in source and sedimentation rate of the region. The clay mineral composition among the individual core at each site show no major changes with depth, except for core TV, which shows higher smectite values at the bottom as compared to the surface.

Clay minerals are commonly used to determine the type and intensity of weathering processes. Smectite is basically the product of chemical weathering. In the present study, smectite shows highest average percentage in core TV (67.30 %) located in the lower middle creek region while the lowest average percentage is seen in core TII (55.11 %) sampled from upper middle creek region. Deccan basalts are the major source for smectite along western continental shelf of India (Rao and Rao, 1995). Bukhari and Nayak (1996), reported higher amounts of smectite in the mouth region of Mandovi estuary which gradually decreased towards the upstream region. Smectite owing to its small size forms aggregate and facilitates settling in high proportions in quiet hydrodynamic conditions. The gradual increase in rate of flocculation for smectite with increase in salinity has been reported by Patchineelam and de Figueiredo (2000). Kaolinite is the product of extreme chemical weathering that occurs in tropical regions where intense seasonal rainfall is followed by dry periods. In the present study, kaolinite exhibits highest average values (12.44 %) in core TI, while core TII shows the lowest average value (9.39 %). Core TI being near the head region with preferably low pH and salinity might have resulted in higher amounts of kaolinite, as attraction between the positive charges on the edges of the particles and negative charges on the planar surfaces of other particles leads to flocculation of this clay mineral in low pH and salinity zone (Schofield and Samson, 1954). On the other hand, illite and chlorite are largely the products of physical weathering. Chlorite and illite have a similar distribution and the amounts are inversely related to that of smectite in almost all the cores studied. Illite (23.64 %) and chlorite (11.86 %) display higher amounts in core TII while the lowest average is seen in core TV (14.75 % and 7.99 %). In core TII, lower amounts of smectite are compensated by higher amounts of illite and chlorite. This may be because; illite and chlorite are more stable than

the other clay minerals. Core TII being away from the main channel of the creek, is sheltered and also closer to urban development resulting in greater transport of terrigenous supply to the sampling location. The study of clay mineral distributions within the Thane creek indicates that the source is basically Deccan basalt and that the formation depends on climatic and physico-chemical conditions.

3.1A.4. Porosity and dry bulk density

Two sediment cores (TI and TII) were analysed for porosity and dry bulk density. For core TI, the porosity values vary from 0.65-0.74 while in core TII the range is 0.53-0.71 with average values of 0.69 and 0.63, respectively.

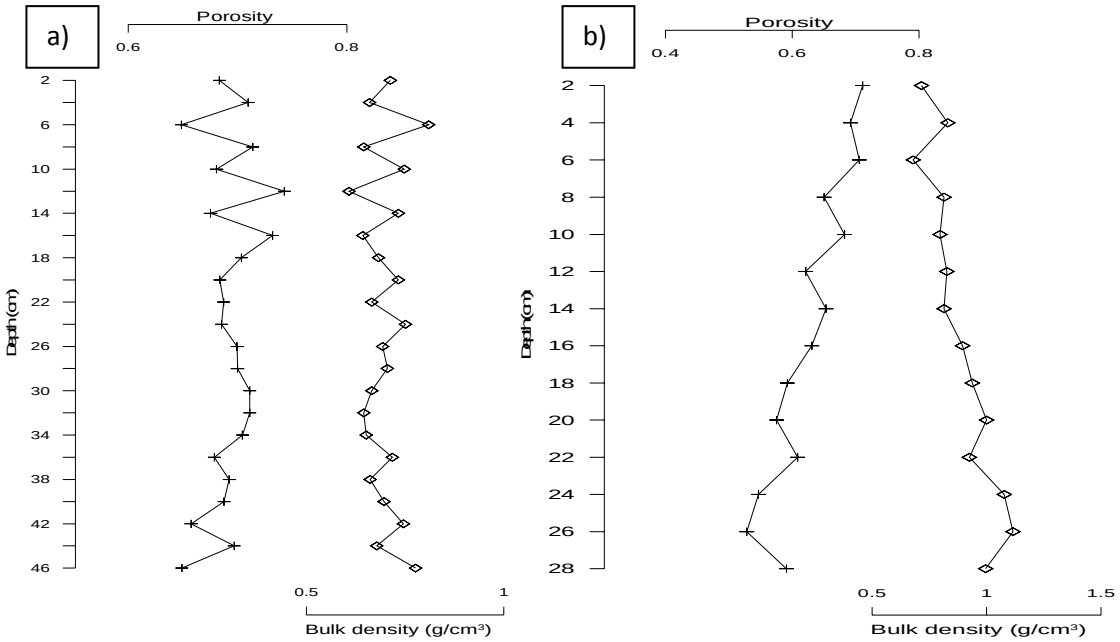

Fig. 3.1A.9. Vertical profiles of Porosity and Bulk density in a) core TI and b) core TII

From the depth profile it is seen that, in core TI (Fig. 3.1A.9), the porosity distribution shows an increasing trend from the bottom to 16 cm while above it large fluctuating trend is seen till the surface. In the case of core TII, a uniform increasing trend is seen from the bottom to the surface of the core. Dry bulk density values range from 0.61-0.81 g/cm^3 for core TI and 0.68-1.12 g/cm^3 for core TII with average values of 0.70 g/cm^3 and 0.89 g/cm^3, respectively. In core TI, the bulk density shows large fluctuation from the bottom to the surface while in core TII, the values display a gradual decreasing trend from the bottom to the surface. In general, in both the cores, porosity and bulk density parameters exhibit opposite trends to each other. The observations are entirely consistent with the grain size analysis (Fig. 3.1A.2a and 3.1A.3a). Also, it is observed that the porosity values, due to sand, in the upper portions of both the cores are much higher than that of the clay-rich sediments at the bottom portions. Lower porosity values exhibited by deeper sediments imply that the void spaces have been squeezed out by consolidation processes and

sediment volume is consequentially decreased. On the other hand, the variation in bulk density is attributable to the relative proportion and specific gravity of solid organic and inorganic particles and to the porosity of the soil.

3.1A.5. Magnetic susceptibility

Magnetic susceptibility is related to total magnetic mineral concentrations in the sediments and, in general, is an expression of detrital input and the subsequent dilution by dia and paramagnetic minerals. Three cores were selected for magnetic susceptibility measurements namely from the creek head (TI), upper (TII) and lower (TV) middle creek regions. The basic parameters analysed to indicate variations in magnetic mineral concentrations are Magnetic susceptibility (χ_{lf}), Anhysteretic Remnant Magnetization (χ_{ARM}) and Saturation Isothermal Remnant Magnetization (SIRM). χ_{lf} represents the total contribution from Fe bearing minerals in the mineral assemblage (Thompson and Oldfield, 1986). It shows the least grain size dependence and is therefore possibly the best parameter for assessing concentrations (Peters and Dekkers, 2003). Further, to evaluate variations in magnetically relevant minerals, the Hard Isothermal Remanent Magnetization (HIRM), the S-ratio, Hard (%) and the other inter-parametric ratio (SIRM/ χ_{lf}) were also examined. Magnetic grain size is indicated by frequency dependent susceptibility (χ_{fd}), χ_{ARM}/χ_{lf} and χ_{ARM}/SIRM. Increase in values of these parameters indicates the increase in fine grained magnetic minerals (single domain). The highest average value for SIRM/ χ_{lf} (15.40 x 10^3A/m) and S-ratio (98 %) are seen in core TI. This core also shows the lowest average values for χ_{ARM} (6480 x $10^{-8}m^3$/kg), χ_{ARM}/SIRM (2.73 x 10^{-5}m/A), χ_{ARM}/χ_{lf} (42.21), HIRM (33.88 %), Hard (1.67 %) and χ_{fd} (1.84 %). In core TV, the highest average values for χ_{lf} (219 x $10^{-8}m^3$/kg), χ_{ARM} (10607 x $10^{-8}m^3$/kg), SIRM (3314 x $10^{-5}Am^2$/kg), HIRM (70 x $10^{-5}Am^2$/kg) and χ_{fd} (2.79 %) are seen while core TII exhibits highest average values for χ_{ARM}/χ_{lf} (68.95), χ_{ARM}/SIRM (5.12 x 10^{-5}m/A) and Hard (3.28 %) and lowest average values for χ_{lf} (120 x $10^{-8}m^3$/kg), SIRM (1631 x $10^{-5}Am^2$/kg), SIRM/ χ_{lf} (13.59 x 10^3A/m) and S-ratio (97 %). The S-ratios calculated are on an average 98 % in the creek region and point to comparatively minor primary high coercivity mineral concentration. Down-core trends of selected mineral magnetic parameters are plotted in Figures 3.1A.10 to 3.1A.12.

From the down-core distribution it is seen that the values in core TI, sampled near the creek head, vary from 99-196 x $10^{-8}m^3$/kg for χ_{lf}, 2461-9395 x $10^{-8}m^3$/kg for χ_{ARM}, 1388-3061 x $10^{-5}Am^2$/kg for SIRM, 1.77-3.48 x 10^{-5}m/A for χ_{ARM}/SIRM, 14.05-16.13 x 10^3A/m for SIRM/ χ_{lf}, 24.90-54.50 for χ_{ARM}/χ_{lf}, -4.48-60.05 x $10^{-5}Am^2$/kg for HIRM, -0.20-3.33 % for Hard, 97-100 %

for S-ratio and 0.77-2.74 % for χ_{fd} with average values of 148 x $10^{-8}m^3/kg$, 6480 x $10^{-8}m^3/kg$, 2288 x $10^{-5}Am^2/kg$, 2.73 x $10^{-5}m/A$, 15.40 x $10^3A/m$, 42.21, 33.88 x $10^{-5}Am^2/kg$, 1.67 %, 98 % and 1.84 %, respectively. The core displays similar vertical patterns (Fig. 3.1A.10) for χ_{lf}, χ_{ARM} and SIRM, i.e. an increase is seen from the bottom to the surface. χ_{ARM}/SIRM and χ_{ARM}/χ_{lf} show identical increasing and decreasing trends. SIRM/χ_{lf} increases from the bottom to 26 cm and then fluctuates upto the surface. HIRM and Hard on the other hand, show similar decreasing trends with a low value at 32 cm depth. S-ratio and χ_{fd} (%) show similar increasing trends from the bottom to the surface. The S-ratio shows an increased peak at 32 cm depth.

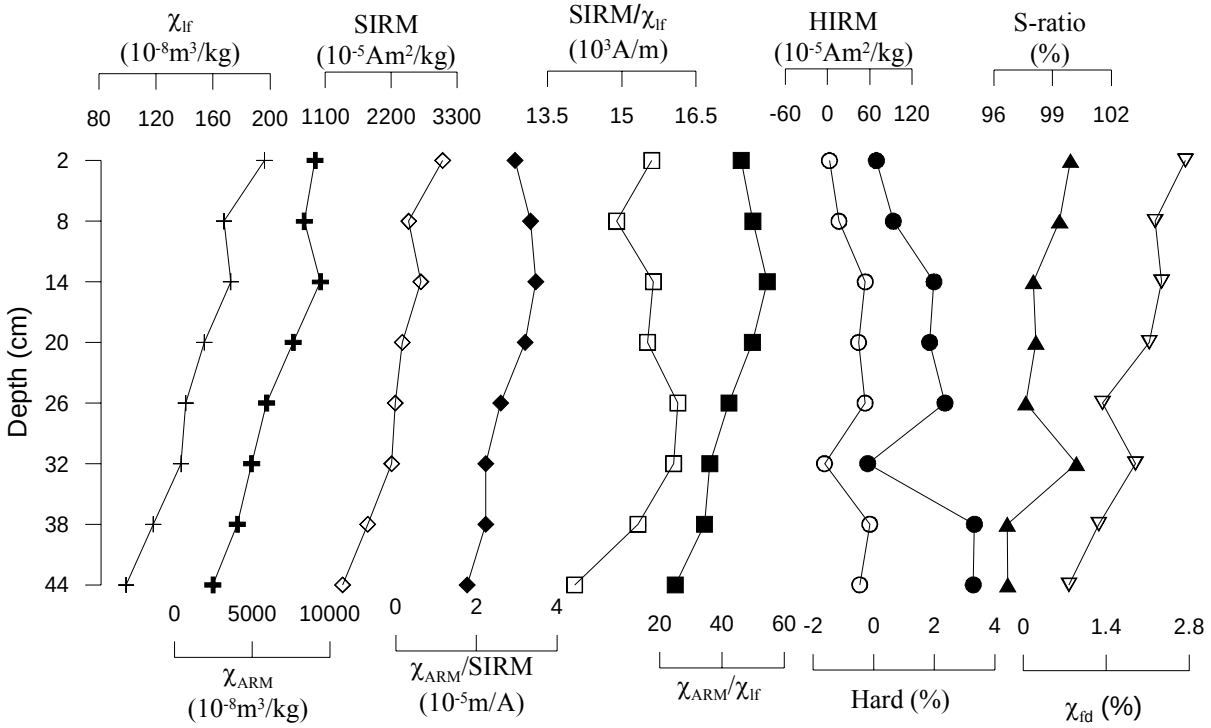

Fig. 3.1A.10. Depth-wise distribution of magnetic susceptibility parameters for core TI

In the case of upper middle creek region (Fig. 3.1A.11), χ_{lf} (range- 109-134 x $10^{-8}m^3/kg$, avg. 120 x $10^{-8}m^3/kg$) and SIRM (range-1480-1797 x $10^{-5}Am^2/kg$, avg. 1631 x $10^{-5}Am^2/kg$) show similar increasing and decreasing trends whereas χ_{ARM} (range- 4786-10568 x $10^{-8}m^3/kg$, avg. 8360 x $10^{-8}m^3/kg$) decreases uniformly from the bottom to the surface. Both χ_{ARM}/SIRM (range- 3.06-6.97 x $10^{-5}m/A$, avg. 5.12 x $10^{-5}m/A$) and χ_{ARM}/χ_{lf} (43.83-90.80, avg. 68.95) after an initial increase at the bottom decreases towards the surface. On the other hand, SIRM/χ_{lf} (range- 13.03-14.31 x $10^3A/m$, avg. 13.39 x $10^3A/m$) after an initial decrease at the bottom increases towards the surface. Also, HIRM (range- 32.87-79.36 x $10^{-5}Am^2/kg$, avg. 53.87 x $10^{-5}Am^2/kg$) and Hard (range- 2.05-4.77 %, avg. 3.28 %) show identical fluctuating trends with alternate decrease and increase, while the S-ratio displays a corresponding opposite trend to both these parameters. χ_{fd}

(range- 1.21-2.63 %, avg. 2.00 %) shows a decrease from the bottom to 8 cm depth and then increases at the surface.

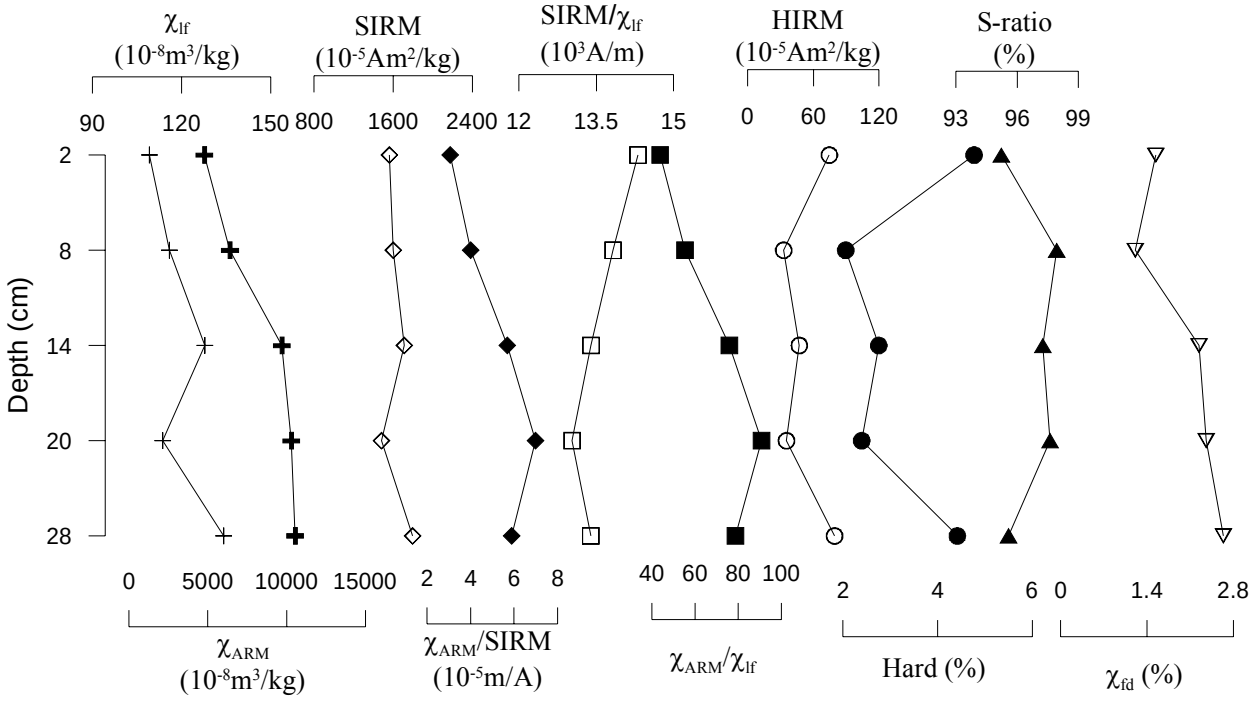

Fig. 3.1A.11. Depth-wise distribution of magnetic susceptibility parameters for core TII

For the lower middle creek region (Fig. 3.1A.12), χ_{lf} (range- 205-238 x $10^{-8}m^3$/kg, avg. 219 x $10^{-8}m^3$/kg) shows parallel variations to SIRM (range- 2975- 3621 x $10^{-5}Am^2$/kg, avg. 3314 x $10^{-5}Am^2$/kg) from the bottom to the surface and also with χ_{ARM} (range- 6656-12797 x $10^{-8}m^3$/kg, avg. 10607 x $10^{-8}m^3$/kg) from the bottom to 20 cm depth. Further above, it decreases. SIRM/χ_{lf} (range- 14.37-16.21 x 10^3A/m, avg. 15.11 x 10^3A/m) shows similar trends with χ_{lf} and SIRM till 14 cm depth and above this, an increase is seen. HIRM (range- 23.45-98 x $10^{-5}Am^2$/kg, avg. 70 x $10^{-5}Am^2$/kg) and Hard (range- 0.79-2.71 %, avg. 2.08 %), also χ_{ARM}/SIRM (range- 1.85-3.81 x 10^{-5}m/A, avg. 3.21 x 10^{-5}m/A) and χ_{ARM}/χ_{lf} (29.93-58.18, avg. 48.34), show identical variations from the bottom to the surface of the core. The S-ratio (range- 97-99 %, avg. 98 %) and χ_{fd} (range- 2.48-3.15 %, avg. 2.79 %) show similar increasing and decreasing trends, except between the depths of 32 and 26 cm, wherein S-ratio decreases and χ_{fd} increases. The profiles of most of the magnetic parameters in the lower middle creek region (core TV) are almost identical to each other and exhibits association similar to that seen in the upper middle creek region (core TII). For example, of χ_{lf} and SIRM; χ_{ARM}/SIRM and χ_{ARM}/χ_{lf}; and HIRM and Hard. In addition, for cores TI and TV, magnetic mineral concentrations are low at the bottom and increase towards the surface.

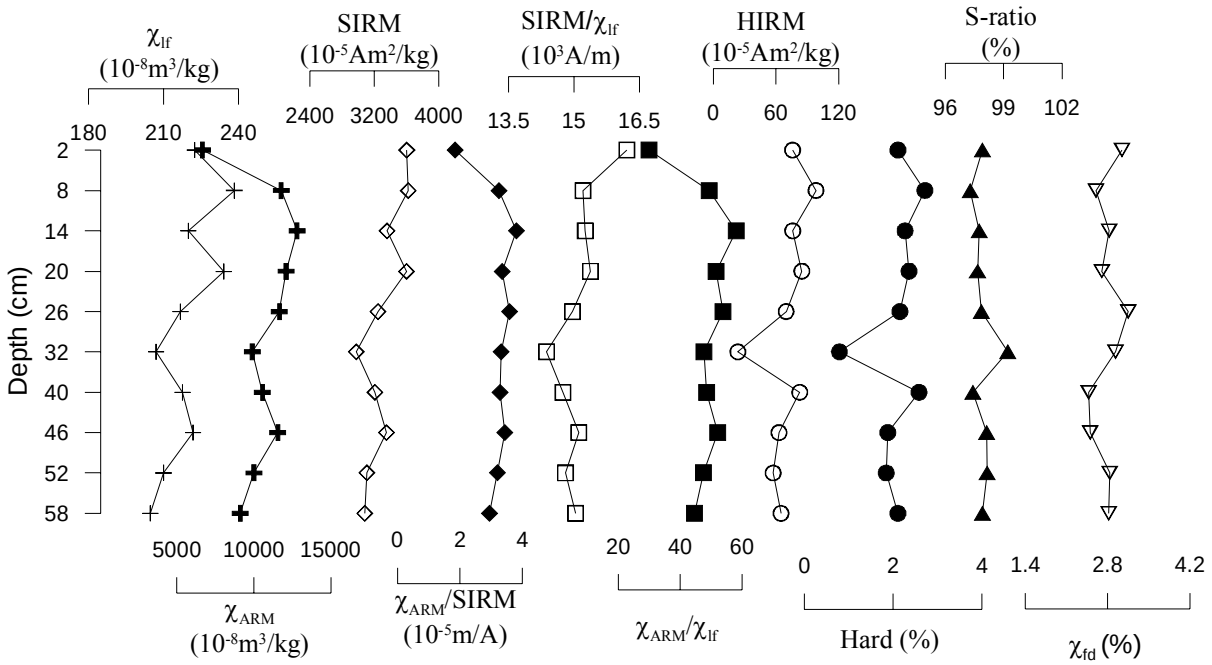

Fig. 3.1A.12. Depth-wise distribution of magnetic susceptibility parameters for core TV

In the present study, the χ_{lf} average value decreases from the head to the lower middle creek region. The χ_{ARM} and SIRM values increase with an increase in concentration of fine magnetic grain size (single domain) (Bloemendal et al., 1992). SIRM is not affected by diamagnetic and paramagnetic minerals but decreases in value with an increase in the concentration of coarse magnetic grains. Therefore, increasing trends of χ_{ARM} and SIRM, from the bottom to the surface in cores TI and TV, points to a single domain mineral. When magnetic signal is controlled by a single magnetic component (Lepland and Stevens, 1996; Maher, 1986), or a mixture of magnetic minerals at a constant ratio (Caitcheon, 1998), χ_{lf} and SIRM exhibit a linear relationship. In such occasions, the inter-parametric ratio SIRM/χ_{lf} can be used to interpret mineral magnetic grain size variations. The ratio increases with decreasing grain size, if magnetic grain size is larger than the grains at the SP/SD boundary (Thompson et al., 1980). χ_{lf} follows similar trend to SIRM, suggesting that susceptibility is due to single domain minerals. The linear relationship of SIRM and χ_{lf} in the creek sediments indicate the predominance of ferrimagnetic components in the sediments.

The χ_{ARM}/χ_{lf} and χ_{ARM}/SIRM vary inversely with magnetic grain size and can be used to assess the relative change in concentrations of finer magnetic grain size. The inter-parametric ratios (SIRM/χ_{lf} and χ_{ARM}/χ_{lf}) are low for multi-domain (MD>1 μm) and super-paramagnetic (SP< 0.03 μm) grains and high for single domain (0.03-1 μm) grains (Maher and Taylor, 1988). The decrease in magnetic mineral concentration and grain size parameters with depth in cores TI and TV (Fig. 3.1A.10 and 3.1A.12) indicate dissolution of both bacterial and lithogenic fine-grained

magnetites, leaving a residue of coarse-grained lithogenic magnetites. For core TII, an opposite trend is seen indicating the dominance of fine-grained magnetites at the surface. HIRM (Stoner et al., 1996) quantifies contributions of high coercivity Fe oxides (hematite, hemoilmenite) and Fe hydroxides (e.g. goethite) to the total remanence while when the S-ratio is close to hundred, the dominant magnetic minerals are ferrimagnetic, and it decreases with increasing contribution of anti-ferromagnetic minerals (Maher, 1986; Verosub and Roberts, 1995). Therefore, the HIRM and S-ratio reflect variations in the coercivity spectrum of the magnetic mineral assemblage and therefore in mineralogy. High S-ratios and low HIRM values for all the studied cores indicate that magnetite is the dominant component of the magnetic material. High concentrations of paramagnetic and diamagnetic components would lead to low χ_{fd} % as is the present case in all the cores studied. In this study, the sediment cores (except TII) show dominant anthropogenic contribution, reflected by significant enhancement of magnetic concentration dependent parameters (χ_{lf}, χ_{ARM} and SIRM) in the uppermost section, followed by rapid decrease with depth. These enrichments of magnetic concentration parameters indicate the presence of fine grained ferrimagnetic (Fe oxides) minerals in the upper part of the sediment cores, which might be derived from anthropogenic activities (Chan et al., 1998; 2001). Further, magnetic mineralogy parameters (S-ratio, Hard and HIRM) of all sediment cores also indicate the abundance of magnetite minerals.

3.1A.6a. Organic matter (TOC, TP and TN)

Organic matter (OM) is an important component of settling particles and sediments in water bodies. It influences a variety of biogeochemical processes and is the most important factor controlling redox conditions, and the cycling of phosphorus, other nutrients and trace metals. Carbon and nutrient concentrations in sediments provide an insight into the historic productivity of an aquatic system. The concentration of organic matter, in general, shows a gradual decrease from the head towards the mouth of the creek. TOC ranges from 0.76-5.00 %, TP from 0.24-1.64 mg/g and TN varies from 0.20-2.89 mg/g for the entire creek region. The average for TOC is 1.96 %, for TP is 0.82 mg/g while for TN it is 0.89 mg/g.

From the head to the mouth region of the creek, TOC ranges from 2.59-5.00 % for core TI, 0.76-2.35 % for core TII, 1.19-2.79 % for core TVI, 1.12-3.12 % for core TIII , 1.10-2.31 % for core TV and 0.78-1.52 % for core TIV, with average values of 3.32, 1.65, 2.17, 1.67, 1.80 and 1.12 %, respectively. TP values range from 0.66-1.64 mg/g for core TI, 0.24-0.40 mg/g for core TII, 0.79-1.07 mg/g for core TVI, 0.57-0.95 mg/g for core TIII, 0.85-1.16 mg/g for core TV and 0.49-0.96 mg/g for core TIV having averages of 1.11, 0.33, 0.92, 0.78, 0.98 and 0.79 mg/g,

respectively. TN concentration for cores near the head (TI) and mouth of the creek vary from 0.72-2.89 mg/g and 1.17-1.86 mg/g with average of 1.46 mg/g and 0.70 mg/g, while in the upper middle creek region the values are 0.35-0.82 mg/g for core TII and 0.30-1.98 mg/g for core TVI having averages of 0.53 mg/g and 0.95 mg/g. The lower middle creek region exhibit range of 0.20-0.52 mg/g and 0.31-1.27 mg/g for cores TIII and TV with average values of 1.40 mg/g and 0.31 mg/g, respectively. At the inner creek end (TI), highest average values of TP and TN are seen while the lowest average value for TP is seen for core TII while core TIII shows the lowest average value for TN.

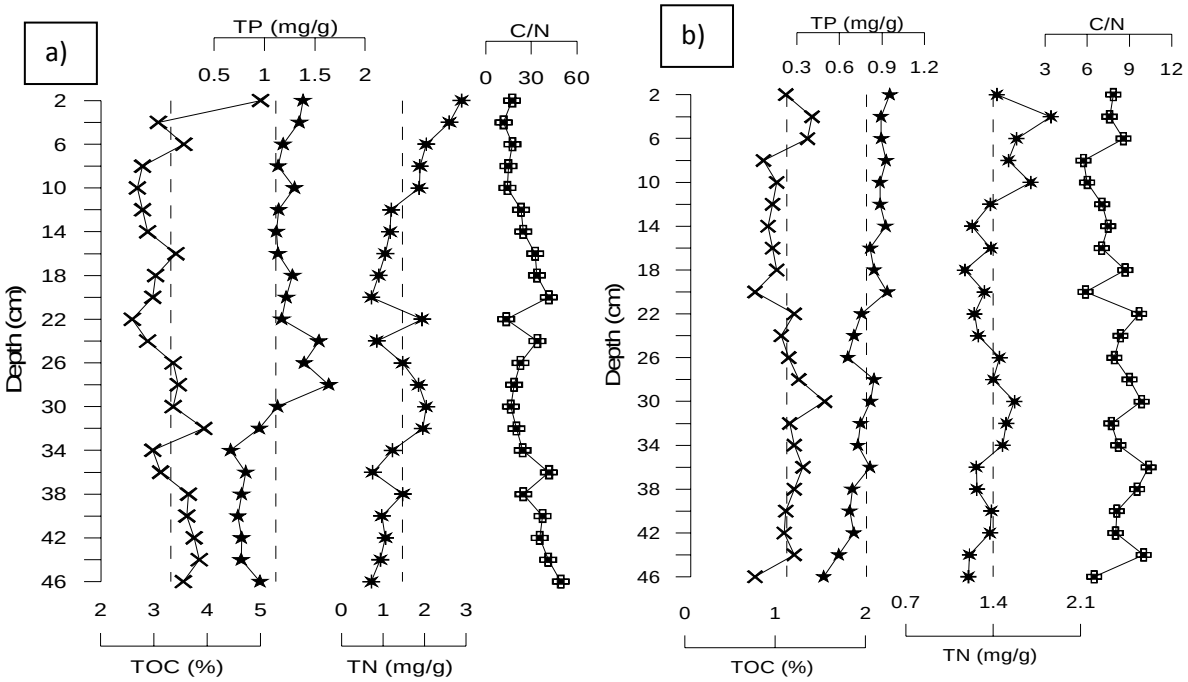

Fig. 3.1A.13. Vertical profiles of Organic matter near the creek a) head (core TI) and b) mouth (core TIV)

Form the depth-wise distribution pattern (Fig 3.1A.13a), near the creek head (core TI), TOC shows a decreasing trend from the bottom to 8 cm depth and further above it increases. On the other hand, TP and TN show increasing trends from the bottom to the surface. However, between the depths of 34 and 22 cm, both the variables display large variations in concentrations. In the upper middle creek region (Fig 3.1A.14), cores TII and TVI, exhibit more or less similar trends with TOC and TN, increasing from the bottom to the surface with few spikes, except for TOC in core TII, whereas TP shows a constant uniform trend. In the lower middle creek region (Fig 3.1A.15), core TIII displays uniform TOC distribution while TP profile increases from the bottom to 32 cm depth and then decreases till 12 cm, followed by an increase towards the surface. TN concentration shows large vertical variations throughout the core. In core TV, TOC and TN show increasing trends with considerable fluctuations while TP decreases from the bottom to the surface. Near the creek mouth (Fig 3.1A.13b), core TIV shows an increase in TP

and TN concentration, while TOC in general decreases from the bottom to the surface, except for positive peaks seen at 30 and 6 cm depths, respectively.

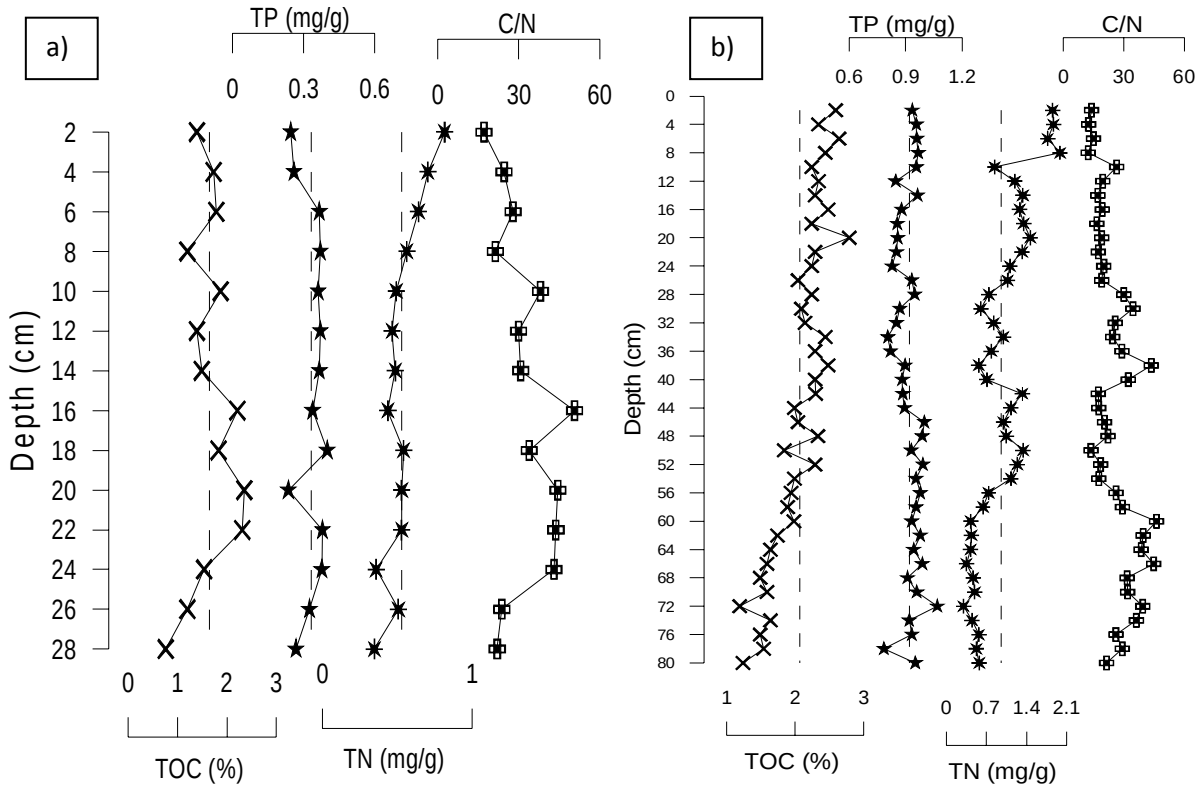

Fig. 3.1A.14. Vertical distribution profiles of Organic matter for upper middle creek region: a) core TII and b) core TVI

In the creek region, the cores collected from the opposite banks show similar down-core profiles both in the upper as well as the lower middle creek regions. Further, the organic matter content of most of the cores studied decreases with depth, as would be expected in any soil or sediment profile due to natural decomposition process. In the uppermost oxic portion of the sediment column, degradation is relatively fast, decreasing in an exponential fashion. The oxidation rate of OM depends on its reactivity, which is initially high and then decreases with time as the more reactive components of the OM are consumed (Westrich and Berner, 1984). Some of this OM is transferred from the oxic zone by biodegradation and bioturbation into the underlying anoxic zone. There is also an upward migration from the anoxic zone as sedimentation proceeds. The percentage of OM is found to be highly correlated with the fine fraction of the sediment (silt + clay). In aquatic environments, organic material can occur as coatings on sediment particles or as discrete particles, thereby facilitating the relationship with grain size (Horowitz and Elrick, 1987). Generally, the organic matter content of sediments increase as the sediment texture becomes finer (Williamson and Wilcock, 1994; Denton et al., 2001). This can be very well witnessed in cores TII, TIV and TVI.

3.1A.6b. C/N ratio

C/N ratio, calculated from percentages of TOC and TN, provide insight into the relative contributions of algal vs. terrestrial organic matter to the sediment i.e. the ratio indicates whether the source of organic matter is autochthonous or allochthonous (Atkinson and Smith, 1983; Perdue and Koprivnjak, 2007). The C/N ratio gives an indication from where the organic material is received in the water column. The C/N ratio in aquatic systems is governed by the mixing of terrestrial and autochthonous OM (e.g., Ostrom and Macko, 1992; Thornton and McManus, 1994; Meyers, 1997). Higher plants are the main organic producers in the terrestrial environment, and consist mainly of cellulose and lignin, which contain few nitrogen compounds. The C/N ratio for marine phytoplankton is 6.6, for fresh marine sediments is 7 to 10, and for terrestrial plants is over 20 (Deevy, 1973; Rullkötter, 2000). The higher the percentage of terrestrial organic matter, the greater the ratio of TOC: TN. Over the entire creek region, C/N values range from 5.72-88.39 with an average of 29.71. The minimum ratio is seen in core TIV (5.72) while the maximum value is seen for core TIII (88.39). The C/N profiles of all the cores are presented in Figures 3.1A.13 to 3.1A.15.

Near the creek head (core TI), C/N ranges from 11.85-49.31 with an average of 26.52 and displays a decreasing trend from the bottom to the surface, except for two increased peaks at 36 and 20 cm depths. At the upper middle creek region, in core TVI, the range of C/N is 12.30-46.15 with an average of 25.41. The C/N values demonstrate an overall increase from the bottom of the core to 60 cm. Above 60 cm, the C/N values decreases to 13.72 at 50 cm, before increasing to 43.59 at 38 cm depth. Above 38 cm, the values decline more rapidly, with a low value of 13.95 at the surface. The other core TII, with a range of 17.03-50.69 and an average of 32.21, shows an increase from the bottom to 16 cm depth followed by a decrease towards the surface. In the case of lower middle creek region, core TIII, with a range of 25.23-88.39 and an average of 55.99, exhibits a fluctuating decreasing and increasing trend. In core TV, C/N values range from 13.12-54.02 with an average of 30.05 and exhibits a trend which points to more influence of freshwater with terrestrial input at depths of 6 cm (26.38) and 18 cm (23.35) to marine dominated organic material, towards the top of the core. Similar observations are also seen for core TVI, which lies in the upper middle creek region, wherein a peak (26.54) is seen at 10 cm depth. This trend of lessening terrestrial influence is significant, as it suggests that either tidal forcing has increased or freshwater and suspended sediment flux to this part of the creek has decreased over time. For core TIV, near the creek mouth, C/N ranges from 5.72-10.35 with an average of 8.05. The C/N ratios remain below 10 for the entire core with the exception of one peak (10.34) at 26 cm depth.

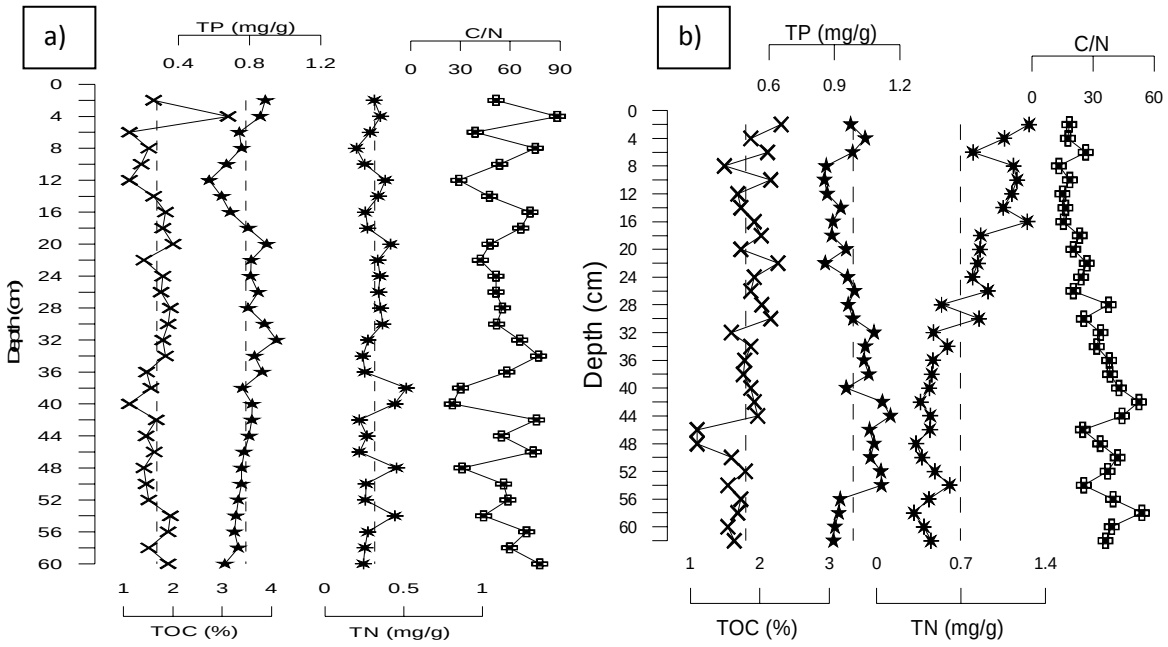

Fig. 3.1A.15. Vertical profiles of Organic matter for lower middle creek region: a) core TIII and b) core TV

In all the cores, except for the lower part of cores TII and TIII, a general decreasing trend from the bottom to the surface is seen. Core TIII has a very variable C/N ratio with high values (>20) suggesting strong influence of terrestrially derived material in the region. As expected due to its central position within the creek, cores TII, TIII, TV and TVI exhibit a C/N ratio profile characteristic of a mixed environment whereby organic material deposited comes from both terrestrial and freshwater/marine sources (Lamb et al., 2006). The ratio for core TIV, which lies near the creek mouth, is close to 10, indicating that this site must be plankton dominated. Low C/N values, accompanied by increased TOC % are often indicative of enhanced algal production. Evidence from C/N ratio analysis suggests that there has been a gradual decrease in the transport of terrestrially derived organic matter or increase of marine dominance over the years to some parts of the creek (TI, TV and TVI). From the head to the mouth of the creek, C/N values, in general show a decreasing trend.

3.1A.7. pH

The pH of the creek region ranges from 6.72-8.90 with an average of 7.77. The pH is found to move towards an alkaline nature with increasing distance from the creek head. The range and average value varies from 6.85-7.99; avg. 7.63 for core TI near the creek head, 7.44-8.19; avg.7.77 for core TII and 7.95-8.90; avg. 8.22 for core TVI, for both the cores sampled from the upper middle creek region, 7.04-8.30; avg.7.69 for core TIII and 6.80-8.45; avg.7.80 for core TV collected from the lower middle creek region while the range is 6.72-8.23; avg.7.49 for core TIV retrieved near the creek mouth.

From the depth-wise distribution (Fig. 3.1A.16), it is seen that pH of cores sampled near the creek head (TI) and mouth (TIV) and also from lower middle regions (TIII and TV) are observed to show a gradual decrease from the bottom to the surface. On the other hand, the values for the core sampled from the upper middle creek region (TII) increases whereas the other core TVI fluctuates from the bottom to the surface. The production of organic acids during organic matter breakdown explains the lower pH in the top layers of cores TI, TIII, TIV and TV. Also soils/sediments with large fraction of humic substances will tend to have a lower pH because humic acids have a wide variety of functional groups such as phenols and carboxyl groups (Alloway, 1995; vanLoon and Duffy, 2005). Soils/sediments rich in carbonates will usually have a high pH because carbonates have the ability to neutralize acidity. This supports the high pH seen in core TII where abundant shells were present.

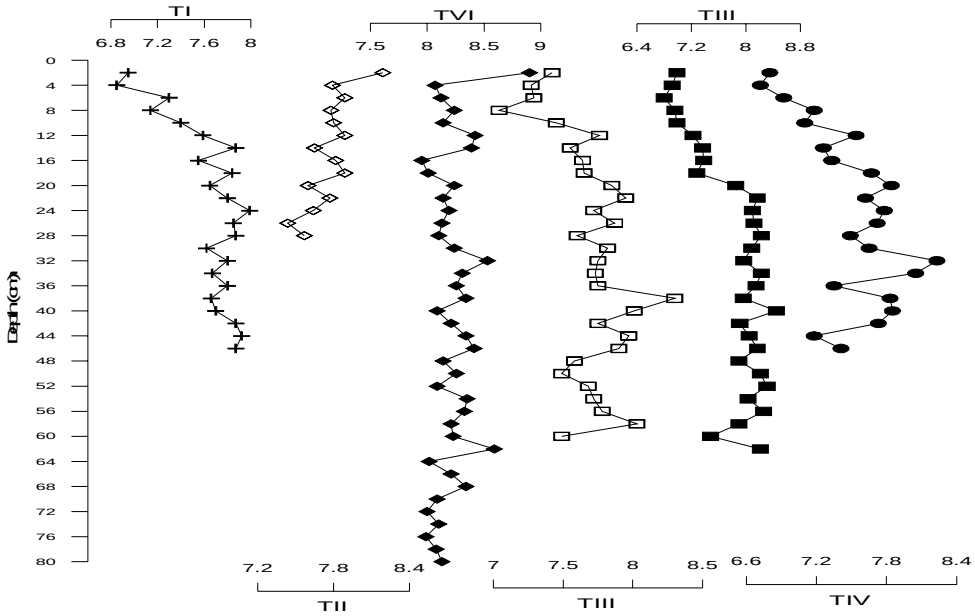

Fig. 3.1A.16. Depth-wise distribution of pH in cores sampled from the creek

3.1A.8. Metal geochemistry

Figures 3.1A.17 to 3.1A.22, represents vertical distribution patterns of metals in all the cores collected from the Thane creek. The abundance of metal concentration in the creek follows the order;

$$Al > Fe > Ca > Mn > V > Zn > Cu > Cr > Ni > Pb > Co$$

In order to account for variations in metal values, the concentration of metals are usually normalised with Al to compensate for the differences in grain size and mineralogical composition. This requires that the normalizer must be an element of natural origin, and must have good correlations with heavy metals and the fine-grained fraction (Mil-Homens et al., 2007). However in the present study, only in core TII and to some extent in core TV, Al showed

good correlations with metals, while the other cores did not show any good positive associations of Al with clay or silt. Therefore, the metals were not normalised with respect to Al.

a) Aluminium (Al)

The Al values in cores collected from the inner (TI), lower middle (TIII and TV) and mouth (TIV) regions of the creek ranges from 8.39-13.08 %, 7.55-14.02 %, 9.31-14.54 %, and 8.16-14.25 % with average values of 10.65, 10.68, 11.19 and 11.51 % respectively, and show an overall increasing trends from the bottom to the surface of the cores. However, in core TIV, considerable fluctuation is seen. In the upper middle creek region in core TII, Al ranges from 9.81-15.49 % with an average of 12.49 % and exhibits a fluctuating increasing trend from the bottom to 8 cm depth and then decreases towards the surface, whereas in core TVI, Al ranging from 9.92-14.20 % and having an average of 11.97 %, although displays some variability in concentrations along its profile, overall there is a decline in concentration along the core length. The fact that there is no overall change in Al concentrations in core TIV, suggests that marine water intrusion into this region of the creek might have not intensified over the periods or that the overall creek discharge might have remained relatively constant over the years. The average values indicate that, in general, the Al distribution over the entire creek is found to remain constant.

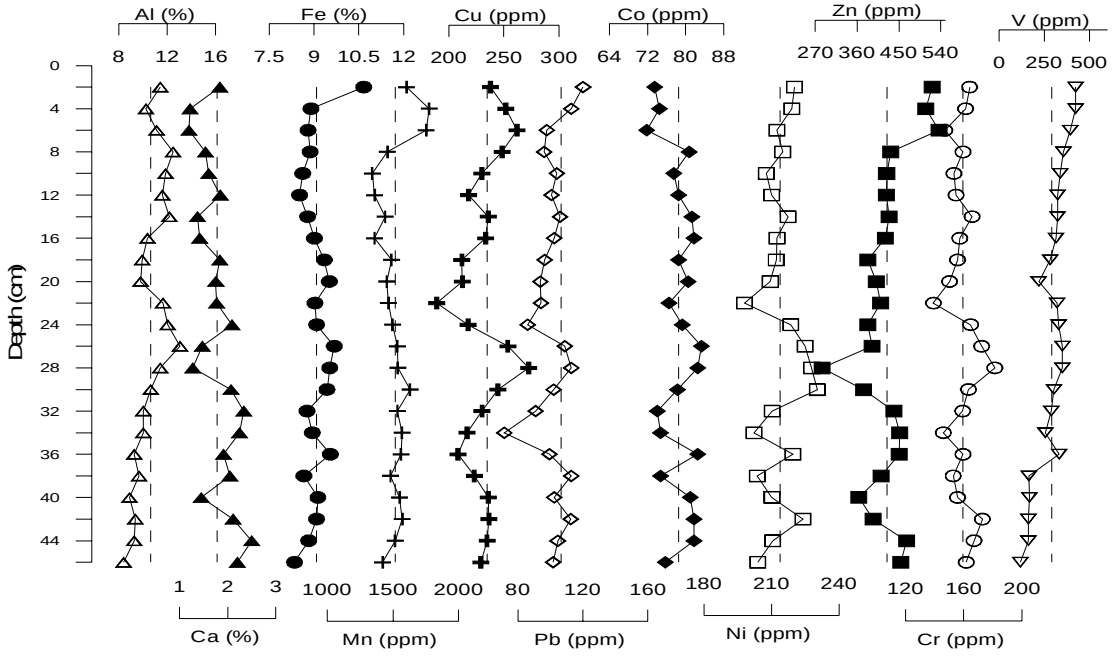

Fig. 3.1A.17. Depth-wise distribution of selected metals in core TI

b) Calcium (Ca)

A fluctuating increasing and decreasing metal trend is seen in core TI (range- 1.19-2.50 %, avg. 1.79 %), collected near the creek head. The metal profile of core from upper middle creek region

(TVI, range- 2.06-3.78 %, avg. 2.81 %) shows an increasing trend from the bottom to the surface with few spikes in between, while core TII (range- 1.74-3.26 %, avg. 2.81 %) initially decreases at the bottom and then increases towards the surface. The trend of Ca concentration in core TIII (range- 1.36-4.25 %, avg. 2.28 %) from the lower middle creek region, displays a sharp increase from the bottom to 16 cm and then shows a decrease for the rest of the core while the other core (TV, range- 1.05-3.42 %, avg. 1.71 %) exhibits a stable distribution from the bottom to 14 cm followed by an increase towards the surface. The core sampled near the creek mouth (TIV, range- 1.32-3.14 %, avg. 2.05 %) shows an almost constant trend with a peak at 34 cm depth. In general, the middle creek region exhibits greater average Ca % as compared to the creek head and the mouth.

c) Iron (Fe)

The Fe distribution in the core sampled from the creek head (TI) ranges from 8.35-10.66 % with 9.09 % average and in general, displays a relatively constant trend throughout the length of the core. On the other hand the core collected from the upper middle creek region, core TVI, ranges from 5.91-8.85 % with 7.40 % average and shows a fluctuating trend only at the bottom (80 to 68 cm) and upper (10 to 2 cm) few sections. However, the other core (TII) from the same region varies from 7.26-8.63 % with 7.83 % average and fluctuates for the entire core length. In the case of lower middle creek region, a decreasing trend is seen in core TIII with a range of 7.11-11.01 % and an average of 9.5 % while the concentration in core TV ranges from 7.32-8.92 % with an average of 8.06 % and exhibits a fluctuating trend for the entire core length. Fe concentration shows fluctuations in the bottom portion (44 to 38 cm) in core TIV (creek mouth) and becomes more uniform with fewer spikes for the rest of the core. The values in core TIV ranges from 6.58-8.24 % and has an average of 7.06 %. In general, the average percentage of Fe is highest (9.09 %) at the creek head (core TI) and decreases towards the creek mouth (7.06 %).

d) Manganese (Mn)

Near the creek head, core TI (range- 1344-1775 ppm, avg. 1518 ppm) increases from the bottom to 30 cm, then decreases from 30 to 10 cm and further above an increase is seen. In the middle creek region, from the bottom to the surface, in cores TII (range- 1743-2787 ppm, avg. 2290 ppm) and TIII (range- 1296-1760 ppm, avg. 1538 ppm) the values fluctuate, TVI (range- 740-1333 ppm, avg. 1014 ppm) uniformly decreases, TV (range- 1653-2518 ppm, avg. 2025 ppm) decreases from the bottom to 24 cm and then increases towards the surface. In the case of core TIV (range- 1612-2110, avg. 1884 ppm), which lies near the creek mouth, a gradual increase is observed from the bottom to 22 cm followed by decreasing and increasing trends till the surface.

In general, Mn concentration shows higher values in the middle creek region and lower values near the creek head and mouth. The highest average value is seen for core TII (2290 ppm) while the lowest is seen for core TI (1518 ppm).

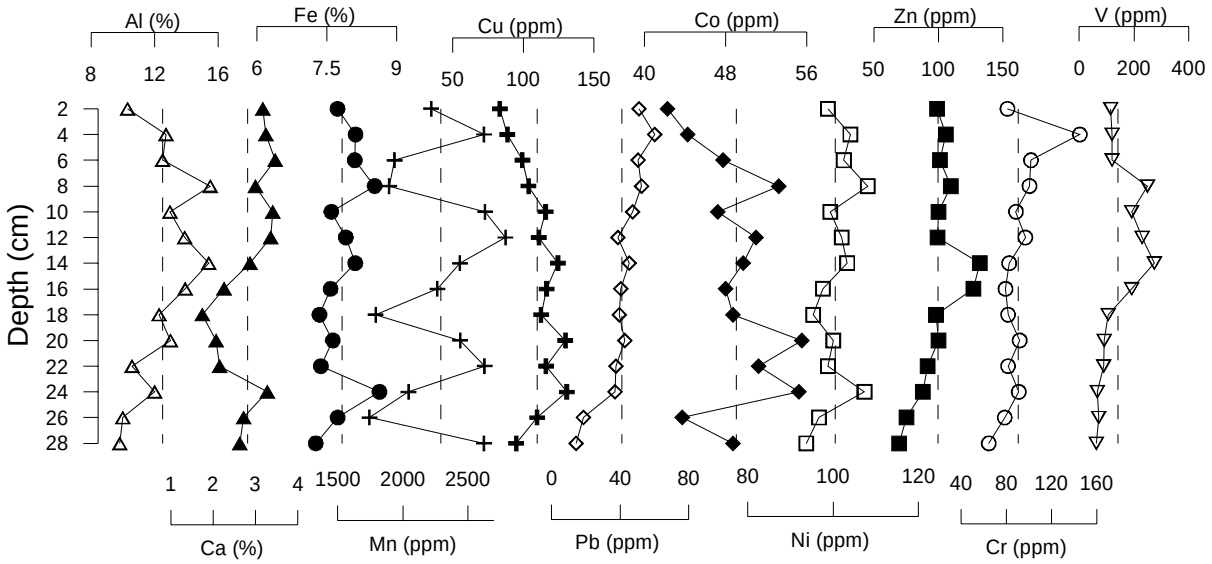

Fig. 3.1A.18. Depth-wise distribution of selected metals in core TII

e) Copper (Cu)

At the inner creek end, core (TI) ranges from 189-273 ppm with an average of 232 ppm and demonstrates a uniform concentration from the bottom to 38 cm depth. Further, from this depth to 28 cm and from 22 to 6 cm, an increasing trend is observed. On the other hand, in the upper middle region, core TVI which ranges from 167-227 ppm with 197 ppm average, increases from the bottom to 46 cm followed by a decrease till the surface while the metal concentration in core TII, having range of 83-131 ppm and average 110 ppm, shows a slight decrease while fluctuating from the bottom to 14 cm and then dropping to low concentrations for the rest of the core. Cores from the lower middle and creek mouth (TIII, TV and TIV) show a gradual increase from the bottom to the surface. Highest average Cu concentration (243 ppm) is seen near the creek mouth while the upper middle creek region (core TII) shows the lowest average value (110 ppm).

f) Lead (Pb)

The range and average values vary from 72-120 ppm, avg.101 ppm for core TI sampled near the creek head; 14-60 ppm, avg.41 ppm for core TII and from 58-129 ppm, avg.91 ppm for core TVI from upper middle creek region; 79-92 ppm, avg.82 ppm for core TIII and 71-92 ppm, avg.82 ppm for core TV collected from lower middle creek region and 81-116 ppm, avg.100 ppm for core TIV sampled near the creek mouth. Cores from the inner creek end, upper middle region and creek mouth (TI, TII, TVI and TIV) show an increasing metal concentration from the bottom to the surface. In the case of lower middle creek region, core TIII, projects a relatively uniform

decreasing trend while core TV exhibits a fluctuating trend. The upper middle creek region (core TII) shows the lowest Pb concentration (41 ppm) when seen for the whole creek region, while the concentrations in the other regions are more or less similar.

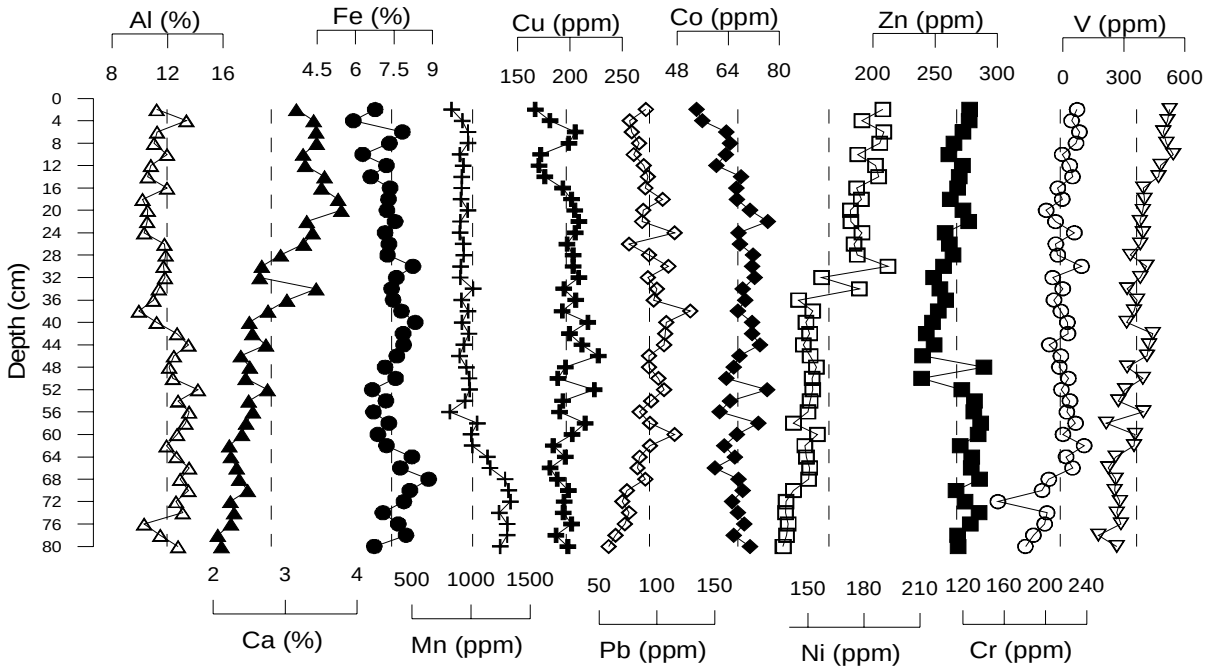

Fig. 3.1A.19. Depth-wise distribution of selected metals in core TVI

g) Cobalt (Co)

The cores from the creek head and mouth (TI and TIV), ranging from 72-83 ppm and 59-70 ppm with averages of 78 and 64 ppm respectively, show fluctuating trends from the bottom to the surface. In the upper middle creek region, core TVI, ranging from 54-77 ppm and having an average of 67 ppm, the metal distribution from the bottom to 14 cm depth, is fairly constant while above it the values decrease. On the other hand, in the case of core TII (range- 42-56 ppm, avg. 49 ppm), an irregular trend is observed from the bottom to 8 cm and further above a decrease is seen. For the lower middle creek region, core TV (range- 32-67 ppm, avg. 45 ppm), the concentration gradually increases towards the surface. In core TIII, ranging from 40-69 ppm with 56 ppm average, from the bottom to 36 cm and from 24 cm till the surface an increasing trend is observed while from 36 to 24 cm depth a decrease is seen. On a whole, the Co values decrease from the head to the mouth region of the creek.

h) Nickel (Ni)

In core TI, having a range of 198-230 ppm with 214 ppm average, representing the inner creek end, from the bottom to 22 cm the values fluctuate while above it a gradual increasing trend is noticed. The core exhibits the highest average Ni concentration. The concentrations are more than twice high compared to all other sites. In the upper middle creek region, core TII (range-

94-108 ppm, avg. 101 ppm), the concentration fluctuates with no definite trend but with two positive peaks at 24 and 8 cm depths, while core TVI (range- 137-193 ppm, avg. 161 ppm) shows a uniform increasing trend. For the lower middle creek region, core TIII (range- 111-138 ppm, avg. 125 ppm), exhibits an increasing trend with a number of spikes. In the case of core TV (range- 85-137 ppm, avg. 113 ppm), from the bottom to 50 cm depth and from 30 cm till the surface, an increase is observed with higher values while from 50 to 30 cm an increasing trend is seen but with relatively lower values. The creek mouth (core TIV), ranging from 128-199 ppm with 182 ppm average, shows a gradual decreasing trend from the bottom to the surface. The core analysis reveals that the upper portions of all the cores, except core TIV, have the highest nickel concentration compared to the bottom portions. The middle region of the creek exhibits lowest average value while the head region has the highest average value.

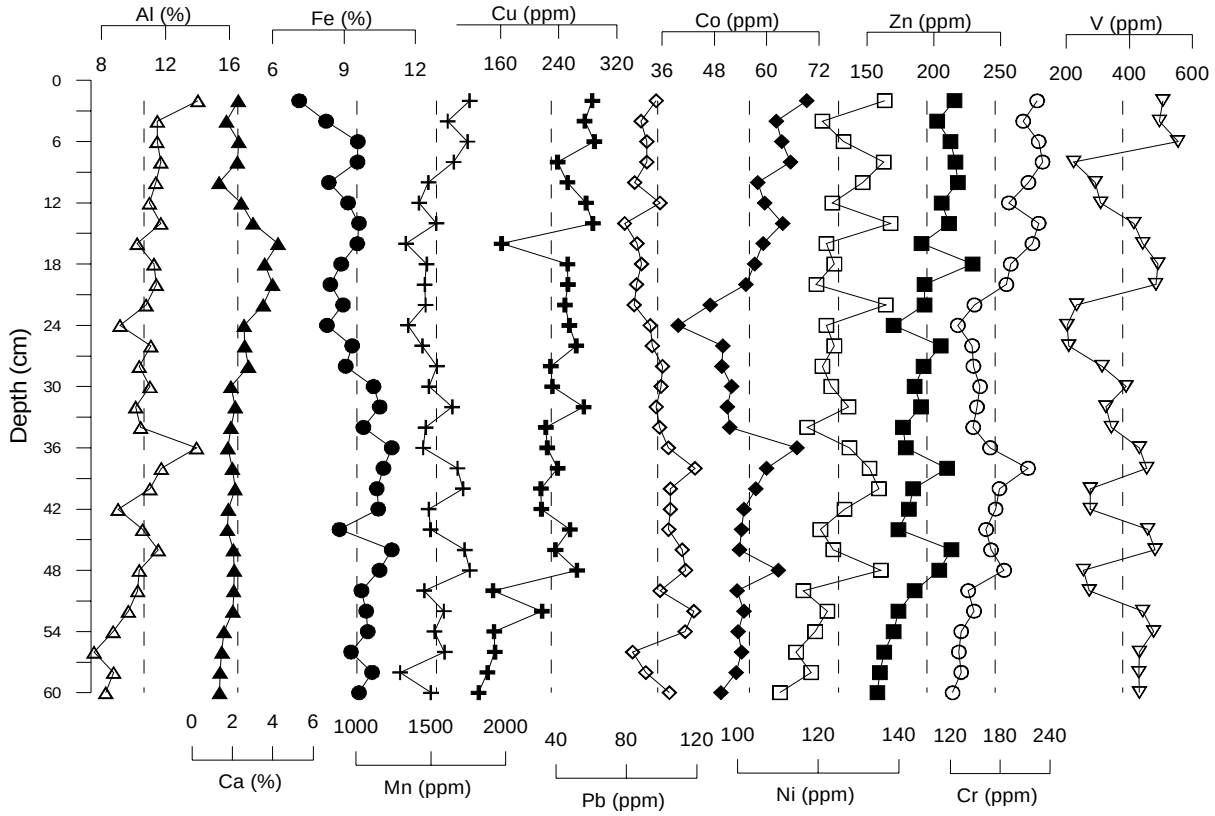

Fig. 3.1A.20. Depth-wise distribution of selected metals in core TIII

i) Zinc (Zn)

Zn concentrations near the creek head (core TI) ranges from 284-536 ppm with an average of 424 ppm. Zn shows fluctuations in the lower portion of the core and then increases in stages uniformly towards the surface, while in the core collected near the creek mouth (core TIV) the metal concentration fluctuates throughout the core length. Zn values, in core TIV, vary from 156-185 ppm with 170 ppm average. The cores TII and TVI, retrieved from upper middle creek region, range from 70-132 ppm and 239-289 ppm with averages of 100 ppm and 268 ppm,

respectively. From the depth-wise distribution plots, core TII shows an increasing trend while in core TVI higher values in the bottom portion followed by sudden decreasing and then an increasing trend towards the surface is seen. Cores TIII and TV, sampled from the lower middle creek region, vary from 158-229 ppm and 109-200 ppm with averages of 192 ppm and 139 ppm, respectively. Both the cores show increasing trends towards the surface with minor fluctuations. In general, in all the cores, the Zn concentrations are found to increase from the bottom to the surface. Also, Zn values are found to gradually decrease from the head to the mouth region of the creek.

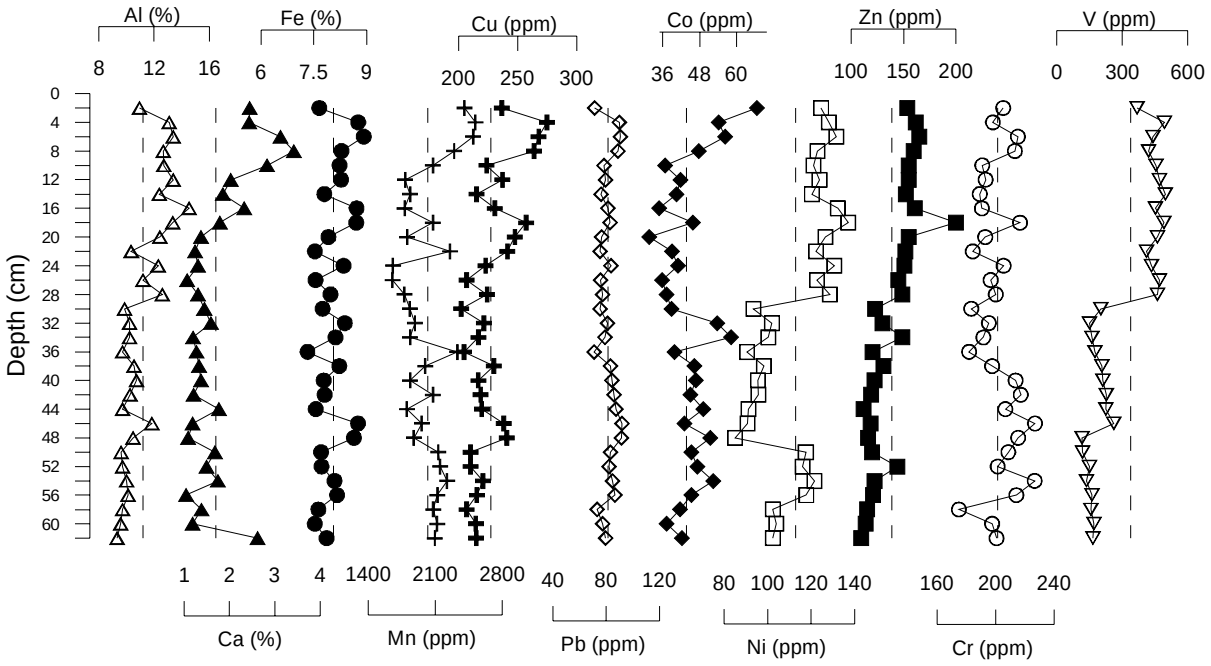

Fig. 3.1A.21. Depth-wise distribution of selected metals in core TV

j) Chromium (Cr)

The Cr concentration in the cores collected from the head to the mouth region of the creek vary from 139-181 ppm with 159 ppm avg. (core TI); 65-145 ppm, avg. 90 ppm (core TII); 154-238 ppm, avg. 214 ppm (core TVI); 123-231 ppm, avg. 174 pm (core TIII); 175-227 ppm, avg. 202 ppm (core TV) and 165-213 ppm, avg. 196 ppm (core TIV). A clear increase towards the surface can be seen in cores collected from the upper middle creek region (cores TII and TVI) and also in one of the cores (TIII) from lower middle creek region. The other core (TV) from lower middle creek region shows an irregular metal trend from the bottom to the surface. The remaining cores, i.e. near the creek head and mouth (TI and TIV), exhibit fluctuating trends with large variations observed in the upper portion of core TIV. It is interesting to note that the upper middle creek region shows the highest average value of 214 ppm (core TVI) and also the lowest average value of 90 ppm (core TII). In general, the values increase from the head to the mouth region of the creek.

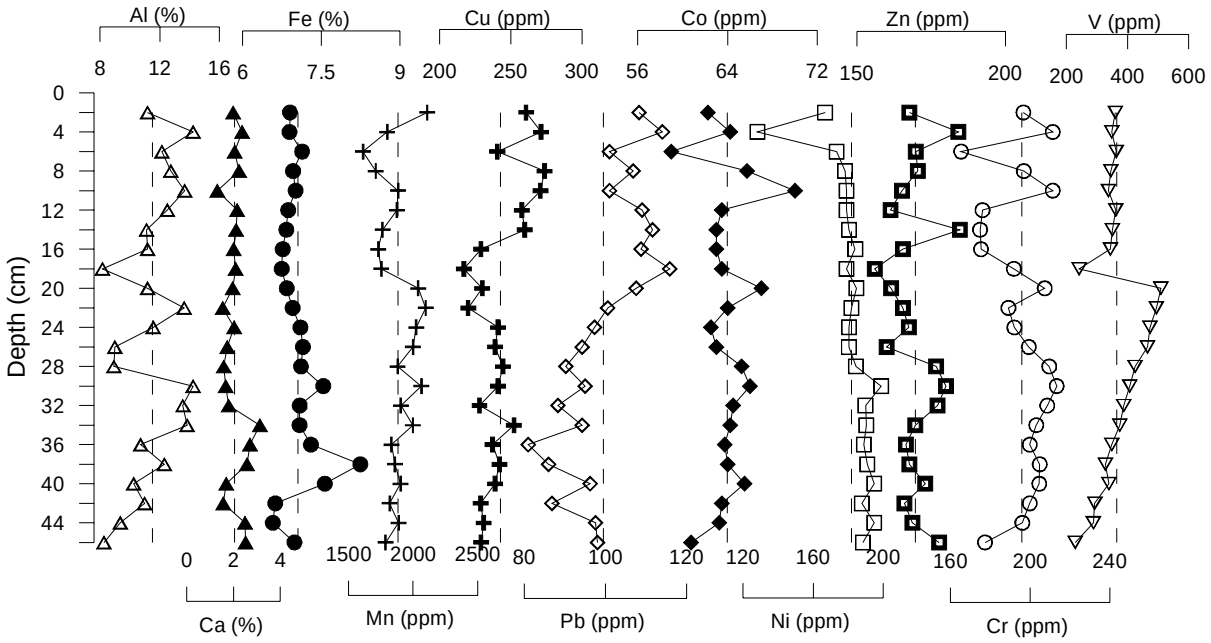

Fig. 3.1A.22. Depth-wise distribution of selected metals in core TIV

k) Vanadium (V)

Core TI (range- 116-423 ppm, avg. 291 ppm) sampled near the creek head, displays a relatively uniform increasing trend of high abundance of the metal. For the upper middle creek region, core TII (63-274 ppm, avg. 141 ppm), from bottom to 14 cm, an increase is seen followed by a decrease towards the surface, while core TVI (range- 176-542 ppm, avg. 363 ppm) exhibits an overall increase towards the surface. The cores from lower middle creek region, core TIII (range- 203-554 ppm, avg. 378 ppm) and core TV (range- 116-496 ppm, avg. 299 ppm) fluctuate irregularly, with no distinct trend observed in the case of core TIII and increases in stages in the case of core TV. On the other hand, core TIV (range- 228-509 ppm, avg. 365 ppm) collected close to the creek mouth exhibits a gradual increase from the bottom to 20 cm depth followed by a drop at 18 cm and then steadily increases towards the surface. The highest average concentration (378 ppm) is seen in the lower middle creek region (core TIII) while the lowest average concentration (141 ppm) is observed in the upper middle creek region (core TII).

In general, of the metals analysed in the creek sediments, the individual metals follow varying patterns. In the creek region, among the metals studied, Al displays the highest average concentration (avg. 11.41 %) while Co has the lowest average concentration (avg. 60 ppm). The creek head exhibits maximum average concentrations of Pb, Co, Ni and Zn with low average values for Al. In the upper middle region (core TII), Cu, Pb, Ni, Zn, Cr and V occur with low average values while Mn, Al and Ca have the highest value at this site. On the other hand, the maximum average concentration of Cr occurs at station TVI (upper middle creek region) with minimum average concentrations of Fe and Mn. Fe, at lower middle creek region (TIII) and Cu,

near creek mouth (TIV), display maximum average concentrations. Minimum average concentrations for Co and Ca occur at station TV (lower middle creek site). The average concentrations of Pb and Cu remain more or less similar throughout the creek except for low values observed for core TII. The average concentrations of Cr and V increase from the creek head to the mouth. Al, in general, shows relatively constant values throughout the creek while Fe, Zn, Ni and Co concentrations decrease with increasing distance from the creek head. Such a trend would be expected for elements of natural, lithogenic origin, which are gradually being diluted with particles of biogenic, authigenic and eventually local anthropogenic origin along the watercourse. The profiles of Al and Fe in sediment cores reveal more or less uniform distribution throughout the length suggesting similar sediment texture and character over its depositional history (Sharma et al., 1994; Ram et al., 2003). Also, it is clear from the figures that trace metal values, in general, show significantly higher concentration in the top 20 cm in each of the cores studied.

When the present metal concentrations are compared (Table 3.1A.1) with studies carried out in the other parts of the country, especially on the west coast of India (Mandovi and Zuari estuaries), it is seen that Fe exhibits lower percentage in the present study region as compared to the Mandovi estuary but higher than the Zuari estuary. In the case of Mn, the present study shows higher amounts than the study carried out by Bhosale and Sahu (1991) in the same region. However, Mandovi and Zuari estuaries project higher concentration of Mn than Thane creek and Ulhas estuary, maybe because of the mining activities being carried out in the Goa region. Among the trace metals, almost all of them show an increment in the present study when compared to the study carried out by Bhosale and Sahu (1991). On the other-hand, the Cr concentrations in the Zuari estuary are found to be comparable with that of the Thane creek and Ulhas estuary in the present study. In general, it is observed that almost all the metals studied show higher concentration in the present study as compared to the study carried out by Bhosale and Sahu (1991). However, we have to keep in mind that the previous study carried out in Mumbai region presented only a spatial distribution and that the present study covers temporal as well as spatial variations. Further, the present study is based on the samples collected from the mudflats region whereas the study of Bhosale and Sahu (1991) was based on the main channel of the estuary and the creek.

Table 3.1A.1. Range of different metals in surface sediments along west coast of India

Area	Fe	Mn	Cu	Pb	Co	Ni	Zn	Cr	V	Reference
Thane creek	-	210-1274	91-240	54-143	34-59	91-130	114-273	29-63	-	Bhosale and Sahu, 1991

Ulhas estuary	-	195-1024	61-150	30-68	31-61	70-133	96-183	30-51	-	Bhosale and Sahu, 1991
Mandovi estuary	2.2-49.7	<DL-1.61%	11.5-77.5	4.5-46.5	2.5-45.3	-	19.9-83.5	-	-	Alagarsamy, 2006
Zuari estuary	7.61-8.72	0.29-0.31	34.34-96.88	-	39.14-52.60	-	70.39-101.95	113-267	-	Dessai and Nayak, 2009
Thane creek	6.77-10.66	836-2405	83-286	51-120	42-74	99-220	99-521	81-231	115-526	Present study
Ulhas estuary	4.09-9.60	759-1904	138-257	54-165	43-105	66-190	125-200	175-288	184-449	Present study

It is a known fact that the geochemical associations of metals provide useful information concerning the absolute levels, source, mobilization, mode of occurrence and biological availability of metal. Core TI, near the creek head, contains more than twice the concentration of metals as compared to the other cores and a reduction in metal content occurs with increasing distance from the creek head. Most of the industries are housed above and along the creek head. During periods of high rainfall and flooding, the core location at TI would receive the sediment-loaded water from the industrial and urban areas first and would therefore receive the larger proportion of contamination. The inner creek with reduced tidal influence, lower salinity and decreased current speed is relatively sheltered, making the conditions conducive for the settlement of suspended load (NIO, 1998). Further, the metal distribution in core TI revealed a general trend of decreasing metal concentration with increasing depth. Therefore, once incorporated into the sediments, it is unlikely that this detrital material is altered significantly by post-depositional processes. As the sediments in this part of the creek contain a greater quantity of fine particles and organic material than those downstream, it is probable that there is an increased potential for adsorption of metals to organic and inorganic particles. Generally, trace metals are more associated with the silt/clay sediment fraction, consisting of particles with a grain size <0.063 mm (Krumgalz et al., 1992). The enrichment of the silt/clay fraction by anthropogenic trace metals is due to the large specific area of this fraction and to the strong adsorptive properties of clay minerals (Krumgalz et al. 1992).! Sediments collected near the mouth of the creek (TIV) reveals a substantial reduction in most of the metal concentrations, as the location of core TIV is more prone to wave action from the sea, causing the sediments to be more uniformly distributed. Therefore, there is evidence for a distance-concentration relationship in the sediment record, with concentrations decreasing with greater distance from the head/input. In general, sediments located within the northern reach of the creek have higher metal concentrations than those in the southern reach.

Variation in metal concentrations can result from natural differences in grain size, mineralogy, organic matter content, diagenetic reactions and anthropogenic inputs. Therefore, these factors

must be considered collectively in any attempt to explain metal distribution or to identify the presence of anthropogenic input of metals in sediments. High Cr and Ni contents in the sediments are interpreted to reflect, in part, the weathering of basic-ultrabasic rocks of the region. Vertical profiles of Fe and Mn show rapid decrease in their concentrations from the surface which might be suggestive of a diagenetic enrichment (Shaw et al., 1990) during which Fe-Mn oxy-hydroxides dissolve in the partly reduced sediment layer producing Fe^{2+} and Mn^{2+} species, which migrate upwards in the sediment column and get precipitated near the oxic-suboxic interface. This phenomenon can explain the subsurface enrichment of Mn along with some metals in cores sampled from the lower middle creek region (cores TIII and TV). The other cores do not show such surface enrichments of Fe and Mn. Most of the metals are likely to be chemically immobilised through formation of their insoluble sulphides (McCaffrey and Thomson, 1980). All these observations support that the early diagenetic remobilization has not significantly affected the vertical distributions of some heavy metals. Instead, they are probably due to contaminant inputs (Cundy and Croudace, 1996; Cundy et al., 1997).

3.1A.9. ^{210}Pb dating

^{210}Pb is one of the dominant isotopes used in geochronologic studies of the recent past environment. All the cores collected from the creek region were subjected to ^{210}Pb analysis to see decay of ^{210}Pb. However, only three of the total cores showed good down-core decay of ^{210}Pb activity. Therefore, the data of those three cores from the creek, namely one from creek head (TI) and the other two from the middle creek region (TII and TV) are presented. The depth profiles of total ^{210}Pb activities along with ^{210}Pb excess activity plots of cores TI, TII and TV are shown in figures 3.1A.23 to 3.1A.25. Good linear relationship between excess ^{210}Pb activity and sediment depths are obtained for cores TI and TII with R^2 values of 0.724 and 0.843 respectively while core TV shows a low R^2 value of 0.541. In core TI, the maximum total ^{210}Pb activity occurs at 4 cm depth (3.57 dpm/g) while the minimum value is seen at a depth of 42 cm. From the depth profile (Fig.3.1A.23) it is seen that, a fluctuating decrease and increase at the bottom is followed by a gradual increase at the surface except at 24 cm (2.61 dpm/g) depth.

In the case of core TII, the maximum total ^{210}Pb activity is present at the surface (2.86 dpm/g) while the minimum value is seen at the bottom (0.44 dpm/g). The vertical distribution profile (Fig.3.1A.24) shows a gradual increasing trend from the bottom to the surface of the core. On the other hand, in core TV, decreasing and increasing trends are observed from the bottom to the surface (Fig.3.1A.25). From 61 cm depth, the total ^{210}Pb activity shows a decrease in value from 1.82 dpm/g to 1.34 dpm/g at 46 cm. Further above, its shows an increase till 32 cm depth (1.98

dpm/g), dropping to 1.68 dpm/g at 24 cm. From this depth till 4 cm, a gradual increase is seen followed by a decline at the surface. The maximum value occurs at 4 cm (2.40 dpm/g) while the minimum is seen at 46 cm depth (1.34 dpm/g).

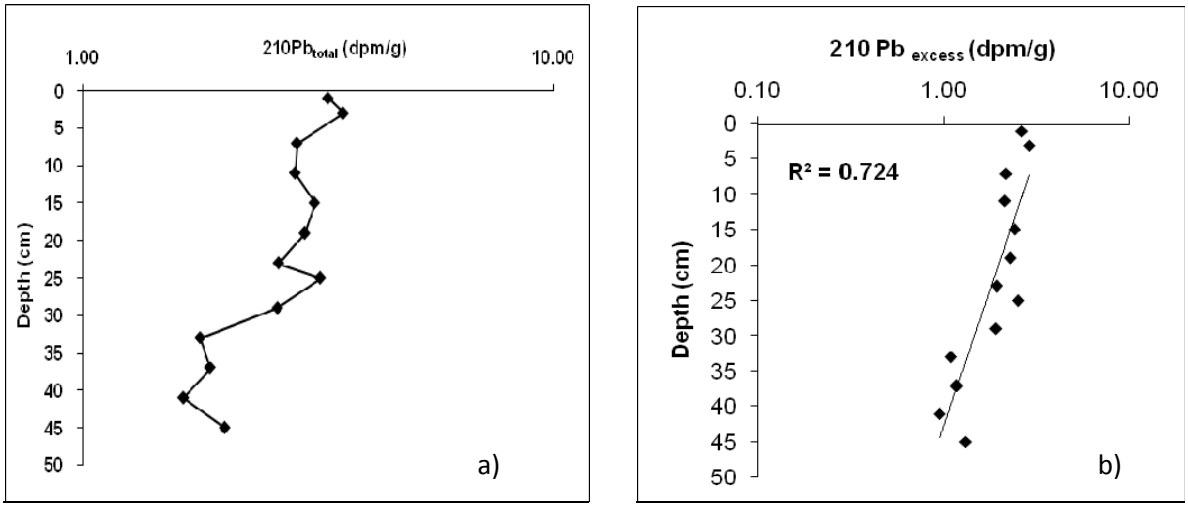

Fig.3.1A.23.Vertical distribution of a) $^{210}Pb_{total}$ and b) $^{210}Pb_{excess}$ activities in core TI

In core TV, a different pattern is noticed between 61 and 46 cm depths. The concentration of ^{210}Pb in these sections decreases. This could indicate a strong physical mixing in the core. In addition, from a general view, the ^{210}Pb concentrations in core TV are a little lower than the average value seen in core TI. This may be because the depositional environment of cores TI and TII are of much lower energy than that of core TV and are also not susceptible to erosion as a result of tidal currents. Moreover, both the cores are farther away from any harbours, sea defences or dredging activities, as compared to core TV, which lies closer to the creek mouth. In cores TI and TII, the decreasing trends of ^{210}Pb activities with depth must be due to a relative constant annual input (Sheets and Lawrence, 1999) and the process of radioactive decay. Under these conditions, the older sediments would be expected to have a lower ^{210}Pb concentration. The results indicate that the deeper sediments in core TI and core TII are not disturbed or mixed, thus supporting valid use of the ^{210}Pb dating technique to determine the sedimentation rate and hence the sediment age.

The sedimentation rate for the cores was calculated employing the Constant Initial Concentration (CIC) model with an assumption of a constant input of the excess ^{210}Pb to the sediment or a constant sedimentation rate (Brugam, 1978; Jha et al., 1999). The sedimentation rate was determined to be 1.46 cm/yr for core TI, 0.24 cm/yr for core TII and 2.72 cm/yr for core TV. Higher sedimentation rate in core TV may be due to higher rate of supply of material from the sea-end as compared to the other cores. Sediment accumulation rates of 19.4 ± 3.3 mm/yr are

reported along the eastern shore of Thane Harbour Complex based on ^{210}Pb dating (Sharma et al., 1994). Core TII was collected from a sheltered area away from the main channel of the creek as compared to cores TI and TV which were collected from the main creek region. The location of core TII very well supports the low sedimentation rate obtained. Sharma et al., (1994) carried out ^{210}Pb dating of core collected from the inner creek region and found a sedimentation rate of 1.46 cm/yr which is same as that obtained for core TI, in the present study, which was also collected from the same location. The results indicate that at the inner creek end the rate of sediment deposition have remained the same over the years.

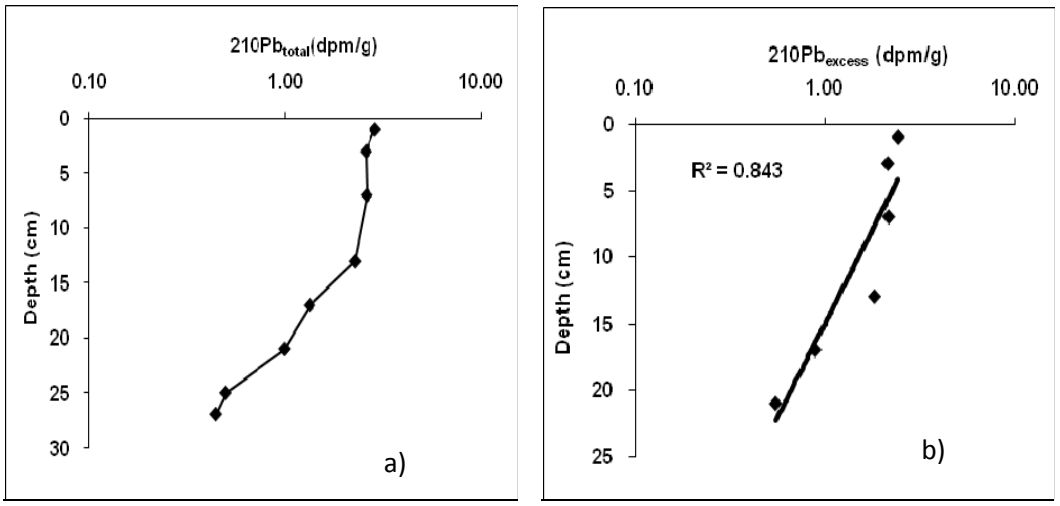

Fig. 3.1A.24. Vertical distribution of a) $^{210}Pb_{total}$ and b) $^{210}Pb_{excess}$ activities in core TII

In the present study, the use of ^{210}Pb ($^{210}P_{excess}$) dating technique, has provided a chronological and undisturbed history of heavy metal deposition spanning a period from ~1970 in core TI and ~1900 in core TII, until the present day. In general, the sedimentation rates in the creek region vary from 0.24-2.72 cm/yr. This estimate is consistent with those cited in previous reports for the Thane creek that ranged from 0.20–4.1 cm/yr (Sharma et al., 1994; Ram et al., 2003).

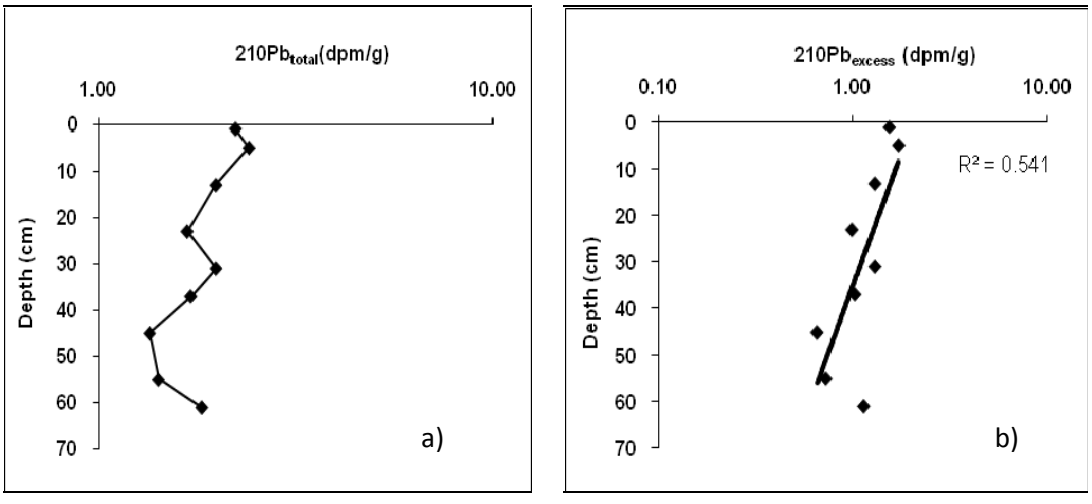

Fig. 3.1A.25. Vertical distribution of a) $^{210}Pb_{total}$ and b) $^{210}Pb_{excess}$ activities in core TV

3.1A.10. Statistical analysis

3.1A.10a. Correlation Analysis

In order to understand the processes involved in the sediment and associated metal distribution in the creek environment, Pearson's correlation analysis at $p< 0.05$ was carried out on the different variables studied for all the cores sampled from the creek. Correlation analysis helps in understanding associations and in-turn variable conditions of deposition. Since Iron (Fe) and Manganese (Mn) hydrous oxides, organic matter content are important carriers of metals (Olsen et al., 1982), in addition to pH and sediment components, the correlation analysis has been discussed accordingly. A high correlation coefficient implies a strong relationship between the variables and, although it is not a measure of quantitative change of one variable with respect to the other, it is a measure of intensity of association between the two variables (Zar, 1984).

Table 3.1A.2. Classification of values based on correlation analysis in the creek region

Stations		Good	Significant
Near creek head	Core TI	0.40-0.51	> 0.51
Upper middle creek region	Core TII	0.50-0.64	> 0.64
	Core TVI	0.30-0.39	> 0.39
Upper middle creek region	Core TIII	0.35-0.45	> 0.45
	Core TV	0.34-0.44	> 0.44
Near creek mouth	Core TIV	0.40-0.51	> 0.51

3.1A.10a1. Sediment components

Particle size is an essential property of sediments, as it affects the physico-chemical behaviour in terms of remobilization, erosion, sedimentation and adsorption capacity (Golterman, 2004). Near the creek head (core TI), sand and silt associates well with each other (r=0.56). However, when the correlations with metals are seen only sand is found to display good association with Ca (r=0.45). The finer sediment fraction (silt and clay) do not show any association with metals except for silt which correlates with Mn but to a lesser extent (r=0.38). In core TII, sampled from the upper middle creek region, silt associates with TP (r=0.55) and to a less extent with TOC (r=0.30). TN, on the other hand, correlates with sand (r=0.49) and clay (r=0.47). Association of sand (r=0.46) and clay (r=0.39) with pH is also observed. The finer sediment fraction exhibits weaker or negative associations with almost all the metals except of silt with Cu (r=0.62) and Co, which correlates to a lesser extent (r=0.30). On the other hand, the sand fraction shows significant correlations with few of the metals viz. with Pb (r=0.72), Ca (r=0.62), and good correlations with Ni (r=0.44), Zn (r=0.46), Cr (r=0.50), V (r=0.56), Al (r=0.53) and to a less extent with Fe (r=0.38). In the other core sampled from the same region but at opposite bank

(core TVI), clay correlates with TP (r=0.33) and TN (r=0.30) while in the case of metals only sand shows correlation with Ca (r=0.34). Sand is observed to be dominant in lower middle creek region (core TIII) compared to other areas, showing significant correlations with almost all the metals, i.e. with Al (r=0.50), Cu (r=0.54), Co (r=0.55), Zn (r=0.65) and Cr (r=0.82) and shows good correlations with Ca (r=0.40) and Ni (r=0.37). Silt and clay show weak or negative correlations. In core TV, retrieved from the same region, no such associations are seen. Sand correlates with Mn (r=0.36), silt with Pb (r=0.49) and Cr (r=0.39) while clay exhibits negative correlations with metals. Organic matter, on the other hand, associates weakly with the sediment components. Near the creek mouth, sand and silt associates well with each other (r=0.43). TP goes well with sand (r=0.37) and silt (r=0.33). However, no good correlations are observed with any of the metals.

From the correlation analysis of sediment components, it is seen that in the creek region the finer sediment fractions do not play a significant role in metal deposition. On the contrary, coarser sediment comprising of sand is found to influence the distribution of few metals to some extent especially on the western reaches of the creek (cores TII and TIII). It is generally accepted that trace metals are mainly concentrated in the clay/silt sediment fraction, consisting of particles of grain sizes <63 μm (Krumgalz et al., 1992). However, many workers have pointed out the fact that larger particles stay in a place longer, often in shallow oxygenated area (Whitney, 1975; Tessier et al., 1982) and therefore may have more time to develop oxide coating and hence adsorb more trace metals than smaller particles. It is also reported that the presence of heavy minerals or coarse fractions of industrial wastes may also increase metal concentrations in the coarser fractions (Thorne and Nickless, 1981; Moore et al., 1989). The increased concentration of metals in the coarser fractions at the present sampling sites may be attributed to inputs from anthropogenic sources. Strong positive correlations of trace metals with sand and negative correlations with silt and clay contents in the present study are reasonable evidence for the above processes.

3.1A.10a2. Organic matter

In core TI (near the creek head), TOC correlates with Fe (r=0.47), Pb (r=0.49), TP and TN significantly with Al (r=0.67, 0.42) and V (r=0.68, 0.66). In addition to this, TN also associates with Mn (r=0.48) and Cu (r=0.43). In the case of core TII (upper middle creek region), TOC and TP associates well with Cu (r=0.45, r=0.42). TOC also correlates with Pb (r=0.39) and Zn (r=0.41). TN exhibits significant associations with pH (r=0.66), Pb (r=0.67) and good associations with Cr (r=0.47). The other core (core TVI) from the same region shows significant

correlation of TOC with TN (r=0.73) and they show significant correlations with Ni (r=0.72, 0.68), Ca (r=0.79, 0.74), V (r=0.67, 0.74) and Cr (r=0.54, 0.41). In addition, TOC also associates significantly with Pb (r=0.48). TP on the other hand displays correlations with Zn (r=0.32) and Al (r=0.51). Of the two cores collected from the lower middle creek region in core TIII organic matter does not show any significant correlation with metals except association of pH with TN (r=0.38) as compared to the other core (core TV). In core TV, good association of TP with pH (r=0.39); significant correlations of TOC with TN (r=0.45), Zn (r=0.45) and good correlations with Ni (r=0.41) and V (r=0.43); TN with Cu (r=0.45), Ni (r=0.67), Zn (r=0.74), Al (r=0.73), Ca (r=0.60) and V (r=0.81) while good correlations are seen of TP with Co (r=0.43). The core collected near the creek mouth (TIV) exhibits good correlation of TN with TOC (r=0.41) and TP (r=0.40). When the association of organic matter with metals is individually examined, TOC correlates well with Fe (r=0.38), Cr (r=0.35) and Al (r=0.44), TP with Cu (r=0.51), Pb (r=0.52) and Al (r=0.37) while TN shows association with Cu (r=0.62), Cr (r=0.36) and Al (r=0.59). The significant relationship of Fe and organic matter with Al indicates that Fe, TOC, TP and TN are closely associated with the aluminosilicate phase, and thus it can be assumed that the detrital minerals might be the predominant carriers of Cu, Pb and Cr in this region of the creek.

The cores collected along the eastern reaches of the creek exhibit better associations of organic matter with metals as compared to the western reaches. In addition, the cores near the head and creek mouth show good metal correlations with the organic matter. The presence of organic matter can potentially increase metal concentrations in sediment by adsorption of metals from surrounding environment onto organic material (Loomb, 2001). The decomposition of organic matter proceeds under anoxic conditions using alternative electron acceptors to oxygen, such as nitrate, Mn and Fe oxides, and sulphate to oxidize (metabolise) organic carbon (Williamson and Wilcock, 1994; Williamson et al., 2003). This process, together with the resulting anoxic conditions, produces large changes to the form of Fe, Mn and S, which are important in binding trace metals in sediment and releasing them to the overlying water (Williamson and Wilcock, 1994). Therefore, the organic matter might be playing an important role in influencing the behaviour of metal deposition in the creek sediments.

3.1A.10a3. pH

In the case of the core collected near the creek head (TI), pH shows good correlations with Co (r=0.45) and Ca (r=0.43). In the upper middle creek region, pH shows good association with Pb (r=0.61) in core TII and Cr (r=0.39) and V (r=0.33) in core TVI. On the other hand, the cores sampled from the lower middle creek region do not display any correlations with metals except

in core TIII with Fe (r=0.37). The pH near the creek mouth (TIV) correlates strongly with Ni (r=0.63) and to a less extent with Fe (r=0.31) and Mn (r=0.35). The pH is one of the important parameters controlling the mobility and retention of heavy metals in soils/sediments. Schlinder (1991) suggests that the pH value of the solution is the master variable that oversees the adsorption of metal ions at surfaces. High pH values promote adsorption whereas low pH can actually prevent the retention of metals by sediment (Belzile et al., 2004). However, in the present study, the role of pH as metal carrier is not significant and varies from site to site.

3.1A.10a4. Fe-Mn oxides/hydroxides

Fe with Ni (r=0.53) and Mn with Cu (r=0.44) exhibit good associations in core TI (creek head). On the other hand in core TII, from the upper middle creek region, Fe is found to display significant correlations with Ni (r=0.95) and good correlations with other metals [Ca (r=0.62), Pb (r=0.46), Cr (r=0.52) and Al (r=0.50)] as compared to Mn which correlates weakly with all the metals. The other core from the same region (core TVI), shows significant correlations of Fe and Mn with each other (r=0.40). However, Fe is found to correlate well with Cu (r=0.30) and Co (r=0.33) while Mn shows association with only Zn (r=0.32). In the lower middle creek region, an opposite association of Fe and Mn is observed between the cores sampled. In core TIII, Mn is found to be the dominant metal carrier showing significant associations with Co (r=0.49) and Ni (r=0.47) and good associations with Zn (r=0.42), Cu (r=0.37), Pb (r=0.36), Cr (r=0.39) and Al (r=0.32), while in core TV, Fe is observed to be the dominant metal carrier wherein Fe shows significant association with Cu (r=0.69), Pb (r=0.67), Zn (r=0.61), Cr (r=0.45), Al (r=0.67) and Ca (r=0.36). Mn also shows significant association but only with few metals [Co (r=0.48) and Ca (r=0.47)] and good association with Cu (r=0.42). Fe shows poor correlation with most of the metals studied in core TIV, sampled near the creek mouth, while Mn correlates significant with only V (r=0.62) but also exhibits good correlation with Cr (r=0.48).

Trace metals are often associated with Mn and Fe oxides/hydroxides in sediments and the chemically or bacterially driven reduction of Mn and Fe oxides/hydroxides may result in the release of Mn, Fe and trace metals (Laslett and Balls, 1995; Zhang et al., 2002). Fe and Mn are mobile metals, influenced by the changes in redox potential. Mn is mobilized from the sediments at oxygen concentrations below 2 mg/l (Fischer et al., 2004; Beard et al., 2003). On the other hand, Fe becomes mobile (i.e. released or precipitated again) at lower redox potential, i.e. at lower oxygen concentrations than Mn. In the present study, the most conspicuous results are the correlations of most of the elements with Fe and Mn in the lower middle creek region. In contrast, correlations are nearly lacking near the creek head and mouth while in the upper middle

region, the correlations are very weak. Generally, the concentrations of Cu, Pb and Zn in the sediments are known to be controlled by the concentrations of Fe-Mn oxy-hydroxide (Balkis and Cagatay, 2001; Youn et al., 1999). This observation can be applied to cores TIII and TV from lower middle creek region. However, in core TII, good association of Fe with Ni and Cr may be due to similar geochemical properties of Ni and Cr with that of Fe (Youn et al., 1999).

3.1A.10a5. Inter-elemental relations

Near the creek head, among the trace metals, Cu correlates significantly with Pb (r=0.54), Ni (r=0.61) and Cr (r=0.60) while Cr associates significantly with Pb (r=0.54), Co (r=0.51) and Ni (r=0.79). Major element Al, is found to show significant associations with V (r=0.72). In core TII, collected from upper middle creek region, Cu with Co (r=0.72); Pb with Cr (r=0.71); Ni with Zn (r=0.65) and Zn with V (r=0.77) show significant associations. In addition to this, associations of Cu with Al (r=0.35); Pb with Ni (r=0.60), Ca (r=0.33) and V (r=0.44); Ni with Cr (r=0.60), Zn (r=0.37), V (r=0.41), Ca (r=0.57); and Cr with Al (r=0.34) and Ca (r=0.42) are also observed. Al shows significant associations with Zn (r=0.81), V (r=0.77), good correlations with Pb (r=0.55), Ni (r=0.59) and Co (r=0.40). Core TVI, sampled from the same region, shows significant association of Cu with Co (r=0.76); Ni with Ca (r=0.84) and V (r=0.74); Cr with Pb (r=0.49), Ni (r=0.52), V (r=0.45) and good correlations with Ca (r=0.32). Ca and V also show a significant correlation (r=0.68) with each other. In the case of cores collected from the lower middle creek region, core TIII, shows significant associations of Cu and Co with Ni (r=0.61, 0.51), Zn (r=0.69, 0.53), Cr (r=0.55, 0.79) and Al (r=0.64, 0.64); Ni with Zn (r=0.61), Cr (r=0.63) and Al (r=0.60); Cr with Zn (r=0.79) and Al (r=0.66); and Zn with Al (r=0.68) and good correlation with Ca (r=0.37). The other core (core TV) exhibits significant correlations of Cu with Pb (r=0.50), Ni (r=0.46), Zn (r=0.63), Al (r=0.66), Ca (r=0.53), V (r=0.50); Cr with Pb (r=0.77); Ni with Zn (r=0.79), Al (r=0.68) and V(r=0.75); Zn with Al (r=0.80) and V (r=0.82); Al with Ca (r=0.48) and V (r=0.87). Good correlations are also observed of Cr with Co (r=0.39); Ca with Zn (r=0.42), Al (r=0.43) and V (r=0.41). Near the creek mouth (core TIV), only Co shows significant association with Cr (r=0.70) while Al associates well with Cu (r=0.39), Zn (r=0.33) and Cr (r=0.33). The remaining elements show weak or negative correlations.

In most of the cores, the inter-elemental correlations are found to show good to significant correlations between the different metals suggesting their similar source or behaviour during deposition or post-depositional processes. Earlier studies of metal distributions in estuarine sediments have found high inter-metal correlations and similar trends in metal chronologies within a given estuary (Santschi et al. 1984; Gersberg et al. 1989; Bricker 1993; Callaway et al.

1998; Hornberger et al., 1999), reflecting the fact that these metals could be coming from similar sources or have similar fate in the environment. Strong correlations between some metals and Al exist in sediments that are relatively uncontaminated (Summers et al., 1996), and weak relationships are indicative of multiple sources of metals from both lithogenous and anthropogenic inputs (Luoma, 1990). Therefore, the presence of positive correlations between Al and most of the metals in both the cores collected from the lower middle creek region and also core TII from upper middle creek region suggest that the metals might be from lithogenic source. On the other hand, multiple sources of metal inputs from anthropogenic and natural sources near the creek head and mouth may explain the weak relationships found between metals and Al in these regions of the creek.

3.1A.10a6. Magnetic susceptibility

The correlation coefficients of Magnetic susceptibility (χ) with other variables are computed separately since only a limited set of samples were analysed for susceptibility parameters. A close relation between χ and metal pollution in soil and sediment was observed in several studies, and χ has also been used as a proxy for heavy metal pollution (Desenfant et al., 2004; Petrovsky et al., 2001). Magnetic properties of sediments have also been used to address problems related to transport, deposition and transformation of magnetic grains in sedimentary environments (Liu et al., 2003a). A recent study carried out by Blaha et al. (2011) on mudflat sediment from Thane creek using magnetic parameters along with Polycyclic Aromatic Hydrocarbon (PAH) data, metal contents and ^{210}Pb dating technique helped in reconstruction of the onset and rise of urban and industrial pollution in the Mumbai region. Further, by comparing the magnetic minerals present in distinct layers and under various sedimentary conditions, different depositional zones were identified by the authors. A special link between χ and heavy metal contents in the uppermost layers of lake or seabed sediment adjacent to industry was also observed in Penny's bay in Hong Kong (Chan et al., 2001). A well known fact is that most of the major pollution sources (e.g. power plants, metallurgy, mining, chemical industry, etc.) emit strongly magnetic iron-containing minerals like magnetite and maghemite (Flanders, 1994; Vassilev and Vassileva, 1997) together with the dangerous heavy metals. Therefore, in order to support the role of magnetic minerals as indicators of anthropogenic source in the present study, correlation analysis at $p < 0.05$, was carried out between the different magnetic parameters studied and metals along with the sediment components.

In core TI (near the creek head), concentration dependent parameters such as χ_{lf}, SIRM and χ_{ARM} are correlated with Fe (r=0.60, 0.62, 0.45), Ni (r=0.55, 0.57, 0.50) and significantly with V

(r=0.85, 0.86, 0.75), indicating anthropogenic origin and its association with coarser magnetic grains. Many previous studies have reported the strong relationships between magnetic parameters and heavy metals in polluted soils (Durza, 1999; Xie et al., 2001). In addition, χ_{ARM}/SIRM, χ_{ARM}/χ_{lf} and χ_{fd} show correlations with Fe (r=0.25, 0.29, 0.47), Ni (r=0.38, 0.43, 0.32), V (r=0.58, 0.62, 0.72) and clay content (r=0.62, 0.63, 0.27) indicating the role of both magnetic concentration and grain size in their association. Stable single domain and smaller grains are concentrated typically in the finest silt and clay fraction (Oldfield et al., 2009). The distribution of most of the metals in the present study (core TI) follows largely the pattern of Fe in the sediments, thus Fe oxides can be one of the factors in the distribution of metals in the sediment. Similar observations have also made in correlation analysis of Fe with the other studied geochemical variables.

In core TV (lower middle creek region) significant associations are seen of χ_{lf} and SIRM with Cu (r=0.87, 0.80), Ni (r=0.49, 0.59), Zn (r=0.66, 0.69) and V (r=0.71, 0.74) and good associations with Cr (r=0.42, 0.31). The correlations between χ_{lf}, Cu and Zn, can be attributed to the incorporation of these elements in the crystalline structure of Fe minerals/molecules (Kukier et al., 2003). On the other hand, core TII (upper middle creek region) does not exhibit any correlations with the metals studied. Magnetic susceptibility of soils is determined by several factors namely, 1) lithological background, since the soil develops on the weathered substrate of certain Fe-containing parent rocks (Jenny, 1941); 2) pedogenic ferromagnetic fraction formed as a result of soil formation (Maher, 1988) and 3) the anthropogenic strongly magnetic fraction accompanying many wastes from industrial production, power plants, car traffic, etc. (Evans and Heller, 2003). Therefore, in cores TI and TV, the metals might be from anthropogenic origin while in core TII, they may be from natural origin. The Bombay harbour lies south of core location TV. Activities such as servicing, scraping and re-painting of the ships while the ships are at anchor results in lot of contamination which might be getting dispersed by strong waves and tides at the mouth and the coarser sediment settles near core TV location which lies on the eastern bank of the creek, where relatively less action of waves and tides are noted. The occurrence of anti-cyclonic eddies in the outer segment, particularly around the islands with high residual velocities, induces strong horizontal mixing thereby enhancing dispersion of contaminants entering the area (Naidu and Sarma, 2001). In core TII, on the other hand, there is no relationship between susceptibility and heavy metal content, where the heavy metal content is rather low in spite of the high susceptibility. In relatively low polluted areas high magnetic susceptibility can be observed, however, this may be due to magnetically strong basement rocks

(i.e. basalts), and might not be accompanied with relevant contents of heavy metals (Magiera et al., 2006).

The strong positive correlation of magnetic susceptibility with metals in cores TI and TV may suggest that the associated elements have a strong anthropogenic signature and input. High χ values reflect high concentrations of magnetic Fe oxides (Thompson et al., 1995). In natural sediment, magnetic Fe oxides are generally proportional to the total Fe oxides, so high concentrations of magnetic Fe oxides in cores TI and TV reflect an external influence. The metals must have adhered with ferrimagnetic minerals and got carried into the sediment. The higher magnetic susceptibility in the superficial sediments could also result from different mechanisms such as diagenetic changes in magnetic mineralogy (Karlin and Levis, 1985, Karlin et al., 1987) or an increased input of detrital magnetite from soil erosion (Maher and Taylor, 1988; Higgitt et al., 1991). Several lines of evidence, however, argue for an anthropogenic origin of the high magnetic susceptibility zone found within the surficial layer of the sediments in the creek. Firstly, the significant correlation between the magnetic susceptibility and heavy metal contents is suggestive of an anthropogenic nature of the magnetic carrier. Secondly, the cores located closer to industrial areas (core TI), the navigation fairway and ship anchorage sites (core TV) show relatively higher magnetic remanence and magnetic susceptibility values. This phenomenon probably implies release of anthropogenic wastes from industries and shipping related activities. So, the good correlations of magnetic parameters with the variations in heavy metals concentration including Fe and Mn, strongly reflect trace metal enrichment in recent years.

3.1A.10b. Factor Analysis

To better understand the general pathways of potential sources of metals and organic matter in the creek system, Factor Analysis was carried out on the data set of each of the cores. Principal components analysis describes the variation of a set of multivariate data as a reduced set of uncorrelated variables, each of which is a particular linear combination of the original variables. In the present study, eigen values greater than 1 are selected. Varimax orthogonal rotation has been employed to transform the analysis matrix and to limit the number of variables loaded in each factor (Buckley et al., 1995). Most of the correlations are taken at >0.70, implying that the extractions of different factors at different sites are reasonable for the study. Component loading (correlation coefficients) measures the degree of closeness between the variables and the Principal components. The largest loading either positive or negative, suggests the meaning of the dimensions; positive loading indicates that the contribution of the variables increases with the

increasing loading in dimension and negative loading indicates a decrease. The values of different factors and percentage variance accounted for the cores are given in Table 3.1A.3-3.1A.8.

3.1A.10b1. Near the creek head (core TI)

The computation of Factor Analysis for this core resulted in four factors accounting for 74.63 % of the total variance. Factor 1 accounts for 26.93 % of the total variance and shows positive loadings of TOC and Fe on Cu, Pb, Ni and Cr. Factor 2 comprises of 20.86 % of the total variance exhibiting positive loadings of sand and silt on Mn and Ca. The third factor displays positive loadings of pH on Co. The fourth factor consisting of TP, Al and to some extent TN shows positive loadings on V. From the observations it can be stated that near the head region of the creek, the major contribution of trace metals come from organic matter (TOC), may be through waste discharge. Some of the metals may also be present as oxides or hydroxides of Fe. Factor 3 highlights the role of pH in retention of some metals in this region of the creek. Thus, TOC, Fe, Mn and pH seem to control the metal associations in this region.

Table 3.1A.3. Varimax normalised factor analysis for core collected near the creek head (TI)

Core TI	Factor 1	Factor 2	Factor 3	Factor 4
Eigen value	4.84	3.75	3.188	1.64
Total Variance	26.93	20.86	17.71	9.13
Sand	0.05	**0.73**	0.07	-0.31
Silt	0.10	**0.92**	-0.08	-0.07
Clay	-0.10	**-0.95**	0.06	0.11
TOC	0.68	0.18	-0.36	-0.41
TP	0.24	-0.17	0.06	**0.80**
TN	0.34	-0.08	-0.70	0.44
pH	-0.19	0.14	**0.78**	-0.32
Fe	0.52	0.14	-0.05	0.26
Mn	0.36	0.40	-0.56	0.11
Cu	**0.72**	0.05	-0.13	0.30
Pb	**0.84**	-0.25	-0.07	-0.04
Co	0.23	-0.05	**0.84**	0.09
Ni	**0.72**	0.36	0.24	0.43
Zn	-0.09	0.07	**-0.82**	-0.10
Cr	**0.77**	0.24	0.45	0.10
V	0.10	0.04	-0.37	**0.87**
Al	0.00	-0.18	0.04	**0.86**
Ca	-0.25	0.40	0.10	-0.62

3.1A.10b2. Upper middle creek region

Core TII: Four factors are computed for core TII resulting in 76.64 % of total variance. Factor 1 with 30.46 % of total variance shows positive loadings of TOC, TN and pH on Pb and to some extent Zn and Cr, while factor 2 with 24.49 % of total variance projects positive loadings of clay

and TN but shows no association with any of the metals. Factor 3 with 12.06 % total variance exhibits positive loadings of Fe and sand on Ni, Cr, Ca and to some extent on Pb. The fourth factor with 9.63 % of total variance displays high positive loadings of Al and sand on Zn and V, and almost all the remaining metals but to a low extent. In general, in this core most of the metals are found to be associated with Al (factors 3 and 4), although to a less extent, indicating the metals are from lithogenic origin.

Table 3.1A.4. Varimax normalised factor analysis for core collected from upper middle creek region (core TII)

Core TII	Factor 1	Factor 2	Factor 3	Factor 4
Eigen value	5.48	4.41	2.17	1.73
Total Variance	30.46	24.49	12.06	9.63
Sand	0.38	0.38	0.51	0.48
Silt	-0.03	**-0.90**	0.01	-0.31
Clay	-0.03	**0.90**	-0.08	0.26
TOC	0.69	-0.46	-0.40	0.12
TP	-0.04	-0.61	0.17	0.19
TN	**0.73**	0.56	0.18	-0.13
pH	0.62	0.44	0.04	0.16
Fe	0.04	-0.24	**0.92**	0.13
Mn	-0.03	0.17	-0.21	0.33
Cu	-0.18	**-0.85**	-0.18	0.27
Pb	**0.81**	0.09	0.42	0.36
Co	-0.27	-0.61	0.02	0.34
Ni	0.18	-0.27	**0.85**	0.25
Zn	0.51	-0.20	0.09	**0.72**
Cr	0.53	0.08	0.59	0.02
V	0.06	0.01	0.27	**0.89**
Al	0.17	-0.26	0.34	**0.86**
Ca	-0.04	0.29	**0.81**	0.05

Core TVI: Five factors are derived accounting 76.69 % of the total variance. Factor 1 with a total variance of 32.03 % exerts high positive loading of TOC and TN on Ni, Cr, V and Ca. The second, third and fifth factor with 16.85, 11.75 and 6.33 % total variance do not show any positive associations with metals, while factor 4, exhibits good positive loadings of pH on Pb and Cr. From the above observation, organic matter, with high percentage of total variance seems be the main metal concentrator in this region.

Table 3.1A.5. Varimax normalised factor analysis for core collected from upper middle creek region (core TVI)

Core TVI	Factor 1	Factor 2	Factor 3	Factor 4	Factor 5
Eigen value	5.76	3.03	2.11	1.75	1.14
Total Variance	32.03	16.85	11.75	9.73	6.33
Sand	0.27	-0.07	0.12	-0.58	0.15

Silt	-0.08	**-0.97**	0.00	0.01	0.17
Clay	0.06	**0.97**	-0.01	0.04	-0.18
TOC	**0.88**	0.07	-0.15	0.14	0.21
TP	-0.14	0.23	0.14	0.03	**-0.77**
TN	**0.84**	0.32	0.06	-0.08	0.07
pH	0.20	0.13	0.37	**0.74**	0.14
Fe	-0.54	0.06	-0.27	0.17	0.54
Mn	**-0.84**	0.18	0.14	-0.35	0.03
Cu	-0.08	0.10	**-0.93**	-0.02	-0.01
Pb	0.34	-0.25	-0.42	0.52	0.18
Co	-0.18	-0.04	**-0.87**	-0.08	0.17
Ni	**0.83**	0.00	0.21	-0.04	0.22
Zn	-0.17	0.14	0.39	-0.31	-0.42
Cr	0.59	-0.17	0.07	0.53	-0.11
V	**0.83**	0.05	0.20	0.15	0.05
Al	-0.37	0.18	-0.10	0.13	**-0.73**
Ca	**0.86**	0.00	0.03	-0.28	0.26

3.1A.10b3. Lower middle creek region

Core TIII: In this core, five factors constitute 73.91 % of the total variance. Factor 1, with total variance of 30.41 %, projects good positive loading of sand and Mn on Cu, Co, Ni, Zn, Cr and Al. The second factor accounts for 14.63 % of the total variance and is dominated by positive loadings of Fe and Mn on Pb. Factor 3 with a total variance of 9.31 % is characterised by good positive loadings of clay, while factor 4 with 9.31 % of total variance shows good loading of TP, TN and pH. Factors 3 and 4 do not show any metal associations. The fifth factor displays 8.62 % total variance but does not exhibit any positive loading among the parameters studied. Good association of Mn with metals, as seen in factors 1 and 2, suggest that Mn oxide might be the main metal carrier in this region.

Table 3.1A.6. Varimax normalised factor analysis for core collected from lower middle creek region (core TIII)

Core TIII	Factor 1	Factor 2	Factor 3	Factor 4	Factor 5
Eigen value	5.47	2.63	1.97	1.68	1.55
Total Variance	30.41	14.63	10.94	9.31	8.62
Sand	**0.73**	-0.40	0.07	-0.31	0.09
Silt	-0.16	0.20	**-0.94**	0.11	0.03
Clay	-0.35	0.09	**0.86**	0.11	-0.09
TOC	-0.22	-0.22	0.06	0.00	**-0.82**
TP	0.05	-0.03	-0.35	0.53	-0.56
TN	0.20	0.12	0.12	0.67	-0.01
pH	-0.32	0.18	-0.11	0.62	0.22
Fe	-0.17	0.68	0.21	0.17	0.30
Mn	0.59	0.56	-0.04	0.09	-0.20
Cu	**0.73**	-0.25	-0.05	0.33	-0.07
Pb	-0.10	**0.82**	-0.10	0.27	0.05
Co	**0.79**	0.27	0.09	-0.35	-0.06

Ni	**0.76**	0.03	-0.11	0.30	0.34
Zn	**0.86**	-0.20	-0.01	0.03	0.05
Cr	**0.91**	-0.13	0.06	-0.21	0.03
V	0.20	0.21	0.21	-0.30	-0.56
Al	**0.81**	-0.05	-0.19	0.12	-0.11
Ca	0.26	-0.67	0.24	0.31	0.07

Core TV: On a whole, four factors are obtained comprising 78 % of total variance in this core. Factor 1 explains 34.87 % of the total variance and is characterised by high positive loadings (>0.70) of TN and to some extent of Al and Fe on Cu, Ni, Zn, V and Ca. This factor could be identified as the natural factor comprising of lithogenic processes involving the weathering of parent material such as rocks and soils. Factor 2 accounts for 22.11 % of the total variance and exhibits good positive loadings of Fe on Cu, Pb and Cr. Factor 2 can be called the Fe-oxide factor as it is observed to control the distribution of most of the metals. Factor 3 with a total variance of 11.99 % shows positive loading of Mn and to a less extent of sand on Co and Ca. The fourth factor shows good loading of silt but with no significant association on metals. From the observations, Fe seems to be the dominant metal carrier in this core.

Table 3.1A.7. Varimax normalised factor analysis for core collected from lower middle creek region (core TV)

Core TV	Factor 1	Factor 2	Factor 3	Factor 4
Eigen value	6.28	3.98	2.16	1.62
Total Variance	34.87	22.11	11.99	9.03
Sand	-0.18	-0.46	0.58	0.13
Silt	-0.01	0.25	-0.02	**0.96**
Clay	0.02	-0.23	-0.01	**-0.96**
TOC	0.42	-0.56	0.19	-0.09
TP	-0.62	0.31	0.18	0.24
TN	**0.88**	-0.23	0.06	0.11
pH	**-0.78**	-0.06	-0.38	-0.20
Fe	0.47	**0.76**	0.01	0.10
Mn	0.11	0.07	**0.87**	-0.19
Cu	0.66	0.52	0.32	0.07
Pb	-0.02	**0.89**	0.11	0.30
Co	-0.09	0.34	**0.72**	0.07
Ni	**0.81**	0.02	0.03	-0.31
Zn	**0.89**	0.10	-0.01	-0.17
Cr	-0.12	**0.73**	0.24	0.22
V	**0.92**	-0.07	-0.17	0.01
Al	**0.90**	0.25	-0.19	0.08
Ca	0.63	0.02	0.51	0.26

3.1A.10b4. Near creek mouth (core TIV)

It is noted that, in this core, five factors account for 72.24 % of the total variance. Factor 1 with a total variance of 21.63 % shows good positive loadings of pH and to some extent of Fe on Ni. On the other hand, factor 2 with a total variance of 18.60 %, exhibits positive loading of TP, TN

and Al on Co, Cr and Cu. Factor 3 shows good positive loading of silt and to a lower extent of TP on V while factor 4 accounts for good loading of TOC, TN, Al and Fe on Zn. The fifth factor projects good positive loadings of Mn on V and to some extent on Cr. organic matter along with Fe seem to be the main metal carriers in this region.

Table 3.1A.8. Varimax normalised factor analysis for core collected near the creek mouth (core TIV)

Core TIV	Factor 1	Factor 2	Factor 3	Factor 4	Factor 5
Eigen value	3.89	3.35	2.81	1.92	1.03
Total Variance	21.63	18.60	15.61	10.65	5.75
Sand	-0.26	-0.21	0.64	0.05	0.16
Silt	0.04	0.00	**0.95**	-0.02	-0.04
Clay	-0.02	0.01	**-0.96**	0.02	0.03
TOC	0.03	-0.04	0.19	**0.86**	0.15
TP	-0.60	0.45	0.43	-0.11	0.07
TN	-0.56	0.45	0.02	0.51	0.15
pH	**0.83**	0.12	0.13	-0.10	0.21
Fe	0.46	0.24	-0.18	0.54	-0.07
Mn	0.32	0.20	0.02	0.08	0.67
Cu	-0.57	0.61	-0.10	0.19	-0.24
Pb	**-0.71**	0.03	0.19	-0.46	-0.06
Co	0.13	**0.84**	-0.13	-0.18	0.31
Ni	**0.84**	-0.02	-0.08	-0.19	-0.01
Zn	-0.22	0.05	-0.10	0.58	-0.21
Cr	0.23	0.58	-0.23	0.33	0.40
V	0.08	0.17	0.44	0.13	**0.70**
Al	-0.22	0.57	0.13	0.46	0.13
Ca	0.16	-0.05	0.12	0.15	-0.75

When the observations of correlation and factor analyses are clubbed together, both the results correlate well with each other. In general, near the creek head, the organic matter is found to be the main carrier of metals. The domestic wastewater received at treatment plants and pumping stations along the creek is estimated to be around 2.6 x 10^5 m^3 day^{-1} and is far in excess to the capacity of treatment plants (Ram, 2004). Wastewater is therefore, often released untreated to the adjacent bay through point discharge (MCGB, 1979). Also, some of the major industries along the creek include fertilizer, petrochemical, thermal power, nuclear, pharmaceutical, chemical and textile, which release wastes into the creek. Thane creek receives industrial wastewater estimated to exceed 1.8 x 10^5 m^3 day^{-1} (MCGB, 1979). Therefore, most of the metals must be adsorbed by the organic matter and get deposited in the sediments. In the upper middle region also, the control of organic matter is seen (core TVI). However, the other core from the same region but collected from a sheltered area representing the creek sub-channel, displays metal associations with Al suggesting a lithogenic origin. On the other hand, at the lower middle creek region, Fe and Mn are the dominant metal carriers. Lastly, near the creek mouth, Fe along with organic

matter again resumes their dominance. The Bombay harbour and Port present at the southern region of the creek brings in large amounts of wastes near the creek mouth. Also, shipping traffic especially in and close to harbours can all act as sources of heavy metal pollution (Forstner and Wittmann, 1981).

In the present study, statistical analysis has been used to reveal the sources and sinks of metals in sediments and to identify the area in which metal distribution is most affected. In this way, the results could confirm whether the creek was indeed under the controlling influence of anthropogenic activities on sediment metal distribution. From the observation of the principal component analysis, it is understood that the industrial zone represented by core TI while the shipyard and port, represented by core TIV, are the main potential sources of metal pollutants and organic matter in the creek indicating that the contents of metals in the creek sediments are clearly of anthropogenic origin while in the middle creek region they are a mix of anthropogenic and lithogenic sources.

3.1A.11. Pollution status of the creek

Human activities around coastal areas have significant negative impacts on the health of the ecosystems and the viability of resources. Therefore, coastal and marine pollution control is required to predict and monitor the consequences of human activities on marine and estuarine ecosystems. To know the extent to which the creek is getting polluted with time, Enrichment factor and Geo-accumulation index was computed.

3.1A.11a. Enrichment Factor (EF)

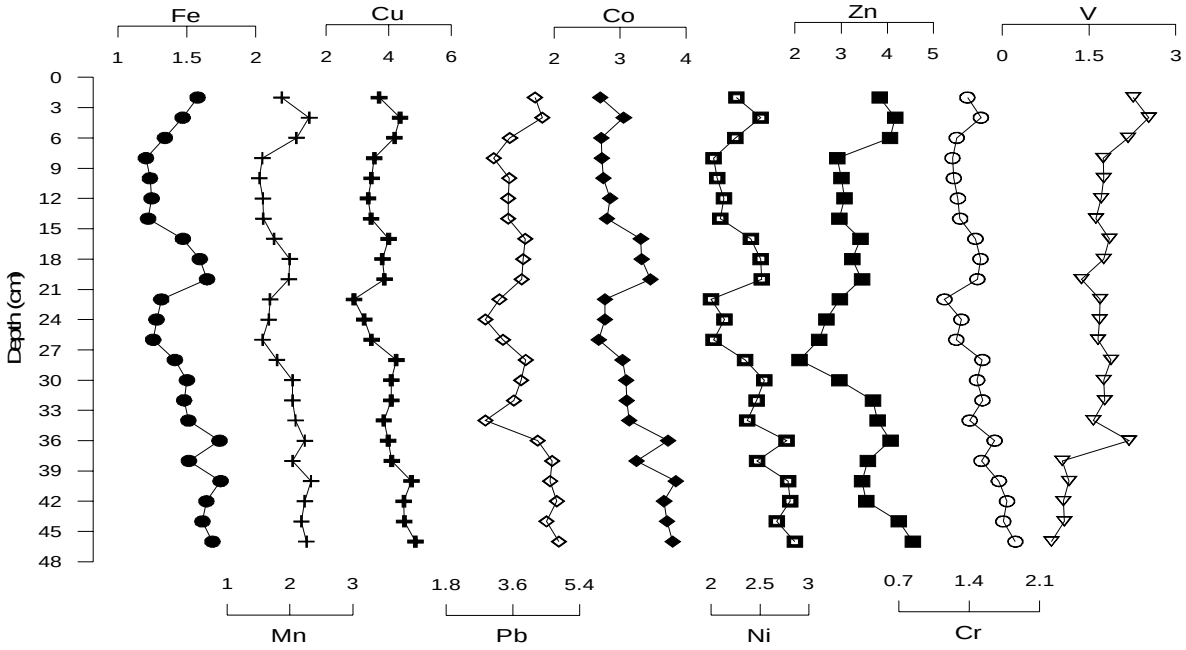

Fig. 3.1A.26. Down-core plots of EF for core collected near the creek head (TI)

Enrichment Factor (EF) has been calculated (Feng et al., 2004) for all the cores using Al as the reference element, to differentiate between the metals originating from anthropogenic (non-crustal) and geogenic (crustal) sources, and to assess the degree of metal contamination. The EF is given by equation (1)

$$EF = (C_n / C_{Al})_{sediment} / (C_n / C_{Al})_{background} \quad (1)$$

where, $(C_n/C_{Al})_{sample}$ is the ratio of concentration of the element (C_n) to that of Aluminium (C_{Al}) in the sediment sample; $(C_n/C_{Al})_{background}$ is the same ratio with background value taken of average shale (Turekian and Wedepohl, 1961).

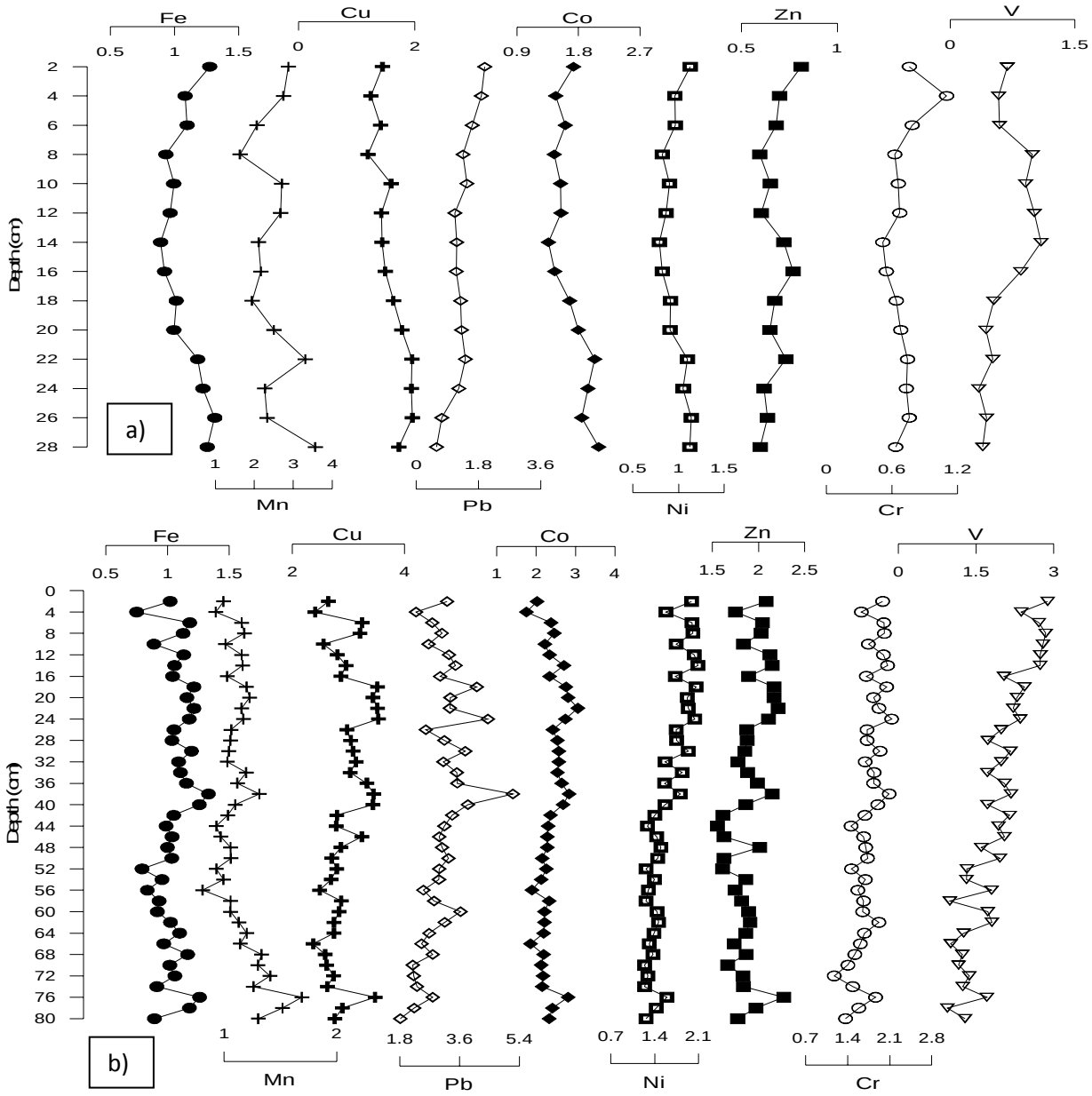

Fig. 3.1A.27. Down-core plots of EF for cores collected from upper middle creek region: a) core (TII) and b) core TVI

Aluminium was selected as the reference element as it is a major constituent of fine grained alumina silicates with which the bulk of the trace metals are usually associated. It is highly

refractory and its concentration is generally not influenced by anthropogenic sources (Schropp and Windom, 1988; Loring, 1991) and also not affected by early diagenetic processes and strong redox effects observed in sediments (OSPAR, 1998; Schneider and Weiler, 1984; Krumgalz et al., 1992).

According to Zhang and Liu (2002), EF values between 0.5 and 1.5 indicate the metal is entirely from crustal material or natural processes, whereas EF values greater than 1.5 suggest that the sources are more likely to be anthropogenic. Figures 3.1A.26 to 3.1A.29 show the down-core plots of EF for the different cores sampled from the creek region. Near the head region of the creek (Fig. 3.1A.26), except for Cr and to some extent Fe, almost all the metals are found to be highly enriched along the entire core length. In the upper middle region of the creek (Fig. 3.1A.27), core TII exhibits considerable enrichment of Mn while in core TVI except for Fe and Mn, almost all the other metals are found to be highly enriched.

When the distributions of EF values are seen in lower middle region of the creek (Fig. 3.1A.28), core TIII from the western bank, displays higher values for all the metals except for Fe, Ni, Zn and Cr. On the other hand in core TV, sampled from the eastern bank of the creek, Fe, Ni and Zn are below the enriched level while the remaining elements point towards an anthropogenic source. Near the creek mouth (Fig. 3.1A.29), the EF values of Fe and Zn are low while enrichment is observed for the remaining elements. The order of average enrichment factor for metals in the creek region is summarized as:

Cu >Pb >Co >Mn >Zn >Ni >V >Cr >Fe

When the average EF values are calculated for the entire creek, the core collected near the creek head shows the highest values for almost all the elements except for Mn, Cr and V while core TII from upper middle creek region exhibits the lowest value. As already confirmed by statistical analysis, core TI is recipient of anthropogenic inputs while in core TII the metals are mostly from lithogenic origin which supports the results of EF values. According to Manta et al. (2002), concentration of some trace metals like Cr, V and Mn seem to be mainly controlled by lithogenic inputs rather than anthropogenic ones while V can also be derived from the oil refinery processes or from domestic heating and automotive traffic (Soldi et al., 1996; Nadal et al., 2004).

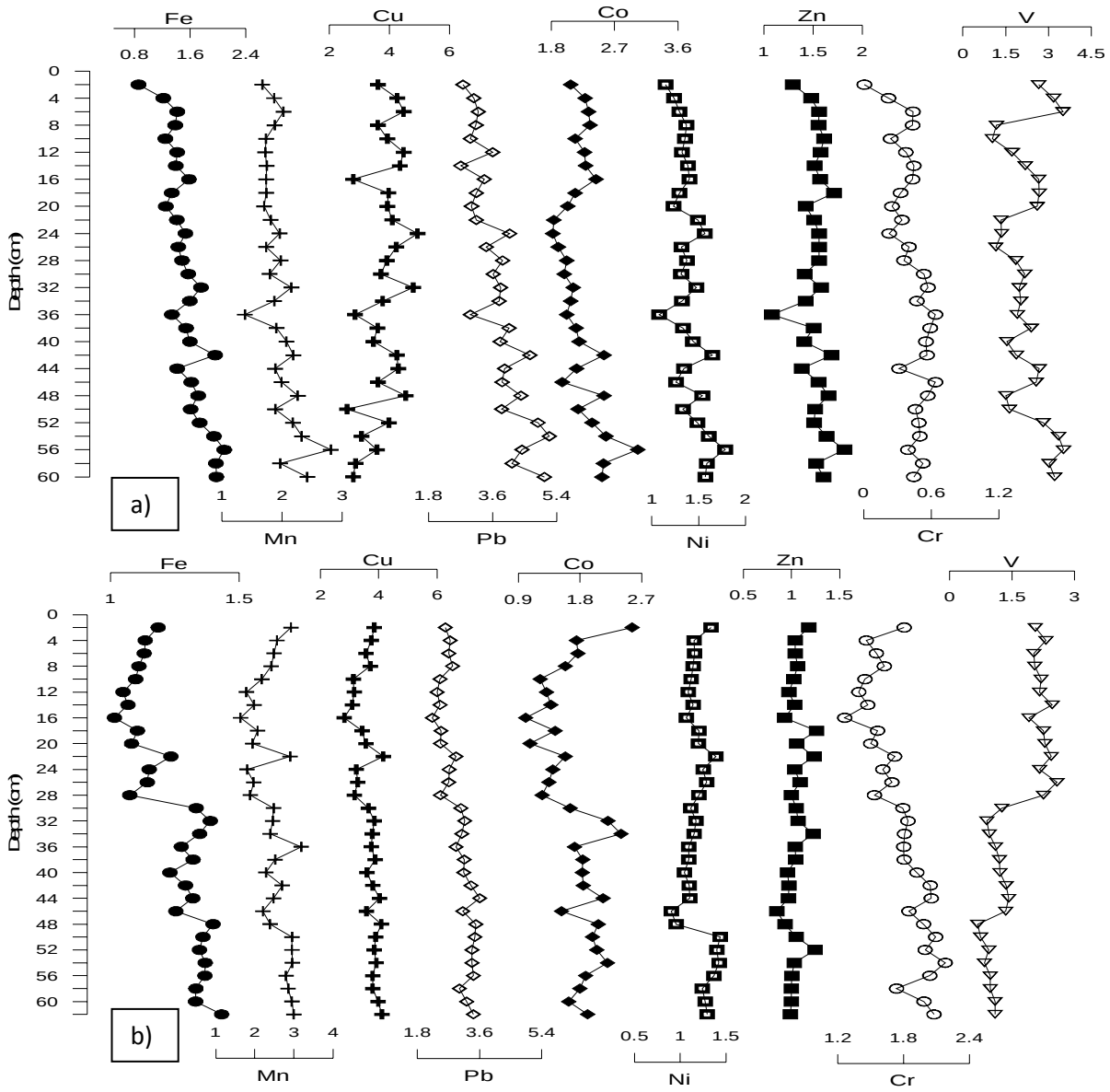

Fig. 3.1A.28. Down-core plots of EF for cores collected from lower middle creek region: a) core TIII and b) core TV

Major refineries are located along the western shore of the creek and discharge their wastes through point sources to the creek. In addition, domestic wastewater releases are also channelled through nallas discharging in the western region of the creek (Rokade, 2009). On the other-hand, the eastern shores are mainly influenced by industrial wastewater from the Thane-Belapur belt. However, when the average EF values of metals from the middle creek region are seen, the cores sampled from eastern bank of the creek shows higher values than the cores collected from the western bank. The reason for such an observation could be due to prevailing strong tidal currents in this area. The effluents from the western bank are transported away from this area and get settled in relatively calm regions i.e. the eastern bank. In general, from the creek head to the mouth a decreasing trend in EF values are observed for almost all the metals indicating dilution of anthropogenic effluents by seawater.

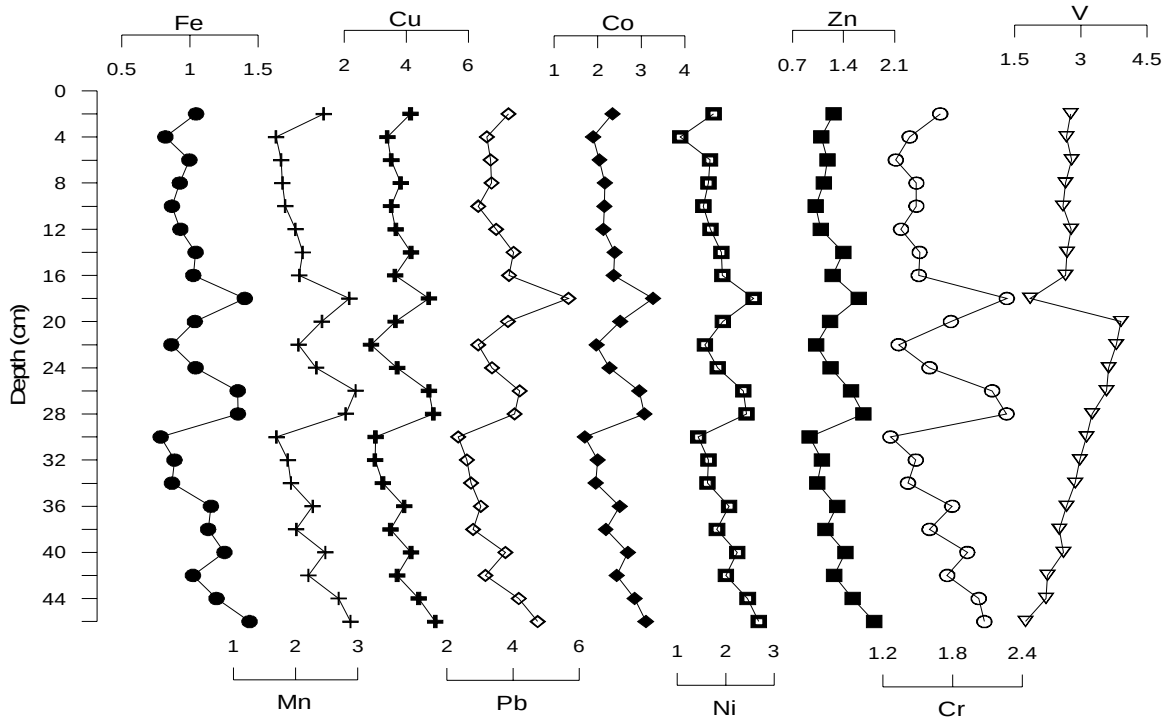

Fig. 3.1A.29. Down-core plot of EF for cores collected near the creek mouth (core TIV)

3.1A.11b. Index of Geoaccumulation (Igeo)

Igeo, which compares present day contaminant concentrations with pre-civilization background values, was used to quantitatively estimate the metal pollution status of the sediments. It is a semi-quantitative approach based on differences between current measurements and subtracted from average global shale measurement taken as background values (Muller, 1979). The Igeo is given by equation (2)

$$\text{Igeo} = \log_2 (Cn/1.5Bn) \qquad (2)$$

where, Cn = the measured concentration of the element n in the sediment fraction; Bn = geochemical background of element n, taken from literature (average global shale) as local or regional background values are unavailable for this region. The factor 1.5 is introduced to include the possible variations of the background values due to lithogenic variations.

Table 3.1A.9. Geoaccumulation index proposed by Muller (1979)

Pollution Intensity	Sediment Accumulation	Igeo class
Very strongly polluted	>5	6
Strongly to very strongly polluted	4-5	5
Strongly polluted	3-4	4
Moderately to strongly polluted	2-3	3
Moderately polluted	1-2	2
Unpolluted to moderately polluted	0-1	1
Practically unpolluted	<0	0

Table 3.1A.9 gives the classification for metal pollution. Class 0 to class 6 represents increasing intensity of pollution, i.e. from unpolluted to very strongly polluted. Figures 3.1A.30 to 3.1A.32 show the distribution plots of Igeo for selected metals in the study area. The core sampled near the creek head (core TI) exhibits moderately polluted class with respect to Cu, Pb, Co, Ni and Zn, while the other metals fall in unpolluted to moderately polluted class (Fig. 3.1A.30a). The core retrieved near the creek mouth (core TIV), shows Cu, Pb and Co to be moderately polluted while the remaining elements are found to be in the unpolluted to moderately polluted class (Fig. 3.1A.30b). In core TII, from upper middle creek, Mn is moderately polluted while Fe, Cu, Pb and Co fall in unpolluted to moderately polluted class. The remaining elements (Ni, Zn, Cr and V) fall in the unpolluted class (Fig. 3.1A.31a). The other core (core TVI), sampled from the same region but on the opposite bank, shows unpolluted to moderately polluted class for all the metals except for Cu, Pb and Co which fall in the moderately polluted class (Fig. 3.1A.31b).

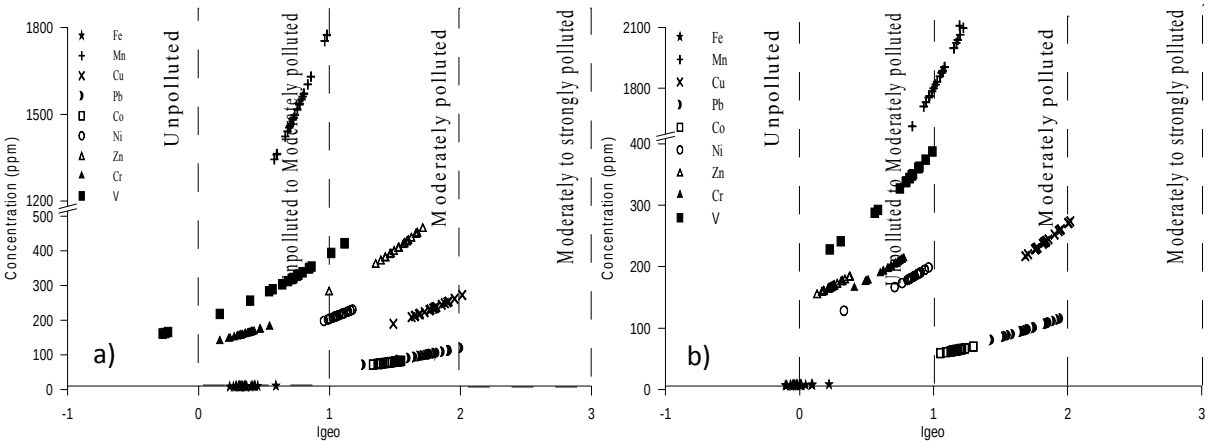

Fig. 3.1A.30. Igeo plots for cores collected near the creek a) head (TI) and b) mouth (TIV)

The lower middle creek region displays moderate pollution with Cu, Pb and Co in core TIII and with Mn and Pb in core TV. In addition to this, in core TV, moderate to strong pollution is observed with respect to Cu. The remaining elements fall in unpolluted to moderately polluted class (Fig. 3.1A.32).

In the creek region, in general, it is seen that in all the cores except for core TII and to some extent in core TV, from the upper and lower middle creek regions respectively, Cu, Pb and Co show level of moderate pollution. The use of anti-fouling paints to cover the underwater parts of the boats, yachts and vessels to protect them from the development of fouling organisms such as algae and barnacles contain metals such as Cu, Pb, Cr and Zn. A large number of small boats and fishing trawlers ply around the creek region. The use of such anti-fouling paints must have resulted in highly localized Cu pollution. On the other hand, emissions from automobiles

consuming leaded petrol are the major source of atmospheric Pb as the atmospheric pathway can be a major source of Pb to marine sediments (Guerra-Garcia and Garcia-Gomez, 2005).

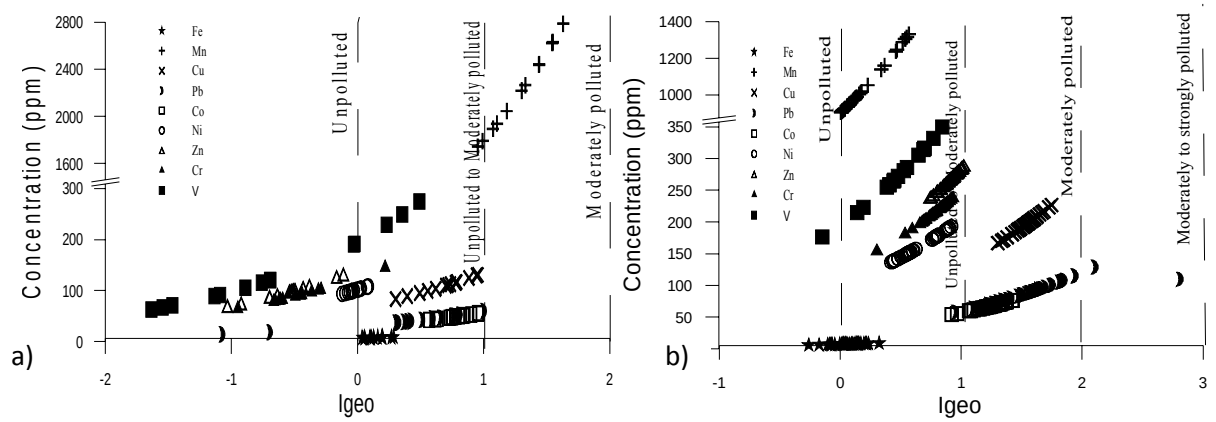

Fig. 3.1A.31. Igeo plots for cores collected from the upper middle creek region: a) core TII and b) core TVI

The major anthropogenic sources of Co include mining and processing of cobalt-bearing ores, the use of cobalt-containing sludge or phosphate fertilizers on soil, the disposal of Co containing waste and atmospheric deposition from activities such as the burning of fossil fuels and smelting and refining of metals (Smith and Carson, 1981). Most of the metals are found to fall in the unpolluted to moderately polluted class implying that the creek might be acting like a passive link and not like an active trap for metals, as previously suggested by Sharma et al. (1994).

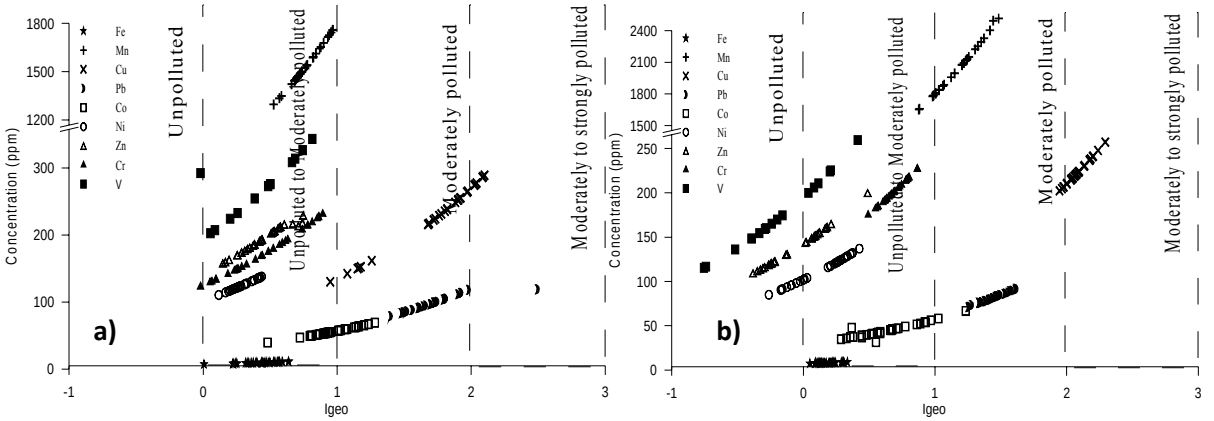

Fig. 3.1A.32. Igeo plots for cores collected from the lower middle creek region: a) core TIII and b) core TV

Also an attempt has been made to compute the EF and Igeo values taking the metal values obtained at the bottom sediments of core TII as the background values, as it gave a record of ~100 years back. From Table 3.1A.10, it can be seen that the EF values for some of the elements lie above 1.5 indicating metal enrichment. In general, not much difference in the computed EF values is observed among the metals, except for Mn which shows low EF values, as compared to the values computed using background value taken from average shale (Turekian and Wedepohl,

1961). This is because, the bottom sediment of core TII has higher concentration of Mn which when computed for EF results in low average values.

Table 3.1A.10. Enrichment values for cores sampled from the creek

Elements	Core TII						Turekian and Wedepohl, (1961)					
	TI	TII	TVI	TIII	TV	TIV	TI	TII	TVI	TIII	TV	TIV
Fe	1.38	1.02	1.00	1.45	1.16	1.00	1.46	1.08	1.06	1.55	1.23	1.06
Mn	0.79	1.02	0.46	0.80	1.00	0.92	1.93	2.49	1.14	1.95	2.46	2.23
Cu	2.51	1.01	1.88	2.44	2.34	2.46	3.92	1.58	2.94	3.82	3.65	3.84
Pb	2.93	1.00	2.34	2.84	2.25	2.70	3.86	1.31	3.08	3.73	2.96	3.54
Co	1.90	1.02	1.44	1.35	1.04	1.45	3.14	1.68	2.38	2.23	1.72	2.39
Ni	2.53	1.02	1.69	1.47	1.26	2.03	2.39	0.96	1.60	1.40	1.19	1.91
Zn	5.06	1.00	2.82	2.27	1.55	1.90	3.40	0.67	1.90	1.53	1.04	1.27
Cr	2.10	1.01	2.50	2.25	2.53	2.41	1.46	0.70	1.74	1.57	1.76	1.67
V	2.38	0.96	2.72	3.18	2.28	2.85	1.66	0.67	1.89	2.24	1.59	1.98

From Table 3.1A.11, it is seen that almost all the elements fall in unpolluted class based on the average values obtained from the bottom sediments of core TII.

Table 3.1A.11. Igeo values for cores sampled from the creek region

Elements	Core TII						Turekian and Wedepohl, (1961)					
	TI	TII	TVI	TIII	TV	TIV	TI	TII	TVI	TIII	TV	TIV
Fe	-0.37	-0.59	-0.67	-0.31	-0.55	-0.74	0.36	0.14	0.06	0.43	0.18	-0.01
Mn	-1.18	-0.60	-1.77	-1.16	-0.77	-0.87	0.75	1.33	0.11	0.77	1.16	1.06
Cu	0.49	-0.60	0.25	0.45	0.46	0.56	1.78	0.69	1.54	1.73	2.11	1.84
Pb	0.71	-0.67	0.54	0.66	0.40	0.69	1.75	0.37	1.61	1.71	1.44	1.72
Co	0.09	-0.59	-0.14	-0.40	-0.73	-0.20	1.46	0.78	1.23	0.97	0.64	1.17
Ni	0.50	-0.59	0.09	-0.27	-0.43	0.27	1.07	-0.02	0.65	0.29	0.13	0.83
Zn	1.49	-0.60	0.84	0.35	-0.13	0.18	1.56	-0.53	0.91	0.44	-0.06	0.25
Cr	0.23	-0.61	0.66	0.33	0.57	0.53	0.35	-0.49	0.78	0.45	0.69	0.65
V	0.38	-0.75	0.73	0.78	0.32	0.76	0.50	-0.63	0.85	0.90	0.54	0.88

Although there are some differences in the results of assessment and classification of heavy metal contamination levels depending on the reference material used, the above results in general, lead to the conclusion that the contamination of Cu, Pb, Co falls in moderately polluted class whereas other heavy metals (Fe, Mn, Ni, Zn, Cr and V) can be classified as not polluted.

3.1A.12. Isocon plots

An Isocon diagram, which compares the average concentration of specific elements from different sites (Grant, 1986; Cundy et al., 1997; Grant, 2005; Singh and Nayak, 2009), has been employed to show the variations in concentration between the sites sampled in the creek region. The examination of the spatial differences of the heavy metal contents in sediments allows the identification of the presence of anthropogenic effects, possible sources of contamination and

effects due to the transport of pollutants from other areas (Massart et al., 1988). In order to plot this diagram, the average concentration of each element along with the sediment components and organic matter contents from each site has been computed. The diagram (Fig.3.1A.33-3.1A.34) indicates a significant difference in the trace metal concentrations between the cores.

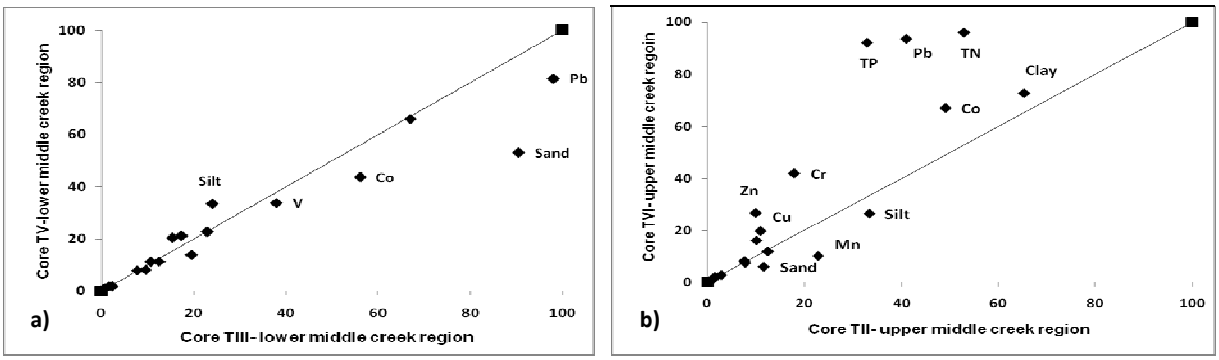

Fig. 3.1A.33. Isocon plots for mudflat cores collected from a) upper and b) lower middle creek regions

When the cores from the upper middle creek region are plotted (Fig.3.1A.33a), core TVI exhibits higher concentrations of TN, TP and clay along with Cu, Pb, Co, Zn and Cr while in core TII all the elements fall on or near the isocon line, except Mn, indicating little variations. For the cores from lower middle region (Fig.3.1A.33b), higher amounts of Pb, Co and V along with sand are seen in core TIII while the other core (TV) represents slightly higher silt percentage. Also, when the cores collected near the creek mouth and head are plotted together (Fig.3.1A.34), TI displays increased amounts of TOC, TP, clay, Mn, Co and Zn as compared to core TIV which shows higher amounts of silt, Cr and V. The high concentrations of TOC and TP in core TI reflects high organic matter fluxes to the sediments as a result of direct discharge of untreated domestic and insufficiently treated industrial wastes which must be acting as good binding sites for metals.

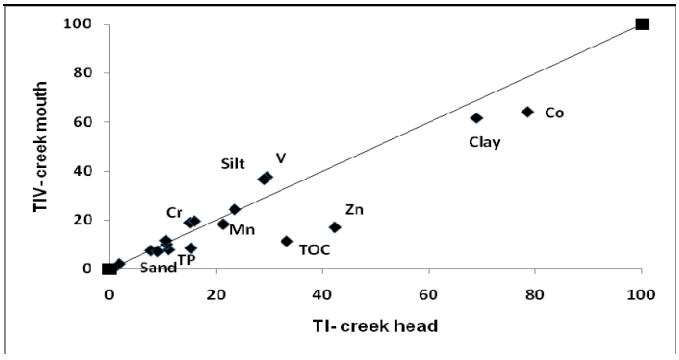

Fig.3.1A.34.Isocon plot for mudflat cores collected near the creek head (TI) and mouth (TIV)

In general, the isocon plots mirror the observations seen in statistical analysis. Although the focus of the present study was the overloaded industrial wastewater and sewage treatment plant

in the creek, other wastewater inputs include, urban storm-waters, untreated sewage (via septic tanks), shipyard and slipway run-off, and agricultural and pastoral run-off. Each of these discharges are a potential source of heavy metals (Choi et al., 2012), as well as organic contaminants. The results of the present study indicate that other factors viz, grain size, organic matter distribution, source rock for sedimentary material, etc., in addition to anthropogenic activities, also influence the enrichment of trace metals in the creek sediments.

3.1B. Thane Mangroves

Two mangrove cores were collected from the Thane creek namely from the upper middle creek region (TIIM) and near the mouth of the creek (TIVM). In order to obtain uniformity in the results, the cores were collected only from the area where *Avecennia marina* mangrove species was present.

3.1B.1. Visual observations

From the bottom to the surface, core TIIM (34 cm long) does not exhibit any distinct trend and is found to be of mixed brown and grey colour while core TIVM (68 cm long) represents gradual change in colour. In this core, from the bottom to 46 cm depth, the colour is dark brown, followed by mixed brown and black colour till 18 cm depth. Above it, brown colour is present till the surface. In both the cores, shells were present randomly in the upper few centimeters.

3.1B.2. Sediment components (sand, silt, clay)

Mangrove forests are known to act as efficient binders and traps of finer sediment. They offer an ideal environment for finer sediment deposition by providing a shelter from wave and tidal energy and by doing so, act as settling basins for suspended material. In the creek, sand, silt and clay in the mangrove regions vary from 0.08-5.96 %, 7.96-54 %, 44.56-91.60 % with average values of 1.28 %, 24.46 % and 74.21 %, respectively. Clay is found to be the dominant sediment component (>70 %) while sand percentage is the lowest (<2 %). In general, sand and silt decrease while clay increases from the the upper middle creek region to the mouth. For the mangrove core sampled from the upper middle creek region (core TIIM), the range is 0.96-5.96 % for sand with 1.94 % average, 19.92-54 % for silt with 33.91 % average and 45-79 % for clay with 64 % average. In the case of mangrove core collected near the creek mouth (core TIVM), sand, silt and clay vary from 0.08-3.32 %, 7.76-27.62 % and 72-92 % with average values of 0.61 %, 15 % and 84 %, respectively. The vertical distribution patterns of sediment components for both the mangrove cores are shown in figure 3.1B.1.

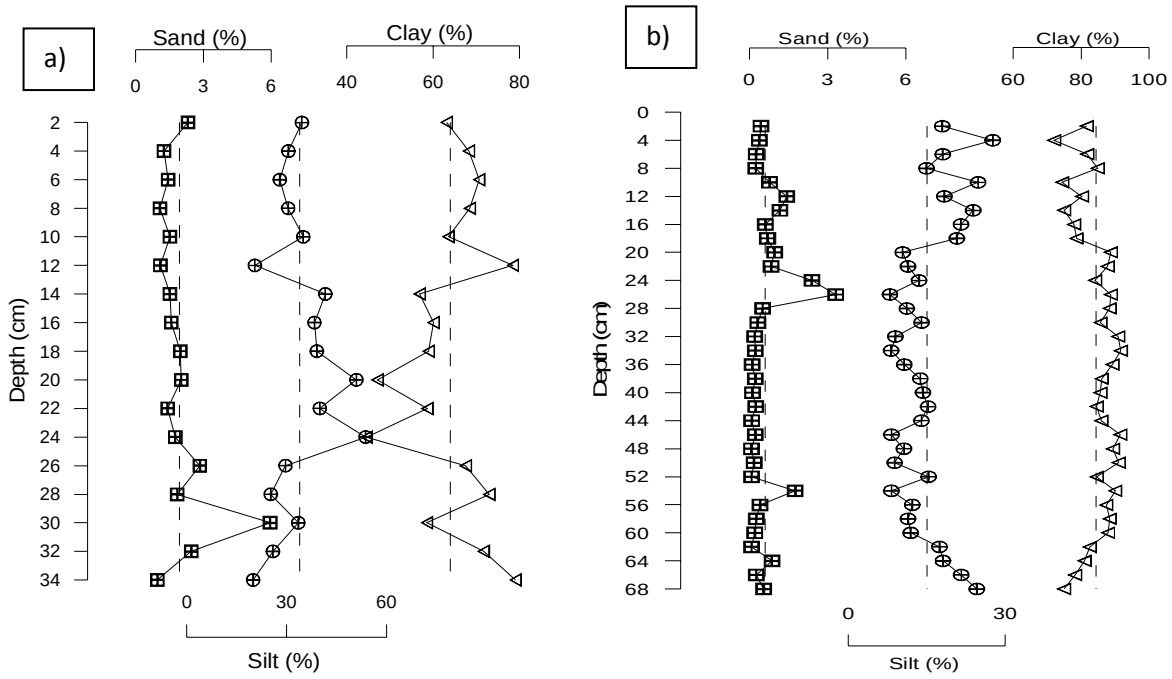

Fig. 3.1B.1. Vertical profiles of sediment components in a) upper middle creek region (core TIIM) and b) near creek mouth (core TIVM)

From the depth profile, it is seen that for core TIIM (Fig. 3.1B.1a), the distribution of sand is constant throughout the core length except at 30 cm depth, where a positive peak is observed. Silt and clay exhibit fluctuating opposite trends to each other with silt increasing and clay decreasing from the bottom to 24 cm. Further above, silt decreases and clay increases from 24 to 6 cm depth followed by an increase towards the surface for silt and a decrease for clay. In the case of core TIVM (Fig. 3.1B.1b), sand percentage is uniform from the bottom to the surface. However, three positive peaks are observed namely at 54, 26 and 12 cm depths. Silt and clay show erratic opposite trends to each other with silt, in general, decreasing from the bottom to 54 cm depth followed by a constant trend upto 20 cm and then increases towards the surface. Similarly, clay displays an increase from the bottom to 54 cm depth followed by a constant trend upto 20 cm and then decreases till the surface. In both the cores, sand percentage is found to be more or less constant. The high silt and clay fraction of the sediment (up to 90 %) indicates that there would be a high capacity to adsorb trace metals in the region.

In order to understand the hydrodynamic condition of sediment deposition in the mangrove regions, ternary diagram proposed by Pejrup (1988) was employed. The details of the diagram have been explained in section 3.1A.5 When the data points are plotted (Fig. 3.1B.2), it is seen that in core TIIM, almost all the subsamples fall in section II while only two subsamples fall in section III of group D indicating relatively less violent to violent hydrodynamic conditions.

However, in the case of core TIVM, the subsamples fall in group I and II of section D reflecting calm to relatively less violent hydrodynamic condition of sediment deposition.

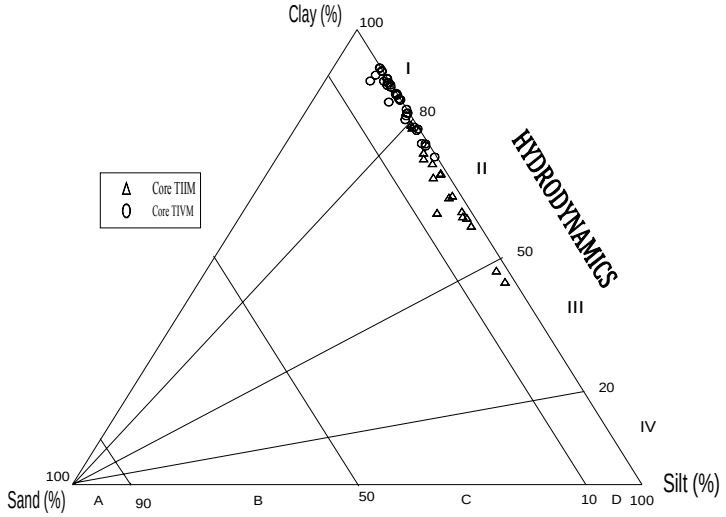

Fig. 3.1B.2. Ternary plot after Pejrup, 1988 for cores in a) upper middle creek region (core TIIM) and b) near creek mouth (core TIVM)

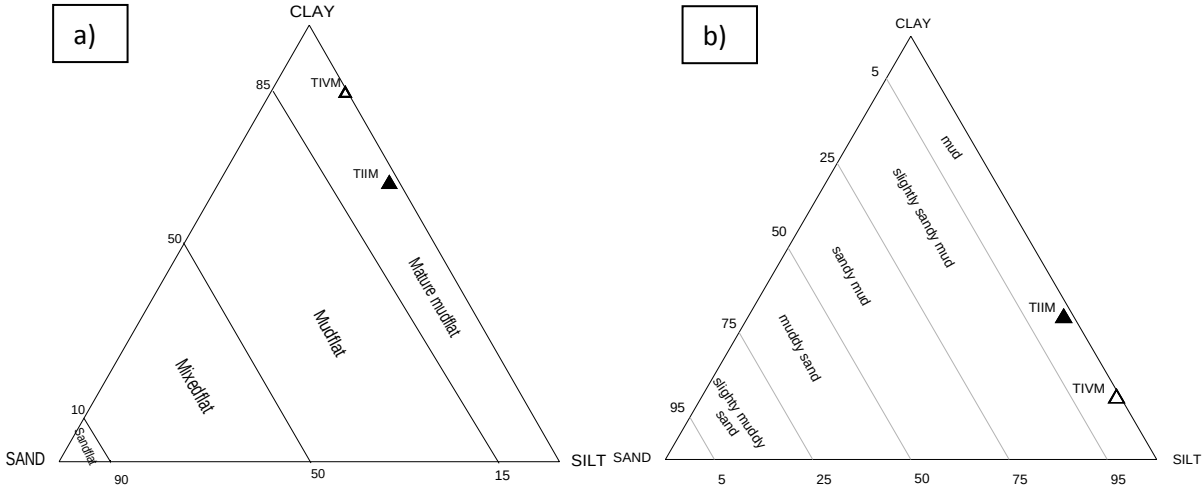

Fig. 3.1B.3. Ternary plots for cores TIIM and TIVM by a) Reineck and Siefert (1980) and b) Flemming (2000)

Based on Reineck and Siefert (1980) diagram (Fig. 3.1B.3a) both the cores fall in Mature Mudflat category, while Flemming (2000) plot (Fig. 3.1B.3b) indicates Mud class for both the cores.

3.1B.3a. Organic matter (TOC, TP, TN) and pH

The ranges of TOC, TP and TN in mangroves of the creek region vary from 0.79-4.18 %, 0.20-1.07 mg/g and 0.30-0.89 mg/g with average values of 1.84 %, 0.72 mg/g and 0.58 mg/g, respectively. For pH, the range is found to vary from 6.88-8.11 with an average value of 7.67. The concentrations of TOC and TP are found to increase while TN decreases from the upper middle creek region (core TIIM) to the creek mouth (core TIVM). pH values are observed to be

more or less constant in the creek region. Figure 3.1B.4 gives the vertical distribution profiles of pH and organic matter for both the mangrove cores. For core TIIM (Fig. 3.1B.4a), TOC (range- 1.34-1.89 %, avg. 1.67 %) shows increasing and decreasing trends from the bottom to 22 cm depth, while further above till the surface an increasing trend is seen. TP (range- 0.20-0.99 mg/g, avg. 0.56 mg/g), on a whole, exhibits a gradual increasing trend from the bottom to the surface whereas TN (range- 0.26-0.60 mg/g, avg. 0.47 mg/g) increases from the bottom to 24 cm and then decreases till 18 cm depth. Further above, it again shows an increase till 8 cm and then decreases towards the surface.

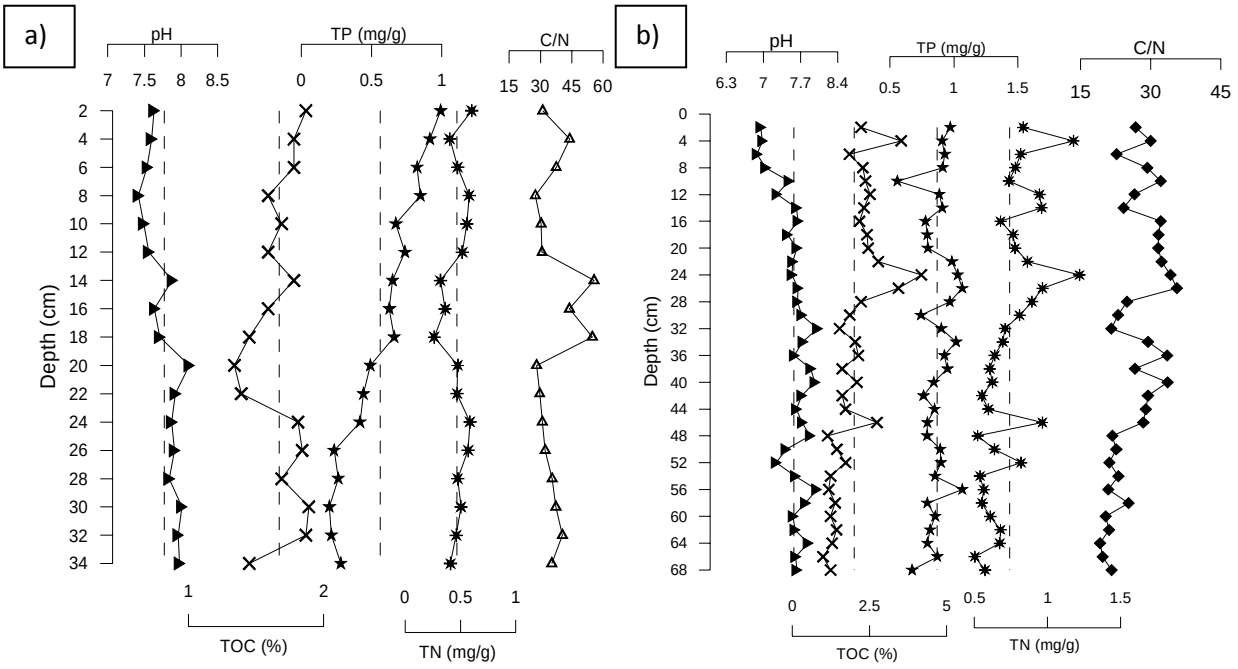

Fig. 3.1B.4. Vertical profiles of pH and organic matter in mangroves of a) upper middle creek region (core TIIM) and b) near creek mouth (core TIVM)

In the case of core TIVM (Fig. 3.1B.4b), TOC (range- 0.94-4.18 %, avg. 2.01 %) shows a gradual increase from the bottom to 22 cm depth and then decreases till the surface with peaks at 46 and 24 cm depths. TP (range- 0.56-1.07 mg/g, avg. 0.87 mg/g) fluctuates throughout the length of the core around the average line. On the other hand, TN (range- 0.50-1.22 mg/g, avg. 0.74 mg/g) decreases from the bottom to 42 cm and above it shows an increasing trend till the surface with two peak values at 24 and 14 cm depths, respectively. pH, in core TIIM (range- 7.42-8.11, avg. 7.77), shows a gradual decreasing trend till the surface whereas, in the case of core TIVM (range- 6.88-8.02, avg. 7.57), from the bottom to 14 cm, the pH trend is uniform and then decreases at the surface. The values in acidic range (6-7) in the upper sediment layer of core TIVM (6-2 cm) are indicative of ongoing oxidative processes.

3.1B.3b. C/N ratio

The mangroves along the creek region show C/N values ranging from 19.17-55.63 with an average value of 31.87. In core TIIM, in the upper middle creek region (Fig. 3.1B.4a), C/N values range from 27.51-55.63 with an average of 37.11 and exhibits a decrease from the bottom to 20 cm followed by increasing and decreasing trends till the surface. On the other hand, in core TIVM sampled near the creek mouth (Fig. 3.1B.4b), the range is 19.17-35.65 with an average of 26.64. In this core, C/N values increase from the bottom to 24 cm and then decrease till 14 cm followed by a fluctuating trend till the surface. In general, in both the mangrove cores, different vertical trends are observed with core TIVM showing an increasing trend of C/N values from the bottom to the surface as compared to core TIIM, which shows a decreasing trend with large fluctuations at the surface. The core near the creek mouth (core TIVM) must be receiving organic matter mainly from the land and marine sources. This is supported by low C/N values. The waves and tides around the region results in better mixing and degradation of organic matter producing a gradual decay with time. Core TIIM, on the other hand, lies at the upper middle creek region away from the main channel of the creek with greater flux of lithogenic matter as compared to the marine source. The high C/N ratio indicates allochthonous, rich organic matter being deposited and only partially degraded.

3.1B.4. Metal geochemistry

Different distribution patterns are found in the vertical profiles of the elements studied. The metals in mangrove cores sampled from the creek range from 7.69-15.26 % for Al, 1.36-3.76 % for Ca, 6.10-9.92 % for Fe, 443-2481 ppm for Mn, 102-155 ppm for Cu, 35-62 ppm for Pb, 42-89 ppm for Co, 112-185 ppm for Ni, 130-198 ppm for Zn, 79-171 ppm for Cr and 65-513 ppm for V with average values of 11.8 %, 2.33 %, 7.97 %, 1442 ppm, 127 ppm, 49 ppm, 57 ppm, 145 ppm, 163 ppm, 122 ppm and 246 ppm, respectively. In general, from the upper middle creek region to the creek mouth Al, Fe, Cu, Co, Zn and V show a decrease while Ca, Mn, Pb, Ni and Cr exhibit an increase in concentrations. The uppermost portions of both the cores contain overall higher concentrations of metals (Fe, Cu, Zn), also Mn and V for core TIIM as compared to the bottom portions.

For core TIIM, the range and average values for the selected metals are 10.61-15.26 %, 13.08 % for Al; 1.36-3.13 %, 1.90 % for Ca; 7.31-9.39 %, 8.73 % for Fe; 443-1664 ppm, 1067 ppm for Mn; 110-155 ppm, 137 ppm for Cu; 35-62 ppm, 47 ppm for Pb; 56-89 ppm, 67 ppm for Co; 112-169 ppm, 124 ppm for Ni; 130-198 ppm, 173 ppm for Zn; 79-112 ppm, 99 ppm for Cr and 131-513 ppm; 304 ppm for V. The plots of down-core metal variations are shown in figures 3.1B.5-

3.1B.6. In core TIIM (Fig. 3.1B.5), Al increases and then decreases from the bottom to 26 cm followed by an increase upto 20 cm depth. Further above till the surface, a decreasing trend is seen. Ca uniformly increases from the bottom to the surface with a peak value at 10 cm depth. On the other hand, Fe and Mn, from the bottom to 22 cm show similar increasing trends while between the depths of 22 to 10 cm, the values for Fe decreases whereas Mn shows an increase. From 8 cm till the surface Fe shows an increasing trend. Cu and Pb show identical trends from the bottom to 10 cm. Above this depth, both the elements show fluctuating opposite trends to each other with Cu increasing and Pb decreasing towards the surface. In the case of Ni and Cr, from the bottom to 30 cm, between 22 and 12 cm depths and from 8 cm till the surface similar increasing and decreasing trends are seen. In general, Ni decreases while Cr increases from the bottom upto 18 cm and then decreases upto the surface. Co displays a gradual decrease from the bottom to the surface, except for a peak value at 12 cm depth. Zn increases with fluctuations from the bottom to 18 cm and then gradually increases till the surface. V fluctuates irregularly from the bottom to the surface with an overall increasing trend.

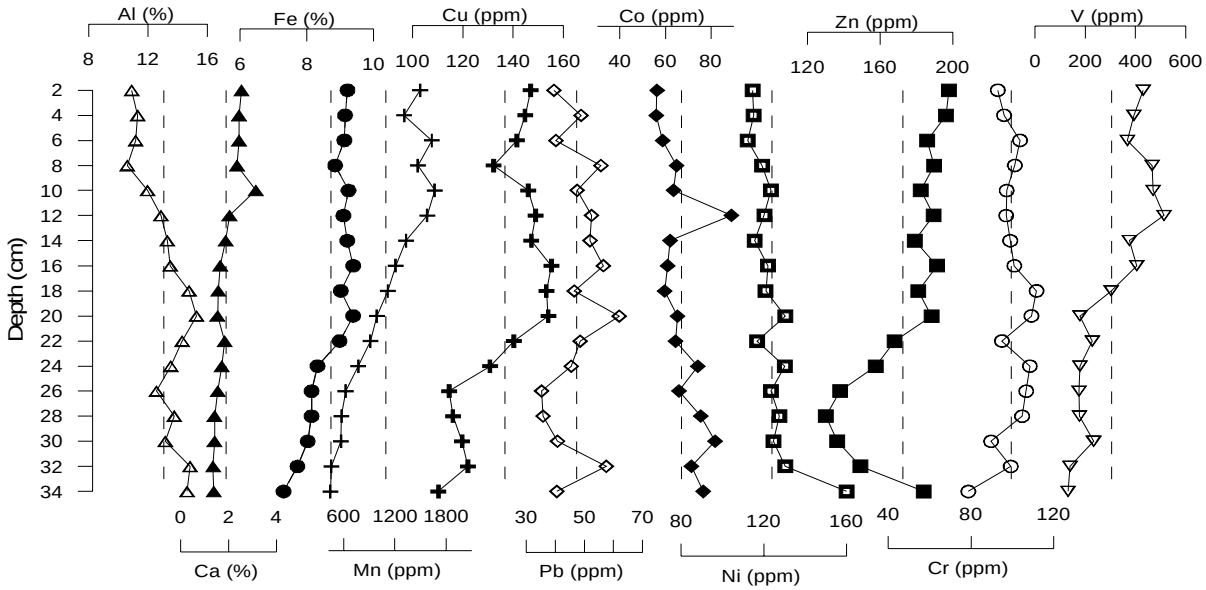

Fig. 3.1B.5. Depth-wise distribution of selected metals in the upper middle creek region (core TIIM)

For the core collected near the creek mouth (core TIVM), the range of metals fluctuate from 7.69-12.74 % for Al, 1.88-3.76 % for Ca, 6.10-9.92 % for Fe, 1484-2481 ppm for Mn, 102-127 ppm for Cu, 42-56 ppm for Pb, 42-55 ppm for Co, 154-185 ppm for Ni, 136-184 ppm for Zn, 120-171 ppm for Cr and 65-300 ppm for V with average values of 10.52 %, 2.75 %, 7.21 %, 1816 ppm, 117 ppm, 50 ppm, 47 ppm, 165 ppm, 153 ppm, 144 ppm and 187 ppm, respectively. From figure 3.1B.6, the distribution of Al is found to be constant throughout the core length while Ca fluctuates from the bottom to the surface. It is seen that Fe increases from the bottom to 62 cm and after dropping at 60 cm, maintains a constant trend in values upto 28 cm depth.

Further above it decreases, followed by a fluctuating increasing trend at the surface. On the other hand, Mn decreases from the bottom to the surface with a fluctuating trend. Cu, Pb and Cr exhibit erratic trends from the bottom to the surface. Co initially increases from the bottom to 60 cm followed by a decrease till 46 cm. Further above, a fluctuating increasing and decreasing trend is observed. Ni and Zn show similar increasing and decreasing trends from the bottom to the surface. V shows a decreasing trend with peaks at 56 and 32 cm depths, respectively.

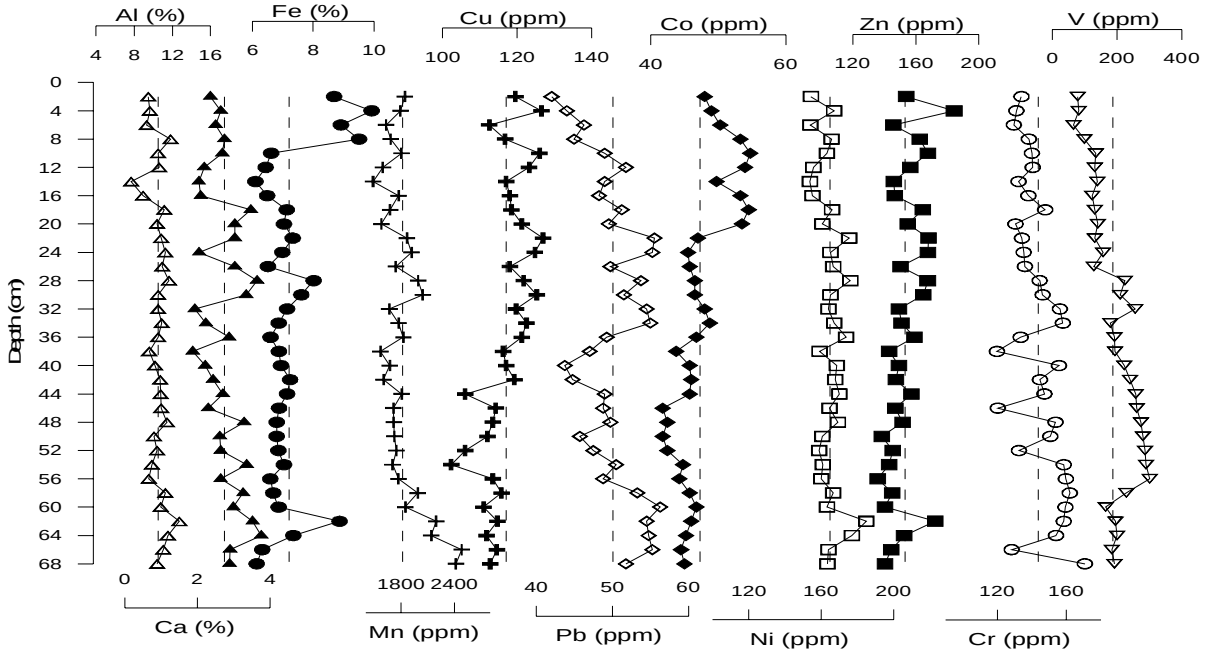

Fig. 3.1B.6. Depth-wise distribution of selected metals near the creek mouth (core TIVM)

In general, along the creek region, most of the metals (Fe, Cu, Co, Zn and V) and major element (Al) in the mangrove regions are found to show a decrease from the upper middle creek region towards the mouth of the creek, while the other major element (Ca) along with Mn, Ni and Cr exhibit an increase. Pb does not display much spatial variation in the creek region. On a whole, high concentrations of metals are found in areas where finest sediments accumulate and organic matter concentrations are also found to be the highest. In core TIVM, near the creek mouth, highest concentration of Mn is seen at the bottom. A study carried out by Sharma et al. (1994) in the Thane creek-Bombay harbour complex, reported higher concentration of Mn with depth in the coastal areas around Thane creek. This was attributed to authogenic source of Mn in the form of hydroxide floccules. Further, they suggested that the dissolved Mn when entering the sea comes in contact with alkaline and oxidizing environments and tends to precipitate as insoluble, finely divided MnO. However, in recent years, increase in organic pollutant loads might have resulted in the decrease of the authigenic Mn precipitation. The high organic matter must have lowered the dissolved oxygen content of water which consequently decreased the flocculation intensity of MnO in the water column resulting in the observed lower Mn concentration.

3.1B.5. Statistical analysis

3.1B.5a. Correlation analysis

Table 3.1B 1. Classification of values based on correlation analysis in the mangrove region

Stations		Good	Significant
Upper middle creek estuarine region	Core TIIM	0.46-0.59	> 0.59
Creek mouth	Core TIVM	0.33-0.43	> 0.43

In both the cores, Pearson's correlation at $p < 0.05$ was computed separately. In core TIIM sampled from the upper middle creek region, when the correlation matrix is seen, among the sediment components sand and clay show weaker or negative associations with all the studied variables except of sand with TOC (r=0.45) and pH (r=0.44) whereas silt shows good associations with Cr (r=0.50), and to a lower extent with Fe (r=0.42) and Cu (r=0.45). In the case of organic matter, TOC and TN correlate to a lower extent (r=0.45) and show negative or poor associations with almost all the studied elements. TP, on the other-hand, exhibits significant associations with most of the elements [Fe (r=0.78), Mn (r=0.91), Cu (r=0.72), Zn (r=0.84), V (r=0.85) and Ca (r=0.78)]. These observations indicate that TOC and TN are not acting as metal carriers in these sediments. pH is found to associate well with Ni (r=0.52) and significantly with Al (r=0.77). Fe and Mn correlate significantly with each other (r=0.84) and also show significant associations with Cu (r=0.94, 0.76), Zn (r=0.66, 0.75), V (r=0.72, 0.93) and Ca (r=0.60, 0.85). In the case of correlations among the metals, Cu correlates significantly with Zn (r=0.73) and V (r=0.64) and also shows correlations with Pb (r=0.54). Other correlations observed are of Ni with Al (r=0.56); Zn with V (r=0.67) and Ca (r=0.57), and Ca with V (r=0.78). The interelemental observations suggest that the mangrove sediments might have the same origin or sources of metals and/or may be influenced by the same factors and processes.

For the mangrove core sampled near the creek mouth (core TIVM), sand is found to associate significantly with TOC (r=0.57) and TN (r=0.48), silt with Co (r=0.42) while clay correlates well with TP (r=0.36), pH (r=0.41) and V (r=0.55). Among the organic matter, TOC with TN (r=0.89), Cu (r=0.62) and Zn (r=0.59) correlates significantly, while associates well with Co (r=0.35). TP and TN correlate well with each other (r=0.34) but do not show any correlation with the rest of the parameters. TN, on the other hand, associates significantly with Cu (r=0.52), Zn (r=0.57) and to some extent with Fe (r=0.33). pH associates with Pb (r=0.41), Cr (r=0.39) and V (r=0.63). Fe correlates significantly only with Zn (r=0.57), while Mn shows better association with Pb (r=0.49), Ni (r=0.42), Al (r=0.45) and Ca (r=0.48). Cu correlates significantly with Co

(r=0.48) and Zn (r=0.64); Pb with Ni (r=0.42), Cr (r=0.34), Al (r=0.49) and Ca (r=0.38); Co with Zn (r=0.41); Ni with Zn (r=0.39), Al (r=0.76) and Ca (r=0.59); Zn with Al (r=0.37); Cr with Ca (r=0.42) and V (r=0.37) while Al goes well with Ca (r=0.56). Extensive correlations of Al with Mn, Pb, Ni, Zn in core TIVM indicates the metals are associated with terrigenous inputs. Furthermore, Zn is also found to associate with Fe, TOC and TN suggesting that this metal might have an anthropogenic and also a natural source in sediments of the study area.

3.1B.5b. Factor analysis

Varimax normalised factor analysis was carried out on both the cores sampled from the mangrove regions resulting in three factors for core TIIM and four factors for core TIVM. The total variance along with eigen values are given in Table 3.1B.2 and 3.1B.3.

Table 3.1B.2. Varimax normalised factor analysis for core TIIM

	Factor 1	Factor 2	Factor 3
Total Variance	42.56	19.79	13.30
Eigen Value	7.66	3.56	2.39
Sand	-0.43	0.24	-0.59
Silt	-0.06	**0.92**	0.15
Clay	0.12	**-0.93**	-0.06
TOC	0.10	0.00	**-0.84**
TP	**0.95**	0.07	0.16
TN	0.13	-0.08	-0.62
pH	**-0.89**	0.22	0.07
Fe	**0.77**	0.50	0.29
Mn	**0.96**	0.09	0.12
Cu	0.65	0.50	0.48
Pb	0.14	0.29	0.64
Co	-0.51	-0.41	-0.11
Ni	-0.68	-0.45	0.27
Zn	**0.73**	-0.04	0.57
Cr	0.04	0.68	-0.01
V	**0.93**	-0.07	0.04
Al	**-0.79**	0.17	0.52
Ca	**0.89**	-0.04	-0.16

Core TIIM: Three factors are extracted resulting in 75.65 % of total variance. Factor 1 accounts for 42.56 % of total variance and shows significant positive loading of TP, Fe and Mn on Cu, Zn, V and Ca. Factor 2, on the other hand with 19.79 % of total variance, exhibits strong positive loadings of silt and good loadings of Fe on Cu and Cr. The third factor (Factor 3) with 13.30 % of total variance displays close associations of Cu, Pb, Zn and Al. Cu and Zn appear to favour terrestrial organic matter (TP) which primarily settles down in the inner part of the creek by adsorption. Sewage and agricultural runoff are considered to be the major anthropogenic source of phosphorus to the coastal marine environment (Kumarsingh et al., 1998). Cu and Zn appear in

factor 1 and also factor 3 indicating natural (weathering) as well as anthropogenic sources (domestic and industrial effluents). Zn and Cu may be derived from natural sources in the soil and sediment and sewage effluent discharges (Benoit, 1999). In this core, TP along with silt, Fe, Mn and Al are found to contribute significantly in metal distribution.

Table 3.1B.3.Varimax normalised factor analysis for core TIVM

	Factor 1	Factor 2	Factor 3	Factor 4
Total Variance	29.44	18.60	14.78	9.44
Eigen Value	5.30	3.35	2.66	1.70
Sand	0.64	-0.09	0.08	-0.43
Silt	0.08	-0.09	**-0.93**	0.17
Clay	-0.16	0.10	**0.92**	-0.12
TOC	**0.93**	-0.12	0.04	0.12
TP	0.36	-0.21	0.61	0.10
TN	**0.87**	-0.12	0.00	0.21
pH	-0.29	0.20	0.30	-0.70
Fe	0.18	0.22	-0.03	**0.89**
Mn	-0.19	0.65	-0.31	-0.16
Cu	**0.72**	0.12	-0.20	0.04
Pb	0.12	0.60	0.07	-0.59
Co	0.45	-0.12	-0.55	0.11
Ni	0.03	**0.88**	0.21	0.07
Zn	0.63	0.50	-0.21	0.41
Cr	-0.48	0.42	-0.02	-0.30
V	-0.62	0.14	0.50	-0.32
Al	0.03	**0.86**	0.21	0.05
Ca	-0.17	**0.77**	-0.04	0.05

Core TIVM: In this core, four factors contribute 72.26 % of the total variance. Factor 1 with 29.44 % of total variance shows positive loading of TOC, TN and sand on Cu, Co and Zn while the second factor with 18.60 % of total variance projects good loading of Mn and Al on Pb, Ni, Zn, Cr and Ca. The third factor results in 14.78 % of total variance and displays good loading of clay and TP on V. The fourth factor has 9.44 % of total variance and exhibits positive loadings of Fe on Zn. The main source of Cu and Zn might be from shipping activities while the remaining elements project a lithogenic source. In this mangrove core, clay, organic matter, Al and also Fe and Mn seem to be strong metal carriers.

From the correlation and factor analyses carried out, two agents controlling the behaviour of the analysed elements were identified in the creek system namely anthropogenic and the terrestrial supply. Since mangrove ecosystems are located in the transition between the continental and marine environments (Cooper, 2001), the sediment for their formation is supplied by land discharges, tidal currents and wave actions (Anthony et al., 2004). In both the mangrove regions, Ca must have a marine origin since biogenic carbonates (especially carbonate shells) are found to constitute an important sediment fraction in the region (Thane creek). Among the metals, Cu

and Zn display an anthropogenic origin while the rest of the metals exhibit a natural source. In general, both the mangroves environments are subjected to similar sediment-metal association with organic matter, Fe-Mn oxides along with finer sediment components as dominant factors in the metal distributions.

3.1B.6. Pollution indicators

3.1B.6a. Enrichment factor

For both the mangrove cores from the creek region, Enrichment factor (EF) was computed. Figures 3.1B.7 and 3.1B.8 give the down-core profiles of EF for both the cores. In core TIIM (Fig. 3.1B.7), Fe, Mn, Ni, Zn and Cr have low EF values (< 1.5) but their values are found to increase towards the surface. The remaining elements show high EF values (> 1.5). Cu, Pb and V show an increase from the bottom to the surface. Although Co displays enriched values, it exhibits no definite trend. When the average EF values are considered, Co (avg. 2.18) displays the highest value while Ni (avg. 1.12) shows the lowest EF value. The remaining elements exhibit a decreasing trend shown by Cu (avg. 1.88), V (avg. 1.49), Pb (avg. 1.46), Fe (avg. 1.15), Mn and Zn (avg. 1.13).

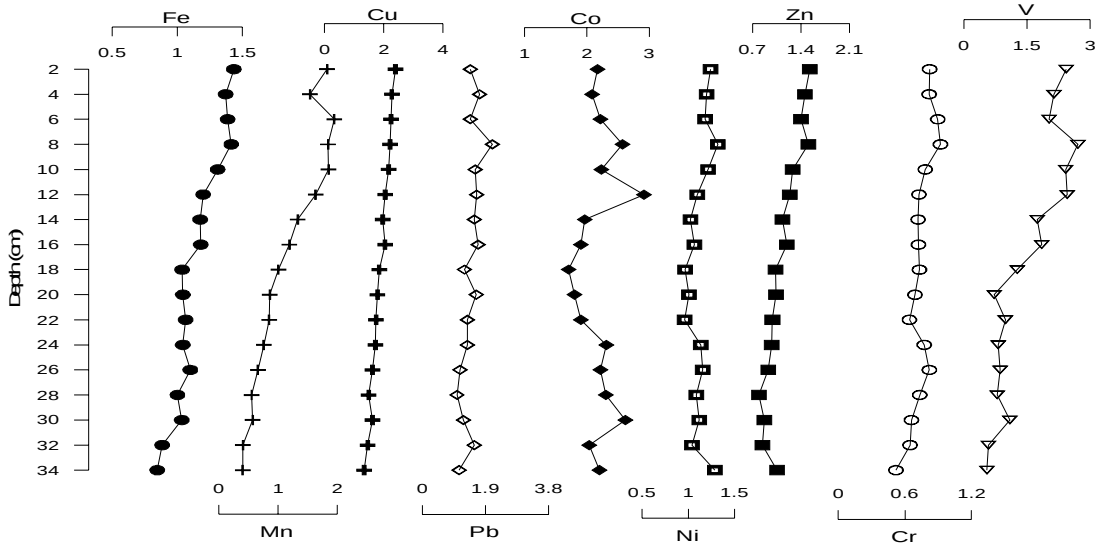

Fig. 3.1B.7. Down-core plot of EF for core collected from the upper middle creek region (core TIIM)

In the case of mangrove core TIVM (Fig. 3.1B.8), Fe, Zn, Cr and V have lower EF values while Mn, Cu, Pb, Co and Ni project enriched concentrations. All the elements show either constant or increasing trends from the bottom to the surface, except for V which shows a decrease. Based on average EF values, Mn shows the highest EF value (average 2.30) followed by Cu (avg. 1.99), Pb and Co (avg. 1.90), Ni (avg. 1.85), Cr (avg. 1.32), Zn (avg. 1.23), Fe (avg. 1.16) and V (avg. 1.09). Municipal and/or industrial wastewater discharges into coastal zones are the most

important sources for contamination of water and sediment with heavy metals (Gonzalez and Brugmann, 1991). In general, in the creek region the average values of EF follow a decreasing order as given below,

Co > Cu > Mn > Pb > Ni > V > Zn > Fe > Cr

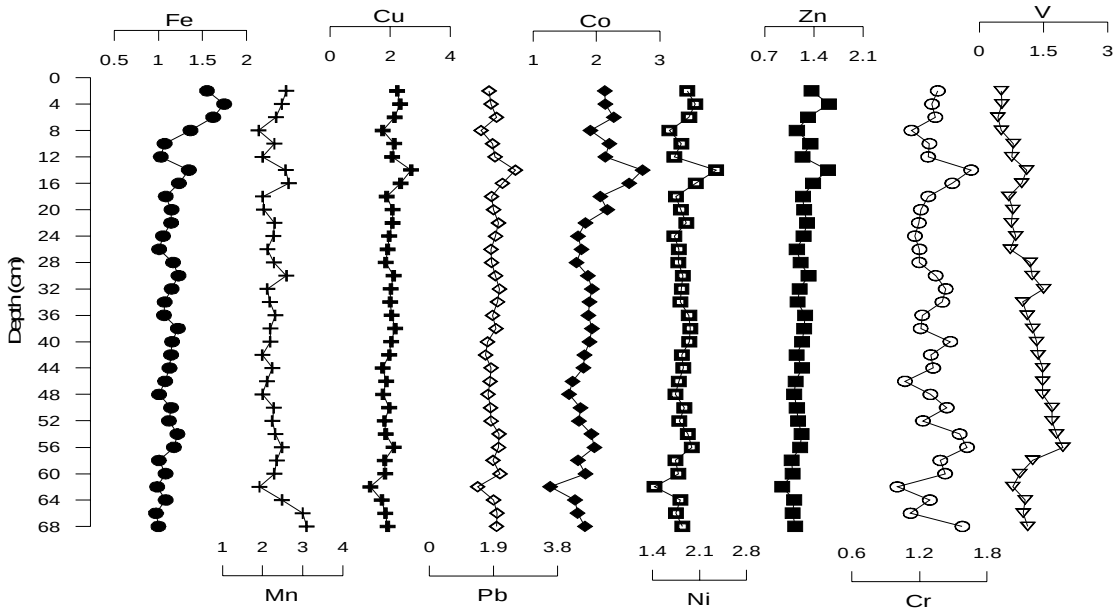

Fig. 3.1B.8. Down-core plot of EF for core collected near the creek mouth (core TIVM)

3.1B.6b. Geoaccumulation Index

Figure 3.1B.9 gives the Igeo plots for both the mangrove cores. The Igeo values suggest that the sites are affected differently for different metals. In core TIIM (Fig. 3.1B.9a), all the subsamples for Co whereas some subsamples for Cu and V fall in the moderately polluted class. The remaining elements fall in the unpolluted to moderately polluted class. In the case of core TIVM (Fig. 3.1B.9b), all the elements fall in unpolluted to moderately polluted class except for few subsamples for Mn which fall in the moderately polluted class. The observation suggests that either the area is well flushed by the incoming tides and sea waves or that the metals get deposited in the mudflat region prior to its entry in the mangrove region.

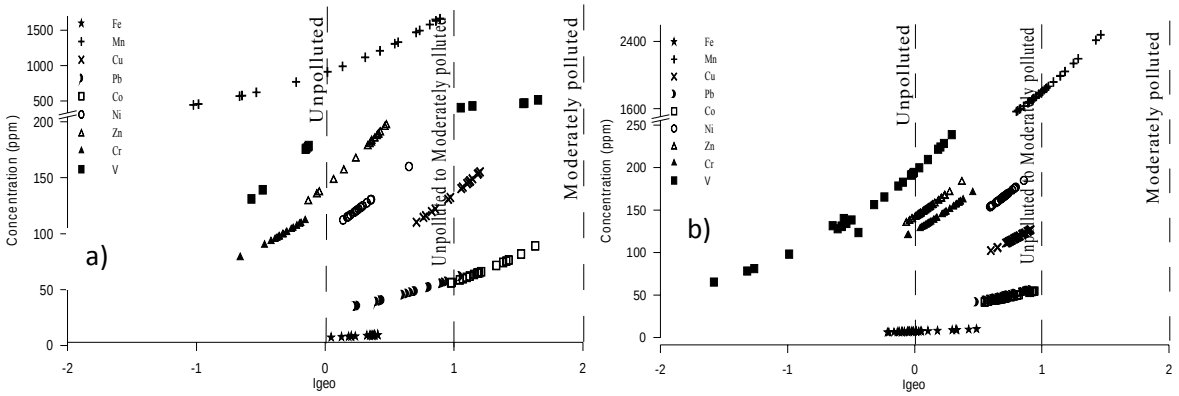

Fig. 3.1B.9. Metal concentration and Igeo plots for mangrove cores collected from a) the upper middle creek region (core TIIM) and b) near the creek mouth (core TIVM)

3.1B.7. Isocon plot

The study of spatial characteristic of sediment distribution is useful in understanding the processes of sediment movement and source of sediments in the creek. Figure 3.1B.10 shows the isocon plot between core TIIM and core TIVM. In core TIIM, V and Co along with silt and sand shows higher concentration while in core TIVM, TOC, TP, Mn, Ca and clay deviate away from the isocon line. The accumulation of sediments is strongly controlled by the nature of substrate as well as the physicochemical conditions controlling dissolution and precipitation. The core TIVM, which lies near the creek mouth, seems to be well flushed by the incoming tides and do not exhibit any metal enrichment as compared to core TIIM lying in upper middle creek region. Core TIIM is well sheltered away from the main channel of the creek and hence provides an ideal environment for deposition of metals.

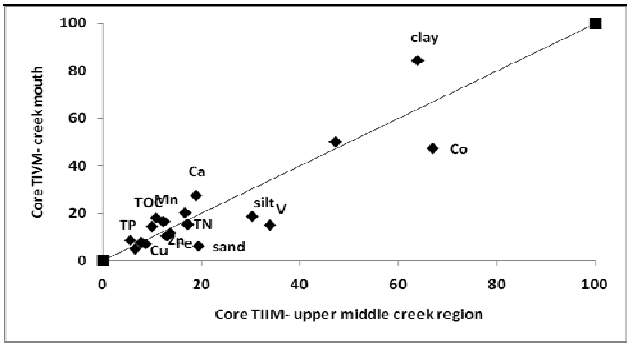

Fig. 3.1B.10. Isocon plot for mangrove cores collected from the upper middle creek region (core TIIM) and near the creek mouth (core TIVM)

3.1B.8. Relationship between the mudflats and mangroves

The examination of the spatial differences of the heavy metals content in sediments allows the identification of the presence of anthropogenic effects, possible sources of contamination and effects due to the transport of pollutants from other areas (Huang and Lin, 2003). Therefore, in order to compare the mudflat and mangrove regions, isocon plots were considered. Figure 3.1B.11 gives the plots of core TII and core TIV of mudflat and core TIIM and core TIVM of mangrove regions.

In the upper middle creek region (Fig. 3.1B.11a), the mangrove core is found to display higher amounts of most of the metals studied as compared to the mudflat core which shows higher Mn and Ca contents. Usually it is thought that high metal concentrations are related to high organic carbon content and finer grain size of the sediments. However, most of the sediment parameters studied (pH, sand, silt, clay, organic matter, Fe, Mn, Al), show similar distribution and contents in both the sub-environments. Also, from the correlation and factor analyses (section 3.1B.5), it is seen that Fe and Mn exhibits better associations with metals in the mangrove region as

compared to the mudflat region which displays good association only with Mn. This association can be partly responsible for the increased metal adsorption in the mangrove region. Strong metal correlations with Al and low value of enrichment factors in the upper creek region especially for core TII mudflat, indicates that the elements present in the sediments are due to natural processes (Fernandes and Nayak, 2012a).

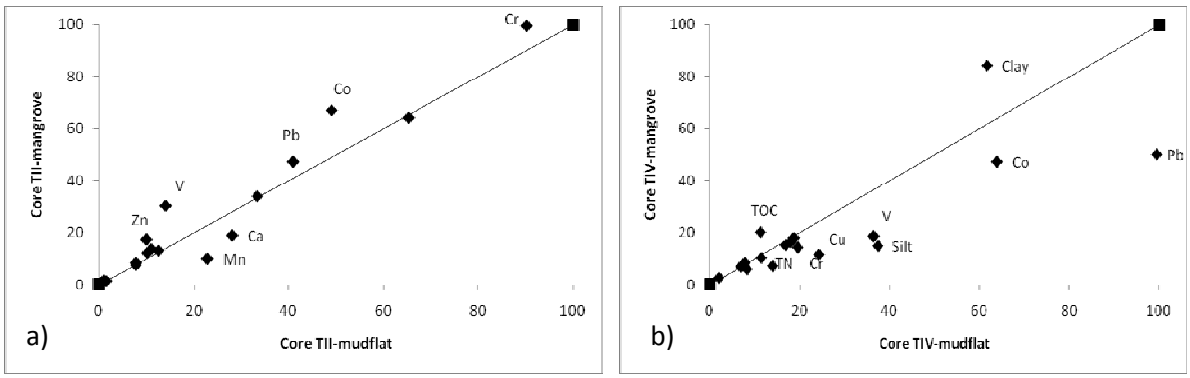

Fig. 3.1B.11. Isocon plots for mudflat and mangrove cores collected from the a) upper middle creek region (core TII) and b) near the creek mouth (core TIV)

The isocon plot of cores sampled near the creek mouth (Fig. 3.1B.11b), shows greater amounts of metals in the mudflat region as compared to the mangrove region. At the near shore zone of the creek, waves are the main agent for bed erosion and sediment suspension. Release of organic matter from sediments can result due to stirring action by strong tidal waves. Further, in estuarine and near-shore environments, flocculation takes place. This is because in salty and brackish waters, the surface charge of particles approaches zero hence repulsion significantly decreases (Wangersky, 1977), and particles can form large aggregations, known as flocs, which may accelerate the sinking and sedimentation of organic particulate matter. Therefore, flocculation and subsequent sedimentation of suspended particulate organic matter at the creek mouth can explain the observed pattern of high metal concentration. On the other hand, the mangroves being at a higher elevation as compared to the mudflats are affected to a lesser extent by re-suspension of sediments caused by tidal current and wave action.

SECTION 2: ULHAS ESTUARY

Seven sediment cores from the intertidal regions, five from mudflats and two from mangroves, covering the entire Ulhas estuary from the head to the mouth, including Northern and Southern banks, were collected during September 2008 (Fig. 3.2A.1). For the purpose of this study, the estuary has been divided into five regions, namely the estuary head region represented by core UIII, upper estuary by core UIV, middle estuary by core UII, lower estuary by core UV while core UI lies near the estuary mouth. All the cores were sampled from mudflats of the main channel of the estuary.

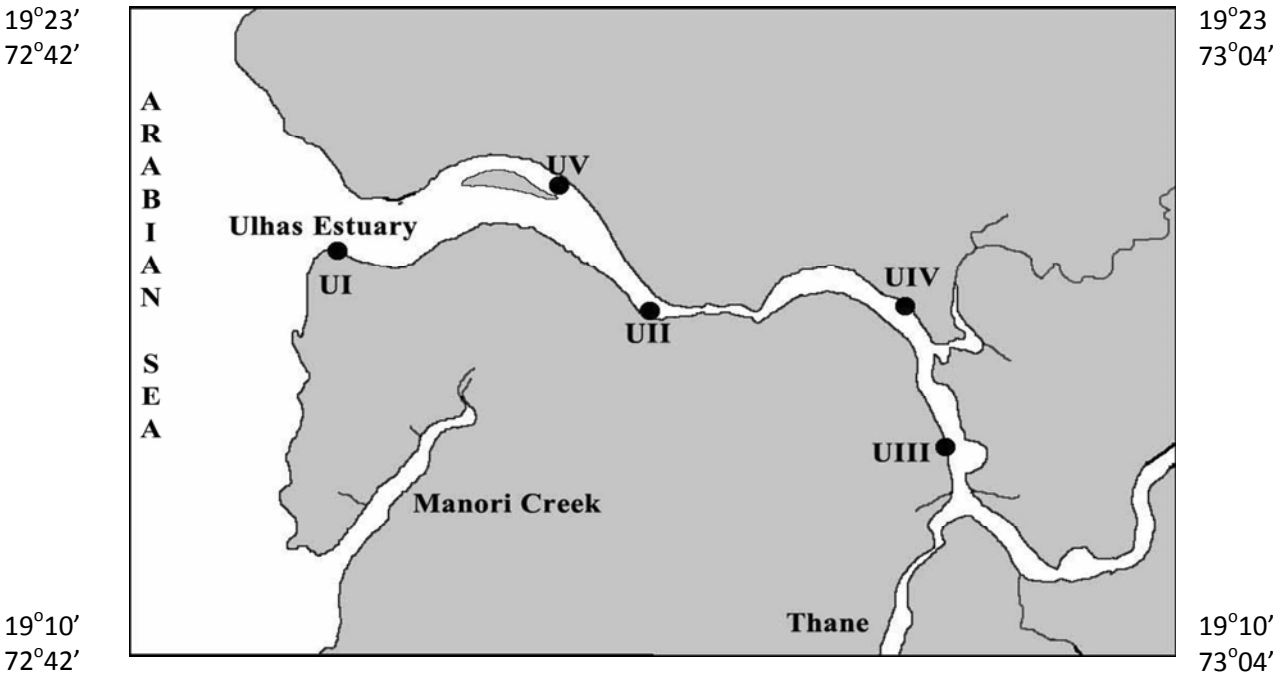

Fig. 3.2A.1. Map showing the sampling locations in Ulhas estuary

3.2A. Mudflats

3.2A.1. Visual description

The sediments of core UIII (70 cm long) collected from the head region of the estuary shows uniform grey colour from the bottom to 14 cm depth while above it, brown colour is seen till the surface. Sediment conditions become increasingly reducing with depth, because of limited diffusion of oxygen across the sediment/water interface (Alongi et al., 1996; Black et al., 1997; Hargrave et al., 1997), often producing visible surface effects, such as black/grey sediments containing iron sulphides. For cores collected from the middle estuary and near the estuary mouth, similar types of colour variations are observed. From the bottom to 30 cm in core UII (60 cm long), and till 22 cm in core UI (26 cm long), mixed colour of brown and black are seen. Further above, till the surface, both the cores exhibit uniform brown colour. In the case of core UIV (60 cm long), sampled from the upper estuarine region, dark brown colour is seen from the bottom to 26 cm depth followed by brown colour upto the surface. Also, between the depths of

26 and 16 cm, presence of sand is noticed. On the other hand, in core UV (28 cm long) retrieved from lower middle estuary, two distinct colour variations are seen, i.e. mixed brown and grey colour from the bottom to 12 cm depth and brown colour for the rest of the core. Additionally, the presence of fragment of carbonate shells are detected in the coarse-grained fraction.

3.2A.2. Sediment components (sand, silt, clay)

In an effort to gain a better understanding of the depositional environment, in terms of identifying areas of potential contamination, the sediment data was classified based on the percentage of sand, silt and clay at each of the sites. The sediment components vary significantly in the region. The upper estuarine site (UIV) has higher average percentage of fine sediments and the values decrease with increasing proximity to the estuary mouth. On a whole, clay is found to be the dominant sediment component with average percentage >50 % while sand is present in low percentage (avg. < 20 %) and for core UV as low as < 2 %. In the entire estuary, sand ranges from 1.88-35.52 %, while silt and clay vary from 18.44-36.64 % and 41.59-69.86 % with average values of 14.02 %, 28.85 % and 57.13 %, respectively. The depth-wise distribution patterns are shown in Figures 3.2A.2 - 3.2A.4.

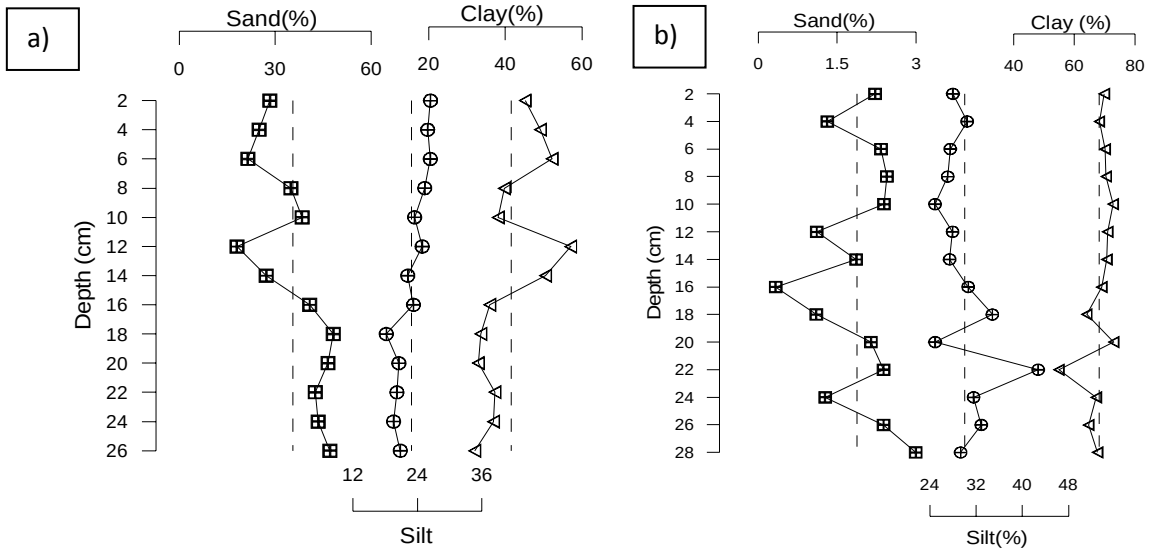

Fig. 3.2A.2. Vertical profiles of sediment component a) near estuary mouth (core UI) and b) lower estuary (core UV)

In core UI (near estuary mouth) sand, silt and clay range from 18.05-48.18 %, 18.22-26.45 % and 32.00-57.04 % with average values of 35.52 %, 22.89 % and 41.59 %, respectively. Sediments at this site show high concentrations of sand throughout the core length. The sediment in core UI can be considered to be sand dominated, and thus reflects a relatively high energy depositional environment with marine derived sand. Sand shows a decrease from the bottom to the surface except for an increased peak seen at 10 cm depth (Fig 3.2A.2a). Silt and clay exhibit an increase towards the surface. However, silt shows a uniform increase while clay fluctuates

irregularly. In general, sand and clay are found to show corresponding opposite trends to each other. In the core collected from lower estuarine region (UV), the range and average values vary from 0.33-2.99 %, 1.88 % for sand, 24.89-42.74 %, 30.01 % for silt and 55-73 %, 68 % for clay. The distribution of sand is found to be very irregular from the bottom to the surface (Fig 3.2A.2b). On the other hand, silt and clay display corresponding opposite trends to each other with silt decreasing and clay increasing upto the surface.

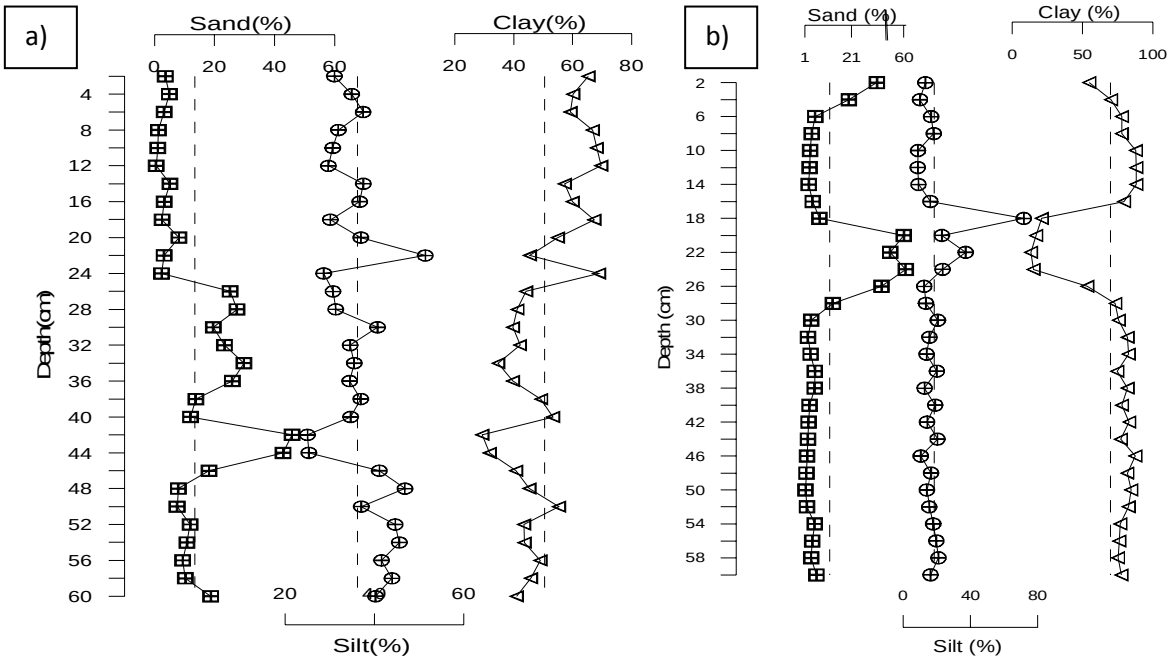

Fig. 3.2A.3. Vertical profile of sediment components in middle (core UII) and upper (core UIV) estuarine regions

In the middle estuarine region (Fig. 3.2A.3a), sand, silt and clay in core UII vary from 0.59-45.76 %, 25.04-51.41 % and 54.88-72.96 % with average values of 13.33 %, 36.27 % and 50.40 %, respectively. The vertical distribution of sand, in general, shows a decreasing trend from the bottom to the surface. Between the depths of 48 and 24 cm, large fluctuations with higher values are seen followed by a gradual decrease upto the surface. Silt decreases and clay increases depth-wise, with irregular fluctuating trends from the bottom to the surface. In the case of upper estuarine region, the values range for core UIV as 1.26-61 % for sand, 8.79-72 % for silt and 13.44-88 % for clay with averages of 11.70 %, 18.44 % and 70 %, respectively. From the depth profile (Fig. 3.2A.3b), it is observed that sand and clay show opposite trends to each other, with sand increasing and clay decreasing in the upper 6 cm. Between 30 and 18 cm depths, sand shows high values and is compensated by low values of clay. Silt, on the other hand, displays more of a constant trend from the bottom to the surface except for a peak at 18 cm depth. In both the cores, it is seen that sand percentage abruptly increases in the middle portion dividing the cores into three layers. The upper and lower layers are dominated by mud while the middle layer

exhibits higher sand contents. Near the inner estuarine region (core UIII), sand, silt and clay range from 2.01-13.65 %, 23.15-64.60 % and 25.20-70 % with average values of 7.65 %, 34.64 % and 55.71 %, respectively. Sand fluctuates irregularly throughout the core (Fig 3.2A.4). Silt and clay project corresponding opposite profiles to each other, with silt increasing and clay decreasing from the bottom to 56 cm depth. Further above, both the components show constant trends till the surface. An increased peak for silt and a decreased peak for clay are noticed at 14 cm depth.

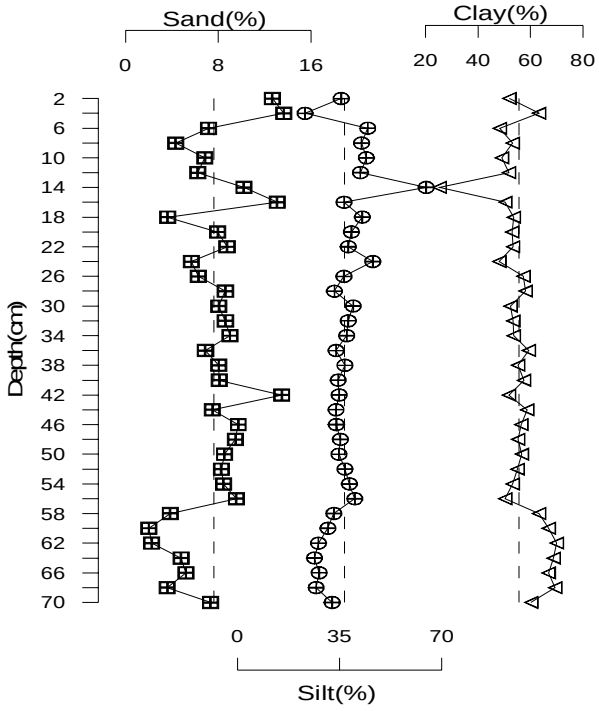

Fig. 3.2A.4. Vertical distribution profile of sediment components for inner estuarine region (core UIII)

Information on grain size distribution helps in understanding and characterizing the depositional environment. In the present study, the grain size distribution patterns show that the Northern bank (core UV) of the estuary has finer material relative to the Southern bank (core UII). This could be attributed to differences in the energy level. The estuarine region due to mixing of sea and river water produces turbulence and creates complex energy conditions. In estuaries, generally fine mud gets deposited near the head and other sheltered regions, while along the main channel and at the mouth, coarser sediments are deposited. From the estuarine inner end to the mouth, a gradual increase in sand percentage and a decrease in silt percentage are observed. Clay, on the other hand, does not show any distinct trend. The dominance of silt in the inner end of the estuary might be due to weak tidal currents. Presence of coarser sediment at the mouth region implies high energy conditions. In general, in most of the cores studied, clay abundance when present alternates with the depth profile of silt. Most of the sediment samples are dominated by clay size material with almost equal portions of sand and silt put together. In

addition, the finer sediment component is high in the surface and tends to decrease down the profile, accompanied by an increase in coarser sediment fraction (sand). The varying thickness of the different layers and the variations in grain size in some of the cores sampled (cores UII and UIV) suggest that sedimentation rates and processes are not the same all along the estuary. Also, variable amounts of deposition in the study sites can explain the inconsistent admixture of sand and clay fractions in the individual cores. Textural variation in the sediments of the estuary can be related to the terrigenous input from the upstream rivers, the bed morphology, and to currents and wave motion. Meandering controls the distribution of energy within river/estuary. The Northern part seems to be with weaker currents and could act as a deposition center of sediments and thus have finer sediments.

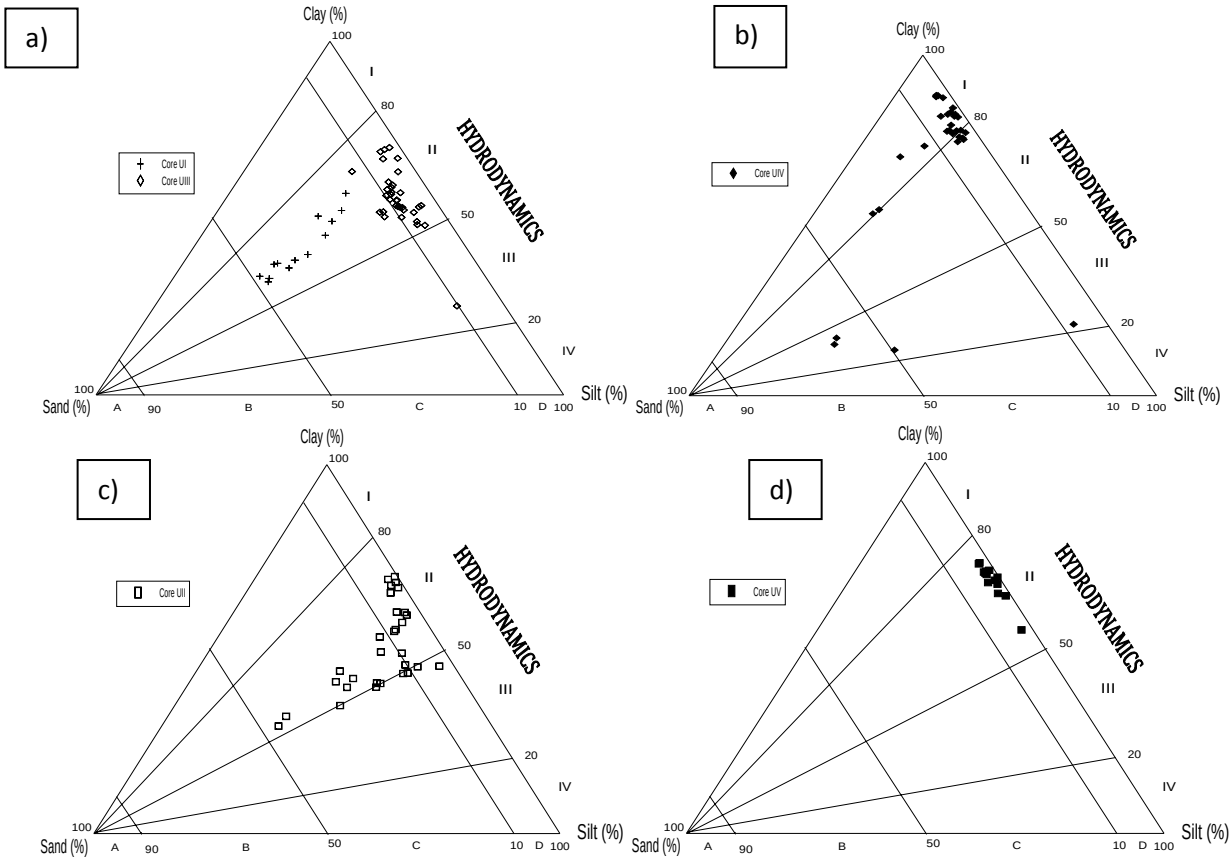

Fig. 3.2A.5. Ternary plots after Pejrup (1988) for cores from the a) estuary mouth (UI) and inner end (UIII), b) upper (UIV), c) middle (UII) and d) lower (UV) estuarine regions

Figure 3.2A.5 is a ternary diagram of the textural classification for soils/sediments proposed by Pejrup (1988), to understand the hydrodynamic conditions, based on the relative proportions of sand, silt and clay size particles in the sediment samples. In the present study, it is seen that for core UIII, almost all the subsamples fall in group II of section D while only two subsamples fall in group II of section C (Fig. 3.2A.5a). This observation suggests presence of relatively less violent hydrodynamic condition resulting in deposition of finer sediments. In the upper estuarine

region (UIV), the subsamples are observed to be scattered with majority of them falling in group I of section D (Fig. 3.2A.5b). The river discharge along with the tidal flow from the sea must be contributing to such an environment, consisting of a mixture of finer and coarser sediments.

In the case of core UII, retrieved from the middle estuarine region, the subsamples are observed to be distributed in sections C and D of group II (Fig. 3.2A.5c) pointing to a less violent hydrodynamic condition composed of coarser and finer sediment samples. The core sampled from the lower estuarine portion (UV) show similar hydrodynamic condition as that of core UIII, with all the subsamples falling in group II of section D (Fig. 3.2A.5d). On the other hand, all the sediment fractions from core UI, near the estuarine mouth, fall in group II of section C (Fig. 3.2A.5a) indicating coarser sediments in relatively less violent hydrodynamic conditions.

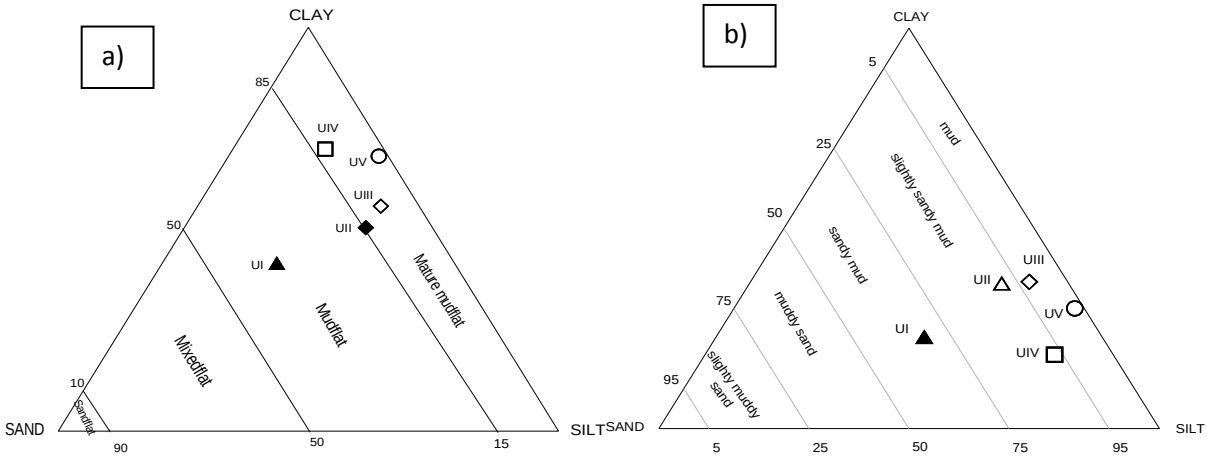

Fig. 3.2A.6. Ternary plots by a) Reineck and Siefert (1980) and b) Flemming (2000)

Also ternary diagram proposed by Reineck and Siefert (1980), was considered for textural identification. When the data points are plotted (Fig. 3.2A.6a), it is observed that the sediments from the upper, middle, lower and inner end of the estuary fall largely in the Mature Mudflat class. On the other hand, the sediments from core UI collected near the estuary mouth fall in the Mudflat class. Another sediment classification on ternary diagram introduced by Flemming (2000) was also applied to the data set. The plot (Fig. 3.2A.6b) shows that the subsamples of core UIII and UV of the estuarine region fall in the Mud class while cores UII and UIV fall in the Slightly Sandy Mud class. The sediments from core UI fall in Sandy Mud class.

3.2A.3. Clay mineralogy

Clay mineral analysis using XRD was performed on subsamples of selected cores namely from the upper (core UIV), lower (core UV) and near the estuary mouth (core UI). The results show that the sediments in the region consist mostly of the minerals smectite, kaolinite, chlorite and illite. Mineral composition is found to be consistent among selected cores, with smectite (avg.

62.66 %) as the major constituent clay mineral followed by illite (avg. 19.14 %), chlorite (avg. 9.85 %) and kaolinite (avg. 8.34 %). In the entire estuary, the percentage of smectite ranges from 48.68-78.33 %, from 7.91-31.02 % for illite, from 5.99-24.16 % for chlorite and from 4.35-12.58 % for kaolinite. The vertical distribution profiles of the cores are shown in figure 3.2A.7.

Clay mineral analysis using XRD was performed on subsamples of selected cores namely from the upper (core UIV), lower (core UV) and near the estuary mouth (core UI). The results show that the sediments in the region consist mostly of the minerals smectite, kaolinite, chlorite and illite. Mineral composition is found to be consistent among selected cores, with smectite (avg. 62.66 %) as the major constituent clay mineral followed by illite (avg. 19.14 %), chlorite (avg. 9.85 %) and kaolinite (avg. 8.34 %). In the entire estuary, the percentage of smectite ranges from 48.68-78.33 %, from 7.91-31.02 % for illite, from 5.99-24.16 % for chlorite and from 4.35-12.58 % for kaolinite. The vertical distributions of the cores are shown in figure 3.2A.7.

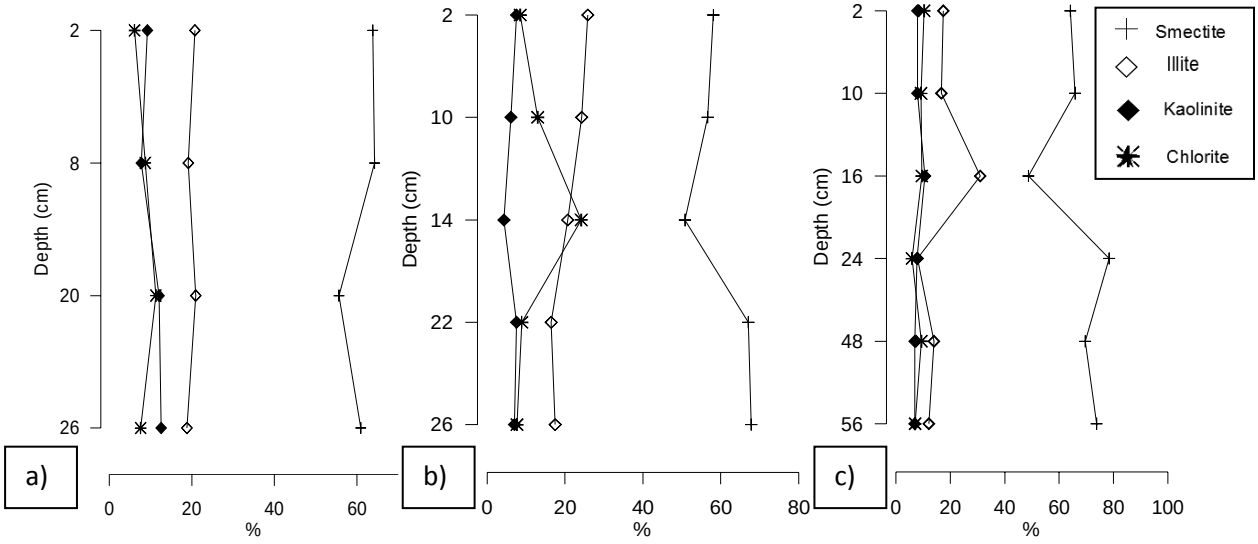

Fig. 3.2A.7. Depth-wise distribution of clay minerals a) near the mouth (core UI) b) lower estuary (core UV) and c) upper estuary (core UIV)

For the core collected near the estuary mouth (UI), the range and average values are 55.64-64.27 %, avg. 61.18 % for smectite; 18.83-21.01 %, avg. 19.95 % for illite; 6.16-11.30 %, avg. 8.46 % for chlorite and 7.79-12.58 %, avg. 10.41 % for kaolinite. From the depth-wise distribution plot (Fig. 3.2A.7a), smectite and illite show opposite trends to each other, with alternate increasing and decreasing patterns. On the other hand, chlorite initially increases at the bottom followed by a decreasing trend towards the surface while kaolinite decreases from the bottom to 8 cm and then increases at the surface. In core UV, from the lower estuarine region, the mineral constituents vary from 50.83-67.79 % for smectite, 16.46-25.87 % for illite, 5.99-10.45 % for chlorite and 4.35-7.59 % for kaolinite with averages of 60.08 %, 20.95 %, 12.43 % and 6.53 %, respectively. Smectite and chlorite show corresponding opposite trends to each other (Fig.

3.2A.7b) while illite and kaolinite exhibit similar decreasing and increasing trends from the bottom to the surface. In the core collected from upper estuary (UIV), smectite ranges from 48.68-78.33 %, illite from 7.91-31.02 %, chlorite from 5.99-10.45 %, kaolinite from 6.99-10.70 % with average values of 66.73 %, 16.53 %, 8.65 % and 8.09 %, respectively. From the down-core plot (Fig. 3.2A.7c), smectite and illite are found to show opposite trends to each other with alternate increasing and decreasing patterns while kaolinite and chlorite display constant trends. The study identified a similar mineral assemblage in the sediments, dominated by smectite which reflects the geology of the study area. The minerals in the estuarine region originate from the weathering of basalt rocks, the primary source of minerals to sediments of the Ulhas estuary.

3.2A.4. Porosity and dry bulk density

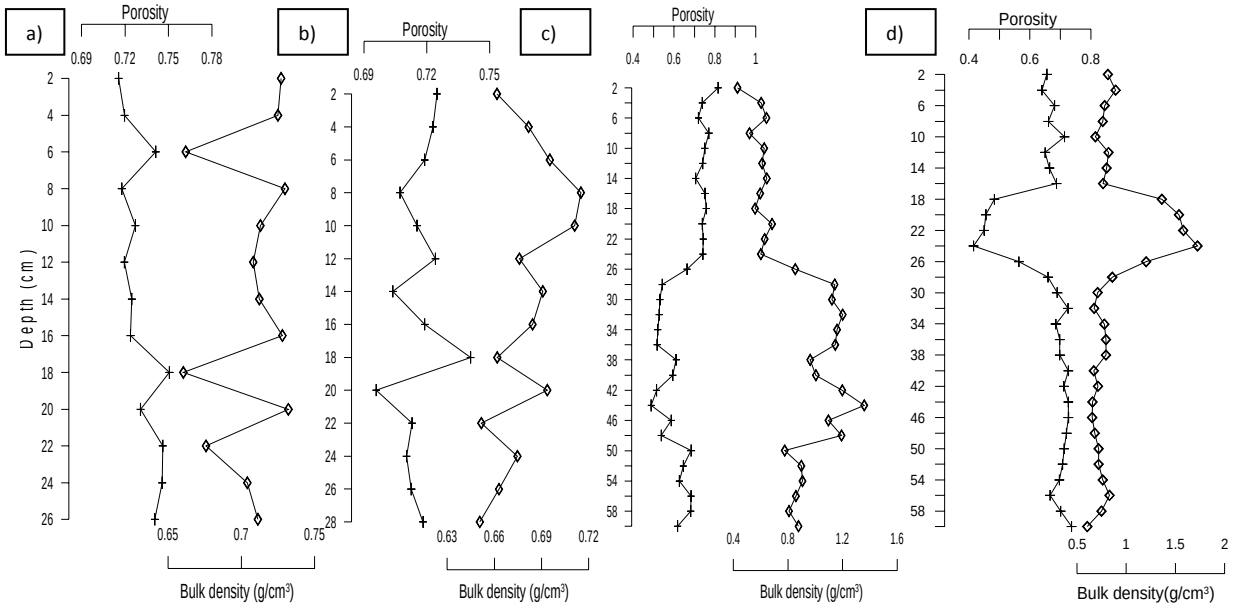

Fig. 3.2A.8. Vertical distribution profiles of Porosity and Dry bulk density in a) core UI, b) core UV, c) core UII and d) core UIV

Four cores sampled from the estuary were selected for porosity and dry bulk density analysis. In the estuarine region porosity varies from 0.42-0.82 while the dry bulk density ranges from 0.43-1.72 g/cm^3 with averages of 0.69 g/cm^3 and 0.78 g/cm^3, respectively. Figure 3.2A.8 gives the vertical distribution profiles for the selected cores. In core UI (Fig. 3.2A.8a), porosity ranges from 0.72-0.75 with an average of 0.73 and exhibits a decreasing trend from the bottom to the surface with minor fluctuations. On the other hand, dry bulk density values vary from 0.66-0.73 g/cm^3 with 0.71 g/cm^3 average and shows large fluctuations from the bottom to the surface. In core UV (Fig. 3.2A.8b), porosity (range- 0.70-0.74, avg. 0.72) and dry bulk density (range- 0.63-0.71 g/cm^3, avg. 0.68 g/cm^3) display an opposite trend.

Cores UII (Fig. 3.2A.8c) and UIV (Fig. 3.2A.8d), range from 0.49-0.82; 0.42-0.72 with averages of 0.65; 0.66 for porosity and 0.43-1.36 g/cm^3; 0.60-1.72 g/cm^3 with averages of 0.87 g/cm^3; 0.87 g/cm^3 for dry bulk density, respectively. Corresponding opposite vertical trends are observed between porosity and bulk density profiles in both the cores. Cores UV and UII show low porosity values at the bottom while cores UI and UIV display lower values at the surface. In cores UII and UIV, a pronounced feature in the porosity and dry bulk density contents are clearly seen between the depths of 24 to 50 cm and again from 16 to 28 cm. This is entirely consistent with the grain-size spectrum (Fig. 3.2A.3) and reflects the fact that the porosity of the sand from the middle unit is much lower than the silt-rich sediments at the top and bottom units (Fig. 3.2A.2). The topmost part of the core is usually covered by a layer of recent sediments, which are poorly consolidated (Winterhalter, 1992), laminated or bioturbated muddy clays or silts.

3.2A.5. Magnetic susceptibility

Three cores were selected from the estuarine region for studying the magnetic susceptibility related parameters viz, cores collected near the estuary mouth, lower and upper estuarine regions. In the estuarine region, the highest average values for χ_{lf} (485 x 10^{-8}m^3/kg), χ_{ARM} (15846 x 10^{-8}m^3/kg), SIRM (8417 x 10^{-5}Am^2/kg) and HIRM (126 x 10^{-5}Am^2/kg) are seen for core UIV, from upper estuary, while maximum values of χ_{ARM}/SIRM (3.19 x 10^{-5}m/A), χ_{ARM}/χ_{lf} (49.81), Hard (2.08 %) and χ_{fd} (2.99 %) are seen for core UV, from the lower estuary. On the other hand core UI, near the estuary mouth shows highest average values of SIRM/χ_{lf} (18.04 x 10^3A/m) and S-ratio (99 %). This core also shows the lowest average values for χ_{ARM} (12186 x 10^{-8}m^3/kg), χ_{ARM}/SIRM (1.57 x 10^{-5}m/A), χ_{ARM}/χ_{lf} (28.17), Hard (1.24 %) and χ_{fd} (1.77 %). Lowest average values of χ_{lf} (220 x 10^{-8}m^3/kg), SIRM (3685 x 10^{-5}Am^2/kg), SIRM/χ_{lf} (15.78 x 10^3A/m), HIRM (72 x 10^{-5} Am^2/kg) and S-ratio (97 %) are seen in core UV. In general, the highest concentrations of most of the magnetic parameters are present at the upper estuarine region while the estuary mouth displays the lowest values. Down-core trends in selected mineral magnetic parameters are plotted in Figures 3.2A.9-3.2A.11.

From the down-core distribution (Fig.3.2A.9), it is seen that the values in core sampled near the estuary mouth (UI), varies from 342-433 x 10^{-8}m^3/kg for χ_{lf}, 8689-12186 x 10^{-8}m^3/kg for χ_{ARM}, 6098-8103 x 10^{-5}Am^2/kg for SIRM, 3065-16148 x 10^{-5}m/A for χ_{ARM}/SIRM, 17.36-19.03 x 10^3A/m for SIRM/χ_{lf}, 20.40-33.78 for χ_{ARM}/χ_{lf}, 14.76-146 x 10^{-5}Am^2/kg for HIRM, 0.24-1.86 % for Hard, 98-100 % for S-ratio and 1.07-3.37 % for χ_{fd}. The core displays similar vertical patterns for χ_{lf} and SIRM, i.e. alternate decreasing and increasing trends are observed from the bottom to the surface. χ_{ARM}, HIRM and Hard form one group while χ_{ARM}/SIRM and χ_{ARM}/χ_{lf}

forms the other group with identical vertical distributions. SIRM/χ_{lf} uniformly decreases from the bottom to the surface while S-ratio and χ_{fd} (%) show increasing trends from the bottom towards the surface.

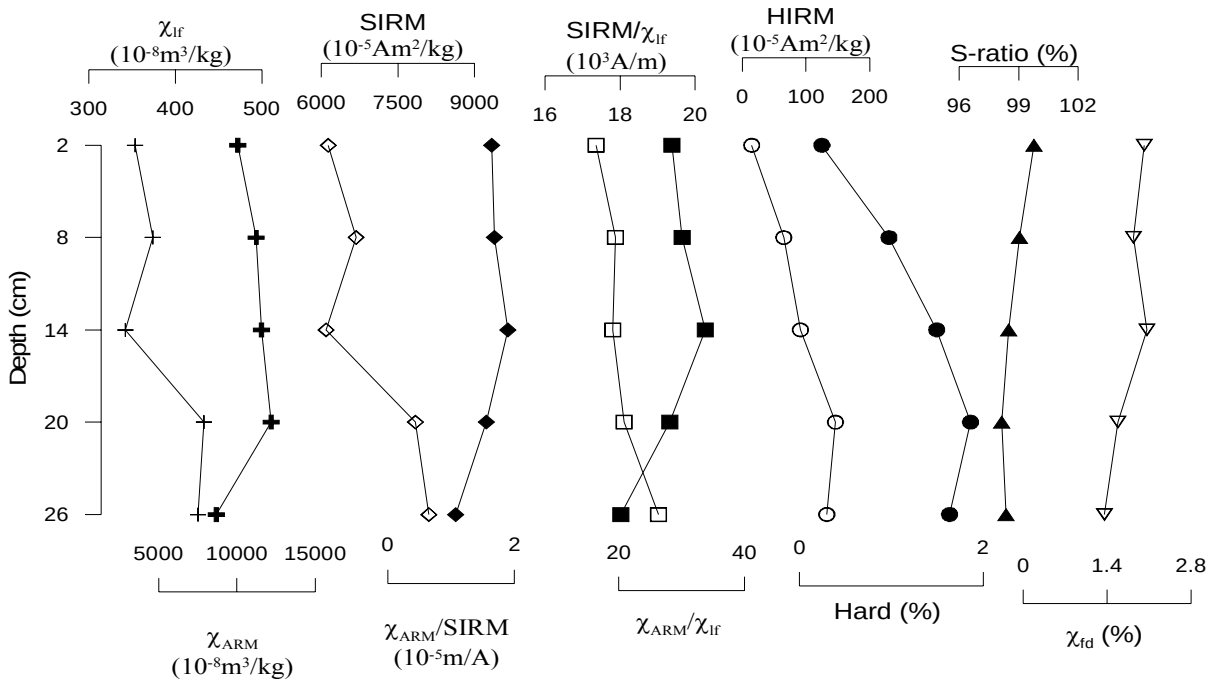

Fig.3.2A.9. Depth-wise distribution of magnetic susceptibility parameters for core UI

In the case of lower middle creek region (Fig. 3.2A.10), χ_{lf} (range- 211-231 x $10^{-8}m^3$/kg, avg. 220 x $10^{-8}m^3$/kg), SIRM (range-3298-3685 x $10^{-5}Am^2$/kg, avg. 3469 x $10^{-5}Am^2$/kg) and χ_{fd} (range- 2.57-3.71 %, avg. 2.99 %) decreases from the bottom to 20 cm and further above increasing trends are observed till the surface. SIRM/χ_{lf} (range- 15.11-16.77 x 10^3A/m, avg. 15.78 x 10^3A/m) exhibits decreasing trends from the bottom to 8 cm and then increases at the surface. χ_{ARM} (range- 6956-14395 x $10^{-8}m^3$/kg, avg. 10956 x $10^{-8}m^3$/kg), χ_{ARM}/SIRM (range- 1.89-4.28 x 10^{-5}m/A, avg. 3.19 x 10^{-5}m/A) and χ_{ARM}/χ_{lf} (31.66-64.72, avg. 49.81) increase uniformly from the bottom to 8 cm and then decrease at the surface. On the other hand, HIRM (range- 46.14-85.81 x 10^{-5} Am^2/kg, avg. 72.24 x $10^{-5}Am^2$/kg) and Hard (range- 1.38-2.33 %, avg. 2.08 %) show similar trends wherein, after initial decrease at the bottom, increases towards the surface are seen. The values of S-ratio (range- 98-99 %, avg. 98 %), increase from bottom to 20 cm and then decrease towards the surface.

For the upper estuarine region (Fig. 3.2A.11), χ_{lf} (range- 218-881 x $10^{-8}m^3$/kg, avg. 485 x $10^{-8}m^3$/kg) shows parallel variations to SIRM (range- 3065-16148 x $10^{-5}Am^2$/kg, avg. 8417 x $10^{-5}Am^2$/kg). χ_{ARM}/SIRM (range- 0.90-4.82 x 10^{-5}m/A, avg. 2.37 x 10^{-5}m/A), χ_{ARM}/χ_{lf} (16.48-67.74, avg. 37.80) and χ_{fd} (range- 1.07-3.37 %, avg. 1.96 %) exhibit identical variations from the

bottom to the surface. SIRM/χ_{lf} (range-13.82-21.02 x 10^3A/m, avg. 18.04 x 10^3A/m) and HIRM (range- -13.17-306 x 10^{-5}Am^2/kg, avg. 126 x 10^{-5}Am^2/kg) project similar trends from the bottom to 20 cm. Above it, SIRM/χ_{lf} decreases and then increases towards the surface while HIRM uniformly increases till the surface. χ_{ARM} (range- 12443-19891 x 10^{-8}m^3/kg, avg. 15846 x 10^{-8}m^3/kg) fluctuates irregularly from the bottom to 20 cm and then decreases towards the surface. Hard (range- -0.20-2.18 %, avg. 1.57 %) and S-ratio (range- 98-100 %, avg. 98 %) show corresponding opposite trends to each other.

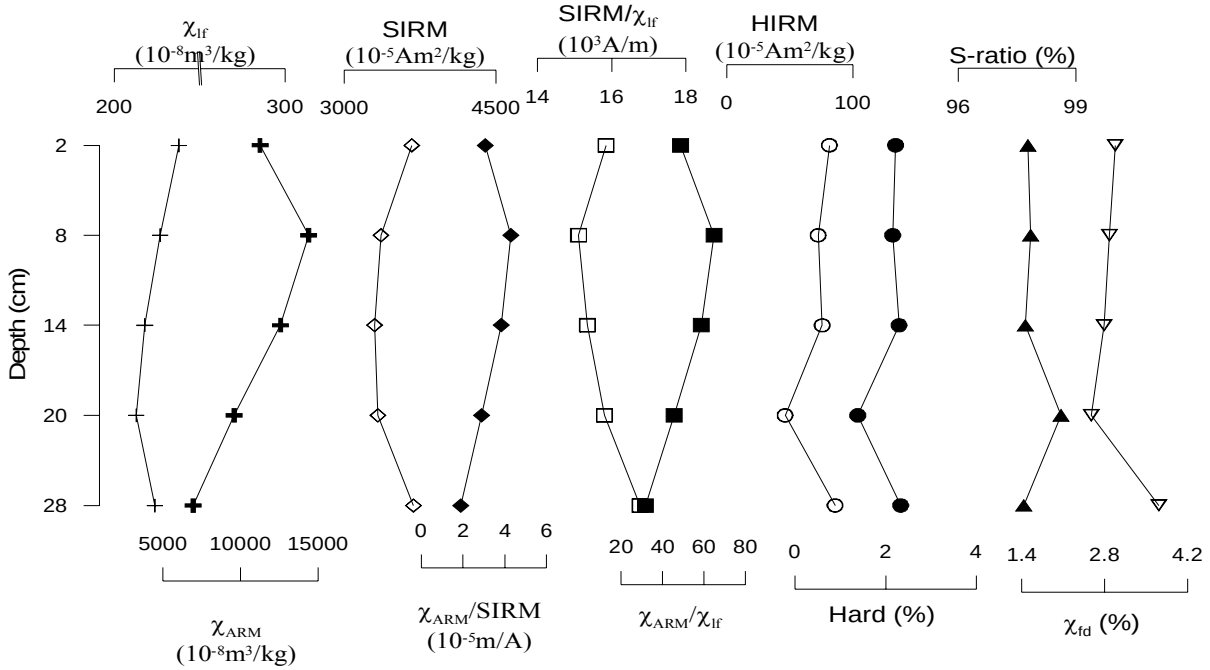

Fig. 3.2A.10. Depth-wise distribution of magnetic susceptibility parameters for core UV

As discussed in section 1 (Thane creek), the ratio χ_{ARM}/χ_{lf} can be used to indicate the grain size of magnetic minerals, with higher values reflecting fine grained single domain (SD) minerals and lower values multi-domain (MD) or supra-paramagnetic (SP) minerals (Banerjee et al., 1981). The high values of χ_{ARM}/SIRM indicate relatively finer ferromagnetic grain assemblages and low values of χ_{ARM}/SIRM indicate coarser ferrimagnetic assemblages. When magnetic signal is controlled by a single magnetic component (Lepland and Stevens, 1996; Maher, 1986), or a mixture of magnetic minerals at a constant ratio (Caitcheon, 1998), χ_{lf} and SIRM exhibit a linear relationship. In such occasions, the interparametric ratio, SIRM/χ_{lf}, can be used to interpret mineral magnetic grain size variations. The ratio increases with decreasing grain size, if magnetic grain size is larger than the grains at the SP/SD boundary (Thompson et al., 1980). The linear relationship of SIRM and χ_{lf} in the estuarine sediments (r=0.98) indicates the predominance of ferrimagnetic components in the sediments. χ_{fd} can indicate the concentration of SP grains in soil, and if it is less than 4 %, MD (Multiple Domain) and SSD (Stable Single Domain) grains dominate (Dearing et al., 1996). High concentrations of paramagnetic and

diamagnetic components would lead to low χ_{fd}. The magnetic grain size of the soils always increases with soil pollution augmenting. The high (close to 100 %) S-ratio for the entire estuary indicates that magnetite, either of natural or anthropogenic origin, is the major magnetic mineral. High S-ratios (of ~98 %) indicate the dominance of an extremely low-coercivity magnetic phase. Due to the geological setting of the sampling site, the sediment can be expected to be magnetically dominated by magnetite from proximal basalt sources. Basalts contain 2-6 % Fe-oxide grains and are enriched with titano-magnetite (Thompson and Oldfield, 1986).

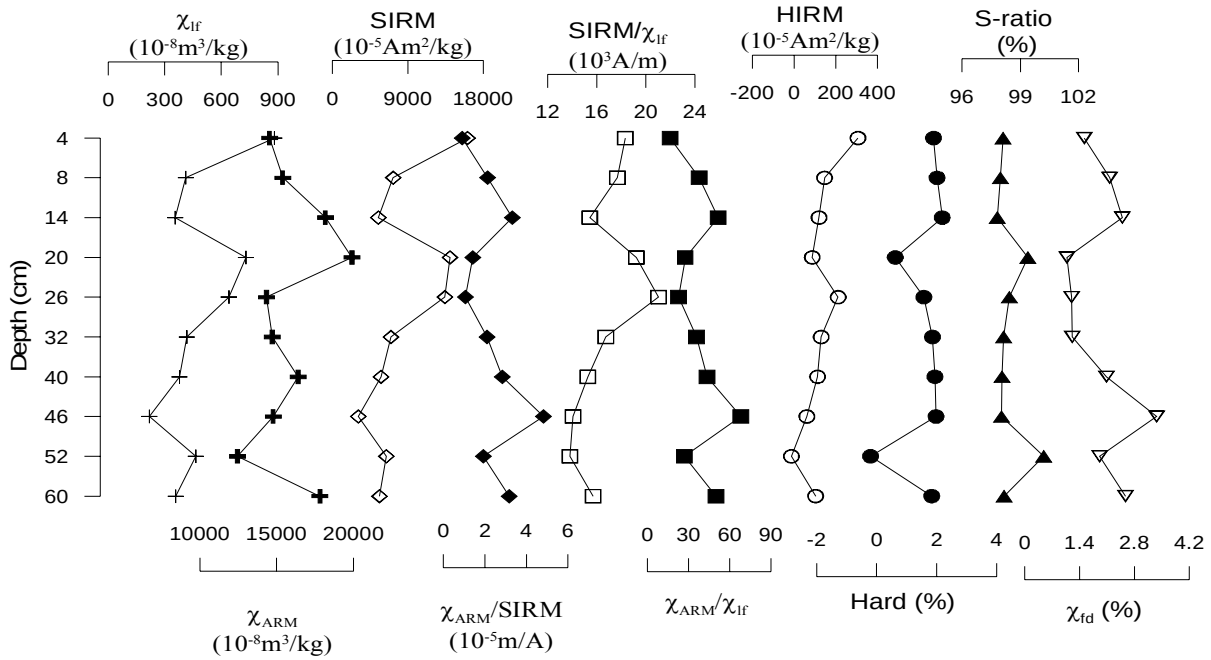

Fig. 3.2A.11. Depth-wise distribution of magnetic susceptibility parameters in upper estuary (core UIV)

In the present study, inspection of the down-core plots of magnetic susceptibility (χ_{lf}) reveals a remarkable degree of consistency within the two cores studied (UI and UV) while in core UIV large fluctuations are seen from the bottom to the surface. Also, higher values of magnetic parameters are found to be concentrated in the upstream region (core UIV), where lot of industrial plants (e.g. glass, heavy machine manufacture, petrochemical works, etc.) are located. χ_{lf} variations in surficial sediments exhibit regional variations in accordance with their mineralogical provinces and the changes in χ_{lf} may largely reflect the source rock composition and strength of the transporting medium. The relatively high χ_{lf} values suggest that the soil is enriched with ferrimagnetic grains probably as a consequence of anthropogenic activities compared to other environmental materials. Based on the sediment components distribution (section 3.2A.1), in core UIV the magnetic parameters display down-core distribution similar to the sand profile with higher sand and χ_{lf} values at the surface and middle portion of the core. Lower values of susceptibility coincide with increase in grain size. The finer grain is dissolved

first due to high surface to volume ratio, which results in reduction of magnetic intensity as well as a shift in grain size towards the coarser end (Karlin and Levi, 1983). These enhancements of magnetic concentration parameters indicate the presence of fine grained ferrimagnetic (Fe oxides) minerals in the upper part of the sediment core, which might be derived from anthropogenic activities (Chan et al., 1998; 2001). The TOC is diamagnetic and the effect of varying TOC content, although little, may have diluted the magnetic susceptibility parameters in the middle portion of the core. Also, reductive diagenesis if present may have resulted in dissolution of magnetite to some extent and therefore decreased χ_{lf} values. The abrupt drop in the χ_{lf}, especially in core UIV, probably marks the extent of the disturbed sediments by human activities such as sand dredging or trawling. The uppermost layer of the sediment has probably been disturbed, causing a re-distribution of anthropogenic wastes and pollutants within this layer.

The ratios of χ_{ARM}/χ_{lf}, χ_{ARM}/SIRM and SIRM/χ_{lf} combined with χ_{lf}, are effective to identify sediment pollution. The significant enhancement of χ_{ARM}, SIRM, Hard and HIRM also suggests soil pollution (Hu et al., 2007). Anthropogenic magnetic particles have different sources, but research works so far have suggested that they are generally dominated by MD and SSD sizes (Hay et al., 1997). In general, the different magnetic parameters reveal that the sediment in the estuary are dominated by fine grained (SSD) (~0.03-0.07 μm) ferrimagnetic minerals.

3.2A.6. a) Organic matter (TOC, TP and TN)

In the estuarine region, TOC varies from 0.47-2.57 %, avg. 1.32 %, TP from 0.12-0.97 mg/g, avg. 0.44 mg/g and TN ranges from 0.34-0.76 mg/g, avg. 0.43 mg/g. The Inner estuarine region (core UIII) shows highest average values for TOC (1.81 %) and TP (0.69 mg/g) while the highest TN concentration (1.31 mg/g) is seen in the middle estuary (core UII). On the other hand, the lower estuary (core UV) shows the lowest average concentration of TOC (0.87 %) while the estuary mouth (core UI) displays lowest average values of TP (0.34 mg/g) and TN (0.33 mg/g). In general, the organic matter in the estuarine region does not exhibit much variation from the inner end to the mouth of the estuary. The vertical distributions of organic matter for the different cores sampled in the estuarine region are given in figures 3.2A.12 to 3.2A.14.

Near the estuary mouth (core UI), range and average values of organic matter are- 0.98-1.64 %, 1.31 % for TOC; 0.30-0.38 mg/g, 0.34 mg/g for TP and 0.15-0.76 mg/g, 0.33 mg/g for TN. From the vertical profile (Fig. 3.2A.12a), TOC exhibits decreasing and increasing trends with larger variations towards the surface as compared to the bottom. In the case of TP, not much deviation from the average line is noticed. TN displays similar down-core trends as TOC from the bottom

to 16 cm depth. Above it, a decrease is seen at 10 cm followed by an increase towards the surface. Core UV, sampled from lower estuarine region, ranges from 0.69-1.43 % for TOC, 0.30-0.52 mg/g for TP and 0.38-1.48 mg/g for TN with averages of 0.87 %, 0.41 mg/g and 0.83 mg/g, respectively. The vertical distribution plot (Fig. 3.2A.12b), shows gradual increase of TN from the bottom to 4 cm depth. Above it, a decrease is seen. On the other hand, TOC fluctuates irregularly throughout the core length. TP shows an increasing trend from the bottom to 14 cm depth while above it, a decreasing trend is noticed except for an increased value at 10 cm depth.

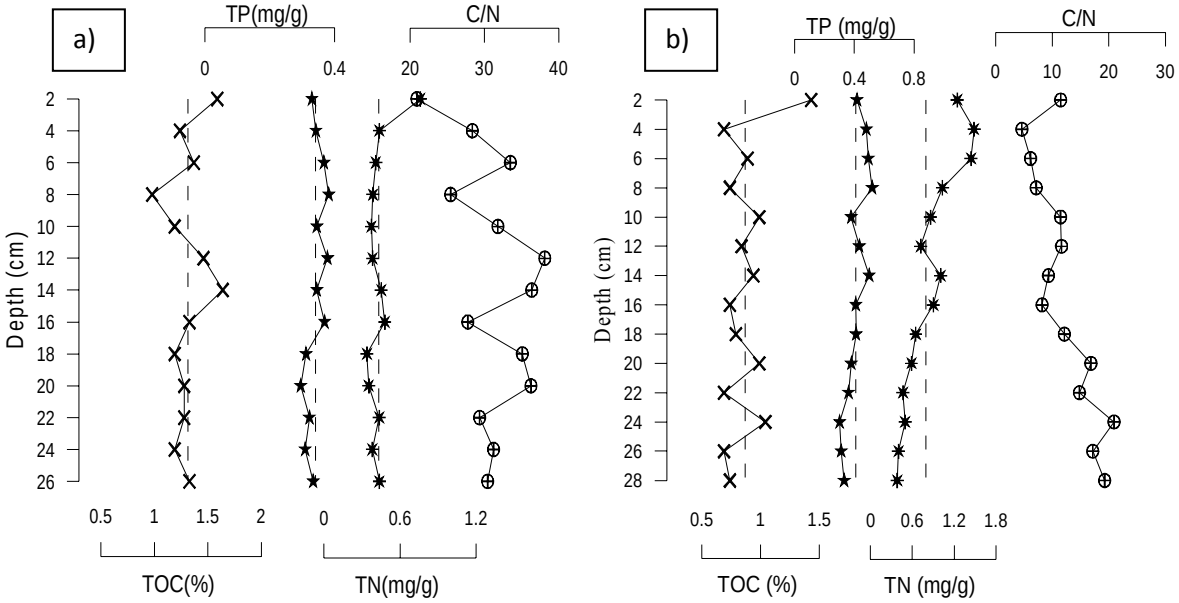

Fig. 3.2A.12. Vertical profiles of Organic matter, a) near estuary mouth (core UI) and b) lower estuarine region (core UV)

In the middle and upper estuarine regions, represented by cores UII and UIV, the organic matter varies from 0.97-1.56 %, avg. 1.28 % and 0.47-1.98 %, avg. 1.35 % for TOC; 0.19-0.64 mg/g, avg. 0.42 mg/g and 0.12-0.56 mg/g, avg. 0.35 mg/g for TP; and 0.28-2.34 mg/g, avg. 1.31 mg/g and 0.23-0.58 mg/g, avg. 0.34 mg/g for TN. For core UII (Fig 3.2A.13a), TOC is found to fluctuate largely from the bottom to 34 cm. Between 34 and 10 cm depths, the concentration remains constant. Above this depth, an increasing trend is noticed upto the surface. TP initially displays a decrease from the bottom to 28 cm depth. Further, an increasing trend till the surface is observed. In the case of TN, a general increasing trend is observed with large fluctuations at the bottom as compared to the surface.

In core UIV (Fig 3.2A.13b), TOC shows large fluctuations from the bottom to the surface of the core whereas variations of TP and TN are restricted around the average line, except near the surface. For core UIII, from inner estuarine end, TOC varies from 1.09-2.57 %, TP from 0.51-0.97 mg/g and TN from 0.13-1.66 mg/g with averages of 1.81 %, 0.69 mg/g and 0.57 mg/g, respectively.

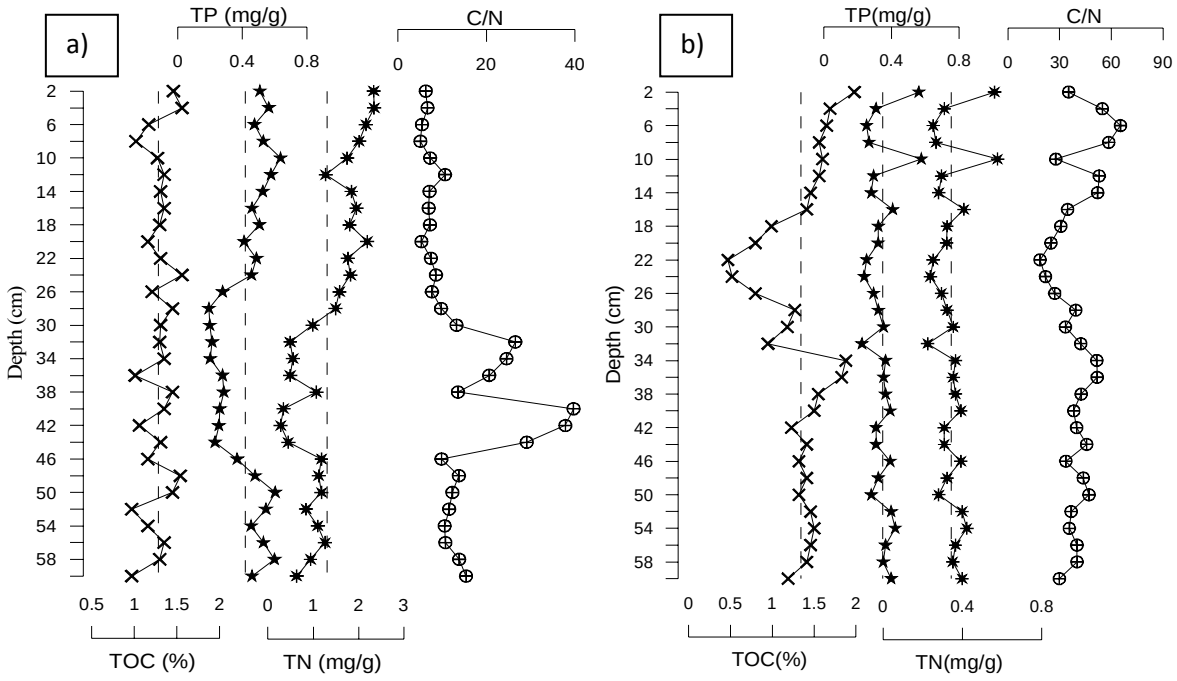

Fig. 3.2A.13. Vertical profiles of Organic matter for a) upper (core UII) and b) middle (core UIV) estuarine regions

From down-core distributions (Fig. 3.2A.14), TOC and TN, in general show an increasing trend from the bottom to the surface with large fluctuations throughout the core length. On the other hand, TP shows an increasing trend from the bottom to the surface, except at depths of 18 to 12 cm, wherein a decreasing trend is observed with higher values between 26 and 18 cm depth.

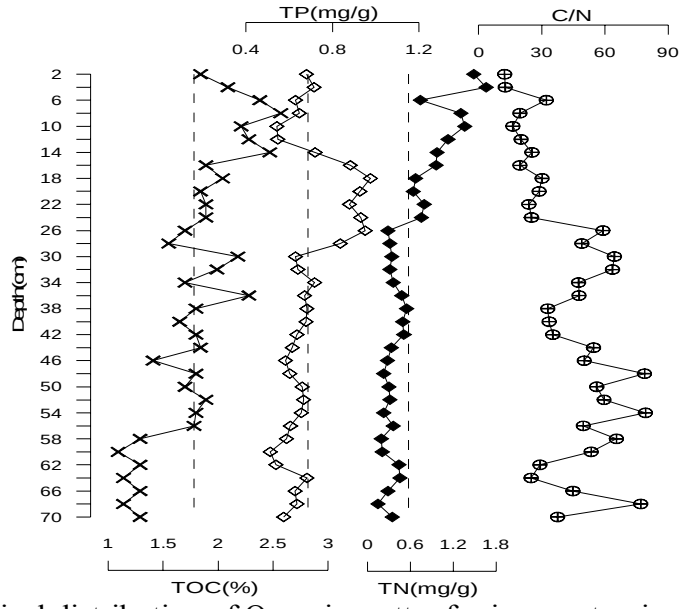

Fig. 3.2A.14. Vertical distribution of Organic matter for inner estuarine region (core UIII)

In estuarine areas, organic matter can be supplied both from autochthonous (such as plants growing on the sediment surface) and allochthonous sources (organic material transported predominantly by the tide or a river). In the present study, sediment organic matter is found to be higher in upper few layers of the cores, which may be because of deposition of fresh material in

the top layer of the sediment. The high organic matter content in the sediments of cores UV, UIV and UIII can be attributed to the inputs by the mangrove swamp bordering the estuary. The general decrease in organic matter content with depth is found to be consistent with classical situation in sediment diagenesis, in which organic carbon decreases with depth (Williamson and Wilcock, 1994). In the mouth area, where sand prevails, organic matter concentrations are lower as compared to the other mud-rich areas. The TOC contents of cores UII and UIV followed the three units that were identified on the basis of particle-size, although there were variations in each unit. Sediment particle size trend seems to play a significant role in controlling the distribution of all organic compounds. For example, the sandy sediments in the middle unit of both the cores revealed minimum concentration of all organic components as compared with the fine grained sediments at the top and bottom units. It is possible that this shift in grain size indicates larger proportion of terrigenous sediments and organic matter in that layer. The TOC concentration in the middle unit are significantly lower than in either the top or bottom units, clearly being diluted by organic-poor coarse grained material in the former. The higher TOC and TP values in the inner estuarine end suggest a sediment supply from urban run-off which accumulates in the narrow estuarine segment. However, the TN is lower in this area than in the southern region (core UII).

3.2A.6. b) C/N ratio

In the estuarine region C/N values range from 5- 79 with an average of 28. Cores UV and UII exhibit minimum values while core UIII has the highest C/N value. The lower and middle estuarine regions have lower C/N values while towards the inner end increasing values are observed. The vertical profiles for C/N are shown in figures 3.2A.12-3.2A.14. For core UI, C/N ranges from 21-38 with an average of 31. From the vertical profile, large fluctuations are observed along the length of the core with a decrease at the surface. In the case of core UV (range- 5-21, avg. 12), a gradual decreasing trend is seen from the bottom to 4 cm depth followed by an increase at the surface. The values of C/N in core UII ranges from 5-40, with an average value of 13. Between the depths of 30 and 46 cm, a large increase in C/N value is seen. The portions above and below this depth exhibit uniform decrease in C/N values, from the bottom to the surface. Highest C/N values are seen in the middle portion, whereas the average values in the bottom portion are similar to the top portion. For core UIV, the range varies from 19-65, with an average of 40. From the bottom to 34 cm depth, an increasing trend is noticed with large fluctuations. Further above till 22 cm depth, a decrease in C/N values is seen. The upper portion of the core, from 22 to 12 cm, shows an increase in value. The surface of the core

is marked with many spikes. In core UIII (range- 12-79, avg. 42), in general, C/N values decreases from the bottom to the surface with large fluctuations.

Overall, almost all the cores display a decreasing trend from the bottom to the surface. Cores UI, UIII and UIV have a very variable C/N ratio with high values (> 20) suggesting strong influence of terrestrially derived material in the region. The C/N ratio reflects both the origin of the carbon and the degree of degradation of OM (Mcdonald et al., 1991). This variable profile is likely the result of the dynamic sedimentation and sediment resuspension regimes that operates in this part of the estuary based on the ^{210}Pb profile of the core. Typically, sediment mixing increases the rate of organic degradation, since bioturbation involves sediment turnover, flushing and oxygenation. At the estuary mouth, deposition and resuspension may be higher than in the extreme upper stations due to stronger tidal currents. Cores UV and UIII experience less riverine influence and hence the allochthonous component of the organic matter is lower. The contents of TOC, TP and TN as well as the C/N ratios for the estuary are slightly elevated close to the mangrove areas (cores UV, UIV and UIII) relative to other parts of the region. Elevated values of C/N ratios indicate contribution of mangroves to the organic matter preserved in the sediments.

3.2A.7. pH

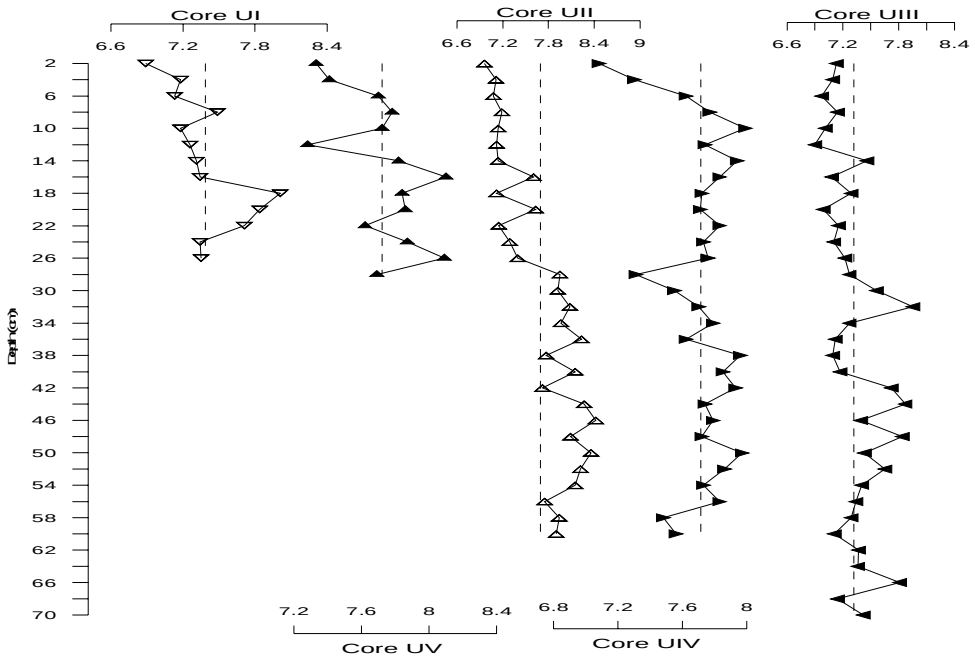

Fig.3.2A.15. Depth-wise distribution of pH in the estuary

In the cores sampled from different regions of the estuary the pH ranges from 6.89-8.01 for core UI, 7.28-8.10 for core UV, 6.96-8.42 for core UII, 7.08-7.99 for core UIV and 6.90-7.95 for core UIII with average values of 7.39, 7.72, 7.70, 7.71 and 7.32, respectively. In general, the pH is

found to be constant in the estuarine region with slightly higher values in the upper, middle and lower estuarine regions. From the bottom to the surface, in all the cores, pH is found to show a decreasing trend.

The sediment pH is found to decrease markedly just below the sediment surface in cores UIII. This decrease can be attributed to oxidation of organic matter and other inorganic chemical species. The production of organic acids during organic matter breakdown explains the lower pH in top layers of the cores. Retention of heavy metals in soils is directly or indirectly affected by the pH. Precipitation and dissolution phenomena of heavy metal-bearing minerals are examples of direct effects. Adsorption and reactions are also pH dependent. Therefore, element retention in soils will be affected indirectly by changes in pH, e.g. hydrolysed metal species (MeOH+) are preferentially adsorbed compared to free metal ions (Herreweghe et al., 2002). At near-neutral to slightly alkaline pH levels, metals tend to be effectively immobilized (Gambrell, 1994). The high pH for the estuarine sediment (core UV) implies it has the potential to retain metals in sediments making the metals become immobile.

3.2A.8. Metal geochemistry

Figures 3.2A.16 to 3.2A.20, present vertical distribution patterns of metals in all the cores collected from the Ulhas estuary. Al did not show good correlations with clay or metals in the estuarine region. Hence, the metals are not normalised with Al. The region is found to contain a wide range of distributions of trace metal concentrations. Fe represents the maximum abundance while Co exhibits the minimum concentration of the studied metals in the present work. Most of the elements are found to show high concentrations in core UIV. Sediments of the western region (core UI), collected near the mouth, exhibits higher values of Fe-oxide-hydroxides and heavy metals compared to the upstream region (core UIII). Core UV shows highest average values for Al, Ca, Mn and Ni while core UI exhibits high values of Fe, Pb, Zn and V. On the other hand, Cu and Co in core UIV and Cr in core UII, display the highest average values. In the present study, the metal contents of the sediments show increasing concentrations from the upstream section of the estuary to the downstream section.

a) Aluminium (Al)

From the estuary mouth to the inner end, Al concentration is found to range from 7.46-8.93 % for core UI, 8.83-12.74 % for core UV, 4.45-7.90 % for core UII, 5.24-14.59 % for core UIV and 5.51-9.95 % for core UIII with averages of 8.23 %, 10.80 %, 6.63 %, 9.80 % and 7.64 %, respectively. Core UV displays the highest average concentration while core UII exhibits the

lowest value. From the bottom to 6 cm, in core UI, Al shows an increasing trend except for a decreased peak at 16 cm. From 6 cm till the surface, a decreasing trend is observed. For core UV, from lower estuary, after an initial decrease at the bottom, an increasing trend is noticed till 4 cm followed by a decrease at the surface. In the middle estuarine region represented by core UII, from the bottom to 50 cm and from 26 cm till the surface, an increasing trend is observed while between the depths of 50 and 26 cm a decreasing trend is seen with some fluctuations. Core UIV, sampled from upper estuarine region, exhibits fluctuating decreasing and increasing trends from the bottom to the surface. The core collected from the inner estuarine end (UIII), shows a gradual decrease in Al from the bottom to the surface except for an increased peak at 56 cm depth.

b) Calcium (Ca)

The range and average of Ca concentration are 1.30-4.41 %, 2.80 % for core UI; 2.90-4.46 %, 3.54 % for core UV; 1.80-5.65 %, avg. 3.05 % for core UII; 1.24-4.54 %, 2.28 % for core UIV and 1.58-4.89 %, avg. 2.82 % for core UIII. The core collected near the estuary mouth (UI) shows a decreasing trend in concentration while in core UV an increasing trend is seen from the bottom to 8 cm followed by a decreasing trend till the surface. In the case of core UII, sampled from middle estuary, a decrease is noticed from the bottom to 54 cm and then an increase is seen till 46 cm depth. Further above till 16 cm, a decreasing trend with large fluctuations is seen which becomes more gradual towards the surface. In general, a more constant trend is observed in core UIV, from upper estuary, except for a large increase seen between depths of 28 and 16 cm. In core UIII, a fluctuating increasing trend is seen from the bottom to 34 cm depth followed by a decrease till the surface. The concentration is found to increase from the mouth to middle estuary and then decrease towards the inner end.

c) Iron (Fe)

Core UI (range- 9.03-10.89 %, avg. 10.02 %), exhibits a decreasing trend, except for two increased values at 22 and 10 cm depths. Core UV (range- 8.32-10.19 %, avg. 9.02 %), displays an increasing trend from the bottom to the surface with minor fluctuations in between the core length. In the case of core UII (range- 4.15-5.04 %, avg. 4.52 %), the values fluctuate around the average line with not much deviations as compared to core UIV (range- 6.91-13.09 %, avg. 8.56 %) which deviates to a large extent from the average line. Core UIII (range- 4.09-5.49 %, avg. 4.51 %), on the other hand, shows a uniform constant trend except for a peak value at 56 cm depth. In general, a decreasing trend is seen from the estuary mouth to the inner end.

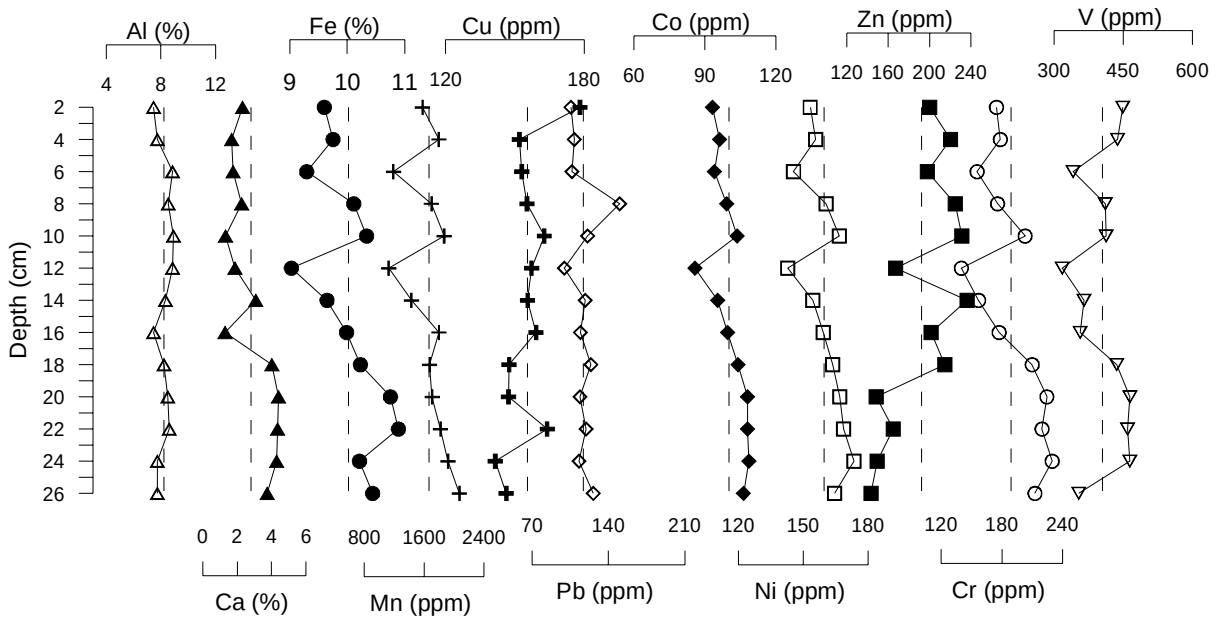

Fig. 3.2A.16. Depth-wise distribution of selected metals near the estuary mouth (core UI)

d) Manganese (Mn)

Mn concentration varies from 1126-2071 ppm with average value of 1666 ppm, in core UI with a decreasing trend from the bottom to 12 cm. Above it till the surface, a fluctuating trend is seen. Core UV (range-1885-2284 ppm, avg. 2077 ppm), increases from the bottom to 18 cm, then decreases till 10 cm depth followed by an increasing trend upto 4 cm. A drop in value is seen at the surface. From the bottom to 48 cm and from 20 cm till the surface, in core UII (range- 635-1320 ppm, avg. 884 ppm), a constant trend is noticed while between the depths of 48 and 20 cm depths, a large fluctuating trend is seen. In core UIV (range- 1545-2626 ppm, avg. 1902 ppm), a fluctuating trend in metal concentration is observed for the entire length with no definite trend, while core UIII ranges from 769-1090 ppm, with an average of 905 ppm and shows a constant trend for the entire core. Highest concentration is seen for core UV while lowest value is observed for core UII.

e) Copper (Cu)

From the down-core plots it is seen that, in core UI, Cu (range- 142-178 ppm, avg. 155 ppm) initially decreases at the bottom and then increases towards the surface with an increased peak at 22 cm depth. In the case of core UV and core UIII, ranging from 166-192 ppm and 117-231 ppm with averages of 173 ppm and 142 ppm, respectively, uniform increasing trends are noticed from the bottom to the surface. For core UII, having range of 87-199 ppm and 126 ppm average value, the values lie close to the average line, except at the surface where an increase is seen. The concentration of Cu varies from 205-345 ppm with an average of 264 ppm for core UIV and

exhibits fluctuating decreasing and increasing trends. Core UII shows the highest average concentration while core UV exhibits the lowest concentration.

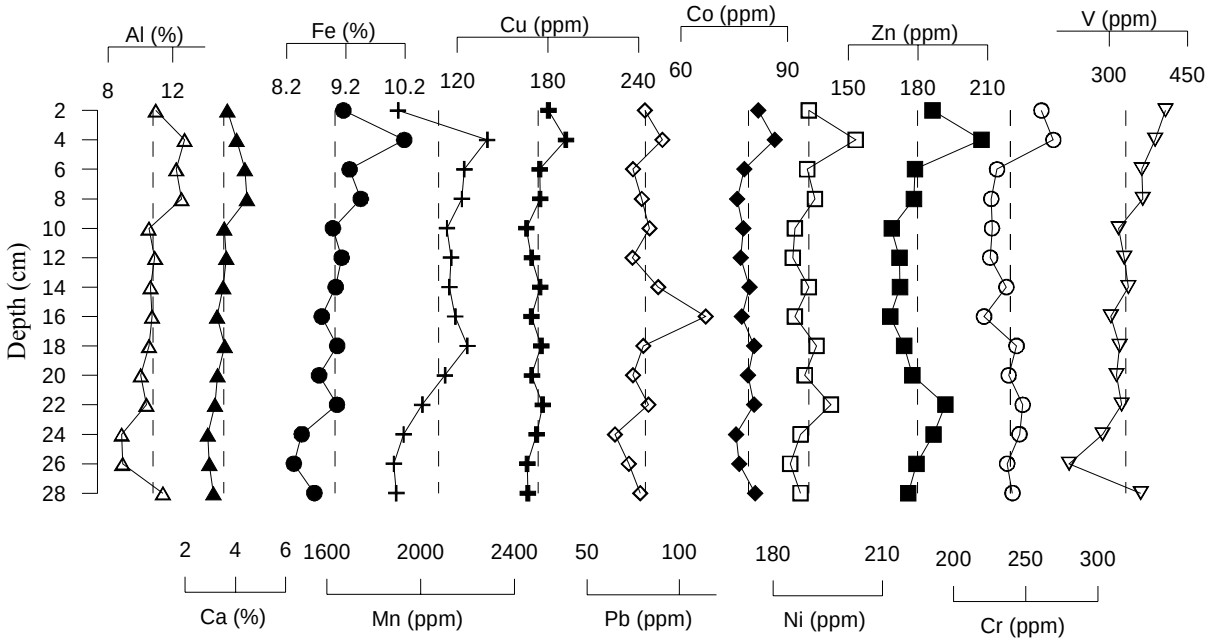

Fig. 3.2A.17. Depth-wise distribution of selected metals in lower estuary (core UV)

f) Lead (Pb)

The concentration ranges from 100-150 ppm with average of 117 ppm at the estuary mouth (UI), while in core UV the range is 65-114 ppm with 82 ppm average. For cores UII and UIV the ranges are from 29-104 ppm and 46-194 ppm with averages of 63 ppm and 95 ppm, respectively. At the inner end (core UIII), the values vary from 26-68 ppm with 43 ppm average value. In core UI, almost all the values lie on the average line, except for a peak at 8 cm depth while in core UV, a fluctuating increasing and decreasing trend is observed from the bottom to the surface. On the other hand in core UII, from the bottom to 32 cm depth and from 14 cm till the surface, an increasing trend is noticed. At the remaining depths, a fluctuating decreasing pattern is seen. For core UIV, an increasing trend in Pb concentration is noticed with larger fluctuations at the upper portion of the core. After an initial decrease, a uniform increasing trend is seen in core UIII. The values, in general, are found to decrease moving from the estuary mouth towards the inner end.

g) Cobalt (Co)

Near the estuary mouth (core UI) the values range from 86-109 ppm with an average of 100 ppm. A decreasing trend is seen from the bottom to the surface except for an increased peak at 10 cm depth. Core UV (range- 76-86 ppm, avg. 79 ppm) and core UIII (range- 41-61 ppm, avg. 48 ppm) exhibit similar trends, i.e. the values lie on/close to the average line. On the other hand in core UII, having range of 31-108 ppm and 71 ppm average, a fluctuating decreasing and increasing trend is seen from the bottom to 22 cm and above it a gradual increasing trend is

observed. Core UIV, varying from 92-139 ppm and having an average of 109 ppm, in general shows an increasing trend from the bottom to the surface with large variations seen at the upper few centimeters of the core. Highest average Co concentration is seen in core UIV and lowest is observed for core UIII.

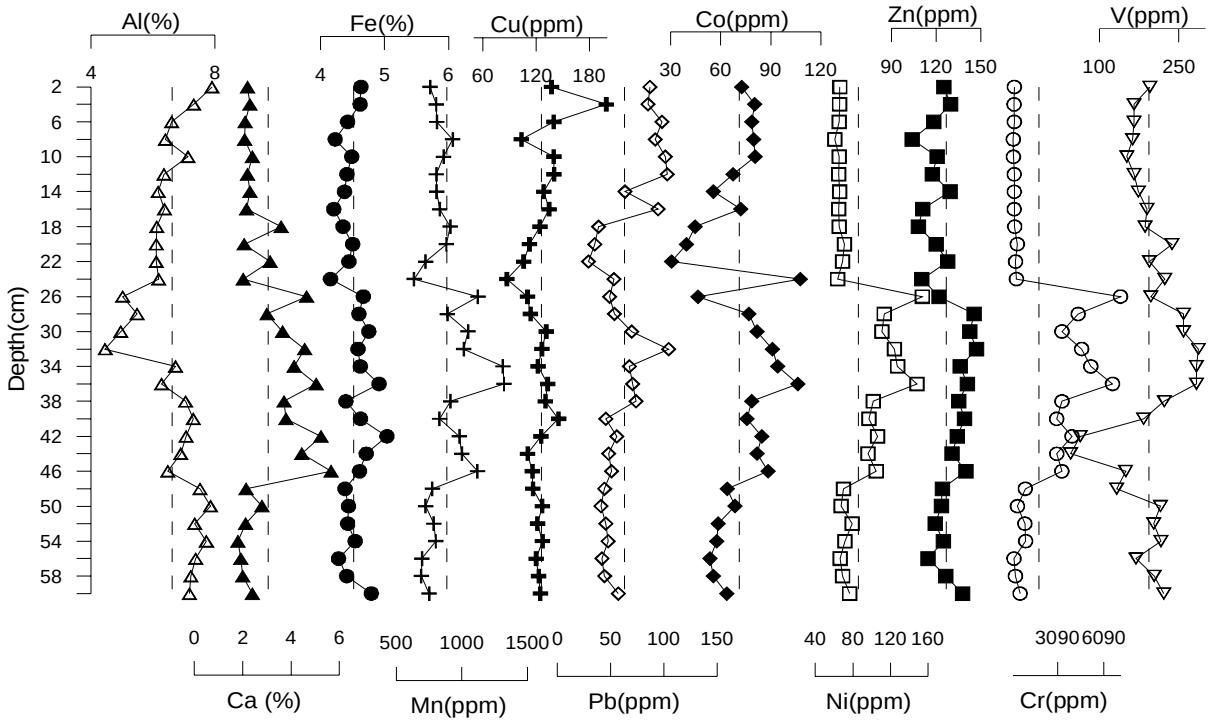

Fig. 3.2A.18. Depth-wise distribution of selected metals in middle region (core UII)

h) Nickel (Ni)

The values of Ni are found to vary from 143-174 ppm with an average of 160 ppm in core UI. After an initial increase at the bottom in core UI, a uniform decreasing trend is observed from 24 to 12 cm depth. Further above, a fluctuating increasing and decreasing trend is seen till the surface. For core UV, the range is 185-203 ppm with an average of 190 ppm. A fluctuating trend is observed for the entire length of the core around the average line. In core UII (range- 61-154 ppm, avg. 86 ppm), from the bottom to 48 cm and from 24 cm till the surface, a constant trend is seen while between the depths of 48 and 24 cm, large fluctuations and higher values are observed. Core UIV and core UIII having ranges of 85-120 ppm and 52-86 ppm and averages of 94 ppm and 72 ppm respectively, exhibit values close to the average line. However, in core UIV slight fluctuations are seen between the depths of 28 and 16 cm. Core UIII, in general shows an increasing trend from bottom to surface. A decrease in Ni concentration is seen from the estuary mouth to the inner end. It is well known that Ni is insoluble at the pH values of marine environment (> 6.7) and exists predominantly as Ni hydroxides (Sunderman and Oskarsson, 1991) which in turn is quickly incorporated in sediments.

i) Zinc (Zn)

The concentrations of Zn is found to vary from 143-237 ppm, 168-207 ppm, 104-147 ppm, 90-221 ppm and 123-230 ppm in cores UI, UV, UII, UIV and UIII with average values 192 ppm, 180 ppm, 127 ppm, 133 ppm and 167 ppm, respectively. The core collected near the estuary mouth (UI) exhibits an increasing trend from the bottom to the surface with large fluctuations while the core sampled from lower estuary (UV) increases from the bottom to 22 cm followed by a decrease till 16 cm. Further above, an increasing trend is observed. In the case of core UII, from the middle estuary, after an initial decrease from the bottom to 56 cm, an increasing trend is noticed till 28 cm. Above it, a fluctuating decreasing trend is seen till the surface. For cores collected from upper and inner end of the estuary, different vertical distributions are seen. In core UIV, a fluctuating decreasing and increasing trend is seen from the bottom to the surface while in core UIII, a decrease from the bottom to 60 cm is followed by an increasing trend till the surface. The estuarine middle region shows the lowest average value while the estuary mouth displays the highest average Zn concentration.

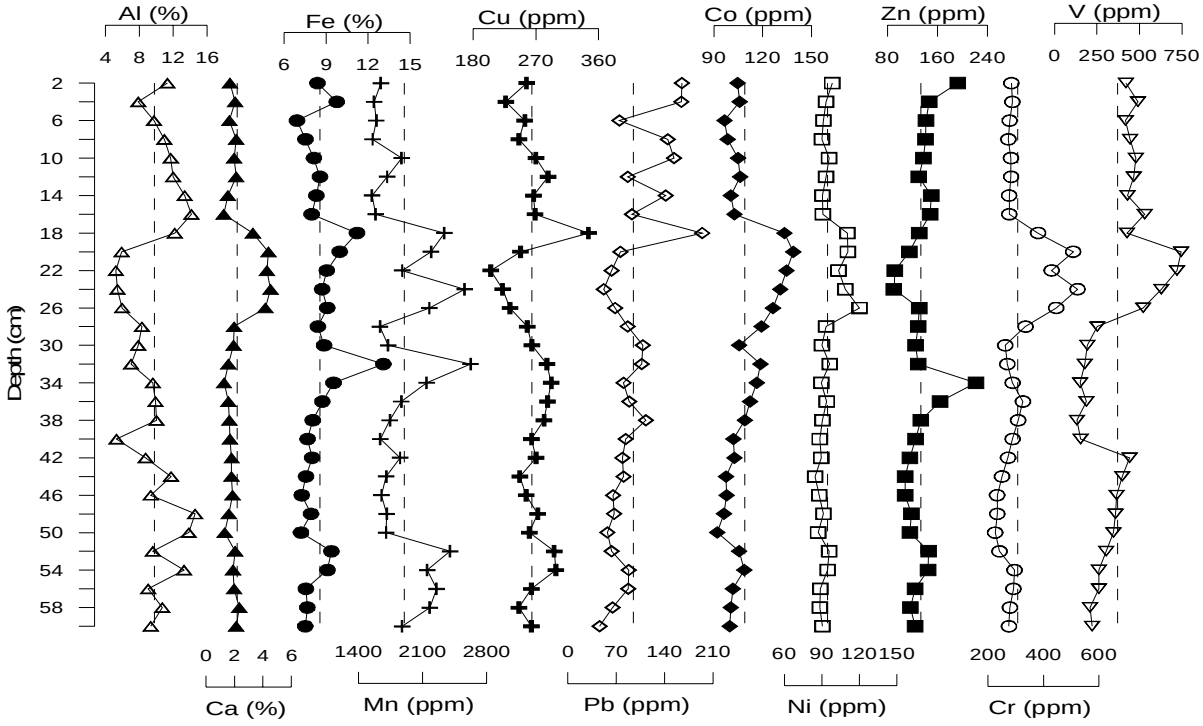

Fig. 3.2A.19. Depth-wise distribution of selected metals in upper region (core UIV)

j) Chromium (Cr)

From the estuary mouth to the inner end, Cr concentration ranges from 140-230 ppm for core UI, 221-269 ppm for core UV, 221-7164 ppm for core UII, 225-522 ppm for core UIV and 90-231 ppm for core UIII ,with averages of 189 ppm, 239 ppm, 1894 ppm, 306 ppm and 173 ppm, respectively. The values decrease from the bottom to the surface, in general, except for an increased peak at 10 cm depth in core UI. In core UV, the values lie near the average line

throughout the core length with slightly higher values at the surface. Between the depths of 46 and 24 cm in core UII, a large increase in Cr concentration is observed while for the rest of the core, a uniform concentration is seen. Similar observation is seen in core UIV, wherein between the depths of 30 and 16 cm, a large increase in Cr concentration is observed while for the rest of the core-length, uniform concentration is seen. In core UIII, the values increase in stages from the bottom to the surface with two distinct decreased peaks seen at 40 and 10 cm depths, respectively. Highest concentration is seen in core UII while core UIII exhibits the lowest value.

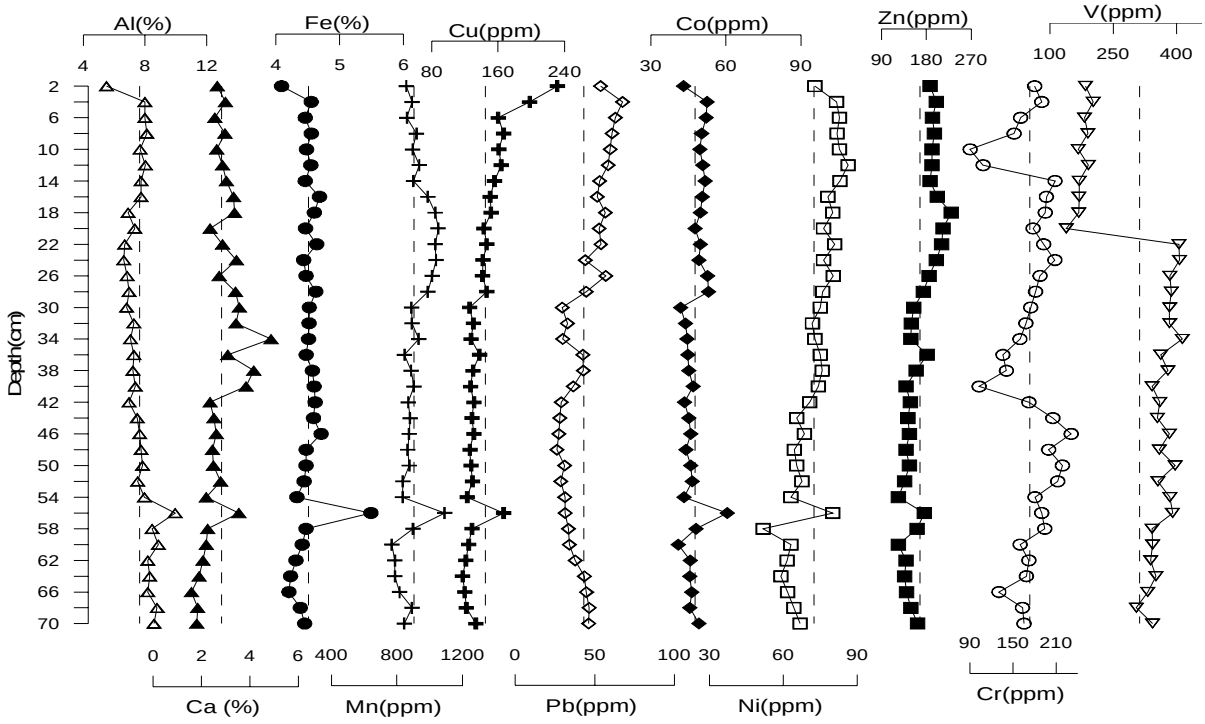

Fig. 3.2A.20. Depth-wise distribution of selected metals in inner end (core UIII)

k) Vanadium (V)

The values of V range from 318-464 ppm with an average of 405 ppm in core UI, 223-407 ppm with an average of 331 ppm in core UV, 45-286 ppm with an average of 193 ppm in core UII, 132-745 ppm with an average of 372 ppm in core UIV and 139-413 ppm with an average of 313 ppm in core UIII. For core UI, after an initial increase from the bottom to 24 cm, a decreasing trend is observed till 12 cm depth followed by a fluctuating increasing trend till the surface. On the other hand, for core UV, except for a decrease at the bottom, a uniform increasing trend is seen from 26 cm till the surface. Large fluctuations are noticed in the middle portion of core UII, as compared to the lower and upper portions of the core. In core UIV, increasing trend is observed from the bottom to the surface with some fluctuations in between, while in core UIII a gradual increasing trend is seen from the bottom to the surface, except for a sharp decrease from 22 to 20 cm depth. In the entire estuary, the distribution of V shows range between 45-745 ppm

with an average of 323 ppm, showing a notable increase farther away from the inner estuary end, towards the sea.

The sampling strategy adopted for the five sites of the estuary, allowed observing and comparing the spatial and temporal variations of metal concentrations in the region. First of all, trace metal concentrations in sediments varied spatially. Metal concentrations, in general, are low in areas with coarse-grained sediment and in areas that are non-depositional. These areas have high bottom stress due to the local hydrodynamic regime and therefore the sediment is continually reworked (Loomb, 2001). However, in the present study, higher metal concentrations are observed in coarser-sediments near the estuary mouth than mud-rich sediments from the eastern upstream part and southern bank of the estuary. For example, core UII, from middle estuarine region shows lowest values for Al, Mn, Zn and V; core UV, sampled from lower estuary has low Fe, Cu, Pb, Co, Ni, Cr contents while core UIV, from upstream region, exhibits low Ca values, although, the above cores have muddy sediments. These observations are not consistent with increasing metal-adsorption sites with decreasing grain size as described in the literature (Loring, 1991; Horowitz et al., 1999). The high metal retention by the coarse fraction can be related to association with high TOC content and, therefore, attributed to the formation of organic coatings over sands, which may increase considerably the adsorption of this fraction, as was observed by Singh et al. (1999), in which oxide coatings contributed in high metal retention capacities of the coarse fraction. Further, sand size particles may also contain minerals like pyroxene, amphiboles, source being deccan basalts and these minerals contain higher contents of Fe and associated elements. The mixing of seawater with fresh water results in formation of floccules formed of small particles cemented either by dissolved organic matter or by sea salts present in the marine sediment. Areas of flocculation often have enriched metal concentrations in sediments. This may be because the settling flocs scavenge other metals from the water column, thereby increasing their metal concentration during deposition, and because the larger aggregated particles tend to have a higher settling velocity, get deposited more rapidly and be transported less distance than smaller discrete particles (Palanques et al., 1995). Also, although the highest concentration of metals are generally found in inshore areas of known anthropogenic inputs, near mouth sediments such as those found in the sandy core UI, distant from known inputs, has metal concentrations within the same range as core UIV which lies closer to industrialised zone. These results indicate the mouth region of the Ulhas estuary is highly contaminated with metals from the industrialized area upstream. This may be also due to the increasing human activities towards the mouth. It appears that contaminants are distributed not only in close proximity to the source but far away as well. Therefore, any assessment of discharges of trace metals to the coastal zone

should consider not only the impact within the immediate vicinity of the outfall but also the impacts that may occur farther afield due to favourable transport and depositional conditions.

Different temporal metal distributions between the sites are also noted. An important observation seen is that there are two groups of samples along the study area where, in one group Co, Ni, Cr and V levels are elevated and in the other group the sediments have a relatively low percentage of fine particles, particularly the group in the middle portion of the cores UII and UIV. A possible explanation is the relationship between Cr and heavy mineral content in the sand fraction. Certain heavy minerals are capable of adsorbing Cr (Padmalal et al., 1997). It might be possible that the sands in the estuary are rich in these heavy minerals. The fact that the metals in these cores showed similar trends suggests that the same processes may have affected them. Al and Fe concentrations from bulk sediment analysis can be used to indicate variations in sediment source and post-depositional diagenetic effects (Ritson et al., 1994). The coinciding of peak values of some metals at the same core depths as Mn and Fe, along with the similarity in profiles in cores UI, UII, UIV and UIII suggests a common controlling factor. Metals such as Cu, Co and Ni, generally bind with insoluble pyrite and are precipitated in the solid phase, but Pb and Zn tend to bind with sulphides that can return to solution (Zheng et al., 2002). This may explain the absence of a substantial increase of solid phase Pb at depths in the sediment, compared to the levels of Co and Ni, which increased to well above surface concentrations. Estuarine sediments, particularly in heavily industrialized urban environments, tend to be anoxic within a few centimeters of the sediment-water interface (Lin et al., 2003). Deeper in the sediment, disturbance of reduced conditions is less probable than in the shallow parts of the estuary. Also, there is a low flushing rate of pore water, and re-suspension by wave and tidal currents is unlikely so that abundant insoluble sulphides can bind metal contaminants as a result of anoxic conditions (Abu-Hilal et al., 1988). This may explain the high solid phase concentration of some metals, observed at depths in the present study (core UI).

All along the estuarine region, no definite trend in spatial metal distribution is seen. A probable reason for this may be the sand dredging activities in Ulhas river estuary along Kalyan, Dombivli and Mumbra. It is understood that larger load of suspended particulate matter takes place due to erosion caused by agriculture, dredging and cutting of mangroves on the riverbanks (Rathod et al., 2002),which is a common sight along the upper stretches of Ulhas river estuary. The narrow channel areas of the estuary have been subject to annual dredging activities which bring about re-suspension of particles from the sediments to the water column and increase the suspended particulate matter in water (Athalye and Goldin, 2002). Martino et al. (2002) have proposed that

re-suspension of metal enriched, fine bed sediment may be a significant agency for metal remobilisation in contaminated turbid estuaries. Therefore, it is likely that dredging the sediment from the river may cause resuspension of contaminated sediments, and may distribute the sediment as far as possible. Therefore, the distribution patterns of trace elements in the profiles can reflect the natural dynamic conditions and also the disturbances due to human dredging activities in this area. However, it should be borne in mind that there is no direct evidence that any of the above sequences are not a result of reworking of older deposits, neither can it be proved, from this study, that post-sedimentation modification of the metal distribution patterns has not taken place through either chemical or biological processes. Nevertheless, there is a close linkage of physical and chemical factors described above (Horowitz and Elrick, 1987) wherein secondary geochemical substrates (organic matter, Fe/Mn oxy-hydroxides) are found to be linked to fine particles, either as the result of coagulation and precipitation of colloids, or as surface coatings on clays (Ip et al., 2007; Jackson, 1998; Kersten and Smedes, 2002).

3.2A.9. ^{210}Pb dating

In Ulhas estuary, out of the three cores selected (UI, UIV and UV) for ^{210}Pb dating, only one core (core UI) sampled near the estuary mouth showed a good decay of ^{210}Pb with depth.

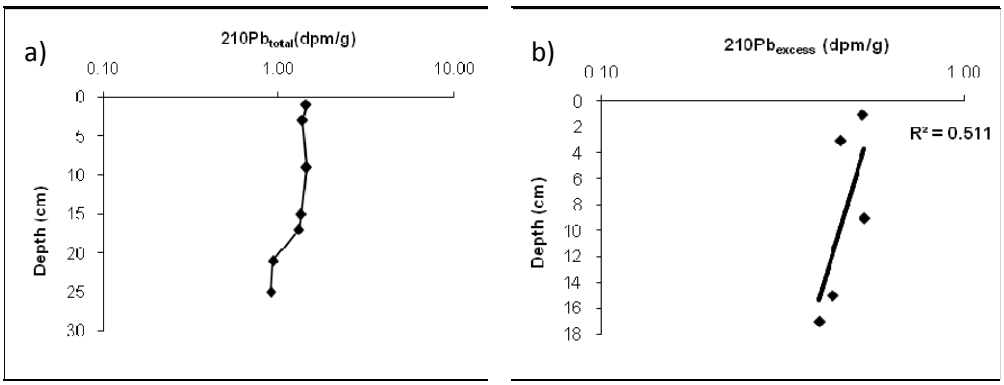

Fig. 3.2A.21. Vertical distribution of a) $^{210}Pb_{total}$ and b) $^{210}Pb_{excess}$ activities in core UI

When the profiles of ^{210}Pb are compared with Pb and redox sensitive elements Fe and Mn, there are no similar peak concentrations, negating the possibilities of mobilization of ^{210}Pb. In core UI, the sedimentation rate was calculated employing the Constant Initial Concentration (CIC) model with an assumption of a constant input of the excess ^{210}Pb to the sediment or a constant sedimentation rate (Brugam, 1978; Jha et al., 1999). The sedimentation rate obtained was 0.24 cm/yr. In the case of the other cores, the total ^{210}Pb profiles did not show a good decay with depth (Fig. 3.2A.22). It shows all the values are more or less same, representing a zone of sediment mixing which must be caused by adding or removing sediments by human activities like dredging. Dredging and sand extraction which are generally conducted in the area and also

bottom trawling by fisherman must have probably resulted in an extensive kneading and resuspension of the surficial sediments. From literature, non-ideal ^{210}Pb behaviour (such as that found in cores UIV and UV) has been attributed to mixing, variation in atmospheric flux due to wind redistribution, migration through the sediment column, particle and hydrology characteristics that influence adsorption and rapid or slow accumulation (Appleby and Piliposian, 2006; Charmasson et al., 1998; San-Miguel et al., 2003; Schottler and Engstrom, 2006). To provide a useful record of anthropogenic input to the coastal system, the sediment must have a relatively high accumulation rate and there should not be significant redistribution of elements throughout the core profile (Cundy et al., 1997; Valette-silver, 1993). So, sedimentation rate in these two cores could not be calculated.

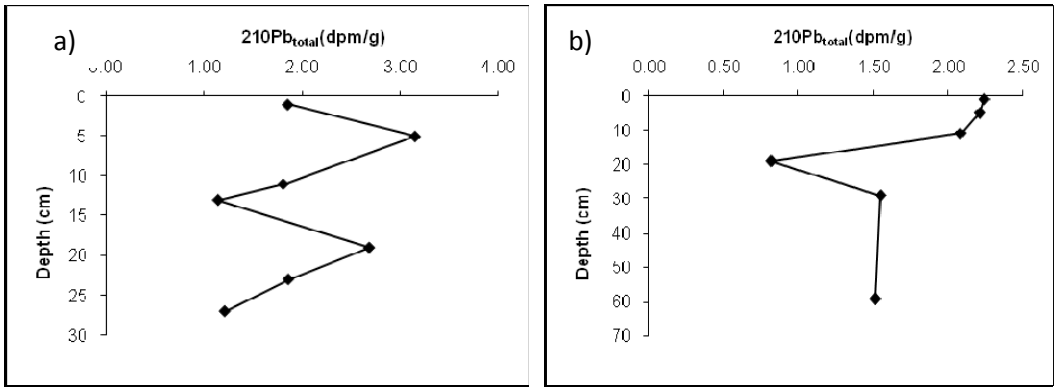

Fig. 3.2A.22. Vertical distribution of $^{210}Pb_{total}$ activities in a) core UV and b) core UIV

High rate of sedimentation (2.96 cm/yr) off Ulhas estuary was reported earlier by Ram et al. (2003) and was attributed to the high sediment transport through Ulhas River during the monsoon season. Thus, it appears that the sedimentation rate increases from 0.24 cm/yr near the estuary mouth (mudflat) to 2.9 cm/y at 25 km offshore. High outflow through the Ulhas estuary to the sea during monsoons transports much of the annual suspended load, generates strong currents and high turbulence in the mouth area that probably do not favour the deposition of fine particles associated with the estuary plume in the vicinity (NIO, 1994).

3.2A.10. Statistical analysis

3.2A.10a. Correlation analysis

All the cores sampled from the estuarine region were subjected to correlation analysis at $p<0.05$. The results of the analysis are discussed below. Three principal factors exert strong control on trace element concentrations in sediments: 1. sorption onto clay minerals (grain-size effect); 2. complexing by organic matter and 3. scavenging by Fe-Mn oxyhydroxides. The correlation analysis is accordingly discussed.

Table 3.2A.1. Classification of values based on correlation analysis in the estuarine region

Stations		Good	Significant
Near estuary mouth	Core UI	0.53-0.66	> 0.66
Lower estuarine region	Core UV	0.51-0.64	> 0.64
Middle estuarine region	Core UII	0.35-0.45	> 0.45
Upper estuarine region	Core UIV	0.35-0.45	> 0.45
Inner estuarine region	Core UIII	0.32-0.42	> 0.42

3.2A.10a1. Sediment components

In core UI, sand is found to show significant association with most of the metals viz, Fe (r=0.89), Mn (r=0.78), Co (r=0.92), Ni (r=0.88), Cr (r=0.89) and Ca (r=0.65). Silt on the other hand displays significant correlations with only clay (r=0.69), TP (r=0.72) and associations to a less extent with Cu (r=0.51) and Zn (r=0.42). Clay correlates with TOC (r=0.52), TP (r=0.59) and shows negative association with almost all the elements studied. For core UV, collected from the lower estuary, amongst the sediment components only silt exhibits some associations with metals [Ni (r=0.36) and Zn (r=0.38)] while sand and clay associates negatively except of clay with TOC (r=0.41), TP (r=0.38), TN (r=0.41) and Al (r=0.36). The core retrieved from the middle estuary (core UII), reflects significant association of sand with most of the metals [Fe (r=0.76), Mn (r=0.62), Ni (r=0.75), Zn (r=0.62), Cr (r=0.77) and Ca (r=0.73)] and negative correlations of silt and clay with all the metals except of clay with TP (r=0.67), TN (r=0.74) and Pb (r=0.39). Core UIV from lower region of the estuary, exhibits significant associations of sand with Co (r=0.74), Ni (r=0.74), Cr (r=0.89), V (r=0.70) and Ca (r=0.85) and to a good extent with Mn (r=0.30); silt with Co (r=0.53), Ni (r=0.42) and Ca (r=0.45); and clay with Cu (r=0.28), Zn (r=0.31) and Al (r=0.48). On the other hand, in core UIII from inner end of the estuary, sand with TOC (r=0.35), TN (r=0.34), TP (r=0.66), Cu (r=0.43) and Ni (r=0.34); silt with Mn (r=0.38), Ni (r=0.57), Zn (r=0.43) and Ca (r=0.35) associates significantly while clay correlates to a low extent with Al (r=0.30) and V (r=0.33).

It appears that finer grain size effect does not exclusively control the distribution of trace metals in most of the cores sampled from the estuary while coarser sediment fraction is found to correlate significantly with most of the metals studied. Metals accumulated to a less extent, or irregularly in fine-grain fractions were also found in a heavily contaminated bay (Ujevic et al., 2000). Tam and Wong (2000) also found that the differences of trace metal concentrations between fine-grained and sand-sized fractions became less significant when the site was more contaminated, which suggest that the excess metals from non-natural sources may be

accumulated in the sand-sized fraction. In the upper estuary, finer fractions are found to correlate significantly with metals. The strong correlation between decreasing sediment size and increasing heavy metal concentration is well documented and suggests that adsorption is the main mechanism by which trace metals accumulate on particles, given that small particle size has a much higher surface area relative to their volume than large particles (Guerra-Garcia and Garcia-Gomez, 2005). The presence of positive correlations between Al and fine grain size (clay) in the upper and inner end of the estuary indicates that alumino-silicate may be the primary metal bearing mineral. Under natural conditions, concentrations of other trace metals in sediments commonly follow a strong, positive linear trend versus Al in a given depositional environment.

3.2A.10a2. Organic matter

The correlation analysis in core UI displays good associations of TOC with TN (r=0.59) and to a less extent with Cu (r=0.42) while TP exhibits correlations with Zn (r=0.44). TN, on the other hand, correlates with only Cu (r=0.67). The core collected from lower estuary (UV) shows significant and good associations of TP and TN with Fe (r=0.77, 0.78), Mn (r=0.75, 0.59), Cu (r=0.50, 0.66), Al (r=0.79, 0.73), V (r=0.89, 0.81) and Ca (r=0.62, 0.68) and also correlations with Ni (r=0.38, 0.42). TOC does not show any correlations with metals. For the core sampled from middle estuarine region (UII), TP and TN correlate well with each other (r=0.53). In addition, TP also associates with Al (r=0.50). TOC shows weak or negative associations with all the metals. In core UIV (upper estuary), TOC correlates significantly with TN (r=0.50), Zn (r=0.72) and Al (r=0.52) while TN associates with only Zn (r=0.43). TP does not show any metal correlations. The inner end of the estuary (core UIII), exhibits significant associations of TOC with TN (r=0.55), Ni (r=0.73), Cu (r=0.46), Zn (r=0.53) and good associations with Pb (r=0.36) and Ca (r=0.40); TP with Mn (r=0.72), Pb (r=0.36), Ni (r=0.39) and Zn (r=0.63); and TN with Cu (r=0.84), Pb (r=0.76), Ni (r=0.66) and Zn (r=0.67).

Positive correlations reveal the affinity of these metals to organic matter. Correlation coefficients between most metals and organic matter are high in most of the cores, indicating that organic matter exerts some control over metal concentrations. Organic matter diagenesis and sediment re-suspension lead to the regeneration of Fe and Mn oxides in sediments, which may alter redox-sensitive heavy metal compositions in the sediment deposits (Breckela et al., 2005). The obtained significant positive correlations between Mn and organic matter in some cores (UIII and UV) and Fe and organic matter in core UV may support this observation.

3.2A.10a3. pH

In core UI, pH correlates well with Fe (r=0.63), Co (r=0.58) and Ca (r=0.68). Good correlations of pH with Pb (r=0.40), Ni (r=0.50) and Cr (r=0.55) are also seen. In core UII significant correlations of pH with Ni (r=0.45), Zn (r=0.54), Cr (r=0.45) and good correlations with Ca (r=0.40) are observed. In core UIII, among the metals only V correlates significantly with pH (r=0.45). The other cores (UV and UIV) do not show any correlations of metals with pH. The estuarine sediments have pH values of ≥ 8. These conditions are favourable for precipitation of Fe-oxides-hydroxides (Parkhurst, 2004), thereby resulting in enrichment of heavy metals by co-precipitation in the uppermost sediment column.

3.2A.10a4. Fe-Mn oxides

Near the estuary mouth (UI), Fe and Mn correlates significantly with each other (r=0.79) and also with Co (r=0.93, 0.80), Ni (r=0.91, 0.86) and Cr (r=0.90, 0.80). Fe also shows good associations with Ca (r=0.63) and V (r=0.62) while Mn shows good correlation with V (r=0.51). In core UV, Fe and Mn associates with each other (r=0.72) and with almost all the metals. Significant correlation of Fe with Cu (r=0.82), Ni (r=0.77), Al (r=0.85), V (r=0.74) and Ca (r=0.79) and good associations with Co (r=0.62), Zn (r=0.53) and to some extent with Cr (r=0.38) are also observed. On the other hand, Mn correlates significantly with only Ca (r=0.68) and shows good associations with Cu (r=0.42), Pb (r=0.41), Al (r=0.62) and Ni (r=0.43). Core UII shows significant associations between Fe and Mn (r=0.56) along with other metals, i.e. Ni (r=0.64, 0.83), Zn (r=0.71, 0.44), Cr (r=0.63, 0.83) and Ca (r=0.65, 0.78). In addition, Mn correlates with Co (r=0.42). In core UIV also, Fe and Mn exhibit significant associations with each other (r=0.62) and some of the metals [Co (r=0.66, 0.57) and Ni (r=0.51, 0.52)]. Correlations of Mn with Cr (r=0.45) and Ca (r=0.46) are also seen. Significant correlation of Fe and Mn with Ni (r=0.38, 0.58), Co (r=0.62, 0.65) and Ca (r=0.44, 0.47) are seen in core UIII. Moreover, associations of Fe with Al (r=0.35) and of Mn with Zn (r=0.70) are also observed.

Al shows good correlations with Fe in the region, however, both metals appear weakly or negatively correlated with the percentage of fine grains (< 63 μm). Since there are no reported anthropogenic sources of Al in the region, the inverse relation may result from dilution of Al and Fe phases in the fine fraction with weathered clays of low scavenging capacity for metals. In general, in all the cores, Fe and Mn are found to correlate well with each other and also with most of the elements studied. This observation suggests that both these redox sensitive elements are the dominant metal carriers in the estuarine region. The biogeochemical cycles of such redox-sensitive metals are of major importance in understanding metal distribution and

behaviour in estuaries, because these oxides readily bind dissolved, cationic metals, removing them from solution as the Mn/Fe oxides precipitate.

3.2A.10a5. Inter-elemental

In core UI, Co and Ni correlate significantly with each other (r=0.96) and also with Cr (r=0.95, 0.94), Ca (r=0.68, 0.62) and V (r=0.59, 0.68). Cr correlates with Ca (r=0.72) and V (r=0.71). Core UV exhibits significant correlations of Cu with almost all the elements i.e. with Co (r=0.74), Ni (r=0.90), Zn (r=0.81), Cr (r=0.76); Co with Ni (r=0.78), Zn (r=0.65) and Cr (r=0.81); Ni with Zn (r=0.82), Cr (r=0.72); Al with Ca (r=0.86), V (r=0.81) and Ca with V (r=0.65). In addition, good associations are seen of Cu with Al (r=0.54), V (r=0.62) and Ca (r=0.48), Co with V (r=0.62) and Al (r=0.44), Ni with Al (r=0.52) and V (r=0.51). In core UII, Pb correlates with Cu (r=0.45) and Co (r=0.49); Zn with Ni (r=0.65); Cr with Co (r=0.38), Ni (r=0.99), Zn (r=0.63), Ca (r=0.82) and Ca with Co (r=0.36), Ni (r=0.81), Zn (r=0.58). For core UIV, significant correlations between Cu and Al (r=0.48); Co with Ni (r=0.84), Cr (r=0.88), Ca (r=0.80) and V (r=0.43); Ni with Cr (r=0.84), Ca (r=0.84) and V (r=0.57); Cr with Ca (r=0.91) and V (r=0.59) and Ca with V (r=0.67) are observed. In the case of core UIII, significant correlations of Cu with Pb (r=0.63), Co (r=0.42), Ni (r=0.59), Zn (r=0.64); Pb with Co (r=0.51), Ni (r=0.64), Zn (r=0.78); Co with Ni (r=0.58) and Zn (r=0.60); Ni with Zn (r=0.75) and Ca (r=0.53) are seen.

High correlation coefficient between the metals indicates their common sources, mutual dependence and identical behaviour during the transport. The absence of correlations among the other metals suggests that the concentrations of these metals are not controlled by a single factor, but a combination of geochemical support phases and their mixed associations. In the present study, the examined metals such as Cu, Co, N and Zn are found to exhibit a common source in cores UV and UIII.

3.2A.10a6. Magnetic susceptibility

The correlation between magnetic susceptibility and heavy metal content has been reported in many of the earlier works (Petrovsky et al., 1998; Durza, 1999; Petrovsky et al., 2001; Shu et al., 2001). Hunt et al. (1984) have also observed a significant correlation of SIRM with Cu, Zn, and Cr in atmospheric particulates. These studies suggested that the magnetic parameters could be a proxy measure of the degree of heavy metal contamination in soils, sediments, and atmospheric particulates. Sheng-Gao et al. (2008) suggested that heavy metals were associated with ferrimagnetic particles in soils, which were attributed to input of traffic emissions and industrial

activities. In various studies, the relationship between magnetic susceptibility and heavy metal concentrations was usually analysed by simple linear regression analysis (Beckwith et al., 1986; Chan et al., 1997; Strzyszcz and Magiera, 1998; Hanesch et al., 2001; Knab et al., 2001). In the present study, the correlation coefficients at $p<0.05$ of Magnetic susceptibility parameters with other variables are separately calculated since only a limited set of samples were analysed for the susceptibility parameters.

In core UI, χ_{lf} and SIRM (r=0.98) correlates with each other and also with SIRM/χ_{lf} (r=0.75, 0.85), HIRM (r=0.80, 0.83), Hard (r=0.65, 0.69), sand (r=0.99, 1.00), Fe (r=0.97, 0.93), Mn (r= 0.78, 0.85), Co (r=0.96, 0.96), Ni (r=0.96, 0.94), Cr (r=0.98, 0.94); χ_{ARM} with χ_{ARM}/χ_{lf} (r=0.78), χ_{ARM}/SIRM with χ_{ARM}/χ_{lf} (r=0.99), χ_{fd} (r=0.90), clay (r=0.82) and Zn (r=0.84); SIRM/χ_{lf} with HIRM (r=0.77), Hard (r=0.69), sand (r=0.81), Fe (r=0.67), Mn (r=0.87), Co (r=0.78), Ni (r=0.73) and Cr (r=0.64); χ_{ARM}/χ_{lf} with χ_{fd} (r=0.86), clay (r=0.79) and Zn (r=0.83); HIRM with hard (r=0.97)), sand (r=0.81), Fe (r=0.83), Mn (r=0.50), Co (r=0.92), Ni (r=0.82), Cr (r=0.72); Hard with sand (r=0.67), Fe (r=0.72), Co (r=0.82), Ni (r=0.70) and Cr (r=0.56); S- ratio with χ_{fd} (r=0.61), silt (r=0.96), Cu (r=0.94); χ_{fd} with silt (r=0.67), clay (r=0.94), Cu (r=0.73) and Zn (r=0.89), indicating the role of both magnetic concentration and grain size in their association.

In core UV, significant correlations are seen of χ_{lf} with SIRM (r=0.70), HIRM (r=0.68), Hard (r=0.58), silt (r=0.57), Fe (r=0.50), Cu (r=0.68), Zn (r=0.76), Cr (r=0.61) and V (r=1.00); SIRM with SIRM/χ_{lf} (r=0.76), HIRM (r=0.65), χ_{fd} (r=0.77), sand (r=0.67), silt (r=0.73), Co (r=0.77), Zn (r=0.56), Cr (r=0.69) and V (r=0.73); χ_{ARM} associates with χ_{ARM}/SIRM (r=0.99) and both together correlate with χ_{ARM}/χ_{lf} (r=0.99, 1.00), Fe (r=0.92, 0.86), Mn (r=0.70, 0.80), Cu (r=0.70, 0.61) and Ni (r=0.96, 0.93); SIRM/χ_{lf} with χ_{fd} (r=0.78), sand (r=0.72), slit (r=0.51), Co (r=0.72); χ_{ARM}/χ_{lf} with Fe (r=0.86), Mn (r=0.79), Cu (r=0.62) and Ni (r=0.93); HIRM with hard (r=0.97), χ_{fd} (r=0.74), silt (r=0.97) and V (r=0.72); Hard with χ_{fd} (r=0.62), silt (r=0.90), Pb (r=0.66) and V (r=0.62); S-ratio with clay (r=0.83); χ_{fd} with sand (r=0.87) and silt (r=0.88). In core UIV, χ_{lf} exhibits good correlations with SIRM (r=0.98) and both together show associations with SIRM/χ_{lf} (r=0.72, 0.84), HIRM (r=0.63, 0.68), sand (r=0.72, 0.78), Co (r=0.59, 0.65), Ni (r=0.59, 0.68), Cr (r=0.60, 0.70) and V (r=0.63, 0.69); χ_{ARM}/SIRM with χ_{ARM}/χ_{lf} (r=0.99), χ_{fd} (r=0.91) and clay (r=0.57); SIRM/χ_{lf} with HIRM (r=0.67), sand (r=0.76), Co (r=0.70), Ni (r=0.79), Cr (r=0.80) and V (r=0.64); χ_{ARM}/χ_{lf} with χ_{fd} (r=0.88) and clay (r=0.51). Significant correlation with magnetic susceptibility and heavy metal contents is suggestive of an anthropogenic source. Core UIV located closer to the industrial zone show relatively higher values of magnetic susceptibility and related parameters.

For Fe, the significant correlation with χ_{lf} can be attributed to the influence of anthropogenic magnetic particulate matter. On the other hand, the correlation between χ_{lf} and Cu and Zn in core UV can be attributed to the incorporation of these elements in the crystalline structure of Fe minerals molecule (Kukier et al., 2003). For Cu, Zn and Mn in core UIV, the correlation with χ_{lf} is not significant. This may be attributed to the fact that these elements do not show an anthropogenic increase. Pb, in the estuarine region, does not show a significant correlation with susceptibility parameters in spite of the high enrichment factor of this metal in the analyzed samples. These results disagree with those reported for other urban areas (Strzyszcz and Magiera, 1998; Durza, 1999; Xie et al., 2001; Hu et al., 2007) which show a significant correlation between χ_{lf} and Pb. A negative or weak correlation appears between χ_{lf} and SIRM with the mud fraction, in all the cores implying that the magnetic minerals must be concentrated in the coarser fraction of sediment. These observations indicate that the magnetic carriers are present mainly in the sand size fraction of the cores. The lack of positive correlation between χ_{lf} and χ_{fd} in sediment of the studied cores indicates that the main susceptibility variations are due to magnetic enhancement as a result of industrial pollution. Many authors reported the positive correlation of χ_{lf} and χ_{fd} in Chinese loess and paleosols (Guo et al., 2001; Zhu et al., 2001; Wang et al., 2003). The S-ratio did not show strong association with heavy metals, indicating that it was not as good indicator of heavy metal content as the magnetic concentration parameters did. Magnetic particles, in the form of fine Fe oxide dusts, could have been released along with other heavy metals from a combination of different sources and introduced into the sediments. The anthropogenic magnetic particles are likely to have come from three sources: (1) emissions from fossil-fuel combustion processes (fly ash); (2) vehicle emissions (vehicular exhaust, abrasion of tyres, brake linings as well as road construction materials) and (3) waste products and dusts from metallurgical and other industries. All three sources might have contributed to the increase of the magnetic susceptibility of the sediments.

3.2A.10b. Factor analysis

In order to confirm the different variable associations, to aid in the identification of parameters controlling trace metal distribution, factor analysis was carried out in all the five cores collected from the estuarine region. The values obtained by varimax rotation are given in Tables 3.2A.2 to 3.2A.3.

3.2A.10b1. Near the estuarine mouth (Core UI)

In factor analysis for core collected near the estuary mouth, the first three principal components accounted for nearly 79.29 % of the total variance, and the variances of Factor 1, Factor 2 and

Factor 3 are 53.68, 14.77 and 10.84 %, respectively. The % variance of Factor 1 is found to be much higher than the other two factors. The first factor exhibits good loadings of sand, Ca, Fe and Mn on Pb, Co, Ni, Cr, and V. This factor likely represents Fe and Mn compounds that seem to be the main binding phases for Pb, Co, Ni, Cr, and V and minor binding phases for Ca. Despite these elements being derived from different industries they are all included in the same factor, which is probably revealing the importance of mixing and homogenising processes originated by tidal and wind regimes, that happen inside the estuary followed by transport and deposition at the estuary mouth. The second factor shows good loadings of Al on Pb and pH while the third factor exhibits good loadings of sand and Ca on Cr and to some extent on Fe, Co, Ni and Cr. The first and third factors show good associations of sand with most of the metals studied. At the estuary mouth, deposition and resuspension of sediment may be higher than in the extreme upper stations due to stronger tidal currents. As a result coarser sediments are found to dominate over finer sediments.

Table 3.2A.2. Varimax rotated factor analysis in core UI

	Factor 1	Factor 2	Factor 3
Total variance	53.68	14.77	10.84
Eigen values	9.66	2.66	1.95
Sand	**0.84**	0.13	0.43
Silt	-0.49	-0.26	-0.73
Clay	**-0.89**	-0.07	-0.30
TOC	-0.64	-0.56	0.19
TP	-0.50	0.24	**-0.75**
TN	-0.09	**-0.93**	0.00
pH	0.41	0.53	0.51
Fe	**0.86**	0.11	0.36
Mn	**0.91**	-0.13	0.09
Cu	-0.13	-0.63	-0.46
Pb	0.64	0.43	-0.34
Co	**0.84**	0.16	0.45
Ni	**0.90**	0.09	0.34
Zn	-0.04	0.05	**-0.75**
Cr	**0.81**	0.03	0.54
V	0.65	-0.27	0.27
Al	-0.28	0.68	-0.07
Ca	0.38	0.07	**0.84**

3.2A.10b2. Lower estuarine region (Core UV)

The core sampled from the lower estuary exhibits a total variance of 84.89 % with four factors. The first factor with 41.79 % total variance shows good positive loadings of TP, TN, Al, Ca, Fe and Mn and to some extent clay on Cu, Ni and V. The significant relationship of Fe and organic matter with Al in this factor indicates that the Fe and organic matter are closely associated with

the aluminosilicate phase, and thus it is assumed that the detrital minerals are the predominant carriers of Cu, Ni and V in the region. The second factor with 22.20 % total variance exhibits good loadings of silt and Fe on Cu, Co, Ni, Zn, Cr and V. The third factor having 13.49 % total variance with good loadings of silt shows associations with Ni but to a low extent. The fourth factor comprises 7.41 % total variance and has good loadings of Mn on Pb. Factor 1 and 2 indicates the metals might be discharged from the same source or have similar depositional activities.

Table 3.2A.3. Varimax rotated factor analysis in core UV

	Factor 1	Factor 2	Factor 3	Factor 4
Total variance	41.79	22.20	13.49	7.41
Eigen values	7.52	4.00	2.43	1.33
Sand	0.06	-0.02	0.03	**-0.90**
Silt	-0.37	0.38	**0.76**	0.06
Clay	0.37	-0.38	**-0.77**	0.08
TOC	-0.19	0.20	**-0.88**	-0.13
TP	**0.91**	0.04	-0.13	0.18
TN	**0.76**	0.31	-0.36	0.22
pH	-0.35	-0.57	0.32	0.27
Fe	**0.81**	0.53	0.02	0.14
Mn	**0.77**	-0.01	0.12	0.48
Cu	0.43	**0.85**	0.05	0.19
Pb	0.25	-0.02	0.11	**0.75**
Co	0.21	**0.85**	0.03	0.07
Ni	0.40	**0.80**	0.34	0.09
Zn	0.06	**0.88**	0.20	-0.10
Cr	-0.14	**0.96**	-0.06	-0.07
V	0.65	0.51	-0.35	-0.14
Al	**0.92**	0.22	0.02	-0.05
Ca	**0.95**	0.06	-0.11	-0.09

3.2A.10b3. Middle estuarine region (Core UII)

A total variance of 76.19 % was produced explaining four factors in the middle estuarine region. The first factor representing 43.93 % of the total variance displays good loadings of pH, sand, Ca, Fe and Mn on Ni, Zn and Cr while factor 2 with 14.26 % of total variance shows good loadings among Cu, Pb and Co. The third factor consisting 9.77 % total variance exhibits good loadings of Ca and Mn on Ni, Cr and V. On the other hand, the fourth factor having 8.24 % total variance shows negative associations between silt and V. Note that elements such as Mn, Ni, Cr and Ca that express moderate to high loadings with both factor 1 and factor 3, are related to more than one geochemical process (Bailey et al., 2005).

Table 3.2A.4. Varimax rotated factor analysis in core UII

	Factor 1	Factor 2	Factor 3	Factor 4
Total variance	43.93	14.26	9.77	8.24
Eigen values	7.91	2.57	1.76	1.48
Sand	**0.85**	-0.11	0.27	0.32
Silt	0.04	-0.30	-0.31	**-0.78**
Clay	**-0.90**	0.28	-0.11	0.09
TOC	-0.27	0.33	-0.05	-0.20
TP	-0.66	-0.01	-0.62	-0.07
TN	**-0.85**	0.10	0.00	0.01
pH	**0.78**	-0.20	-0.06	-0.29
Fe	**0.80**	0.19	0.11	0.22
Mn	0.53	0.13	0.64	0.21
Cu	0.05	**0.79**	-0.33	-0.06
Pb	-0.27	**0.76**	0.21	0.20
Co	0.31	0.58	0.26	0.23
Ni	0.68	0.04	0.68	0.03
Zn	**0.78**	0.29	0.23	-0.28
Cr	0.68	0.04	0.66	0.09
V	-0.01	0.15	0.54	**-0.71**
Al	0.07	0.08	**-0.88**	0.04
Ca	0.69	0.00	0.48	0.31

3.2A.10b4. Upper estuarine region (Core UIV)

Factor analysis in the upper estuarine region (core UIV) produced four factors resulting in a total variance of 77.47 %. Factor 1 with 43.81 % total variance shows good loadings of sand, silt, Ca on Co, Ni, Cr and V. Variables included in Factor 2 accounts for 15.35 % total variance and results in good loadings of pH and TP. Factor 3 having 11.01 % total variance exhibits good loadings of Fe and Mn and to some extent silt on Cu, Co and Ni. Factor 4 with total variance of 7.30 % displays good loadings of silt and Al on Cu and Pb. In almost all the factors the role of finer fraction (silt) is seen reflecting the binding of heavy metals and as such their distribution patterns are controlled by the fine grained fraction in the core.

Table 3.2A.5. Varimax rotated factor analysis in core UIV

	Factor 1	Factor 2	Factor 3	Factor 4
Total variance	43.81	15.35	11.01	7.30
Eigen values	7.89	2.76	1.98	1.31
Sand	**0.92**	-0.02	0.03	-0.32
Silt	0.43	0.28	0.39	0.55
Clay	**-0.92**	-0.13	-0.23	-0.03
TOC	-0.59	-0.67	-0.27	0.20
TP	-0.61	0.38	-0.20	-0.07
TN	-0.18	-0.56	-0.14	0.20
pH	-0.17	0.60	0.03	0.22
Fe	0.25	-0.11	**0.81**	0.13
Mn	0.22	0.19	**0.82**	-0.11
Cu	-0.45	-0.09	0.53	0.63
Pb	0.12	-0.46	0.02	0.66

Co	**0.78**	0.04	0.57	-0.03
Ni	**0.81**	0.04	0.39	0.04
Zn	-0.24	**-0.85**	0.16	0.18
Cr	**0.89**	0.11	0.27	-0.18
V	**0.81**	0.19	-0.34	0.11
Al	-0.44	-0.07	-0.32	0.66
Ca	**0.88**	0.31	0.19	-0.17

3.2A.10b5. Inner estuarine end (Core UIII)

Total variances of 82.07 % with five factors were extracted in the core collected in the inner estuarine region.

Table 3.2A.6. Varimax rotated factor analysis in core UIII

	Factor 1	Factor 2	Factor 3	Factor 4	Factor 5
Total variance	38.71	15.52	11.46	9.28	7.10
Eigen values	6.97	2.79	2.06	1.67	1.28
Sand	0.18	0.36	0.00	0.01	**0.73**
Silt	0.16	**0.81**	0.09	0.08	0.00
Clay	-0.21	**-0.86**	-0.08	-0.08	-0.26
TOC	0.39	**0.79**	-0.01	-0.02	0.10
TP	0.15	0.08	-0.02	**0.93**	0.14
TN	**0.89**	0.28	-0.07	0.01	0.05
pH	-0.59	0.00	-0.14	-0.31	0.48
Fe	-0.16	0.30	**0.87**	0.11	0.14
Mn	0.14	0.29	0.50	**0.74**	0.07
Cu	**0.82**	0.20	0.07	0.06	0.28
Pb	**0.89**	0.02	0.04	0.25	-0.24
Co	0.41	0.12	**0.79**	0.26	0.03
Ni	0.55	0.65	0.25	0.30	-0.08
Zn	**0.70**	0.27	0.20	0.55	-0.02
Cr	-0.21	-0.14	0.11	0.28	**0.77**
V	**-0.85**	-0.14	0.03	0.09	0.06
Al	-0.08	-0.35	0.67	-0.53	-0.22
Ca	-0.15	0.67	0.12	0.40	-0.08

The first factor accounts for 38.71 % total variance and shows good loadings of TN on Cu, Pb, Co, Ni and Zn. These strong loadings suggest that associations with TN control the abundance and distribution of Cu, Pb, Co, Ni and Zn in this core. The second factor with 15.52 % of total variance projects good loadings of TOC, silt and Ca on Ni. The third factor having 11.46 % of total variance displays good loadings of Al, Fe and Mn on Co. This factor likely represents Fe and Mn compounds that seem to be the main binding phases for Co. The fourth factor with 9.28 % of total variance shows good loadings of TP, Ca and Mn on Zn while the fifth factor accounts for 7.10 % total variance with positive loadings of sand and to some extent pH on Cr.

Generally, the results of correlation and factor analyses agree with each other. In the present study, the result of factor analysis corresponds well with coefficient correlation matrix with Fe and Mn as the dominant metal carriers followed by organic matter. The results obtained in factor

analysis suggest that Ca might have a distinct marine source, comprising of biogenic carbonates, present in high concentration in sediments with coarser grain size. This is in good agreement with the results obtained in correlation analysis, confirming that Ca has a distinct (i.e. marine) source, comprising biogenic carbonates, present in high concentration in sediments with coarser grain size. Carbonates which are linked to coarser particles can play an important role in the distribution of Mn in estuarine systems as they are important nucleation centres for Mn oxides (Dassenakis et al., 1995). Consequently carbonates play a similar role as clays by acting as a carrier for the metal binding substrate (Mn oxides) but do not strongly bind metals themselves, therefore acting more as a diluent in the latter case (Campbell et al., 1988). In most of the cores, the correlations of Fe with Al, organic matter and fine-grained fraction are not too strong, suggesting that apart from being a constituent of clay minerals and as coatings on the surface of clay particles, the distribution of Fe is also controlled by other factors. In the estuarine region, except at the inner end of the core, finer fraction does not play any role in metal association. Induced mixing in the shallow estuary clubbed with dredging activities winnows out the fine grain material, pollutants discharged into this region are not likely to accumulate in the immediate vicinity and are exported towards the sea. The fact that many metals with elevated levels did not cluster together in the statistical analyses reflects the different sources and controls on their behaviour such as human activity and the local environment. The modes of delivery of trace metals to the estuary from industries are probably diverse and could include erosion, transportation and deposition by wind, water of contaminated soils near major industrial sites and also dissolved metals which could accumulate in sediments via surface and ground water flows. These observations suggest a double balanced process, between (i) the removal of metal from the water column, estuaries and coastal inputs into the sediments and (ii) the metal inputs (diffusion, desorption) from the sediments to the water column.

3.2A.11. Pollution indices

3.2A.11a. Enrichment factor (EF)

The vertical plots of EF are shown in figures 3.2A.23 to 3.2A.27. From Fig. 3.2A.23, in core UI, it is seen that most of the metals show an increment towards the surface. Throughout the core, the EF values of almost all the elements are more than 1.5. The individual metals followed varying patterns, but on average higher concentrations of Cu, Zn and V are present towards the surface while for Fe, Mn, Pb, Co, Ni and Cr the values are found to be within the lower end of the core. In general the order of average EF values in the core are Pb > Co >Cu >V >Mn >Ni >Cr >Fe >Zn. For core UV, from lower estuary, the average EF trend is Co >Pb >Cu >Mn >Cr

>Ni >V >Fe >Zn. From the down-core plot (Fig. 3.2A.24), almost all the elements show similar decreasing trends from the bottom to 8 cm depth while further above till the surface of the core an increasing trend is seen.

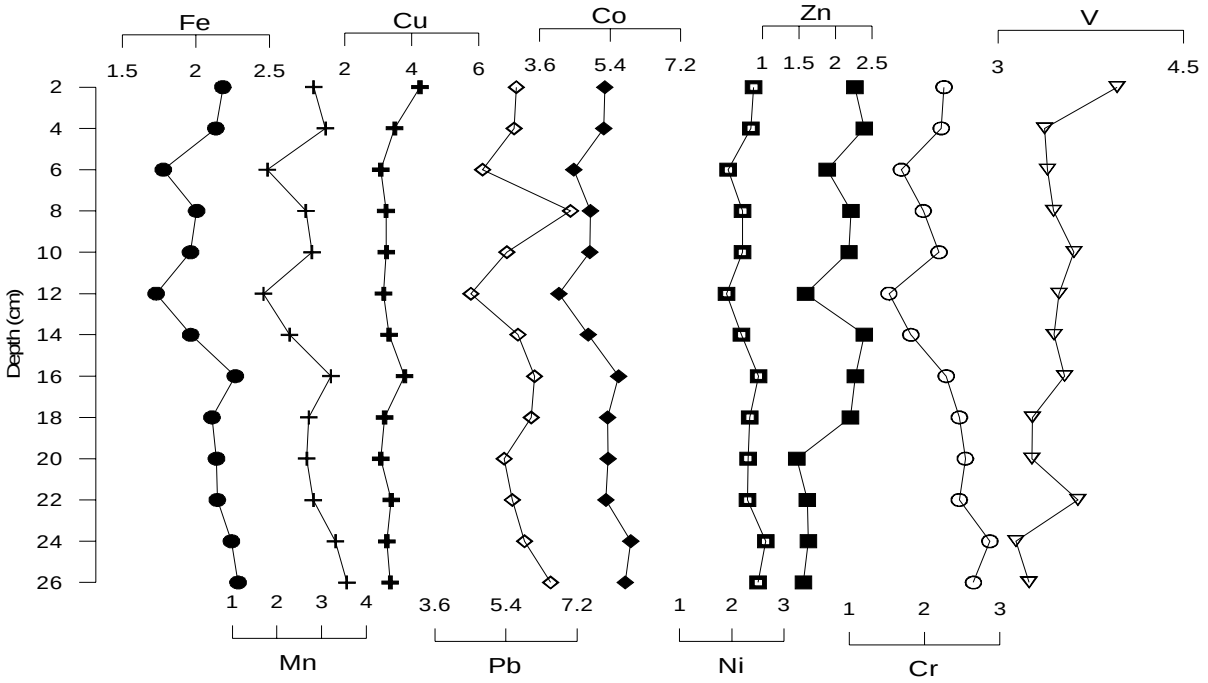

Fig. 3.2A.23. EF plot for core collected near the estuary mouth (UI)

For core UII, the trend of average EF is Cr > Co > Pb > Cu > V > Mn > Zn > Ni > Fe. Larger variations are observed in the middle portion of the core as compared to lower and upper portions of the core (Fig. 3.2A.25). Also, the values are found to decrease towards the surface of the core. Enrichment in most of the elements in the middle portion of the core is related to fluctuations in grain size, since their concentration show a relatively similar pattern to sand concentration.

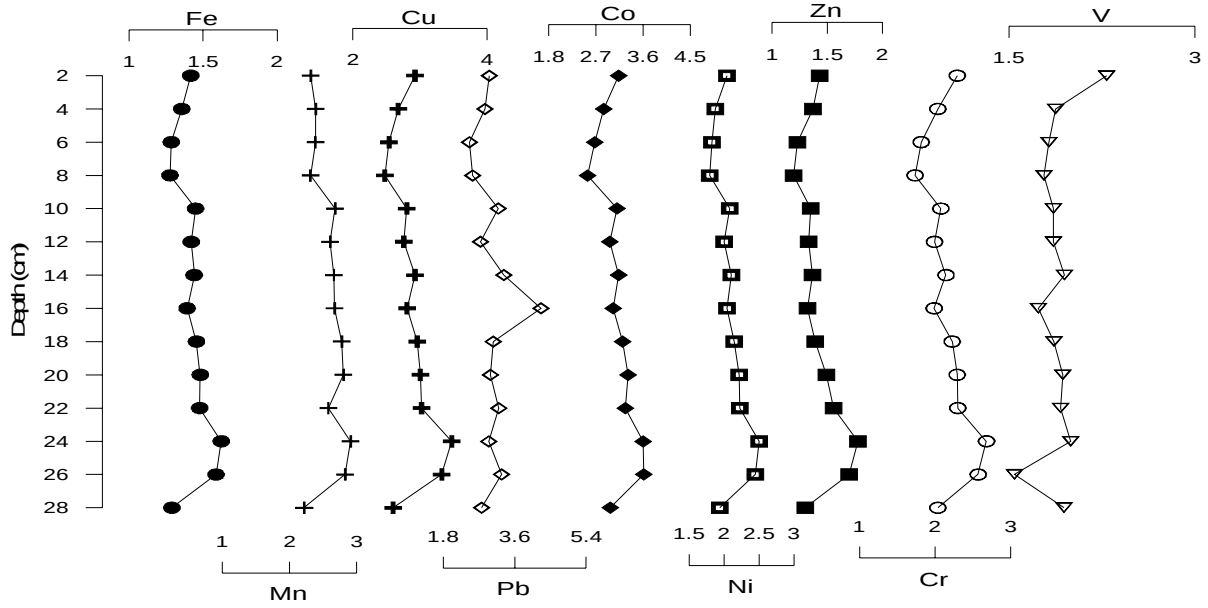

Fig. 3.2A.24. EF plot for core collected in the lower estuary (UV)

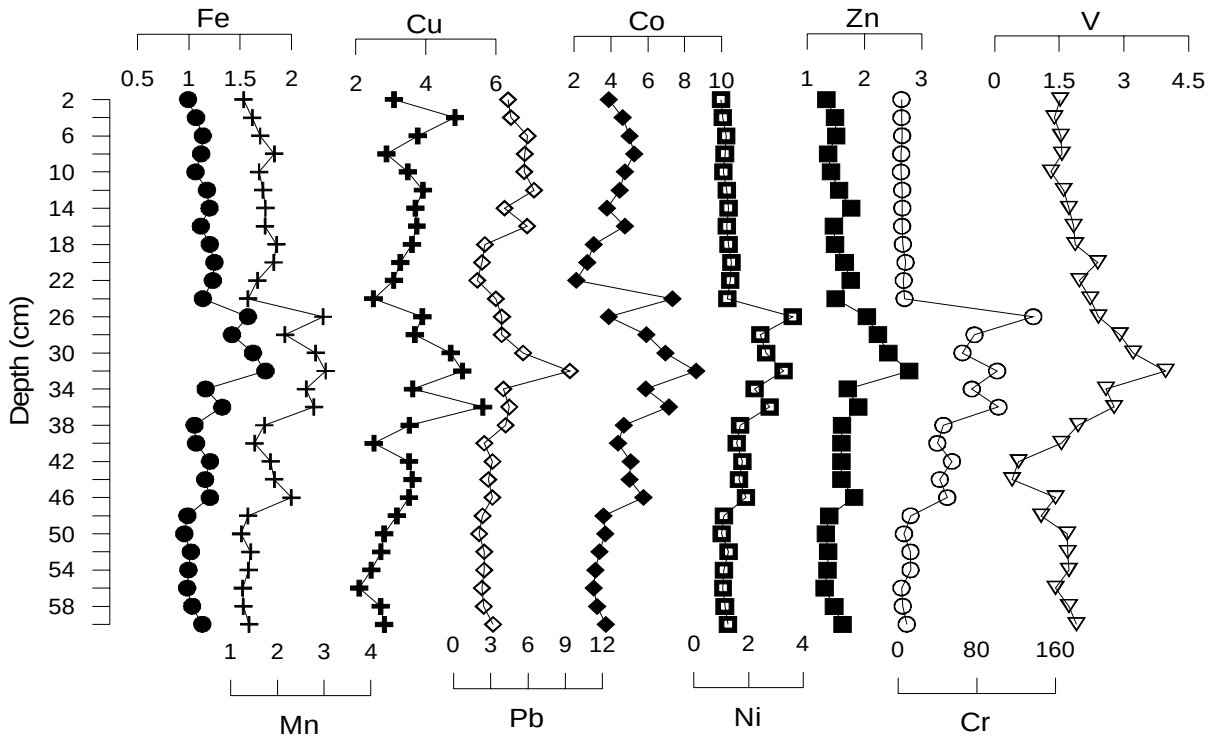

Fig. 3.2A.25. EF plot for core collected in the middle estuary (UII)

In core UIV, the average EF values follow the trend, Co > Cu > Pb > Cr > Mn > V > Fe > Ni > Zn. All the elements between the depths of 28 and 18 cm, show an enrichment which again are found to be similar to sand percentage profile (Fig. 3.2A.26). Higher EF values are seen at the middle portion and to some extent at lower portion of the core as compared to the upper portion. In core UIII, the trend of EF value is Cu > Co > V > Pb > Cr > Zn > Mn > Ni > Fe. Most of the elements exhibit a constant trend from the bottom to the surface, except for Cr and V, which fluctuate considerably (Fig. 3.2A.27). In all the elements, except for V, enrichments have been maintained upto the surface. This indicates that the enrichments are clearly related to anthropogenic contamination.

From the distribution profiles it is seen that Fe and Ni concentrations at all stations are at natural concentration level (EF < 1.5). For other metals, concentration levels in all the sites are higher than natural levels. The EF of trace metals of mudflats in the present study are higher than the previous study carried out by Bhosale and Sahu (1991) on estuarine sediments. The enrichment of metals in the sediments most likely reflects the degree of urbanization of the surrounding terrain where specific anthropogenic sources contribute metals.

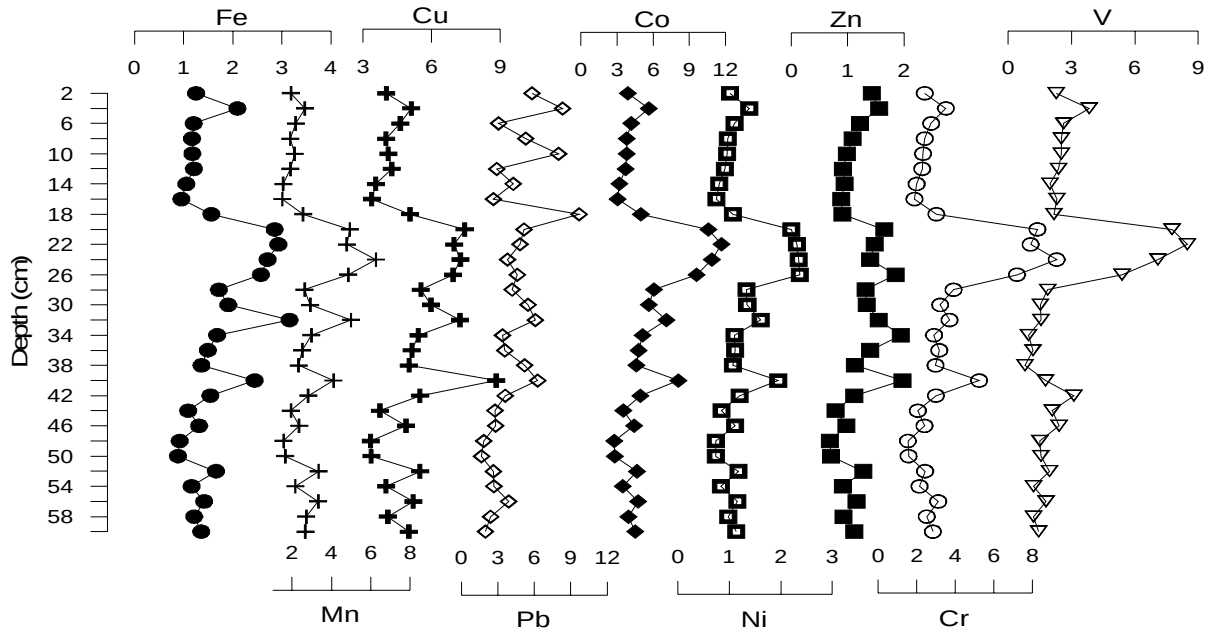

Fig. 3.2A.26. EF plot for core collected in the upper estuary (UIV)

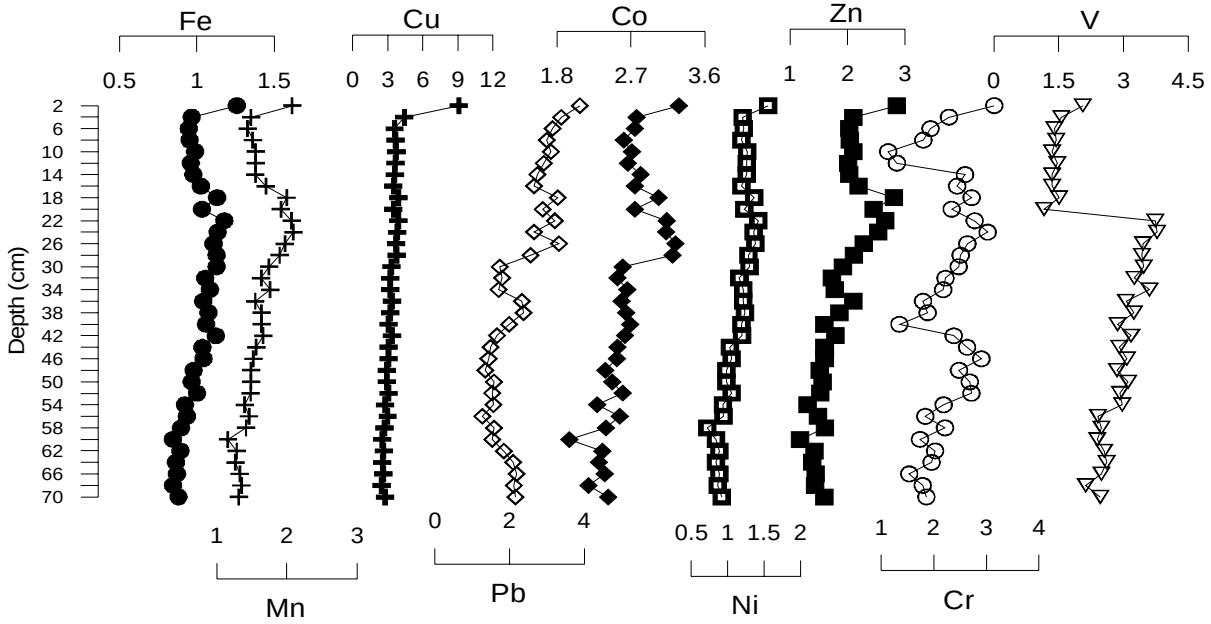

Fig. 3.2A.27. EF plot for core collected near the inner end (UIII)

The distribution of the heavy metal enrichment within the study area can be explained in terms of the proximity of the cores (eastern) to the potential sources of contaminants. Since the western core (UI) was located adjacent to the anchorage site and the navigation fairway, it was conceivably more vulnerable to contamination by shipping discharges and wastes. Particles enriched in heavy metals probably settled through the water column without substantial lateral disbursement by water currents. The cores from the upstream region also showed appreciable amounts of metal enrichment. Industrial activities capable of contributing to elevated concentrations of heavy metals include the plastic industry, automobile and boat fuel, construction, galvanizing iron and steel products, and electroplating (Forstner and Wittmann,

1979; Moore and Romamoorthy, 1984). A number of industries situated in Kalyan-Ulhasnagar industrial zone, in the upstream region, fall into these categories, thus leading to elevated concentrations of Cu, Pb, Co, Cr and Zn in the Ulhas estuary due to proximity to these sources of contamination. The estuary receives effluent from domestic sewage from surrounding localities. Also, there was higher level of TOC at these stations with significant positive correlations between the metals and TOC, showing that incorporation of metals by flocculation with organics influenced their concentration in sediment. It is, however, possible that the frequent dredging in the estuary results in the removal and transport of contaminated sediment particles, such that a build up of metal levels is ameliorated. This may also explain the variable status of enrichment between the different sampling sites.

3.2A.11b. Igeo

Based on Igeo values, in core UI, Cu, Co and Pb fall in moderately polluted class while the remaining elements fall in unpolluted to moderately polluted class (Fig. 3.2A.28a). A few subsamples for Pb fall in moderately to strongly polluted class. For core UV, Mn, Cu, Pb and Co fall in moderately polluted class while the remaining elements fall in unpolluted class (Fig. 3.2A.28b). In core UII, the elements, Fe, Mn, Ni and V are classified as unpolluted, Cu and Pb are unpolluted to moderately polluted while Co and few samples of Cu are moderately to strongly polluted. On the other hand, the subsamples for Cr ranges from moderately polluted to strongly polluted class (Fig. 3.2A.29a).In the case of core UIV (Fig. 3.2A.29b), Cu, Pb, Co and Cr fall in moderately polluted class while a few subsamples of all the above elements also fall in moderately to strongly polluted class. In core UIII, only Cu falls in moderately polluted class while the remaining elements fall in unpolluted to moderately polluted class (Fig. 3.2A.30).

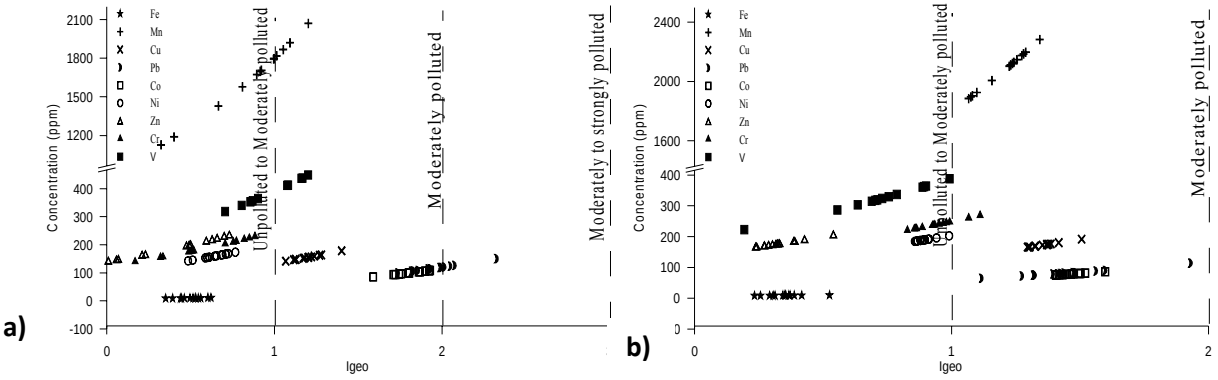

Fig. 3.2A.28. Igeo plot for cores collected near the a) estuary mouth (UI) and b) lower estuary (UV)

Based on the Igeo classification, the magnitude of heavy-metal pollution in sediments of the estuary is as follows, Co > Cu > Pb > Cr > Mn> V> Zn> Ni > Fe. According to the Igeo classification, the studied sites are highly polluted with respect to most trace metals. Co released

into the atmosphere is deposited on soil, and Co released to water may sorb to particles and settle into sediment or sorb directly to sediment. Other sources include the burning of fossil fuels, sewage sludge, phosphate fertilizers, mining and smelting of Co ores, processing of cobalt alloys and industries that use or process cobalt compounds.

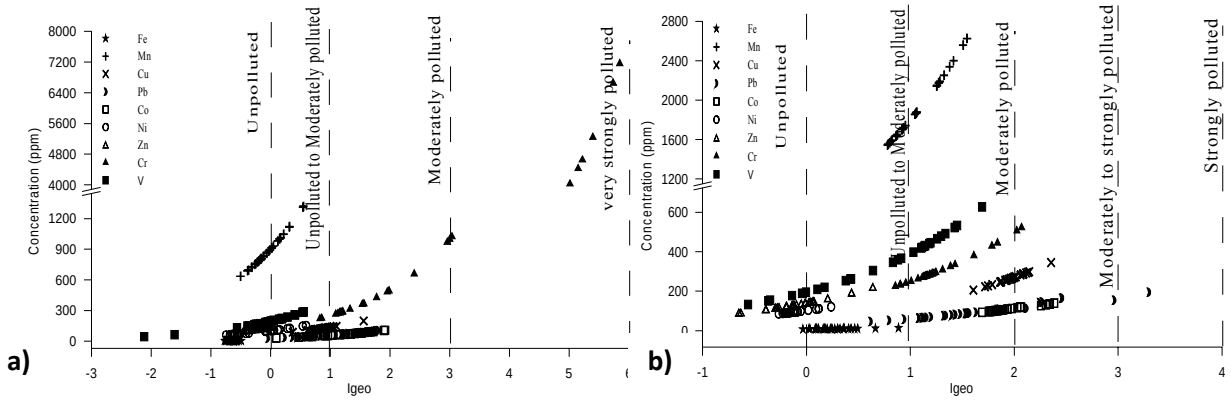

Fig. 3.2A.29. Igeo plot for core collected in the a) middle (UII) and b) upper (UIV) estuary

Important anthropogenic inputs of Cu in estuarine and coastal waters include sewage sludge dumpsites, municipal waste discharge, and antifouling paints (Kennish, 1998). Cu has a high affinity for clay mineral fractions, especially those rich in coatings containing organic carbon and Mn oxides (Callender, 2003) and as a result, residues are often elevated in sediments near localized sources of inputs (Denton et al., 1997).

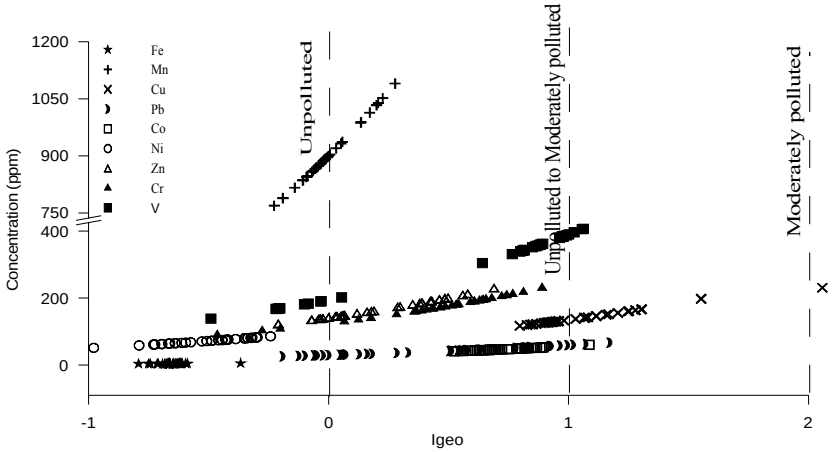

Fig. 3.2A.30. Igeo plot for core collected in the inner estuary (UIII)

Abu-Hilal et al. (1988) and Laxen (1983) attributed high Pb concentrations to several sources such as boat exhaust systems, spillage of oil, and other petroleum products from mechanized boats employed for fishing and the discharge of sewage effluents into water. In addition to these sources, atmospheric input of Pb generated from the automobile exhaust emission can be attributed as the most significant source to the investigated areas. Moreover, it did not follow the vertical distribution of any of the controlling factors considered for metals accumulation in sediments (e.g. Al, Fe, Mn, clay or OM). This indicates the increased land-based activities as

well as using leaded gasoline in the last four decades. Major coastal marine contributors of Cr are dominated by input from rivers, urban runoff, domestic and industrial wastewaters and sewage sludge (Denton et al., 1997). Also, other main sources in the aquatic environment include the waste stream from electroplating and metal finishing industry (Callender, 2003; Finkelman, 2005).

An attempt to compute EF and Igeo, using the values of the bottom sediment in core UI, which showed a record of 120 yrs back, could not be achieved as the bottom values were higher than the surface as well as that seen for the other cores in the estuarine region.

3.2A.12. Isocon plots

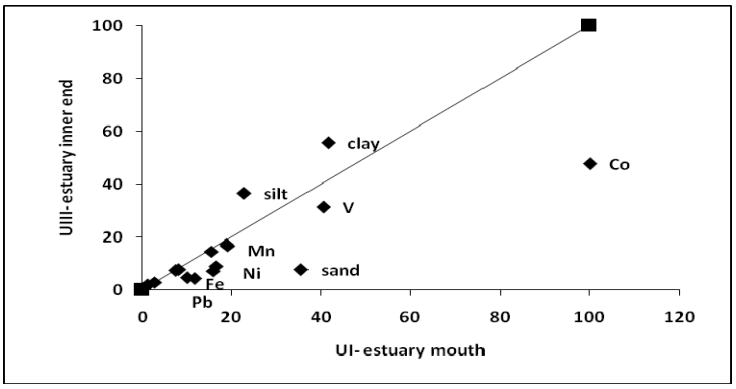

Fig. 3.2A.31. Isocon plot for cores collected near the estuary mouth (UI) and inner end (UIII)

The spatial distribution patterns of geochemical characteristics and heavy metals are illustrated in the form of an isocon diagram. When isocon diagram comparing cores collected from the estuary mouth and the inner end is plotted (Fig. 3.2A.31), it is observed that almost all the metals show higher concentration in the core collected from the mouth region as compared to the core from the inner end. Spatial and temporal fluctuations in metal concentrations may be caused by changing environmental processes/parameters, such as water flow rate, pH, salinity, turbidity, temperature and organic matter (Baeyens et al., 2005; Hatje et al., 2003; Teasdale et al., 2003).

On the other hand, when cores from the northern (UV) and southern (UII) banks of the estuary are plotted on the isocon diagram (Fig. 3.2A.32), the core from the northern bank shows enrichment of most of the metals along with clay while in the case of core from the southern region high amounts of silt, Cr and Mn are seen. The higher sand percentage in core UII must be acting as a metal diluent.

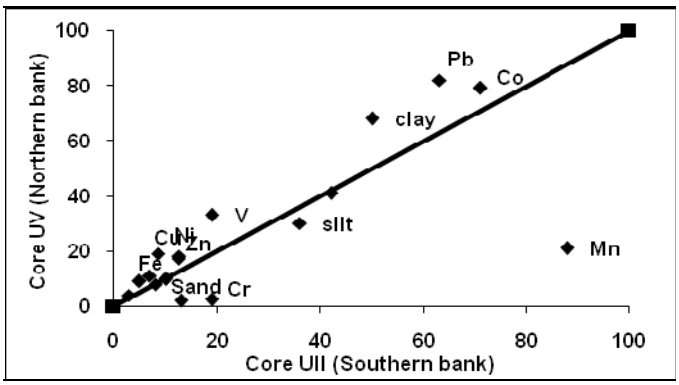

Fig. 3.2A.32. Isocon plot for cores collected from Northern (UII) and Southern (UV) banks

In general, the area of the study possesses two very different situations. One, present in the upper reaches of the estuary with metals presenting enrichment (from diffuse and point sources) and high C/N ratios. The other developing in the outer perimeter of the estuary near mouth, open to the main body of water and, as a consequence mainly of hydrodynamics, staying free from heavy metal concentration to some extent and demonstrating low C/N ratios.

3.2B. Mangroves

Two mangroves cores, representing *Avicennia marina* were sampled from the Ulhas estuary, one from lower estuarine region (UVM) and the other from upper estuarine region (UIVM).

3.2B.1. Visual observations

In core UVM, from lower estuarine region, from the bottom to 44 cm dark brown colour is observed while above it till the surface brown colour is seen. The other core from upper estuary (UIVM) shows a fluctuating trend in colour variations. From the bottom to 34 cm depth, grey colour is seen while above it till 28 cm, the sediment is found to be sandy of brown colour. Further, from 28 to 4 cm grey colour is again noticed. At the surface the core is of brown colour.

3.2B.2. Sediment components (sand, silt, clay)

The sediment components in the mangrove regions of the estuary vary from 0.05-67.40 % for sand, 6.36-54.29 % for silt and 26.24-84.88 % for clay with averages of 6.11 %, 24.63 % and 69.30 %, respectively. From the vertical distribution plot (3.2B.1a) it is seen that in core UVM, sand (range-1.89-67.40 %, avg. 11.88 %), silt (range-6.36-38.21 %, avg. 22.10 %) and clay (range-26.24-77.92 %, avg. 66.02 %) exhibit a constant trend with minor peaks. On the other hand in core UIVM (3.2B.1b), sand (range-0.05-2.13 %, avg. 0.34 %) displays a uniform trend except for two increased peaks at 36 and 6 cm depths compensated by clay. Silt (range-15.02-54.29 %, avg. 27.15 %) and clay (range-45.60-84.88 %, avg. 72.59 %) do not deviate much from

the average line. The bulk of the sediment appears to be made up of finer sediments (silt and clay) which make up at least 40 % and over 80 % of some samples.

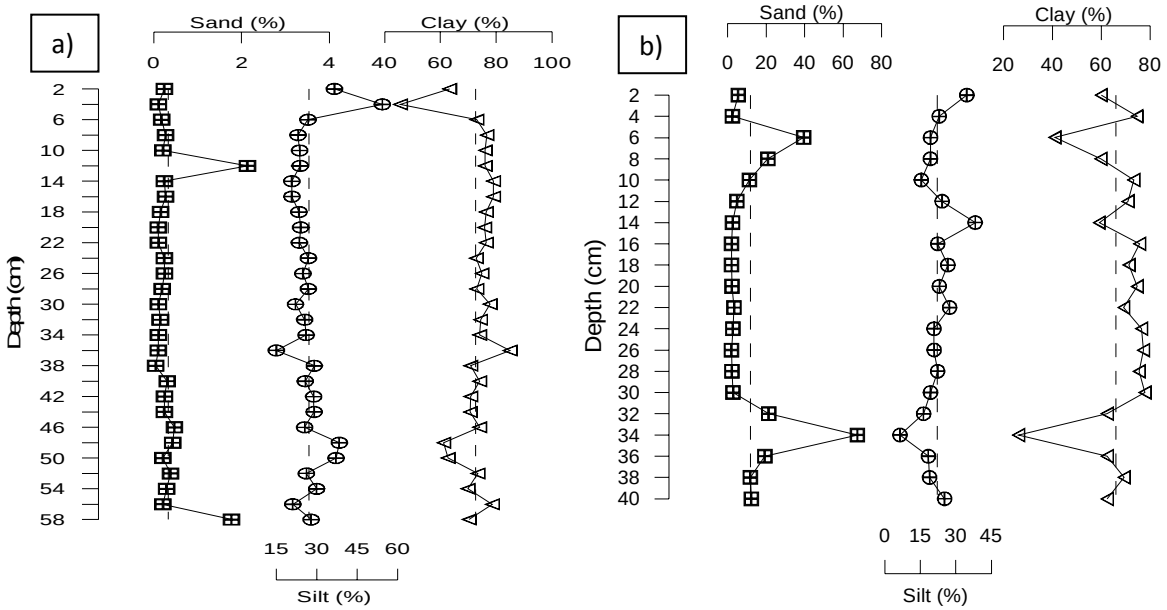

Fig. 3.2B.1. Vertical profiles of sediment component a) lower (UVM) and b) upper (UIVM) estuarine regions

Based on ternary plot of Pejrup (1988), core UVM falls in group II of section D while in core UIVM some samples fall in group II of sections C and D (3.2B.2). In both the cores the sediment deposition seems to occur under relatively less violent hydrodynamic conditions. The plots by Reineck and Siefert (1980) indicate both the cores fall in Mature Mudflat category (Fig. 3.2B.3a) while in the case of plot by Flemming (2000), core UVM fall in mud class whereas core UIVM fall in Slightly Sandy Mud category (Fig. 3.2B.3b).

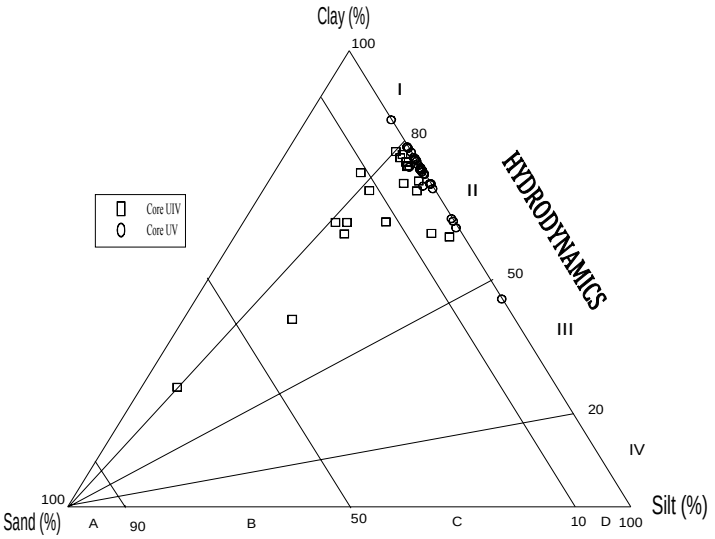

Fig. 3.2B.2. Ternary plot after Pejrup, 1988 for cores from the upper (UIVM) and lower (UVM) estuarine regions

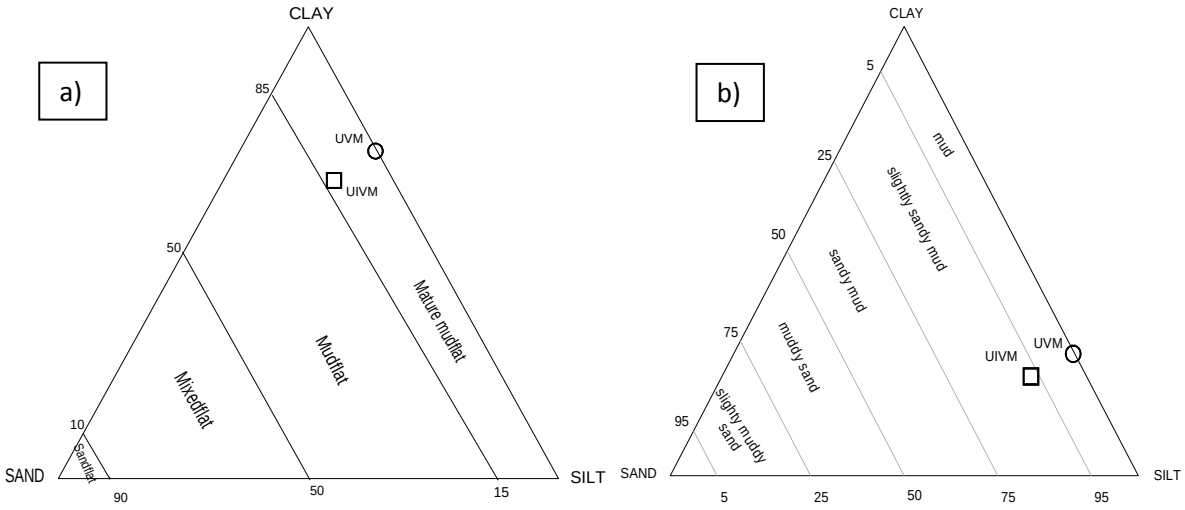

Fig. 3.2B.3. Ternary plots by a) Reineck and Siefert (1980) and b) Flemming (2000)

3.2B.3. a) Organic matter (TOC, TP and TN) and pH

In the estuarine region, the organic matter varies from 0.25-1.85 % for TOC, 0.28-1.04 mg/g for TP and 0.33-0.94 mg/g for TN with average values of 0.98 %, 0.50 mg/g and 0.55 mg/g, respectively. When the depth-wise distribution is seen (3.2B.4a), core UVM with TOC ranging from 0.25-1.84 % having average of 0.89 % decreases from the bottom to the surface, while TN varying from 0.33-0.87 mg/g, average 0.54 mg/g lies close to the average line, except for few fluctuations in the middle portion of the core. pH (range- 6.98-7.95, avg. 7.43) and TP (range- 0.31-0.61 mg/g, avg. 0.43 mg/g) show similar vertical profiles, i.e. an increasing trend is observed from the bottom to the surface of the core.

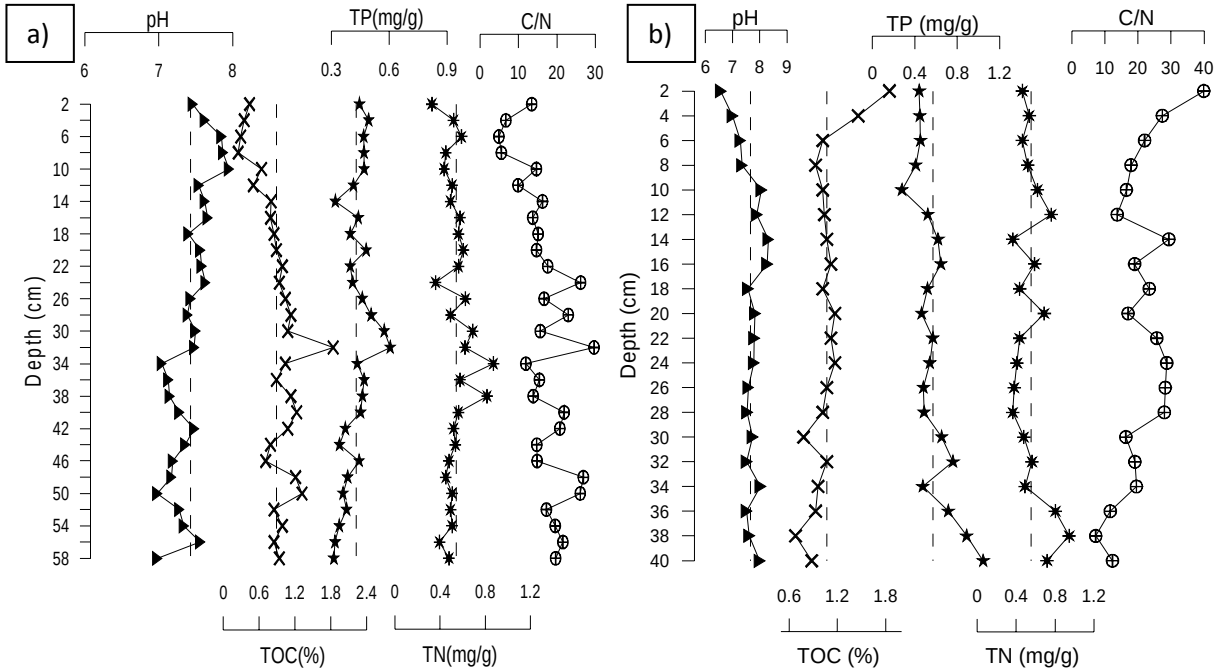

Fig. 3.2B.4. Vertical profiles of Organic matter for a) lower (core UVM) and b) upper (core UIVM) estuarine regions

In core UIVM (3.2B.4b), pH (range- 6.57-8.31, avg.7.66) gradually decreases from the bottom to the surface, TOC (range- 0.68-1.85 %, avg.1.07 %) exhibits an increasing trend while TN (range- 0.37-0.94 mg/g, avg.0.55 mg/g) shows a decreasing trend from the bottom to the surface. TP (range- 0.28-1.04 mg/g, avg.0.57 mg/g), on the other hand, decreases from bottom to 10 cm followed by an increase towards the surface. In both the cores no large variation in the organic matter profiles are seen. Preferential preservation of the organic matter could be attributed to anoxic conditions existing in mangrove areas owing to the high input of material in the mangrove stand.

3.2B.3. b) C/N ratio

In core UVM, C/N ranges from 4.92-29.68 with average value of 16.84 while the C/N ratio in core UIVM (range-7.21-39.87, avg. 21.12), in general, increases from the bottom to the surface (3.2B.4). However, in both the cores, the depth profiles do not show any smooth trend but fluctuates along the core. Although upper mangrove sediment (core UVM) have C/N ratios that are lower than 20, may be owing to mixing of nitrogen rich material derived from marine primary producers such as phytoplankton and algae, this signature is not reflected in the underlying sediments. The observed trend in the C/N values can be attributed to the progressive decrease in the influence of land derived materials, including the mangrove litter. In the case of core UIVM, C/N ratios indicate terrestrial influence in the region.

3.2B.4. Metal geochemistry

In the estuarine mangrove region the elements vary from 7.77-14.15 % for Al, 0.72-3.53 % for Ca, 7.87-11.32 % for Fe, 1097-2888 ppm for Mn, 110-283 ppm for Cu, 44-170 ppm for Pb, 49-154 ppm for Co, 53-144 ppm for Ni, 107-217 ppm for Zn, 132-475 ppm for Cr and 106-520 ppm for V, having average values of 11.28 %, 1.78 %, 9.16 %, 2030 ppm, 191 ppm, 93 ppm, 89 ppm, 141 ppm, 152 ppm, 247 ppm and 284 ppm, respectively.

Core UVM: In the core collected from lower estuarine mangrove region, the distribution of range and average values are 7.77-13.69 %, 10.94 % for Al; 1.34-3.13 %, 2.01 % for Ca; 8.59-10.25 %, 9.58 % for Fe; 1097-2443 ppm, 1741 ppm for Mn; 110-131 ppm, 124 ppm for Cu; 44-82 ppm, 55 ppm for Pb; 49-59 ppm, 53 ppm for Co; 144-175 ppm, 152 ppm for Ni; 107-190 ppm, 138 ppm for Zn; 132-183 ppm, 152 ppm for Cr and 106-356 ppm; 227 ppm for V. The metals depth profile is shown in figure 3.2B.5. Ca, Cu, Zn and Cr show an increasing trend from the bottom to the surface. Al, Mn and Co exhibits a decreasing trend from the bottom to the surface. Fe initially shows an increase from the bottom to 50 cm followed by a fluctuating

decreasing trend till 30 cm depth. Further above, a gradual increasing trend is observed. Pb gradually increases from the bottom to 14 cm and then decreases towards the surface. Ni, on the other hand, decreases from the bottom to 34 cm and then increases towards the surface with minor fluctuations. V displays a decrease in values in steps from the bottom to the surface.

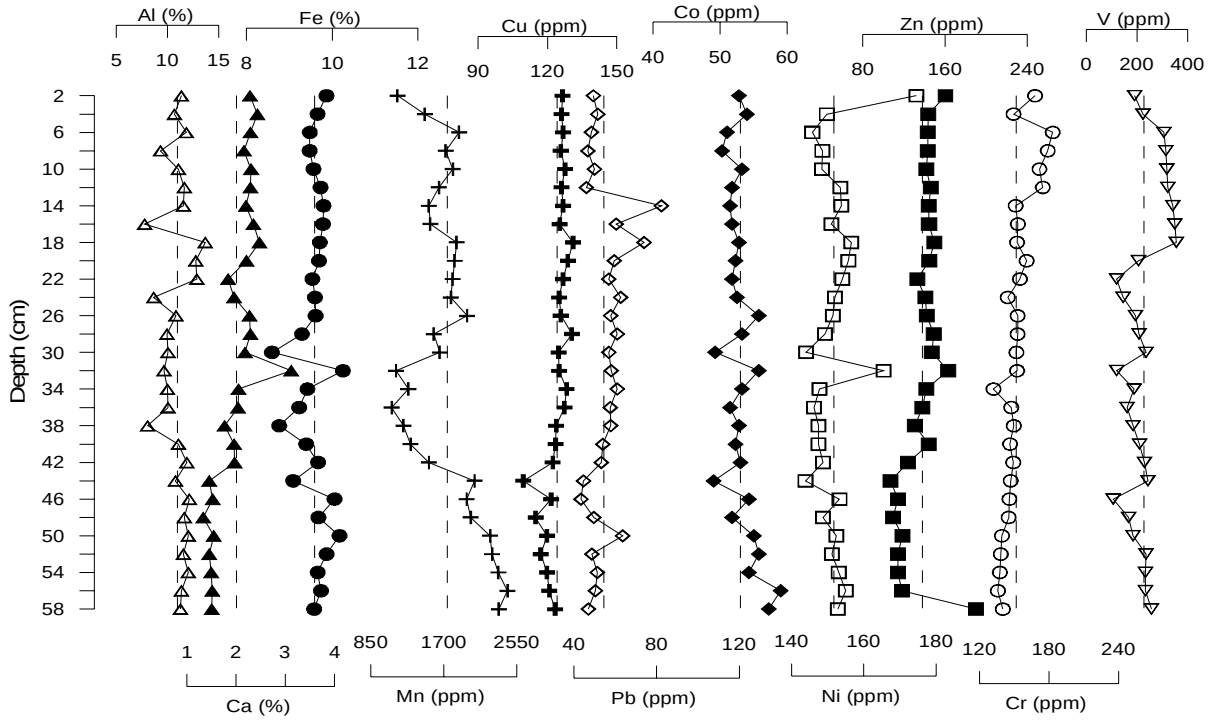

Fig. 3.2B.5. Depth-wise distribution of selected metals in lower estuarine mangrove region (core UVM)

Core UIVM: For the core retrieved from the upper estuarine region, the elements range from 9.42-14.15 % for Al, 0.72-3.53 % for Ca, 7.87-11.32 % for Fe, 1821-2888 ppm for Mn, 206-283 ppm for Cu, 92-170 ppm for Pb, 106-154 ppm for Co, 114-153 ppm for Ni, 137-217 ppm for Zn, 280-475 ppm for Cr and 204-520 ppm for V with average values of 11.61 %, 1.54 %, 8.74 %, 2319 ppm, 258 ppm, 130 ppm, 125 ppm, 129 ppm, 165 ppm, 342 ppm and 340 ppm, respectively. From the down-core profile (Fig. 3.2B.6), Al, Co and Cr exhibit a decrease from the bottom to the surface of the core while Zn displays an increasing trend from the bottom to the surface. Ca and Pb show increasing trends from the bottom to 10 cm depth. Above it, decreasing trends are seen. Fe, Mn, Cu, Ni and V project increasing and decreasing trends from the bottom to the surface.

Metals in sediments are concentrated by physical (grain size, surface area) or chemical (cation exchange capacity, mineralogy, concentration of geochemical substrates) factors (Horowitz et al., 1989). By employing both of these concepts, the geochemistry of sediments can provide insights into the processes that affected the sediment-trace element distributions. In core UIVM, almost all the elements except for Ca, Fe and Ni, show high concentration than core UVM. This

may be due to the presence of high organic matter in the former. Also in both the cores, increment in Fe concentration is observed at the surface. Fe enrichment in surficial sediments is often a diagenetic feature, resulting from post-depositional redistribution of Fe by dissolution caused by microbial reduction and precipitation caused by chemical oxidation. In general, these reduction and oxidation processes are more variable in upper layers than in deeper layers. This suggests a dynamic fate of trace metals (dissolution, precipitation, and adsorption) especially in the top 5 cm, where biological activity is also concentrated. Bioturbation, physical mixing and oxidation processes (e.g. organic matter degradation) can play important roles in sediment geochemistry and result in deeper penetration of oxic conditions (Fenchel, 1996; Thamdrup et al., 1994) causing fluctuations in the redox boundaries, contributing to a non-steady state in the sediment (Li et al., 2000a).

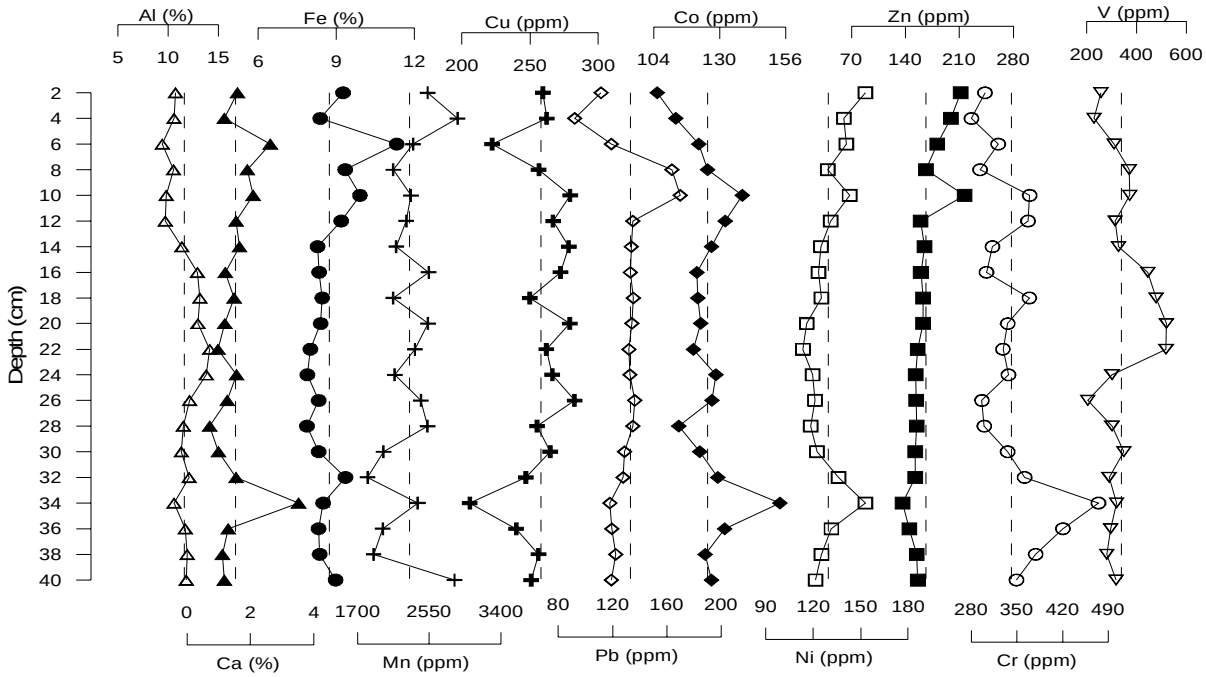

Fig. 3.2B.6. Depth-wise distribution of selected metals in upper estuarine mangrove region (core UIVM)

3.2B.5. Statistical analysis

Table 3.2B.1.Classification of values based on correlation analysis in the estuarine region

Stations		Good	Significant
Lower estuarine region	Core UVM	0.36-0.46	> 0.46
Upper estuarine region	Core UIVM	0.43-0.55	> 0.55

3.2B.5a. Correlation analysis

In both the cores, Pearson's correlation at $p < 0.05$ was computed separately (Table 3.2B.1). From correlation matrix, in core UVM, the sediment components do not show any association

with metals while in the case of organic matter only TP shows significant correlation with Ca (r=0.51), Cu (r=0.71) and Cr (r=0.47). pH, on the other hand, exhibits significant associations with Ca (r=0.51), Cr (r=0.71) and V (r=0.47). Fe and Mn displays good associations with Al (r=0.37, 0.44) and Co (r=0.52, 0.40). In addition, Fe also correlates with Ni (r=0.62). Among the elements, Cu correlates with Pb (r=0.46), Zn (r=0.66) and Cr (r=0.40); Co with Ni (r=0.37) and Cr with V (r=0.42). The elements in this group do not correlate with the finer fraction, which indicates that the dynamic environmental conditions exert no significant control over them (Borrego et al., 2004). In core UVM, Fe-Mn, organic matter and pH are found to contribute significantly in the metal distributions. The presence of organic matter as metal carrier in the mangrove core infers that the metals might have been transported as organic debris to the mangrove region. Further, change in pH condition and reduction of organic matter might be facilitating in trapping of metals in the region.

In core UIVM, among the sediment components, sand associates significantly with Ca (r=0.87), Co (r=0.64), Ni (r=0.61) and Cr (r=0.63); clay with Cu (r=0.83) and good associations of silt with TOC (r=0.47) and Cu (r=0.50) are seen. TOC correlates with Mn (r=0.47) and Zn (r=0.62) while TP and TN associate well with each other (r=0.48) but do not show association with any of the metals studied. In the case of redox sensitive elements, Fe and Mn, only Fe shows significant associations with Ni (r=0.55) and good associations with Zn (r=0.49) and Ca (r=0.52), while Mn does not show any correlations with metals. Among the metals, only Co with Cr (r=0.79) and Zn with Ni (r=0.49) display correlations. In general, coarser sediments, TOC along with Fe are found to be the dominant metal carriers in the region.

3.2B.5b. Factor analysis

The loadings between principal factors and geochemical variables of both the mangrove cores are given in Table 3.2B.2 and 3.2B.3

Core UVM: Factor analysis in core UVM resulted in five factors amounting to 74.39 % of total variance. The first factor accounts for 24.56 % of total variance and shows good loadings of pH on Cr and V. The second factor with 16.39 % total variance displays good loadings of TP and Ca on Cu and Zn and also to some extent on Ni and Cr. Factor 3 with 14.27 % total variance exhibits good loadings of Al and Fe on Co and Ni while the fourth factor with 11.56 % total variance shows good loadings of clay on Pb and to some extent on Cu, Pb and V. Clays have high specific surface area and can directly trap heavy metals; they may also act as a substrate for

organic matter flocculation (Keil et al., 1994) which in turn adsorb metals. The fifth factor with 7.61 % total variance has good loadings of Pb.

Table 3.2B.2. Varimax rotated factor analysis in core UVM

	Factor 1	Factor 2	Factor 3	Factor 4	Factor 5
Total variance	24.56	16.39	14.27	11.56	7.61
Eigen values	4.42	2.95	2.57	2.08	1.37
Sand	0.08	-0.10	0.13	0.06	**-0.91**
Silt	-0.05	-0.04	0.15	**-0.92**	0.04
Clay	0.06	0.05	-0.16	**0.92**	-0.01
TOC	**-0.82**	0.10	0.03	0.16	0.19
TP	0.02	**0.78**	-0.30	-0.15	0.17
TN	-0.40	0.31	-0.57	0.20	0.12
pH	**0.83**	0.23	0.07	0.08	0.23
Fe	-0.04	-0.03	**0.87**	-0.11	0.01
Mn	0.05	**-0.78**	0.28	0.05	-0.19
Cu	0.20	**0.76**	0.14	0.34	0.03
Pb	-0.19	0.29	0.19	0.49	0.50
Co	-0.47	-0.11	0.60	-0.03	-0.27
Ni	-0.07	0.36	**0.77**	-0.12	-0.04
Zn	0.06	**0.74**	0.16	0.16	-0.47
Cr	**0.81**	0.39	-0.05	-0.01	-0.10
V	0.66	-0.05	0.00	0.36	-0.18
Al	0.13	-0.37	0.53	0.05	0.04
Ca	0.27	**0.89**	0.12	0.11	0.14

Core UIVM: Four factors representing 75.56 % of total variance were produced by varimax rotation. Factor 1 is responsible for 32.39 % of the explained variance, and mainly comprises of silt, clay and Cu. This factor is found to be dominated by finer sediment fraction. The second factor with 22.89 % variance shows good loadings of TOC and Mn on Zn. The third factor with 11.82 % variance has good loadings of pH on Pb and Co while the fourth factor having 8.47 % variance exhibits good loadings of pH, TP and Al on V but to a low extent and negative loading on Fe. The negative correlations of heavy metals with Fe indicate the possibility of absence of Fe- oxides as the main controller in the geochemistry of mangrove sediments at this location. Although organic matter plays an important role in the development of the oxidizing/reducing environment within the core sediments, it does not seem to be a major carrier of the metals in core UIVM. Ca, a major component of the core sediments, has little direct influence on the geochemistry of the metals other than to act as a diluent. The data also suggest that association of the metals with the aluminosilicate fraction is limited in core UIVM.

Table 3.2B.3. Varimax rotated factor analysis in core UIVM

	Factor 1	Factor 2	Factor 3	Factor 4
Total variance	32.39	22.89	11.82	8.47
Eigen values	5.83	4.12	2.13	1.52
Sand	**-0.96**	-0.08	-0.05	-0.18
Silt	0.61	0.38	-0.19	0.10
Clay	**0.89**	-0.10	0.16	0.18

TOC	0.21	**0.74**	-0.37	-0.25
TP	0.06	-0.64	-0.41	0.45
TN	0.05	**-0.80**	-0.16	-0.15
pH	-0.13	-0.31	0.63	0.40
Fe	-0.26	-0.02	0.03	**-0.78**
Mn	0.11	0.49	-0.25	-0.04
Cu	**0.86**	0.06	0.35	0.01
Pb	0.15	-0.11	**0.90**	-0.18
Co	-0.70	-0.38	0.45	0.01
Ni	-0.55	0.17	-0.28	-0.68
Zn	0.32	0.40	-0.06	**-0.76**
Cr	**-0.72**	-0.47	0.09	0.12
V	0.08	0.15	0.56	0.37
Al	0.28	0.09	0.10	**0.84**
Ca	**-0.86**	0.16	0.18	-0.37

3.2B.6. Pollution Indices

3.2B.6a. Enrichment factor (EF)

Core UVM: Mn (2.13) shows highest average EF value while Zn (1.08) exhibits the lowest value. From the depth-wise plot (Fig. 3.2B.7), greater fluctuation are seen in the middle portion of the core as compared to upper and lower portions for all the elements. Mn shows high enrichment at the bottom as compared to the surface. Almost all the elements, except for Mn, show a decrease in EF values at the bottom.

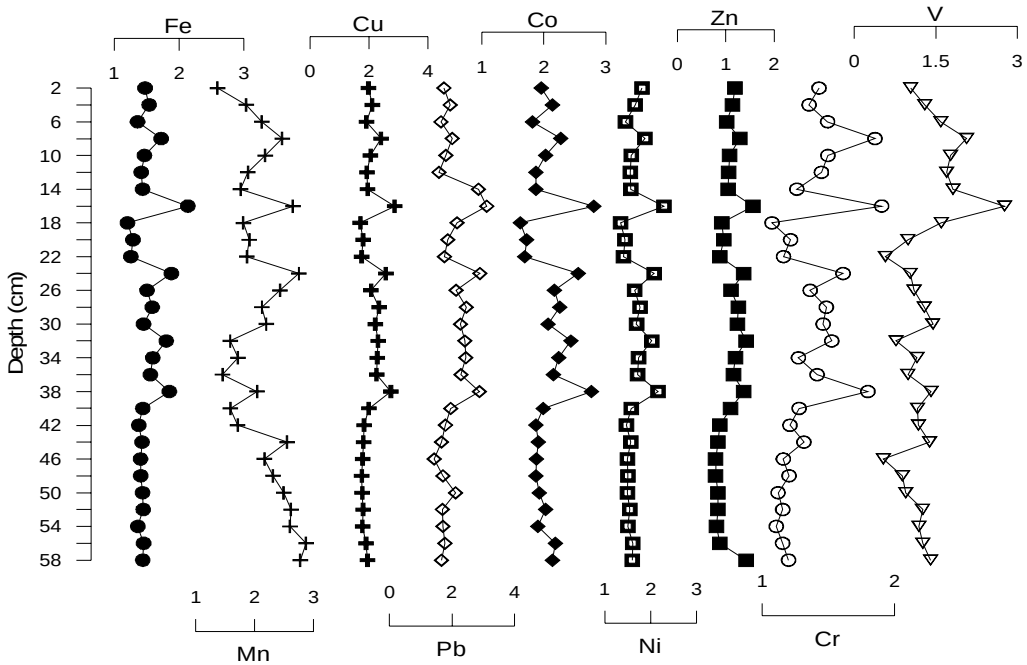

Fig. 3.2B.7. Depth-wise distribution of EF in lower estuarine mangrove region (core UVM)

Core UIVM: Highest average EF value is seen for Pb (4.66) while lowest for Zn (1.23). Mn and Cu; Fe, Ni and Zn; and Cr with Co show similar vertical profiles. Pb gradually increases from the bottom to 8 cm depth and then decreases at the surface while V shows large fluctuations along the length of the core. All the metals, except Mn, Co, Cu, Cr and Pb, maintain EF values

without significant variations throughout the core. The order of abundance of EF for different elements in core UVM is Mn > Co > Pb > Cu > Ni > Fe > Cr > V > Zn while in core UIVM, the order is Pb > Co > Cr > Cu = Mn > V > Ni > Fe > Zn.

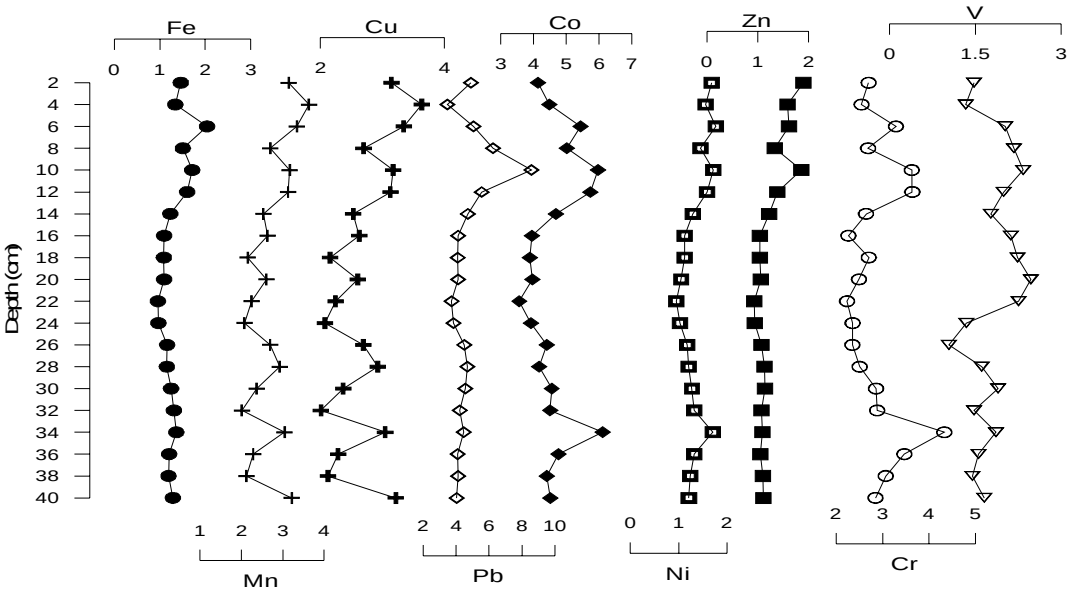

Fig. 3.2B.8. Depth-wise distribution of EF in upper estuarine mangrove region (core UIVM)

3.2B.6b. Igeo

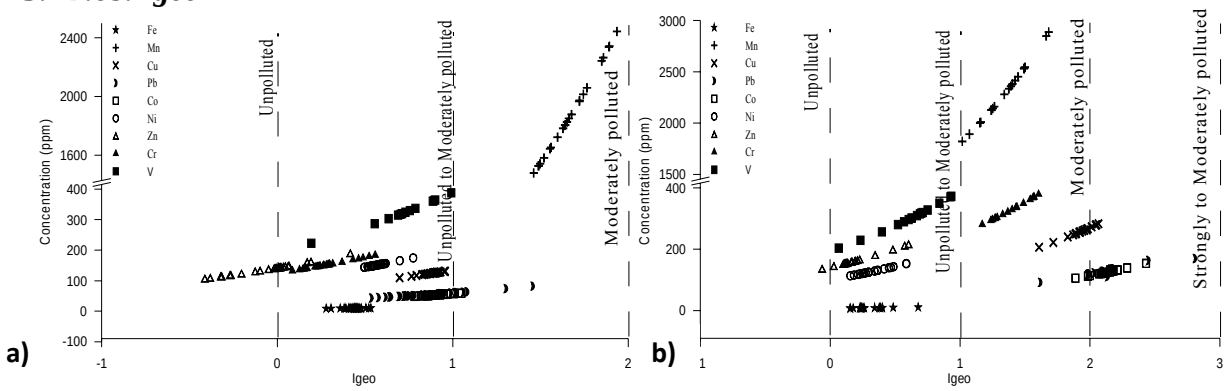

Fig. 3.2B.9. Igeo plots for mangrove cores collected in the a) lower (UVM) and b) upper (UIVM) estuary

In core UVM (Fig. 3.2B.9a), Mn falls in moderately polluted class while the remaining elements fall in unpolluted to moderately polluted class. On the other hand, in core UIVM (Fig. 3.2B.9b), Pb and Co fall in strongly to moderately polluted class; Mn, Cu and Cr in moderately polluted class while Fe, Ni, Zn and V fall in unpolluted to moderately polluted class.

3.2B.7. Isocon plot

When the mangroves from the lower and upper estuarine regions are plotted together on the isocon diagram (Fig. 3.2B.10), most of the elements are found to be higher in the upper estuarine mangrove core than the lower estuarine core. Large number of industries and major towns in the basin of Ulhas River, discharge waste water into the estuary (Fernandes and Nayak, 2010). Also,

rivers flowing along urban areas bring pollutants to downstream, which get incorporated in the sediments of the intertidal regions. These processes must have resulted in an increased accumulation and higher concentrations of metals in the mangrove sediments from the upper estuarine region where industries are located than the lower estuarine mangrove region. The flushing duration also has a major influence on the capacity of an estuary to withstand contamination by dispersing contaminants. Estuaries which are more open and have larger tidal ranges usually have greater rates of flushing, decreasing the likelihood of metal enrichment (Deeley and Paling, 1999).

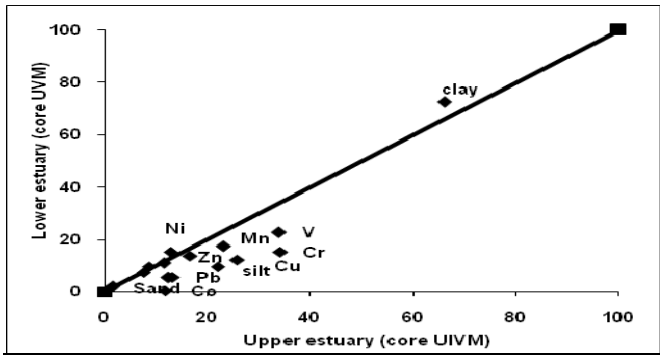

Fig. 3.2B.10. Isocon plot for mangroves cores collected from the lower (UVM) and upper (UIVM) estuary

3.2B.8. Relationship between the mudflats and mangroves

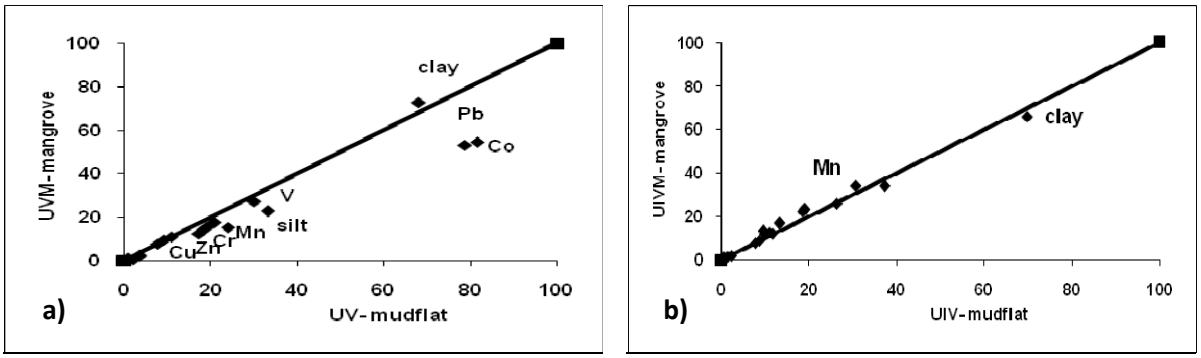

Fig. 3.2B.11. Isocon plot for cores collected from mudflats and mangroves of the a) lower (UV, UVM) and b) upper (UIV, UIVM) estuary

In general, estuarine mudflats being at lower elevation are generally subjected to strong hydrodynamic conditions such as tidal action, mixing and freshwater discharge and hence are more dynamic compared to mangroves which being situated at a higher elevation, has very low water exchange. However, when the distributions of the different sediment parameters are plotted on the isocon diagram, the mudflat region in lower estuary (Fig. 3.2B.10a) is found to be dominated by higher amounts of almost all the metals studied while the mangrove core exhibits higher clay percentage. In the case of mudflat and mangrove cores from the upper estuarine region (Fig. 3.2B.10b), not much variation in metal distribution are seen. Intertidal areas are

highly dynamic systems which are constantly influenced by local energy levels. The mudflats receive a large input of nutrients, sediment and organic matter from the sea and land discharges of river water and sewage, etc. Areas such as intertidal mudflats in enclosed bays or estuaries will be most susceptible to pollutants as dispersion is low and the finer substrata in these areas will act as a sink (Nedwell, 1997; Ahn et al., 1995; Somerfield et al., 1994).

3.2B.9. Mudflats - Thane creek vs. Ulhas estuary

When the distribution of different variables are seen in the creek and estuarine regions (Fig. 3.2B.12), the creek exhibits higher amounts of organic matter along with clay, Mn, Zn and Pb contents. The fluxes of metals and organic matter through domestic wastewater have gone up in recent years in the creek region from 2.5 x 10^5 m^3/d to 3.16 x 10^6/d (Rokade, 2009). On the other hand in the estuarine region, greater amounts of sand, Cu, Cr and Co are seen.

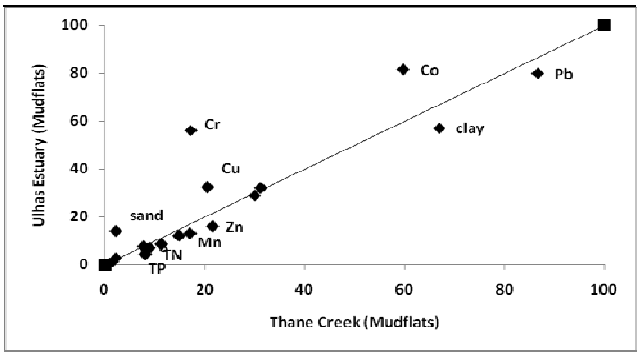

Fig. 3.2B.12. Isocon plot for mudflat cores collected from Thane creek and Ulhas estuary

3.2.10. Mangroves- Thane creek vs. Ulhas estuary

When the mangrove cores from the creek and estuarine region are compared (Fig. 3.2B.13), it is seen that higher amounts of most of the elements studied are seen in the estuarine region as compared to the creek which shows only high TOC and clay content. The observation indicates that in the estuarine region, the mangroves are acting as strong metal sink. Also, the higher values in the estuarine region may be because the mangrove cores were sampled in contaminated areas as compared to the creek region.

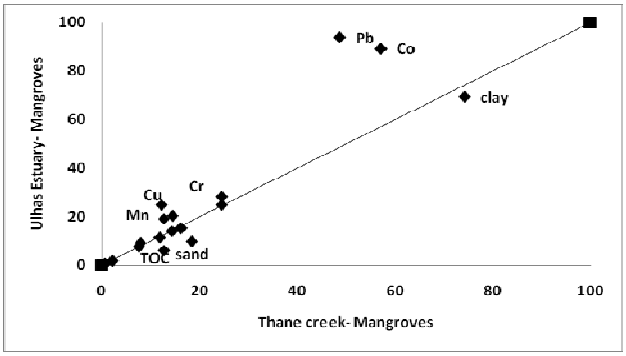

Fig. 3.2B.13. Isocon plot for mangrove cores collected from the Thane creek and Ulhas estuary

SECTION 3: MANORI CREEK

Considering the small area of the creek, three sediment cores were sampled from Manori creek, two from the mudflats (cores ManI and ManII) and one from the mangrove region (core ManIIM), as shown in the figure 3.3A.1.

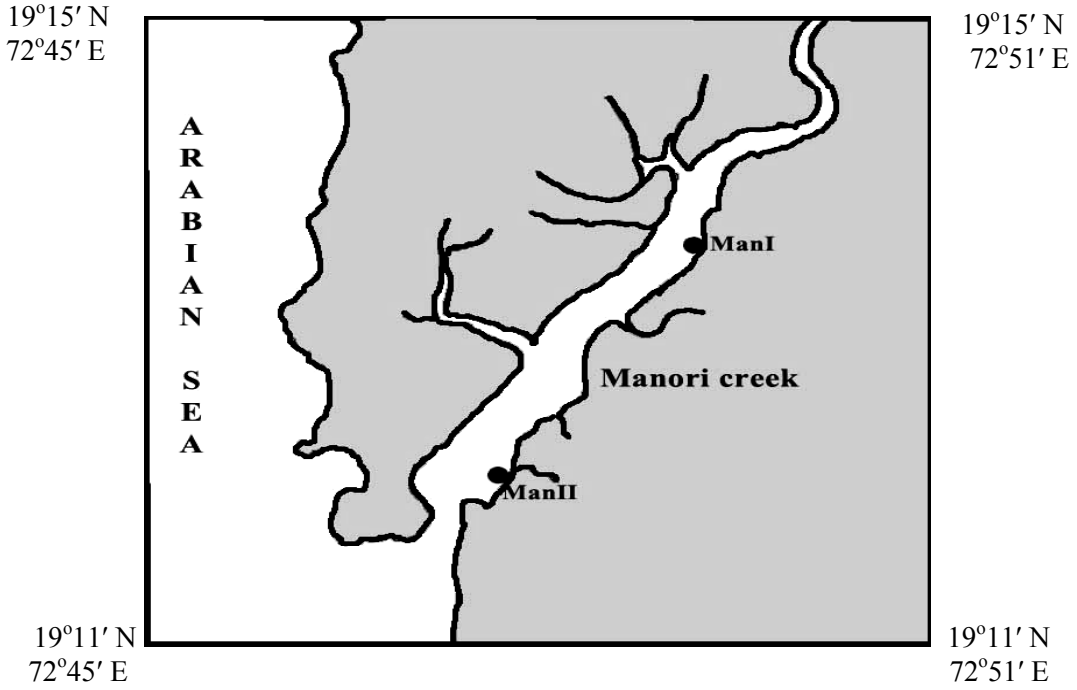

Fig. 3.3A.1. Map showing the sampling locations in Manori creek

3.3A. Mudflats

3.3A.1. Visual description

Based on the variations in the sediment colour, the sediment cores could be divided into two vertical zones.

1. Brown colour from 0-14 cm in core ManI and from 0-18 cm in core ManII.
2. Mixed brown and grey colour from 14-50 cm in core ManI and uniform grey colour from 18-42 cm in core ManII with slight smell of H_2S in the lower portions of both the cores.

3.3A.2. Sediment components (sand, silt and clay)

The range of the sediment components in core ManI varies from 0.46-4.41 % for sand, 25.77-47.40 % for silt and 51.23-71.94 % for clay with average values of 1.51 %, 40.49 % and 58.00 %, respectively. For core ManII, the range and average values are 0.33-3.90 %, 1.60 % for sand, 36.69-54.32 %, 46.45 % for silt and 43.57-62.80 %, 51.95 % for clay. The down-core plots of cores ManI and ManII for sand, silt and clay are shown in Figure 3.3A.2. For core ManI, sand percentage is found to decrease from the bottom to 26 cm and also from 18 to 8 cm depth. Highest percentage of sand (4.41 %) is seen at 6 cm, while at 28 cm depth the lowest percentage

(0.46 %) is observed. Silt and clay show corresponding opposite increasing and decreasing trends to each other, with clay exhibiting a prominent peak (71.94 %) at 18 cm depth which corresponds to the lowest percentage of silt (25.77 %). The lowest percentage of clay (51.23 %) is noted at 50 cm depth while silt percentage is highest at 44 cm depth (47.40 %).

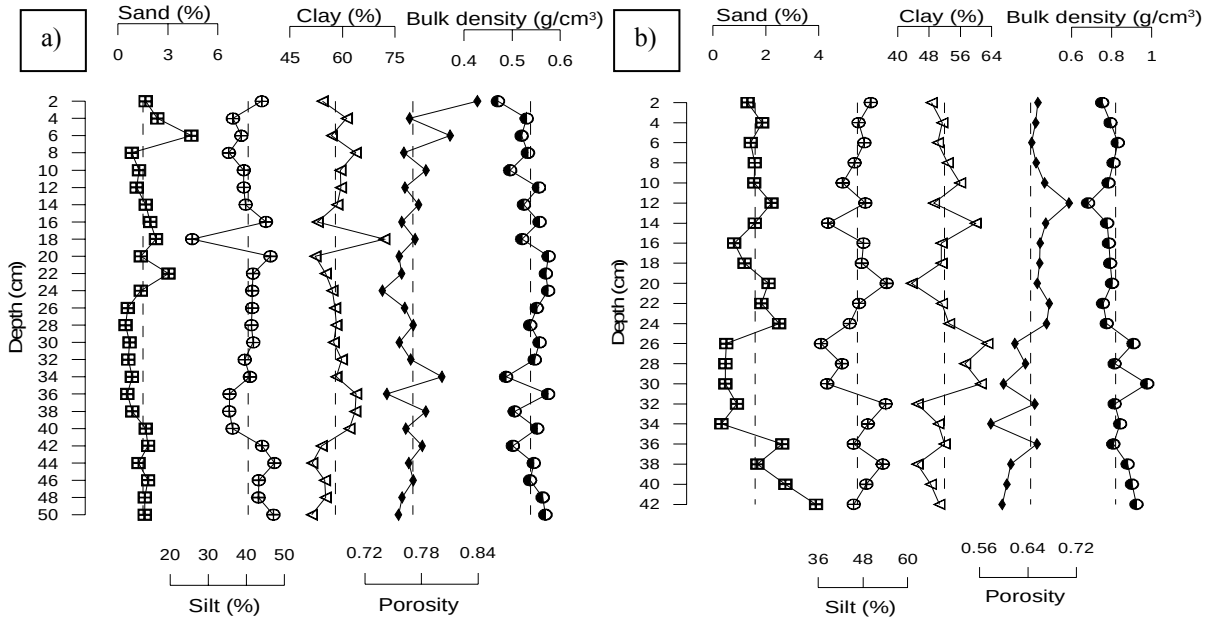

Fig. 3.3A.2. Vertical profiles of sediment components near the creek a) head (core ManI) and b) mouth (core ManII)

In core ManII, sand percentage is found to decrease from the bottom to the surface with sharp increases seen at 36, 24 and 12 cm depths. Decrease in sand percentage is more drastic between 42 and 34 cm depths and becomes more gradual later towards the surface. The highest value (3.90 %) is seen at 42 cm while the lowest value (0.33 %) is observed at 34 cm depth. Silt and clay show corresponding opposite trends to each other. In the upper 10 cm, silt percentage is found to increase while the percentage of clay decreases upto the surface. The highest percentage of silt is seen at 20 cm depth (54.32 %) which also corresponds to the lowest percentage of clay (43.57 %), while the highest percentage of clay is seen at 26 cm depth (62.80 %) which corresponds to the lowest percentage of silt (36.69 %). Both the cores are found to be dominated by finer sediment fractions. Core ManI, collected from the inner region of the creek, shows higher percentage of clay (58 %) than core ManII (51.95 %) which lies closer to the mouth of the creek. Silt percentage is found to be higher in core ManII (46.45 %) than in core ManI (40.49 %), while sand percentage is found to be of similar range in both the cores.

3.3A.3. Porosity and dry bulk density

In cores ManI and ManII, the sediment porosity and dry bulk density show corresponding opposite trends (Fig.3.3A.2). However, in core ManI, large fluctuations in sediment porosity (range- 0.74-0.84, avg. 0.77) and dry bulk density (range- 0.47-0.58 g/cm^3, avg. 0.54 g/cm^3) are

observed from 40 to 34 cm depth whereas in the case of core ManII, such fluctuations are seen from 36 to 26 cm depth. The observed increase in dry bulk density with depth in both the cores may be due to sediment consolidation. In core ManI, at 24 cm depth the lowest porosity value (0.738) is observed whereas the highest value (0.839) is seen at 2 cm depth. The lowest dry bulk density (0.470 g/cm^3) is seen at 2 cm whereas the highest (0.576 g/cm^3) is observed at 20 cm depth. In the case of core ManII, 34 and 12 cm depths correspond to the lowest (0.596) and highest (0.708) values of porosity while 12 and 30 cm depths correspond to the lowest (0.683 g/cm^3) and the highest (0.977 g/cm^3) values of dry bulk density. Sediment dry bulk density and porosity are found to vary in the different sediment layers of the same area. This may be because the lower layers of sediments are being compressed by the weight (overburden pressure) of upper sediment layers. Dry bulk density values are found to be relatively high in core ManII as compared to core ManI, while porosity values are higher in core ManI than in core ManII. Since both the cores have similar sediment granulometry, these observations indicate a disturbed condition in core ManI wherein the sediments must have not settled with time creating more voids as compared to core ManII which reflects a more stable and compact sedimentary condition.

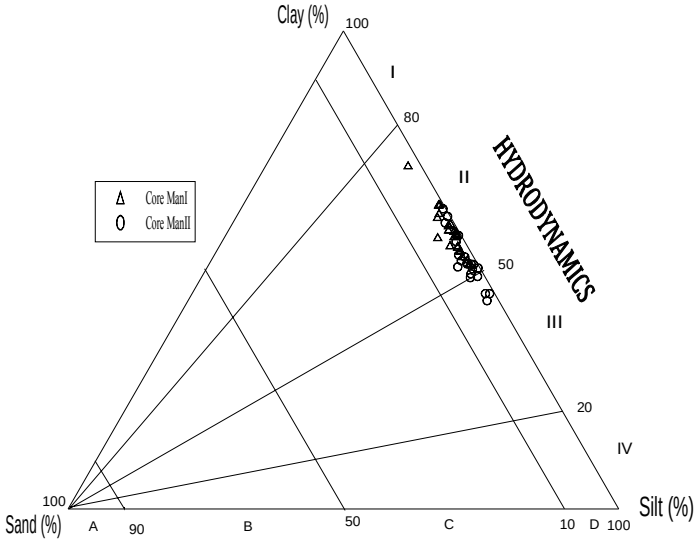

Fig. 3.3A.3. Ternary plot after Pejrup (1988) for cores near the creek head (ManI) and the mouth region (ManII)

Further, in order to understand the hydrodynamic condition of the depositional environment of the study area, ternary diagram proposed by Pejrup (1988) has been used. In the present study, it is seen that the sediment fractions from both the cores fall largely under group II of section D (Fig. 3.3A.3), indicating that the sediment deposition took place under relatively less violent conditions. Also textural class of sediment is understood in more detail by plotting the sediment component data on the ternary diagram proposed by Reineck and Siefert (1980). When the data

points are plotted (Fig. 3.3A.4a), it is observed that the sediments fall largely in the Mature Mudflat class for both the cores. Another sediment classification on ternary diagram introduced by Flemming (2000) is also applied to the data set. The plot (Fig. 3.3A.4b) shows that both the cores fall in the Mud class.

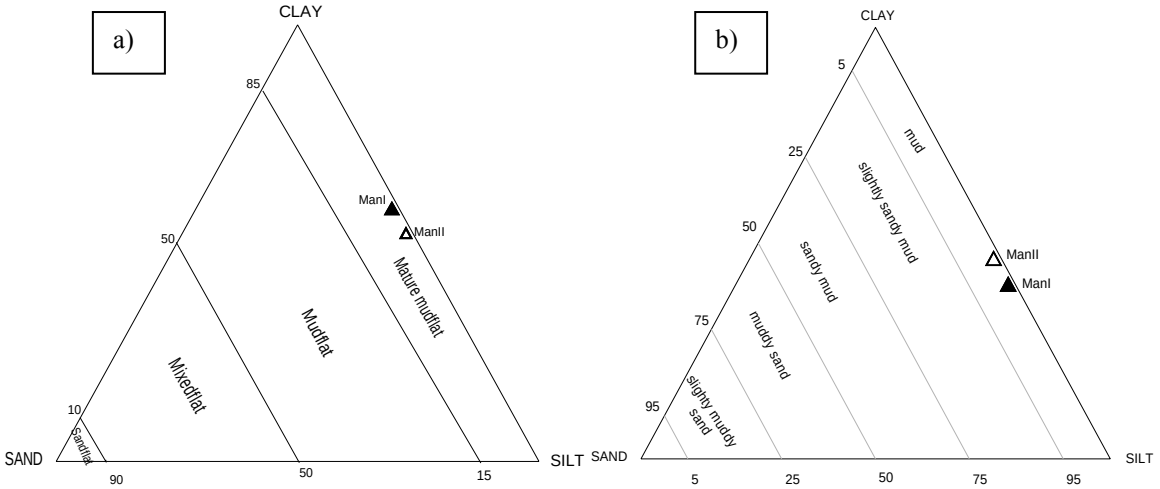

Fig. 3.3A.4. Ternary plots after a) Reineck and Siefert (1980) and b) Flemming (2000)

3.3A.4. Clay mineralogy

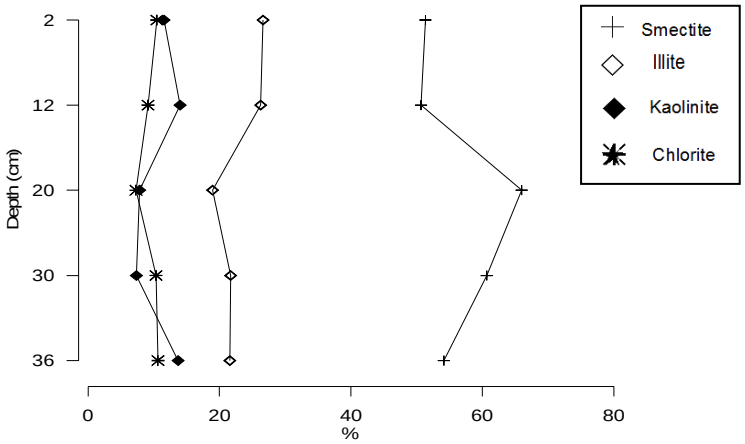

Fig. 3.3A.5. Depth-wise distribution of clay minerals in core ManII

Clay mineral analysis using XRD was performed on selected subsamples of core collected near the creek mouth (ManII). The vertical distribution for the core is shown in Figure 3.3A.5. From the figure, Smectite (range- 50.66-65.94 %, avg. 56.55 %), is found to be the dominant mineral followed by illite (range- 18.93-26.61 %, avg. 23.00 %), kaolinite (range- 7.33-13.98 %, avg. 10.89 %) and chlorite (range- 7.27-10.62 %, avg. 9.56 %). From the bottom to the surface, it is seen that smectite increases till 20 cm and then decreases towards the surface. In the case of illite and kaolinite, initially a decrease is seen at the bottom followed by an increasing trend towards the surface. On the other hand for chlorite, a decrease from the bottom to 20 cm depth is seen and further above an increasing trend is observed.

3.3A.5a. Organic matter and pH

The range and average concentrations of pH, TOC, TP and TN for core ManI vary from 7.14-8.39, 7.88; 2.00-3.02 %, 2.39 %, 0.40-1.12 mg/g, 0.81 mg/g and 0.28-2.99 mg/g, 1.62 mg/g while for core ManII the ranges are 7.16-8.14, 0.52-1.28 %, 0.20-0.80 mg/g and 0.73-2.03 mg/g with average values of 7.61, 0.73 %, 0.54 mg/g and 1.35 mg/g, respectively. The average values of pH, TOC, TP and TN are found to be higher in core ManI than in core ManII.

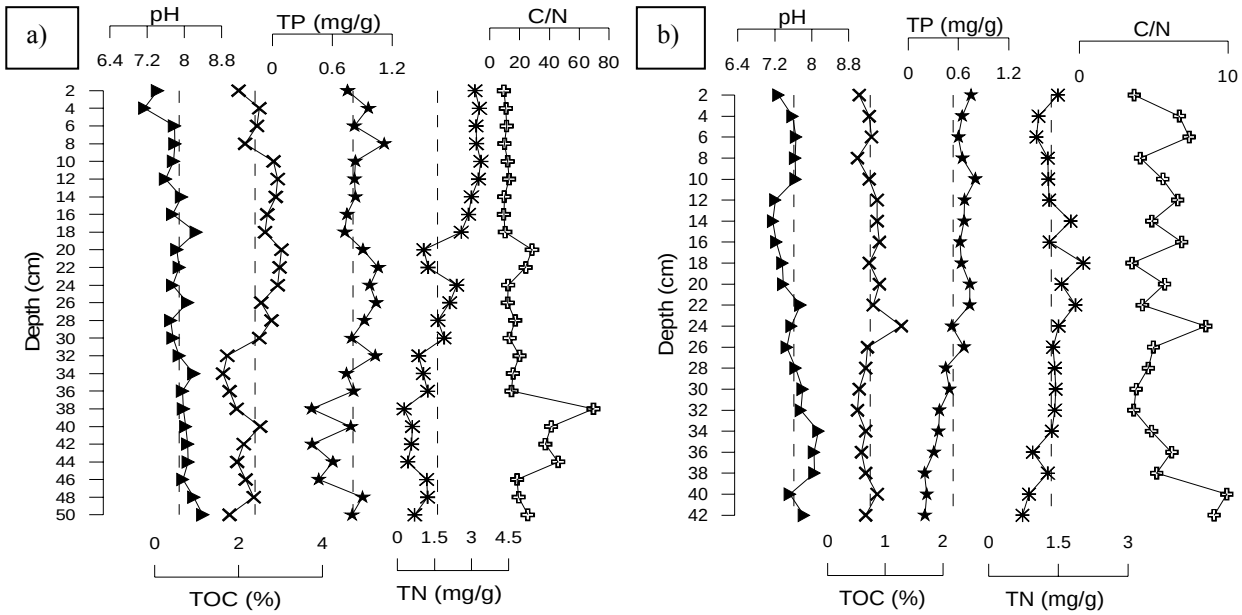

Fig. 3.3A.6. Vertical profiles of organic matter near the creek a) head (core ManI) and b) mouth (core ManII)

When the depth-wise distributions of these components are viewed in core ManI (Fig. 3.3A.6a), pH in general is found to exhibit a decreasing trend with minor fluctuations from the bottom to surface while TOC shows a decrease in the lower portion followed by an increase in the upper portion of the core. The pH is highest at 50 cm (8.39) and lowest at 4 cm (7.14) depth, whereas highest percentage (3.02 %) of TOC is seen at 20 cm depth while the lowest percentage (2.00 %) is seen at the surface. On the other hand, TP concentration is found to increase with fluctuating trends from the bottom to 24 cm depth and then shows a decreasing trend between 24 to 18 cm and again from 8 cm till the surface. The TN values show initial fluctuating trend from the bottom to a depth of 20 cm with an overall increasing trend while further above, a linear increasing trend is observed till the surface. Both TP (0.40 mg/g) and TN (0.28 mg/g) show the lowest concentration at 38 cm depth while the highest concentration is seen at 8 cm for TP (1.12 mg/g) and at 14 cm depth for TN (2.99 mg/g).

In core ManII (Fig. 3.3A.6b), pH in general shows a decreasing trend with minor fluctuations from the bottom to the surface. The highest (8.14) and lowest (7.16) pH values are noted at 34 and 14 cm depths, respectively. TOC is found to decrease from the bottom to 32 cm depth, and

then increase upto 12 cm followed by a decrease till the surface. The highest (1.28 %) and lowest percentage (0.52 %) of TOC occurs at 24 and 8 cm depths, respectively. TP shows a constant increasing trend from the bottom to the surface while TN increases from the bottom to 18 cm depth and then shows a gradual decrease till the surface. The lowest concentration of TP (0.20 mg/g) and TN (0.73 mg/g) are observed at 42 cm depth while the highest concentration is seen at 10 cm for TP (0.80 mg/g) and at 18 cm depth for TN (2.03 mg/g).

3.3A.5b. C/N ratio

Organic matter in the sediments of intertidal regions of estuaries comes from autochthonous (produced in an estuary) and allochthonous (supplied from the sea and rivers) sources (Wada et al., 1987; Cifuentes et al., 1988). C:N ratios are often used to differentiate marine from terrestrial organic matter (Redfield et al., 1963; Atkinson and Smith, 1983; Perdue and Koprivnjak, 2007) i.e. the ratio indicates whether the source of organic matter is autochthonous or allochthonous. If they are from a terrestrial source, the ratio of TOC: TN would generally be >20. The higher the percentage of terrestrial organic matter, the greater the ratio of TOC: TN. The TOC and TN contents of marine sediments reflect processes such as rates of sedimentation and environmental aspects of deposition. Since estuarine sediments incorporate a mixture of these two sources, relative changes in the C/N ratio can indicate changes in the proportions of organic carbon sources to the estuary. Information on the distribution of these elements is therefore important for the evaluation and reconstruction of past environments.

In the present study, TOC: TN ratio varies from 9.31 to 69.64, averaging 20.33 for core ManI and from 3.54 to 9.92 for core ManII, with an average of 5.73. The ratio of TOC/TN in the sediments of the inner part of the creek is found to show an increase with depth (Fig. 3.3A.6a), which reflects, to some extent the changes in the source of organic matter in recent years. If carbon, nitrogen and phosphorus in the sediments are generated from the same source, they should have a good correlation. However, it can be seen that the correlation between TN and TOC is weaker near the mouth of the creek ($r=0.16$; $p< 0.05$), indicating different sources while a good correlation exists between TOC and TN in the inner area ($r =0.56$; $p< 0.05$), which implies a similar source and/or are subjected to similar processes. The ratio of TOC/TN is found to be much greater in the inner part than near the mouth of the creek. This is probably because of greater contribution of terrestrial matter by the river Dahisar which drains into the creek while additional organic matter comes from land-based plants. Also, as the inner part of the creek is small and narrow, the waste water drainage from nearby industries and agricultural activities results in relatively high accumulation of external organic matter. On the other hand, the

sediments near the mouth of the creek receive more marine based organic matter resulting in the observed low TOC/TN ratio. The sediment samples at the bottom of core ManII show elevated TOC/TN ratio, which presumably represents greater input of eroded material from the surrounding land as can be concluded from the high sand percentage observed in the lower portion of the core. The increased input of sand might have resulted from increased precipitation during that period.

The study of vertical distribution of TOC, TN and their ratio (TOC/TN) can also be used to indicate diagenesis (Wakeham, 2002). In core ManI, elevated values of TOC/TN ratio observed between 46-36 cm and 24-18 cm depths; and in core ManII, a decreasing trend from bottom to 34 cm depth followed by an erratic TOC/TN profile towards the surface may be attributed to diagenetic degradation. As nitrogen is more labile than carbon, organic matter degradation usually results in an increase in C/N ratio (Meyers, 1997), later decreasing due to nitrogen immobilization (Benner et al., 1991). Grey/black colour along with H_2S smell observed in the lower portions of both the cores point towards formation of H_2S, indicating anaerobic conditions in the sediments. The diagenetic profile tends to be more defined with anaerobic degradation than with aerobic degradation (Berner, 1980; Boudreau, 1997). However, the ratio is observed to be relatively homogenous in the upper half of core ManI. This may be because, bacterial and animal activities are most intense and electron acceptors are more energetic in the surface layer of the sediments (Aller, 1982) and lead to oxidation of organic matter. This form of distribution could also be the result of rapid deposition (i.e. high sedimentation rates), wherein the organic material is quickly moved below the more diagenetically active zone, thus suffering less degradation. According to Hedges and Keil (1995), the rapid sediment deposition protects the buried organic material from contact with the main oxidizing agents found in the overlying sea water such as oxygen, nitrate and sulfate.

3.3A.6. Metal geochemistry

The concentration ranges of selected metals in cores ManI and ManII are 6.0-8.72, 4.23-8.28 % for Al; 2.11-2.81, 1.46-2.81 % for Ca, 9.30-17.88, 8.90-11.94 % for Fe; 831-1294, 744-1274 ppm for Mn; 152-196, 133-186 ppm for Cu; 91-173, 50-75 ppm for Pb; 20-58, 21-42 ppm for Co; 53-153, 20-67 ppm for Ni; 237-348, 117-188 ppm for Zn; 170-361, 117-164 ppm for Cr and 184-306, 186-314 ppm for V. The averages are 7.57 %, 7.25 % for Al; 2.45 %, 1.74 % for Ca; 14.05 %, 10.26 % for Fe; 1013 ppm, 1026 ppm for Mn; 176 ppm, 157 ppm for Cu; 128 ppm, 62 ppm for Pb; 4 ppm 3, 36 ppm for Co; 89 ppm, 42 ppm for Ni; 276 ppm, 166 ppm for Zn; 263 ppm, 143 ppm for Cr and 249 ppm, 267 ppm for V. When the average concentrations of the

selected metals are seen, all the metals except for Mn and V show higher concentrations in core ManI as compared to core ManII. The plots of the metals for cores ManI and ManII are represented graphically in Figures 3.3A.7 and 3.3A.8, respectively.

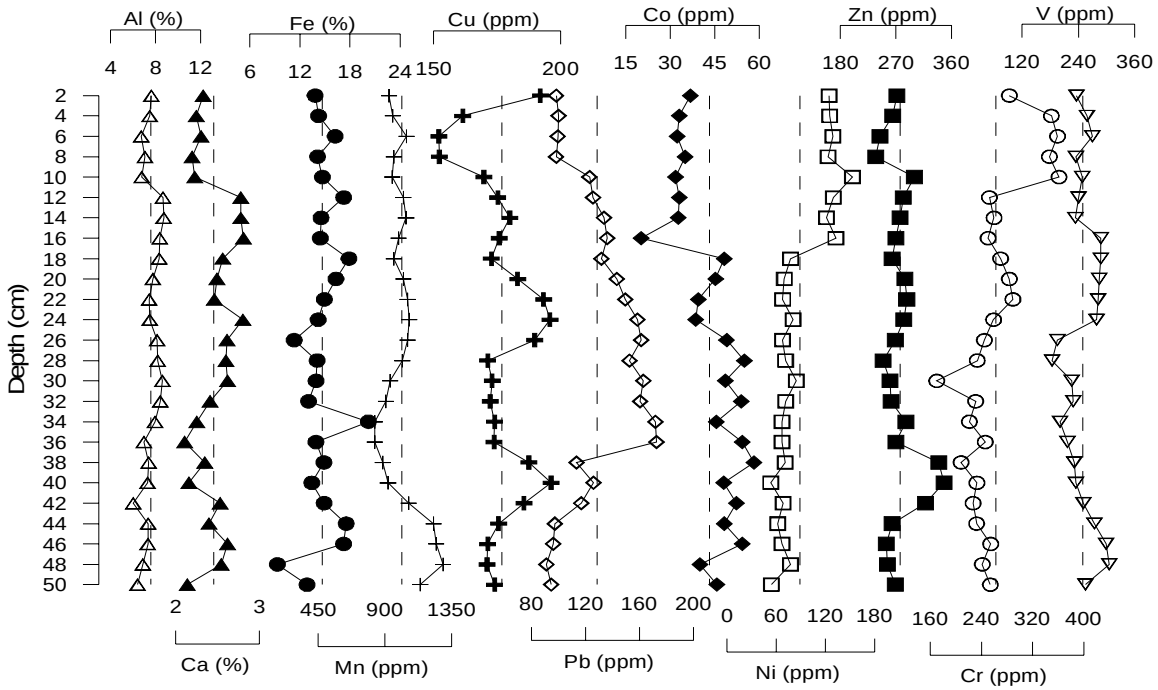

Fig. 3.3A.7. Depth-wise distribution of selected metals in core ManI

In core ManI, the distribution pattern of Al is observed to be constant with minor decreases at 42 and 10 cm depths. An increasing trend with minor fluctuations is seen for Ca from the bottom to 12 cm depth which is then followed by a decreasing trend till the surface. Fe is found to exhibit a fluctuating pattern while Mn and Co show decreasing trends with minor initial fluctuations from the bottom to the surface (Fig. 3.3A.7). Zn shows an increase from the bottom to 10 cm depth with an increased peak at 40 cm. Further, a decrease at 8 cm depth is followed by an increasing trend till the surface. Cu, in general, shows a decreasing trend from the bottom to 8 cm depth with increased values seen at 42 and 24 cm depths, respectively. Above 8 cm depth, an increasing trend is seen till the surface. Pb concentration is found to increase from the bottom to 36 cm depth and further above a systematic decrease till the surface is seen. Ni and Cr, in general, show increasing trend from the bottom to the surface with slight fluctuations in between and drastic increase from 18 to 16 cm and from 12 to 10 cm depths, respectively. For V, an initial decrease is followed by a constant increasing trend and then a decrease towards the surface is seen.

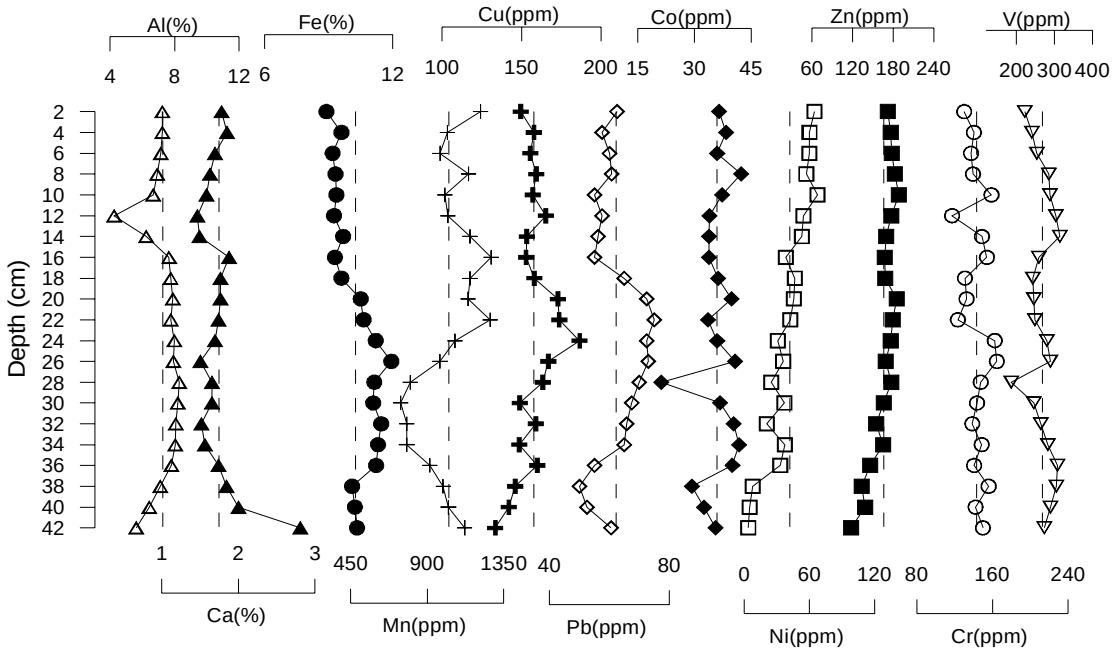

Fig. 3.3A.8. Depth-wise distribution of selected metals in core ManII

For core ManII (Fig. 3.3A.8), the elements, Al and Ca, show corresponding opposite trends from the bottom to 32 cm, wherein Al increases and Ca decreases. Further above, they show similar increasing and decreasing trends. The vertical distribution profiles of Fe and Pb show similar trends. For Fe, an increasing trend is seen from the bottom to 26 cm while Pb shows this trend till 22 cm depth. Further, a systematic decreasing trend is observed till 16 cm depth for both the elements. Above this, Pb shows a fluctuating increasing trend till the surface whereas Fe shows a gradual decreasing trend. Mn profile shows a decrease from bottom to 30 cm depth and then increases upto 22 cm depth which is followed by a decrease till 6 cm depth and then an increase. Cu shows an increase from the bottom to 24 cm depth, followed by a decrease towards the surface. Co, on the whole, shows a decreasing trend from the bottom to surface with increased peaks observed at 34, 28 and 8 cm depths. Ni shows an increasing trend from the bottom to the surface whereas Zn increases from the bottom to 10 cm depth. Above this depth, it shows a decreasing trend till the surface. Cr displays an increasing trend from the bottom to 24 cm followed by a fluctuating decreasing trend towards the surface. V initially shows an increase from the bottom to 36 cm, followed by a decrease till 28 cm depth. From 26 to 18 cm depth and 14 cm till the surface, a decreasing trend is seen while between 28 and 26 cm and 18 to 14 cm depths, V shows an increase.

High concentration of metals can accumulate in sediments within a relatively short time (Stumm and Baccini, 1978). It is known that metals display a different degree of affinity to organic and inorganic compounds and that it is an important factor influencing metal distribution (Lu et al.,

1983). The similarity between the profiles of Cu, Pb and Zn in the mudflat core ManII indicates that either these elements have undergone similar early-diagenetic remobilization and re-precipitation around the redox boundary or that all three elements are derived from the same source. The geochemical variations in metal distribution is associated with the extent to which the precipitation or dissolution of Fe and Mn oxides/hydroxides act as specific ‘‘sink’’ or source of heavy metal (Lacuraj and Maria, 2006). The lack of coincident peaks between the redox sensitive elements Fe and Mn and most of the selected trace metals point out that early diagenetic remobilization has not significantly affected the vertical distributions of these trace metals. The observed subsurface enrichment of Cu, Ni and Zn in core ManI and Ni and Zn in core ManII may be due to contaminant input in recent years. A weak correlation of Cu, Pb and Zn with clay and TOC in core ManI further supports a contaminant source.

The interaction of different factors, such as the distance of element sources to estuary, the chemical characteristics of the element, the combination of elements in estuarine sediments, the hydraulic conditions in the estuary, etc., result in the observed spatial distribution pattern of chemical components in the estuarine sediments. The concentration of metals in sediments that are located seaward (ManII) are found to be low for most of the studied elements as compared to the sediments in the inner part of the creek (ManI), where enriched metal concentrations are observed. The low metal contents in core ManII might be due to the mixing of enriched particulate material coming from upstream, with relatively clean marine sediments near the creek mouth (Soto-Jimenez and Paez-Osuna, 2001). The landward to seaward decrease of sediment metal concentrations in estuaries have been explained by two mixing mechanisms. The first suggested mechanism is that solubilisation of metals from the suspended matter occurs as a result of physicochemical factors during the mixing of freshwater and seawater (Jouanneau et al., 1983). Alternately, fluvial sediments enriched with metals may be diluted by the landward incursion of less enriched marine sediments into the estuaries (Forstner and Muller, 1974). The silt-clay type of sediments present near the riverside (core ManI), are observed to be rich in organic matter contents and thus have higher cation exchange capacity and large surface area. Finer sediments are able to trap metal rich ions, while sandy type sediments being organically poor have little ability to retain the metal ions. This nature of sediments might have resulted in the higher metal concentrations seen in core ManI as compared to core ManII. The increment of organic matter deposition to coastal waters has been related to intensive use of inorganic fertilizers, the population growth (Cornwell et al., 1996) and the increasing sewage inputs of particulate sedimentary matter (Stull et al., 1986). Therefore, the enrichments of organic matter as well as trace metals found in core ManI are likely related to the urban settlements established

around the creek in recent years, leading to increments in population and growing agricultural developments that must have resulted in sewage load being washed down the creek.

3.3A.7. Isocon plot

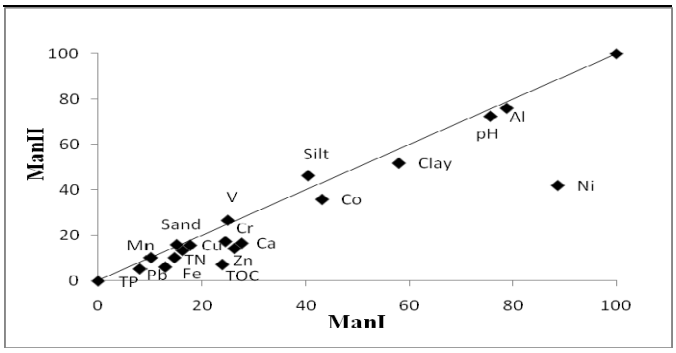

Fig. 3.3A.9. Isocon plot for cores collected near the creek head (ManI) and mouth (ManII)

Further, an Isocon diagram, which compares the average concentrations of specific elements from different sites (Cundy et al., 1997; Singh and Nayak, 2009), has been employed to show the variations in concentration between the two study sites. In order to plot this diagram, the average concentration of each element along with the sediment components and organic matter from each site has been calculated. The diagram (Fig. 3.3A.9) indicates a significant difference in the trace metal concentrations between the two mudflat cores. Core ManI exhibits higher concentrations of Ni, Cr, Zn, Ca, Co and also TN, TP and TOC while in core ManII, all the elements fall on or near the isocon line indicating little variations. The high concentrations of TOC, TP and TN in core ManI reflects high fluxes of organic matter to the sediments as a result of direct discharge of untreated domestic wastes and insufficiently treated industrial wastes which must be acting as good binding sites for metals.

3.3A.8. ^{210}Pb activity

Further, to support the understanding of metal associations and its consequent deposition, ^{210}Pb dating was carried out on both the sediment cores collected from the creek region. The activity of total ^{210}Pb is found to be lower in core ManII as compared to core ManI (Fig. 3.3A.10). The maximum total ^{210}Pb activity is found at 14 cm depth (2.69) in core ManI while in core ManII, the highest total ^{210}Pb activity (1.99) is seen at the surface. The results obtained for the two cores differ considerably. The factors that influence the accumulation of ^{210}Pb include sediment grain-size and organic matter content (Wang et al., 2005).

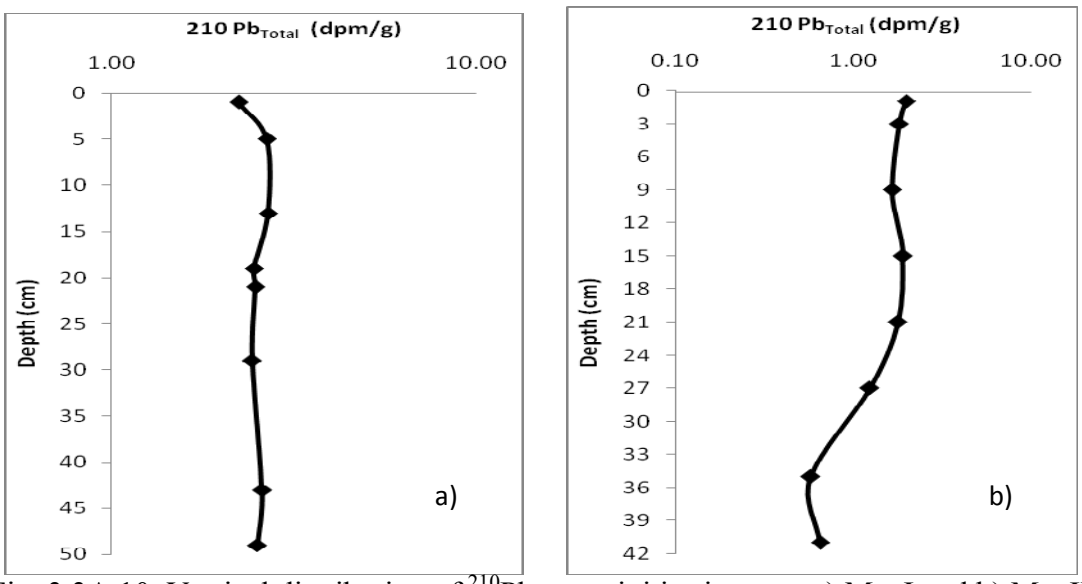

Fig. 3.3A.10. Vertical distribution of $^{210}Pb_{total}$ activities in cores a) ManI and b) ManII

Lead-210 activity does not show any definite trend with depth in core ManI. In this core, the ^{210}Pb activity is seen to be very disturbed even though the core granulometry contains higher finer sediment fractions. Also, the decay pattern does not correspond to the exponential form that would result from the radioactive decay law. Rather, it indicates temporal changes in the sedimentation rate. On the other hand, core ManII shows a better decreasing trend in ^{210}Pb activity with depth as compared to core ManI, suggesting that the downcore decrease in ^{210}Pb activity supports the idea that core ManII is a more compact and deposited in undisturbed sedimentary environment than core ManI.

Irregular profile of ^{210}Pb activity in core ManI may be explained by complex hydrodynamics and changing sedimentary environment or rapid changes in sediment supply, source or energy conditions (Andrew et al., 2003). It may also be due to disruptions in the normal process of sediment accumulation or mixing of the surficial sediments by physical or biological processes. In core ManII, the sedimentation rate is found to be 1.46 cm/yr so the bottom of the core corresponds to 1970's. Residential developments were scarce before 1970s, but increased markedly since then, especially around the vulnerable creek area. The modified land use and land cover with the developments around the creek may be probably the major source of sediments and increased sediment supply to the creek. The changes in the sediment load must have affected the accumulation of materials and contaminants in the creek.

3.3A.9. Statistical analysis

3.3A.9a. Correlation analysis

Three principal factors exert strong control on trace element concentrations in sediments namely sorption onto clay minerals (grain-size effect), complexing by organic matter and scavenging by Fe-Mn oxyhydroxides. Core ManI shows significant correlations of TN and good correlations of TOC with metals such as Ni (r=0.76, 0.34), Cr (r=0.45, 0.27) and Al (r=0.45, 0.33) while in core ManII, organic matter (TOC, TP and TN) is found to show good associations with Cu (r=0.52, 0.51, 0.49), Mn (r=0.36, 0.46, 0.25), while TP and TN also correlates with Pb (r=0.31, 0.52), Ni (r=0.87, 0.33) and Zn (r=0.87, 0.52). The comparatively lower metal values seen at ManII indicates concentrations are diluted by seawater at this location. These observations reflect an anthropogenic origin for metals at ManI which are transported by the current to ManII during ebb tides (Fernandes and Nayak, 2012b). No significant correlations were observed for Fe and Mn with other metals in both the cores except for Pb with Fe (r=0.55) in core ManII. This indicates that the metals in ManI and ManII are affected to a less extent by Fe and Mn hydroxides. The good positive relationship between Ni and Cr (r=0.65) in ManI and of Cu with Pb (r=0.62) and Zn (r=0.66) in ManII suggest that the source of the metal input might be similar or from anthropogenic source. Significant correlations observed between organic matter (TOC, TP and TN) and some of the metals indicate a significant role of organic matter in the process of trapping and incorporating the metals into the sediments.

3.3A.9b. Factor Analysis

Table 3.3A.1. Factor analysis matrix after varimax rotation for core ManI

	Factor 1	**Factor 2**	**Factor 3**	**Factor 4**
Variance (%)	25.52	18.93	14.82	10.06
pH	**-0.60**	-0.15	-0.22	-0.01
TOC	0.35	-0.01	**0.72**	0.22
TP	**0.64**	-0.07	0.07	-0.47
TN	**0.77**	0.19	0.49	0.05
Sand	0.28	-0.03	-0.03	**0.76**
Silt	-0.12	**-0.88**	0.06	-0.04
Clay	0.07	**0.88**	-0.05	-0.10
Fe	-0.14	0.37	0.18	0.45
Mn	-0.04	**-0.78**	0.02	0.38
Cu	-0.59	-0.08	0.47	-0.07
Pb	-0.17	0.27	0.44	**-0.64**
Co	**-0.75**	0.10	-0.26	-0.34
Ni	**0.80**	0.18	0.16	0.25
Zn	**-0.62**	0.31	0.12	0.18
Cr	**0.74**	0.14	-0.27	0.42
Al	0.14	0.21	**0.71**	-0.41
Ca	0.02	-0.27	**0.87**	0.04
V	0.06	-0.34	0.10	**0.75**

In the present study, eigen values greater than 1 are selected with varimax orthogonal. In core ManI, four factors accounts for 69.33 % of the total variance (Table 3.3A.1). The first factor shows significant positive loadings on TP, TN, Ni and Cr and good loading on TOC. Thus Factor

1 is associated with the organic matter component and hence can be called the "Organic matter controlled factor (I)". This factor explains the significant role of organic matter in the binding of certain heavy metals (Murray et al., 1999; Eimers et al., 2002). Factor 2 with significant positive loadings on clay and good loadings on Fe, Zn, Pb and Al suggests the associations of these metals with finer sediment fractions and aluminosilicates. This factor can be called the "Clay controlled factor", assuming the elements to be enriched in the clay fraction. Factor 3 is found to have high significant positive loadings for TOC, Al and Ca and good loadings on TN, Cu and Pb. This factor may be called the "Organic matter controlled factor (II)". Factor 4 shows significant positive loadings on Sand, V and good loadings on Fe, Cr, Mn, Ni and TOC. This factor may be called the "Fe-Mn oxide controlled factor". Fe-Mn oxides along with organic matter are generally considered predominant metal sorbents due to their large surface area (Forstner and Wittmann, 1979).

Table 3.3A.2. Factor analysis matrix after varimax rotation for core ManII

	Factor 1	**Factor 2**	**Factor 3**	**Factor 4**
Variance (%)	27.32	20.81	12.25	10.87
pH	-0.13	**-0.76**	-0.07	-0.28
TOC	0.22	0.23	0.13	**0.81**
TP	0.45	**0.84**	0.11	-0.10
TN	**0.71**	0.33	0.02	-0.02
Sand	-0.52	0.00	-0.25	**0.66**
Silt	-0.04	-0.08	**-0.93**	0.02
Clay	0.13	0.07	**0.92**	-0.14
Fe	0.42	**-0.78**	0.29	0.06
Mn	-0.07	**0.62**	-0.23	0.50
Cu	**0.78**	0.22	0.08	0.32
Pb	**0.86**	-0.15	0.06	0.12
Co	0.01	0.10	-0.01	-0.26
Ni	-0.01	**0.87**	0.00	-0.34
Zn	**0.64**	**0.64**	0.13	-0.20
Cr	-0.10	-0.37	**0.66**	0.15
Al	**0.69**	-0.44	0.05	-0.24
Ca	-0.52	-0.30	-0.27	0.44
V	-0.52	0.02	0.29	0.18

In core ManII, a four-factor model explaining 71.25 % of total variance has been adopted (Table 3.3A.2). Factor 1 has high significant positive factor loadings for TN, Cu, Pb, Zn, Al and good loadings on TP, Fe and TOC and can be called the "Organic matter controlled factor". Factor 2 exhibits high positive loadings for TP, Ni, Zn, Mn and good loadings on TN, TOC and Cu. This factor can be called "Mn- oxide controlled factor". Factor 3 shows significant positive loadings for clay, Cr and good loadings on Fe and V. This factor can be called the "Clay controlled factor". Factor 4 has high significant positive loadings for TOC and sand and good loadings on Cu, Mn and Ca. This factor may be related to marine sedimentation processes and as such must

have mainly originated from marine sources. This factor can be called the "Marine controlled factor".

3.3A.10. Pollution indices

3.3A.10a. Enrichment Factor (EF)

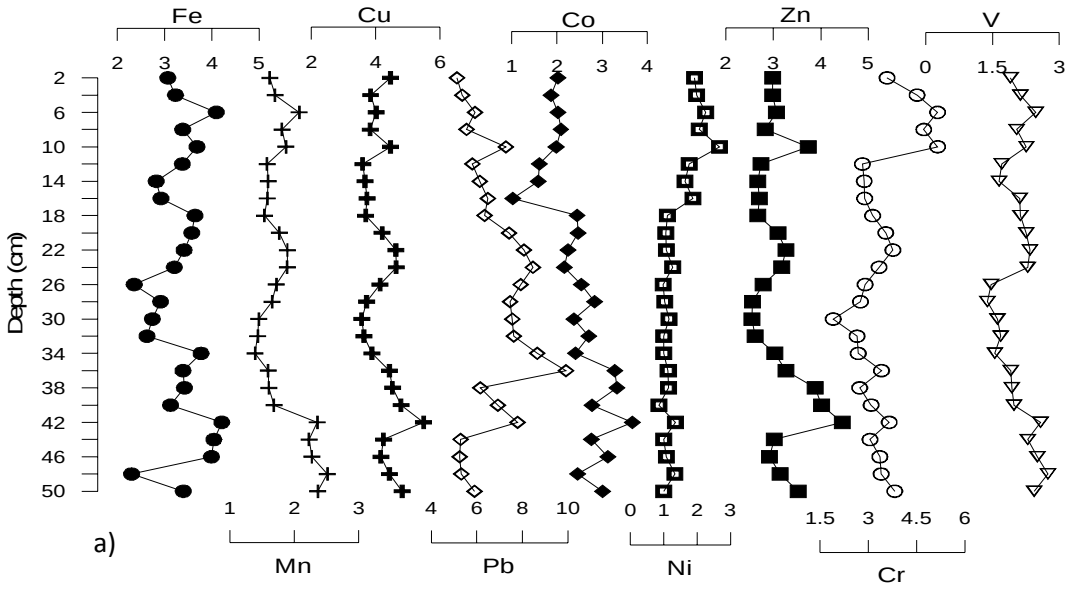

Fig. 3.3A.11. Down-core plot of EF for core collected near the creek head (ManI)

The vertical plots of EF are shown in figures 3.3A.11-3.3A.12. The computed average values of EF show core ManI to be highly enriched with metals (Fe, 3.31; Mn, 1.81; Cu, 4.19; Pb, 6.79; Co, 2.43; Ni, 1.39; Zn, 3.11; Cr, 3.39 and V, 1.75) as compared to core ManII (Fe, 2.44; Mn, 1.94; Cu, 3.95; Pb, 3.49; Co, 2.13; Ni, 0.66; Zn, 1.97; Cr, 1.94; V, 1.89), which suggests that the creek facilitates more concentration of metals near the head region than near the mouth possibly due to availability of more finer sediments (clay) and higher percentage of organic matter. Enrichment at this region can also be attributed to both the direct discharges from point sources such as wastewaters discharges and river carrying contaminants, influenced by the hydrological and sedimentation conditions in the creek.

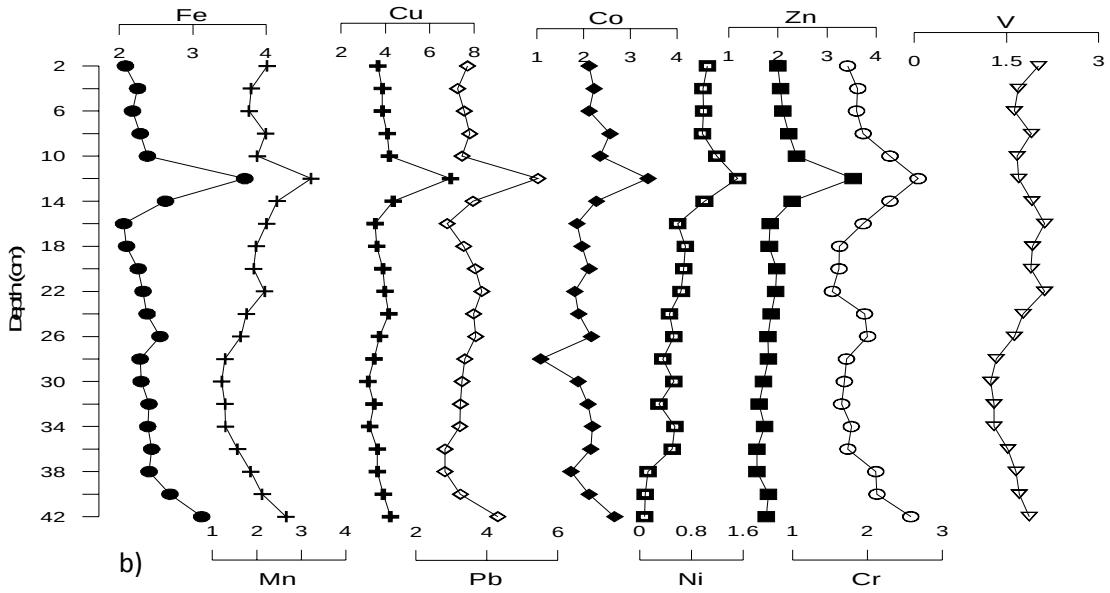

Fig. 3.3A.12. Down-core plot of EF for core collected near the creek mouth (ManII)

3.3A.10b. Index of Geoaccumulation (Igeo)

Figures 3.3A.13 (a & b) show the distribution of Igeo for selected metals in the study area. From the plots it is observed that Ni, Co and Mn in core ManI, are all found to fall in class 1 whereas Fe, Cu, Zn and Cr fall in class 2. Pb is found to fall in class 3. In core ManII, Ni falls in class 0, while Fe, Mn, Co, Zn and Cr fall in class 1. Cu and Pb fall in class 2.

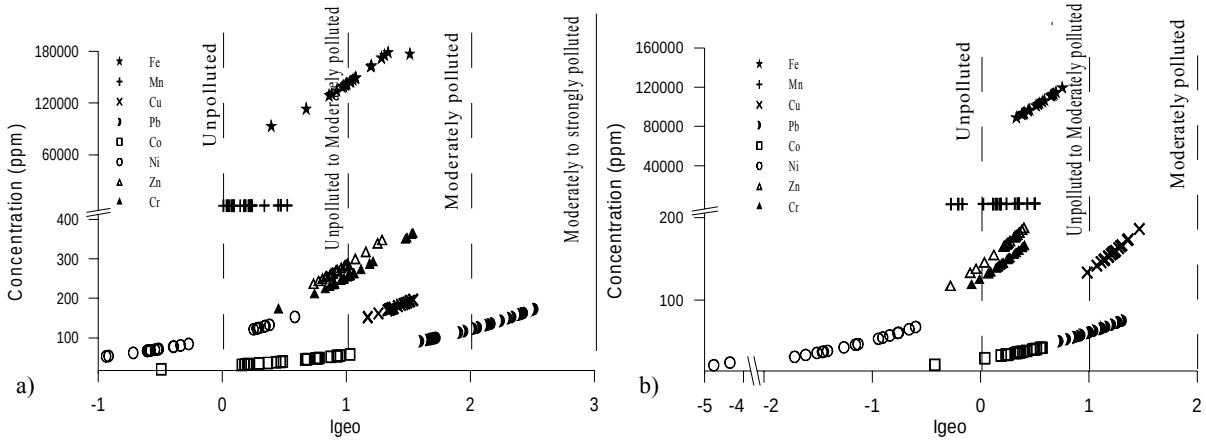

Fig. 3.3A.13. Igeo plots for core collected near the creek a) head (ManI) and b) mouth (ManII)

The concentration of Pb is found to be significantly higher in both the cores and may be attributed to the deposition of Pb particulates released by vehicles and through atmospheric input of Pb from the use of leaded petrol by motor vehicles as well as fishing boats that operate in the creek. The sources of Cu include power plants, industrial areas, the use of copper sulphate as a fungicide in vineyards (Fernandez, 2000). The use of slurry as a fertiliser containing appreciable amounts of Cu, Zn, Fe and Mn, have also been observed to be an important Cu source (Lopez, 2002). Another possible source of Cu could be the anti-fouling products present in boat paints. Also the agricultural activities around the study area may have contributed to the observed high

levels of Pb and Cu, since these metals can occur as impurities in fertilizers and in metal-based pesticides, compost and manure. Industrial activities may represent a primary source for Cr, Ni and Co, extensively used in the paint, chemical factories and textile works which are operational in the area. Additionally, Ni and Co might be linked to emissions from domestic heating systems (De Miguel et al., 1999).

Different metals bind with Fe-Mn oxides, finer sediment fractions and organic matter through adsorption, co-precipitation and complexation in sediment-water interface. In the studied cores, organic matter (TOC, TP and TN), clay and Fe-Mn oxides are found to be the dominant metal carriers. However, their order of significance is found to vary at both the sites. In core ManI, the order of significance is found to be: organic matter > clay > Fe-oxide whereas in core ManII organic matter is followed by Mn-oxide and clay. Differences in the depositional environments of the cores are further reflected by the varying metal associations observed in the two regions. Different factors such as low energy mechanical processes, bioturbation, salinity, pH, sediment components and organic matter concentration in sediments influence the mobility of metals, and consequently their distribution (Guieu et al., 1998; Sauve et al., 2000; Bostick et al., 2001). From factor analysis it is seen that "the organic matter controlled factor", shows maximum amount of total variance in both the cores, indicating good correlation of organic matter with most of the variables studied. In core ManII, the first factor (F1) shows association of organic matter with Cu, Pb, Al and Zn while in core ManI, this component is found to associate with only Ni and Cr. However, in core ManI, in addition to factors F1 and F3 which comprises of Cu, Pb, Al and Ca is also found to be controlled by organic matter but to a lesser extent. The elements in core ManI may be remobilised by physical disturbance (Petersen et al., 1997), organic matter diagenesis and sediment re-suspension (Breckela et al., 2005) wherein regeneration of Fe and Mn oxides may have altered heavy metal associations with organic matter in the sediments. Changes in the oxidation status of sediments are found to influence pH (Gambrell, 1994) which inturn affects the mobility of metals. Decreasing pH values from bottom to surface observed in core ManI must have decreased the strength of metal association. High pH values promote adsorption whereas low pH can actually prevent the retention of metals by sediments (Belzile et al., 2004). Therefore in core ManI, sediment mixing might be responsible for the observed metal profiles. Similar observations have also been made in other reservoirs, e.g., in Humber Estuary (Lee and Cundy, 2001). As seen from the Pb activity profile (Fig. 3.3A.10a), core ManI is found to be disturbed which is also supported by field observations of mixed brown and grey colour seen for major portion of the core as well as from high porosity observations. On the other hand, core ManII showed good down-core decay of ^{210}Pb activity (Fig. 3.3A.10b) and low porosity values

pointing towards a compact undisturbed sedimentary environment. Therefore, the differences in the metal associations with the carrier phase in core ManI as compared to core ManII is clearly due to the changing sediment supply and post-depositional processes in core ManI (Fernandes et al., 2011).

3.3B. Mangroves

3.3B.1 Visual description

From the bottom to 8 cm depth, a mixed brown and black colour is seen while above it, till the surface brown colour is observed for the mangrove core. The black colour indicates presence of ferrous sulphide and pyrites (FeS_2) produced when sulphide in the sediment reacts with Fe (Williamson et al., 2003).

3.3B.2. Sediment components (sand, silt, clay) and Organic matter (TOC, TP, TN)

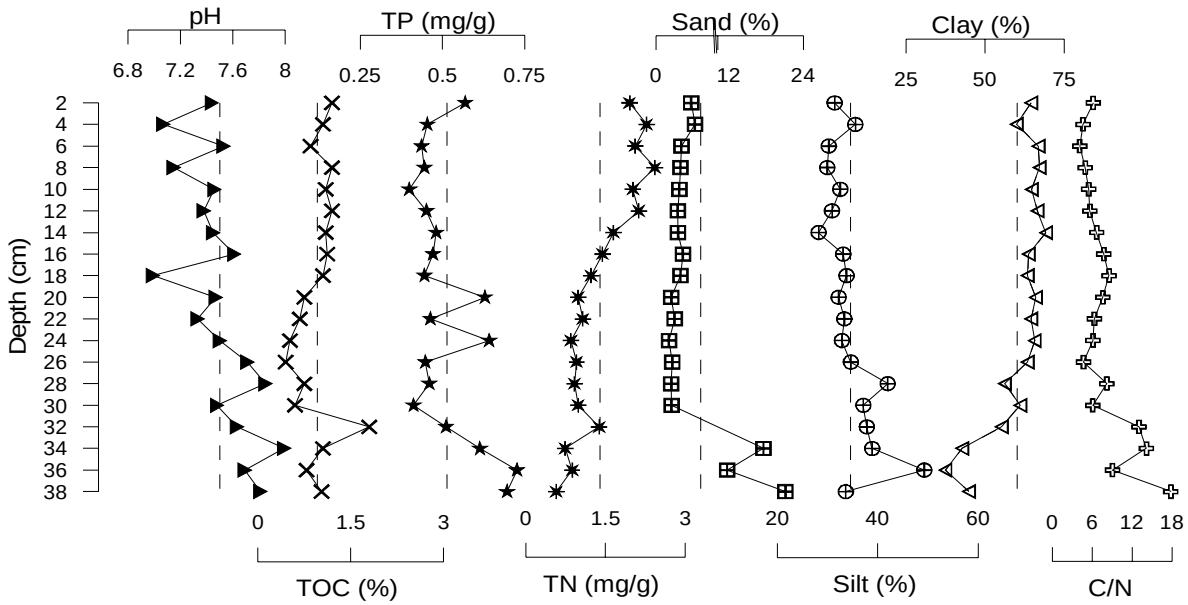

Fig. 3.3B.1. Vertical profiles of organic matter and sediment components in mangrove core (ManIIM)

The sediment components of mangrove core shows a range of values from 1.52-21.49 % for sand, 28.33-49.27 % for silt, 37.44-69.20 % for clay and 0.45-1.80 % for TOC. For TN and TP, the values are found to range from 0.58-2.43 mg/g and from 0.40-0.73 mg/g respectively. The results of the core sediments for the sites show that, in general, the sediments are mainly composed of silt and clay with very low sand content. From the depth-wise distribution (Fig. 3.3B.1) it is seen that, TOC and TN show an increase from the bottom to the surface while TP after a decreasing trend from bottom to 10 cm depth, shows an increase towards the surface. Sand exhibits a decrease from the bottom to 30 cm depth, while a constant trend is seen above 30 cm. In the case of silt and clay, both show corresponding opposite trends to each other with silt

decreasing and clay increasing from the bottom to the surface of the core. The C/N values range from 4.13-17.82 and are found to decrease from the bottom to the surface of the core. When higher plant tissues degrade, C/N values fall, on the one hand, because carbon mineralizes faster than nitrogen, and on the other hand, the bacteria, decomposing these materials produce some nitrogen (Meyers and Lallier-Vergès, 1999; Marchand et al., 2005).

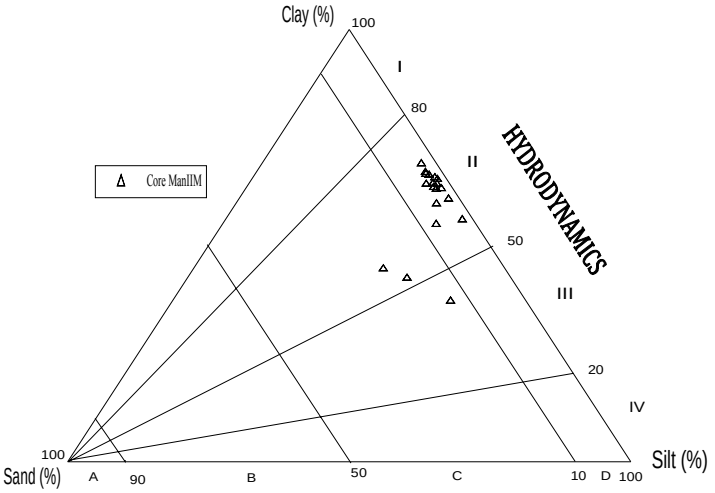

Fig. 3.3B.2. Ternary plot after Pejrup (1988) for mangrove core near the creek mouth (ManIIM)

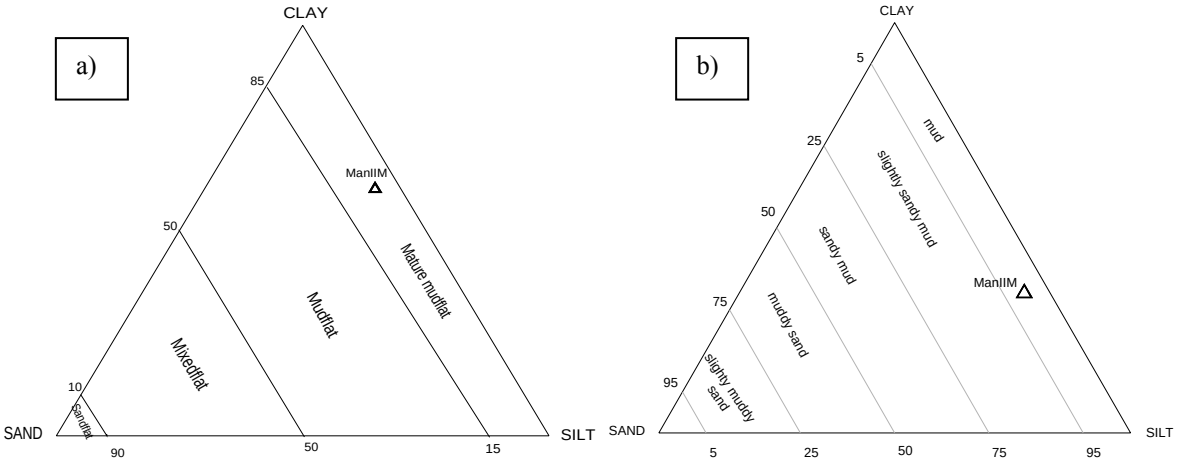

Fig. 3.3B.3. Ternary plots after a) Reineck and Siefert (1980) and b) Flemming (2000)

From the ternary diagram proposed by Pejrup (1988) (Fig. 3.3B.2), the sediment fractions of the mangrove core fall largely under group II of section D, with few samples in group C, indicating that the sediment deposition took place under relatively less violent conditions. Also textural class of sediment was determined by ternary diagram proposed by Reineck and Siefert (1980) and Flemming (2000). When the data points are plotted (Fig. 3.3B.3), it is observed that the sediments fall largely in the Mature Mudflat and Mud class, respectively.

3.3B.3. Metal geochemistry

The plot of selected metals (Al, Ca, Fe, Mn, Cu, Pb, Co, Ni, Zn, Cr and V) is presented graphically with depth in Figure 3.3B.4. The concentration of metals in the sediment are found to range from 6.15 to 8.21 % for Al, 1.58 to 3.17 % for Ca, 9.07 to 14.52 % for Fe, 813 to 1456 ppm for Mn, 53 to 200 ppm for Cu, 24 to 100 ppm for Pb, 22 to 41 ppm for Co, 44 to 102 ppm for Ni, 85 to 208 ppm for Zn, 54 to 258 ppm for Cr and from 162 to 336 ppm for V.

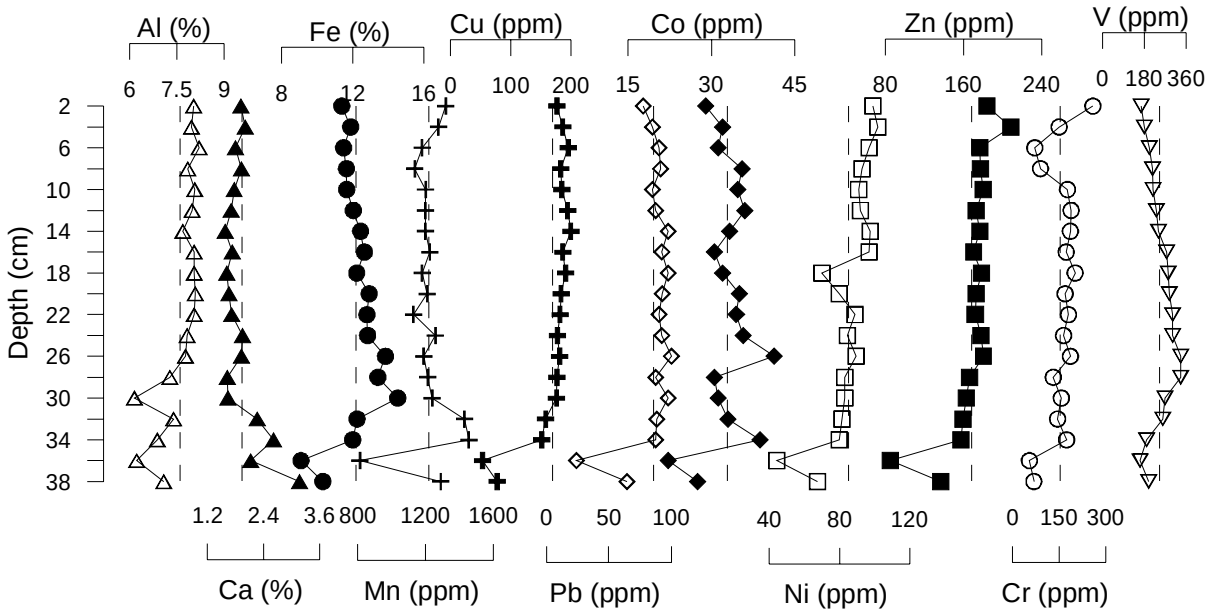

Fig. 3.3B.4. Depth-wise distribution of selected metals in mangrove core ManIIM

In the mangrove core (Fig. 3.3B.4), Al shows an increasing trend from the bottom to the surface with minor initial fluctuations at the bottom, showing maximum peak at 6 cm and minimum peak at 30 cm depth while Ca uniformly decreases from the bottom to the surface. Fe and Mn show similar decreasing and increasing trends from the bottom to 34 cm depth while from 34 to 22 cm depth, both the elements show corresponding opposite trends. Fe shows an increase till 30 cm depth and then a decrease till 22 cm with a prominent peak at 30 cm depth. In the case of Mn, a decreasing trend from 34 to 22 cm depth with a slight increased peak at 24 cm depth is observed. Further above, from 22 to 10 cm depth, both the metals again show a similar fluctuating behaviour of a decreasing trend. In the remaining portion of the core, i.e. from 10 cm upto the surface, Fe and Mn show alternate opposite decreasing and increasing trends. Zn along with Cr; and Cu along with Pb show similar decreasing and increasing trends from the bottom to the surface. The trends of Co and Ni are similar to Cu and Pb from bottom to 22 cm depth while above 22 cm upto the surface, the behaviour of Ni is found to be opposite from the other trace metals namely; Cu, Pb, Zn and Cr. In the case of V, an increasing trend from the bottom to 28 cm depth followed by a constant decreasing trend upto the surface is seen.

When the depth-wise distribution of the metals is observed (Fig. 3.3B.4), the redox-sensitive elements viz. Fe and Mn are found to correlate well with each other and accordingly control the vertical distribution of most of the metals, especially in the lower portion of the core. This significant correlation between Fe and Mn suggests the presence of Fe/Mn compounds and their strong association to the geochemical matrix. According to the study of Zabetoglou et al. (2002), Fe and Mn oxides/hydroxides have a high affinity with most trace metals and Fe often correlates with concentrations of other metals in aquatic environments. Cu, Pb, Co, Ni, Zn, Cr and V show positive correlations with Fe and Mn revealing their adsorption onto the oxyhydroxides of Fe and Mn and also their complexation with organic material playing an important role in their distribution patterns (Samuel and Phillips, 1988). A better metal-metal association in the core can be explained in terms of identical source and/or identical behaviour of the metals during their transportation (Kumar et al., 1998). Further, the presence of metals in sediments is controlled by grain size and organic matter. TN, Fe, Co and Zn are found to show peaks at 4 cm depth. Under sub-oxic conditions, the degradation of sedimentary organic matter involves the use of trace metals (e.g. Mn and Fe) as secondary oxidants and the reduction of Fe and Mn results in the mobilization and upward diffusion of these metals to oxic surface sediments where they are reprecipitated either as oxides, or occasionally as carbonates (Farmer and Lovell, 1984). TN, TP and TOC are found to show a peak at 8 cm depth which coincides with Pb and Co. Sediment organic matter has higher ion exchange capacity than sediment colloids and plays an important role in cation exchange capacity (Matagi et al., 1998). Another prominent peak of Fe, Pb, Co, Ni, Zn and Cr is seen at 26 cm depth, which indicates remobilization of the metals by Fe and Mn. Below the redox boundary, reduction of Fe^{3+} to Fe^{2+} can result in release of surface-adsorbed trace metals (Bourg, 1988). In general, when the depth-wise distributions of metals are studied, in recent years, the concentrations of most of the metals are found to be higher when compared to the bottom sediments (Fernandes et al., 2012).

3.3B.4. Statistical analysis

3.3B.4a. Correlation analysis

Organic carbon and clay contents are major controlling factors that have influence on the binding of heavy metals (De Groot et al., 1976; Fletcher et al., 1994; Williams et al., 1994). This can be demonstrated by correlating heavy metal concentrations with organic matter and clay content. The significant correlation at $p<0.05$ are observed between TN and Cu ($r=0.51$), Ni ($r=0.65$), Zn ($r=0.53$); and TOC with TN ($r=0.46$) indicates that they have a common source. This suggests that, probably these metals may have been introduced to the creek via organic materials. In

coastal environments such as in mangroves, the associations between organic matter, granulometric fractions, heavy metals and base cations act as functions of ionic strength of sediment solution and surface cation complexation (Hussein and Rabenhurst, 2001). Also in the core, the concentrations of TOC, TN, Ni, Zn and Cu are found to increase near the surface as compared to the bottom. The increase of chemical material deposition in the coastal waters can be related to intensive applications of inorganic fertilizers and also to the population growth (Cornwell et al., 1996). Further, increasing inputs of land derived sedimentary matter (Stull et al., 1986); and organic C and N-contained materials (Finney and Huh, 1989) associated with urban wastes, must have also contributed to the increase of these elements. In the case of sediment components, all the elements studied show strong correlations with clay. The core was collected further away from the main channel of the creek. Due to lack of vigorous water motion, the fine sediments tend to settle on the bottom along with organic matter. Fine material, with a larger surface to volume (or weight) ratio, has a greater potential to scavenge both inorganic and organic pollutants from the water column (Madiseh et al., 2009). Fernandes and Nayak (2009) found similar observation in a study carried out in estuarine mudflats of the Mandovi River.

3.3B.4b. Factor analysis

Factor Analysis was carried out in an attempt to further clarify the major controlling factors that determine the distribution of heavy metals in the sediment. Eigen values greater than 1 are selected with varimax rotation. Three factors accounted for 77 % of the total variance. Factor 1 explains 49.90 % of the total variance and shows good positive loadings of TN and clay on Cu, Ni, Zn and Al and negative loadings on Ca. This seems to be the granulometric factor and sorption/desorption on the fine-grained minerals and organic matter. Also this can be identified as the Al factor in which Cu appears to be associated with aluminosilicates, and both are slightly diluted by carbonates. The second factor accounts for 15.80 % of the total variance and exhibits good positive loadings of Fe on V. The third factor describes 12.96 % of the total variance and shows good positive loadings of Fe and Mn on Cu, Pb, Co, Ni, Zn, Cr and to a low extent on clay, Al and V. The second and third factors are due to different processes and therefore can be called the process factors.

Table 3.3B.1. Factor analysis matrix after varimax rotation for core ManII

	Factor 1	**Factor 2**	**Factor 3**
Variance (%)	49.90	15.80	12.96
pH	**-0.80**	0.09	0.07
TOC	0.09	**-0.75**	0.17
TP	-0.67	-0.21	-0.36
TN	**0.81**	-0.49	0.06

Sand	**-0.80**	-0.51	-0.18
Silt	-0.58	0.20	-0.56
Clay	**0.84**	0.22	0.42
Fe	0.16	**0.71**	0.62
Mn	-0.24	-0.28	**0.88**
Cu	**0.71**	0.24	0.63
Pb	0.39	0.32	**0.83**
Co	0.11	0.24	**0.76**
Ni	0.62	-0.12	0.65
Zn	0.62	0.01	**0.72**
Cr	0.28	0.16	0.58
Al	0.68	-0.14	0.39
Ca	**-0.76**	-0.55	0.02
V	0.04	**0.84**	0.34

3.3B.5. Pollution Indices

3.3B.5a. Enrichment Factor (EF)

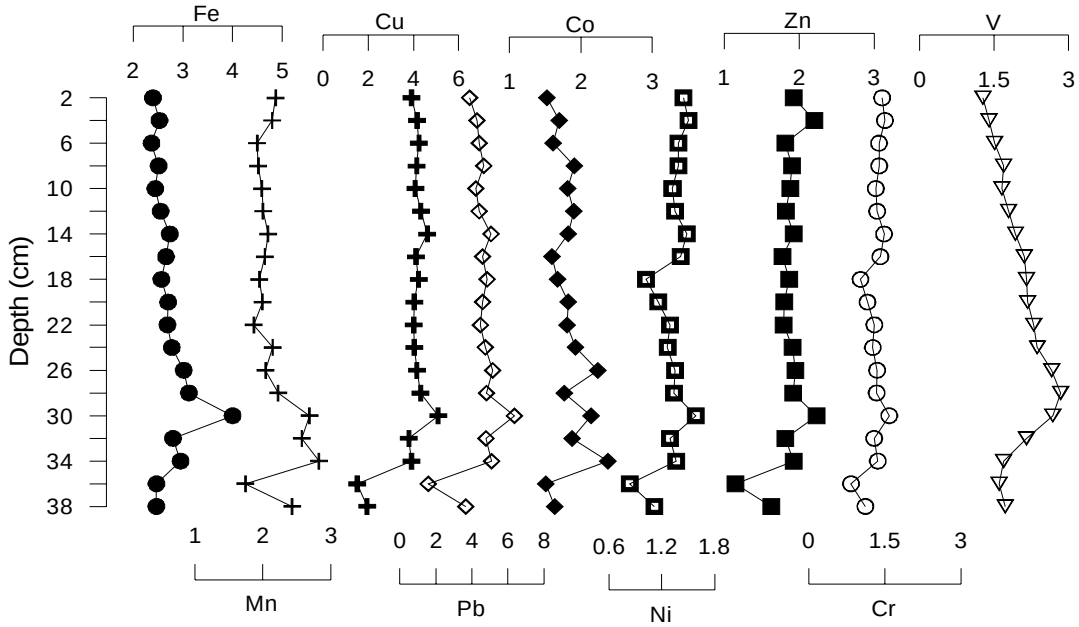

Fig. 3.3B.5. Down-core plots of EF for core collected from mangrove region (ManIIM)

The calculation of EF shows that most of the selected metals are enriched in the mangrove sediments. Pb and Cu (avg. 4.50 and 3.93) have the highest EF values among the metals studied. Co, Zn, Cr, V, Mn and Fe have minor enrichments (avg. 1.82, 1.86, 1.93, 1.98, 2.14 and 2.73 respectively) whereas Ni exhibits the lowest EF value (avg. 1.31). Factors like enhanced organic matter content, flocculation due to varying salinity regimes (Sholkovitz, 1976) and transportation

of deep shore sediments to the coastal zone (Rubio et al., 2000; Seralathan et al., 2006, Ramesh et al., 2006) contribute significantly towards the enrichment of heavy metals in sediments.

When the EF is observed for the entire length of the core (Fig. 3.3B.5), high values are seen in the upper portion as compared to the lower portion of the core for some of the metals. This clearly indicates the creek is getting enriched with metals of anthropogenic origin. The enhanced values of trace metals might have resulted from an increase in anthropogenic fluxes related to the urban and industrial development in recent years.

3.3B.5b. Index of Geoaccumulation (Igeo)

Karbassi et al. (2006) elaborated that I_{geo} values can be used effectively and are more meaningful in explaining the sediment quality. The I_{geo} index proposed by Muller (1979), show that all the metals fall within Class 1 and Class 2 (Fig. 3.3B.6) of Muller's grade scale (Table 3.1A.9). This suggests that the mangrove sediments of the creek are moderately polluted with Pb and Cu while unpolluted with respect to the remaining metals.

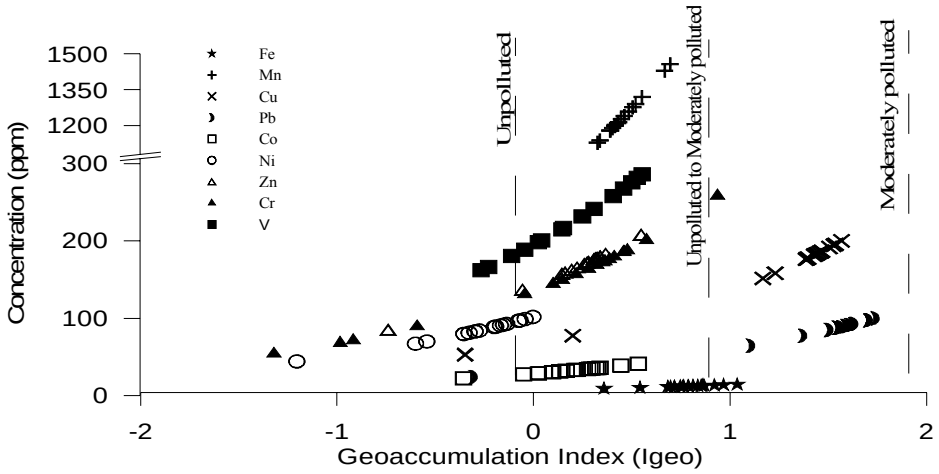

Fig. 3.3B.6. Igeo plot for mangrove core collected near the creek mouth (ManIIM)

From the values of I_{geo} calculated, vehicular traffic in the populated stretch of this creek as well as mechanized boats for fishing may have lead to the emission of Pb and its deposition at local scale. The increasing use of Cu as anti-bio-fouling agent on fishing trawlers and other commercial boats being operated in the study area might be one of the reasons for the increase in Cu concentration in recent years (Fernandes and Nayak, 2010).

3.3B.6. Isocon plot

Based on the isocon plot between the mudflat and mangrove regions at site ManII (Fig. 3.3B.7), higher concentration of Ni and Pb are seen in the mangrove region as compared to the mudflat area. This might be because of the higher clay contents present in the mangrove area. The low

hydrodynamic condition in mangroves favours the accumulation of finer sediment and organic matter. Clay minerals have a higher surface area to volume ratio and can absorb material into their lattice framework (Loomb, 2001). The mangrove core was sampled further away from the main channel of the creek than the mudflat core. Areas that are sheltered from strong tidal currents are subject to lesser amounts of erosion and are liable to be storage areas or sinks for contaminated sediments (Rees et al., 1996). However, for the mudflat region, higher amounts of V and Co are seen which can be attributed to the higher percentage of silt in the region. The major physical factor that controls fate and transport of contaminants is the energy of the overlying water flow (Birch et al., 2001). In high energy systems, sediments tend to be coarse-grained, usually metal poor, with low sorptive capacity (Birch et al., 2001; Horowitz, 1991). In low energy systems, sediments tend to be fine-grained, bearing considerable natural metal loads and acquire additional contaminant content because of the high sorptive capacity of the fine particles (Kersten and Smedes, 2002).

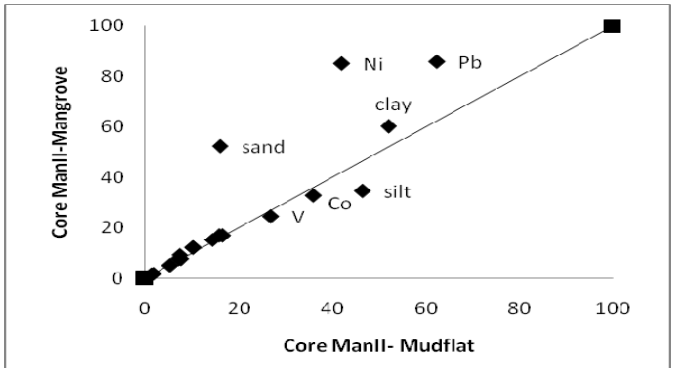

Fig. 3.3B.7. Isocon plot for cores collected from mudflat and mangrove regions

SECTION 4: VERSOVA CREEK

Two mudflat cores were sampled from the creek region representing the mouth (VI) and the head (VII) regions (Fig. 3.4.1).

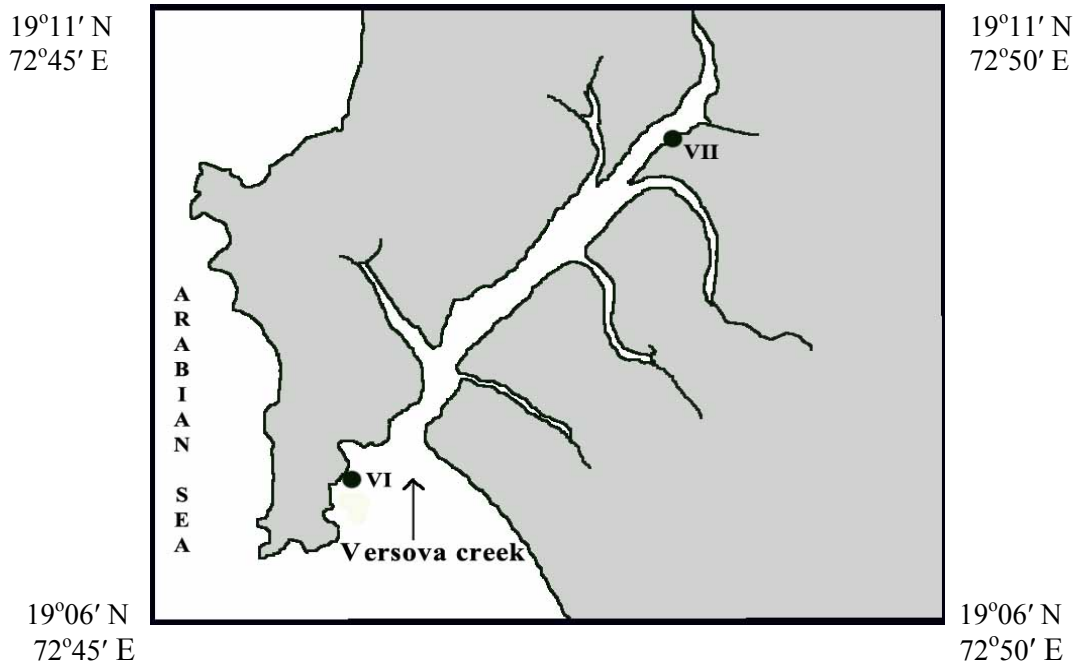

Fig. 3.4.1. Map showing the sampling locations in Versova creek

3.4.1. Visual description

The colour difference between the two sediment cores of the creek was noted. From the bottom to 58 cm, core VI, is found to be of dark grey colour while above it till the surface grey colour is observed. The other core (VII) exhibits mixed brown and black colour from the bottom to 32 cm depth and above it black colour is seen.

3.4.2. Sediment components and organic matter

In core VI, the range of the different parameters analysed are 7.34-8.45 for pH, 0.56-2.55 % for TOC, 0.14-0.64 mg/g for TP, 0.21-1.11 mg/g for TN, 1.58-24.97 % for sand, 43.86-76.07 % for silt and 12.76-45.80 % for clay with average values of 7.83, 1.46 %, 0.29 mg/g, 0.57 mg/g, 8.12 %, 63.96 % and 27.92 %, respectively. On the otherhand, for core VII, the pH, TOC, TP, TN, sand, silt and clay ranges from 6.75-8.28, 1.65-8.18 %, 0.27-0.91 mg/g, 0.47-0.91 mg/g, 1.83-28.95 %, 24.73-57.72 % and 24-62.72 %, having average of 7.64, 6.24 %, 0.54 mg/g, 0.60 mg/g, 8.66 %, 40.53 % and 50.82 %, respectively. From the depth distribution plot (Fig. 3.4.2), in core VI, pH is found to decrease from the bottom to 56 cm, followed by an increasing trend till 16 cm depth. Further, a decreasing trend is observed at the surface. In the case of organic matter, TOC and TP, in general exhibit increasing trends from the bottom to surface. However, TN shows large fluctuations along the length of the core with an overall increase in the upper portion of the

core. Among the sediment components, sand shows an increasing trend from the bottom to the surface, with two increased peaks seen at depths of 66 and 40 cm. Silt and clay display opposite trends to each other.

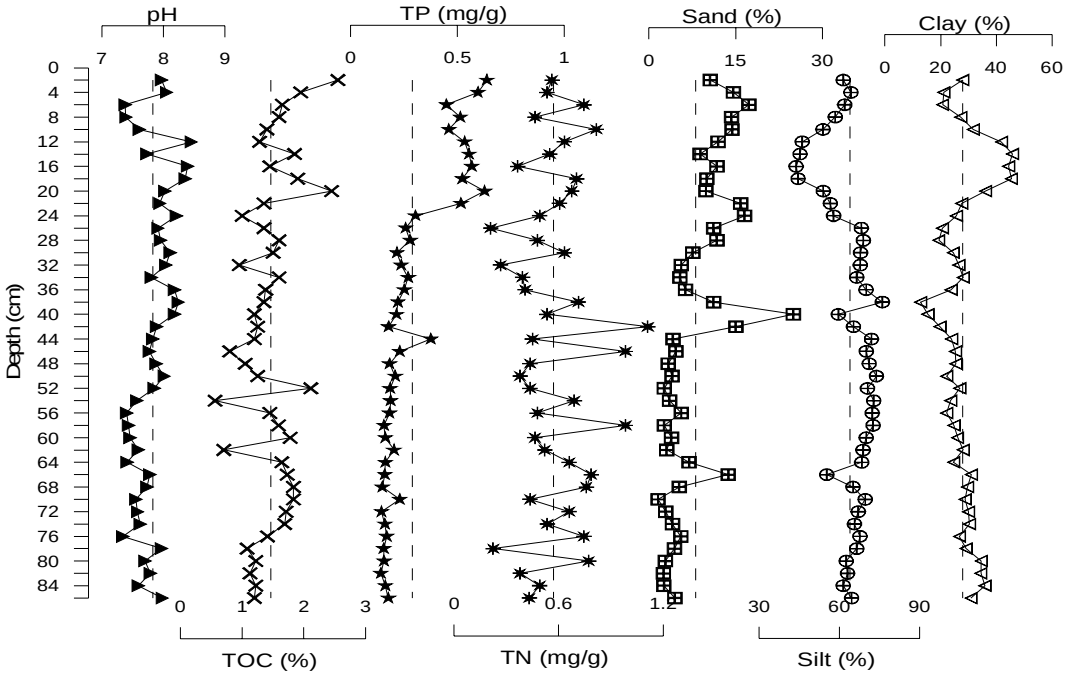

Fig. 3.4.2. Vertical profiles of organic matter and sediment components in core VI

In core VII (Fig. 3.4.3), pH gradually decreases from the bottom to the surface of the core. TOC and TN, on the other hand, increase towards the surface. TP initially increase from the bottom to 20 cm, then decreases towards the surface with large fluctuations. Among the sediment components, sand increases from the bottom to 34 cm and then gradually decreases upto the surface. Silt and clay decrease from the bottom to 36 cm and then further above exhibit corresponding opposite trends, with silt decreasing and clay increasing from the bottom to the surface of the core. Higher average sand percentage is observed in core VII as compared to core VI. Heavy land drainage and strong tidal currents could be the reason for the dominance of sand at the upper end of the creek. The sediment distribution pattern indicates that the mouth region is dominated by silt fractions while near the creek head clay is found to be the dominant component. The grain size distribution in the creek region shows mud to be the dominant sediment fraction, comprising about 88-91%.

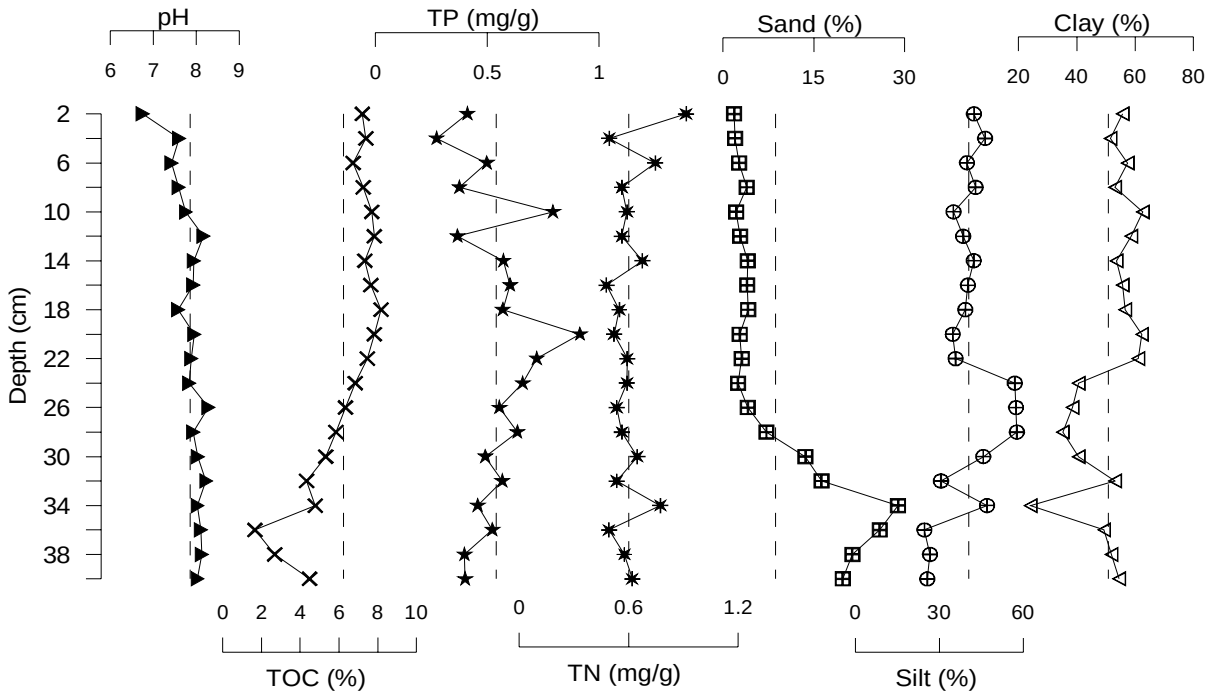

Fig. 3.4.3 Vertical profiles of organic matter and sediment components in core VII

Ternary diagram by Pejrup (1988) show the sediment fractions for core VII fall largely under group II of section C and D (Fig. 3.4.4), while few subsamples also fall in group III, indicating that the sediment deposition took place under relatively less violent conditions. For core VI, mostly all the samples fall in group III of section C and D. The distribution pattern indicates that the sediment deposition took place under relatively violent hydrodynamic condition.

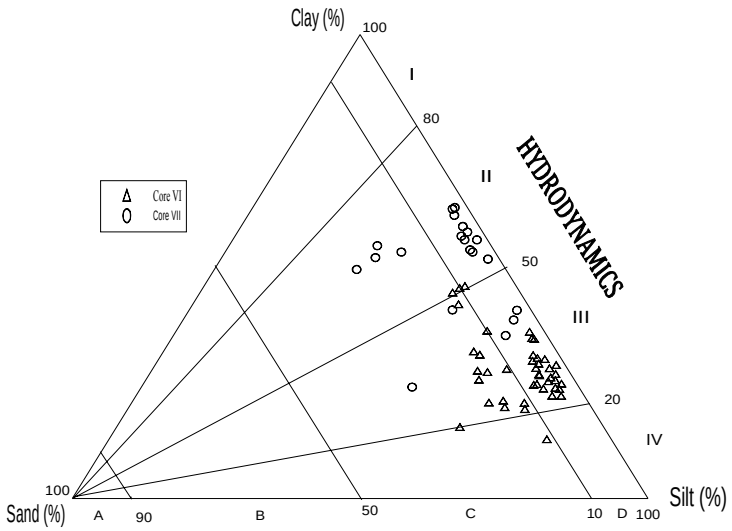

Fig. 3.4.4.Ternary plot after Pejrup (1988) for cores near the creek head (VII) and mouth (VI)

Ternary diagram proposed by Reineck and Siefert (1980) and Flemming (2000) (Fig. 3.4.5) show that for both the cores of the creek fall in the Mature Mudflat and Mud class, respectively.

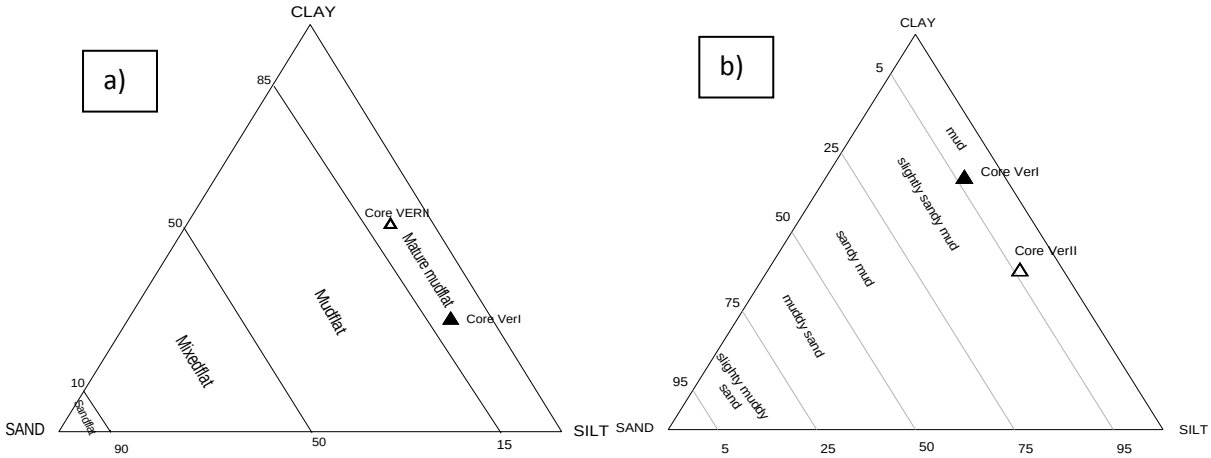

Fig. 3.4.5. Ternary plots by a) Reineck and Siefert (1980) and b) Flemming (2000)

3.4A.3. Clay mineralogy

Clay mineral analysis using XRD was performed on selected subsamples of core VI. The results show that the sediments in the region consist mostly of the mineral smectite (range- 48.55-66.56 %, avg. 54.65 %), illite (range- 16.37-27.71 %, avg. 22.42 %), kaolinite (range- 6.44-21.59 %, avg. 14.16 %) and chlorite (range- 7.41-10.63 %, avg. 8.78 %).

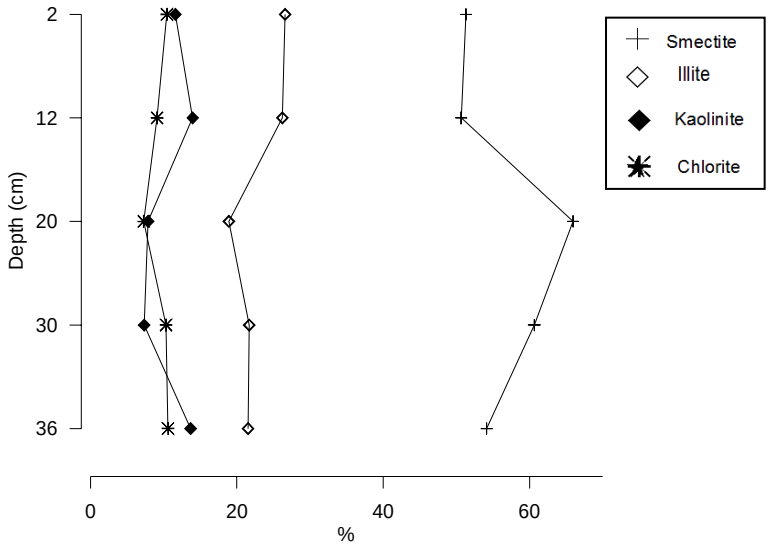

Fig. 3.4.6. Depth-wise distribution of clay minerals in core VI

The vertical distribution of clay minerals for the core is shown in figure 3.4.6. From the depth-wise distribution, smectite and illite show opposite trends to each other with alternate increasing and decreasing patterns. On the otherhand, kaolinite initially decreases at the bottom followed by an increasing trend towards the surface while chlorite decreases from bottom to 20 cm and then increases at the surface.

SECTION 5: NHAVA-SHEVA

Two sediment cores were sampled from the creek, one from the mudflat region and the other from a mangrove region (Fig. 3.5.1). A distance of 50 m was maintained between the sub-environments.

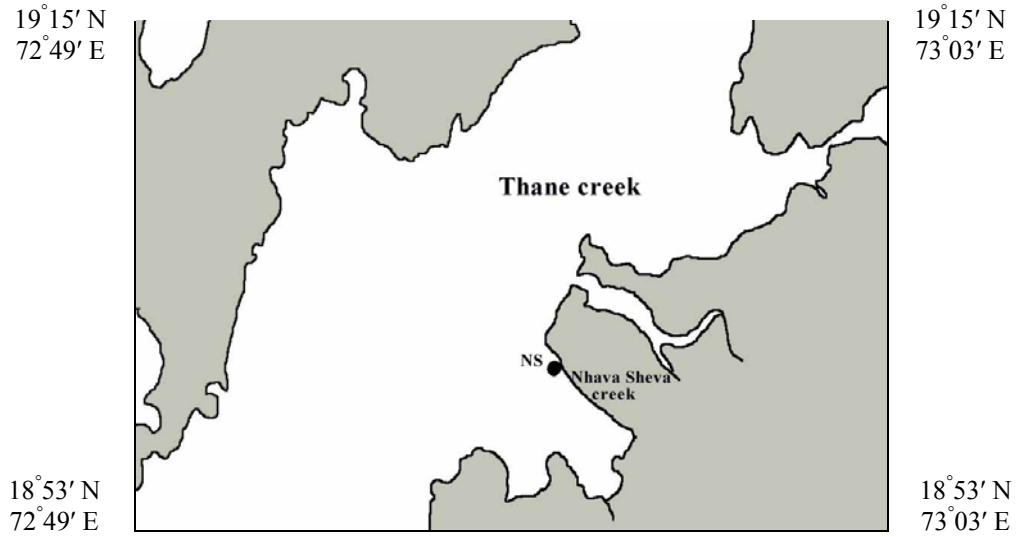

Fig. 3.5.1. Map showing the sampling locations in Nhava-Sheva creek

3.5.1. Visual description

The mudflat core shows distinct variation in colour from the bottom to the surface. The lower portion of the core, from the bottom to 16 cm displays grey colour while from 16 to 10 cm depth grey and black colour is seen. Further above, brown colour is noticed. In the mangrove core, from the bottom to 28 cm dark brown colour is seen followed by brown colour till the surface.

3.5.2. Sediment components and Organic matter

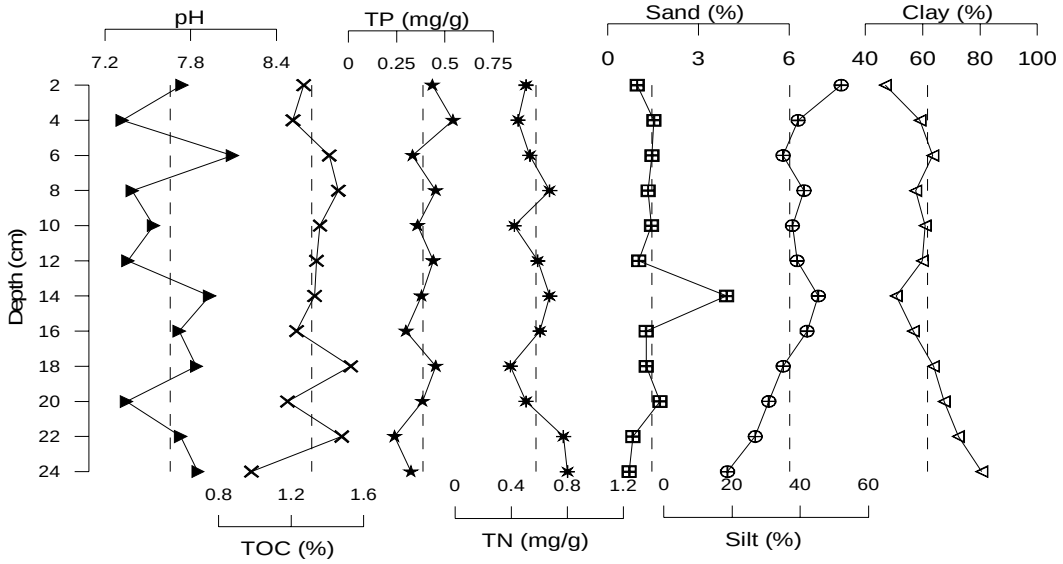

Fig. 3.5.2. Vertical profiles of sediment components and organic matter in mudflat core (NS)

In the mudflat core (Fig. 3.5.2) from the depth profile it is seen that pH (range- 7.32-8.09, avg. 7.66) fluctuates largely from the bottom to surface with no distinct trend while TP (range- 0.24-0.54 mg/g, avg. 0.39 mg/g) exhibits an increasing trend from the bottom to the surface. TOC (range- 0.98-1.53 %, avg. 1.32 %) and TN (range- 0.40-0.80 mg/g, avg. 0.58 mg/g) decrease from the bottom to the surface with some fluctuations.

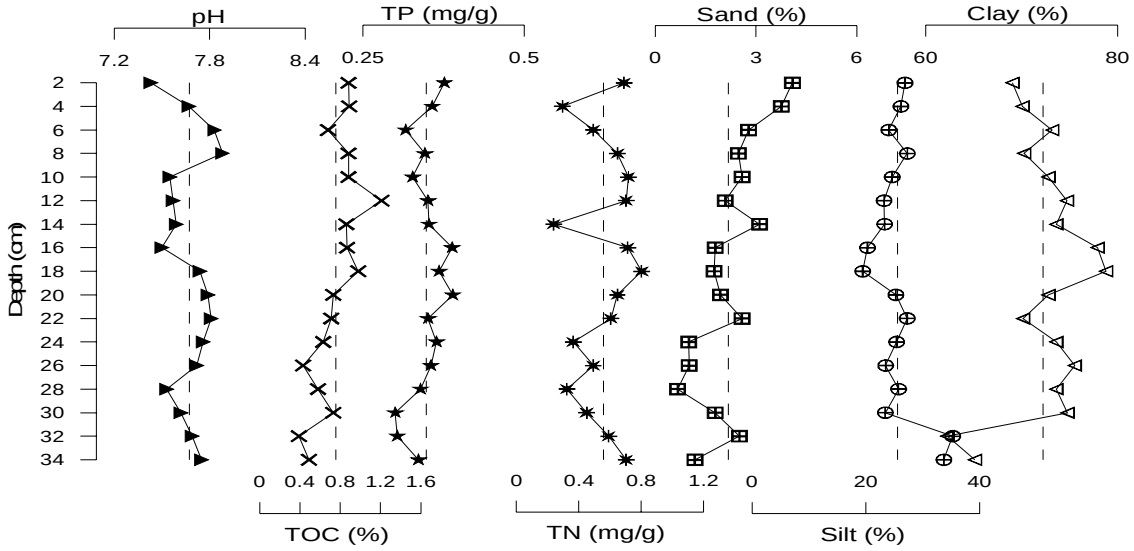

Fig.3.5.3.Vertical profiles of sediment components and organic matter in mangrove core (NS-M)

Among the sediment components, sand (range- 0.71-3.93 %, avg. 1.45 %) does not deviate much from the average line except for an increased peak seen at 14 cm depth. Silt (range- 18.65-52 %, avg. 36.88 %) and clay (range- 47-80.64 %, avg. 61.67 %) display corresponding opposite trends, with silt increasing and clay decreasing from the bottom to 14 cm depth. Further above, increasing and decreasing trends are noticed. For the mangrove core (Fig. 3.5.3), pH (range- 7.43-7.88, avg. 7.67) projects decreasing and increasing trends from the bottom to the surface. Among the organic matter, TOC (range- 0.39-1.21 %, avg. 0.75 %) and TP (range- 0.30-0.39 mg/g, avg. 0.35 mg/g) exhibit increasing trends from the bottom to surface with minor fluctuations while TN (range- 0.24-0.80 mg/g, avg. 0.56 mg/g) displays erratic trends from the bottom to the surface of the core. Sand (range- 0.67-4.09 %, avg. 2.18 %) increases from the bottom to surface of the core while silt (range- 19.44-35.25 %, avg. 25.57 %) decreases from the bottom to 18 cm and further above increases upto the surface. Clay (range- 62.24-78.80 %, avg. 72.25 %), on the other hand, increases from the bottom to 18 cm depth and then decreases towards the surface of the core. The high mud content indicates the prevalent hydrodynamics and presence of mangrove roots, which are well developed and helped to retain the finer fraction with the dense grid of vertical pneumatophores and aerial roots. This structure traps floating

detritus and reduces flow, eventually creating conditions wherein suspended clay and silt particles settle in the creek (Soto-Jimenez and Paez-Osuna, 2001).

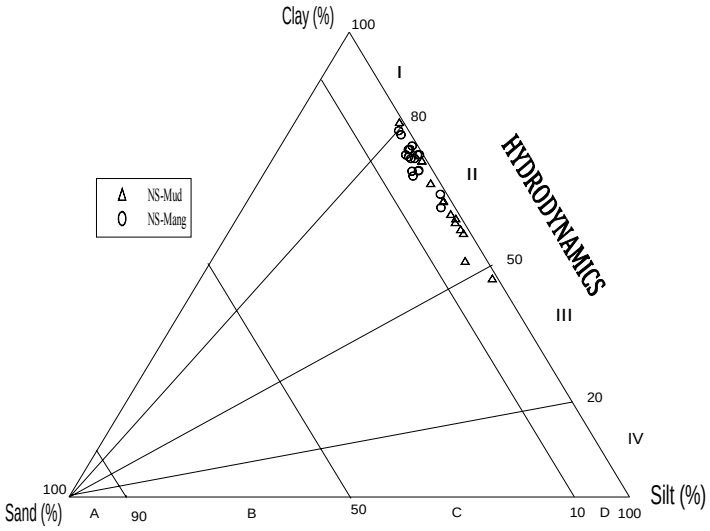

Fig. 3.5.4. Ternary plots for mudflat (NS) and mangrove region (NS-M) after Pejrup (1988)

Ternary diagram after Pejrup (1988) show that the sediment fractions of both the cores fall largely under group II of section D (Fig. 3.5.4), indicating that the sediment deposition took place under relatively less violent conditions. Ternary diagrams by Reineck and Siefert (1980) (Fig. 3.5.5a) and Flemming (2000) (Fig. 3.5.5b) show that both the cores of the creek fall in the Mature mudflat and Mud class, respectively.

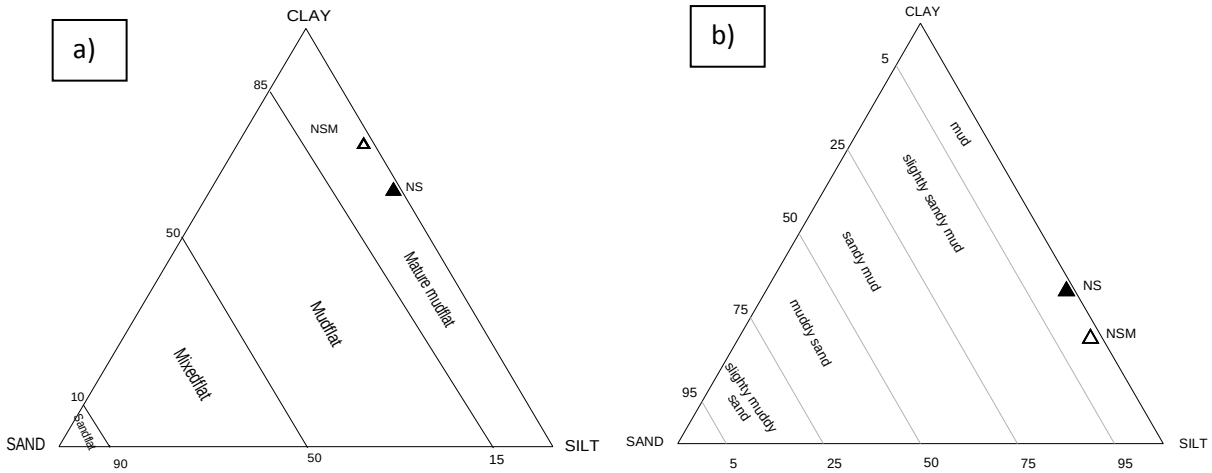

Fig. 3.5.5. Ternary plots for mudflat (NS) and mangrove region (NS-M) after a) Reineck and Siefert (1980) and b) Flemming (2000)

Chapter 4

SPECIATION

4.1. Introduction

Heavy metals are present in different chemical forms viz., metal carbonates, oxides, sulphides, organo-metallic compounds and lattice structure bound. However, only part of the metal present can be easily remobilized. Site-specific chemical and physical conditions greatly influence the form in which metals occur in the environment and thus the degree to which they are sorbed to sediments and soils. Chemical processes at the sediment-water interface are complex and are governed by physicochemical characteristics such as grain size, organic matter, redox potential or ionic strength change, resulting in the release of bound metal into solution (Wepener and Vermuelen, 2005). Unlike many organic contaminants that lose toxicity with biodegradation, metals cannot be degraded and their toxic effects can therefore be long lasting (Clark, 1992). Because, metals can be either adsorbed onto sediments or accumulated by benthic organisms to toxic levels, bioavailability and toxicity depend upon the amounts of metal bound to the sediment (Yu et al., 2001). Chemical speciation can be defined as the identification and quantification of the different chemical species, forms or phases present in the sediment.

Many sequential extraction procedures (SEPs) are available for analyzing metal species in various kinds of soils and environmental samples and can provide information on origin, mode of occurrence, biological and physiochemical availability, mobilization and transport of metals in sediment which makes the procedures valuable tools in contaminant analysis (Zimmerman and Weindorf, 2010). Quantification of contaminants in soils is typically done using chemical solutions of varying, but specific strengths and reactivities to release metals from the different soil fractions (Ryan et al., 2008). The procedure proposed by Tessier et al. (1979) is the most commonly used protocol for sequential extraction and has been used for this study. Although different SEPs are available, many of the fractionation procedures tend to be the same. The theory behind all sequential extraction procedures (SEPs) is that the most mobile metals are removed in the first fraction and continue to be extracted in order of decreasing mobility. Tessier et al. (1979) determined that the five most common fractions that could be affected by various environmental conditions were exchangeable, carbonate bound, Fe and Mn oxide bound, organic matter bound and residual. Metals, especially of anthropogenic input, are expected to associate with the first four fractions and metals found in the residual fraction are considered to be of natural occurrences derived from the parent rock (Ratuzny et al., 2009).

Metals present in sediments or soils can be toxic to organisms which are directly exposed to them. In the solid phase, metal ions can be retained on organic and inorganic soil components by various sorption mechanisms (e.g., ion exchange or surface complexation); or they can exist as

minerals or be co-precipitated with other minerals (e.g., carbonates) in the soil. Metals are found in all sediments; however, a large amount of the total metals in most sediment is in the residual fraction as part of the natural minerals that make up the sediment particles. These residual metals are not bio-available. The remaining forms of metals in sediments are adsorbed to or complexed with various sediment components and may be bio-available. In oxidized sediments, metals may be adsorbed to clay particles, Fe, Mn and Al oxide coatings on clay particles or dissolved and particulate organic matter. As the concentration of oxygen in sediment decreases, usually because of microbial degradation of organic matter, the metal oxide coatings begin to dissolve, releasing the adsorbed metals. In oxygen-deficient sediments, many metals react with sulphide produced by bacteria and fungi to form insoluble metal sulphides. Metals may be released from sorbed or complexed phases into sediment pore water in ionic, bio-available forms during changes in oxidation/reduction potential. Microbial degradation of organic matter may also release adsorbed metals to pore water.

Rivaro et al. (2005) carried out speciation of metals in Albanian coastal sediments and observed that high percentage of Cr, Cu, Ni and Mn were present in the labile fractions, which revealed recent river input of these metals, related to mining and industrial wastewater discharge. A study was carried out by Nemati et al. (2011), wherein sequential extraction procedure was applied for partitioning of heavy metals in river core sediments in Malaysia. The results showed the element concentrations, from top to bottom layers, decreased predominantly indicating the pollution was of recent years. Arias et al. (2008), analysed short sediment cores, dredged from the dry dock of a former shipyard, to establish the distribution of 12 metals into four speciation fractions. Fractionation studies showed that three of the metals were mobile, being preferentially associated with non-residual fractions. Sequential chemical extraction of metals (Cu, Ni, Mn, Fe, Pb, Cr, and Zn) from core sediments of the Orogodo River was carried out by Iwegbue (2011), with a view of providing information on the phase distribution of these metals with respect to depths and seasons. The speciation patterns indicated that majority of the metals existed either in the Fe-Mn oxides or residual form in the top sections of the core. At the deeper sections, the metals occurred predominantly in the residual form. Metals in the Fe-Mn oxides and organic bound forms may be remobilized as a result of changes in the pH and redox potential of the sediments. Prasad et al. (2006) carried out fractionation of Fe, Zn, Cu, Pb, Mn and Cd in the sediments of the Achankovil River, Western Ghats, India using a sequential extraction method, to understand the metal availability in the basin for biotic and abiotic activities. The results showed that maximum amount of the metals were bound to the non-residual fractions (mainly Fe-oxides) indicating the non-residual phase to be the most important phase for majority of the

heavy metals studied. Yu et al. (2010) studied chemical speciation of heavy metals (Cu, Zn, Ni, Cr, Mn, Co, Fe, V and Pb) in the intertidal surface sediments from Quanzhou Bay using a modified BCR sequential extraction procedure in order to evaluate the potential mobility and the possible transfer of heavy metals from sediments to the surrounding environment. The results showed that Mn occupied the highest percentage in the acid-soluble fraction, and Pb and Cu presented the highest percentages in the reducible fraction. The highest percentages of Fe, V, Cr, Zn, Ni and Co were found in the residual fraction.

Therefore, the total metal concentration alone does not accurately measure the fraction biologically available to aquatic and terrestrial organisms. Further, so far, no study has been focused on metal fractionation in the aquatic sediments of the Thane creek and the Ulhas estuary. Hence, speciation study was carried out in the region, to have a better understanding of metal origin and bioavailability. The percentage of metal extracted was calculated from the ratio between the concentration of the element in each fraction and the sum of concentrations in all the fractions. The elements Cu, Pb, Co, Zn and Cr were selected in view of their anthropogenic character, and Fe and Mn, because of their sensitivity to diagenetic changes. The lack of reference materials for these extraction methods can be overcome by comparing the sum of the concentrations obtained in each individual step with the total metal concentration (Ramos et al., 1994; Fernandes, 1997).

4.2. Thane creek

Speciation analyses were carried out for three mudflat cores namely; near the creek head (TI), lower middle creek region (TV) and near the creek mouth (TIV). The metal range obtained for the different fractions is given in Table 4.1. The results of sequential chemical extractions, showing the distribution of metals in the different phases of sediment from the creek are shown in Figures 4.1-4.7.

Fe: From the depth-wise distribution plots (Fig. 4.1), in all the cores, the F1 and F4 fractions show a decreasing trend from the bottom to the surface with minor fluctuations. In the case of F2 fraction in core TI, the values initially decrease at the bottom followed by slight increase with large fluctuations towards the surface. For cores TV and TIV, similar down-core trends are seen wherein the values gradually decrease from the bottom to the surface except for increased peak at 26 cm in core TV and at 16 cm depth in core TIV. In core TI, the F3 fraction shows large variations. From the bottom to 18 cm, a decrease is noticed followed by an increasing trend till 10 cm depth. Further above a decreasing trend is observed. For core TV, after an initial decrease

at the bottom, an increasing trend is seen till the surface while for core TIV, a decrease from the bottom to 18 cm depth followed by an increasing trend upto the surface is observed. The F5 fraction in core TI increases from the bottom to 26 cm depth, then decreases till 10 cm followed by an increasing trend upto the surface. In core TV, the F5 fraction exhibits fluctuation while a gradual increasing trend is seen in the case of core TIV. In all the three cores, the total Fe content displays similar trends with the F5 fraction.

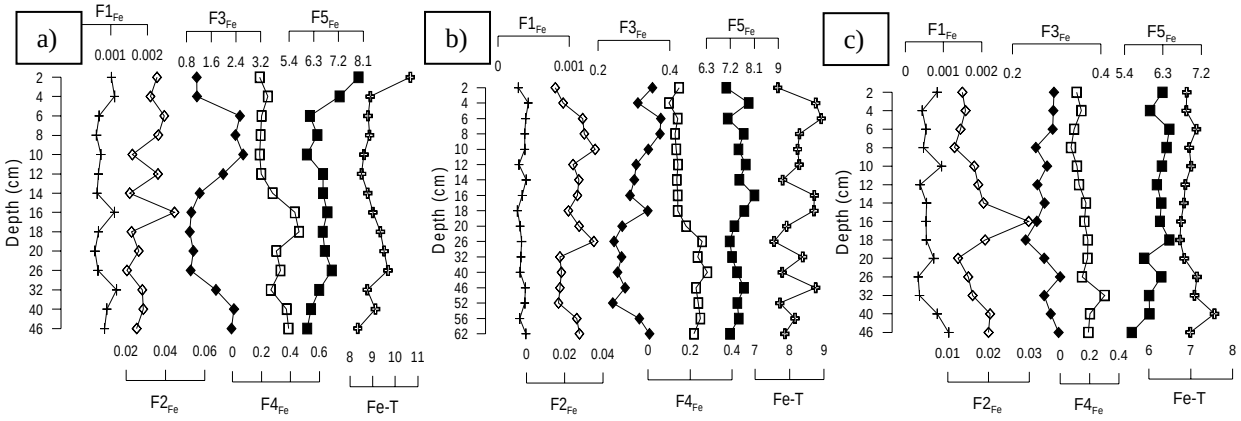

Fig. 4.1. Plots of different fractions of Fe in a) core TI b) core TV and c) core TIV

In all the three cores studied, highest amounts of Fe are present in the residual fraction (> 90 %) followed by Fe-Mn oxide, organic/sulphide, carbonate and exchangeable phases. Negligible amounts of exchangeable fractions of Fe are found in all the core samples. These results are in agreement with the study of Moalla et al. (1997), who mentioned that most of the Fe exists as crystalline Fe oxides (goethite, limonite and magnetite). The high Fe percentage in the residual fraction indicates that the sediment is relatively unpolluted with respect to this element.

Mn: The vertical distributions of the different fractions for all the cores are shown in Figure 4.2. For core TI, the F1 fraction shows a constant trend from the bottom to the surface except for an increased peak at 14 cm depth. In core TV, a gradual increasing trend is seen from the bottom to the surface while in core TIV after an initial increase from the bottom to 32 cm, a decreasing trend is observed till 12 cm. Further above, slight increasing trend is seen till the surface. The F2 fraction in core TI decreases from the bottom to the surface while in core TIV after an initial increase, a decrease is seen till the surface.

In core TV, the F2 fraction displays a decreasing trend from the bottom to 12 cm followed by an increase till 8 cm depth. Further above, a decreasing trend is seen. The F3 fraction, in core TI, exhibits a uniform increasing trend from the bottom to the surface while in cores TV and TIV similar profiles are seen, wherein decreasing trends from the bottom to 10 cm in core TV and 8 cm in core TIV, are followed by increasing trends till the surface. In the case of the F4 fraction,

cores TV and TIV exhibit increasing trends from the bottom to the surface while core TI shows a decreasing trend from the bottom to the surface, except for an increased peak at 26 cm depth. All the three cores display increasing trends for the F5 fraction from the bottom to the surface. In cores TI and TV, the down-core profiles of total Mn are similar to the profiles of the F5 fractions. In the case of core TIV, total Mn profile goes well with the F4 fraction.

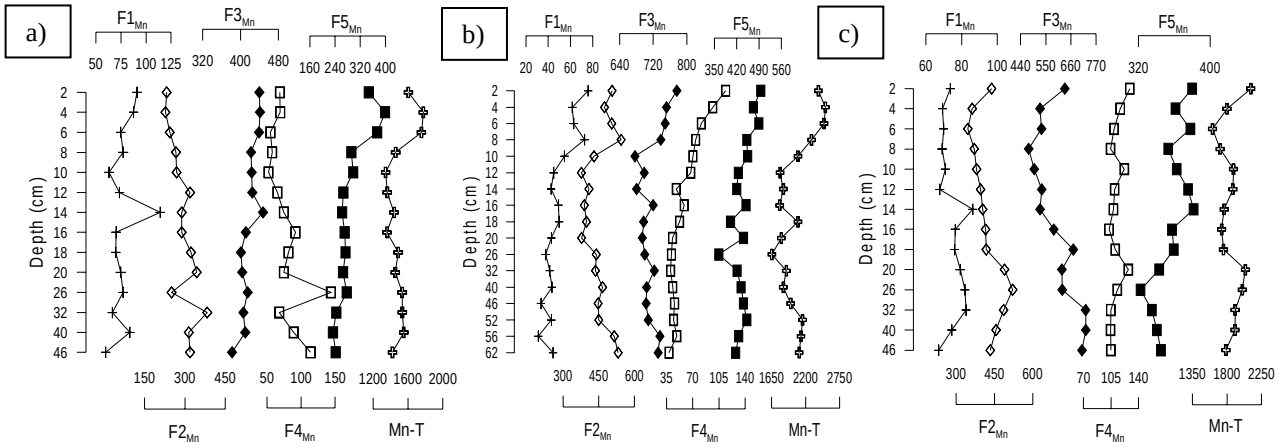

Fig. 4.2. Plots of different fractions of Mn in a) core TI b) core TV and c) core TIV

The association of Mn with different fractions in all the three cores follows the order: Fe-Mn oxides > carbonate > residual > organic/sulphide > exchangeable. The low percentages of Mn in the residual fraction can be attributed to the relatively large ionic radius of Mn which makes its retention by soil silicates difficult. In the present study, Mn is found to be associated primarily with the oxide and carbonate fractions. Also, considerable amounts of Mn are found in all of the four fractions (F1, F2, F3 and F4). Such trend has been noted by other researchers (Usero et al., 1998; Ngaim and Lim, 2001). The study conducted by Akcay et al. (2003) have demonstrated that Mn exhibits an exceptional environmental behaviour by distributing mainly in the unstable form bounded to exchangeable, carbonate and Fe/Mn-oxide. The different chemical forms of Mn can affect the solubility and mobility of the metal from sediments. These results indicate that considerable amounts of Mn may be released into the environment if conditions become more acidic or if the sediments are subjected to more reducing conditions (Yuan et al., 2004). Therefore, Mn in the creek sediments might have higher mobility and availability.

Cu: From the vertical depth profiles (Fig. 4.3), the F1 and F2 fractions, in core TI show decreasing trends while in cores TV and TIV increasing trends from the bottom to the surface are seen. For the F3 fraction, in core TI and TIV similar trends are noticed, wherein decreasing trends from the bottom to 8 cm depth for core TI and 18 cm depth for core TIV, are followed by increasing trends till the surface. The F4 fraction fluctuates throughout the length of core TI. In core TV, it exhibits an increasing trend while core TIV shows a decreasing trend from the

bottom to the surface. In all the three cores, the F5 fraction displays an overall increasing trend from the bottom to the surface. The total Cu contents in all the three cores, display similar trends with their respective F5 fractions.

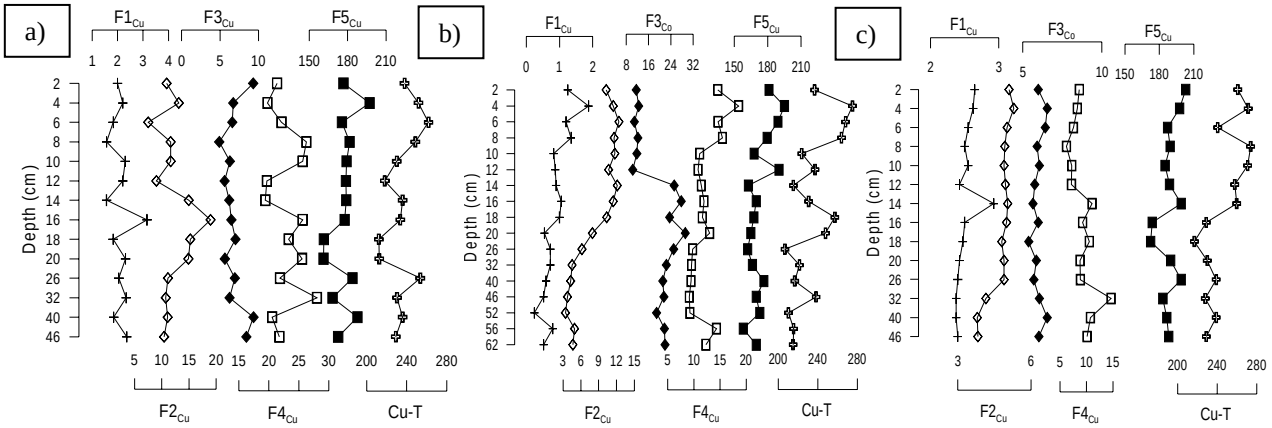

Fig. 4.3. Plots of different fractions of Cu in a) core TI b) core TV and c) core TIV

The partitioning percentage of Cu in the sediments is of the order: residual > organic/sulphide > carbonate > Fe-Mn oxide > exchangeable in core TI while in core TV the order is residual > Fe-Mn oxide > organic/sulphide > carbonate > exchangeable. In core TIV the order is residual > organic/sulphide > Fe-Mn oxide > carbonate > exchangeable. In sediments of cores TI and TIV, Cu is largely bound to the organic fraction reflecting the formation of stable organo-metallic complexes. Similar results were observed by Zhou et al. (1998) and Ramos et al. (1999), who reported that Cu primarily binds with organic matter. The metals in F4 fraction may be released into the environment if conditions become more oxidising. The high Cu in residual and organic/sulphide fractions may indicate that the sediment is relatively unpolluted.

Pb: From the down-core plots (Fig. 4.4), it is seen that the F1 fraction fluctuates from the bottom to the surface in all the three cores studied, with an overall decreasing trend. The F2 fraction in core TI fluctuates with no definite trend while in core TV an increasing trend is noticed. In core TIV, increasing and decreasing trends are seen from the bottom to the surface. The F3 fraction shows a decreasing trend in core TI while in cores TV and TIV a decrease is seen at the bottom followed by an increase towards the surface. In core TI, the F4 fraction increases from the bottom to the surface while in core TV an increase from the bottom to 26 cm depth is followed by a decreasing trend till the surface. On the other hand in core TIV, the F4 fraction decreases from the bottom to 12 cm depth followed by an increasing trend till the surface. The F5 fraction in core TI decreases from the bottom to 6 cm and further above, an increasing trend is seen. Core TV shows a decreasing trend from the bottom to the surface while in core TIV an increasing trend is seen with large fluctuations towards the upper portion of the core. In cores TI and TV and to some extent in core TIV, the total Pb content displays similar trends to the F5 fractions.

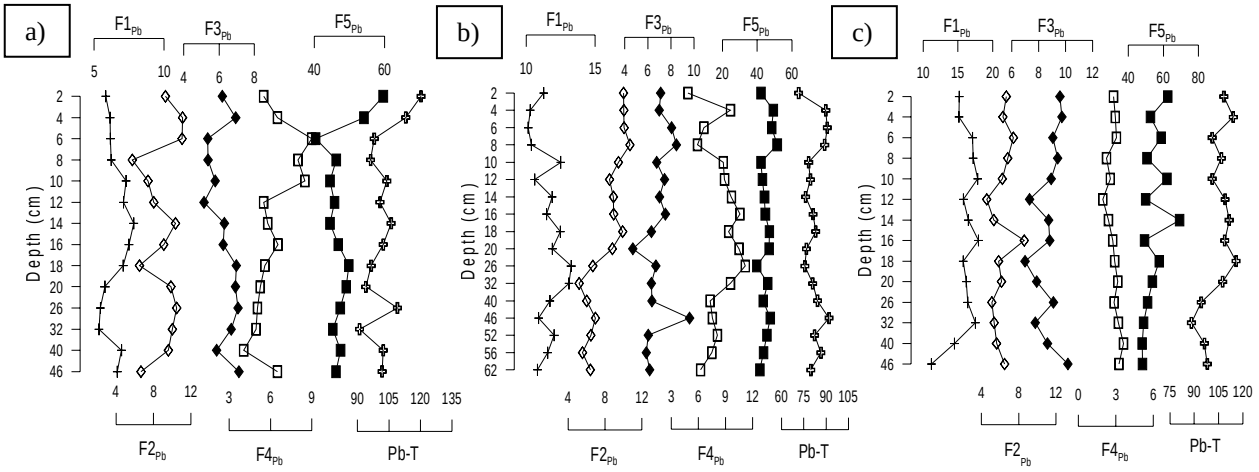

Fig. 4.4. Plots of different fractions of Pb in a) core TI b) core TV and c) core TIV

The Pb profiles at all the sites show major portions bound to the residual fraction followed by carbonates > exchangeable > Fe-Mn oxide > organic/sulphide in core TI, exchangeable > organic/sulphide > carbonates > Fe-Mn oxide in core TV while in core TIV the order is exchangeable > Fe-Mn oxide > carbonates > organic/sulphide. Next to residual, the carbonate fraction is another important phase for Pb in core TI. A number of studies have found that Pb can be associated with carbonates (Lopez-Sanchez et al., 1996; Izquierdo et al., 1997). Carbonates can be an important absorbent for Pb when organic matter and Fe-Mn oxides are less abundant in the aquatic system. The carbonate form is a loosely bound phase and liable to vary with changes in the environmental conditions. It is observed that Pb in the exchangeable fractions of core TIV is higher than that in the other sediment cores. This might be the effect of low pH in core TIV sediments. The low pH of the sediments might have resulted in an increase in solubility and potential bioavailability of Pb in the creek system (Sims, 1986). However, higher percentages of Pb are present in the residual fractions which indicate that the sediment is relatively unpolluted with respect to this element.!

Co: From the vertical distribution plots (Fig. 4.5), the F1 fraction in core TI decreases while in core TIV increases, from the bottom to the surface. In the case of core TV, the F1 fraction fluctuates, showing an increasing trend from the bottom to 14 cm followed by a decreasing trend till the surface. The F2 fraction in core TI, after an initial increase at the bottom exhibits decreasing trend till the surface while in cores TV and TIV, large fluctuating trends are seen with an overall increasing trend towards the surface. For the F3 fraction in core TI and core TIV, increasing trends are seen from the bottom to the surface while in core TV almost constant trend is noticed with a slight increase at the surface. Core TI exhibits a decreasing trend, while cores TV and TIV display increasing trends with minor fluctuations from the bottom to the surface for the F4 fraction. The F5 fraction, in core TI, increases from the bottom to the surface while for

core TIV a decreasing trend is seen. An increasing and decreasing trend is observed in the case of core TV. Among the three cores studied, only in core TIV, the total Co contents show depth profile similar to the F5 fraction.

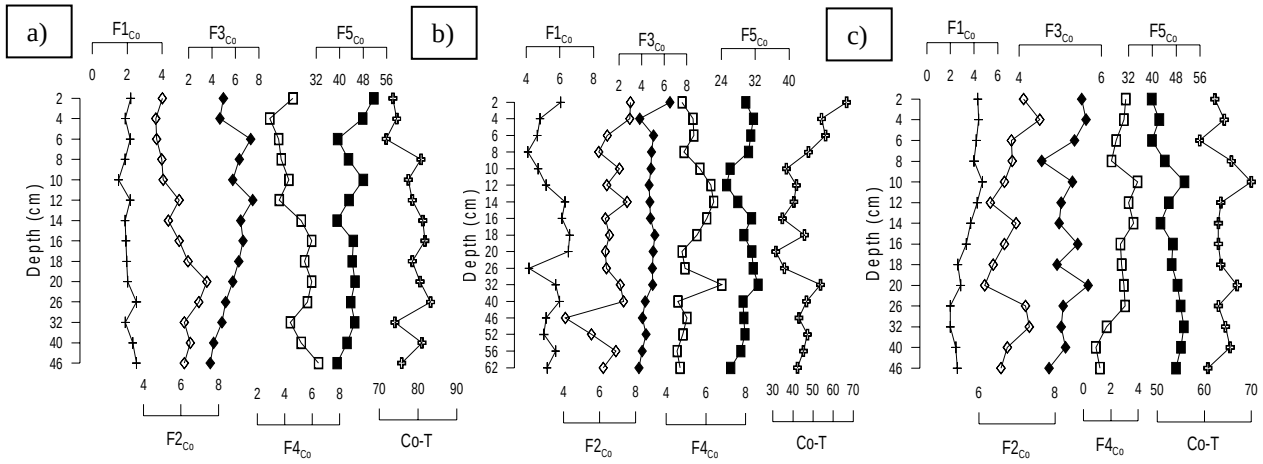

Fig. 4.5. Plots of different fractions for Co in a) core TI b) core TV and c) core TIV

The percentage in the five fractions of Co follow the order, residual > carbonates > organic/sulphide > Fe-Mn oxide > exchangeable in core TI, residual > carbonates > exchangeable > organic/sulphide > Fe-Mn oxide in core TV and residual > carbonates > Fe-Mn oxide > exchangeable > organic/sulphide in core TIV. The high Co content associated with carbonates could be explained by assuming that Co might have co-precipitated with Ca carbonates as suggested by Sposito (1984). Anthropogenically derived Co has been found to preferentially associate with Fe and Mn oxides in estuarine sediments (Chiffoleau et al., 1994), but this behaviour was not observed in the present cores. The dominance of the residual fraction of Co in the creek sediments is probably due to the low levels of total Co in the sediments. Most of the Co may have come from the parent material of geological origin and may exist in the residual form in the sediments. The anthropogenic sources seem to be less important for Co in these sediments.

Zn: In core TI, the F1 fraction distribution is found to increase from the bottom to the surface while in core TV, a decreasing trend is seen (Fig. 4.6). However, in core TIV large fluctuation in the F1 fraction is seen. The F2 fraction, in cores TI and TV, after an initial decrease increases towards the surface while in core TIV, from the bottom to the surface, an increasing trend is seen except for a decreased peak at 6 cm depth. In core TI, the F3 fraction fluctuates and decreases at the bottom followed by an increasing trend at the surface. In core TV, it increases uniformly towards the surface while core TIV projects alternate increasing and decreasing trends with a decrease at the surface. The F4 fraction exhibits an increase from the bottom to 16 cm in core TI, further above a decrease is seen till 10 cm depth followed by an increasing trend till the surface.

In the case of core TV, from the bottom to 16 cm depth, a decreasing trend is noticed while further above an increasing trend is seen. For core TIV, a uniform increasing trend is seen. Core TIV shows an increasing trend for the F5 fraction while cores TI and TV show large fluctuations along the core depth, with no definite trends. In all the three cores, the total Zn content displays similar trends to that of the F5 fraction.

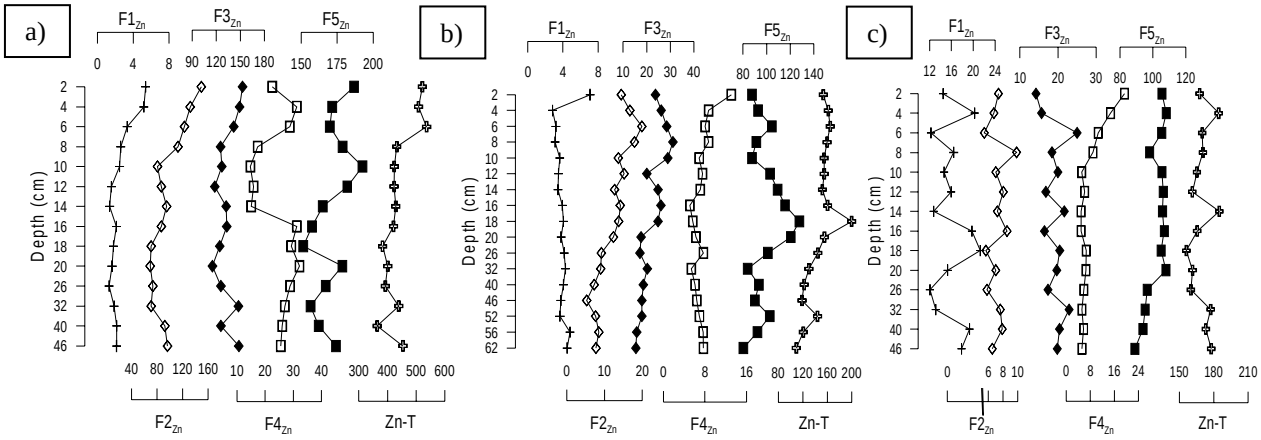

Fig. 4.6. Plots of different fractions of Zn in a) core TI b) core TV and c) core TIV

Zn distribution at all the sites show significant amounts bound to the residual fraction. In cores TI and TV similar trends in metal fractionation are observed, wherein the residual fraction is followed by Fe-Mn oxide > carbonates > organic/sulphide > exchangeable. In the case of core TIV, the residual fraction is followed by Fe-Mn oxide > exchangeable > organic/sulphide > carbonates. A considerable amount of Zn appears associated with carbonates (22 %) in core TI, which can be attributed to the relatively high stability of Zn carbonates under the pH-Eh conditions common in soils (Vaithiyanathan et al., 1993). This observation supports the role of carbonates in scavenging Zn introduced into the creek through pollution. Other authors (Carrol et al., 1998; O'Day et al., 1998; Harrington et al., 1998) have proposed that Zn occurs mainly in the reducible fraction of the non-residual sediment fractions due to its strong bonding with the Fe oxides. The association of Zn with the Fe and Mn oxides of soils and sediments has been widely recognized by Kuo et al. (1983) and Gonzalez et al. (1994), showing that the Zn adsorption onto these oxides has high stability constants. The observations indicate that the sediment is relatively unpolluted by this element.

Cr: In cores TI and TV (Fig. 4.7), the F1 and F2 fractions show decreasing trends from the bottom to the surface while in core TVI increasing trends are seen. For the F3 fraction, cores TI and TIV, exhibit decreasing trends at the bottom while increasing trends are observed towards the surface. For core TV, an increasing trend is noticed from the bottom to the surface. For the F4 fraction, increasing trends are seen for cores TI and TIV with minor fluctuations. In core TI,

the F5 fraction, in general exhibits an increasing trend with slight fluctuations while in core TV, increasing and decreasing trends are noticed from the bottom to the surface. Core TIV shows a decreasing trend from the bottom to the surface. In all the three cores, the total Cr content displays similar trends to that of the F5 fraction.

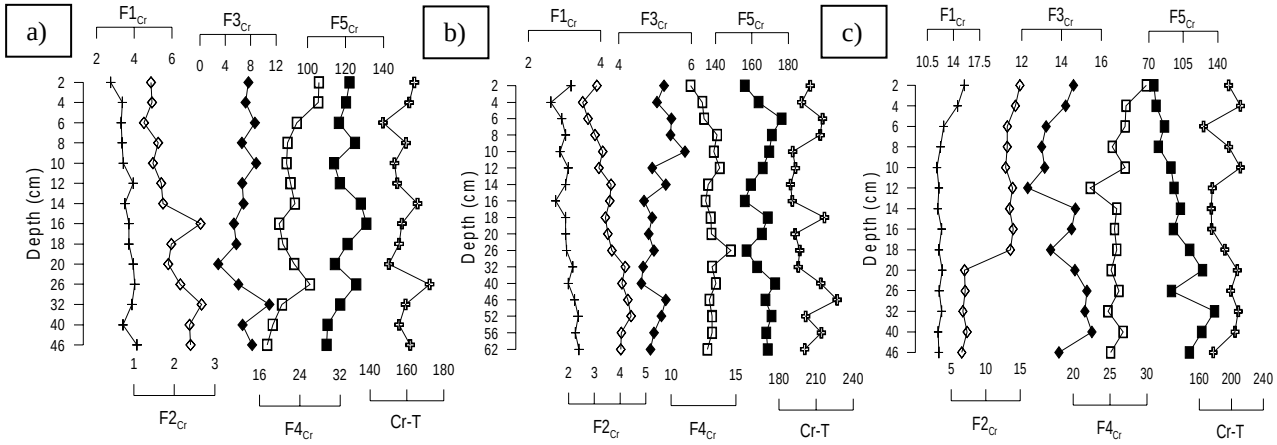

Fig. 4.7. Plots of different fractions of Cr in a) core TI b) core TV and c) core TIV

In cores TI and TIV, Cr fractionation exhibits similar trends with residual > organic/sulphide > Fe-Mn oxide > exchangeable > carbonates while in core TV, residual > organic/sulphide > Fe-Mn oxide > carbonates > exchangeable pattern is seen. Under oxic and suboxic conditions Cr typically sorbs to Fe, and especially Mn, oxides (Davison, 1993; Guo et al., 1997; Achterberg et al., 1997). Under anoxic conditions, reduced Cr is not readily incorporated into sulphides (Huerta-Diaz et al., 1998), but instead tends to associate with organic matter (Otero and Macias, 2002). Also Guo et al. (1997) reported that under reducing conditions, the behaviour of Cr is controlled primarily by insoluble large molecular humic materials. The observations indicate that most of the Cr in the sediment occurs in highly resistant minerals and therefore is unlikely to be released to pore-waters through dissociation (Yuan et al., 2004). We can conclude that the high percentage of Cr in residual and organic/sulphide fractions may indicate that the sediment is relatively unpolluted by this element.

Table 4.1. Range of metals for different fractions in the cores from the Thane creek region

Station	Fraction	Fe (%)	Mn (%)	Cu (%)	Pb (%)	Co (%)	Zn (%)	Cr (%)
Near creek head (TI)	F1	0.007- 0.014	5.36-9.62	0.69-1.36	6.74-10.46	2.32-4.35	0.33-1.06	1.70-2.92
	F2	0.25-0.54	18.54-32.83	3.52-8.18	8.03-15.36	7.31-11.12	17.46-28.89	0.82-1.72
	F3	11.30-29.63	34.22-38.33	2.16-4.24	7.15-9.74	6.63-12.80	28.69-36.55	1.97-7.04
	F4	2.02-5.73	4.65-12.37	8.27-13.00	5.48-12.51	4.68-11.10	3.55-8.11	12.24-17.29
	F5	67.98-85	20.59-32.55	77-83	56.15-69	67-77	35.07-46.12	75-80
Lower middle creek region (TV)	F1	0.003-0.005	1.76-3.86	0.12-0.78	11.93-17.10	8.04-12.37	1.92-4.85	1.41-1.77
	F2	0.20-0.46	23.37-30.14	1.66-5.78	6.48-13.24	8.60-14.66	4.29-12.11	1.37-2.25

	F3	3.03-4.90	39.24-44.22	4.62-13.54	5.68-11.62	7.18-11.85	11.01-20.50	2.34-2.99
	F4	1.19-3.53	2.18-5.80	4.45-7.75	6.42-14.42	8.75-13.11	3.10-8.95	6.27-7.97
	F5	92-95	23.00-27.61	77-85	51.26-59.23	52.79-61.43	60-75	86-88
Near creek mouth (TIV)	F1	0.005-0.019	4.05-5.73	1.09-1.31	14.11-21.20	2.96-7.18	7.73-13.37	6.33-10.30
	F2	0.17-0.45	24.09-31.42	1.81-2.54	5.21-9.85	9.31-12.09	3.43-6.50	3.41-9.97
	F3	3.33-5.00	34.66-42.72	2.52-3.12	7.82-12.85	7.39-9.22	8.82-15.89	7.62-9.95
	F4	1.11-4.60	6.03-8.48	2.97-6.96	2.35-4.48	1.39-5.89	3.19-12.05	12.62-19.90
	F5	91-95	19.34-26.35	87-91	56.33-67.78	66.44-76	63.75-70	50.12-69.89

Core TI, sampled near the creek head, showed higher concentration of most of the metals in the first three fractions as compared to the other cores. The sediment speciation results in all the cores display similar spatial distributions of each metal. Mn appears to have the greatest amount of variability among the fractions. Profiles of the different fractions of Cu and also Mn in core TV are similar and show significant positive correlations between the different fractions. This could be indicative of an equilibrated distribution of the high concentrations measured between the different sediment fractions. The order of abundance of metals in the different fractions of the creek sediment is as follows,

Exchangeable: Pb > Mn > Co > Cr > Cu > Zn > Fe in core TI, Pb > Co > Mn > Zn > Cr > Cu > Fe in core TV and Pb > Zn > Cr > Co > Mn > Cu > Fe in core TIV. The higher amounts of Pb in the exchangeable fraction of all the three cores confirm the anthropogenic source of this element.

Carbonate bound: Mn > Zn > Pb > Co > Cu > Cr > Fe in core TI, Mn > Co > Pb > Zn > Cu > Cr > Fe in core TV and Mn > Co > Pb > Cr > Zn > Cu > Fe in core TIV

Fe-Mn oxides bound: Mn > Zn > Fe > Co > Pb > Cr > Cu in core TI, Mn > Zn > Co > Cu > Pb > Fe > Cr in core TV and Mn > Zn > Pb > Cr > Co > Fe > Cu in core TIV.

Organic/sulphide bound: Cr > Cu > Pb > Co > Mn > Zn > Fe in core TI, Pb > Co > Cr > Cu > Zn > Mn > Fe in core TV and Cr > Mn > Zn > Cu > Co > Pb > Fe in core TIV.

Residual: Cu > Cr > Fe > Co > Pb > Zn > Mn in core TI, Fe > Cr > Cu > Zn > Co > Pb > Mn in core TV and Fe > Cu > Co > Zn > Pb > Cr > Mn in core TIV. Cu and Fe are mainly present in the crystalline structures of the residual fraction, a distribution which is generally considered to limit availability for uptake (Dicks and Allen, 1983).

4.3. Ulhas estuary

Speciation analyses were carried out in three mudflat cores of the estuarine region, i.e. near the estuary mouth (UI), the lower estuary (UV) and the upper estuary (UIV). The metal range obtained for the different fractions is given in Table 4.2. The partitioning patterns of heavy metals in the sediment cores from the sequential extraction results are shown in Figures 4.8-4.14.

Fe: From the vertical distribution profile (Fig. 4.8), in cores UI and UIV, the F1 fractions show a constant trend, except for core UI, which shows an increase towards the surface. Core UV fluctuates along the entire length of the core. The F2 fraction, for cores UI and UV, decrease from the bottom to the surface while for core UIV, it maintains a uniform trend except for an increment seen from 26 to 18 cm depth. In core UI, the F3 fraction decreases from the bottom to the surface while in core UIV an increase is seen. For core UV, a constant trend is noticed, except for a slight increase at the surface. The F4 fraction, in core UI, shows minor fluctuations while in core UV an increasing trend is seen from the bottom to 12 cm, followed by a decreasing trend till the surface. In core UIV, in general, an increasing trend is observed from the bottom to the surface. However, between the depths of 32 and 16 cm, a decrease is seen. For the F5 fraction, all the cores exhibit increasing and decreasing trends throughout the length of the core. In all the three cores, the total Fe content display similar trends to that of the F5 fractions.

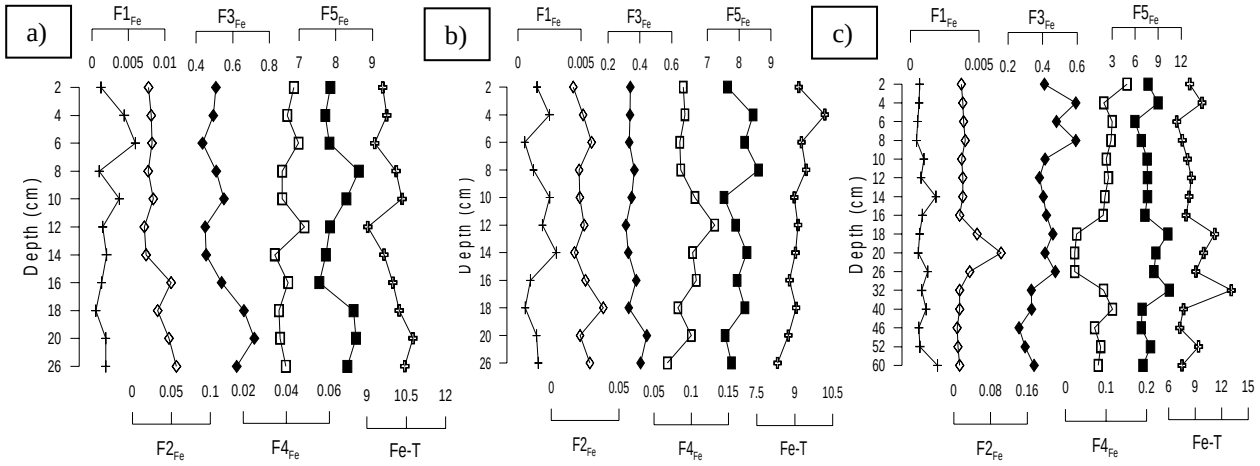

Fig. 4.8. Plots of different fractions of Fe in a) core UI b) core UV and c) core UIV

In all the three cores, Fe association with different fractions follows the order: residual > Fe-Mn oxide > organic/sulphide > carbonates > exchangeable. Fe is mainly found in the silicate lattice fraction which can be explained by its participation in alumino-silicates. The amounts in the other fractions, except the one associated with oxides, are negligible. The exchangeable and carbonate fractions are found to be minor contributors for Fe. No relevant differences can be established based on the sampling locations. High percentages of Fe in the Fe-Mn oxides fraction imply presence of significant amount of Fe in poorly crystalline hydroxides. This can be explained by the precipitation effect of the Fe-Mn oxy-hydroxides in water. Under strong oxidizing condition and neutral pH value, Fe^{2+} can be transformed to Fe^{3+} rapidly and precipitated as Fe-oxy-hydroxide (Stum and Morgan, 1996; Pizzarro et al., 2003).

Mn: For core UI, the F1 fraction maintains a uniform trend except for a decreased peak at 12 cm depth (Fig. 4.9). In core UV, it decreases from the bottom to 18 cm followed by alternate increasing and decreasing trends till the surface. On the other hand, in core UIV, it uniformly increases from the bottom to the surface. The F2 fraction, for cores UI and UV, display decreasing trends from the bottom to the surface while in core UIV, it shows a constant trend with a decreased peak at 16 cm depth. The F3 fraction, in core UI, shows a decreasing trend from the bottom to 6 cm followed by an increase towards the surface while, in core UV and core UIV, a uniform trend is seen except for slight fluctuations in the deeper portions of the cores. In the case of F4 fraction, in core UI, large fluctuations are seen with overall decreasing trend from the bottom to the surface while for core UV, an increasing trend is seen from the bottom to the surface. In core UIV, a decreasing trend is seen from the bottom to 20 cm followed by an increasing trend till the surface, with large fluctuations. For the F5 fraction, core UI and UIV exhibit decreasing trends from the bottom to the surface, with core UIV exhibiting large variations especially in the lower portion of the core. In core UV, a uniform increasing trend is seen from the bottom to 4 cm with a decrease at the surface. In all the three cores, the total Mn content displays similar trends to that of the F5 fractions.

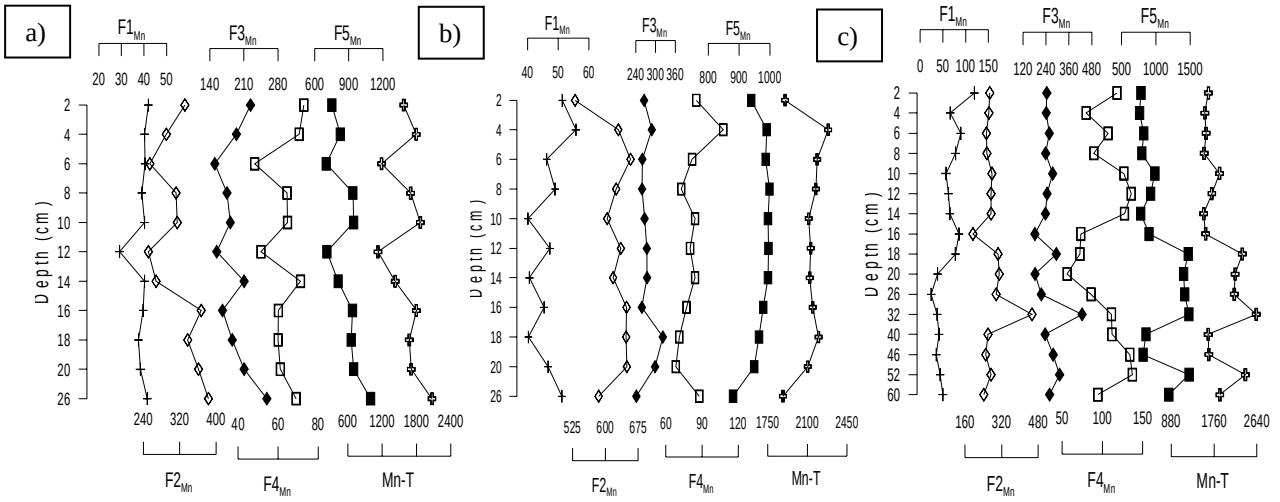

Fig. 4.9. Plots of different fractions of Mn in a) core UI b) core UV and c) core UIV

In all the three cores, the observed trends in metal fractionation are residual > carbonates > Fe-Mn oxide > organic/sulphide > exchangeable. The higher level of Mn in carbonate fraction is most likely due to the similarity in ionic radii to that of Ca, which allows them to substitute for Ca in the carbonate phase (Pedersen and Price, 1982; Zhang et al., 1988). Mn is abundant in the Earth's crust; the radius of Mn^{2+} (0.91) is similar to that of Ca^{2+} (1.08) and Mg^{2+} (0.8), so the replacement of Ca^{2+} and Mg^{2+} by Mn is easier (Liu et al., 2005). Other studies also reported that Mn was mainly in carbonates (Wartel et al., 1991; Boughriet et al., 1994).

Cu: For cores UI, UV and UIV (Fig. 4.10.), the F1 fractions show decreasing trends from the bottom to the surface. However, in core UIV, large fluctuations are observed between the depths of 32 and 16 cm. The F2 fraction for core UI displays a decreasing trend while, in core UV and UIV, increasing trends are seen from the bottom to the surface. The F3 fraction for cores UI and UV, project decreasing trends from the bottom to the surface while in core UIV, it maintains a uniform trend. The F4 fraction for cores UI and UIV exhibits increasing trends from the bottom to the surface while, for core UV, it maintains a uniform trend. The F5 fraction, in core UI, shows an increasing trend from the bottom to 12 cm followed by a decreasing trend till the surface while, for core UV, a decreasing trend is seen from 18 to 10 cm followed by an increasing trend till the surface. Core UIV maintains a uniform trend, except between depths of 20 and 12 cm, where large increases in values are seen. In all the three cores, the total Cu content displays similar trends to that of the F5 fraction.

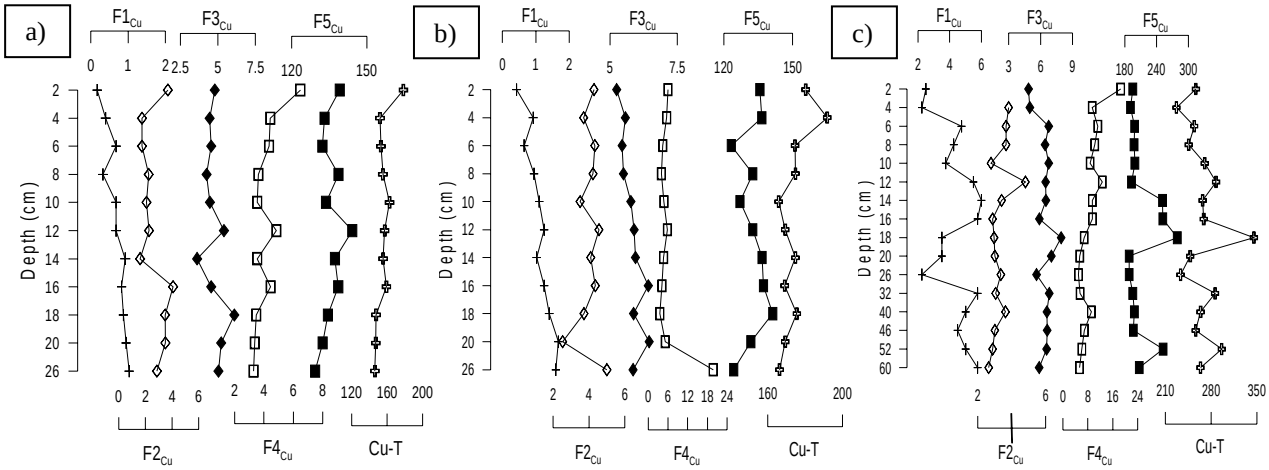

Fig. 4.10. Plots of different fractions of Cu in a) core UI b) core UV and c) core UIV

In core UI, the trend in metal fractionation is residual > Fe-Mn oxide > organic/sulphide > carbonates > exchangeable, in core UV it is residual > organic/sulphide > Fe-Mn oxide > carbonates > exchangeable while in core UIV it is residual > organic/sulphide > Fe-Mn oxide > exchangeable > carbonates. In this study, 88-92 % of total Cu is found in the residual fraction, indicating that it is mainly of lithogenic origin. This coincides with the results of researches carried out in the Pearl River Estuary and East China Sea (Liu et al., 2003b; Yuan et al., 2004), wherein higher amounts of Cu were present in the residual fraction. In cores UV and UIV, appreciable amounts of Cu are present in the organic fraction. Cu can easily form complexes with organic matter due to the high stability constant of the organic-Cu complex (Kotoky et al., 2003). Many studies have also reported high concentrations of Cu associated with the organic matter in the sediment (Jones, 1987; Fernandes, 1997; Zhou et al., 1998; Dollar et al., 2001). Organic matter exhibits a high degree of selectivity for divalent ions and hence the organic bound Cu fraction is an important fraction in the sediments and is not available to the biological

activity (Mcbride, 1994). The Cu in the F4 fraction decreased with increasing depths in cores UI and UIV. This may be due to decrease in the organic matter contents of the cores with depth (Abollino et al., 2002).

Pb: In core UI (Fig. 4.11), the F1 fraction decreases while, in core UIV, it increases from the bottom to the surface. In core UV, a decrease is seen from the bottom to 14 cm while above it an increasing trend is seen. In the case of the F2 fraction, core UI exhibits a decreasing trend while core UV displays increasing trend from the bottom to the surface. Core UIV exhibits an increase upto 18 cm followed by a decrease towards the surface. The F3 fraction in core UI decreases from the bottom to the surface while in cores UV and UIV it maintains a constant trend except for an increased peak at 18 cm for core UIV. The F4 fraction for core UI decreases with fluctuations while for core UIV an increasing trend is seen from the bottom to the surface. Core UV, on the other hand, maintains a uniform trend with an increased peak at 14 cm depth. For the F5 fraction for core UI not many variations are seen with depth. Core UV exhibits increasing and decreasing trends while in the case of core UIV an increasing trend is observed with large fluctuations towards the upper portion of the core. In all the cores, the total Pb content displays similar trends to that of the F5 fraction.

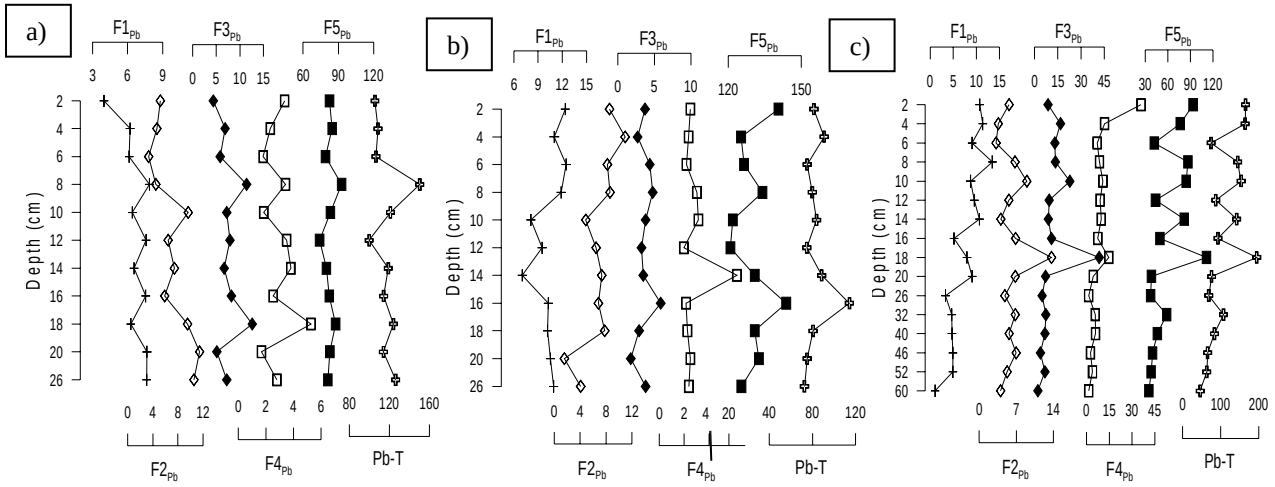

Fig. 4.11. Plots of different fractions of Pb in a) core UI b) core UV and c) core UIV

In core UI, the proportion of Pb fractions follow the order, residual > Fe-Mn oxide > carbonates > exchangeable > organic/sulphide while in core UV, the trend is residual > exchangeable > carbonates > organic/sulphide > Fe-Mn oxide. For core UIV, the order is residual > Fe-Mn oxide > organic/sulphide > exchangeable > carbonates. The concentrations of Pb associated with Fe-Mn oxides, residual and organic fractions in core UIV are markedly higher in the top 15 cm of the core than those in the deeper layers. Most of Pb is present in the Fe-Mn oxide fraction in cores UI and UIV which is in agreement with other studies (Jones and Turki, 1997; Ramos et al., 1994) indicating that Pb can form stable complexes with Fe and Mn oxides. The accumulation of

anthropogenic Pb in the oxide fraction is in accordance with earlier findings which showed that Fe and Mn hydrous oxides are important scavengers of Pb in soils/sediments and play an important role in controlling its mobility in the environment (Burt et al., 2003; Kaasalainen and Yli-Halla, 2003; Singh et al., 2005; Davidson et al., 2006; Cuong and Obbard, 2006). It should also be noted that oxide association does not guarantee the immobilization of contaminant elements in the subsurface, so metals associated with Fe and Mn oxides are still labile and may be released upon decomposition of the oxides under reduced conditions, consequently having a significant impact on soil quality and biota (Chlopecka, 1996). In all the cores, large amounts of Pb are present in the exchangeable form indicating that Pb in these samples is more in bio-available fractions. Similar results were reported by Hung et al. (1993), Fernandes (1997), Zhou et al. (1998) and Li et al. (2000), who mentioned that such chemical partitioning pattern of Pb confirms the anthropogenic sources of Pb in the sediment and can also affect the solubility and mobility of Pb from the sediments. Therefore, Pb in the sediments at this site might have high mobility and availability.

Co: From the vertical depth profile (Fig. 4.12), in core UI, the F1 fraction displays a constant trend from the bottom to 14 cm followed by a sharp decreased peak at 14 cm depth. Further above, an increasing trend is seen till 8 cm followed by a decrease till the surface. In core UV, the F1 fraction increases from the bottom to 10 cm and then decreases towards the surface while in core UIV, an increasing trend is seen from the bottom to the surface with minor fluctuations. The F2 fraction for core UI decreases gradually from the bottom to the surface while in core UIV, an increasing trend is observed with an increased peak at 20 cm depth. After some fluctuations at the bottom, core UV maintains a uniform trend till the surface. In core UI, the F3 fraction decreases from the bottom to the surface while in cores UV and UIV, increasing and decreasing trends are observed with larger fluctuations in core UIV as compared to core UV. The F4 fractions, in cores UI and UV, display increasing trends from the bottom to the surface, while in core UIV it shows large variations with overall increasing trend. In all the three cores, the F5 fraction exhibit decreasing trends from the bottom to the surface with some fluctuations. In cores UI and UIV, the total Co content displays similar trends to that of the F5 fraction.

The metal fractionation trend in core UI is residual > Fe-Mn oxide > carbonates > organic > exchangeable, in core UV the trend is residual > Fe-Mn oxide > organic > carbonates > exchangeable while in core UIV it is residual > Fe-Mn oxide > organic > exchangeable > carbonates. Fe-Mn oxide phase is found to be significant contributor of Co. Similar observations were made by Calmano and Forstner (1983) and Jones and Turki (1997). The high Co in the

residual and Fe-Mn oxide fractions may indicate that Co in the sediments is less mobile than the other elements studied.

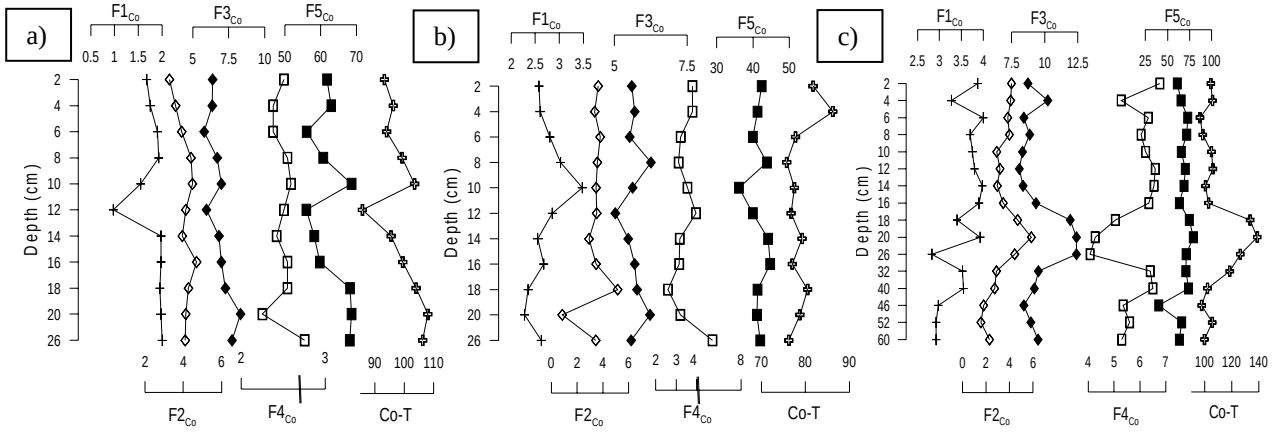

Fig. 4.12. Plots of different fractions of Co in a) core UI b) core UV and c) core UIV

Zn: The F1 and F2 fractions in cores UV and UIV (Fig. 4.13), display increasing trends from the bottom to the surface while in core UI, both the fractions show decreasing trends. In the case of cores UV and UIV, the F3 fractions exhibit decreasing trends in the lower portions while increasing trends are seen for the upper portions of the cores. All the three cores display increasing trends from the bottom to the surface with minor fluctuations for the F4 fractions. The F5 fraction, for core UI, increases from the bottom to 18 cm and further above a decrease is seen. On the other hand for core UV, a decreasing trend is noticed from the bottom to 6 cm followed by large fluctuations at the surface. In core UIV, an increasing trend from the bottom to the surface is observed. In all the three cores, the total Zn content displays similar trends to the F5 fraction.

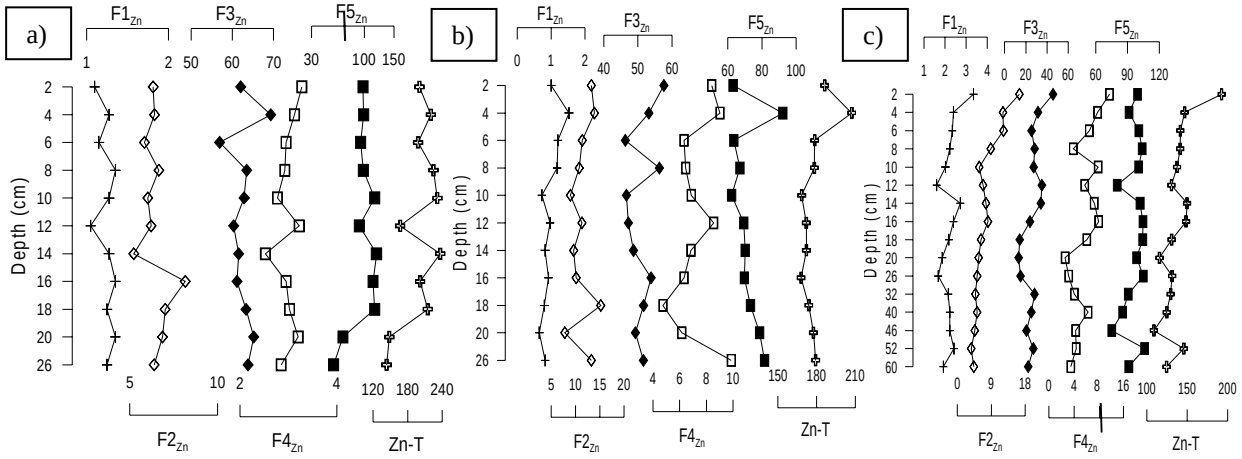

Fig. 4.13. Plots of different fractions of Zn in a) core UI b) core UV and c) core UIV

In all the three cores, the metal fractionation trends are residual > Fe-Mn oxide > carbonates > organic > exchangeable. The low percentage of Zn in the F1 fractions are due to the fact that Zn can be easily absorbed and utilized by organisms in the aquatic environment (Campbell, 1995).

The residual fraction made the most important contribution to the Zn concentration followed by the Fe-Mn and carbonate fractions. Rubio et al. (2001) suggested that Zn is fixed mainly to the oxy-hydroxides during deposition. The high percentage of Zn in Fe-Mn oxides/hydroxides confirmed the known ability of this phase to scavenge Zn from aqueous phase (Isuare et al., 2005). The results of this study are in agreement with previous works (Skvaria, 1998; Broughiet et al., 2007). Zn amounts associated with organic matter and/or sulphides are low (1.83-5.06 %) which can be explained, not only by the relatively weak bond of Zn with the organic matter, but by the tendency of this metal to form sulphides, depending on the redox potential of the soil. Chester et al. (1985) found that higher percentages of Zn were associated with carbonates in polluted surficial stream sediments compared with cleaner samples. In the case of core UI, in the upper few centimeters of the core, Zn in carbonate fraction is found to be higher than the Fe-Mn oxide fraction. Calcium carbonate forms complexes with Zn as a double salt ($CaCO_3 \cdot ZnCO_3$) in the sediment (Li et al., 2000b). Post-depositional processes may have influenced the observed distribution of Zn, since it has been suggested that Zn which is mobilized during the dissolution of Fe and Mn oxides, may be repartitioned to carbonates (Zwolsman et al., 1993).

Cr: The F1 fractions, in cores UI and UIV (Fig. 4.14), show increasing trends from the bottom to the surface while in core UV, a constant trend is seen. The F2 fractions, in cores UI and UV, decreases from the bottom to the surface while in core UIV, an increasing trend is seen except for a decreased peak at 18 cm depth. In the case of the F3 fractions, in cores UI and UV, decreasing trends are seen while in core UIV large fluctuations are observed especially at the bottom. Core UI displays an increasing trend, for the F4 fraction, from the bottom to 8 cm while above it a decreasing trend is seen till the surface. On the other hand, core UV, projects an increasing trend from the bottom to the surface. For core UIV, from the bottom to 18 cm a fluctuating decreasing trend is seen while above it, an increasing trend is noticed. For the F5 fraction, cores UI and UV, exhibit decreasing trends in the lower portions while increasing trends are observed in the upper portions of the cores. Core UIV maintains a constant trend along the core length except for an increment from 32 to 16 cm depth. In cores UI and UIV and to some extent in core UV, the total Cr content displays similar trends with the F5 fractions.

The speciation of Cr in the sediments is in the order of residual > exchangeable > Fe-Mn oxide > carbonates > organic in core UI, and residual > organic > Fe-Mn oxide > exchangeable > carbonates in cores UV and UIV. High amounts in the residual fraction indicate that most of the Cr in the sediments occurs in highly resistant minerals and therefore is unlikely to be released to pore-waters through dissociation (Yuan et al., 2004). $CaCO_3$ in the carbonate phase is not a

significant contributing factor to the heavy metal content of sediments (Paropkari et al., 1980). Significant percentage contribution of Cr in the F4 fraction has been reported in the literature (Iwegbue et al., 2007; Belzunce-Segarra et al., 2008).

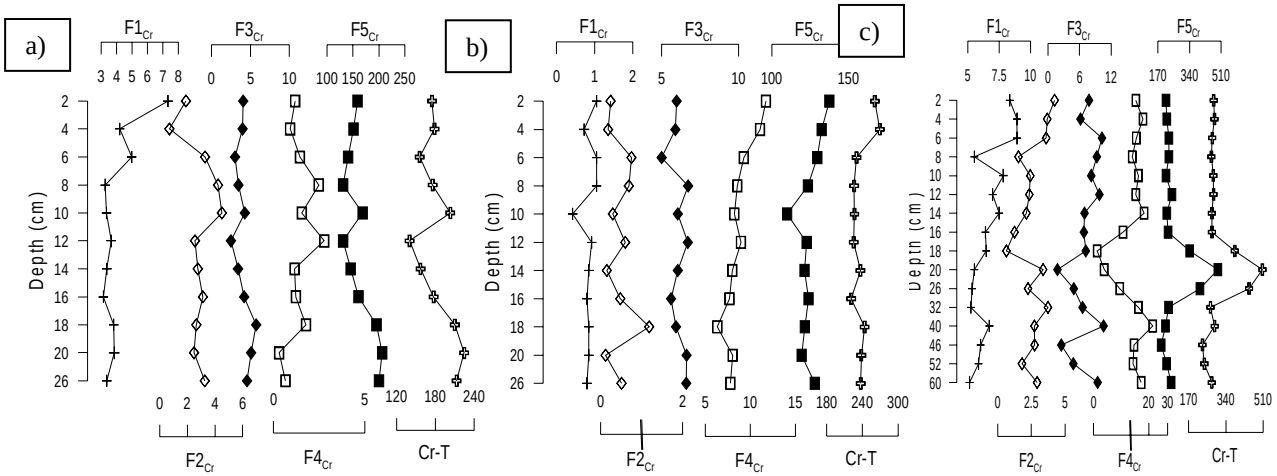

Fig. 4.14. Plots of different fractions of Cr in a) core UI b) core UV and c) core UIV

Table 4.2. Range of metals for different fractions in cores from the estuarine region

Station	Fraction	Fe (%)	Mn (%)	Cu (%)	Pb (%)	Co (%)	Zn (%)	Cr (%)
Near estaury mouth (UI)	F1	0.01-0.07	2.25-3.38	0.11-0.72	4-7.61	1.41-2.72	0.64-1.08	1.59-4.23
	F2	0.18-0.63	19.18-23.46	1.09-2.67	3.48-10.55	4.34-6.21	2.73-5.50	0.44-2.93
	F3	5.21-7.67	10.62-15.72	2.47-4.11	4.41-10.41	8.26-9.77	32.17-54.57	1.73-2.75
	F4	0.40-0.58	3.74-5.13	2.32-4.20	1.54-4.35	2.52-3.32	1.32-2.57	0.14-1.94
	F5	91.41-93.87	52.88-61.31	90.20-93.40	72.20-82.98	78.90-81.94	36.48-63.11	90.70-94.64
Lower middle estuarine region (UV)	F1	0.01-0.04	1.97-2.77	0.28-1.14	4.16-8.12	4.12-6.65	0.46-0.93	0.34-0.75
	F2	0.20-0.45	28.35-32.35	1.71-3.19	1.06-7.18	1.59-9.02	5.48-10.42	0.07-1.16
	F3	3.73-5.45	12.80-15.75	3.46-4.37	1.19-3.48	0.09-11.61	31.31-40.17	3.43-4.91
	F4	0.82-1.57	3.39-5.19	2.26-12.60	1.27-12.38	4.56-12.49	3.26-6.29	4.65-7.49
	F5	93.04-94.88	47.17-50.16	79.44-90.68	77.10-89	68.49-76.59	44.03-55.18	87.79-89.54
Upper middle estuarine region (UIV)	F1	0.01-0.03	1.22-7.81	1.07-2.66	2.40-13.84	2.97-5.09	1.24-2.08	1.10-3.52
	F2	0.10-1.12	12.16-18.74	0.98-2.58	3-12.02	1.86-5.56	2.56-9.18	0.18-1.71
	F3	3.07-7.87	9.18-18.36	2.13-3.38	4.85-22.07	8.78-14.40	10.71-27.13	0.36-4.18
	F4	0.24-1.84	2.83-8.87	2.24-8.22	2.67-23.28	4.05-9.15	2.11-8.16	0.11-8.72
	F5	90.30-95.94	51-70.47	86.40-92.94	56.58-80.07	68.29-77.56	55.43-80.85	83.36-97.63

The upstream region (core UIV) of Ulhas estuary, representing the combined effect of the lithology, land use patterns and soil conditions, show higher values of metals in the F1, F2 and F3 fractions as compared to the downstream regions of the estuary. This observation suggests that supply of metals in the estuarine system via the sediment dissolution and soil erosion has been a significant factor which has been increasing in recent times. Also, from the bottom to the surface, the metal concentration is found to increase, except for upper few layers of some of the cores. This may be due to the post diagenetic disturbances taking place in this region like dredging, resuspension etc.

The occurrence of metals in the different sediment fractions are in the following order:
Exchangeable: Pb > Mn > Cr > Co > Zn > Cu > Fe for core UI, Pb > Co > Mn > Cu> Zn > Cr > Fe for core UV and Pb > Co > Mn > Cr > Cu > Zn > Fe for core UIV.
Carbonate bound: Mn > Pb > Co > Zn > Cu > Cr > Fe for core UI, Mn > Zn > Co > Pb > Cu> Cr > Fe for core UV and Mn > Pb > Zn > Co > Cu > Cr > Fe for core UIV.
Fe-Mn oxides bound: Zn > Mn > Co > Pb > Fe > Cu > Cr for core UI, Zn > Mn > Co > Cr > Fe > Cu > Pb for core UV and Zn > Mn > Pb > Co > Fe > Cu > Cr for core UIV.
Organic/sulphide bound: Mn > Co > Cu > Pb > Zn > Cr > Fe for core UI, Co > Cr > Zn > Mn > Cu > Pb > Fe for core UV and Pb > Co > Mn > Cr > Zn > Cu > Fe for core UIV.
Residual: Fe > Cr > Cu > Co > Pb > Mn > Zn for core UI, Fe > Cu > Cr > Pb > Co > Zn > Mn for core UV and Fe > Cu > Cr > Co > Zn > Pb > Mn for core UIV.

4.4. Speciation - Thane vs. Ulhas region

Comparison of the pattern of metal speciation between the two study sites indicate the importance of partitioning the total metal content into bio-available and residual fractions, in order to identify areas of anthropogenic contamination.

Different phases behave differently in the sedimentary diagenetic environment, and thus have different potentials for re-mobilization and for uptake by biota. It is evident from the results that major portions of the metals studied are bound in different forms with different strengths. Among the metals analysed in the three cores of Thane creek, the element which showed the highest average percentage in the F1 phase is Pb in cores TI (8.66 %), TV (14.47 %) and TIV (18.21 %). In the Ulhas estuary also higher amounts of Pb are seen in the F1 fractions, i.e. for core UIV (8.12 %), core UV (6.71 %) and core UI (6.27 %). The exchangeable fraction corresponds to the metal species that are most easily available for plant uptake, which can be released by merely changing the ionic strength of the medium (Norvell, 1984). The F2 fraction is highest for Mn in core TI (25.19 %), core TV (26.33 %), core TIV (26.96 %) and also in cores UI (21.33 %), UV (31.14 %) and UIV (16.03 %). The carbonate-bound sediment fraction is affected less by environmental changes, such as microbial sediment activity. The metal content bound to carbonates is sensitive to pH changes and this can become mobilized when the pH is low. The enrichment of some elements in the F1 and F2 fractions may be a result of recent anthropogenic inputs. At the same time, reductive dissolution of Fe-Mn oxides may also lead to increasing concentrations in the two fractions (Yuan et al., 2004). Higher percentages of Pb and Mn in the exchangeable and carbonate fractions indicate that the metals in the creek and estuarine sediments are potentially more available for exchange and/or release into the

environment. Singh et al. (2005) and Jain (2004) suggested that a large part of the metals introduced by human activities are present in the exchangeable fraction and the fraction dissolved with acetic acid (carbonates). With regards to the reducible Fe-Mn associated phase (F3), core TI (36.30 %), core TV (41.85 %) and core TIV (38.10 %) show highest amounts of Mn while cores UI (38.31 %), UV (35.98 %) and UIV (18.75 %) exhibit greater amounts of Zn. The Fe-Mn oxides fraction includes the metal oxides/ hydroxides soluble under slightly acidic pH, as well as the metals associated with reducible amorphous Fe-Mn oxy-hydroxides (Velimirovic et al., 2011). In the organic fraction (F4), the highest percentage is seen for Cr in cores TI (14.46 %) and TIV (15.98 %) while core TV exhibits presence of Pb (10.42 %). In the Ulhas estuary, higher values of Mn (4.29 %) in core UI, Co (6.55 %) in core UV and Pb (8.37 %) in core UIV are observed. Calmano et al. (1993) reported a rather high proportion of metals strongly bound to the organic/sulphide fraction. Organic fraction may be associated with various forms of organic material such as living organisms, detritus, or coatings on mineral particles through complexation or bioaccumulation processes. This form of metals can exist in sediment for longer periods and can also be released with organic matter decomposition (Velimirovic et al., 2011). Metals bound to the easily reducible phase (Fe/Mn oxides) and to organic matter/sulphides may be better held by a scavenging effect, i.e., this fraction acts as a sink of metals.

In the creek region, Cu (80.05 %) in core TI and Fe in core TV (93.59 %) and core TIV (93.12 %) display highest percentage in the residual fraction while in the estuary, higher amounts of Fe are present in the residual fraction in all the three cores studied. Metals associated with residual fractions, usually form part of the crystalline structure of minerals, remain relatively stable and inert, and are not easily released into the mobile and bio-available phases (Tessier et al., 1979; López-Gonzáles et al., 2006; Wong et al., 2007). In both the regions, therefore, trace metals associated with the residual fraction, suggests that their concentrations are controlled significantly by transport processes with fine particles as carriers. The heavy metals bound to the residual fraction (F5) contain mainly primary and secondary minerals, which may hold metals within their crystal structure and so the residual fraction (F5) is identified as a stable fraction (Fuentes et al., 2008). These metals are not expected to be released in solution over a reasonable time span under the conditions normally encountered in nature (Lasheen and Ammar, 2009).

When the depth-wise distribution trends of the metals in the different fractions are observed, the concentration of metals in fractions 1 and 2 are found to be higher in the upper portions of the core as compared to the lower portions, for some of the elements at the two sampling sites (Zn in

core TI; Mn, Cu and Co in core TV; Co and Cr in core TIV; Zn and Cr in core UIV). The sub-surface enrichment may be due to the contamination deposited from the surface waters, which indicates enrichment leading to pollution in recent years. This is because the pollutants are always absorbed by surface sediment first, and then sinks into deeper positions by chemical exchange (Nemati et al., 2011). When the results are analysed for the other fractions for both the study sites, it is seen that for most of the cores, for example, Fe in core TV, Co in cores TI and TIV, F3 content decreases while F4 content increase with depth. This could be caused by the dissolution of oxy-hydroxides under reduced conditions generated by tidal inundation. When dissolution happens, adsorbed and co-precipitated ions of these compounds are liberated to interstitial water and could become part of another sedimentary phases (sulphides, carbonates) or be liberated to the solution. In marine environments under anoxic conditions, sulphide anions (generated by sulphate reduction) are likely to be present. Liberated ions can react with these sulphide anions and form the corresponding metal sulphide, the majority of these compounds are insoluble. So, it is probable that a metallic transfer from fraction F3 to fraction F4 takes place. The opposite process could also occur in two different ways. First, the oxygenation of anoxic sediments may occur, during which sulphides will be oxidized to sulphates and accompanying ions will be liberated. These ions could be attracted by Fe-Mn oxy-hydroxides, neo-formed or present in the sediment in upper levels. Second, in oxic sediments the liberated metal ions, released due to organic matter decomposition, would be captured by oxy-hydroxides among other possible ligands (Alvarez-Iglesias et al., 2003). This could be the case for Mn in cores TV and TIV, Cu in core TV, Pb in core TI and Cr in core UV where F4 content decreases with increase in depth, whereas F3 content increases. Therefore, an opposite trend could be expected between sedimentary fractions F3 and F4 for the metals studied. On the other hand, both fractions (F3 and F4) of Fe for cores TV, TIV and core UI, and Cu in core UV simultaneously increase in their contribution with depth. This can be explained as in the marine environment most of the metal may precipitate as sulphide in organic matter rich sediments and get adsorbed and concentrated in oxy-hydroxides (Marcet-Miramontes et al., 1997). The residual fraction (F5) is found to show an increasing trend with increasing depth for most of the elements at both the studied sites. This implies that the elements are not readily available for mobilization in the deeper sections of the core.

The spatio-temporal metal variation results show that at both the sites, the residual fraction is found to be predominant and the contribution of the other four fractions to the total metal concentration is only minimal except for Mn. The relative content of a metal in the residual phase can be used as a measure of the contribution of natural sources, and also of the degree of

contamination, with a higher percentage of residual phase indicative of lower levels of pollution (Singh et al., 2005). In Thane creek and Ulhas estuary, the contents of Fe are generally over 90 % in the residual fraction. Since the concentration of Fe in the mobile fraction is found to be very low, it may be concluded that the sediments are not polluted with regard to this metal at both the sites. The heavy metal distributions in the non-residual phases (F1+F2+F3+F4) varied with the element analyzed and with the sampling site.

Considering the percentage of metals extracted in the most labile fractions (F1+F2+F3+F4), the order of mobility from most to least bio-available, in Thane creek is: Mn (75.05 %) > Zn (59.77 %) > Pb (37.05 %) > Co (29.45 %) > Fe (22.77 %) > Cr (22.60 %) > Cu (19.95 %) for core TI; Mn (74.43 %) > Pb (43.64 %) > Co (42.78 %) > Zn (31.38 %) > Cu (19.01 %) > Cr (13.01 %) > Fe (6.41 %) for core TV while in core TIV the trend seen is Mn (77.02 %) > Cr (39.40 %) > Pb (38.42 %) > Zn (33.04 %) > Co (28.18 %) > Cu (10.65 %) > Fe (6.88 %). In Ulhas estuary it is, Zn (44.84 %) > Mn (41.27 %) > Pb (22.64 %) > Co (19.37 %) > Cu (8.27 %) > Cr (7.16 %) > Fe (5.64 %) for core UI; Mn (51.32 %) > Zn (49.70 %) > Co (27.22 %) > Pb (16.02 %) > Cr (11.44 %) > Cu (11.40 %) > Fe (6.38 %) for core UV and Mn (40.73 %) > Pb (35.06 %) > Zn (29.78 %) > Co (25.03 %) > Cr (10.59 %) > Cu (9.87 %) > Fe (7.04 %) for core UIV. Mn and Zn are present in greater percentage (>50 %) in the labile fractions in the samples collected near the creek mouth (TI) as compared to the other two regions (TV and TIV) wherein only Mn is present in higher amounts in the labile fractions. In core TI and to some extent in core TIV, Zn concentrations are significantly higher than Pb concentrations in the bio-available fractions (Table 4.3), especially in the upper portions of the cores. Several authors have reported (Karczewska, 1996; Wilson and Pyatt, 2007) the relatively high mobility of Zn in the soil environment, which makes it considerably more mobile than Pb. According to McLean and Bledsoe (1992), Zn gets readily adsorbed on clay minerals, carbonates or hydrous oxides and is present in the exchangeable form. Perez-Cid et al. (1996) stated that Zn is the most labile metal because of its stronger affinity to non-residual fractions. The results also agree with the findings reported by other authors for industrialized areas (Chlopecka, 1996; Guevara-Riba et al., 2004; Davidson et al., 2006). Core TI being closer to the industrialised areas is more prone to contaminant input.

In the case of the estuarine region, only core UV shows higher amounts of Mn (>50 %) as compared to the other two cores. In general, Mn is found to be the most bio-available element while Fe is observed to be the least bio-available element in the creek and the estuarine regions. However, significant fractions of Cu, Pb and Zn in the Thane creek sediments sampled near the

head region (TI), and Pb in all the cores of the Ulhas estuary which supports input from most of the human population and industrial activities, are present in labile forms, so a potential pollution risk may exist. In general, the average concentrations of non-residual fractions of almost all the metals in sediments are greater in the Thane creek (12.02 % for Fe; 75 % for Mn; 16.54 % for Cu; 39.70 % for Pb; 33.47 % for Co and 25 % for Cr) than in the Ulhas estuary (6.35 % for Fe; 44.44 % for Mn; 9.84 % for Cu; 24.57 % for Pb; 23.87 % for Co and 9.73 % for Cr). Therefore, these results indicate that heavy metals in sediments from the creek are potentially more available for exchange and/or release into the marine environment relative to those from the estuary.

4.5. Correlation factor

Mn, Fe, and organic matter (OM) have been identified as the three most important sediment components for metal partitioning (Murray, 1987; Shea, 1988). A number of studies have demonstrated that OM, Fe and Mn oxides/hydroxide content in sediments are important not only in controlling the binding of metals to sediments but also in the bioavailability and toxicity of metals (Ford et al., 1997; Muller et al., 2002). Different metals bind with Fe, Mn and OM through adsorption, co-precipitation and complexation in sediment-water interface. The metal fraction bound to reducible (Fe oxides and hydroxides) and oxidized (organic) fraction can be mobilized when environmental conditions become increasingly reducing or oxidizing (Bryan and Langston, 1992). Also metals bound to sediment fractions have a potential for remobilisation due to microbial activity (Jones and Turki, 1997). The reducing micro-organisms in sediment are able to reduce insoluble Fe (III) oxides to soluble Fe (II) oxides and thereby releasing metals associated with the oxide phase, whereas oxidizing micro-organisms in sediments might oxidize the organic sediment constituent and expel the metals associated with the organic fraction. In order to evaluate the OM and Fe-Mn on the metal distributions in the sediments, correlation factor at $p < 0.05$ was investigated.

4.5.1. Role of OM in distribution of metal fractions

Relations between organic matter and metal species are investigated in both the studied sites.

Thane creek

In core TI, TOC and TN show good correlations with F1 (r=0.57, 0.43) and F5 (r=0.51, 0.53) fractions of Fe; F5 (r=0.51, 0.43) fraction of Pb; F1 (r=0.51, 0.82), F2 (r=0.41, 0.73) and F3 (r=0.67, 0.61) fractions of Zn. The remaining elements do not exhibit good correlations. In core TV, TOC and TN display significant associations with F1 (r=0.50, 0.64) and F4 (r=0.53, 0.65)

fractions of Mn; F2 fractions of Cu (r=0.48, 0.87), Pb (r=0.41, 0.81) and Zn (r=0.47, 0.75); F2 (r=0.66, 0.35) and F3 (r=0.57, 0.53) fractions of Co. In core TIV, TOC and TN exhibit good correlations with F3 (r=0.57, 0.64) fraction of Cu; F2 (r=0.68, 0.58) fraction of Co, F4 (r=0.50, 0.42) fraction of Zn; F1 (r=0.47, 0.40) and F4 (r=0.45, 0.31) fractions of Cr.

The other correlations observed are TOC with F3 fraction of Cu (r=0.72); F1 (r=0.41) fraction of Co, TP with F5 fraction of Fe (r=0.59); F3 (r=0.42) and F5 (r=0.63) fractions of Mn; F5 fraction of Co (r=0.53); F4 (r=0.78) and F5 (r=0.44) fractions of Cr, TN with F3 (r=0.66) and F5 (r=0.78) fractions of Mn; F3 (r=0.50) and F4 (r=0.71) fractions of Cr in core TI. In core TV, TP with F5 fraction of Co (r=0.56), TN with F1 (r=0.63) and F4 (r=0.41) fractions of Cu; F3 (r=0.69) fraction of Zn. In core TIV, TP with F5 (r=0.59) fraction of Fe; F4 (r=0.48) and F5 (r=0.65) fractions of Mn; F1 (r=0.55) and F2 (r=0.80) fractions of Cu; F1 (r=0.61) and F5 (r=0.57) fractions of Pb; F1 (r=0.69), F3 (r=0.40), F4 (r=0.65) fractions of Co; F4 (r=0.43), F5 (r=0.85) fractions of Zn and F2 fraction of Cr (r=0.71).

Ulhas estuary

In core UI, TOC and TN display significant associations with F4 (r=0.50, 0.83) fraction of Cu and F1 (r=0.45, 0.81) fraction of Cr; F4 (r=0.49, 0.72) fraction of Cr in core UV; in core UIV, F4 fraction of Fe (r=0.88, 0.31), F4 fraction of Pb (r=0.58, 0.47) and F4 (r=0.74, 0.58) fraction of Zn. In addition to this other correlations observed are TP with F4 fractions of Fe (r=0.49) and Cr (r=0.68); TN with F1 fraction of Mn (r=0.40) in core UI; TP and TN with F5 fractions of Fe (r=0.79, 0.46) and Mn (r=0.76, 0.51); F2 fraction of Pb (r=0.71, 0.78); F1 fraction of Zn (r=0.63, 0.79) in core UV. TP with F1 fractions of Fe (r=0.44) and Cu (r=0.48); F4 fraction of Mn (r=0.60); TOC with F1 (r=0.68) and F4 (r=0.47) fractions of Mn; F2 (r=0.46) and F4 (r=0.82) fractions of Cu; F1 fraction of Pb (r=0.51); F4 fraction of Co (r=0.72); F1 (r=0.62), F2 (r=0.68), F3 (r=0.82) fractions of Zn; F1 (r=0.74), F3 (r=0.51) and F4 (r=0.58) fractions of Cr in core UIV.

Metals complexed with OM are generally described by anion exchange or organic-metallic complexation. Carbonyl, phenolic, hydroxyl, and carbonyl functional groups are assumed to be primarily responsible for the binding (Horsfall and Spiff, 2005). Cu is preferentially retained in OM by complexation rather than by ion exchange (Balasoiu et al., 2001; Kotoky et al., 2003). The correlation between OM and Cu is much stronger than those with Pb and Zn in cores from Ulhas estuary. In aquatic systems, organic materials exhibit a high degree of selectivity for divalent ions and the probable order of binding strength for metal ions onto OM is Cu > Pb > Zn

(Jonasson, 1977). Thus, the organically bound form is an important phase for Cu in the estuarine sediments. No clear relationships between Cu and TOC in the F4 fraction are seen in the creek, indicating that this phase might represent more than organic-bound Cu or that TOC is not a useful measure of OM capable of binding trace metals (Mortimer and Rae, 2000), in this region. The Zn concentration upto 5 % is reported to be bound in the humic acid fraction of the soil (Bodek et al., 1988). The good correlations of Zn in core TI and core UIV with the organic fraction may be due to the scavenging effect. It can be concluded that the OM content is a relevant factor in the distribution of metal among the fractions and plays an important role in the distribution of these metals in the sediments.

4.5.2. Role of Fe-Mn in distribution of fractions

In aquatic redox chemistry, the geochemical and ecological importance of Fe and Mn has been recognised. Here, Fe and Mn oxides/hydroxides are referred as total Fe and total Mn.

Thane creek

In core TI, the associations are: total Fe with F5 fraction of Fe (r=0.78), Co (r= 0.60) and Pb (r=0.74); total Mn with F5 (r=0.73) fraction of Mn, F2 (r=0.60) fraction of Pb, F1 (r=0.65), F2 (r=0.67) and F3 (r=0.55) fractions of Zn; total Fe and total Mn with F4 (r=0.59, 0.56) fraction of Cr. In core TV, F3 (r=0.67) fraction with total Mn, and F5 (r=0.53) fraction with total Fe of Fe; total Mn with all the five fractions of Mn (F1=0.70, F2=0.67, F3=0.73, F4=0.72 and F5=0.73); F1 (r=0.60), F4 (r=0.74) and F5 (r=0.58) fractions of Cu; F2 (r=0.48) and F5 (r=0.48) fractions of Pb; F2 (r=0.50) and F4 (r=0.61) fractions of Zn; F3 (r=0.48) fraction of Cr; F3 (r=0.50) and F5 (r=0.63) fractions of Pb with total Fe. In core TIV, F3 fractions of Fe (r=0.48) and Cu (r=0.59); F4 (r=0.54) fraction of Pb correlates with total Fe while F2 (r=0.71) and F4 (r=0.68) fractions of Mn associates with total Mn.

Ulhas estuary

In core UI, total Fe and total Mn associate with F2 (r=0.69, 0.66) and F3 (r=0.88, 0.61) fractions of Fe; F2 (r=0.74, 0.49) and F5 (r=0.54, 0.52) fractions of Pb; F1 (r=0.57, 0.48), F3 (r=0.92, 0.67) and F5 (r=0.89, 0.78) fractions of Co; F1 (r=0.76, 0.65) and F3 (r=0.51, 0.64) fractions of Zn; F3 (r=0.81, 0.67) and F5 (r=0.80, 0.62) fractions of Cr. In addition, F5 (r=0.70) fraction of Fe also shows association with total Fe. For Mn, all the fractions (F1=0.56, F2=0.82, F3=0.60, F4=0.61 and F5=0.89) correlate with total Mn while F2 (r=0.81), F3 (r=0.50) and F5 (r=0.89) fractions also associate with total Fe. In core UV, total Fe and total Mn show correlation with F5 (r=0.64, 0.63) fractions of Fe and Mn. F1 (r=0.85, 0.45) fraction of Zn, F2 (r=0.79) fraction of

Mn with total Mn, F2 (r=0.80) fraction of Pb with total Fe. For core UIV, total Fe and total Mn associate significantly with F5 (r=0.97, 0.74) fraction of Fe; F2 (r=0.84, 0.74), F3 (r=0.59, 0.60) and F5 (r=0.69, 0.96) fractions of Mn and F3 (r=0.50, 0.52) fraction of Co.

The high correlation values of Mn associating with total Fe and total Mn in Thane creek as compared to Ulhas estuary cores can be attributed to the finer texture of the soil which contributes to a higher accumulation rate (Shuman, 1985). Oakley et al. (1981) reported that hydrous Mn oxides exhibit more extensive isomorphic substitution than amorphous Fe oxides and show greater conditional equilibrium constants for the heavy metals than Fe oxides. Shuman (1985) stated that Fe oxides may be of greater consequence than the Mn-oxide fraction in the Zn chemistry, in contrast to the data presented by Tipping et al. (1985) who found larger amounts of Zn in the Mn-oxide fraction which can be applied for cores from the creek region. Pattan et al. (1995) found that Cr, one of the redox sensitive metals, co-precipitated with authigenic Mn-oxy-hydroxide. This can be applied to core TV. Singh and Subramaniam (1984) explained that Mn-Fe oxides act as efficient scavengers for many of the heavy metals (Fe, Mn, Cu, Zn, etc). Relatively higher concentration of Zn and other heavy metals associating with the F3 fraction at both the sites may be caused by the adsorption of these elements by the colloids of Mn and Fe as explained by Jenne (1968). The sorption of Zn with Fe in the sediment may strongly hinder their mobility in the aquatic environment. Further, the positive correlations of Pb with the total Mn and total Fe in core UI, suggest that Pb carbonates might be incorporated with Mn oxides and amorphous Fe oxides as reported by Todorovic et al. (2001). It should be pointed out that oxide association does not guarantee the immobilization of contaminant elements in the subsurface, so metals associated with Fe and Mn oxides are still labile and may be released upon decomposition of the oxides under reduced conditions, consequently having a significant impact on soil quality and biota (Chlopecka, 1996) as stated earlier.

In cores from the Ulhas estuary, distinct association between the different elements are not observed. This may be attributed to frequent sediment resuspension caused by dredging activities, which strongly disturbs the spatial distribution of heavy metals in sediments. The data on correlation analysis showed the capacity of Fe-Mn oxy-hydroxides (F3) and organic matter-sulphides (F4) to retain trace metals (Tessier et al., 1979; Ramos et al., 1994; Mortimer and Rae, 2000).

4.6. Sediment Quality Guidelines

If the concentration of metals incorporated in sediments exceed threshold values, a direct risk to detrital and deposit-feeding benthic organisms can occur, which may represent a long-term contamination source to higher trophic levels (Mendil and Uluözlü, 2007). Therefore, eco-toxicological effects of heavy metal contaminations in sediments was determined using Sediment Quality Guidelines (SQGs) defined by MacDonald et al. (2000), developed for marine and estuarine ecosystem (Bakan and Ozkoc, 2007). The different concentration terms used (TEL, PEL, ERL and ERM) are already explained earlier. Generally the primary purpose of SQG is to monitor and protect the aquatic biota from the harmful and toxic effects related with sediment-bound contaminants (MacDonald et al., 2000; Spencer and Macleod, 2002; McCready et al., 2006). These guidelines evaluate the degree to which the sediment-associated chemical status which might adversely affect aquatic organisms and are designed to assist sediment assessors and managers responsible for the interpretation of sediment quality (Caeiro et al., 2005). Sediment quality criteria have also been derived using the Apparent Effects Threshold (AET) approach. This approach determines the concentration of a particular toxicant above which a statistically significant ($p<0.05$) biological effect is always observed, e.g. increase in toxicity in sediment toxicity tests, damage to benthic infaunal community structure, histopathological abnormalities in fish (Chapman and Mann, 1999). It is assumed that when the threshold AET concentration of a particular toxicant is exceeded under field conditions, any observed effects are due to the contaminant of interest. An advantage of the AET approach is that criteria are developed from field conditions using both chemical and biological information. As reported by many authors, both approaches have their own limitations, e.g. the SQG do not account for the physico-chemical attributes of the sediments such as grain size, organic matter content, sulphides, chemical species and complexes that may increase or decrease the potential for toxic effects at a specific area (Ingersoll et al., 2000); and limitations to AET approach are that a large data set is required, the criteria are developed on a chemical by chemical basis and that the method does not account for the effects of multiple toxicants (Giesy and Hoke, 1990). Therefore, a combination of these approaches can be a good option to give a more comprehensive and accurate assessment on the contamination status of heavy metals in the region.

The data sets of metals in the bio-available fractions (sum of the first four fractions) of both the study sites, Table 4.3, are compared with the SQG and AET using SQUIRT (Screening Quick Reference Table). SQG for elements such as Fe, Mn and Co are not available. From Table 4.3, it is seen that for elements such as Cu, Pb, Zn and Cr in all the cores of Ulhas estuary and for Pb, Cu, Zn in core TIV, Pb, Cr and Zn in core TV and Pb in core TI of Thane creek, the bio-

available fractions of the elements are below TEL, PEL, ERL and ERM values indicating low risk of adverse effects on organisms. On the other hand, Cu and Zn in core TI, Cu in core TV are below PEL and ERM but above TEL and ERL. Cr values, in cores TI and TIV, are above TEL but below PEL, ERL and ERM. Based on AET values, Mn and Co show elevated values exceeding AET, suggesting these two elements are potentially bio-available and thus indicate their toxicity to environment. The remaining elements have values far below the AET values indicating no harm to the biota with respect to these elements.

Table 4.3. Screening Quick Reference table for heavy metals in marine sediment (Buchman, 1999)

Element	Thane Creek			Ulhas Estuary			TEL	PEL	ERL	ERM	Apparent effects threshold (AET)
	Near creek head(TI)	Lower middle (TV)	Near creek mouth (TIV)	Near estuary mouth (UI)	Lower estuary (UV)	Upper estuary (UIV)					
Fe (%)	1.97	0.51	0.45	0.61	0.48	0.53	-	-	-	-	22% (Neanthes)
Mn (ppm)	866	1278	1208	609	1023	701	-	-	-	-	260 (Neanthes)
Cu (ppm)	44.08	40.63	22.47	12	17	23	31.6	149	34	270	390 (Microtox and Oyster Larvey)
Pb (ppm)	27.94	34.97	33.76	24	25	34	35.8	128	46.7	218	-
Co (ppm)	18.33	22.02	17.99	15	16	22	-	-	-	-	10 (Neanthes)
Zn (ppm)	256.06	45.44	50.41	73	71	42	121	459	150	410	410 (Infaunal community)
Cr (ppm)	34.89	24.79	63.97	12	16	28	31.6	111	81	370	62 (Neanthes)

Analysis of the partitioning of metals in the sediments indicates that the percentage of metals associated with fractions 1 to 4 differ considerably between the sites and this may indicate relative differences in bio-availability. In general, bio-availability depends on the nature of metal particle associations, the mechanisms of metal release from sediments and the variation in exposure routes (Chapman et al., 1998). In the absence of anthropogenic influences, trace metals in sediments are mainly associated with silicates and primary minerals and therefore have limited mobility. Chemical elements introduced from human activity show greater mobility and are associated with other sediment phases, such as carbonates, oxides, hydroxides and sulphides (Heltai et al., 2005). However, Thane creek experiences very high sediment accumulation rates varying from 0.24-2.72 cm/yr. Consequently, maximum metal concentrations occur several centimeters below the sediment surface. In comparison with the Ulhas estuary, it is less likely to present a risk to burrowing organisms, as these sediments are far less likely to be disturbed by dredging activities. However, should significant agitation and mixing with oxygenated water occur, as would happen to material dredged from the shipping channel, oxidative degradation of organic matter would be enhanced resulting in potential mobilisation of Cu, Zn and Cr. Therefore, the elements Cu, Zn and Cr enriched in sediments near the creek head might be released to the water column if there is a change in the environmental condition. Benthic

invertebrates are an important link in the transfer of substances to higher trophic levels because of their close association with sediments and their ability to accumulate metals (Burgos and Rainbow, 2001). Hence, although metal concentrations in the bio-available fractions are low in the Ulhas estuary, contaminated sediments at relatively shallow depths in estuary experiencing erosion, may present considerable risk to sediment dwelling biota.

4.7. Risk Assessment Code (RAC)

In some earlier studies (Jain, 2004; Ghrefat and Yusuf, 2006), the Risk Assessment Code (RAC) has been used to assess environmental risks and estimate the possible damage to benthic organisms caused by contaminated sediments. This is because, in sediments, metals are bound to both, different fractions and with different bonding strengths, with the latter influencing the bio-availability of the metal in the environment (Bacon and Davidson, 2008; Filgueiras et al., 2002). The RAC considers the percentage fraction of metals that are exchangeable and associated with carbonates. In this fraction, the metals are weakly bound to the sediment and present a greater environmental risk, since they are more available to the aquatic system. When RAC percentage is less than 1, the sediment is at no risk to the aquatic environment. Percentages of 1-10 reflect low risk, 11-30 % corresponds to medium risk and 31-50 % has high risk. Above 50 %, the sediment poses a very high risk, and is considered dangerous, with metals easily able to enter the food chain (Jain, 2004; Perin et al., 1985). The RAC was determined for the selected seven metals and the values interpreted in accordance with the RAC classifications. Although RAC does not take into account the total metal concentration, it may be useful to assess the environmental risk using sequential extraction as a characterization method.

It can be seen (Table 4.1) that the percentage of Mn associated with the exchangeable and carbonate-bound fraction (F1 and F2) ranges from medium to high risk; Fe and Cu exhibit low risk; Pb, Co, Zn and Cr displays low to medium risk in the Thane creek while in the Ulhas estuary (Table 4.2), Fe, Cu, Co, Zn and Cr project low risk; Mn and Pb show low to medium risk. In general, the RAC as applied to the present study reveals that Mn mostly exists in the labile fraction and therefore falls under the high-risk category and can easily enter the food chain. Because of its toxicity and availability, it can pose serious problems to the ecosystem. The total content of Mn in the sediments is also quite high and its association with labile fractions may cause deleterious effects. Speciation patterns of Co, Zn, Pb and Cr show low to medium risk, while Fe and Cu do not show any risk to the environment.

It is remarkable that in spite of the higher total content of metals at location UIV (in an industrial area), the distribution of the studied metals among the fractions is fairly similar for all the estuarine sampling sites studied. This can be explained by taking into account that sediments can, to a certain extent, accumulate heavy metals without drastically changing the distribution among fractions, if pH value remains in a common range. In general, the small amounts of metals in exchangeable form and the fraction associated with carbonates reduce the leaching potential, although their accumulation in organic complexes and inorganic precipitates enables them to become mobile whenever the chemical equilibrium of the sediment shifts. Greater percentage of metals present in the residual category indicates lower pollution, because this inert phase corresponds to detrital or lattice bound metals that cannot be remobilized as discussed earlier. It should be pointed out that extraction results do not necessarily prove the existence of any of the defined phases in sediments, but merely reflect the chemical behaviour of metals within the different extracting solutions (Coetzee, 1993). This study has confirmed the fact that the knowledge of the total heavy metal content of sediments is not enough to exactly recognize the effect of physico-chemical processes on the behaviour of heavy metals. One has also to know the mobility of the heavy metals in sediments, which can be effectively studied by sequential extraction experiments.

Chapter 5

SUMMARY

Sediments are sinks for elements in aquatic systems and are recognized as one of the largest host of pollutants. Sediments provide information on the various processes such as sedimentation, hydrodynamics, sediment contaminant interaction, sediment-organism interaction and historical contaminants. Changes in contamination, biological status and physical characteristics of coastal marine systems during the past have often led to significant variations in the composition of accumulating sediments. Human activities bring marked geochemical variations in coastal sediments. The signals of these variations are often challenging to interpret due to various sedimentological, geochemical and post-depositional factors affecting the profiles. However, by using a sufficient number of parameters and their analyses, employing sophisticated multivariate methods, much information can be extracted from the geochemical data. Thus, the analysis of sediments can aid in reconstructing the history of changes and understanding human impact on the ecosystem.

Mumbai, one of the natural bays, necessitates monitoring for pollution due to the rapid increase in population and development of industries. The purpose of this study was to characterize the distribution of heavy metals in sediments along intertidal regions of Mumbai coast, with the goal of improving the understanding of the fate of contaminants in wetland sediments. Five creeks/estuaries along Mumbai coast were selected for the present study namely, Thane creek and Ulhas estuary which comprised the larger water bodies, and Manori creek, Versova and Nhava-Sheva creeks consisted the smaller water bodies,. This thesis is an attempt to study the spatial and temporal distribution of metals in different sub-environments such as mudflat and mangrove sediments along with the probable sources and factors accountable for the variations. In addition, to identify and quantify the metal forms, to gain a precise understanding of the potential and actual impacts of elevated metal levels in the sediment**,** metal speciation has been studied in the different fractions of the sediment core. The important factors that control the sources and processes occurring in sediments which are known to control the speciation, are also studied.

The methodology comprised of using multiple geochemical proxies, such as sediment characteristics, organic matter content, bulk elemental chemistry, metal speciation, magnetic susceptibility parameters, clay mineralogy and radioisotope chronology. Statistical analysis comprising of Pearson’s correlation matrix and Factor analysis, was attempted to understand the various geochemical sources and processes determining the transport and fate of the metals in the sediments. In order to determine the pollution status of the region, various pollution indices such as Enrichment Factor (EF) and Index of Geo-accumulation (Igeo) were computed. Also,

sediment quality guidelines were employed to know the pollution status with respect to biota. Further, based on metal speciation results, Risk Assessment Code (RAC) was used to assess the environmental risks and estimate the possible damage to benthic organisms caused by the contaminated sediments.

Based on spatial and temporal variations, mudflat cores collected from the head to the mouth of the Thane creek, showed a gradual decrease in sand and clay percentages and an increase in silt percentage. The cores collected from the opposite banks, showed similar down-core profiles for sediment components, both in the upper as well as the lower middle creek regions. Further, the organic matter content of most of the cores studied showed a gradual decrease from the head towards the mouth of the creek and also decreased with depth. The core, sampled near the creek head, contained more than twice the concentration of most of the metals studied as compared to the other cores and a reduction in metal content occurred with increasing distance from the creek head. In general, sediments located within the northern reach of the creek had higher concentrations than those in the southern reach. ^{210}Pb dating, on mudflat cores, showed a sedimentation rate of 1.46 cm/yr near the creek head, 0.24 cm/yr in the upper middle creek region and 2.72 cm/yr in the lower middle creek region. From the observation of the principal component analysis, the industrial zone represented by the core sampled near the creek head and the shipyard and port area, represented by the core collected from lower creek region, were the main potential sources of metal pollutants and organic matter in the creek indicating that the contents of metals in the creek sediments were clearly of anthropogenic origin while in the middle creek region they were a mix of anthropogenic and lithogenic sources.

In the mangrove regions, from the correlation and factor analyses carried out, the mangroves environments were found to be subjected to similar sediment-metal associations with organic matter, Fe-Mn oxides along with finer sediment components as dominant factors in the metal distribution. Based on Igeo, Cu, Pb and Co were found to fall in the moderately polluted class in the mudflat region while in the mangrove region, few subsamples of Mn and Co were in the moderately polluted class. The remaining elements were in the unpolluted to moderately polluted class. In the upper middle creek region, the mangrove core was found to display higher values for most of the metals studied as compared to the mudflat core while cores sampled near the creek mouth showed higher values for metals in the mudflat region as compared to the mangrove region.

In the Ulhas estuary, from inner estuarine end to the mouth region, a gradual increase in sand percentage and a decrease in silt percentage were observed. The organic matter did not exhibit much variation from the head to the mouth of the estuary. The metal content of the sediments showed increasing concentrations moving from the upstream section of the estuary to the downstream section. The metal distribution showed large fluctuation with depth which was related to the frequent dredging activities carried out in the region. Based on ^{210}Pb dating only one of the mudflat cores collected near the estuary mouth showed good down-core decay, with a sedimentation rate of 0.24 cm/yr. The result of factor analysis corresponded well with correlation matrix, with Fe and Mn as the dominant metal carriers followed by organic matter. When the concentrations of the different sediment parameters were plotted on the Isocon diagram, the mudflat region in the lower estuary was found to be dominated by higher values for almost all the metals studied while the mangrove core exhibited higher clay percentage. In the case of mudflat and mangrove cores from the upper estuarine region, not much variation in metal distribution was seen. Based on Igeo, in the mudflat region, Cu, Pb and Co was found to fall in the moderately polluted class while the remaining elements were in the unpolluted class. In the mangrove core from the lower estuary, Mn falls in moderately polluted class whereas in the core from upper mangrove region, Pb and Co fall in strongly to moderately polluted class; Mn, Cu and Cr in moderately polluted class while Fe, Ni, Zn and V fall in unpolluted to moderately polluted class.

In addition, Magnetic susceptibility parameters showed presence of fine grain ferrimagnetic minerals dominated by magnetite in the Thane creek and Ulhas estuary. Based on XRD analysis, Smectite was found to be the dominant clay mineral in the study area followed by kaolinite, illite and chlorite. XRD analysis clearly showed that the basalt rock was the dominant clay mineral source in the study area. When the distributions of different variables are compared between the creek and estuarine regions using the Isocon plot, the creek exhibited higher values of organic matter along with clay, Mn, Zn and Pb contents. On the other hand in the estuarine region, greater values for sand, Cu, Cr and Co were seen. When the mangrove cores from the creek and estuarine region were compared using the isocon plot, it was seen that higher values for most of the elements studied were seen in the estuarine region as compared to the creek which showed only high TOC and clay content. The observation indicated that in the estuarine region, the mangroves were acting as strong metal sink.

The geochemical trends, when viewed together in the two large water bodies, are found to be strongly site-specific and depend on the local geochemical background, basin characteristics and

anthropogenic metal and nutrient loading. The Ulhas estuary study site is a good example of a transportation zone characterized by diverse sediments ranging from sand, silt and clay and low organic carbon content. The site had high hydrodynamic energy due to its exposure to tidal and coastal currents and therefore fine particulates associated with metals had a tendency to move on. These conditions of high hydro-dynamism, high sedimentation rate, high clay/silt fraction, which retain more pollutants due to the higher surface/volume and high organic matter content, served as a favourable environment for metal enrichment. Mangroves bordering the estuarine region further acted as efficient traps of sediments, organic matter and also provided shelter from wave and tidal energy hence acted as settling areas for suspended material making it an excellent example of a zone of accumulation. In contrast, the Thane creek had high percentage of fine sediments (comprised up to 90 % clay/silt) and high organic matter content, a characteristic of areas of low hydrodynamic energy which implied that the creek was acting like a passive link and not like an active trap for metals.

Among the smaller water bodies studied, in Manori creek, the head region (core ManI) showed the highest metal concentration along with organic matter while the creek mouth (core ManII) had the lowest concentration. ^{210}Pb activity did not show any definite trend with depth in core ManI. On the other hand, core ManII showed a better decreasing trend in ^{210}Pb activity with depth, suggesting that the down-core decrease in ^{210}Pb activity supported the idea that core ManII was more compact and deposited in undisturbed sedimentary environment than core ManI. Statistical analysis indicated organic matter (TOC, TP and TN), clay and Fe-Mn oxides were found to be the dominant metal carriers in the region. In the mangrove region, when the depth-wise distributions of metals are studied, in recent years, the concentrations of most of the metals were found to be higher when compared to the bottom sediments. Igeo suggested that the mangrove sediments of the creek were moderately polluted with Pb and Cu while unpolluted with respect to the remaining metals.

In Versova creek, the sediment component distribution pattern indicated that the mouth region was dominated by silt fractions while near the creek head, clay was found to be the dominant component. The grain size distribution in the creek region showed mud to be the dominant sediment fraction, comprising about 88-91%. In Nhava-Sheva creek, the mangrove and mudflat cores showed the dominance of clay component while sand percentage was found to be low.

In order to study Metal speciation in the sediments, the conventional speciation scheme (Tessier et al, 1979) was applied to selected sediment cores from the Thane creek and Ulhas estuary.

Seven metals namely Fe, Mn, Cu, Pb, Co, Zn and Cr were studied in vertical sections of the cores. The speciation results showed that in Thane creek, core TI, sampled near the creek head had higher metal concentration of Mn and Zn in the bio-available fractions in the upper few centimeters of the core indicating that there might be a risk to the biota if the environmental conditions change. For Ulhas estuary, almost all the elements studied were in the residual phase. The results of spatio-temporal metal variation showed that at both the sites, the residual fraction was found to be predominant and the contribution of the other four fractions to the total metal concentration was only minimal except for Mn. The residual fraction was found to show an increasing trend with increasing depth for most of the elements at both the sites. This implied that the elements were not readily available in the deeper sections of the core. In general, the average concentrations of non-residual fractions of almost all the metals studied were greater in the Thane creek than in the Ulhas estuary. These results indicated that heavy metals in the creek sediments were potentially more available for exchange and/or release into the marine environment relative to those from the estuary. The Risk Assessment Code (RAC), applied to the present study, revealed that Mn mostly existed in the labile fraction and therefore was under the high-risk category and could easily enter the food chain. Speciation patterns of Co, Zn, Pb and Cr showed low to medium risk to the aquatic environment. Fe and Cu did not show any risk to the environment.

On the basis of the research findings of the present study, the following recommendations are made for future investigations on metal pollution in the Mumbai region;

- Investigations to be undertaken to evaluate the bioaccumulation potential of Mn in the creek and estuarine regions. This will provide important data both from the public health and ecological point of view.
- The Sediment Quality Guidelines (SQG) used in the present study were developed in the U.S and cannot be expected to apply equally to all sediment types and sets of environmental conditions, and therefore, should be utilized for guideline purposes only. Appropriate SQGs for the sediments to be developed.
- Investigation to include other organic compounds like TBT, dioxins, the persistent organic pollutants (POPs) and the alkylated PAHs needs to be carried out.

REFERENCES

Abollino, O., Aceto, M., Malandrino, M., Mentasti, E., Sarzanini, C. and Petrella, F. (2002). Heavy metals in agricultural soils from Piedmont, Italy: Distribution, speciation and chemometric data treatment. Chemosphere, 49, 545-557.

Abu-Hilal, A., Badran, M. and Vaugelas, J. (1988). Distribution of trace elements in Callichirus laurae burrows and nearby sediments in the Gulf of Aquaba, Jordan (Red Sea). Marine Environmental Research, 25, 233-248.

Achterberg, E. P., Van Den Berg, C. M. G., Boussemart, M. and Davison, W. (1997). Speciation and cycling of trace metals in Esthwaite Water: A productive English lake with seasonal deep-water anoxia. Geochimica et Cosmochimica Acta, 61, 5233-5253.

Adamo, P., Arienzo, M., Imperato, M., Naimo, D., Nardi, G. and Stanzione, D. (2005). Distribution and partition of heavy metals in surface and sub-surface sediments of Naples city port. Chemosphere, 61(6), 800-809.

Aguilera, A. and Amils, R. (2005). Tolerance to cadmium in Chlamydomonas sp. (Chlorophyta) strains isolated from an extreme acidic environment, the Tinto River (SW, Spain). Aquatic Toxicology, 75, 316-329.

Ahn, I. Y., Kang, Y. C. and Coi, J. W. (1995). The influence of industrial effluents on intertidal benthic communities in Panweol, Kyeonoggi Bay (Yellow Sea) on the West coast of Korea. Marine Pollution Bulletin, 30(3), 200-206.

Akcay, H., Oguz, A. and Karapire, C. (2003). Study of heavy metal pollution and speciation in Buyak Menderes and Gediz river sediments. Water Research, 37, 813-822.

Alagarsamy, R. (2006). Distribution and seasonal variation of trace metals in surface sediments of the Mandovi estuary, west coast of India. Estuarine, Coastal and Shelf Science, 67, 333-339.

Alagarsamy, R. (2009). Environmental magnetism and application in the continental shelf sediments of India. Marine Environmental Research, 68, 49-58.

Aller, R. (1982). The effects of macrobenthos on chemical properties of marine sediments and overlying water. In: P.L. McCall & M.J.S. Tevesz (eds.), Animal-sediments relations. Plenum Press, New York, 53-102p.

Alloway, B. J. (1995). The origins of heavy metals in soils. In Heavy Metals in Soils. 2nd edition, (ed. B. J. Alloway): Blackie Academic and Professional.

Alongi, D. M., Boyle, S. G., Tirendi, F. and Payn, C. (1996). Composition and behaviour of trace metals in post-oxic sediments of the Gulf of Papua, Papua New Guinea. Estuarine, Coastal and Shelf Science, 42(2), 197-211.

Alvarez-Iglesias, P., Rubio, B. and Vilas, F. (2003). Pollution in intertidal sediments of San Simon Bay (Inner Ria de Vigo, NW of Spain): total heavy metal concentrations and speciation. Marine Pollution Bulletin, 46, 491-521.

Andrew, B. C., Lan, W. C. and Alejandro, C. (2003). Reconstructing historical trends in metal input in heavily- disturbed, contaminated estuaries: Studies from Bilbao, Southampton Water and Sicily. Applied Geochemistry, 18, 311-325.

Angelidis, M. O. (1995). The Impact of Urban Effluents on the Coastal Marine Environment of Mediterranean Islands. Water Science Technology, 32(9-10), 85-94.

Anon (2006). Indian Tide Table. Part I. Indian and Selected Foreign Ports, Geodetic and Research Branch. Government of India, Surveyor General of India.

Anthony, E. J. (2004). Sediment dynamics and morphological stability of estuarine mangrove swamps in Sherbro Bay, West Africa. Marine Geology, 208, 207-224.

Appleby, P. G. and Piliposian, G. T. (2006). Radiometric dating of sediment records from mountain lakes in the Tatra Mountains. Biologia Bratislava, 61(Suppl 18), 51-64.

Apte, S. C. and Day, G. M. (1998). Dissolved metal concentrations in the Torres Strait and Gulf of Papua. Marine Pollution Bulletin, 36, 298-304.

Apte, S. C., Batley, G. E., Bowles, K. C., Brown, P. L., Creighton, N., Hales, L. T., Hyne, R. V., Julli, M., Markich, S. J., Pablo, F., Rogers, N. J., Stauber, J. L. and Wilde, K. (2005). A comparison of copper speciation measurements with the toxic response of three sensitive freshwater organisms. Environmental Chemistry, 2, 320-330.

Apte, S. C., Rowland, R. and Patney, H. (2000). Size distribution of copper complexing ligands in tropical freshwaters. Chemical Speciation and Bioavailability, 12, 79-88.

Arias, R., Barona, A., Ibarra-Berastegi, G., Aranguiz, I. and Elıas, A. (2008). Assessment of metal contamination in dregded sediments using fractionation and Self-Organizing Maps. Journal of Hazardous Materials, 151, 78-85.

Athalye, R. P. and Goldin, Q. (2002). Studies on the intertidal sediments of Thane creek and Ulhas river estuary. In: Goldin Quadros (ed.), Proceedings of the National Seminar on Creeks, Estuaries and Mangroves, Pollution and Conservation. Zoology Department, Thane, 66-71.

Athalye, R. P., Patil, N. N., Borkar, U., Quadros, G. and Somani, V. U. (2003). Study of Flora, Intertidal Macrobenthic Fauna and Fishery of Ulhas River Estuary and Thane Creek to assess the pollution status and decide mitigative strategy. B. N. Bandodkar College of Science, Thane and MMRDA Mumbai project, 211p.

Atkinson, M. J. and Smith, S. V. (1983). C: N: P ratios of benthic marine plants. Limnology and Oceanography, 28, 568-574.

Bacon, J. R. and Davidson, C. M. (2008). Is there a future for sequential chemical extraction? Analyst, 133, 25-46.

Baeyens, W., Leemakers, M., De Gieter, M., Nguyen, H. L., Parmentier, K., Panutrakul, S. and Elskens, M. (2005). Overview of trace metal contamination in the Scheldt estuary and effect of regulatory measures. Hydrobiologia, 540, 141-154.

Bailey T. C., Barcellos, C. and Krzanowski, W. J. (2005). Use of spatial factors in the analysis of heavy metals in sediments in a Brazilian coastal region. Environmetrics, 16, 563-572.

Bakan, G. and Ozkoc, H. B. (2007). An ecological risk assessment of the impact of heavy metals in surface sediments on biota from the mid-Black Sea coast of Turkey. International Journal of Environmental Studies, 64 (1), 45-57.

Balasoiu, C. F., Zagury, G. J. and Deschenes, L. (2001). Partitioning and speciation of chromium, copper and arsenic in CCA contaminated soil: influence of soil composition. Science of the Total Environment, 280, 239-255.

Balkis, N. and Cagatay, M. N. (2001). Factors controlling metal distributions in the surface sediments of the Erdek Bay, Sea of Marmara, Turkey. Environment International, 27, 1-13.

Banerjee, S. K., King, J. and Marvin, J. (1981). A rapid method for magnetic granulometry with applications to environmental studies. Geophysical Research Letters, 8, 333-336.

Batley, G. E., Apte, S. C. and Stauber, J. L. (2004). Speciation and bioavailability of trace metals in water, Progress since 1982. Australian Journal of Chemistry, 57, 903-919.

Beard, W. C., Davidson, G., Benne, T. T. S. J. and Rhoton, F. E. (2003). Evaluation of the Potential for Trace Element Mobilization Resulting from Oxygenating Sediments from a Small Mississippi Reservoir. USD A-ARS National Sedimentation Laboratory Research Report No. 37, 69p.

Beckwith, P. R., Ellis, J. B., Revitt, D. M. and Oldfeld, F. (1986). Heavy metal and magnetic relationships for urban source sediments. Physics of the Earth and Planetary Interiors, 42, 67-75.

Belzile, N., Chen, Y., Gunn, J. and Dixit, S. (2004). Sediment trace metal profiles in lakes of Killarney Park, Canada: from regional to continental influence. Environmental Pollution, 130, 239-248.

Belzunce-Segarra, M. J., Prego, R., Wilson, M. J., Bacon, J. and Santos-Echeandia, J. (2008). Metal speciation in surface sediments of the Vigo Ria (NW Iberian Peninsula). Scientia Marina, 72(1), 119-126.

Benner, R., Fogel, M. L. and Sprague, E. K. (1991). Diagenesis of belowground biomass of Spartina alterniflora in salt-marsh sediments. Limnology and Oceanography, 36(7), 1358-1374.

Benoit, G., Wang, E. X., Nieder, W. C, Levandowsky, M. and Breslin, V. T. (1999). Sources and history of heavy metal contamination and sediment deposition in Tivoli South bay, Hudson River, New York. Estuaries, 22, 169.

Benson, N. U., Udosen, E. D. and Akpabio, O. (2008). Interseasonal distribution and partitioning of heavy metals in subtidal sediment of Qua Iboe Estuary and associated Creeks, Niger Delta (Nigeria). Environmental Monitoring and Assessment, 146, 253-265.

Berner, R. (1980). Early diagenesis: a theoretical approach. Princeton University Press, New York, 421p.

Bhosale, U. and Sahu, K. C. (1991). Heavy metal pollution around the island city of Bombay, India. Part II: Distribution of heavy metals between water, suspended particles and sediments in a polluted aquatic regime. Chemical Geology, 90, 285-305.

Birch, G. F. (2003). A test of normalization methods for marine sediment, including a new post-extraction normalization (PEN) technique. Hydrobiologia, 492, 5-13.

Birch, G. F., Robertson, E., Taylor, S. E. and MCconchie, D. M. (2000). The use of sediments to detect human impact on the fluvial system. Earth and Environmental Science, 39, 1015-1028.

Birch, G. F., Taylor, S. E. and Matthai, C. (2001). Small-scale spatial and temporal variance in the concentration of heavy metals in aquatic sediments: a review and some new concepts. Environmental Pollution, 113, 357-372.

Biscaye, P. E. (1965). Mineralogy and sedimentation of deep sea clay in the Atlantic Ocean and adjacent sea and oceans. Bulletin Geological Society of America, 76, 803-832.

Black, K. D., Fleming, S., Nickell, T. D. and Pereira, P. (1997). The effects of ivermectin, used to control sea lice on caged farmed salmonids, on infaunal polychaetes. ICES Journal of Marine Science, 54, 276-279.

Blaha, U., Basavaiah, N., Deenadayalan, K., Borole, D. V. and Mohite, R. D. (2011). Onset of Industrial Pollution recorded in Mumbai mudflat sediments, using integrated magnetic, chemical, ^{210}Pb dating, and Microscopic methods. Environmental Science and Technology, 45 (2), 686-692.

Blasco, F. (1975). Mangroves of India (Les Mangroves de' Inde), Institute Francias De Pondichery, Travaux de la section. Scientifique et Technique, Tome XIV, Fascicule 1, 175p.

Bloemendal, J., King, J. W., Hall, F. R. and Doh, S. J. (1992). Rock magnetism of Late Neogene and Pleistocene deep sediments: relationship to sediment source, diagenetic processes and sediment lithology. Journal of Geophysical Research, 97, 4361-4375.

Bodek, I., Lyman, W. J., Reehl, W. F. and Rosenbalt, D. H. (1998). Environmental Inorganic Chemistry. Pergamon Press.

Borkar, M. U., Quadros, G. and Athalye, R. P. (2007). Threats to the mangroves of Thane creek and Ulhas river estuary, India. Journal of Coastal Development, 11 (1), 48-56.

Borrego, J., Lopez-Gonzalez, N. and Carro, B. (2004). Geochemical signature as markers in Holocene sediments of the Tinto River estuary (Southwestern Spain). Estuarine, Coastal and Shelf Science, 61, 631- 641.

Bostick, B. C., Hansel, C. M., La Force, M. J. and Fendoref, S. (2001). Seasonal fluctuations in zinc speciation within a contaminated wetland. Environmental Science and Technology, 35, 3823-3829.

Boudreau, B. (1997). Diagenetic models and their implementation: modelling transport and reactions in aquatic sediments. Springer-Verlag, Berlin, 414p.

Boughriet, A., Wartel, M. and Cordier, C. (1994). Chemical speciation of some particulate elements in the English Channel, and impact of human activities on the magnetic behavior of suspended matter. Marine Pollution Bulletin, 28, 541-556.

Bourg, A. C. M. (1988). Metals in aquatic and terrestrial systems: sorption, speciation and mobilization, In: Salomons, W. and Forstner, U. (Eds), Chemistry and Biology of solid waste dredged materials and mine tailings, 3-32p.

Boyko, T., Scholger, R., Stanjek, H. and MAGPROX Team. (2004). Topsoils magnetic susceptibility mapping as a tool for pollution monitoring: repeatability of in situ measurements. Journal of Applied Geophysics, 55, 249-259.

Bradl, H. B. (2005). Sources and Origins of Heavy Metals. In Heavy Metals in the Environment; origin, interaction and remediation, (ed. H. B. Bradl).

Breckela, E. J., Emersona, S. and Balistrieri, L. S. (2005). Authigenesis of trace metals in energetic tropical shelf environments. Continental Shelf Research, 25(11), 1321-1337.

Bricker, S. B. (1993). The history of Cu, Pb, and Zn inputs to Narragansett Bay, Rhode Island as recorded by salt-marsh sediments. Estuaries, 16, 589-607.

Broughriet, A., Proix, N., Billon, G., Recourt, P. and Ouddane, B. (2007). Environmental impacts of heavy metal discharges from a smelter in Deule-canal sediments (Northern France); concentration levels and chemical fraction. Water, Air and Soil Pollution, 180, 83-95.

Bruder-Hubscher, V., Lagarde, F., Leroy, M. J. F., Coughanowr, C. and Enguehard, F. (2002). Application of a sequential extraction procedure to study the release of elements from municipal solid waste incineration bottom ash. Analytica Chimica Acta, 451, 285-295.

Brugam, R. B. (1978). Human disturbance and the historical development of Linsley Pond. Ecology, 59, 19-36.

Bryan, G. W. and Langston, W. J. (1992). Bioavailability, accumulation and effects of heavy metals in sediments with special reference to United Kingdom Estuaries: a review. Environmental Pollution, 76, 89-131.

Buchman, M. F. (1999). NOAA screening quick reference tables. NOAA HAZMAT Report 99-1. Seattle, WA, Coastal Protection and Restoration Division, National Oceanic and Atmospheric Administration, 12p.

Buckley, D. E., Smith, J. N. and Winters, G. V. (1995). Accumulation of contaminant metals in marine sediments of Halifax Harbour, Nova Scotia: Environmental factors and historical trends. Applied Geochemistry, 10(2), 175-195.

Budhu, M. (1999). Soil mechanics and foundation. John Wiley and Sons Incorporation, 14-18p.

Bukhari, S. S. and Nayak, G. N. (1996). Clay minerals in identification of provenance of sediments of Mandovi estuary, Goa, west coast of India. Indian Journal of Marine Science, 25, 341-345.

Burgos, M. G. and Rainbow, P. S. (2001). Availability of cadmium and zinc from sewage sludge to the flounder, Platichthys flesus via a marine food chain. Marine Environmental Research, 51, 417-431.

Burt, R., Wilson, M., Mays, M. D. and Lee, C. W. (2003). Major and trace elements of selected pedons in the USA. Journal of Environmental Quality, 32, 2109-2121.

Byrne, R. H., Kump, L. R. and Cantrell, K. J. (1988). The influence of temperature and pH on trace metal speciation in seawater. Marine Chemistry, 25, 163-181.

Caeiro, S., Costa, M. H., Ramos, T. B., Fernandes, F., Silveira, N., Coimbra, A., Medeiros, G. and Painho, M. (2005). Assessing heavy metal contamination in Sado Estuary sediment: an index analysis approach. Ecological Indicators, 5(2), 151-169.

Caitcheon, G. C. (1998). The significance of various sediment magnetic mineral fractions for tracing sediment sources in Killimicat Creek. Catena, 32, 131-142.

Calace, N., Ciardullo, S., Petronio, B. M., Pietrantonio, M., Abbondanzi, F., Campisi, T. and Cardellicchio, N. (2005). Influence of chemical parameters (heavy metals, organic matter, sulphur and nitrogen) on toxicity of sediments from the Mar Piccolo (Taranto, Ionian Sea, Italy). Microchemical Journal, 79(1-2), 243-248.

Callaway, J. C., Delaune, R. D. and Patrick, W. H. Jr. (1998). Heavy metal chronologies in selected coastal wetlands from northern Europe. Marine Pollution Bulletin, 36, 82-96.

Callender, E. (2003). Heavy metals in the environment - historical trends. In Treatise on geochemistry, Volume 9. Edited by B. Sherwood Lollar, D.H. Holland and K.K. Turekian. Elsevier Inc, San Diego, California, 67-105p.

Calmano, W. and Forstner, U. (1983). Chemical extraction of heavy metals in polluted river sediments in central Europe. Science of the Total Environment, 28, 77-90.

Calmano, W., Forstner, U. and Hong, J. (1994). Mobilization and Scavenging of Heavy Metals Following Resuspension of Anoxic Sediments from the Elbe River, in C. Alpers and D. Blowes (eds), Environmental Geochemistry of Sulfide Oxidation. American Chemical Society, 298-321.

Calmano, W., Hong, J. and Förstner, U. (1993). Binding and mobilization of heavy-metals in contaminated sediments affected by pH and redox potential. Water Science and Technology, 28, 223-235.

Campbell, P. G. C., Lewis, A. G., Chapman, P. M., Crowder, A. A., Fletcher, W. K., Imber, B., Luoma, S. N., Stokes, P. M. and Winfrey, M. (1988). Biologically Available Metals in Sediments. NRCC No. 27694. National Research Council of Canada, Ottawa, Canada.

Campbell, P. G. C. (1995). Metal speciation and bioavailability in aquatic system. In Interaction between trace metals and aquatic organisms a critique of free-ion activity model, eds. A. Tessier and D. Turner, 45–102. England: John Wiley and Sons, Ltd.

Cantwell, M. G., Burgess, R. M. and Kester, D. R. (2002). Release and phase partitioning of metals from anoxic estuarine sediments during periods of simulated resuspension. Environmental Science and Technology, 36, 5328-5334.

Carrol, S. A., O'Day, P. A. and Piechowski, M. P. (1998). Rock-water interactions, controlling zinc, cadmium and lead concentrations in surface waters and sediments. Environmental Science and Technology, 32, 956-965.

Chandra, S. (2002). Investigations into the Lami municipal dump as a source of heavy metal contamination, Thesis, University of the South Pacific (USP).

Chan, L. S., Ng, S. L., Davis, A. M., Yim, W. W. S. and Yeung, C. H. (2001). Magnetic properties and heavy-metal contents of contaminated seabed sediments of Penny's Bay, Hong Kong. Marine Pollution Bulletin, 42 (7), 569-583.

Chan, L. S., Yeung, C. H., Yim, W. W. S. and Or, O. L. (1998). Correlation between magnetic susceptibility and distribution of heavy metals in contaminated sea-floor sediments of Hong Kong Harbour. Environmental Geology, 36, 77-86.

Chapman, P. M. and Mann, O. S. (1999). Sediment Quality Values (SQVs) and Ecological Risk Assessment (ERA). Marine Pollution Bulletin, 38, 339-344.

Chapman, P. M., Wang, F., Janssen, C., Persoone, G. and Allen, H. (1998). Ecotoxicology of metals in aquatic sediments: binding and release, bioavailability, risk assessment and remediation. Canadian Journal of Fisheries and Aquatic Sciences, 55, 2221-2243.

Charmasson, S., Bouisset, P., Radakovitch, O., Pruchon, A. S. and Arnaud, M. (1998). Long-core profiles of 137Cs, 134Cs, 60Co and 210Pb in sediment near the Rhône River (Northwestern Mediterranean Sea). Estuaries, 21(3), 367-378.

Chen, Z., Kostaschuk, R. M. and Yang, M. (2001). Cases and solutions: heavy metals on tidal flats in the Yangtze Estuary, China. Environmental Geology, 40(6), 742-749.

Chester, R., Kudoja, W. M., Thomas, A. and Towner, J. (1985). Pollution connaissance in stream sediments using non-residual trace metals. Environmental Pollution (Series B), 10, 213-238.

Chiffoleau, F., Cossa, D., Auger, D. and Truquet, I. (1994). Trace metal distribution, partition and fluxes in the Seine estuary (France) in low discharge regime. Marine Chemistry, 47, 145-158.

Chlopecka, A. (1996). Assessment of form of Cd, Zn and Pb in contaminated calcareous and gleyed soils in southwest Poland. Science of the Total Environment, 188, 253-262.

Choi, K. Y., Kim, S. H., Hong, G. H. and Chon, H. T. (2012). Distributions of heavy metals in the sediments of South Korean harbours. Environmental and Geochemical Health, 34, 71-82.

Chouksey, M. K., Kadam, A. N. and Zingde, M. D. (2004). Petroleum hydrocarbon residues in the marine environment of Bassein-Mumbai. Marine Pollution Bulletin, 49, 637-647.

Cifuentes, L. A., Sharp, J. H. and Fogel, M. L. (1988). Stable carbon and nitrogen isotope biogeochemistry in the Delaware estuary. Limnology and Oceanography, 35, 1102-1115.

Clark, M. W., McConchie, D. M., Lewis, D. E. and Saenger, P. (1998). Redox stratification and heavy metal partitioning in *Avicennia* dominated mangrove sediments, a geochemical model. Chemical Geology, 149, 147-171.

Clark, R. B. (1992). Marine Pollution. Oxford University Press, Oxford.

Coetzee, P. P. (1993). Determination of Speciation of Heavy Metals in Sediments of the Hortbees port: dam by sequential chemical extraction. Water SA, 9 (4), 291-300.

Cooper, J. A. G. (2001). Geomorphological variability among microtidal estuaries from the wave-dominated South African coast. Geomorphology, 40, 99-122.

Cornwell, J. C., Conley, D. J., Owens, M. and Stevenson, J. C. (1996). Sediment chronology of the Eutrophication of Chesapeake bay. Estuaries, 19, 488-499.

Cundy, A. B. and Croudace, I. W. (1996). Sediment accretion and recent sea level rise in the Solent, southern England: inferences from radiometric and geochemical studies. Estuarine, Coastal and Shelf Science, 43, 449-467.

Cundy, A. B., Croudace, I. W., Thomson, J. and Lewis, J. T. (1997). Reliability of salt marshes as geochemical recorders of pollution input: a case study from contrasting estuaries in southern England. Environmental Science and Technology, 31, 1093-1101.

Cuong, D. T. and Obbard, J. P. (2006). Metal speciation in coastal marine sediments from Singapore using a modified BCR-sequential extraction procedure. Applied Geochemistry, 21, 1335-1346.

Dassenakis, M., Degaita, A. and Scoullos, M. (1995). Trace metals in sediments of a Mediterranean estuary affected by human activities (Acheloos river estuary, Greece). Science of the Total Environment, 168, 19-31.

David, C. P. (2003). Heavy metal concentrations in growth bands of corals: a record of mine tailings input through time (Marinduque Island, Philippines). Marine Pollution Bulletin, 46(2), 187-196.

Davidson, C. M., Urquhart, G. J., Ajmone-Marsan, F., Biasioli, M., da Costa Duarte, A. and Davison, W. (1993). Iron and manganese in lakes. Earth-Science Reviews**,** 34,119-163.

Davidson, C. M., Urquhart, G. J., Ajmone-Marsan, F., Biasioli, M., da Costa Duarte, A., Dıaz-Barrientos, E., Grcman, H., Hossack, I., Hursthouse, A. S., Madrid, L., Rodrigues, S. and Zupan, M. (2006). Fractionation of potentially toxic elements in urban soils from five European cities by means of a harmonised sequential extraction procedure. Analytica Chimica Acta, 565, 63-72.

Davutluoglu, O. I., Seckin, G., Ersu, C. B., Yilmaz, T. and Sari, B. (2011). Heavy metal content and distribution in surface sediments of the Seyhan River, Turkey. Journal of Environmental Management, 92, 2250-2259.

Dearing, J. A., Dann, R. J. L., Hay, K., Lees, J. A., Loveland, P. J., Maher, B. A. and O'Grady, K. (1996). Frequency-dependent susceptibility measurements of environmental materials. Geophysics Journal International, 124, 228-240.

Deeley, D. M. and Paling, E. I. (1999). Assessing the Ecological Health of Estuaries in Australia. Marine and Freshwater Research Laboratory, Land and Water Resources Research and Development Corporation Occasional Paper 17/99, Institute for Environmental Science, Murdoch University.

Deevy, E. (1973). Sulfur, nitrogen and carbon in the biosphere. In: G.M. Woodwell & E.V. Peacan (eds.). Carbon and the biosphere. USAEC, Washington D.C., 182-190p.

De Groot, A. J., Salomons, W. and Allersma, E. (1976). Processes affecting heavy metals in estuarine sediments, In J.D. Burton and P.S. Liss (Eds). Estuarine Chemistry, London. Academic Press, 131-153p.

De Miguel, E., Llamas, J. F., Chacón, E. and Mazadiego, L. F. (1999). Sources and pathways of trace elements in urban environment: A multi-elemental qualitative approach. Science of the Total Environment, 235, 355-357.

Denton, G. R. W., Bearden, B. G., Concepcion, L. P., Siegrist, H. G., Vann, D. T. and Wood, H. R. (2001). Contaminant Assessment of Surface Sediments from Tanapag Lagoon, Saipan, Water and Environmental Research Institute of the Western Pacific, Technical Report No. 93, University of Guam, Mangilao, Guam.

Denton, G. R. W., Wood, H. R., Concepcion, L. P., Siegrist, H. G., Eflin, V. S., Narcis, D. K. and Pangelinan, G. T. (1997). Analysis of In-Place Contaminants in Marine Sediments from Four Harbour Locations on Guam: A Pilot Study, Water and Environmental Research Institute of the Western Pacific, Technical Report No. 87, University of Guam, Mangilao, Guam.

De Schamphelaere, K. A. C. and Janssen, C. R. (2004). Development and field validation of a biotic ligand model predicting chronic copper toxicity to Daphnia magna. Environmental Toxicololgy and Chemistry, 23, 1365-1375.

Desenfant, F., Petrovsky, E. and Rochette, P. (2004). Magnetic signature of industrial pollution of stream sediments and correlation with heavy metals: case study from South France. Water, Air and Soil Pollution, 152 (1-4), 297-312.

Dessai, D. V. G. and Nayak, G. N. (2009). Distribution and speciation of selected metals in surface sediments, from the tropical Zuari estuary, central west coast of India. Environmental Monitoring and Assessment, 158, 117-137.

Dhage, S. S., Chandorkar, A. A., Kumar, R., Srivastava, A. and Gupta, I. (2006). Marine water quality assessment at Mumbai West Coast. Environment International, 32, 149-158.

Dicks, D. M. and Allen, M. E. (1983). Correlation of copper distribution in a freshwater sediment system to bioavailability. Bulletin of Environmental Contamination and Toxicology, 30, 37-43.

Dollar, N. L., Souch, C. J., Filippelli, G. M. and Mastalerz, M. (2001). Chemical fractionation of metals in wetland sediments: Indiana Dunes National Lakeshore. Environmental Science and Technology, 35, 3608-3615.

Dolphin, T. J., Hume, T. M. and Parnell, K. E. (1995). Oceanographic processes and sediment mixing on a sandflat in an enclosed sea, Manukau Harbour, New Zealand. Marine Geology, 128, 169-181.

Durve, V. S. and Bal, D. V. (1961). Hydrology of Kalwa Backwaters and Adjoining Area. Journal of University of Bombay, 29, 39-48.

Durza, O. (1999). Heavy metals contamination and magnetic susceptibility in soils around metallurgical plan. Physics and Chemistry of the Earth. Part A: Solid Earth and Geodesy, 24 (6), 541-543.

Eimers, M. C., Evans, R. D. and Welbourn, P. M. (2002). Partitioning and bioaccumulation of cadmium in artificial sediment systems, Applications of a stable isotope tracer technique. Chemosphere, 46, 543-551.

Eggleton, J. and Thomas, K. V. (2004). A review of factors affecting the release and bioavailability of contaminants during sediment disturbance events. Environment International, 30, 973-980.

Erickson, R. J., Benoit, D. A., Mattson, V. R., Nelson, Jr., H. P. and Leonard, E. N. (1996). The effects of water chemistry on the toxicity of copper to fathead minnows, Environmental Toxicology and Chemistry, 15, 181-193.

Essien, J. P., Antai, S. P. and Olajire, A. A. (2009). Distribution, seasonal variations and ecotoxicological significance of heavy metals in sediments of Cross River Estuary mangrove swamp. Water, Air and Soil Pollution, 197, 91-105.

Evans, M. and Heller, F. (2003). Environmental Magnetism. Principles and Applications of Enviromagnetics, vol. 86. Academic Press. An imprint of Elsevier Science, International Geophysics Series.

Fang, G. and Yang, H. (2010). Heavy Metals in the River Sediments of Asian Countries of Taiwan, China, Japan, India, and Vietnam during 1999-2009. Environmental Forensics, 11, 201-206.

Farmer, J. G. and Lovell, M. A. (1984). Massive diagenetic enhancement of manganese in Loch Lomond sediments. Environmental Technology letters, 5, 257-270.

Fenchel, T. (1996). Worm burrows and oxic microniches in marine sediments. 2. Distribution patterns of ciliated protozoa. Marine Biology, 127, 297-301.

Feng, H., Han, X., Zhang, W. and Yu, L. (2004). A preliminary study of heavy metal contamination in Yangtze River intertidal zone due to urbanization. Marine Pollution Bulletin, 49, 910-915.

Fergusson, J. E. (1990). The Heavy Elements: Chemistry, Environmental Impact and Health Effects, Pergamon Press, Oxford, England.

Fernandes, H. M. (1997). Heavy metal distribution in sediments and ecological risk assessment: the role of diagenetic processes in reducing metal toxicity in bottom sediment. Environmental Pollution, 97, 317-325.

Fernandes, L. and Nayak, G. N. (2009). Distribution of sediment parameters and depositional environment of mudflats of Mandovi estuary, Goa, India. Journal of Coastal Research, 25, 273-284.

Fernandes, L. and Nayak, G. N. (2012b). Geochemical assessment in a creek environment: Mumbai, west coast of India. Environmental Forensics, 13, 43-54.

Fernandes, L. and Nayak, G. N. (2012a). Heavy metals contamination in mudflat and mangrove sediments (Mumbai, India). Chemistry and Ecology, 1-21.

Fernandes, L. and Nayak, G. N. (2010). Sources and Factors Controlling the Distribution of Metals in Mudflat Sedimentary Environment, Ulhas Estuary, Mumbai. Indian Association of Sedimentologists, 29, 71-83.

Fernandes, L., Nayak, G. N. and Ilangovan, D. (2012). Geochemical Assessment of Metal Concentrations in Mangrove Sediments along Mumbai Coast, India. International Journal of Civil and Geological Engineering, 6, 15-20.

Fernandes, L., Nayak, G. N., Ilangovan, D. and Borole, D. V. (2011). Accumulation of sediment, organic matter and trace metals with space and time, in a creek along Mumbai coast, India. Estuarine, Coastal and Shelf Science, 91, 388-399.

Fernandez, J. A. (2000). An extended study of heavy metal deposition in Galicia (NW Spain) based on moss analysis. Science of the Total Environment, 254, 31-34.

Filgueiras, A. V., Lavilla, I. and Bendicho, C. (2002). Chemical sequential extraction for metal partitioning in environmental solid samples. Journal of Environmental Monitoring, 4, 832-857.

Finkelman, R. B. (2005). Sources and Health Effects of Metals and Trace Elements in our Environment: An Overview in T.A. Moore, A. Black, J.A. Centeno, J.S. Harding, D. A. Trumm (ed.), Metal Contaminants in New Zealand, Resolutionz Press, Christchurch, New Zealand, 25-46p.

Finney, B. P. and Huy, C. (1989). History of metal pollution in the Southern California Bight: an update. Environmental Science and Technology, 23, 294-303.

Fischer, R., Wol, F. C., Rahner, D., Paul, L., Deppe, T. and Steinberg, C. E. W. (2004). Fixation of manganese and iron in freshwater sediments through electrochemically initiated processes I: Principles and laboratory studies. Aquatic Science, 66 (1), 95-102.

Flanders, P. (1994). Collection, measurements and analysis of airborn magnetic particulates from pollution in the environment. Journal of Applied Physics, 75, 5931-5936.

Flemming, B. W. (2000). A revised textural classification of gravel-free muddy sediments on the basis of ternary diagrams. Continental Shelf Research, 20, 1125-1137.

Fletcher, C. A., Bubbs, J. M. and Lester, J. N. (1994). Magnitude and distribution of contaminants in five salt marshes on the Essex coast, United Kingdom I. Addressing the problem, site description and physic-chemical parameters. Science of the Total Environment, 155, 312-345.

Flynn, W. (1968). The determination of low levels of polonium-210 in environmental samples. Analytica Chimica Acta, 43, 221-227.

Folk, R. L. (1974). Petrology of sedimentary rocks. Hemphill, Austin, Texas, 177p.

Ford, R. G., Bertsch, P. M. and Farley, K. J. (1997). Changes in transition and heavy metal partitioning during hydrous iron oxide aging. Environmental Science and Technology, 31(7), 2028-2033.

Forstner, U. and Muller, G. (1974). Schwermetalle in Flussen und Seen. Springer, Berlin.

Forstner, U. and Wittmann, G. T. W. (1979). Metal pollution in the aquatic environment. Springer, Berlin, 386p.

Forstner, U. and Wittman, G. T. W. (1981). Metal Pollution in the Aquatic Environment, 2nd edn. Springer-Verlag, Berlin, 486p.

Fox, L. E. and Wofsy, S. C. (1983). Kinetics of removal of iron colloids from estuaries. Geochimica et Cosmochimica Acta, 47, 211-216.

Fuentes, A., Lloréns, M., Sáez, J., Aguilar, Ma. I., Ortuño, J. F. and Meseguer, V. F. (2008). Comparative study of six different sludges by sequential speciation of heavy metals. Bioresource Technology, 99, 517-525.

Furness, R. W. and Rainbow, P. S. (2000). Heavy Metals in the Marine Environment, in R. W. Furness & P. S. Rainbow (ed.), Heavy Metals in the Marine Environment, CRC Press, Inc, Florida, United States of America, 1-3p.

Gallon, C., Tessier, A., Gobeil, C. and Beaudin, L. (2005). Sources and chronology of atmospheric lead deposition to a Canadian Shield lake: inferences from Pb isotopes and PAH profiles. Geochimica et Cosmochimica Acta, 69, 3199-3210.

Gallon, C., Tessier, A., Gobeil, C. and Carignan, R. (2006). Historical perspective of industrial lead emissions to the atmosphere from a Canadian smelter. Environmental Science and Technology, 40, 741-747.

Gambrell, R. P. (1994). Trace and Toxic Metals in Wetlands - A Review. Journal of Envionmental Quality, 23, 883-891.

Gangaiya, P., Tabudravu, J., South, R. and Sotheeswaran, S. (2001). Heavy metal contamination of the Lami coastal environment, Fiji, South Pacific. Journal of Natural Science, 19, 24-29.

Garcia, C. A. B., Barreto, M. S., Passos, E. A. and Alves, J. P. H. (2009). Regional Geochemical Baselines and Controlling Factors for Trace Metals in Sediments from the Poxim River, Northeast Brazil. Journal of Brazilian Chemical Society, 20(7), 1334-1342.

Gautam, P., Blaha, U., Appel, E. and Neupane, G. (2004). Environmental magnetic approach towards the quantification of pollution in Kathmandu urban area, Nepal. Physics and Chemistry of the Earth, 29(13-14), 973-984.

Gersberg, R. M., Trindade, F. and Nordby, C. (1989). Heavy metals in sediments and fish of the Tijuana Estuary. Journal of Border Health, 5, 5-15.

Ghrefat, H. A., Abu-Rukah, Y. and Rosen, M. A. (2011). Application of geoaccumulation index and enrichment factor for assessing metal contamination in the sediments of Kafrain Dam, Jordan. Environmental Monitoring and Assessment, 178, 95-109.

Ghrefat, H. and Yusuf, N. (2006). Assessing Mn, Fe, Cu, Zn, and Cd pollution in bottom sediments of Wadi Al-Arab Dam, Jordan. Chemosphere, 65, 2114-2121.

Giesy, J. P. and Hoke, R. A. (1990). Freshwater sediment quality criteria: Toxicity bioassessment. In Sediments: Chemistry and Toxicity of In-Place Pollutants (Baudo, R., Giesy, J., and Muntau, H., Eds), CRC Press Inc, Boca Raton, FL, 265-332p.

Goddu, S. R., Appel, E., Jordanova, D. and Wehland, F. (2004). Magnetic properties of road dust from Visakhapatnam (India) - relationship to industrial pollution and road traffic. Physics and Chemistry of the Earth, 29, 985-995.

Godoy, J. M., Moreira, I., Wanderley, W., Simões Filho, F. F. L. and Mozeto, A. A. (1998). An alternative method for the determination of excess ^{210}Pb in sediments. Radiation Protection Dosimetry, 75, 111-115.

Golterman, H. (2004). Chemistry of phosphate and nitrogen compounds in sediments. Dordrecht: Kluwer.

Gonzalez, H. and Brugmann, L. (1991). Heavy metals in littoral deposits off Havana City, Cuba. Chemistry and Ecology 5, 171-179.

Gonzalez, M. J., Ramos, L. and Hernandez, L. M. (1994). Distribution of trace metals in sediments and relationship with their accumulation in earthworms. International Journal of Environmental Analytical Chemistry, 57, 135-150.

Grant, J. A. (1986). The isocon diagram - a simple solution to Gresens' equation for metasomatic alteration. Economic Geology, 81, 1976-1982.

Grant, J. A. (2005). Isocon analysis: A brief review of the method and applications, Element and Isotope Mobility during Water-Rock Interaction Processes (Dini, A., Corteel, C. And Deyhle, A., eds.). Physics and Chemistry of the Earth, 30(17-18), 997-1004.

Grasshoff, K. (1999). Methods of Seawater Analysis, Verlag Chemie, Weinheim, 205p.

Guerra-Garcia, J. M. and Garcia-Gomez, J. C. (2005). Assessing pollution levels in sediments of a harbour with two opposing entrances. Environmental implications, Journal of Environmental Management, 77(1), 1-11.

Guevara-Riba, A., Sahuquillo, A., Rubio, R. and Rauret, G. (2004). Assessment of metal mobility in dredged harbour sediments from Barcelona (Spain). Science of the Total Environment, 321, 241-255.

Guieu, C., Martin, J. M., Tankere, S. P. C., Mousty, F., Trincherini, P., Bazot, M. and Dai, M. H. (1998). On trace metal geochemistry in the Danube River and Western Black Sea. Estuarine, Coastal and Shelf Science, 47 (14), 471-485.

Guo, B., Zhu, R. X., Bai, L. X. and Florindo, F. (2001). Rock magnetic properties of a loess/palaeosol couple along an N-S transect in Chinese Loess Plateau. Science of China (D), 44, 1099-1109.

Guo, T. Z., Delaune, R. D. and Patrick, W. V. (1997). The effect of sediment redox chemistry on solubility-chemically active forms of selected metals in bottom sediments receiving produced water discharge spill. Science and Technology Bulletin, 4, 165-175.

Hanesch, M. and Scholger, R. (2002). Mapping of heavy metal loadings in soils by means of magnetic susceptibility measurements. Environmental Geology, (42), 857-870.

Hanesch, M., Scholger, R. and Dekkers, M. (2001). The application of fuzzy c-means cluster analysis and non-linear mapping to a soil data set for the detection of polluted sites. Physics and Chemistry of the Earth, 26, 885-891.

Hanesch, M., Scholger, R. and Rey, D. (2003). Mapping dust distribution around an industrial site by measuring magnetic parameters of tree leaves. Atmospheric Environment, 37, 5125-5133.

Hani, A. and Kariminejad, M. (2010). Toxic Metal Distribution in Soils of Kaveh Industrial City, Iran**.** World Applied Sciences Journal, 8 (11), 1333-1342.

Hargrave, B. T., Philips, G. A., Doucette, L. I., White, M. J., Milligan, T. G., Wildish, D. J. and Cranston, R. E. (1997). Assessing benthic impacts of organic enrichment from marine aquaculture. Water, Air and Soil Pollution, 99, 641-650.

Harikumar, P. S and Jisha, T. S. (2010). Distribution pattern of trace metal pollutants in the sediments of an urban wetland in the southwest coast of India. International Journal of Engineering Science and Technology, 2(5), 840-850.

Harrington, J. M., Laforce, M. J., Rember, W. C. and Fendorf, S. E. (1998). Phase association and mobilization of iron and trace elements in Coeur d'Alene lake, Idaho. Environmental Science and Technology, 32, 65-656.

Hatje, V., Apte, S. C., Hales, L. T. and Birch, G. F. (2003). Dissolved trace metal distribution in Port Jackson estuary (Sydney Harbour), Australia. Marine Pollution Bulletin, 46, 428-434.

Hay, K. L., Dearing, J. A., Baban, S. M. J. and Loveland, P. J. (1997). A preliminary attempt to identify atmospherically–derived pollution particles in English topsoils from magnetic susceptibility measurements. Physics and Chemistry of the Earth, 22, 207-210.

Hedges, J. and Keil, R. (1995). Sedimentary organic matter preservation: an assessment and speculative synthesis. Marine Chemistry, 49, 81-115.

Heltai, G., Percsich, K., Halász, G., Jung, K. and Fekete, I. (2005). Estimation of ecotoxicological potential of contaminated sediments based on a sequential extraction procedure with supercritical CO_2 and subcritical H_2O solvents. Microchemical Journal, 79, 231-237.

Herreweghe, S. V., Swennen, R., Cappuyns, V. and Vandecasteele, C. (2002). Chemical associations of heavy metals and metalloids in contaminated soils near former ore treatment plants: a differentiated approach with emphasis on pH statleaching. Journal of Geochemical Exploration, 76, 113-138.

Heugens, E. H., Jager, T., Creyghton, R., Kraak, M. H., Hendriks, A. J., Van Straalen, N. M. and Admiraal, W. (2003). Temperature-dependent effects of cadmium on Daphnia magna: accumulation versus sensitivity. Environmental Science and Technology, 37, 2145-2151.

Higgitt, S. R., Oldfield, F. and Appleby, P. G. (1991). The record of land use change and soil erosion in the late Holocene sediment of the Petit Lac d'Annecy, Eastern France. The Holocene, 1, 14-28.

Hirose, K. (2006). Chemical speciation of trace metals in seawater: a review. Analytical Sciences, 22(8), 1055-1063.

Hoffmann, V., Knab, M. and Appel, E. (1999). Magnetic susceptibility mapping of roadside pollution. Journal of Geochemical Exploration, 66 (1-2), 313-326.

Ho, H. H., Swennen, R. and Damme, V. (2010). Distribution and contamination status of heavy metals in estuarine sediments near Cua Ong harbour, Ha long bay, Vietnam. Geologica Belgica, 13(1-2), 37-47.

Hornberger, M. I., Luoma, S. N., Van Geen, A., Fuller, C. and Anima, R. (1999). Historical trends of metals in the sediments of San Francisco Bay, California. Marine Chemistry, 64, 39-55.

Horng, C. S., Huh, C. A., Chen, K. H., Huang, P. R., Hsiung, K. H. and Lin, H. L. (2009). Air pollution history elucidated from anthropogenic spherules and their magnetic signatures in marine sediments offshore of southwestern Taiwan. Journal of Marine Systems, 76, 468-478.

Horowitz, A. J. and Elrick, K. A. (1987). The relation of stream sediment surface area, grain size and composition to trace element chemistry. Applied Geochemistry, 2, 437-451.

Horowitz, A. J. (1991). A Primer on Sediment-trace Element Chemistry, second ed. Lewis Publishers Inc., Chelsea, Michigan.

Horowitz, A. J., Elrick, K. A. and Hooper, R. P. (1989). The prediction of aquatic sediment-associated trace element concentrations using selected geochemical factors. Hydrological Processes, 3, 347-364.

Horowitz, A. J., Meybeck, M., Idlafkih, Z. and Biger, E. (1999). Variations in trace element geochemistry in the Seine River Basin based on floodplain deposits and bed sediments. Hydrological Processes, 13, 1329-1340.

Horsfall, M. and Spiff, A. I. (2005). Speciation and bioavailability of heavy metals in sediment of Diobu River, Port Hanourt, Nigeria. European Journal of Scientific Research, 60, 20-26.

Hou, X., Parent, M., Savard, M. M., Tassé, N., Bégin, C. and Marion, J. (2006). Lead concentrations and isotope ratios in the exchangeable fraction: tracing soil contamination near a copper smelter. Geochemistry: Exploration Environment Analysis, 6, 229-236.

Huan, F., Weiguo, Z., Li, J., Michael, P. W., Qiufeng, Z., Dekui, Y., Jianhua, T. and Lizhong, Yu. (2010). Short- and long-term sediment transport in western Bohai Bay and coastal areas. Chinese Journal of Oceanology and Limnology, 28 (3), 583-592.

Huang, K. and Lin, S. (2003). Consequences and implications of heavy metal spatial variations in sediments of the Keelung River drainage basin, Taiwan. Chemosphere, 53, 1113-1121.

Huerta-Diaz, M. A., Tessier, A. and Carignan, R. (1998). Geochemistry of trace metals associated with reduced sulphur in freshwater sediments. Applied Geochemistry, 13, 213-233.

Hung, T. C., Meng, P. J. and Wu, S. J. (1993). Species of copper and zinc in sediments collected from the Antarctic Ocean and the Taiwan Erhjin Chi coastal area. Environmental Pollution, 80, 223-230.

Hunt, A., Jones, J. and Oldfield, F. (1984). Magnetic measurement and heavy metals in atmospheric particulates of anthropogenic origin. Science of the Total Environment, 33, 129-139.

Hussein, A. H. and Rabenhorst, M. C. (2001). Tidal inundation of transgressive coastal areas: pedogenesis of salinization and alkalinization. Soil Science Society of America Journal, 65, 536-544.

Hu, X. F., Su, Y., Ye, R., Li, X. Q. and Zhang, G. L. (2007). Magnetic properties of the urban soils in Shanghai and their environmental implications. Catena, 70, 428-436.

IMD (2007). Annual climate summary 2007: Indian Meteorological Department, Govt. of India, Pune, India, 27p.

Ingersoll, C. G., Macdonald, D. D., Ning, W., Judy, L. C., Field L. J., Pam, S. H., Nile, E. K., Rebekka, A. L., Corinne, S. and Dawn, E. S. (2000). Prediction of sediment toxicity using consensus-based freshwater sediment quality guidelines. United States Geological Survey (USGS) final report for the U.S. Environmental Protection Agency (USEPA), Great Lakes National Program Office (GLNPO).

Ip, C. C. M., Xi, X. D., Zhang, G., Wai, O. W. H. and Li, Y. S. (2007). Trace metal distribution in sediments of the Pearl River Estuary and the surrounding coastal area, South China. Environmental Pollution, 147(2), 311-323.

Isuare, M., Manceau, A., Geoffrey, N., Laboudigue, A. and Tamura, N. (2005). Zinc mobility and speciation in soil covered by contaminated dredged sediment using micrometer-scale and bulk-averaging X-ray fluorescence, absorption and diffraction techniques. Geochimica et Cosmochimica Acta, 69(5), 1173-1198.

Iwegbue, C. M. A. (2011). Chemical fractionation of metals in core sediments of Orogodo River, southern Nigeria. Toxicological and Environmental Chemistry, 93(7), 1341-1358.

Iwegbue, C. M. A., Eghwrudje, M. O., Nwajei, G. E. and Egboh, S. H. O. (2007). Chemical speciation of heavy metals in the Ase River sediment, Niger Delta, Nigeria. Chemical Speciation and Bioavailibility, 19(3), 117-127.

Izquierdo, C., Usero, J. and Gracia, I. (1997). Speciation of heavy metals in sediments from salt marshes on the southern Atlantic coast of Spain. Marine Pollution Bulletin, 34(2), 123-128.

Jackson, M. L. (1958). Soil chemical analysis. New York: Prentice Hall.

Jackson, T. A. (1998). Mercury in aquatic ecosystems. In: Langston, W.J., Bebianno, M.J. (Eds.), Metal Metabolism in Aquatic Environments. Chapman & Hall, London, 77-138p.

Jagtap, T. G., Untawale, A. G. and Inamdar, S. N. (1994). Study of mangrove environment of Maharashtra coast using remote sensing data. Indian Journal of Marine Sciences, 23(2), 90-93.

Jain, C. K., Gurunadha Rao, V. V. S., Prakash, B. A., Mahesh Kumar, K. and Yoshida, M. (2010). Metal fractionation study on bed sediments of Hussainsagar Lake, Hyderabad, India. Environmental Monitoring and Assessment, 166, 57-67.

Jain, C. K. (2004). Metal fractionation study on bed sediments of River Yamuna, India. Water Research, 38(3), 569-578.

Jarvis, I. J. and Jarvis, K. (1985). Rare earth element geochemistry of standard sediments: a study using inductively coupled plasma spectrometry. Chemical Geology, 53, 335-344.

Jenne, F. A. (1968). Controls of Mn, Fe, Co, Ni, Cu and Zn concentrations in the soils and water: The significance of hydrous Mn and Fe oxides, in: R. F. Gould (ed.), Trace in Organics in the Waters, Advances in Chemistry Series 73,Washington DC, American Chemistry Society, 337-387p.

Jenny, H. (1941). Factors of Soil Formation. A System of Quantitative Pedology. Dover, New York.

Jha, S. K., Chavan, S. B., Pandit, G. G. and Sadasivan, S. (2003). Geochronology of Pb and Hg pollution in a coastal marine environment using global fallout 137-Cs. Journal of Environmental Radioactivity, 69, 145-157.

Jha, S. K., Krishnamoorthy, T. M., Pandit, G. G. and Nambi, K. S. V. (1999). History of accumulation of mercury and nickel in Thane Creek, Mumbai, using ^{210}Pb dating technique. Science of the Total Environment, 236, 91-99.

Jonasson, I. R. (1977). Geochemistry of sediment/water interactions of metals, including observations on availability. In Fluid Transport of Sediment-associated Nutrients and Contaminants, eds H. Shear and A. E. P. Watson, pp. 255-271. IJC/PLUARG, Windsor (Ontario).

Jones, R. W. (1987). Organic facies. In: Brooks, J., Welte, D. (Eds.), Advances in Petroleum Geochemistry. Academic Press, New York, 1-90p.

Jones, B. and Turki, A. (1997). Distribution and speciation of heavy metals in surficial sediments from the Tees Estuary, north-east England. Marine Pollution Bulletin, 34, 768-779.

Jouanneau, J. M., Ethcheber, H. and Latouche, C. (1983). Improvishment and decrease of metallic elements associated with suspended matter in the Gironde estuary. In proceedings of a NATO Advanced Conference on trace metals in Seawater, (eds) C. S. Wong, E. Boyle, K.W.

Kaasalainen, M. and Yli-Halla, M. (2003). Use of sequential extraction to assess metal partitioning in soils. Environmental Pollution, 125, 225-233.

Kapicka, A., Petrovsky, E., Ustjak, S. and Machackova, K. (1999). Proxy mapping of fly ash pollution of soils around a coal-burning power plant: a case study in the Czech Republic. Journal of Geochemical Exploration, 66, 291-297.

Karbassi, A. R., Bayati, I. and Moattar, F. (2006). Origin and chemical partitioning of heavy metals in riverbed sediments. International Journal of Environmental Science and Technology, 3(1), 35-42.

Karczewska, A. (1996). Metal species distribution in top and sub-soil in an area affected by copper smelter emissions. Applied Geochemistry, 11, 35-42.

Karlin, R. and Levi, S. (1983). Diagenesis of magnetic minerals in recent hemipelagic sediments. Nature, 303, 327-330.

Karlin, R., Lyle, M. and Health, G. R. (1987). Authigenic magnetite formation in suboxic marine-sediments. Nature, 326, 490-493.

Keil, R. G., Montlucon, D. B., Prahl, F. R. and Hedges, J. I. (1994). Sorptive preservation of labile organic matter in marine sediments, Nature, 370, 549-552.

Kennish, M. J. (1998). Trace metal-sediment dynamics in estuaries: pollution assessment. In: Ware, G.W. (Ed.), Review Environmental Contamination Toxicology, vol. 155. Springer, Berlin, 69-110p.

Kersten, M. and Smedes, F. (2002). Normalization procedures for sediment contaminants in spatial and temporal trend monitoring. Journal of Environmental Monitoring, 4, 109-115.

Knab, M., Appel, E. and Hoffman, V. (2001). Separation of the anthropogenic portion of heavy metal contents along a highway by means of magnetic susceptibility and fuzzy C-means cluster analysis, European Journal of Environment Engineering and Geophysics, 6, 125-140.

Kotoky, P., Bora, B. J., Baruah, N. K., Baruah, J., Baruah, P. and Borah, G. C. (2003). Chemical fraction of heavy metals in soils around oil installation, Assam. Chemical Speciation and Bioavailability 15(4), 115-125.

Kristensen, E. (2000). Organic matter diagenesis at the oxic/anoxic interface in coastal marine sediments, with emphasis on the role of burrowing animals. Hydrobiologia, 426, 1-24.

Krumgalz, B. S., Fainshtein, G. and Cohen, A. (1992). Grain size effect on anthropogenic trace metals and organic matter distribution in marine sediments. Science of the Total Environment, 116, 15-30.

Kukier, U., Ishak, Ch. F., Sumner, M. E. and Miller, W. P. (2003). Composition and element solubility of magnetic and non-magnetic fly ash fractions. Environmental Pollution, 123, 255-266.

Kulkarni, V. A., Jagtap, T. G., Mhalsekar, N. M. and Naik, A. N. (2010). Biological and environmental characteristics of mangrove habitats from Manori creek, West Coast, India. Environmental Monitoring and Assessment 168 (1-4), 587-596.

Kumar, A., Kaur, I. and Mathur, R. P. (1998). Water quality and metal enrichment in bed sediments of the rivers Kali and Hindon, India. Environmental Geochemistry and Health, 20, 53-60.

Kumarsingh, K., Hall, L. A., Chang, A. M. and Stoute, V. A. (1998). Phosphorus in sediments of a shallow bank influenced by sewage and sugar factory effluents in Trinidad, West Indies. Marine Pollution Bulletin, 36, 185-192.

Kuo, S., Heilman, P. E. and Baker, A. S. (1983). Distribution and forms of copper, zinc cadmium, iron and manganese in soils near a copper smelter. Soil Science, 135, 101-119.

Lacuraj, C. and Maria, S. (2006). Geochemical index of trace metals in the surficial sediments from the western continental shelf of India, Arabian Sea. Environmental and Geochemical Health, 28, 509-518.

Lala, K. D. (2004). Water Supply of Thane Municipal Corporation, Proceedings of One Day Seminar on-Pollution of Water Bodies In urban Area (case Study), Vidya Prasarak Mandal's Polytechnic, Thane. Sponsored by AICTE, N. Delhi, 6-9p.

Lamb, A. L., Wilson, G. P. and Leng, M. J. (2006). A review of coastal palaeoclimate and relative sea-level reconstructions using $\delta^{13}C$ and C/N ratios in organic material. Earth-Science Review, 75, 29-57.

Lasheen, M. R. and Ammar, N. S. (2009). Assessment of metals speciation in sewage sludge and stabilized sludge from different wastewater treatment plants, Greater Cairo. Egypt. Journal of Hazardous Material, 164, 740-749.

Laslett, R. E. and Balls, P. W. (1995). The behaviour of dissolved Mn, Ni and Zn in the Forth, an industrialized, partially mixed estuary. Marine Chemistry, 48, 311-328.

Laxen, D. P. H. (1983). The Chemistry of Metal Pollution in water. In Pollution causes, effects and control (ed.), Roy. M. Horrison, The Royal Society of Chemistry, London, WIVOBN, 104p.

Lecoanet, H., Leveque, F. and Ambrosi, J. P. (2003). Combination of magnetic parameters: an efficient way to discriminate soil-contamination sources (south France). Environmental Pollution, 122, 229-234.

Lee, S. V. and Cundy, A. B. (2001). Heavy metal contamination and mixing processes in sediments from the Humber estuary, Eastern England. Estuarine, Coastal and Shelf Science, 53, 619-636.

Lepane, V., Morriset, M., Viitak, A., Laane, M. and Alliksaar, T. (2010). Partitioning of metals between operational fractions in the sediment record from Lake Peipsi. Chemistry and Ecology, 26(4), 35-48.

Lepland, A. and Stevens, R. L. (1996). Mineral magnetic and textural interpretations of sedimentation in the Skagerrak, eastern North Sea. Marine Geology, 135, 51-64.

Lin, C. H., Pedersen, J. A. and Suffet, I. H. (2003). Influence of aeration on hydrophobic organic contaminant distribution and diffusive flux in estuarine sediments. Chemosphere, 37(16), 3547-3554.

Liu, C., Yun, F., Xiao, B., Cho, S. J., Moon, Y. T., Morkoç, H., Abouzaid, M., Ruterana, R., Yu, K. M. and Walukiewicz, W. (2005). Structural analysis of ferromagnetic Mn-doped ZnO thin films deposited by radio frequency magnetron sputtering. Journal of Applied Physics, 97, 126107.

Liu, J., Zhu, R. and Li, G. (2003a). Rock magnetic properties of the fine-grained sediment on the outer shelf of the East China Sea: implication for provenance. Marine Geology, 193, 195-206.

Liu, W. X., Li, X. D., Shen, Z. G., Wang, D. C., Wai, O. W. H. and Li, Y. S. (2003b). Multivariate statistical study of heavy metal enrichment in sediments of the Pearl River Estuary. Environmental Pollution 121, 377-388.

Li, X. D., Wai, O. W. H., Li, Y. S., Coles, B. J., Ramsey, M. H. and Thornton, I. (2000a). Heavy metal distribution in the sediment profiles of the Pearl River Estuary, South China. Applied Geochemistry, 15, 567-581.

Li, X., Shen, Z., Wai, O. W. H. and Li, Y. (2000b). Chemical partitioning of heavy metal contaminants in sediments of the Pearl River Estuary. Chemical Speciation and Bioavailability, 12(1), 17-25.

Long, E. R., Field, L. J. and MacDonald, D. D. (1998). Predicting toxicity in marine sediments with numerical sediment quality guidelines. Environmental Toxicology and Chemistry, 17 (4), 714-727.

Long, E. R., MacDonald, D. D., Smith, S. L. and Calder, F. D. (1995). Incidence of adverse biological effects within ranges of chemical concentrations in marine and estuarine sediments. Environmental Management, 19, 81-97.

Loomb, C. A. M. (2001). Muddy Sedimentation in a Sheltered Estuarine Marine, Westpark Marina, Auckland, New Zealand, Thesis, The University of Waikato.

Lopez, A. M. (2002). Cattle as biomonitors of soil arsenic, copper, and zinc concentrations in Galicia (NW Spain). Archives of Environmental Contamination and Toxicology, 43, 103-108.

López-González, N., Borrego, J., Ruiz, F., Carro, B., Lozano-Soria, O. and Abad, M. (2006). Geochemical variations in estuarine sediments: Provenance and environmental changes (Southern Spain). Estuarine, Coastal and Shelf Science, 67, 313-320.

Lopez-Sanchez, J. F., Rubio, R., Samitier, C. and Rauret, G. (1996). Trace metal partitioning in marine sediments and sludges deposited off the coast of Barcelona (Spain). Water Research, 30, 153-159.

Loring, D. H. (1991). Normalization of heavy-metal data from estuarine and coastal sediments. ICES Journal of Marine Science, 48, 101-115.

Lu, J. I., Li, C. S., Wang, W. H. and Peng, A. (1983). Chemical behaviour of mercury in Ji Yun river. In Proceedings of International Conference of Heavy Metals in the Environment, Heidelberg, Edinburgh, CEP Consultants Ltd., 780-783.

Luoma, S. N. (1983). Bioavailability of trace metals to aquatic organisms: a review. Science of the Total Environment, 28, 1-23.

Luoma, S. (1990). Processes affecting metal concentrations in estuarine and coastal marine sediments. In R. Furness & P. Rainbow (Eds.), Heavy metals in the marine environment, Boca Raton, FL, USA: CRC, 51-66p.

Lu, S. G. (2003). Chinese Soil Magnetism and Environment. Beijing, China: Higher Education Press; (in Chinese).

Lu, S. G., Xue, Q. F., Zhu, L. and Yu, J. Y. (2008). Mineral magnetic properties of a weathering sequence of soils derived from basalts in eastern China. Catena, 73, 23-33.

MacDonald, D. D., Ingersoll, C. G. and Berger, T. A. (2000). Development and evaluation of consensus-based sediment quality guidelines for freshwater ecosystems. Archives of Environmental Contamination and Toxicology, 39, 20-31.

Madiseh, S. D., Savary, A., Parham, H. and Sabzalizadeh, S. (2009). Determination of the level of contamination in Khuzestan coastal waters (Northern Persian Gulf) by using an ecological risk index. Environmental Monitoring and Assessment, 159, 521-530.

Magiera, T., Strzyszcz, Z., Kapicka, A. and Petrovsky, E. (2006). Discrimination of lithogenic and anthropogenic influences on topsoil magnetic susceptibility in Central Europe. Geoderma, 130, 299-311.

Maher, B. A. and Taylor, R. M. (1988). Formation of ultrafine-grained magnetite in soils. Nature, 366, 368-370.

Maher, B. A. and Thompson, R. (1999). Quaternary Climates, Environments and Magnetism. Cambridge University Press, Cambridge.

Maher, B. A. (1986), Characterization of soils by mineral magnetic measurements. Physics of the Earth and Planetary Interiors, 42, 76-92.

Maher, B. A. (1988). Magnetic properties of some synthetic sub-micron magnetites in soils. Geophysical Journal of the Royal Astronomical Society, 94, 83-96.

Mance, G. (1987). Pollution Threat of Heavy Metals in Aquatic Environments, Elsevier Applied Science Publishers Ltd, New York, United States of America.

Manta, D. S., Angelone, M. and Bellanca, A. (2002). Heavy metals in urban soils: a case study from the city of Palermo (Sicily), Italy. Science of the Total Environment, 300, 229-243.

Marcet-Miramontes, P., Andrade-Couce, M. L. and Montero-Vilariño, M. J. (1997). Contenidoy enriquecimiento de metales en sedimentos de la Ría de Vigo (España). Thalassas, 13, 87-97.

Marchand, C., Disnar, J. R., Lallier-Verge's, E. and Lottier, N. (2005). Early diagenesis of carbohydrates and lignin in mangrove sediments subject to variable redox conditions (French Guiana). Geochimica et Cosmochimica Acta, 69, 131-142.

Martino, M., Turner, A., Nimmo, M. and Millward, G. E. (2002). Resuspension, reactivity and recycling of trace metals in the Mersey Estuary, UK. Marine Chemistry, 77, 171-186.

Massart, D. L., Vanderginste, B. G. M., Deming, S. N., Michotte, Y. and Kaufman, L. (1988). Chemometrics: A Textbook, Elsevier, Amsterdam.

Matagi, S. V., Swai, D. and Mugabe, R. (1998). A Review of Heavy Metals Mechanism in Wetlands. African Journal of Tropical Hydrobiology Fisheries, 8, 23-35.

Mcbride, M. B. (1994). Environmental Chemistry of Soils. Oxford University Press, New York.

McCaffrey, R. J. and Thomson, J. (1980). A record of the accumulation of sediment and trace metals in a Connecticut salt marsh. In Estuarine physics and chemistry: Studies in Long Island, ed. by B. Saltzman, New York: Academic Press, 165-236p.

McCready, S., Birch, G. F. and Long, E. R. (2006). Metallic and organic contaminants in sediments of Sydney Harbour, Australia and vicinity - a chemical dataset for evaluating sediment quality guidelines. Environment International, 32, 455-465.

McDonald, T. J., Mahlon, K. C., Rafalska, J. K. and Fox, R. G. (1991). Source and maturity of organic matter in glacial and Cretaceous sediments from Prydz Bay, Antarctica, ODP Holes 739C and 741A. In Barron, J., Larsen, B., et al., Proc. ODP, Sci. Results, 119: College Station, TX (Ocean Drilling Program), 407-416p.

MCGB (1979). Report to Municipal Corporation of greater Bombay upon methods for treatment and disposal of waste water from greater Bombay, Vol I (Metcalf and Eddy Inc and Environmental Engineering Consultants Joint Venture, Bombay), 5.1-5.5.

McLean, J. E. and Bledsoe, B. E. (1992). Behaviour of metals in soils. USEPA Ground Water Issue. EPA/540/S-92/018.

Mendil, D. and Uluözlü, O. D. (2007). Determination of trace metal levels in sediment and five fish species from lakes in Tokat, Turkey. Food Chemistry, 101, 739-745.

Mendiguchía, C., Moreno, C., Mánuel-Vez, M. P. and García-Vargas, M. (2006). Preliminary investigation on the enrichment of heavy metals in marine sediments originated from intensive aquaculture effluents. Aquaculture, 254, 317-325.

Metcalf and Eddy/EEC, (1979). Methods for treatment and disposal of waste water from Greater Bombay. Vol. I. Studies on waste water disposal and submarine outfall around Bombay. Project Report. National Institute of Oceanography, Bombay, 250p.

Meyers, P. A. and Lallier-Vergès, E. (1999). Lacustrine sedimentary organic matter records of Late Quaternary paleoclimates, Journal of Paleolimnology, 21, 345-372.

Meyers, P. A. (1997). Organic geochemical proxies of paleoceanographic, paleolimnologic and paleoclimatic processes. Organic Geochemistry, 27(5-6), 213-250.

Mil-Homens, M., Stevens, R. L., Cato, I. and Abrantes, F. (2007). Regional geochemical baselines for Portuguese shelf sediments. Environmental Pollution, 148(2), 418-427.

Miller, J. R., Hudson-Edwards, K. A., Macklin, M. G. and Lechner, P. J. (2000). Heavy metal contamination of the Pilcomayo River, Bolivia. In: Nriagu J (ed) Eleventh International Conference on Heavy Metals in the Environment (CD-ROM). University of Michigan, School of Public Health, Ann Arbor.

Mishra, V. (2002). Study of Macrofauna of Mangrove Mudflats of Ulhas River Estuary, Ph.D. Thesis, University of Mumbai. 253p.

Moalla, S. M. N., Awadallah, R. M., Rashed, M. N. and Soltan, M. E. (1997). Distribution and chemical fractionation of some heavy metals in bottom sediments of Lake Nasser. Hydrobiologica, 364, 31-40.

Mohapatra, B. C. and Rengarajan, K. (2000). Heavy metal toxicity in the Estuarine, Coastal and Marine Ecosystems of India. CMFRI Special Publication, 69, 121p.

Moore, J. N., Brook, E. J. and Johns, C. (1989). Grain size partitioning of metals in contaminated, coarse-grained river floodplain sediment: Clark Fork River, Montana. Environmental Geology and Water Research, 14, 107-115.

Moore, J. W. and Romamoorthy, S. (1984). Heavy metals in natural waters: applied monitoring an impact assessment, Springer-Verlag, New York.

Moreno, E., Sagnotti, L., Dinares-Turell, J., Winkler, A. and Cascella, A. (2003). Biomonitoring of traffic air pollution in Rome using magnetic properties of tree leaves. Atmosphere and Environment, 37, 2967-2977.

Morris, A. W. and Bale, A. J. (1981). Laboratory simulation of chemical processes induced by estuarine mixing; the behaviour of iron and phosphate in Estuaries. Estuarine, Coastal and Shelf Science, 13, 1-10.

Mortimer, R. J. G. and Rae, J. E. (2000). Metal speciation (Cu, Zn, Pb, Cd) and organic matter in oxic to suboxic salt marsh sediments, Severn Estuary, southwest Britain. Marine Pollution Bulletin, 40(5), 377-386.

MPCB (2005). Report on environment status of Mumbai region. Mumbai: Maharashtra Pollution Control Board.

Muller, B., Granina, L., Schaller, T., Ulrich, A. and Wehrli, B. P. (2002). As, Sb, Mo, and other elements in sedimentary Fe/Mn layers of Lake Baikal. Environmental Science and Technology, 36(3), 411-420.

Muller, G. (1979). Schwermetalle in den sedimenten des Rheins - Veranderungen seit (1971). Umschau, 79, 778-783.

Munksgaard, N. C. and Parry, D. L. (2001). Trace metals, arsenic and lead isotopes in dissolved and particulate phases of North Australian coastal and estuarine seawater. Marine Chemistry, 75, 165-184.

Murphy, J. and Riley, J. P. (1962). A modified single solution method for determination of phosphate in natural waters. Analytica Chimica Acta, 26, 31-36.

Murray, K. S., Cauvent, D., Lybeer, M. and Thomas, J. C. (1999). Particle size and chemical control of heavy metals in bed sediment from the Rouge River, southeast Michigan. Environmental Science and Technology, 33, 397-404.

Murray, W. (1987). Mechanisms controlling the distribution of trace elements in oceans and lakes. Advances in Chemistry Series, 216, 153-184.

Mutsaddi, K. B. (1964). A Study of Gobioid, Boleopthalmus Dussumieri (Cuv. & Val.), Ph. D. Thesis, University Of Bombay, 11-45p.

Nadal, M., Schuhmacher, M. and Domingo, D. L. (2004). Metal pollution of soils and vegetation in an area with petrochemical industries. Science of the Total Environment, 321(1-3), 59-69.

Naidu, V. S. and Sarma, R. V. (2001). Numerical modelling of tide-induced currents in Thane Creek; West coast of India. Journal of Waterway, Port, Coastal, and Ocean Engineering, 127, 241-244.

Nedwell, S. F. (1997). Intraspecific variation in the responses to copper by two estuarine invertebrates. Unpublished Ph.D. thesis. University of Hull.

Nemati, K., Bakar, N. K. B., Abas, M. R. and Sobhanzadeh, E. (2011). Speciation of heavy metals by modified BCR sequential extraction procedure in different depths of sediments from Sungai Buloh, Selangor, Malaysia. Journal of Hazardous Materials, 192, 402-410.

Neser, G., Kontas, A., Unsalan, Esin Uluturhan, E., Altay, O., Darılmaz, E., Kucuksezgin, F., Tekogul, N. and Yercan, F. (2012). Heavy metals contamination levels at the Coast of Aliağa (Turkey) ship recycling zone. Marine Pollution Bulletin, 64, 882-887.

Ngaim, L. S. and Lim, P. E. (2001). Speciation patterns of heavy metals in tropical estuarine anoxic and oxidized sediments by different sequential extraction schemes. Science of the Total Environment, 275, 53-61.

Nies, D. H. (1999). Microbial heavy metal resistance. Applied Microbiology and Biotechnology, 51, 730-750.

NIO (1998). Flora and fauna in MbBT area. National Institute of Oceanography, Mumbai, 412p.

NIO (1994). Release of wastewater in Ulhas estuary and environmental impact predictions. National Institute of Oceanography, Goa, 190p.

Norvell, W. A. (1984). Comparison of chelating agents for metals in diverse soil materials. Soil Science Society of America Journal, 48, 1285-1292.

Oakley, S. M., Nelson, P. O. and Williamson, K. J. (1981). Model of trace-metal partitioning in marine sediments. Environmental Science and Technology, 15, 474-480.

O'Day, P. A., Carrol, S. A. and Waychunas, G. A. (1998). Rock– water interactions, controlling zinc, cadmium and lead concentrations in surface waters and sediments, UST ri-state mining district. 1. Molecular identification using X-ray absorption spectroscopy. Environmental Science and Technology, 32, 943-955.

Oldfield, F. (1999). Environment magnetism: the range of applications. In: Walden, J., Smith, J. P., Oldfield, F. (Eds.), Environmental magnetism, a practical guide, quaternary research association. Technical Guide, 6, 212-222p.

Oldfield, F., Hao, Q., Bloemendal, J., Gibbs-Eggar, Z., Patil, S. and Guo, Z. (2009). Links between bulk sediment particle size and magnetic grain-size: general observations and implication for Chinese loess studies. Sedimentology, 56, 2091-2106.

Olsen, C. R., Cutshall, N. H. and Larsen, I. L. (1982). Pollutant particle associations and dynamics in coastal marine environments: a review. Marine Chemistry, 11, 501-533.

OSPAR (1998). OSPAR guidelines for the Management of Dredged Material. Annex 43 (Ref. B-8.2) of Ministerial Meeting of the OSPAR Commission, 32p.

Ostrom, N. E. and Macko, S. A. (1992). Sources, cycling, and distribution of water column particulate and sedimentary organic matter in Northern Newfoundland Fjords and bays: A stable isotope study. Organic Matter-Productivity, Accumulation and Preservation in Recent and Ancient Sediments- (Whelan, J. and Farrington, J. W., eds.), Columbia Univ. Press, New York, 55-81p.

Otero, X. L. and Macias, F. (2002). Variation with depth and season in metal sulfides in salt marsh soils. Biogeochemistry, 61, 247-268.

Padmalal, D., Maya, K. and Seralathan, P. (1997). Geochemistry of Cu, Co, Ni, Zn, Cd and Cr in the surficial sediments of a tropical estuary, southwest coast of India: a granulometric approach. Environmental Geology, 31, 85-93.

Palanques, A., Dias, J. and Farran, M. (1995). Contamination of heavy metals in the suspended and surface sediment of the Gulf of Cadiz (Spain): the role of sources, currents, pathways and sinks. Oceanologica Acta, 18(4), 469-477.

Palanques, A., Masqué, P., Puig, P., Sanchez-Cabeza, J. A., Frignani, M. and Alvisi, F. (2008). Anthropogenic trace metals in the sedimentary record of the Llobregat continental shelf and adjacent Foix Submarine Canyon (northwestern Mediterranean). Marine Geology, 248, 213-227.

Parkhurst, D. (2004). PHREEQC, version 2.11. U.S. Geological Survey Water-Resources, Denver, Colorado.

Paropkari, A. Z., Topgi, R. S., Rao, C. M. and Murthy, P. S. N. (1980). Distribution of Fe, Mn, Ni, Co, Cu and Zn in non-lithogenous fractions of sediments of Gulf of Kutch. Indian Journal of Marine Science, 9, 54-56.

Patchineelam, S. M. and De Figueiredo, A. M. (2000). Preferential settling of smectite on the Amazon continental shelf. Geo-Marine Letters, 20, 37-42.

Patel, B., Bangera, V. S., Patel, S. and Balaoi, M. C. (1985). Heavy metals in Bombay Harbour Area. Marine Pollution Bulletin, 16, 22-28.

Patel, B., Mulay, C. D. and Ganguly, A. K. (1975). Radioecology of Bombay harbour- a tidal estuary. Estuarine, Coastal Marine Science, 3, 13-42.

Patil, A. R. (1982). Study of Heavy Metals (Cu, Cd & Hg) in the Aquatic Environment of Ulhas Mula-Mutha River. M.Sc Thesis, University of Mumbai.

Patrick, W. H., Gambrell, R. P. and Khalid, R. A. (1977). Physiochemical factors regulating solubility and bioavailability of toxic heavy metals in contaminates dredge sediment. Journal of Environmental Science and Health, 12, 475-492.

Pattan, J. N., Rao Ch, M., Higgs, N. C., Colley, S. and Parthiban, G. (1995). Distribution of major, trace and rare-earth elements in surface sediments of the Wharton Basin, Indian Ocean. Chemical Geology, 121(1-4), 201-215.

Pedersen, T. F. and Price, N. B. (1982). The geochemistry of manganese carbonate in Panama Basin sediments. Geochimica et Cosmochimica Acta, 46, 59-68.

Pejrup, M. (1988). The triangular diagram used for classification of estuarine sediments: a new approach. In de Boer, P. L., van Gelder, A., Nios, S. D., (Eds), Tide – influenced sedimentary environments and facies. Reidel, Dordrecht, 289-300p.

Pempkowiak, J., Sikora, A. and Biernacka, E. (1999). Speciation of heavy metals in marine sediments vs their bioaccumulation by mussels. Chemosphere, 39(2), 313-321.

Perdue, E. M. and Koprivnjak, J. F. (2007). Using the C/N ratio to estimate terrigenous inputs of organic matter to aquatic environments. Estuarine, Coastal and Shelf Science, 73, 65-72.

Perez-Cid, B., Lavilla, I. and Bendicho, C. (1996). Analytical assessment of two sequential extraction schemes for metal partitioning in sewage sludge. Analyst, 121, 1479-1484.

Perin, G., Craboledda, L., Lucchese, M., Cirillo, R., Dotta, L., Zanette, M. L. and Orio, A. A. (1985). Heavy metal speciation in the sediments of Northern Adriatic sea - a new approach for environmental toxicity determination, in: T.D. Lekkas (Ed.). Heavy Metal in the Environment, 2, 454-456.

Peters, C. and Dekkers, M. J. (2003). Selected room temperature magnetic parameters as a function of mineralogy, concentration and grain size. Physics and Chemistry of the Earth, 28, 659-667.

Petersen, V., Willer, E. and Willamowski, C. (1997). Remobilization of trace elements from polluted anoxic sediments after resuspension in toxic water. Water, Air and Soil Pollution, 99, 515-522.

Petrovsky, E. and Ellwood, B. B. (1999). Magnetic monitoring of air- land- and water-pollution. In. Mahar, B.A. and Thompson, R. (eds.) Quaternary Climates, Environments and Magnetism, 279-322, Cambridge Univ. Press, Cambridge, 390p.

Petrovsky, E., Kapicka, A., Jordanova, N. and Boruvka, L. (2001). Magnetic properties of alluvial soils contaminated with lead, zinc and cadmium. Journal of Applied Geophysics, 48, 127-136.

Petrovsky, E., Kapicka, A., Zapletal, K., Sebestova, E., Spanila, T., Dekkers, M. J. and Rochette, P. (1998). Correlation between magnetic parameters and chemical composition of lake sediments from Northern Bohemia-preliminary study. Physics and Chemistry of the Earth, 23, 1123-1126.

Pizzarro, J., Aangelica Rubio, M. and Castill, X. (2003). Study of chemical speciation in sediment. An approach to vertical distribution of metal distribution in Rapel reservoir (Chile). Journal of Chilean Chemical Society, 48, 45-50.

Prasad, M. B. K., Ramanathan, A. L., Shrivastav, S. K., Anshumali and Saxena, R. (2006). Metal fractionation studies in surficial and core sediments in the Achankovil River basin in India. Environmental Monitoring and Assessment, 121, 77-102.

Praveena, S. M., Aris, A. Z. and Radojevic, M. (2010). Heavy Metals Dyanamics and Source in Intertidal Mangrove Sediment of Sabah, Borneo Island. EnvironmentAsia, 379-383.

Quadros, G., Sukumaran, S. and Athalye, R. P. (2009). Impact of the changing ecology on intertidal polychaetes in an anthropogenically stressed tropical creek, India. Aquatic Ecology, 43, 977-985.

Rabouille, C., Amouroux, D. and Jouanneau, P. A. J. (2007). Biogeochemical and contaminant cycling in sediments from human-impacted coastal lagoon- Introduction and summary. Estuarine, Coastal and Shelf Science, 72(3), 387-392.

Ram, A., Borole, D. V., Rokade, M. A. and Zingde, M. D. (2009). Diagenesis and bioavailability of mercury in the contaminated sediments of Ulhas estuary, India. Marine Pollution Bulletin, 58, 1685-1693.

Ram, A. (2004). Mercury burden in coastal marine sediments of northwest coast of India in relation to pollution, Ph.D. thesis, University of Mumbai.

Ram, A., Rokade, M. A. and Zingde, M. D. (1998). Mercury in sediments of Ulhas estuary. In: International conference on environmental science (abstract). Regional research laboratory, Trivandrum, 52p.

Ram, A., Rokade, M. A., Borole, D. V. and Zingde, M. D. (2003). Mercury in sediments of Ulhas estuary. Marine Pollution Bulletin, 46, 846-857.

Ramesh, R., Kumar, A., Inamdar, A. B., Mohan, P. M., Prithviraj, M. and Ramachandran, S. (2006). Tsunami characterization and mapping in Andaman and Nicobar islands, G.V. Rajamanickam (Ed.) 26th December 2004 tsunami causes, effects remedial measures, pre and post tsunami disaster management, a geoscientific perspective, New Delhi: New Academic Publisher, 150-174p.

Ramos, I., Hernandez, L. M. and Gonzalez, M. J. (1994). Sequential extraction of copper, lead, cadmium and zinc in the soil from or near Donana National Park. Journal of Environmental Quality, 23, 50-57.

Ramos, I., Gonzalez, M. J. and Hernandez, L. M. (1999). Sequential extraction of copper, lead, cadmium and zinc in sediments from Ebro River Spain: Relationship with levels detected in earthworms. Bulletin of Environmental Contamination and Toxicology, 63, 301-308.

Rao, V. P. and Rao, B. R. (1995). Provenance and distribution of clay minerals in the sediments of the western continental shelf and slope of India. Continental Shelf Research, 15, 1757-1771.

Ratheesh, K. C. S., Joseph, M. M., Gireesh Kumar, T. R., Renjith, K. R., Manju, M. N. and Chandramohanakumar, N. (2010). Spatial Variability and Contamination of Heavy Metals in the Inter-tidal Systems of a Tropical Environment. International Journal of Environmental Research, 4(4), 691-700.

Rathod, S. D. and Patil, N. N. (2009). Assessment of some hydrological parameters of Ulhas river estuary, in the vicinity of Thane city, Maharashtra state. Journal of Aquatic Biology, 24(2), 103-108.

Rathod S. D., Patil, N. N., Quadros, G. and Athalye, R. P. (2002). Qualitative Study of Fin Fish and Shell Fish Fauna of Thane Creek and Ulhas River Estuary. Proceeding of The National Seminar on creek, estuaries and mangroves - Pollution and Conservation, 135-141.

Ratuzny, T., Gong, Z. and Wilke, B. M. (2009). Total concentrations and speciation of heavy metals in soils of the Shenyang Zhangshi Irrigation Area, China. Environmental Monitoring and Assessment, 156 (1-4), 171-180.

Redfield, A. C., Ketchum, B. H. and Richards, F. A. (1963). The influence of organisms on the composition of sea-water. In: Hill N (ed) In the sea, 2nd edn. Wiley, New York, 26-77p.

Rees, J. G., Williams, T. M., Nguli, M. M., Kairu, K. K. and Yobe, A. C. (1996). Contaminant transport and storage in the estuarine creek systems of Mombasa, Kenya. British Geological Survey Technical Report WC/96/42, 67p.

Riba, I., DelValls, T. A., Forja, J. M. and Gómez-Parra, A. (2004). The influence of pH and Salinity values in the toxicity of heavy metals in sediments to the estuarine clam *Ruditapes philippinarum*. Environmental Toxicology and Chemistry, 23(5), 1100-1107.

Rijstenbil, J. W. and Gerringa, L. J. A. (2002). Interactions of algal ligands, metal complexation and availability, and cell responses of the diatom *Ditylum brightwellii* with a gradual increase in copper. Aquatic Toxicology, 56, 115-131.

Ritson, P. I., Esser, B. K., Niemeyer, S. and Flegal, A. R. (1994). Lead isotopic determination of historical sources of lead to Lake Erie, North America. Geochimica et Cosmochimica Acta, 58 (15), 3297-3305.

Rivaro, P., Grotti, M., Ianni, C. and Magi, E. (1998). Heavy metals distribution in the Eolian Basin (South Tyrrhenian Sea). Marine Pollution Bulletin, 36, 880-886.

Rokade, M. A. (2009). Heavy metal burden in coastal marine sediments of northwest coast of India in relation to pollution. PhD thesis, University of Bombay.

Rubio, B., Nombela, M. A. and Vilas, F. (2000). Geochemistry of major and trace elements in sediments of the Ria de Vigo (NW Spain): An assessment of metal pollution. Marine Pollution Bulletin, 40, 968-980.

Rubio, B., Pye, K., Rae, J. E. and Rey, D. (2001). Sedimentological characteristics, heavy metal distribution and magnetic properties in sub-tidal sediments, Ria de Pontevedra, NW Spain. Sedimentology, 48, 1277-1296.

Rullkötter, J. (2000). Organic matter: the driving force for early diagenesis. In: H.D. Schulz & M. Zabel (eds.). Marine Geochemistry. Springer-Verlag, Berlin, 129-172p.

Ryan, P. C., Hillier, S. and Wall, A. J., (2008). Stepwise effects of the BCR sequential chemical extraction procedure on dissolution and metal release from common ferromagnesian clay minerals: a combined solution chemistry and X-ray powder diffraction study. Science of the Total Environment, 407(1), 603-614.

Sahuquillo, A., Lopez-Sanchez, J. F., Rubio, R., Rauret, G., Thomas, R. P., Davidson, C. M. and Ure, A. M. (1999). Use of a certified reference material for extractable trace metals to assess sources of uncertainty in the BCR three-stage sequential extraction procedure. Analytica Chimica Acta, 382, 317-327.

Sangode, S. J., Vhatkar, K., Patil, S. K., Meshram, D. C., Pawar, N. J., Gudadhe, S. S., Badekar, A. G. and Kumaravel, V. (2010). Magnetic susceptibility distribution in the soils of Pune Metropolitan Region: implications to soil magnetometry of anthropogenic loading. Current Science, 98, 516-527.

Samuel, N. L. and Phillips, D. J. H. (1988). Distribution, variability and impacts of trace elements in San Francisco Bay. Marine Pollution Bulletin, 19, 413-425.

San-Miguel, E. G., Perez-Moreno, J. P., Bolıvar, J. P. and Garcıa-Tenorio, R. (2003). Validation of isotope signatures in sediments affected by anthropogenic inputs from uranium series radionuclides. Environmental Pollution, 123, 125-130.

Santschi, P. H., Hohener, P., Benoit, G. and Bucholtz Ten Brink, M. (1990). Chemical processes at the sediment-water interface. Marine Chemistry, 30, 269-315.

Santschi, P. H., Nixon, S., Pilson, M. and Hunt, C. (1984). Accumulation of sediments, trace metals (Pb, Cu) and total hydrocarbons in Narrangansett Bay, Rhode Island. Estuarine, Coastal and Shelf Science, 19, 427-449.

Sarkar, S. K., Franciskovic-Bilinski, S., Bhattacharya, A., Saha, M. and Bilinski, H. (2004). Levels of elements in the surficial estuarine sediments of the Hugli River, northeast India and their environmental implications. Environment International, 30(8), 1089-1098.

Sauve, S., Hendershot, W. and Allen, H. E. (2000). Solid-solution partition of metals in contaminated soils: Dependence on pH, total metal burden, and organic matter. Environmental Science and Technology, 34, 1125-1131.

Schlinder, P. W. (1991). The regulation of heavy metal concentrations in natural aquatic systems. In Heavy Metals in the Environment 1. (Ed) Vernet, J. P., Elsevier, Amsterdam, London, New York and Toyko, 95-124p.

Schneider, B. and Weiler, K. (1984). A quick grain size correction procedure for trace metal contents of sediments. Environmental Technology Letters, 5, 245-256.

Schofield, R. K. and Samson, H. R. (1954). Flocculation of kaolinite due to the attraction of oppositely charged crystal faces. Discussion of the Faraday Society, 18, 135-145.

Schottler, S. P. and Engstrom, D. R**.** (2006). A chronological assessment of Lake Okeechobee sediments using multiple dating markers. Journal of Paleolimnology, 36, 19-36.

Schropp, S. J. and Windom, H. L. (1988). A guide to the interpretation of metal concentrations in estuarine sediments. Coastal Zone Management Section, Department of Environmental Regulation, Florida, 74p.

Sedgwick, J. S. (2005). Contamination and Remediation of Soil at a Former Orchard Site, Hamilton, North Island, New Zealand, Thesis, The University of Waikato.

Seralathan, P., Srinivasalu, S., Ramanathan, A. L., Rajamanickam, G.V., Nagendra, R. and Singarasubramanian, S. R. (2006). Post tsunami sediments characteristics of Tamilnadu Coast, G. V. Rajamanickam (Ed.), 26th December 2004 tsunami causes, effects remedial measures, pre and post tsunami disaster management, a geoscientific perspective, New Delhi: New Academic Publisher, 124- 149p.

Sharma, P., Borole, D. V. and Zingde, M. D. (1994). 210-Pb geochronology and trace element composition of the sediments in the vicinity of Bombay, west coast of India. Marine Chemistry, 47, 227-241.

Shaw, T. J., Gieskes, J. M. and Jahnke, R. A. (1990). Early diagenesis in differing depositional environments: the responses of transition metals in pore water. Geochimica et Cosmochimica Acta, 54, 1233-1246.

Shea, D. (1988). Developing National Sediment Quality Criteria. Environmental Science and Technology, 11, 1256-1261.

Sheets, R. W. and Lawrence, A. E. (1999). Temporal dynamics of airborne lead-210 in Missouri (USA): implications for geochronological methods. Environmental Geology, 38, 343-348.

Sheng-Gao, L., Shiqiang, B. A. I. and Lixia, F. U. (2008). Magnetic Properties as Indicators of Cu and Zn contamination in soils. Pedosphere, 18, 479-485.

Sholkovitz, E. R. (1976). Flocculation of dissolved organic and inorganic matter during the mixing of river water and seawater. Geochimica et Cosmochimica Acta, 40, 831-845.

Sholkovitz, E. R. (1978). The flocculation of dissolved Fe, Mn, Cu, Ni, Co and Cd during estuarine mixing. Earth Planetary Science Letters, 41, 77-86

Shu, J., Dearing, J. A., Morse, A. P., Yu, L. and Yuan, N. (2001). Determining the sources of atmospheric particles in Shanghai, China, from magnetic and geochemical properties. Atmospheric Environment, 35, 2615-2625.

Shuman, L. M. (1985). Fractionation method for soil microelements. Soil Science, 140(l), 11-22.

Siegel, F. R. (2002). Environmental Geochemistry of Potentially Toxic Metals. Springer, Berlin, 148p.

Simpson, S. L. and Batley, G. E. (2003). Disturbances to metal partitioning during toxicity testing Fe(II)-rich estuarine porewaters and whole-sediments. Environmental Toxicology and Chemistry, 22, 424-432.

Sims, J. T. (1986). Soil pH effects on the distribution and plant availability of manganese, copper and zinc. Soil Science Society of America Journal, 50, 367-313.

Singare, P. U., Lokhande, R. S. and Pathak, P. P. (2010). Soil Pollution along Kalwa Bridge at Thane Creek of Maharashtra, India. Journal of Environmental Protection, 1, 121-128.

Singh, K. P., Mohan, D., Singh, V. K. and Malik, A. (2005). Studies on distribution and fractionation of heavy metals in Gomti river sediments - a tributary of the Ganges, India. Journal of Hydrology, 312, 14-27.

Singh, A. K., Hasnain, S. I. and Banerjee, D. K. (1999). Grainsize and geochemical partitioning of heavy metals in sediments of the Damodar River Atributary of the lower Ganga, India. Environmental Geology, 39(1), 90-98.

Singh, K. T. and Nayak, G. N. (2009). Sedimentary and Geochemical Signatures of Depositional Environment of Sediments in Mudflats from a Microtidal Kalinadi Estuary, Central West Coast of India. Journal of Coastal Research, 25(3), 641-650.

Singh, S. K. and Subramanian, V. (1984). Hydrous Fe and Mn oxides-scavengers of heavy metals in the aquatic environment, CRC Critical Review in Environment Control, 14(1), 33-90.

Skvaria, J. (1998). A Study on the trace metal speciation in the Ruzin reservoir sediment. Acta Montanistica Slovaca, 3(2), 177-182.

Smith, D. S., Bell, R. A. and Kramer, J. R. (2002). Metal speciation in natural waters with emphasis on reduced sulphur groups as strong metal binding sites. Journal of Comparitive Biochemical Physiology, 133, 65-74.

Smith, I. C. and Carson, B. L. (1981). Trace metals in the environment. Ann Arbor, MI, Ann Arbor Science Publishers.

Soldi, T., Pesavento, M. and Alberti, G. (1996). Separation of vanadium (V) and (IV) by sorption on an iminodiacetic chelating resin. Analytical Chimica Acta, 323 (1), 27-37.

Somerfield, P. J., Gee, J. M. and Warwick, R. M. (1994). Soft sedimental meiofaunal community structure in relation to a long term heavy metal gradient in the Fal estuary system. Marine Ecology Progress Series, 105 (1-2), 79-88.

Soto-Jimenez, M. F. and Paez-Osuna, F. (2001). Distribution and normalization of heavy metal concentrations in mangrove and lagoon sediments from Mazatlan Harbor (SE Gulf California). Estuarine, Coastal and Shelf Science, 53, 259-274.

Spencer, K. L. and MacLeod, C. L. (2002). Distribution and partitioning of heavy metals in estuarine sediment cores and implications for the use of sediment quality standards. Hydrology and Earth Science System, 6(6), 989-998.

Sposito, G. (1984). The Surface Chemistry of Soils. Oxford University Press, New York, 113p.

Stoner, J. S., Channell, J. E. T. and Hillaire-Marcel, C. (1995). Magnetic properties of deep sea sediments off southwest Greenland: Evidence for major differences between the last two deglaciations. Geology, 23, 241-244.

Stoner, J. S., Channell, J. E. T. and Hillaire-Marcel, C. (1996). The magnetic signature of rapidly deposited detrital layers from the deep Labrador Sea: Relationship to North Atlantic Heinrich layers. Paleoceanography, 11(3), 309-325.

Stordal, M. C., Gill, G. A., Wen, L. S. and Santschi, P. H. (1996). Mercury phase speciation in the surface waters of three texas estuaries: Importance of colloidal forms. Limnology and Oceanography, 41, 52-61.

Strzyszcz, Z. and Magiera, T. (1998). Magnetic susceptibility and heavy metals contamination in soils of Southern Poland. Physics and Chemistry of the Earth, 23 (9-10), 1127-1131.

Stull, J. K., Baird, R. B. and Heesen, T. K. (1986). Marine sediment core profiles of trace constituents offshore of a deep wastewater outfall. Journal of Water Pollution Continental Federation, 58, 985-991.

Stumm, W. and Baccini, P. (1978). Man-made chemical perturbation of lakes. In: Lerman A (ed) Lakes. Chemistry, geology and physics. Springer, New York, 91-126p.

Stum, W. and Morgan, J. J. (1996). Aquatic chemistry: Chemical equilibria and rates in natural water. New York: John Wiley and Sons Inc., 1022p.

Summers, J. K., Wade, T. L., Engle, V. D. and Malaeb, Z. A. (1996). Normalization of metal concentrations in estuarine sediments from the Gulf of Mexico. Estuaries, 19, 581-594.

Sunderman, F. W. (Jr.) and Oskarsson, A. (1991). Nickel. In: Merian E (ed.) Metals and Their Compounds in the Environment: Occurrence, Analysis and Biological Relevance. VCH, Weinteim, Cambridge, 1101-1126p.

Suresh, G., Ramasamy, V., Meenakshisundaram, V., Venkatachalapathy, R. and Ponnusamy, V. (2011). Influence of mineralogical and heavy metal composition on natural radionuclide concentrations in the River sediments. Applied Radiation and Isotopes, 69, 1466-1474.

Swart, D. H. (1983). Physical aspects of sandy beaches - a review. In: (eds. A. McLachlan & T. Erasmus) Sandy beaches as ecosystems. The Hague, The Netherlands: Junk, 5-44p.

Tam, N. F. Y. and Wong, Y. S. (2000). Spatial variation of heavy metals in surface sediments of Hong Kong mangrove swamps. Environmental Pollution, 110(2), 195-205.

Tandel, S. S. (1986). Influence of Biotic and Abiotic Factors on a Catfish Mystus gulio (Ham.) from Thane Creek, near Thane City, Ph. D. Thesis, University of Bombay; 7-25p.

Teasdale, P. R., Apte, S. C., Ford, P. W., Batley, G. E. and Koehnken, L. (2003). Geochemical cycling ans speciation of copper in waters and sediments of Macquaire Harbour, Western Tasmania. Estuarine, Coastal and Shelf Science, 57, 475-487.

Templeton, D. M., Ariese, F., Cornelis, R., Danielsson, L., Muntau, H., Van Leeuwen, H. P. and Lobinski, R. (2000). Guidelines for terms related to chemical speciation and fractionation of elements. Definitions, structural aspects, and methodological approaches. Pure and Applied Chemistry, 72(8), 1453-1470.

Tessier, A., Campbell, P. G. C. and Bisson, M. (1982). Particulate trace metal speciation in stream sediments and relationship with grain size: Implication for geochemical exploration. Journal of Geochemical Exploration, 16, 77-104.

Tessier, A., Campbell, P. G. C. and Bisson, M. (1979). Sequential extraction procedure for the speciation of particular trace metals. Analytical Chemistry, 51, 844-851.

Thamdrup, B., Fossing, H. and Jorgensen, B. B. (1994). Manganese, iron, and sulfur cycling in a coastal marine sediment, Aarhus Bay, Denmark. Geochimica et Cosmochimica Acta, 58, 5115-5129.

Thompson, R. and Oldfield, F. (1986). Environmental Magnetism. Allen and Unwin Publishers Ltd., U.K., 227p.

Thompson, R., Bloemendal, J., Dearing, J. A., Oldfield, R., Rummery, T. J., Stober, J. C. and Turner, G. M. (1980). Environmental applications of magnetic measurements. Science, 207, 481-486.

Thompson, R., Oldfield, F. and Yan, Y. J. (1995). Environmental Magnetism. Geological Publishing House, Beijing.

Thorne, L. T. and Nickless, G. (1981). The relation between heavy metals and particle size fractions within the Severn Estuary (U.K. inter-tidal sediments). Science of the Total Environment, 19, 207-213.

Thornton, S. F. and McManus, J. (1994). Application of organic carbon and nitrogen stable isotope and C/N ratios as source indicators of organic matter provenance in estuarine systems: evidence from the Tay Estuary, Scotland. Estuarine, Coastal and Shelf Science, 38, 219-233.

Tipping, E., Hetherington, N.B., Hilton, J., Thompson, D.W., Bowles, E. and Hamilton-Taylor, J. (1985). Artifacts in the use of selective chemical extraction to determine distributions of metals between oxides of manganese and iron. Analytical Chemistry, 57, 1944-1946.

TMC-ES (2000). Environmental status report prepared by the pollution control cell of Thane Municipal Corporation, 118p.

Todorovic, Z., Polic, P., Djordjevic, D. and Antonijevic, S. (2001). Lead distribution in water and its association with sediment constituents of the Barje lake (Leskovac, Yugoslavia), Journal of Serbian Chemical Society, 66(10), 697-708.

Turekian, K. K. and Wedepohl, K. H. (1961). Distribution of the elements in some major units of the Earth's crust. Geological Society of American Bulletin, 72, 175-192.

Ujevic, I., Odžak, N. and Barić, A. (2000). Trace metal accumulation in different grain size fractions of the sediments from a semi-enclosed bay heavily contaminated by urban and industrial wastewaters. Water Research, 34(11), 3055-3061.

Usero, J., Gamero, M., Morillo, J. and Garcia, I. (1998). Comparative study of three sequential extraction procedures for metals in marine sediments. Environment International, 24, 478-496.

Vaithiyanathan, P., Ramanathan, A. I. and Subramanian, V. (1993). Transport and distribution of heavy metals in Cauvery River. Water, Air and Soil Pollution, 71, 13-28.

Valette-Silver, N. J. (1993). The use of sediment cores to reconstruct historical trends in contamination of estuarine and coastal sediment. Estuaries, 16, 577-588.

Van Cappellen, P. and Wang, Y. (1996). Cycling of iron and manganese in surface sediments: A general theory for the coupled transport and reaction of carbon, oxygen, nitrogen, sulfur, iron and manganese. American Journal of Science, 296, 197-243.

vanLoon, G. W. and Duffy, S. J. (2005). Environmental Chemistry - a Global Perspective: Oxford University Press.

Vasconcelos, M., Leal, M. F. C. and Van-Den-Berg, C. M. G. (2002). Influence of the nature of the exudates released by different marine algae on the growth, trace metal uptake, and exudation of Emiliania huxleyi in natural seawater. Marine Chemistry, 77, 187-210.

Vassilev, S. and Vassileva, Ch. (1997). Geochemistry of coals, coal ashes and combustion wastes from coal-fired power stations. Fuel Processes and Technology, 51, 19-45.

Velimirovic, M. B., Prica, M. D., Dalmacija, B. D., Roncevic, S. D., Dalmacija, M. B., Becelic, M. D. and Trickovic, J. S. (2011). Characterisation, Availability, and Risk Assessment of the Metals in Sediment after Aging. Water, Air and Soil Pollution, 214 (1-4), 219-229.

Venkatachalapathy, R., Veerasingam, S., Basavaiah, N., Ramkumar, T., Deenadayalan, K. (2011a). Environmental magnetic and geochemical characteristics of Chennai coastal sediments, Bay of Bengal, India. Journal of Earth System Science, 120(5), 885-895.

Venkatachalapathy, R., Veerasingam, S., Basavaiah, N., Ramkumar, T., Deenadayalan, K. (2011b). Environmental magnetic and petroleum hydrocarbons records in sediment cores from the north east coast of Tamil Nadu, Bay of Bengal, India. Marine Pollution Bulletin, 62, 681-690.

Vernet, J. P. (1991). Heavy Metals in the Environment, Elsevier Science Publishers B. V, New York, USA.

Verosub, K. L. and Roberts, A. P. (1995). Environmental magnetism: past, present, and future. Journal of Geophysical Research. 100, 2175-2192.

Versteeg, J. K., Morris, W. A. and Rukavina, N. A. (1995). The utility of magnetic properties as a proxy for mapping contamination in Hamilton Harbor sediment. Journal of Great Lakes Research, 21, 71-83.

Vijay, R., Khobragade, P. and Sohony, R. A. (2010). Water quality simulation of sewage impacts in west coast of Mumbai, India. Water Science and Technology, 62(2), 279-287.

Von Gunten, H. R., Sturm, M. and Moser, R. N. (1997). 200-year record of metals in lake sediments and natural background concentrations. Environmental Science and Technology, 31, 2193-2197.

Wada, E., Minagawa, M., Mizutani, H., Tsuji, T., Imaizumi, R. and Karasawa, K. (1987). Biogeochemical studies on the transport of organic matter along the Otsuchi River Watershed, Japan. Estuarine, Coastal and Shelf Science, 25, 321-336.

Wakeham, S. (2002). Diagenesis of organic matter at the water-sediment interface. In: A. Gianguzza, E. Pelizzeti & S. Sammartano (eds.), Chemistry of marine water and sediments. Springer, Berlin, 146-164p.

Walkey, A. and Black, J. A. (1934). The determination of organic carbon by rapid titration method. Soil Science, 37, 29-38.

Wang, A., Shu, G. and Jianjun, J. (2005). Contemporary sedimentation rates on salt marshes at Wanggang, Jiangsu, China. Acta Geographica Sinica, 60(1), 61-70 (in Chinese).

Wangersky, P. J. (1977). The role of particulate matter in the productivity of surface waters. Helgolander Wissenschaftliche Meeresuntersuchungen, 30, 546-564.

Wang, G. and Liu, J. (2003). Characteristic of element geochemistry and high-resolution sedimentation records in Xianghai wetlands. Scientia Geographica Sinica, 23(2), 208-212.

Wang, X. Y., Lu, H. Y., Li, Z., Deng, C. L., Tan, H. B. and Song, Y. G. (2003). Paleoclimatic significance of mineral magnetic properties of loess sediments in northern Qinghai-Tibetan Plateau. Chinese Science Bulletin, 48**,** 2126-2133.

Wang, Y. and Van Cappellen, P. (1996). A multicomponent reactive transport model of early diagenesis: Application to redox cycling in coastal marine sediments. Geochimica et Cosmochimica Acta, 60, 2993-3014.

Wang, Y. P., Shi, Y. J., Wang, H., Lin, Q., Chen, X. C. and Chen, Y. X. (2007). The influence of soil heavy metals pollution on soil microbial biomass, enzyme activity, and community composition near a copper smelter. Ecotoxicology and Environmental Safety, 67, 75-81.

Wartel, M., Skiker, M., Auger, Y., Boulghrienta, A. and Puskaric, E. (1991). Seasonal variation of Mn^{2+} adsorption on to calcareous surfaces in the English Channel, and its implication on the manganese distribution coefficient. Marine Chemistry, 36, 85-105.

Wepener, V. and Vermeulen, L. A. (2005). A note on the concentrations and bioavailability of selected metals in sediments of Richards Bay Harbour, South Africa. Water SA, 34(4), 589-595.

Westrich, J. T. and Berner, R. A. (1984). Role of sedimentary organic matter in bacterial sulfate reduction: The G model tested. Limnology and Oceanography, 29, 236-249.

Whitney, P. R. (1975). Relationship of manganese-iron oxides and associated heavy metals to grain size in stream sediments. Journal of Geochemical Exploration, 4, 251-263.

Wilde, K. L., Stauber, J. L., Markich, S. J., Franklin, N. M. and Brown, P. L. (2006). The effect of pH on the uptake and toxicity of copper and zinc in a tropical freshwater alga (Chlorella sp.). Archives of Environmental Contamination and Toxicology, 51, 174-185.

Williamson, B., Lewis, G., Mills, G. and Vant, B. (2003). Contaminants on the coast, in J. R. Goff, S. L. Nichol and H. L. Rouse (eds.), The New Zealand Coast: Te Tai o Aotearoa, Dunmore Press, Palmerston North, New Zealand, 237-259p.

Williams, J. P., Bubbs, J. M. and Lester, J. N. (1994). Metal accumulation within saltmarsh environments: A review. Marine Pollution Bulletin, 28, 277-290.

Williamson, R. B. and Wilcock, R. J. (1994). The Distribution and Fate of Contaminants in Estuarine Sediments: Recommendations for environmental monitoring and assessment, Technical Publication No. 47, Auckland Regional Council, Auckland, New Zealand.

Wilson, B. and Pyatt, F. B. (2007). Heavy metal dispersion, persistence, and bioaccumulation around an ancient copper mine situated in Anglesey, UK. Ecotoxicology and Environmental Safety, 66, 224-231.

Winterhalter, B. (1992). Late-quaternary stratigraphy of Baltic Sea basins - A review. Bulletin of Geological Society of Finland, 64, 189-194.

Wong, C. S. C., Wu, S. C., Duzgoren-Aydin, N. S., Aydin, A. and Wong, M. H. (2007). Trace metal contamination of sediments in an e-waste. Environmental Pollution, 145, 434-442.

Xie, S., Dearing, J. A., Boyle, J. F., Bloemendal, J. and Morse, A. P. (2001). Association between magnetic properties and element concentrations of Liverpool street dust and its implications. Journal of Applied Geophysics, 48, 83-92.

Youn, S. T., Koh, Y. K. and Ryu, S. O. (1999). Distribution characteristics of surface sediments and metal elements in Hampyong Bay, the south-western coast of Korea. Journal of Environmental Science, 8, 677-684.

Yuan, C., Shi, J., He, B., Liu, J., Liang, L. and Jiang, G. (2004). Speciation of heavy metals in marine sediments from the East China Sea by ICP-MS with sequential extraction. Environment International, 30, 769-783.

Yu, R., Hu, G. and Wang, L. (2010). Speciation and ecological risk of heavy metals in intertidal sediments of Quanzhou Bay, China. Environmental Monitoring and Assessment, 163, 241-252.

Zabetoglou, K., Voutsa, D. and Samara, C. (2002). Toxicity and heavy metal contamination of surficial sediments from the Bay of Thessaloniki (Northwestern Aegean Sea) Greece. Chemosphere, 49, 17-26.

Zar, J. H. (1984). Biostatistical Analysis. Prentice-Hall, Englewood Cliffs.

Zhang, H., Davidson, W., Mortimer, R. J. G., Krom, M. D., Hayes, P. J. and Davies, I. M. (2002). Localised remobilization of metals in a marine sediment. Science of the Total Environment, 296, 175-187.

Zhang, J. and Liu, C. L. (2002). Riverine composition and estuarine geochemistry of particulate metals in China–Weathering features, anthropogenic impact and chemical fluxes. Estuarine, Coastal and Shelf Science, 54, 1051–1070.

Zhang, J., Huang, W. W. and Martin, J. M. (1988). Trace metals distribution in Huanghe (Yellow River) estuarine sediments. Estuarine, Coastal and Shelf Science, 26, 499-526.

Zheng, Y., Anderson, R. F., Van Geen, A. and Fleisher, M. Q. (2002). Remobilisation of authigenic uranium in marine sediments by bioturbation. Geochimica et Cosmochimica Acta, 66 (10), 1759-1772.

Zhou, H. Y., Cheung, R. Y. H., Chan, K. M. and Wong, M. H. (1998). Metal concentrations in sediments and Tilapia collected from inland waters of Hong Kong. Water Research, 32, 3331-3340.

Zhu, R. X., Deng, C. L. and Jackson, M. (2001). A magnetic investigation along a NW-SE transect of the Chinese Loess Plateau and its implications. Physics and Chemistry of the Earth, 26, 867-872.

Zimmerman, A. J. and Weindorf, D. C. (2010). Heavy metal and trace metal analysis in soil by sequential extraction: A review of procedures. International Journal of Analytical Chemistry, ID-387803.

Zingde, M. D. and Desai, B. N. (1981). Mercury in Thane Creek, Bombay harbour. Marine Pollution Bulletin, 12, 237-241.

Zingde, M. D. (1989). Marine pollution-what are we heading for? In: Somayajulu BLK, editor. Ocean science-trends and future directions. New Delhi: Indian National Science Academy.

Zingde, M. D. (2002). Proceedings of the National Seminar on Creeks, Estuaries and Mangroves - Pollution and Conservation, 28th to 30th November, 2002, Thane, Ed. by: Quadros, G., 3-7p.

Zourarah, B., Maanan, M., Robin, M. and Carruesco, C. (2009). Sedimentary records of anthropogenic contribution to heavy metal content in Oum Er Bia estuary (Morocco). Environmental Chemistry Letters, 7, 67-78.

Zwolsman, J. J. G., Berger, G. W. and Van Eck, G. T. M. (1993). Sediment accumulation rates, historical input, postdepositional mobility and retention of major elements and trace metals in salt marsh sediments of the Scheldt Estuary, SW Netherlands. Marine Chemistry, 44, 73-94.

Zwolsman, J. J. G., Eck, B. T. M. and Van der Weijden, C. H. (1997). Geochemistry of dissolved trace metals in the Scheldt estuary, southwestern Netherlands: Impact of seasonal variability. Geochimica et Cosmochimica Acta, 61, 1635-1652.